F.F. (Russ) Knapp
Ashutosh Dash

Radiopharmaceuticals for Therapy

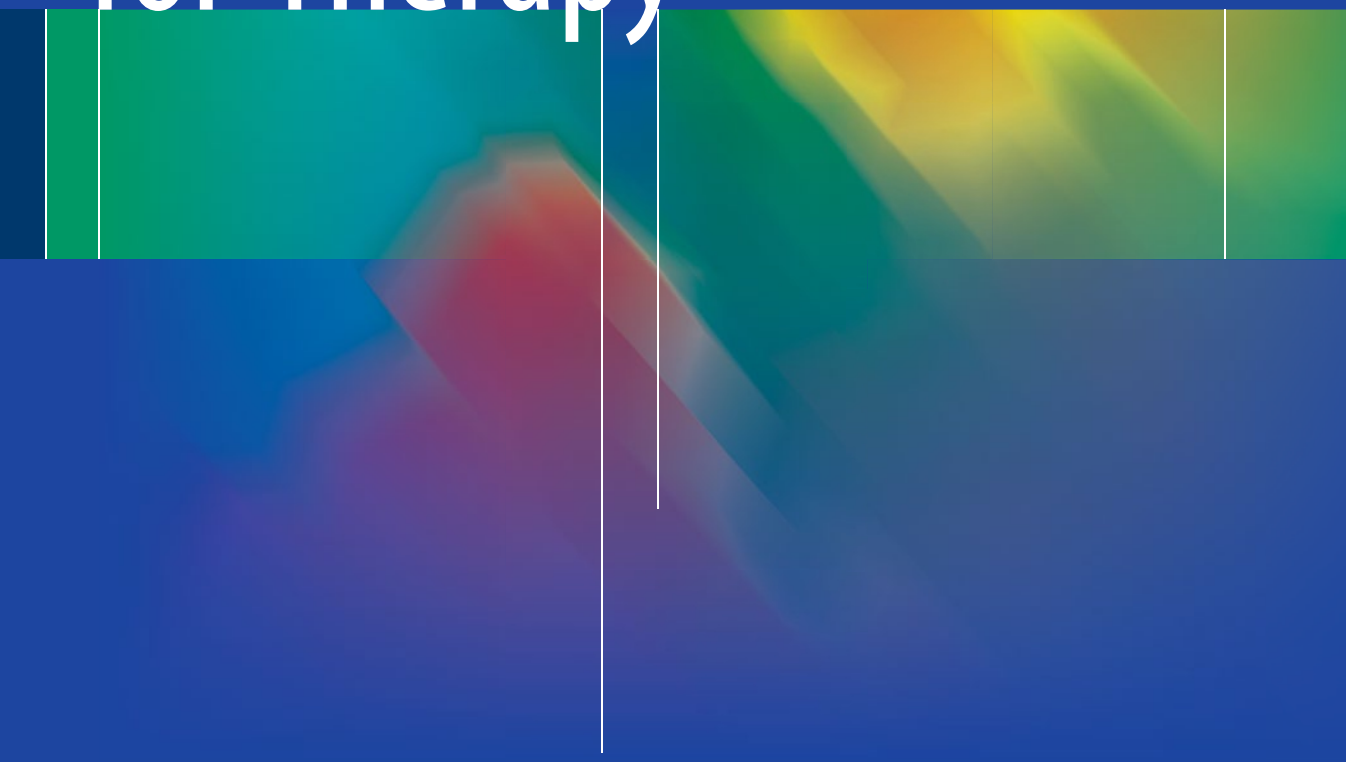

Springer

Radiopharmaceuticals for Therapy

F.F. (Russ) Knapp • Ashutosh Dash

Radiopharmaceuticals for Therapy

Springer

F.F. (Russ) Knapp
Nuclear Security and Isotope Division
Oak Ridge National Laboratory
OAK RIDGE
USA

Ashutosh Dash
Isotope Production and
Applications Division
Bhabha Atomic Research Centre
Mumbai
India

ISBN 978-81-322-2606-2 ISBN 978-81-322-2607-9 (eBook)
DOI 10.1007/978-81-322-2607-9

Library of Congress Control Number: 2015960843

Springer New Delhi Heidelberg New York Dordrecht London

Printed on acid-free paper

Springer (India) Pvt. Ltd. is part of Springer Science+Business Media (www.springer.com)

The authors dedicate this book to their families, mentors, and colleagues who have so strongly affected their professional careers. Russ Knapp offers his dedication to his parents, who inspired and supported a strong interest in science at an early age; to his wife and best friend Toni, who for over 50 years encouraged and, even in many cases, tolerated his professional work; and to their children Michael and Gina, who have made his more important personal life such a joy. He also expresses his personal thanks to his deceased important friend, Mr. A. P. Callahan, who as a mentor and colleague had taught him so much about science and life. Ashutosh Dash gives his dedication to his wife Sarita and son Shaswat, who stood by him through thick and thin, lifted him up when he was low, pushed him forward at difficult times, and never complained at all when times were difficult. Through lonely and difficult times, they gave him strength and encouraged him. He also expresses his personal thanks to Dr. Russ Knapp for believing, encouraging, understanding, and tolerating through the whole process of completing this book.

Foreword

The use of radioactivity for treatment of disease is more than a century old and began with the use of naturally occurring radium-226 in the early part of the twentieth century. However, the field of radionuclide therapy (RNT) had not progressed as rapidly as probably anticipated due to the early failure due to absence of suitable targeting mechanisms. The use of artificially produced phosphorus-32 for the treatment of *polycythemia vera* beginning in the 1930s was a positive step which had stimulated the growth of this field. The major breakthrough for RNT, however, was the use of iodine-131 for the treatment of thyroid cancer which began in 1946. The uptake of radioactive iodide anions is governed by a well-defined mechanism involving the sodium iodide symporter protein and is the most basic and finest example of molecular nuclear medicine. Normal thyroid tissue takes up around 30 % of ingested iodine, which represents the highest targeting that a drug can achieve. Iodine-131 continues to be widely used post surgically for the ablation of remnant cancer cells. Although a variety of radiopharmaceuticals were subsequently introduced in later years for treatment of some types of cancer and for palliation of pain due to bone metastases, widespread/routine use has not yet gained broad acceptability. Generally, the majority of the patients who have undergone unsuccessful treatment by alternative nonradioactive strategies who have few other options for success are often referred for nuclear medicine RNT as a last resort and mainly for palliative therapy. In fact, none of the other therapeutic radiopharmaceuticals introduced in the last century have been anywhere nearly successful like the use of iodine-131 for the treatment of thyroid cancer.

In this regard, introduction of peptide receptor radionuclide therapy (PRRNT) in the beginning of the current millennium for the treatment of neuroendocrine tumors (NETs) with beta-emitting is an important seminal exception. PRRNT utilizes low molecular weight radiolabeled peptides targeting to specific cell surface receptors which are very often upregulated on cancer cells. Although several radioisotopes have been identified that are used for PRRNT, lutetium-177 and yttrium-90 are two key examples as radionuclides used for both PRRNT and radioactive antibody targeting. Currently, PRRNT using somatostatin analog peptides is the most efficacious mode of therapy for the treatment of inoperable NETs. However, NETs are tumors with relatively low incidence, and hence the total number of patients benefitted is still very small. Another important developing theme is the use of alpha-emitting radioisotopes for therapy, and the commercialization and

routine clinical introduction of the Xofigo® (radium-223 chloride) for the treatment of castration-resistant prostate cancer is an important advance for the therapeutic arena.

However, the real success of PRRNT, as an example, will be demonstrated when suitable radiopharmaceuticals are developed for the treatment for major cancer entities, and success in this direction is already on the horizon. The pharmacophore, N-acetyl aspartyl glutamate (NAAG), radiolabeled with ^{68}Ga, for instance, is providing excellent PET images of patients presenting with prostate cancer. Adenocarcinoma of the prostate gland overexpresses prostate-specific membrane antigen (PSMA) which is targeted by NAAG. Because this is a small peptide, the radioactivity not attached to the targeted cancer cells is rapidly excreted, thereby providing excellent PET images of the cancer-affected areas. Lutetium-177-labeled NAAG is also under evaluation for the treatment of prostate cancer, and the male patient population who can benefit from this PET technology is very large and is expected to dramatically change the trajectory of targeted therapy.

Growth in the development of therapeutic radiopharmaceuticals is linked to advances in many related disciplines, and molecular biology identifies suitable targets for different types of cancer. An in-depth understanding of the biochemical reactions occurring within the body is important to provide information which will help identify new targets. Once suitable target-seeking molecules are identified, subsequent detailed research is required to develop a successful therapeutic radiopharmaceutical. These efforts include an evaluation for modification of the target-seeking pharmacophore to provide suitable radiolabeling without compromising the affinity to the target. In addition, both in vitro and in vivo biological studies are required to demonstrate the targeting property, and preclinical evaluation and finally the demonstration of the clinical efficacy must be established. A major goal which presents these challenges is the subsequent use in humans. Current regulations in most countries mandate that a radiopharmaceutical undergoes the same phase 0, I, II, and III studies before its market introduction as a product. Compliance with these regulatory requirements is difficult for a commercial radiopharmaceutical manufacturer to justify, since the modest market volume for therapeutic radiopharmaceuticals will often not qualify the high investment required for a clinical trial. The usual short shelf lives of radiopharmaceuticals do not allow large-scale manufacturing, and it is difficult for patent holders to overcome the competition of use of generic radiopharmaceutical products. Hence, most discoveries in the therapeutic radiopharmaceutical arena are not used to the most effective extent for the benefit of mankind. Nevertheless, the scientists working in this area put forth extensive efforts to develop new therapeutic radiopharmaceuticals.

There are many young colleagues who wish to work in the fascinating multidisciplinary field of therapeutic radiopharmaceuticals, which, by nature, requires broad knowledge in many fields, which includes radioisotope production, chemistry, radiochemistry, and biology and physiology. There is extensive literature available on therapeutic radiopharmaceuticals; however, a primary source which will provide basic knowledge is highly useful, not only for new investigators in this area but also for those scientists, physicians, and

other professionals already working in the field of nuclear medicine. For these reasons this book on "radiopharmaceuticals for therapy" authored by Prof. F. F. (Russ) Knapp and Dr. A. Dash is expected to fill an important niche in the literature. The 17 chapters span all key aspects describing the development and use of therapeutic radiopharmaceuticals. The expertise and extensive experience of these authors are reflected in the appropriate selection of chapters and their contents. This book will be highly useful to scientists and nuclear medicine physicians working in this fascinating field, and I am honored to have been given the opportunity to provide the Foreword to *Therapeutic Radiopharmaceuticals*.

Cochin, India M.R.A. Pillai, PhD, DSc

Acknowledgments

The authors extend their sincere appreciation to Dr. M. R. A. Pillai, Ph.D., D.Sc., for his vision in conceiving the important need for a book on therapeutic radiopharmaceuticals and for providing the *Foreword*. He had initially recommended this book to Springer Verlag and had encouraged the authors to move forward. The authors also thank their families for their patience and their colleagues who have helped in many different ways and who had provided information and insights which encouraged the authors. Special thanks are also extended to Mr. Mark Dickey, a senior member of the ORNL technical library staff, for his enthusiastic assistance in identifying and obtaining reference and reprint materials.

Contents

Part III Therapeutic Radiopharmaceuticals for Cancer Therapy

Abbreviations

ADME	Adsorption, distribution, metabolism, and excretion
AE	Auger electron
BFCA	Bifunctional chelating agent
CD	Cluster of differentiation
Ci	Curie
C-K	Coster–Kroenig
CT	Computed tomography
DES	Drug eluting stent
DNA	Deoxyribonucleic acid
DOTA	1, 4, 7, 10-tetraazacyclododecane-1, 4, 7, 10-tetraacetic acid
DTPA	Diethylenetriamine pentaacetic acid
EC	Electron capture
HAMA	Human automouse antibody
HCC	Hepatocellular carcinoma
HDR	High-dose radiation
HEHA	1, 4, 7, 10, 13, 16-hexaazacyclohexane-N, N′, N″, N‴, N⁗, N⁗′-hexanoic acid
HER-2	Receptor tyrosine-protein kinase erbB-2 (CD340)
HSA	High specific activity
HSA	Human serum albumin
IC	Internal conversion
IT	Isomeric transition
IVRT	Intravascular radiation therapy
LATO	Late acute thrombotic occlusion
LER	Lower extremity revascularization
LET	Linear energy transfer
LSA	Low specific activity
MABG	Meta-astatobenzyl guanidine
mCi	Millicurie
MDP	Methylene diphosphonate
MeV	Mega (million) electron volts
MIBG	Metaiodobenzylguanidine
MIBI	Methoxy isobutyl nitrile (ligand)
MRI	Magnetic resonance imaging
MTB	Maximal tolerated dose
NIS	Sodium iodide transporter
NMSC	Nonmelanoma skin cancer

PET	Positron emission tomography
PLA	Polylactic acid
PPRT	Peptide receptor radionuclide therapy
RAD	Radiation adsorbed dose
RAIT	Radioimmunotherapy
RBE	Relative biological effectiveness
RDG	Arginine–glycine–aspartate acid (tripeptide sequence)
RNT	Radionuclide therapy
SA	Specific activity
σ	Sigma, neutron cross section, cm^{24}
SIRC	Surgically created resection cavity
SIRT	Selective internal radiation therapy
SKID	Severe combined immunodeficiency
SPECT	Single-photon emission computerized tomography
Super-C–K	Super Coster–Kroenig
TACE	Trans-arterial chemoembolization
TARE	Trans-arterial radioembolization
TART	Trans-arterial radionuclide therapy
TATE	Peptide sequence
TOC	Peptide sequence, $DOTA^0$–Phe^1–Tyr^3
US	Ultrasound

Part I

Radiopharmaceuticals

1 Introduction: Radiopharmaceuticals Play an Important Role in Both Diagnostic and Therapeutic Nuclear Medicine

1.1 Introduction: Use of Radioisotopes in Nuclear Medicine

As a foundation for a discussion of the development and use of therapeutic radiopharmaceuticals, it is first necessary to provide an introduction to the field of nuclear medicine and how radioisotopes are used in this board-certified clinical specialty for both diagnostic and therapeutic applications. In the field of nuclear medicine, unsealed radioactive agents known as radiopharmaceuticals are administered generally intravenously for either diagnostic or therapeutic applications (McCready 2000; Ercan and Caglar 2000). These specialists and their staff are specially trained in the safe handling, storage, and disposal of radioactive materials. Special licensing is required, radiopharmaceuticals must be approved by regulatory bodies for use, and certified radiopharmacists are required for the formulation and dispensing of these radioactive substances. Diagnostic applications in nuclear medicine use low activity tracer levels of generally gamma- or positron-emitting radioisotopes which are generally produced in nuclear reactors and accelerators (Chap. 5). In contrast, therapeutic applications utilize particle-emitting radionuclides for induction of radiotoxicity to kill cells in the targeted tissue. The substrate or targeting moiety (vector) to which the radionuclide is chemically attached is designed to favor the accumulation of the administered radiopharmaceutical at the targeted cell, tissue, or organ. The radiation emitted from the accumulated radioactivity is then detected by external measuring devices such as a gamma camera or positron emission tomographic camera to reconstruct images for diagnostic purposes. For therapeutic applications in nuclear medicine, particles emitted from radioactive decay of selected radioisotopes deliver cytotoxic levels of radiation to the target site. After site-specific accumulation of the radiopharmaceutical to the target site, cytotoxic ionizing radiation is delivered to induce un-repairable double-strand DNA breaks which result in subsequent cell death (Hoefnagel 1998; Aerts et al. 2014; Wheldon 1994). It should also be noted that in the form of sealed radioactive sources, therapeutic radioisotopes are also used in other clinical specialties, most notably in brachytherapy practiced in radiation oncology. In these applications, permanently often reusable sealed radioactive sources are introduced adjacent to the target tissue for limited time periods and then removed, or permanently implanted, such as well-established methods for treatment of prostate cancer (Connell and Hellman 2009; Gerber and Chan 2008). This book focuses on the description of unsealed radioactive materials which are used for nuclear medicine therapy.

F.F. (Russ) Knapp, A. Dash, *Radiopharmaceuticals for Therapy*, DOI 10.1007/978-81-322-2607-9_1

1.2 Key Examples of Nuclear Medicine

1.2.1 Nuclear Medicine Imaging

For imaging tissue anatomy, function, and metabolism, radioisotopes which decay by emission of gamma photons, X-rays, and positrons (β^+) are targeted to specific organs and disease entities (James and Gambhir 2012; Zanzonico 2012). The radiopharmaceutical agents are generally administered intravenously and for some applications either orally or by inhalation, with the radioactive agent then localizing in the targeted specific organ or tissue. The emission of radiation from the localized radioactive agent is then detected by scintillation cameras and other instruments and the detector data is then processed in the computer into either two-dimensional (planar imaging) or three-dimensional (tomographic imaging) images of the radiopharmaceutical distribution. These data can also be used for several important applications on organ function to quantitate time–activity curves or the uptake and release kinetics of radioactivity over time. Images obtained from stationary camera devices are referred as scintigraphs, while the use of a linear moving or rotating camera system in two dimensions is called a scan. The use of the latter tomographic technology is currently most widely used for many applications, where the gamma camera is rotated around the patient to obtain three-dimensional images (Kjaer 2006). The development and clinical applications of radioisotopes and radiopharmaceuticals in nuclear medicine are widely described in the literature (Bhattacharyya and Dixit 2011; Britton 1997; Ercan and Caglar 2000; Hoefnagel 1991; Leeds 1990; Penner et al. 2009; Volkert and Hoffman 1999).

Modern gamma cameras provide tomographic images, and this technology is commonly referred to as single-photon emission computed tomography (SPECT). Another major nuclear medicine imaging modality is positron emission tomography (PET) which provides very high-resolution images and detects the coincidence photon events which occur after positron emission of radioisotopes such as carbon-11 (^{11}C) and fluorine-18 (^{18}F). Nuclear medicine imaging is thus unique, because it provides information about both structural and functional changes involved in a disease process and offers unique opportunities and can determine the presence of metabolic and functional abnormalities based on biological changes mostly at the cellular level rather than changes in anatomy, which are often only detected at later stages of the disease. Traditional radiology-based imaging technologies such as X-ray computed tomography (CT), ultrasound (US), and magnetic resonance imaging (MRI) are almost used exclusively for evaluation of anatomy. Nuclear medicine imaging using planar scanning, SPECT, and PET, however, can thus often reveal metabolic and physiological abnormalities generally not detected by static forms of anatomic imaging such as CT and US, although some unique physiologic applications are possible with the MRI modality. Important instrumental developments have progressed over the last two decades, however, by the combination of traditional anatomically based imaging modalities and radioisotope-based technologies. Current state-of-the-art imaging instruments are thus now widely used which simultaneously utilize both PET and SPECT in conjunction with MRI and CT in hybrid imaging instruments for accurate assessment of radiopharmaceutical targeting data with anatomical images (i.e., PET-CT, PET-MRI, SPECT-CT).

1.2.2 Molecular Imaging

Molecular imaging is a special nuclear medicine application where engineered radiopharmaceutical agents are specifically targeted for the detection and evaluation of functional changes at a specific cellular level, which allows monitoring of body function to measure specific chemical and biological processes (Bentzen and Gregoire 2011; Garden et al. 1989; Howard et al. 2015; Hunter and Eisbruch 2011; Maletz et al. 2012; Schlegel 2010; Simpson et al. 2009; Wolbarst and Hendee 2006). Molecular imaging can often uniquely identify disease processes at very early

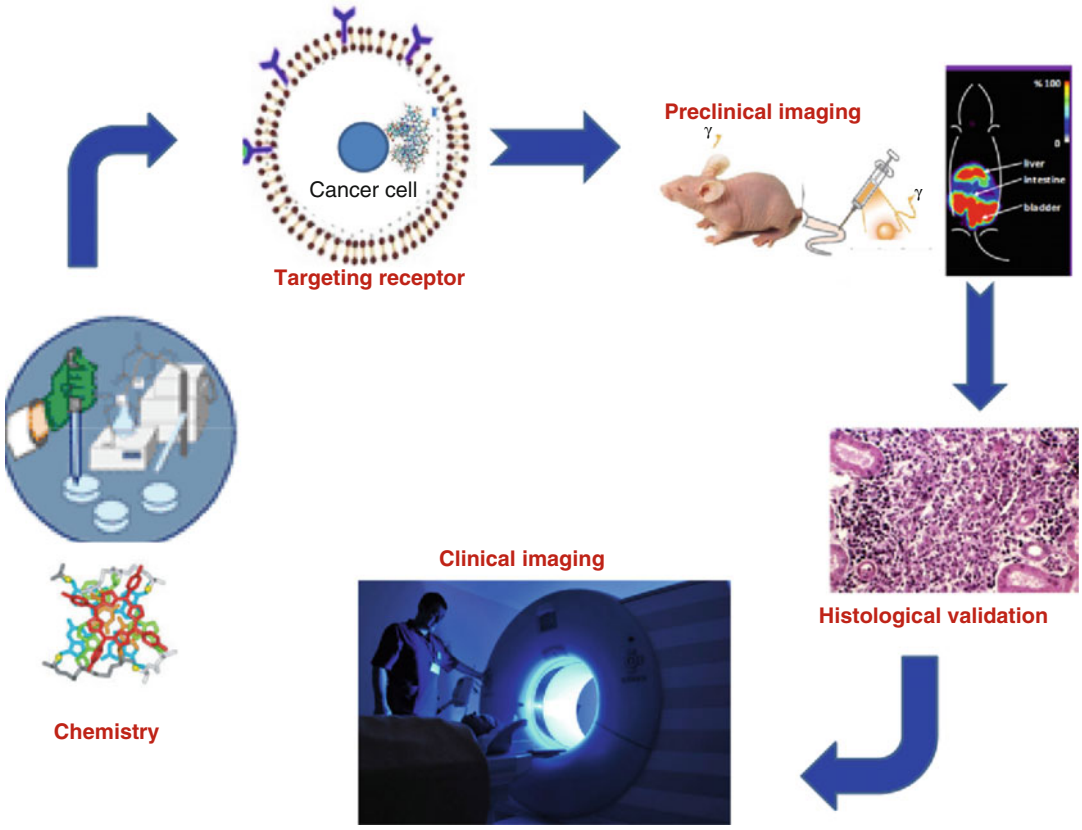

Fig. 1.1 The cycle of the development of molecular imaging agents

stages before clinical symptoms are observed. Several examples include the use of radiolabeled peptides to detect tumors. Nuclear medicine imaging thus plays a critical role at every phase of disease assessment, which includes diagnosis and staging, treatment planning, monitoring response to therapy, and monitoring recurrence and residual disease. In cancer management these technologies can detect disease conditions which may often be occult and be undetected by other imaging modalities. Imaging can also assess the severity of disease, including the degree of spread throughout the body. Although initial cancer staging has been historically accomplished by various diagnostic techniques such as CT and MRI, the relatively recent broad availability of SPECT and PET nuclear imaging technologies has resulted in new opportunities in cancer management, for example, for staging, upstaging, or downstaging specific cancer entities. In planning cancer treatment, nuclear medicine imaging often provides important information for selecting the most effective therapy based on the unique biologic characteristics of a particular patient and the molecular properties of the tumor. This "personalized" approach for patient management is important for evaluation of response to ongoing therapy, and such functional imaging technologies offer advantages not available through anatomic imaging alone. This critical advantage can allow midcourse alteration of treatment, if necessary, as opposed to the presentation of structural changes revealed by other imaging modalities. Nuclear imaging is also highly useful for detection of residual disease or surveillance for recurrence (Akkas et al. 2014; de Haas et al. 2012; Kostakoglu et al. 2013; Kurdziel et al. 2008). The key components which comprise the development of molecular imaging (MI) agents are depicted in Fig. 1.1.

1.2.3 In Vivo Function Tests

In this process a radiopharmaceutical is administered, and the adsorption, distribution, metabolism, and excretion (ADME) properties are documented (Dalvie 2000; Giron et al. 2008). Functional processes that can be assessed include tissue blood flow and metabolism, protein–protein interactions, expression of cell receptors in normal and abnormal cells, cell–cell interactions, neurotransmitter activity, cell trafficking and homing, tissue invasion, and programmed cell death. By providing information on these processes, nuclear medicine imaging offers a broad array of tools for probing normal and disease-related states of tissue function and response to treatment. The time–activity curves of the organs of interest are obtained which reflect organ function. In vivo quantification of radiopharmaceuticals has great potential as a tool in assessing the function of an organ or organ systems. Key examples include kidney function tests, neurological disorders, cardiovascular disease, bile flow, lymphatic drainage, thyroid structure and function, small-bowel transit gastric emptying assessment, acute GI bleeding, hepatic hemangiomas, reticuloendothelial function renal, artery stenosis, and inflammatory bowel disease (Alazraki 1993; Bomanji and Siraj 1995; Eberlein et al. 2011; El-Maghraby et al. 2006; Ganz and Serafini 1989; Messa et al. 1995; Notghi and Harding 1995; Prvulovich and Bomanji 1998; Ross 1991).

1.2.4 Nuclear Medicine Therapy

The primary focus of this book is the use of unsealed radioactive sources for nuclear medicine therapy, which is commonly referred to as radionuclide therapy (RNT). In this therapeutic modality, high activity levels of generally particle-emitting radioisotopes attached to tissue-targeting agents are administered to deliver high radiation doses to targeted tissues. Principal established clinical applications include cancer therapy (Chaps. 9 and 10), treatment of metastatic bone pain (Chap. 12), and treatment of inflammatory processes such as rheumatoid arthritis (Chap. 14). Key examples of developing technologies using therapeutic radiopharmaceuticals include treatment of nonmelanoma skin cancer in delicate anatomical areas (Chap. 13) and therapy of hyperplasia which often occurs after arterial angioplasty (Chap. 15). These applications and the radiopharmaceuticals which are employed are discussed in subsequent chapters. A large variety of disease-targeting radiopharmaceuticals to which are attached radionuclides which emit alpha (α), beta (β^-), or Auger (AE)/conversion (CE) electron particulate radiation are used for RNT. Unlike conventional external beam therapy—under the purview of radiation oncology—RNT is practiced in the nuclear medicine arena and targets diseases at the cellular rather than on a gross anatomical level (Cuaron et al. 2009: Dash et al. 2013; Eary 1991; Gabriel 2012; Srivastava and Dadachova 2001; Yeong et al. 2014). This concept is a blend of a tracer moiety that mediates a site-specific accumulation followed by induction of cytotoxicity with the short-range biological effectiveness of the particulate radiation. The proximal contact between the radionuclide and the cells targeted for destruction enables the absorbed radiation to be concentrated at the target site with the minimal injury to adjacent healthy tissue.

1.3 Radiopharmaceuticals

In contrast to the common use of nonradioactive therapeutic routine pharmaceuticals, radiopharmaceuticals are generally administered at subpharmacologic dose in very high specific activity (radioactivity/unit mass). Radiopharmaceuticals can consist in some instances of a radionuclide in ionic form—such as iodine-131 (^{131}I) for treatment of thyroid cancer or strontium-89 (^{89}Sr) for bone pain palliation (Chap. 12)—but these agents are generally represented by pharmaceutical targeting agents to which the radioisotope is chemically attached. These carrier molecules are represented by a broad range of molecules, which include chelating agents, small molecules, drugs, peptides, proteins, or particles. Similar to

conventional pharmaceuticals, the radiopharmaceutical targeting agents are administered by oral, intra-arterial, intravenous, intratumoral, intra-portal, and intracavity routes. The administered radiopharmaceuticals accumulate in the organ or tissue of interest through a variety of well-established known biological mechanisms, for which these agents are designed and developed. The radionuclides attached to the radiopharmaceuticals provide the radiation component (radioactivity), while the carrier molecule targets specifically diseased tissues or cells. These radiopharmaceutical carrier molecules to which radionuclides are attached are often called vectors and often consist of small organic molecules such as a drug, carbohydrate, lipid, nucleic acid, peptide, fragment of antibody, or even very large whole antibodies (Cutler et al. 2013; Dash et al. 2013). The synthetic chemical and biological issues associated for vector selection, development, and preparation are challenging and key factors to provide these agents for preclinical evaluation with a goal of eventual clinical application and are based on the ability of radiopharmaceuticals to accumulate selectively on/or/in a cell, tissue, or organ.

The activity doses of radiopharmaceutical used for diagnostic imaging applications vary depending on the extent of accumulation at the target site, the residence time, release kinetics, type of investigation being conducted, and the imaging technology which is employed. The goal is to limit the activity levels which are required for imaging to minimize the radiation dose to no targeted tissues. Often millicurie (mCi) levels of radioactivity are adequate for diagnostic studies, whereas several hundreds of mCi of activity are often required for therapeutic applications. Radiopharmaceuticals are formulated in various chemical and physical forms and require production and dispensing under good manufacturing conditions (GMP). There are several hundred radiotracers which have been developed over the last decades which have potential radiopharmaceutical use in humans. The radioisotopes used for both diagnostic and therapeutic applications are generally produced in research reactors and accelerator facilities or are available from radionuclide generator systems, as described in Chaps. 5, 6, 7, and 8. Although some imaging and therapeutic agents are produced or dispensed in-house in a hospital-based radiopharmacy under carefully controlled conditions, most radiopharmaceutical agents are delivered for clinical use in a ready-to-use form by commercial manufacturers or from a central radiopharmacy.

Radiopharmaceuticals are available in a wide variety of chemical and physical forms which include radionuclides in inorganic forms, such as $Na^{131}I$ (thyroid therapy), $^{90}SrCl_2$ (bone pain palliation), and $Na^{99m}TcO_4$ (thyroid imaging). Radionuclides are generally attached by complexation to suitable chelating groups, and these entities are then used for imaging or therapy. Key diagnostic examples include ^{99m}Tc-MDP (methylene diphosphonate) for bone imaging and ^{99m}Tc-MIBI (methoxy isobutyl isonitrile), which is widely used for assessment of regional myocardial perfusion. In addition, radionuclides can be complexed to a suitable chelating agent which is attached to the targeting vector, and key examples in this class include ^{99m}Tc-Hynic-TOC (a somatostatin analog peptide) used for tumor detection and therapy management evaluation. In addition, another important strategy is covalent linkage of radionuclides to drug molecule, and examples include ^{131}I-MIBG (MIBG: metaiodobenzylguanidine) for the treatment of adrenal-based tumors, primarily in children. Finally, therapeutic radionuclides can also be attached by chemical chelation to a carrier vector such as ^{99m}Tc-UBI (UBI, ubiquicidin). Key examples of different types of widely used radiopharmaceuticals and their uses are provided in Table 1.1.

The development and use of radiopharmaceuticals is truly a multidisciplinary process. Key strategies for radiopharmaceutical development include a number of physiological issues which are required to insure that the expected targeting and kinetics are optimized. Radiopharmaceuticals should exhibit rapid blood clearance and, when appropriate, possess high membrane permeability to facilitate cellular accumulation. The agents should also exhibit slow metabolism before delivery and after accumulation at the target site and minimal accumulation in nontarget organs. In addition, limited transport and biochemical transformation should

Table 1.1 Examples of key diagnostic and therapeutic radionuclides and radiopharmaceutical agents used in nuclear medicine applications

Radionuclide	Agent	Chemical form	Application
Diagnostic radiopharmaceuticals			
^{18}F	^{18}F[FDG]	Vector-link	Imaging cell proliferation
^{123}I	^{123}I-MIBG	Vector-link	Imaging medullary carcinoma
^{99m}Tc	$Na^{99m}TcO_4$	Ionic	Thyroid scanning
^{99m}Tc	^{99m}Tc-MDP	CA	Bone imaging
^{99m}Tc	^{99m}Tc-DTPA	CA	Renal agent for estimation of glomerular filtration rate (GFR) estimation
^{99m}Tc	^{99m}Tc-MIBI	CA	Cardiac imaging
^{99m}Tc	^{99m}Tc-ECD	CA	Brain imaging
^{99m}Tc	^{99m}Tc-hynic-TOC	Vector-CA	Imaging neuroendocrine tumors
^{99m}Tc	^{99m}Tc-hynic-RGD	Vector-CA	Imaging neo-angiogenesis
^{99m}Tc	^{99m}Tc-UBI		Imaging infection
Therapeutic radiopharmaceuticals			
^{131}I	$Na^{131}I$	Ionic	Thyroid scanning, treatment of hyperthyroidism and thyroid cancer
^{131}I	^{131}I-MIBG		Treatment of medullary carcinoma
^{177}Lu	^{177}Lu-DOTATATE	Vector-CA	Treatment of neuroendocrine tumors
^{89}Sr	$^{89}SrCl_2$	Ionic	Bone pain palliation
^{90}Y	Zevalin®	Vector-CA	Treatment of non-Hodgkin's lymphoma

CA chelating agent, *Vector-CA* vector attached chelating agent

occur to facilitate kinetic modeling of the tracer. These data are generated from time–activity curves and serial imaging and allow an estimation of radiation dose to both target and nontarget organs. Radiopharmaceutical development encompasses a variety of disciplines and capabilities including radionuclide production (Chaps. 5, 6, 7, and 8) with subsequent radiochemical processing, purification, and analysis to provide the radionuclides with requisite purity. Other key capabilities and resources include the organic synthesis of chelating agents or vectors for radiolabeling with the appropriate properties, and the development of radiolabeling methods ensures high radiochemical yields. Rapid and efficient purification procedures are required to obtain high radiochemical purity of the final products. From a pharmaceutical perspective, reliable technologies are required for the routine production of sterile, pyrogen-free products with minimum inconvenience achieved either through kit formulation procedure or through the use of automated synthesis modules. Finally, simple quality control procedures are required to ensure the purity and assurance for human use.

1.3.1 Diagnostic Radiopharmaceuticals

The use of radiopharmaceuticals for imaging organ function and disease involvement is the unique capability of nuclear medicine. Radiopharmaceuticals used in diagnostic nuclear medicine procedures generally emit either gamma radiation or positrons, and the half-lives of radionuclides for imaging applications generally span from minutes to several hours. Although it is not a goal of this book to discuss these diagnostic agents in detail, Table 1.2 provides a

summary of commonly used radionuclides for diagnostic radiopharmaceuticals.

1.3.2 Nuclear Medicine Imaging

Radiopharmaceuticals are administered to patients and then redistributed by well-established physiological principles which depend on specific properties of the targeting agent. All radiopharmaceuticals are carefully designed and have well-defined properties which govern adsorption, distribution, metabolism, and excretion (ADME). Nuclear medicine imaging is conducted at defined time points which are evolved as the imaging protocols (Zanzonico 2012). Usually imaging commences after clearance of blood pool activity. The evolution of nuclear medicine imaging has taken many twists and turns as both equipment technology and new radiopharmaceuticals have been developed over the past decade. The commonly used planar, SPECT, and PET imaging techniques are discussed in more detail below.

Table 1.2 Key examples of radionuclides used for diagnosis in nuclear medicine

Radionuclide	Half-life	Emission
^{15}O	2.1 min	Positron
^{11}C	20.4 min	Positron
^{68}Ga	60 min	Positron
^{18}F	109.8 min	Positron
^{99m}Tc	6 h	Gamma
^{111}In	2.8 days	Gamma
^{123}I	13.2 h	Gamma

1.3.2.1 Planar Imaging

A schematic representation of planar and SPECT imaging principles is illustrated in Fig. 1.2. Detection and subsequent image reconstruction of gamma rays emitted by radiopharmaceuticals is accomplished by scintillation cameras also referred to as Anger or gamma cameras (Fig. 1.2a). The gamma rays emitted by the radionuclide are detected by the scintillation crystal, which is usually thallium-activated sodium iodide (Anger 1958; Erickson 1992; Tapscott 1998; Pexman 1973; Telander and Loken 1967). The ionizations produced within the sodium iodide crystals emit secondary radiations which are converted to light photons via sodium iodide scintillation detectors, and photodiodes then convert the secondary radiation to light photons which are amplified by a series of photomultiplier tubes before measurement as a current pulse. Reconstruction is accomplished using computer software which converts the current detected at different points corresponding to the crystal to images. These images are traditionally called scintigraphs and are displayed as two-dimensional views of the targeted site region of interest. Such 2D images, known as planar scintigrams, are often of poor quality due to the superposition of nontarget activity from the 3D body which restricts the measurement of organ function and prohibits accurate quantification of that function. However, in some cases, such as bone scintigraphy, planar imaging is a common and cost-effective application. Computer processing of the planar scintigrams can increase the accuracy with

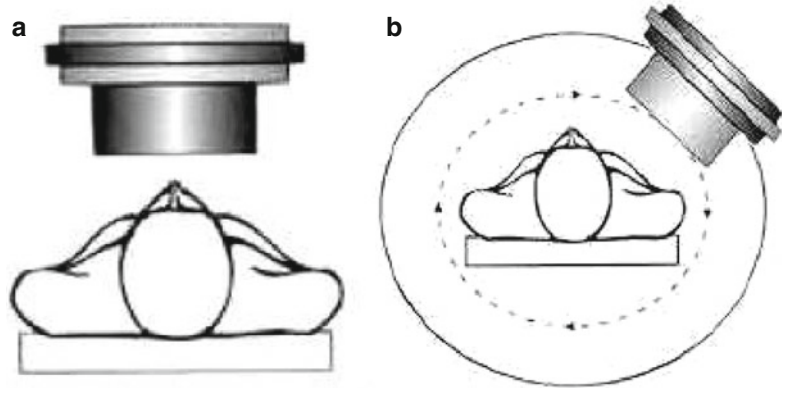

Fig. 1.2 Orientation and patient placement for planar and SPECT imaging. (**a**) 2D planar scan. (b) 3D SPECT, single-photon emission computed tomography

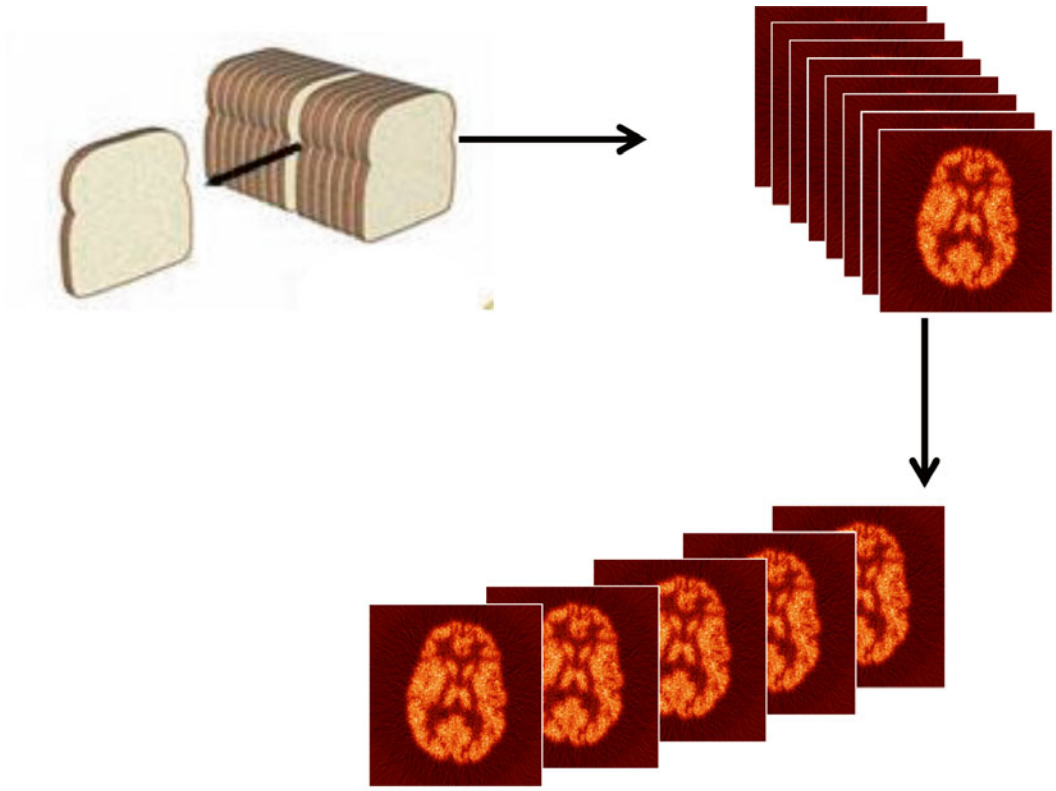

Fig. 1.3 The principal of single-photon emission computed tomography (SPECT)

which the image approximates the activity distribution, selectively enhance normal or abnormal structures of interest, and optimize the use of the display system presenting the image (MacIntyre et al. 1994; Zaidi 2006).

1.3.2.2 Single-Photon Emission Computed Tomography (SPECT)

SPECT is a 3D tomographic technique that uses the imaging data from many angles which are then reconstructed in different planes. SPECT uses a combination of a rotating gamma camera with a powerful computerized calculation system which allows the acquisition of cross-sectional images (Fig. 1.2b). This technique evolved to three-dimensional imaging acquisition which can be performed within a realistic time frame. SPECT has the capability for mapping physiological function and metabolic activity and thereby providing more specific information concerning organ function for the evaluation of function or physiology. The development of SPECT led to improved imaging of the heart, lung, liver, kidney, bone, and inflamed or infected tissues. SPECT also allows the identification of metastases and determination of the extent of a cancer. SPECT provides the activity distribution in different sections of the object at different depths and in turn to accurately determine the location of the lesion as well as metastasis.

SPECT is a technique whereby cross-sectional images of tissue function can be produced by reconstructing data in slices of the total organ thereby greatly minimizing the removal of the effect of overlying and underlying radioactivity as depicted in Fig. 1.3.

The functional information obtained by SPECT is complementary to planar images, obtained by projections of the organ under investigation (Eberl et al. 2006; Jaszczak 2006; Horger and Bares 2006; Schillaci 2006; Schillaci et al. 2007; Krausz and Israel 2006). Schematic representation of single-photon emission computed tomography

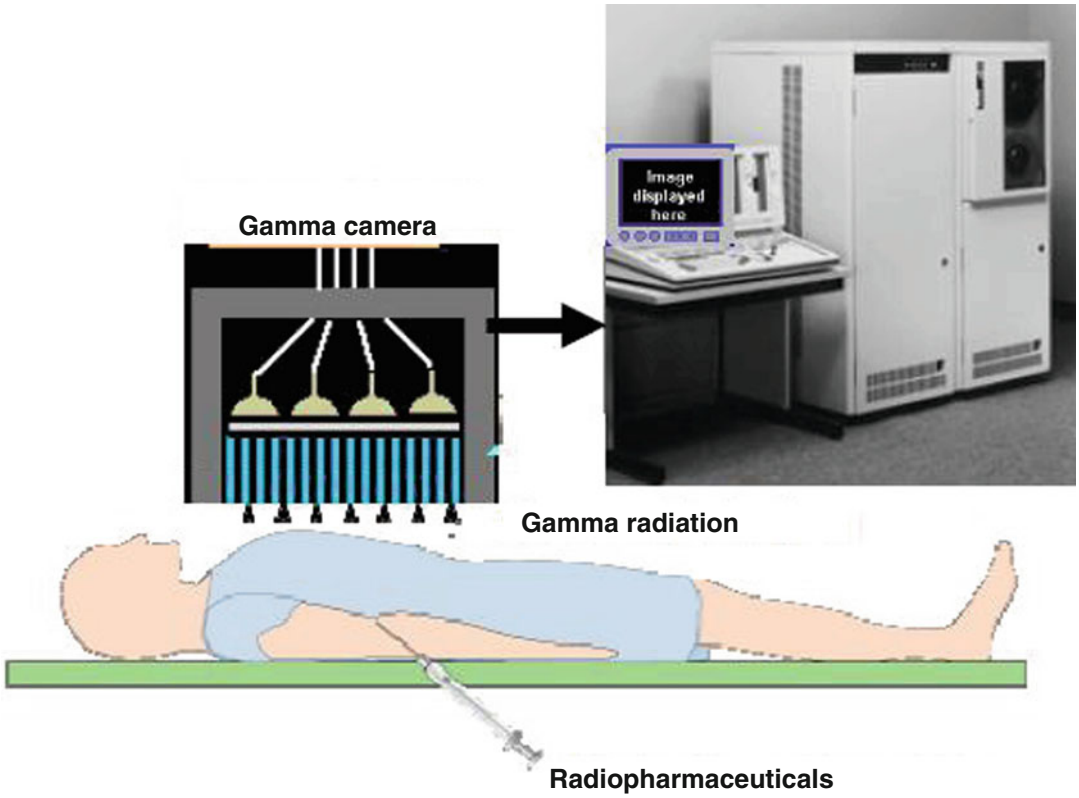

Fig. 1.4 Single-photon emission computed tomography (SPECT)

(SPECT) in a clinical setup is depicted in Fig. 1.4. The advantages of SPECT over planar scintigraphy include better spatial localization, improved detection of abnormal function, and, importantly, greatly improved quantification. In general SPECT images have poorer spatial resolution than the 2D images from which they are reconstructed. Of course capital costs and costs for maintenance of SPECT instrumentation are much higher than for planar imaging instruments.

Radioisotopes used for SPECT are limited to those that emit gamma rays with an energy range that is suitable for the gamma camera such as thallium-201 (^{201}Tl), technetium-99m (^{99m}Tc), and iodine-123 (^{123}I). The spatial resolution of SPECT systems is in the range of 10–14 mm.

1.3.2.3 Positron Emission Tomography (PET)

Positron emission tomography (PET) is a powerful diagnostic imaging modality which has become a dominant imaging method in the field of nuclear medicine (Coleman 1999; Gambhir 2002; Delbeke and Martin 2001; Kubota 2001; Mankoff and Bellon 2001; Mammatas et al. 2015; Mercer 2007; Wood et al. 2007; Riemann et al. 2008; Solomon et al. 2003). This technology requires radionuclides that decay with the emission of positrons (β^+). The concept of simultaneous detection (coincidence detection) is based on $\beta^+ + \beta^-$-annihilation by positron interaction with an electron from the surrounding environment after traveling a short distance (3–5 mm), resulting in the emission of two 511 keV gamma rays traveling in opposite directions. In PET, image acquisition is then based on the detection of the two gamma rays in a coincidence mode. A valid annihilation event requires a coincidence within 12 ns between the two detectors placed on opposite sides of the scanner. In a PET instrument, the patient is positioned within a ring of scintillation detectors. If two events are detected simultaneously in opposing detectors, it is

assumed that an annihilation occurred somewhere on an imaginary line connecting these two detectors. By acquiring a large number of such events, e.g., 10^6, tomographic reconstruction methods can be used to reconstruct two-dimensional images of the tracer distribution. Schematic representation of single detector ring of positron emission tomographic (PET) scanner is depicted in Fig. 1.5.

The higher sensitivity of this technology and its excellent quantification of regional tissue tracer concentrations are the distinct advantages of PET over SPECT, and these advantages have been harnessed to maximize the use of the tracer principle to visualize and measure biologic processes with PET (Zaidi 2006; Gholamrezanejhad et al. 2009). On the other hand, SPECT offers the possibility to widen the observational time window owing to the longer half-life of single-photon emitters and offers the possibility to observe biological processes in vivo several hours or days after administration of the labeled compound (Meikle et al. 2005).

A total of about 2350 fixed or mobile PET facilities are estimated to be in operation in the USA alone. SPECT and PET are not necessarily competitive with one another, but instead, have progressed on different parallel tracks with a focus on providing diagnosis information (Alavi and Basu 2008; Gholamrezanejhad et al. 2009; Jansen and Vanderheyden 2007; Mariani et al. 2008; Rahmim and Zaidi 2008). While both SPECT and PET have the capability for the detection of cancers and related metabolic abnormalities using the appropriate radiopharmaceutical agents, these technologies generally do not provide the anatomical information required for precise localization of lesions. For this reason, the most contemporary hybrid imaging systems encompass capabilities for the simultaneous registration of both PET images with computed tomography (CT) and magnetic

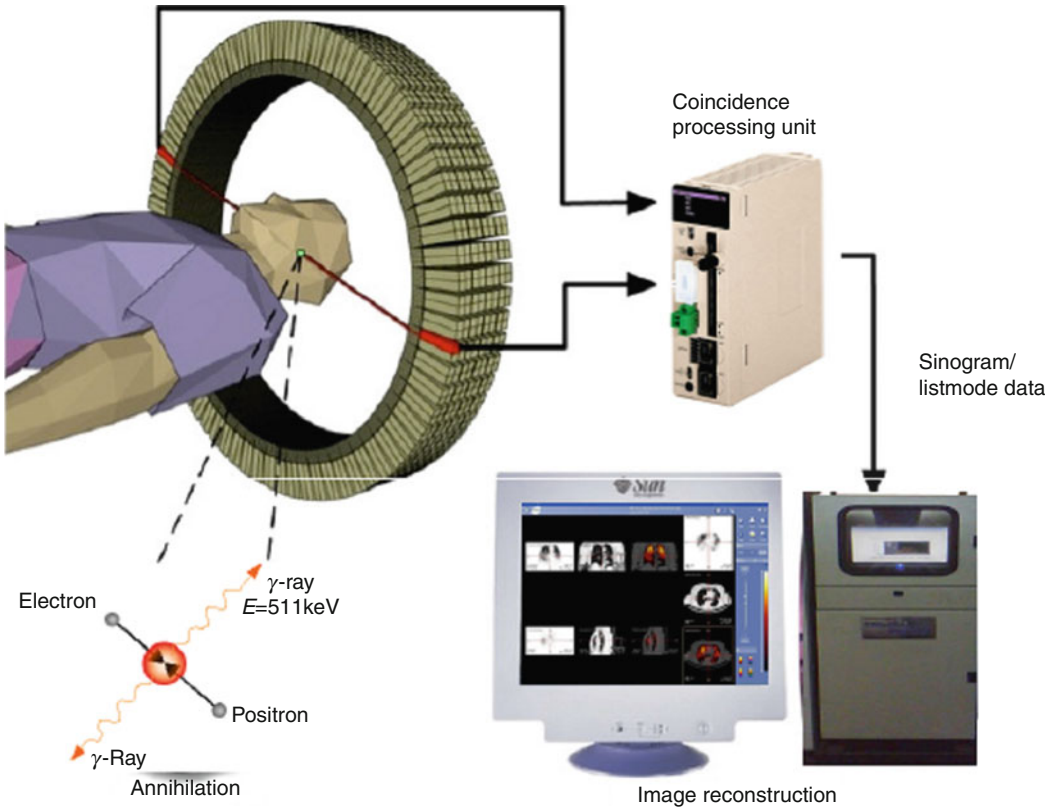

Fig. 1.5 Typical positron emission tomography (PET) system and patient orientation

resonance imaging (MRI) which offers excellent anatomic detail, in conjunction with the functional information provided by the PET capability. An earlier initial strategy involved software-based fusion of independently performed scintigraphic (PET or SPECT) and radiological images (CT), but these methods were time consuming and impractical for routine use. Introduction of hybrid PET-CT as well as PET-MR has now allowed co-registration of data from both the imaging modalities. The PET-CT and PET-MR images provide additional information which has greatly improved diagnostic accuracy and has greatly impacted patient management, especially for oncological applications (Beyer et al. 2011; Bockisch et al. 2009; Brandon et al. 2011; Chowdhury and Scarsbrook 2008; Delbeke and Sandler 2000; Delbeke et al. 2009; Keidar et al. 2003; Kuikka et al. 1998; Mariani et al. 2010; Patton et al. 2000; Schillaci et al. 2004; Utsunomiya et al. 2006).

1.4 Therapeutic Radiopharmaceuticals

In contrast to the goal of limiting tissue radiation dose for diagnostic applications, nuclear medicine therapy is designed to deliver therapeutic doses of ionizing radiation to specific disease sites for cure, disease control, or pain palliation. The ionizing radiation induces irreversible damage to nuclear DNA by induction of double-strand breaks, thereby inhibiting further proliferation of these cells (Fig. 1.6).

In radionuclide therapy, the biological effect is obtained by energy absorbed from the radiation emitted by the radionuclide. Therefore, a radionuclide used for targeted therapy must emit particulate radiations which have relatively short path lengths thereby depositing the radiation energy in a small volume of cells to spare surrounding nontarget tissues. Radionuclides used for targeted therapy decay by alpha, beta, or Auger electron emission, as described in

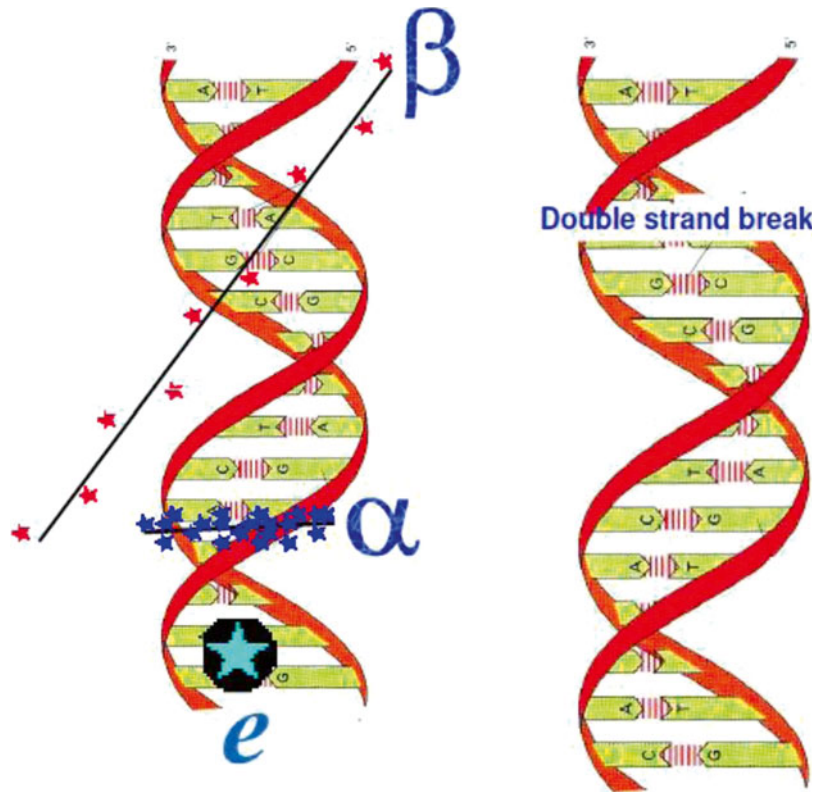

Fig. 1.6 Schematic of DNA strand breaks mediated by ionizing radiation

Chaps. 2, 3, and 4. Within each radionuclide category, there are multiple radionuclides with a variety of range in soft tissues, half-lives, and chemical properties which offer the attractive possibility of optimizing targeted radionuclide therapy to specific therapeutic applications. Production issues and availability and costs are also important parameters which are discussed in Chaps. 5, 6, 7, and 8. Unlike tumor-directed drugs and toxins, which kill only the directly targeted cells, a unique feature of many radioactive emissions (i.e., beta) is that they can often exert a "bystander" or "cross-fire" effect, potentially destroying adjacent tumor cells even if they are not targeted by the radiopharmaceutical. In most cases this characteristic is advantageous, since it is unusual for delivery of the therapeutic radiopharmaceutical to every target cell to be labeled, especially for therapy of solid tumors, because of blood supply and anatomical and physiological barriers. In other cases, dose delivery to only the targeted cell may be a necessity, such as the use of very short-range alpha-emitting radioisotopes (Chap. 3) for the treatment of blood-borne diseases such as some types of leukemia. A systemically administered targeted radiotherapeutic agent has the potential to eliminate primary tumor sites as well as metastases and other malignant cell populations which may be undetectable by diagnostic imaging.

The efficacy of a therapeutic radiopharmaceutical depends on the radiotoxic nature of the radiation emitted and the targeting ability of the radiopharmaceutical vector used for carrying the radionuclide to the disease sites. The choice of a radionuclide for use in therapeutic radiopharmaceuticals is based on several criteria. Radionuclides that decay by alpha-particle emission (α), beta-particle emission (β^-), electron capture (EC), and internal conversion (IC) leading to the emission of Auger and Coster–Kronig (C–K) electrons are suitable for radionuclide therapy. These radiations have high linear energy transfer (LET) and deliver localized radiation. The treatment efficacy with a particular radionuclide can vary depending on the size of the tumor to be treated and intratumor distribution of the tracer. In addition, the nature and energy of the particulate radiation must match with the uptake and distribution of the radiopharmaceutical. The size of the tumor or site/cavity for treatment should match with the appropriate tissue range of radionuclide emissions. Radionuclides that emit β^- particles can induce damage in a cell volume extending up to several millimeters, while alpha particles can induce damages within a few cell volumes. In contrast, Auger and C–K electrons are effective only when they are localized within the cell nucleus to damage DNA. The physical half-life of the radionuclide should also be matched with the in vivo biolocalization and clearance properties of the vector that is used for carrying the radionuclide to the site of interest. The decay product of the radionuclide should be preferably stable or have a very long half-life. The emission of gamma photons—preferably of low abundance—is also advantageous and allows imaging to track the radiopharmaceutical uptake as well as to allow biokinetic data for low-dose imaging for dosimetry estimates and for staging of disease state as well as for monitoring response to therapy. The radionuclide should be available at highest standards of purity, which include radionuclidic, radiochemical, and chemical purity, and should be available either carrier-free (i.e., every atom is radioactive) or with very high specific activity (SA, activity per unit mass). For practical considerations, the radionuclide should have favorable chemical properties enabling radiolabeling with wide range of biomolecules. As discussed in detail in Chaps. 5, 6, 7, and 8, large-scale cost-effective production feasibility ultimately decides the success of a radionuclide to emerge as a choice for therapy (Zimmermann 2013).

1.4.1 Traditional Applications of Therapeutic Radiopharmaceuticals

Therapeutic radiopharmaceuticals have traditionally been used in nuclear medicine for the treatment of a variety of various diseases which are briefly discussed as a prelude for the more detailed recent developments and the use of various newer agents described in detail in the

subsequent chapters. Phosphorous-32 as ^{32}P-orthophosphate ($^{32}PO_4^{3-}$) is an early example which has been traditionally used for the treatment of elderly patients with *polycythemia vera* and essential thrombocytopenia (low blood platelet count) and is one of the earliest applications of radionuclide therapy. However, this mode of therapy is now rarely followed due to the availability of other more recent modes of therapy. Use of ^{131}I for the treatment of thyroid cancer patients has been practiced for many decades and is a unique and still widespread therapeutic example of successful radionuclide therapy. Iodine-131 as sodium iodide is one of the remarkable radiopharmaceuticals and a magic bullet since about one third of the orally administered dose is taken up in a normal thyroid for direct in vivo incorporation into the thyroglobulin macromolecule. Such large concentration of radioactivity allows near total destruction of remnant cancer tissues post surgery. Stimulation of the thyroid by injection of recombinant thyroid-stimulating hormone enhances the efficacy of the therapy. This well-established and historical technology has been widely discussed in the literature and is not described in this book. Iodine-131 is also traditionally used for therapy of other types of cancer. Metaiodobenzylguanidine (MIBG) is a catecholamine analog similar to noradrenaline, which accounts for the uptake of this radiopharmaceutical in catecholamine storage vesicles. The ^{131}I-mIBG agent is used for the treatment of medullary carcinomas such as neuroblastoma and pheochromocytoma. This is an established specialized therapy which is not discussed in this book. However, the use of radiolabeled peptides for therapy of neuroendocrine gastroenteropancreatic (NE-GEP) tumors is described in detail in Chap. 10.

1.4.2 Current and New Therapeutic Applications

1.4.2.1 Peptide Receptor Radionuclide Therapy (PRRT)

The use of radiolabeled peptides for the targeting and treatment of receptors expressed on specific cancer entities is a rapidly growing clinical specialty (PRRT). The overexpression of many peptide receptors on human tumor cells compared to normal tissues makes these receptors attractive molecular targets for radiotherapy. The most commonly used peptide-based therapy is the use of somatostatin (SST) analogs for the treatment of neuroendocrine tumors (NETs). As discussed in Chap. 10, NETs usually overexpress somatostatin receptors, thus enabling the therapeutic use of somatostatin analogs able to reduce signs and symptoms of hormone hypersecretion, improve quality of life, and slow tumor growth. Peptide receptor radionuclide therapy is thus an effective treatment option for patients with well-differentiated somatostatin receptor-expressing neuroendocrine tumors. There are several analogs of somatostatin which have been synthesized and evaluated, and Tyr3-octreotate (TATE) and Tyr3-octreotide (TOC) predominantly target sst2 receptors. PRRT with ^{90}Y- or ^{177}Lu-labeled somatostatin analogs, DOTATOC and ^{177}Lu-DOTATATE, has demonstrated impressive results on tumor response, overall survival, and quality of life in patients with gastroenteropancreatic neuroendocrine tumors (GEP-NETs). Besides somatostatin receptor-targeting peptides, as described in Chap. 10, there are multiple other radiopeptide analogs which are being developed as diagnostic and therapeutic agents. Some of these peptide analogs, including cholecystokinin, gastrin, gastrin-releasing peptide, arginine–glycine–aspartate (RGD) peptides, and glucagon-like peptide 1 analogs, have shown promise in preclinical studies.

1.4.2.2 Radioimmunotherapy

Radioimmunotherapy (RIT) uses large macromolecular monoclonal antibodies as vectors for transport of the radioactivity to cancer cells. The radiolabeled antibodies are directed against various antigens overexpressed on tumor cells or blood vessels formed during angiogenesis. RIT combines the synergistic effects of both radiation and immunotherapy with manageable local and systemic side effects. Radionuclides emitting β^--particles such as ^{90}Y and ^{131}I are used for RIT. The improved effectiveness of antibodies

labeled with beta-emitting radionuclides relates to the phenomenon of "cross-fire" or "bystander" effect, where tumor cells within close range of the targeted cell are also killed due to secondary radiations. Non-Hodgkin's lymphomas (NHLs) are a heterogeneous group of lymphoreticular malignancies which exhibit a wide range of aggressive behavior. The majority of NHLs are B-cell lymphomas, with the follicular and diffused large B-cell lymphomas constituting up to 50 % of NHL cases. The currently US FDA-approved therapeutic agent for the management of lymphomas is ^{90}Y ibritumomab tiuxetan (Zevalin®, Cell Therapeutics Inc, Seattle, WA, and Schering AG, Berlin, Germany; FDA approved in 2002). Earlier, ^{131}I tositumomab had been commercially available and also used for the same indication, but this agent no longer has market approval (Bexxar, GlaxoSmithKline, Research Triangle Parks, NC; FDA approved in 2003).

1.4.2.3 Treatment of Hepatocellular Carcinoma (HCC) and Hepatic Malignancies

As described in Chap. 11, hepatocellular carcinoma (HCC) is a malignant tumor of liver hepatocytes which may be present either as primary liver cancer or as metastatic/secondary liver tumors. Radioembolization by delivering β^--emitting radionuclides (transarterial radioembolization, TART) in colloidal form through the hepatic artery is one of the therapies for the treatment of these inoperable/non-resectable liver malignancies. Radioembolization exploits HCC preferential blood supply from the hepatic artery to deliver the radioactive particles which localize in hepatic end-arterioles thereby allowing localized delivery of therapeutic doses. Thus, this methodology essentially represents a flow-directed mode of treatment that is dependent on neo-angiogenesis. Lipiodol labeled with ^{131}I and lipiodol labeled with ^{90}Y are the two early agents used for this therapy. More recently, such therapy with ^{90}Y microspheres has emerged as the mainstream modality due to the availability of approved products. Commercially available microspheres formed from glass (TheraSphere®; MDS Nordion, Ottawa, ON, Canada) and microspheres made of resin (SIR-Spheres®; Sirtex Medical, Sydney, Australia) are the two commercially available microsphere devices in which ^{90}Y is incorporated. TheraSphere® consists of ^{90}Y embedded into glass microspheres of ~25 μm diameter size which is approved by the US Food and Drug Administration for the treatment of unresectable HCC. SIR-Spheres® consists of biocompatible resin-based microspheres containing ^{90}Y and was granted approval for metastatic colorectal cancer in 2002. In addition to these commercially available agents, a variety of new radiopharmaceuticals are being developed and evaluated for the treatment of HCC as described in Chap. 11.

1.4.2.4 Bone Pain Palliation Therapy

As discussed in detail in Chap. 12, bone metastases are a common complication and the principal cause of pain in cancer patients. Bone metastases may occur in almost all cancers at different frequencies; however, prostate, lung, and breast cancers have maximum probability for such metastases. Radiopharmaceutical treatment of metastatic bone pain is an effective modality that provides palliation of pain to multiple areas of the skeleton simultaneously without the significant soft tissue toxicity. A wide range of radionuclides, especially beta-emitting radionuclides such as ^{177}Lu, ^{32}P, ^{186}Re, ^{188}Re, ^{153}Sm, and ^{89}Sr, have been used for clinical management of bone pain. Of these, ^{32}P and ^{89}Sr are used in the inorganic ionic form, whereas the others are used in the form of complexes with bone-seeking chelates. More recently, ^{223}Ra (Xofigo®) has emerged as a leader in the treatment of bone pain from prostate cancer refractory to chemical castration.

1.4.2.5 Nonmelanoma Skin Cancer Therapy

Clinical implementation of a relatively new radionuclide-based technology described in Chap. 13 may offer the best therapeutic regimen for treatment of nonmelanoma skin cancers, especially in delicate areas of the face and neck regions where surgical removal can result in difficult to resolve scarring. Radioisotopes being evaluated for this application primary involve ^{188}Re and ^{32}P skin applications.

1.4.2.6 Radiosynovectomy: Therapy of Arthritis (Radiosynoviorthesis)

Another important clinical application of therapeutic radioisotopes is the treatment of inflamed synovial joints. This technique is referred to as radiosynovectomy or radiosynoviorthesis and involves the restoration of inflamed and damaged synovial membrane of the joints after intra-articular injection of radionuclide-based preparations to patients with rheumatoid arthritis. This technology is practiced essentially worldwide, except interestingly in the USA, because of regulatory fear of consequences of in vivo radioisotope leakage. In this procedure, a beta-emitting radionuclide in colloidal or particulate form is injected into the articular cavity to deliver radiation dose to the inflamed synovium without excessive irradiation of surrounding tissue. Chapter 14 discusses the agents used for this application. Since the synovial thickness of different joints, principally including the knee, wrist, and finger vary substantially, selection of a radionuclide for radiosynovectomy is critical and is therefore primarily based on the size of the joint to be treated. Thus, for smaller joints lower-energy β^- emitters such as ^{169}Er are preferable. Several other β^--emitters have been evaluated or have entered routine use for this indication and include ^{165}Dy, ^{166}Ho, ^{32}P, $^{186/188}$Re, ^{90}Y, and, more recently, ^{177}Lu.

1.4.2.7 Therapy of Arterial Restenosis following Balloon Angioplasty

Finally, an additional unique therapeutic radioisotope application involves the intraluminal application of beta-emitting radioisotopes, currently limited to ^{188}Re, for the inhibition of the hyperplastic response of smooth muscle cell proliferation following arterial wall damage after balloon angioplasty as described in Chap. 15.

1.5 Historical Timeline of Nuclear Medicine

Nuclear medicine is gifted with contributions from scientists across different disciplines including chemistry, biology, physics, engineering, and medicine. Nuclear medicine evolved into the current status thanks to a series of discoveries and landmark events. The following timeline highlights some important dates in the history of nuclear medicine:

1896 Henri Becquerel discovers radioactivity.

1897 Marie Curie isolates radium from pitchblende.

1903 Alexander Graham Bell suggested placing radium sources in or near tumors for therapeutic purposes.

1913 Frederick Proescher intravenously injects radium for therapy of various diseases.

1924 Georg de Hevesy performed the first radiotracer studies in animals using ^{210}Pb and ^{210}Bi.

1925 Herrman Blumgart and Otto Yens used bismuth-214 (radium-C) to determine the arm-to-arm circulation time in patients.

1932 Ernest Orlando Lawrence constructed the first cyclotron, providing high-energy particles suitable for radionuclide production.

1935 O. Chievitz and George de Hevesy administered phosphate labeled with phosphorus-32 to rats and demonstrated the renewal of the mineral constituents of the bone.

1936 John Hundale Lawrence first applied the artificial radionuclide ^{32}P to treat leukemia. (John 1936)

1938 John Livingood and Glenn Seaborg discovered iodine-131 and cobalt-60.

1938 Emilio Segre and Glenn Seaborg discovered ^{99m}Tc, which is still the mostly used radionuclide in nuclear medicine.

1939 Joseph Gilbert Hamilton, Mayo Soley, and Robley Evans published the first paper on the diagnostic uses of iodine-131 in patients.

1939 Charles Pecher observed uptake of strontium-89 in bone metastases.

1940 The Rockefeller Foundation funded the first cyclotron dedicated for biomedical radionuclide production at Washington University in St. Louis.

1941 Saul Hertz gave a patient the first therapeutic dose of iodine-130.

1942 Enrico Fermi demonstrated the first controlled chain reaction.

1946 Allen Reid and Albert Keston discovered iodine-125, which became important in the field of radioimmunoassay.

1946 Samuel M. Seidlin, Leo D. Marinelli, and Eleanor Oshry treated a patient with thyroid cancer with iodine-131, an "atomic cocktail."

1947 Benedict Cassen used radioiodine to determine whether a thyroid nodule accumulates iodine, helping to differentiate benign from malignant nodules.

1947 George Moore used iodine-131-labeled diiodofluorescein to "probe" the brain for tumors at surgery.

1949 B. Silverstone used phosphorus-32 to detect brain tumors at surgery with a probe detector.

1950 K.R. Crispell and John P. Storaasli used iodine-131-labeled human serum albumin (RISA) for imaging the blood pool within the heart.

1950 Abbott Laboratories sold the first commercial radiopharmaceutical (^{131}I-labeled human serum albumin).

1951 The US Food and Drug Administration approved $Na^{131}I$ for use with thyroid patients. It was the first regulatory approved radiopharmaceutical.

1951 Benedict Cassen, Lawrence Curtis, Clifton Reed, and Raymond Libby automated a scintillation detector to "scan" the distribution of radioiodine within the thyroid gland.

1953 Gordon Brownell and H.H. Sweet built a positron detector based on the detection of annihilation photons by means of coincidence counting.

1953 Robert F. Schilling invented a test of vitamin B12 absorption, which plays a key role in nuclear hematology.

1954 David Kuhl invented a photorecording system for radionuclide scanning. This development moved nuclear medicine further in the direction of radiology.

1955 Rex Huff measured the cardiac output in man using iodine-131 human serum.

1955 George V. Taplin used iodine-131-labeled rose bengal to image the liver. He also used radioiodinated hippuran to measure kidney function with scintillation detectors.

1957 The first ^{99}Mo/^{99m}Tc generator was constructed at the Brookhaven National Laboratory in the USA.

1957 H. Knipping used xenon-133 to measure lung ventilation.

1958 Hal Anger invented the scintillation camera, an imaging device that made possible to conduct dynamic studies.

1959 Solomon Berson and Rosalyn Yalow invented the technique of radioimmunoassay to detect insulin antibodies in human serum.

1959 Picker X-Ray Company delivered the first 3-inch rectilinear scanner.

1960 John McAfee and Henry Wagner imaged the kidneys with radiomercury-labeled chlormerodrin.

1961 Allis-Chalmers installed the first US "medical center" cyclotron at Washington University Medical School. The cyclotron was designed by M.M. Ter-Pogossian.

1962 David Kuhl introduced emission reconstruction tomography. This method later became known as SPECT and PET. It was extended in radiology to transmission X-ray scanning, known as CT.

1962 Nuclear Chicago delivered the first commercial Anger camera to Ohio State University.

1963 Henry Wagner first used radiolabeled albumin aggregates for imaging lung perfusion in normal persons and patients with pulmonary embolism.

1963 George V. Taplin developed albumin aggregates for study of phagocytosis by the reticuloendothelial system.

1963 B. Ansell and B.M. Cook used radiolabeled colloids for radiation synovectomy.

1964 The FDA exempted the "new drug" requirements for radiopharmaceuticals regulated by the Atomic Energy Commission.

1964 Paul Harper and Katherine Lathrup developed radiotracers labeled with Tc-99m for the study of the brain, thyroid, and liver.

1968 Henry Wagner and colleagues used xenon-133 ventilation scans to diagnose pulmonary embolism.

1969 C.L. Edwards reported the accumulation of gallium-67 in cancer.

1970 W.C. Eckelman and P. Richards developed Tc-99m "instant kit" radiopharmaceuticals. The first one was Tc-99m-DTPA.

1970 The FDA announced that it would gradually withdraw the exemption granted to radiopharmaceuticals and start regulating them as drugs. The change would be completed by January 20, 1977.

1971 Gopal Subramanian and John McAfee introduced Tc-99m-labeled phosphates for bone imaging.

1972 David Kuhl performed the first quantitative measurement of cerebral blood volume in living patients.

1973 H. William Strauss introduced the exercise stress-test myocardial scan.

1973 Elliot Lebowitz introduced thallium-201 for myocardial perfusion imaging, first proposed by Kawana.

1973 David Goldenberg demonstrated that radiolabeled antibodies against a human tumor antigen (CEA) could target and image human tumors in animals.

1976 John Keyes developed the first general purpose single-photo emission computed tomography (SPECT) camera.

1976 N. Firusian used strontium-89 to reduce pain from metastatic bone disease.

1976 Ronald Jaszczak developed the first dedicated head SPECT camera.

1977 The FDA required manufacturers to obtain an approved new drug application for new and existing radiopharmaceuticals. The requirements are essentially the same as those for other prescription drugs.

1977 New England Nuclear received FDA approval to distribute thallium-201 for myocardial perfusion and the diagnosis and location of myocardial infarction.

1978 David Goldenberg used radiolabeled antibodies to image tumors in humans.

1981 J.P. Mach used radiolabeled monoclonal antibodies for tumor imaging.

1981 K.A. Krohn, D.R. Vera, and S.M. Steffen developed the first Tc-99m-labeled receptor ligand.

1982 Steve Larson and Jeff Carrasquillo treated cancer patients with malignant melanoma using iodine-131-labeled monoclonal antibodies.

1983 William Eckelman and Richard Reba carried out the first successful SPECT imaging of a neuroreceptor in humans.

1983 Henry Wagner carried out the first successful PET imaging of a neuroreceptor using himself as the experimental subject.

1987 Medi-Physics received FDA approval to market the first brain perfusion imaging radiopharmaceutical, iodine-123 IMP.

1985 D.E. Troutner and W.A. Volkert discover ^{99m}Tc-PnAO, the first technetium-based tracer which crossed the blood-brain barrier (BBB).

1988 Ceretec® (^{99m}Tc-HMPAO) for brain perfusion introduced by Amersham was approved by the FDA for the diagnosis of stroke.

1989 The first positron-emitting radiopharmaceutical (^{82}Rb) has been approved for myocardial perfusion imaging.

1990 Alan Fischman used indium-111-labeled chemotactic peptides to detect foci of infection.

1990 Steve Lamberts and Eric Krenning imaged endocrine tumors with somatostatin receptor-binding radiotracers.

1992 The FDA approved the first monoclonal antibody radiopharmaceutical for tumor imaging.

1993 Medi-Physics/Amersham received FDA approval to market strontium-89 chloride for relief of bone pain.

1994 Mallinckrodt received FDA approval to market the first peptide radiopharmaceutical that binds somatostatin receptors for imaging granulomatous and autoimmune diseases.

1995 ADAC Laboratories shipped the first SPECT camera with coincidence detection capability, suitable for combined SPECT and PET imaging.

1996 PET became an accepted tool for brain studies.

1997 Validation of ^{123}I-*beta*-CIT in assessing dopamine transporters in the diagnosis of Parkinson's disease.

1998 FDG PET studies were for the first time used to assess the response of an initial dose of chemotherapy to predict the response to subsequent high-dose chemotherapy.

1999 Sentinel node studies approved by HCFA for improved diagnosis and management of cancers.

2000 The first commercial PET/CT is launched by CTI.

2000 *Time Magazine* recognizes Siemens Biograph as the invention of the year.

2001 16.9 million nuclear medicine procedures were performed in the USA.

2003 FDA gives approval to IDEC Pharmaceuticals for clinical use of Zevalin™, a radioimmunotherapy agent.

2004 FDA approves the use of Bexxar™ for use in lymphoma.

2007 There were 1.8 million PET or PET/CT procedures performed in this year in the USA only.

2008 The first hybrid PET/MRI system for humans, created by Siemens, was installed.

2008 Nuclear medicine has gone through a global crisis due to acute shortage of ^{99}Mo. This has impacted patient access to care.

2009 FDA in September 2009 approved ^{90}Y-ibritumomab tiuxetan as part of the first-line treatment of follicular non-Hodgkin's lymphoma.

2013 The US Food and Drug Administration (FDA) approved radium Ra 223 dichloride (Xofigo® Injection, Bayer HealthCare Pharmaceuticals Inc.) for the treatment of patients with castration-resistant prostate cancer (CRPC), symptomatic bone metastases, and no known visceral metastatic disease.

The orphan drug designation has been granted by both the US Food and Drug Administration (FDA) and the European Medicines Agency (EMA) for use of gallium-68 DOTATATE as a diagnostic agent for the management of gastroenteropancreatic neuroendocrine tumors (GEP-NETs).

1.6 Summary

Nuclear medicine imaging and radionuclide therapy have been in use for over half a century, and this field continues to grow as new radiopharmaceuticals and upgraded imaging modalities emerge. With the availability of a large number of diagnostic agents, SPECT and PET are matured technologies and represent the mainstay of functional diagnostic imaging. While PET has seen the maximum growth in the last 15 years, the next phase of growth of nuclear medicine is expected to be in radionuclide therapy. Nuclear medicine therapy is not expected to be an answer for the treatment of all types of cancers and chronic disease entities, but there are other niche areas that will emerge wherein nuclear medicine therapy can offer better solutions with alternative technologies. For this reason, radionuclide therapy should not be regarded to be in competition with other treatment modalities. Nuclear medicine therapy is a multidisciplinary procedure that involves a close understanding between specialists in many areas, including nuclear medicine, oncology, surgery, interventional radiology, and radiopharmaceutical scientists. Diagnostic imaging together with radionuclide therapy will be capable of providing patient-specific therapy in many cases.

The full potential of targeted radionuclide therapy can only be realized if new developments in radionuclide technology and availability and carrier-targeting molecules continue to expand. With the appropriate combination of an optimally engineered targeting vector and a suitable radionuclide, the benefit of radionuclide therapy is expected to substantially increase. For a very long time, the use of ^{131}I for the treatment of thyroid cancer patients was the sole example of a therapeutic success based on radionuclide therapy. Advances in nuclear medicine are possible, thanks to the identification of new biological targets and the discovery of suitable targeting vectors, and many more new agents are expected to be available for radionuclide therapy. However, the difficulties and expense to

obtain regulatory approval for new radiopharmaceuticals in a timely manner will continue to be detrimental factors for enhancing the scope of radionuclide therapy. The subsequent chapters in this book address the broad topic of nuclear medicine therapy, in terms of its development, advances, current practices, and future directions.

References

Aerts A, Impens NR, Gijs M, et al. Biological carrier molecules of radiopharmaceuticals for molecular cancer imaging and targeted cancer therapy. Curr Pharm Des. 2014;20(32):5218–44.

Akkas BE, Demirel BB, Vural G. Prognostic factors affecting disease-specific survival in patients with recurrent and/or metastatic differentiated thyroid carcinoma detected by positron emission tomography/computed tomography. Thyroid. 2014;24(2):287–925.

Alavi A, Basu S. Planar and SPECT imaging in the era of PET and PET-CT: can it survive the test of time? Eur J Nucl Med Mol Imaging. 2008;35(8):1554–9.

Alazraki NP. Radionuclide imaging in the evaluation of infections and inflammatory disease. Radiol Clin North Am. 1993;31(4):783–94.

Anger H. Scintillation camera. Rev Sci Instr. 1958;29: 27–33.

Bentzen SM, Gregoire V. Molecular imaging-based dose painting: a novel paradigm for radiation therapy prescription. Semin Radiat Oncol. 2011;21(2):101–10.

Beyer T, Freudenberg LS, Townsend DW, et al. The future of hybrid imaging—part 1: hybrid imaging technologies and SPECT/CT insights. Imaging. 2011;2(2):161–9.

Bhattacharyya S, Dixit M. Metallic radionuclides in the development of diagnostic and therapeutic radiopharmaceuticals. Dalton Trans. 2011;40(23):6112–28.

Bockisch A, Freudenberg LS, Schmidt D, et al. Hybrid imaging by SPECT/CT and PET/CT: proven outcomes in cancer imaging. Semin Nucl Med. 2009;39(4):276–89.

Bomanji JB, Siraj QH. Tumour imaging. Br J Hosp Med. 1995;54(2–3):70–5.

Brandon D, Alazraki A, Halkar RK, et al. The role of single-photon emission computed tomography and SPECT/computed tomography in oncologic imaging. Semin Oncol. 2011;38(1):87–108.

Britton KE. Towards the goal of cancer-specific imaging and therapy. Nucl Med Commun. 1997;18:992–1005.

Chowdhury FU, Scarsbrook AF. The role of hybrid SPECT-CT in oncology: current and emerging clinical applications. Clin Radiol. 2008;63(3):241–51.

Coleman RE. PET in lung cancer. J Nucl Med. 1999; 40(5):814–20.

Connell PP, Hellman S. Advances in radiotherapy and implications for the next century: a historical perspective. Cancer Res. 2009;69:383–92.

Cuaron JJ, Hirsch JA, Medich DC, et al. A proposed methodology to select radioisotopes for use in radionuclide therapy. AJNR Am J Neuroradiol. 2009;30:1824–9.

Cutler CS, Hennkens HM, Sisay N, et al. Radiometals for combined imaging and therapy. Chem Rev. 2013; 113(2):858–83.

Dalvie D. Recent advances in the applications of radioisotopes in drug metabolism, toxicology and pharmacokinetics. Curr Pharm Des. 2000;6(10):1009–28.

Dash A, Knapp FF, Pillai MRA. Targeted radionuclide therapy-an overview. Curr Radiopharm. 2013;6(3):152–80.

de Haas HJ, van den Borne SW, Boersma HH, et al. Evolving role of molecular imaging for new understanding: targeting myofibroblasts to predict remodeling. Ann N Y Acad Sci. 2012;1254:33–41.

Delbeke D, Martin WH. Positron emission tomography imaging in oncology. Radiol Clin North Am. 2001;39(5):883–917.

Delbeke D, Sandler MP. The role of hybrid cameras in oncology. Semin Nucl Med. 2000;30(4):268–80.

Delbeke D, Schöder H, Martin WH, et al. Hybrid imaging (SPECT/CT and PET/CT): improving therapeutic decisions. Semin Nucl Med. 2009;39(5):308–40.

Eary JF. Nuclear medicine in cancer diagnosis. Lancet. 1991;354:853–7.

Eberl S, Chan HK, Daviskas E. SPECT imaging for radioaerosol deposition and clearance studies. J Aerosol Med. 2006;19(1):8–20.

Eberlein U, Bröer JH, Vandevoorde C, et al. Biokinetics and dosimetry of commonly used radiopharmaceuticals in diagnostic nuclear medicine – a review. Eur J Nucl Med Mol Imaging. 2011;38(12):2269–81.

El-Maghraby TA, Moustafa HM, Pauwels EK. Nuclear medicine methods for evaluation of skeletal infection among other diagnostic modalities. Q J Nucl Med Mol Imaging. 2006;50(3):167–92.

Ercan MT, Caglar M. Therapeutic radiopharmaceuticals. Cur Pharm Des. 2000;6:1085–121.

Erickson JJ. Development of the scintillation camera. Am J Physiol Imaging. 1992;3–4:98–104.

Gabriel M. Radionuclide therapy beyond radioiodine. Wien Med Wochenschr. 2012;162(19–20):430–9.

Gambhir SS. Molecular imaging of cancer with positron emission tomography. Nat Rev Cancer. 2002;2(9): 683–93.

Ganz WI, Serafini AN. The diagnostic role of nuclear medicine in the acquired immunodeficiency syndrome. J Nucl Med. 1989;30(12):1935–45.

Garden KL, Bones PJ, Bates RH. From living being to medical image-bridging the dimensionality gap. Australas Phys Eng Sci Med. 1989;4:186–204.

Gerber DE, Chan TA. Recent advances in radiation therapy. Am Fam Physician. 2008;78:1254–62.

Gholamrezanejhad A, Mirpour S, Mariani G. Future of nuclear medicine: SPECT versus PET. J Nucl Med. 2009;50(7):16N–8.

Giron MC, Portolan S, Bin SA, Mazzi U, Cutler CS. Cytochrome P450 and radiopharmaceutical metabolism. Q J Nucl Med Mol Imaging. 2008;52(3): 254–66.

Hoefnagel CA. Radionuclide therapy revisited. Eur J Nucl Med. 1991;18:408–31.

Hoefnagel CA. Radionuclide cancer therapy. Ann Nucl Med. 1998;12:61–70.

Horger M, Bares R. The role of single-photon emission computed tomography/computed tomography in benign and malignant bone disease. Semin Nucl Med. 2006;36(4):286–94.

Howard SA, Rosenthal MH, Jagannathan JP, et al. Beyond the vascular endothelial growth factor axis: update on role of imaging in nonantiangiogenic molecular targeted therapies in oncology. AJR Am J Roentgenol. 2015;204(5):919–32.

Hunter KU, Eisbruch A. Advances in imaging: target delineation. Cancer J. 2011;17(3):151–4.

James ML, Gambhir SS. A molecular imaging primer: modalities, imaging agents, and applications. Physiol Rev. 2012;92(2):897–965.

Jansen FP, Vanderheyden JL. The future of SPECT in a time of PET. Nucl Med Biol. 2007;34(7):733–5.

Jaszczak RJ. The early years of single photon emission computed tomography (SPECT): an anthology of selected reminiscences. Phys Med Biol. 2006;51:R99–115.

Keidar Z, Israel O, Krausz Y. SPECT/CT in tumor imaging: technical aspects and clinical applications. Semin Nucl Med. 2003;33(3):205–18.

Kjaer A. Molecular imaging of cancer using PET and SPECT. Adv Exp Med Biol. 2006;587:277–84.

Kostakoglu L, Fardanesh R, Posner M, et al. Early detection of recurrent disease by FDG-PET/CT leads to management changes in patients with squamous cell cancer of the head and neck. Oncologist. 2013;18(10): 1108–17.

Krausz Y, Israel O. Single-photon emission computed tomography/computed tomography in endocrinology. Semin Nucl Med. 2006;36(4):267–74.

Kubota K. From tumor biology to clinical Pet: a review of positron emission tomography (PET) in oncology. Ann Nucl Med. 2001;15(6):471–86.

Kuikka JT, Britton KE, Chengazi VU, Savolainen S. Future developments in nuclear medicine instrumentation: a review. Nucl Med Commun. 1998;19(1): 3–12.

Kurdziel KA, Ravizzini G, Croft BY, et al. The evolving role of nuclear molecular imaging in cancer. Expert Opin Med Diagn. 2008;2(7):829–42.

Leeds NE. The clinical application of radiopharmaceuticals. Drugs. 1990;40(5):713–21.

MacIntyre WJ, Saha GB, Go RT. Planar imaging with single-head large-field-of-view cameras: are they still the workhorse? Semin Nucl Med. 1994;24(1):11–6.

Maletz KL, Ennis RD, Ostenson J, et al. Comparison of CT and MR-CT fusion for prostate post-implant dosimetry. Int J Radiat Oncol Biol Phys. 2012;82(5): 1912–7.

Mammatas LH, Verheul HM, Hendrikse NH, et al. Molecular imaging of targeted therapies with positron emission tomography: the visualization of personalized cancer care. Cell Oncol. 2015;38(1):49–64.

Mankoff DA, Bellon JR. Positron-emission tomographic imaging of cancer: glucose metabolism and beyond. Semin Radiat Oncol. 2001;11(1):16–27.

Mariani G, Bruselli L, Duatti A. Is PEt always an advantage versus planar and SPECT imaging? Eur J Nucl Med Mol Imaging. 2008;35(8):1560–5.

Mariani G, Bruselli L, Kuwert T, et al. A review on the clinical uses of SPECT/CT. Eur J Nucl Med Mol Imaging. 2010;37(10):1959–85.

McCready VR. Milestones in nuclear medicine. Eur J Nucl Med. 2000;27(Suppl):S49–79.

Meikle SR, Kench P, Kassiou M, Banati RB. Small animal SPECT and its place in the matrix of molecular imaging technologies. Phys Med Biol. 2005;50:R45–6.

Mercer JR. Molecular imaging agents for clinical positron emission tomography in oncology other than fluorodeoxyglucose (FDG): applications, limitations and potential. J Pharm Pharm Sci. 2007;10(2):180–202.

Messa C, Fazio F, Costa DC. Clinical brain radionuclide imaging studies. Semin Nucl Med. 1995;25(2):111–43.

Notghi A, Harding LK. The clinical challenge of nuclear medicine in gastroenterology. Br J Hosp Med. 1995; 54(2–3):80–6.

Patton JA, Delbeke D, Sandler MP. Image fusion using an integrated, dual-head coincidence camera with X-ray tube-based attenuation maps. J Nucl Med. 2000;41(8): 1364–8.

Penner N, Klunk LJ, Prakash C. Human radiolabeled mass balance studies: objectives, utilities and limitations. Biopharm Drug Dispos. 2009;30:185–203.

Pexman JH. Gamma camera or rectilinear scanner. Proc R Soc Med. 1973;66(8):830–3.

Prvulovich EM, Bomanji JB. The role of nuclear medicine in clinical investigation. BMJ. 1998;316:1140–6.

Rahmim A, Zaidi H. PET versus SPECT: strengths, limitations and challenges. Nucl Med Commun. 2008;3: 193–207.

Riemann B, Schäfers KP, Schober O, Schäfers M. Small animal PET in preclinical studies: opportunities and challenges. Q J Nucl Med Mol Imaging. 2008;52(3):215–21.

Ross DS. Evaluation of the thyroid nodule. J Nucl Med. 1991;32(11):2181–92.

Schillaci O. Single-photon emission computed tomography/computed tomography in lung cancer and malignant lymphoma. Semin Nucl Med. 2006;36(4):275–85.

Schillaci O, Danieli R, Manni C, et al. Is SPECT/CT with a hybrid camera useful to improve scintigraphic imaging interpretation? Nucl Med Commun. 2004;25(7):705–10.

Schillaci O, Filippi L, Manni C, et al. Single-photon emission computed tomography/computed tomography in brain tumors. Semin Nucl Med. 2007;37(1):34–47.

Schlegel W. If you can't see it, you can miss it: the role of biomedical imaging in radiation oncology. Radiat Prot Dosimetry. 2010;139(1–3):321–6.

Simpson DR, Lawson JD, Nath SK, et al. Utilization of advanced imaging technologies for target delineation in radiation oncology. J Am Coll Radiol. 2009; 6(12):876–83.

Solomon B, McArthur G, Cullinane C, et al. Applications of positron emission tomography in the development of molecular targeted cancer therapeutics. BioDrugs. 2003;17(5):339–54.

Srivastava S, Dadachova E. Recent advances in radionuclide therapy. Semin Nucl Med. 2001;31(4):330–41.

Tapscott E. Nuclear medicine pioneer: Hal O. Anger. First scintillation camera is foundation for modern imaging systems. J Nucl Med. 1998;39(3):15N, 19N, 26N-27N.

Telander GT, Loken MK. Comparison of the scintillation camera with a conventional rectilinear scanner using technetium-99m pertechnetate in a tumor brain phantom. J Nucl Med. 1967;8(7):487–501.

Utsunomiya D, Shiraishi S, Imuta M, et al. Added value of SPECT/CT fusion in assessing suspected bone metastasis: comparison with scintigraphy alone and nonfused scintigraphy and CT. Radiology. 2006; 238(1):264–71.

Volkert WA, Hoffman TJ. Therapeutic radiopharmaceuticals. Chem Rev. 1999;99:2269–92.

Wheldon TE. Targeting radiation to tumours. Int J Radiat Biol. 1994;65:109–16.

Wolbarst AB, Hendee WR. Evolving and experimental technologies in medical imaging. Radiology. 2006; 238(1):16–39.

Wood KA, Hoskin PJ, Saunders MI. Positron emission tomography in oncology: a review. Clin Oncol. 2007; 19:237–55.

Yeong C-H, Cheng M-H, Ng K-H. Therapeutic radionuclides in nuclear medicine: current and future prospects. J Zhejiang Univ Sci B. 2014;15(10):845–63.

Zaidi H. Recent developments and future trends in nuclear medicine instrumentation. Z Med Phys. 2006;16(1): 5–17.

Zanzonico P. Principles of nuclear medicine imaging: planar, SPECT, PET, multi-modality, and autoradiography systems. Radiat Res. 2012;177(4):349–64.

Zimmermann RG. Why are investors not interested in my radiotracer? The industrial and regulatory constraints in the development of radiopharmaceuticals. Nucl Med Biol. 2013;40:155–66.

Therapeutic Radionuclides Decay with Particle Emission for Therapeutic Applications

2

2.1 Introduction

Unsealed radioactive sources are administered by certified medical staff, and the use of ^{131}I-iodide for ablation of thyroid tissue and surgical remnants is the classic example in endocrinology. While application of sealed radioactive sources such as ^{192}Ir in radiation oncology generally involves the use of afterloading devices, for instance, unsealed radioactive sources for the selective delivery of radiation to target tissues or organs without significantly affecting normal tissues are known as radionuclide therapy and are practiced by nuclear medicine specialists. This promising treatment option has been available for more than 70 years but had been for many years confined for radiation therapy of limited diseases, with the treatment of thyroid cancer the most prominent example.

Over the last 40–50 years, rapid and widespread interest in radionuclide therapy has been the driving force behind extensive research focused on the design, development, testing, and clinical evaluation of many novel radiopharmaceuticals. Production of radionuclides which are required for radionuclide therapy (Chaps. 5, 6, 7, and 8) is the first step in the development of therapeutic radiopharmaceuticals and also the most crucial aspect for the success as well as sustainable growth of radionuclide therapy. Development of production and processing technologies has been an area of intense research since there are a variety of therapeutic radionuclides which differ based on their physical half-lives, type of particle emission (β^-, σ, Auger), particle emission energy, specific activity, and chemistry (Ehrhardt et al. 1998; Karenlin and Toporov 1998; IAEA 2012; Mausner et al. 1988; Neves et al. 2005; Qaim 2012; Ruth et al. 1989; Troutner 1987; Volkert et al. 1991; Yeong et al. 2014; Zhuikov 2014). While the production of therapeutic radionuclides requires a thorough understanding of the nuclear reactions and decay schemes, development and implementation of processing methods require knowledge of the appropriate aqueous solution chemistry. This chapter discusses the key aspects related to the production of important therapeutic radionuclides, embracing current and possible future needs in the rapidly advancing field of radionuclide therapy. While both research reactors and accelerators are the principal technologies which offer the possibility for sustainable production of a wide range of radionuclides, there are several issues and challenges that must be considered in order to fully realize their potential (Ehrhardt et al. 1998; IAEA 2012; Mausner et al. 1988; Neves et al. 2005; Qaim 2012; Ruth et al. 1989; Troutner 1987; Volkert et al. 1991; Yeong et al. 2014; Zhuikov 2014). Depending on both the demands and applications, efficient production of therapeutic radionuclides plays a key role for current opportunities in technology development and to fulfill future research needs for radionuclides of emerging interest that appear promising for radionuclide therapy.

F.F. (Russ) Knapp, A. Dash, *Radiopharmaceuticals for Therapy*, DOI 10.1007/978-81-322-2607-9_2

Radionuclide therapy utilizes unsealed radioactive sources designed to deliver therapeutic doses of ionizing radiation to specific disease sites and is an attractive treatment option either for curative intent or for disease control and palliation (Chatal and Hoefnagel 1999; Joensuu and Tenhunen 1999). This methodology combines the advantages of target selectivity similar to that of brachytherapy or external beam radiotherapy and at the same time is systemically similar to chemotherapy. Systemic administration strategies offer the prospect of treating disseminated metastatic tumors (McDougall 2000; Volkert and Hoffman 1999). The basic principle primarily underlines the administration of a radiopharmaceutical for selective accumulation at the diseased tissue either to ablate or damage cells through the emission of energetic β^--particles, α-particles, or Auger electrons (e^-) (Britton 1997; Heeg and Jurisson 1999; McEwan 1997; Serafini 1994). The targeting feature of radionuclide therapy is achieved either by the intrinsic targeting properties of some radionuclides or by conjugating the radionuclide to specific carrier molecules. Therapeutic radiopharmaceuticals generally consist of two entities, which include the radionuclide, which is the radiation source, and a targeting moiety that determines tissue localization. In light of the explicit need to deliver sufficient cytotoxic radiation to the target cells while not causing unmanageable side effects, it is imperative that the radiopharmaceutical accumulates selectively in the diseased tissue, clears rapidly from the blood and other normal organs, and has rapid transit through the excretory organs, in order to minimize radiation damage to normal tissues.

Over the years, radionuclide therapy has undergone rapid and continual evolutionary cycles, relying on empirically prepared radiopharmaceuticals and presently progressing to the use of intelligent design of specific agents for targeted therapy. As the development of therapeutic radiopharmaceuticals has progressed, the use of the metallic radionuclides as well as novel target-specific pathways is now a hallmark (Spencer et al. 1987; Hoefnagel 1991; Stöcklin et al. 1995; O'Donoghue et al. 1995; Ercan and Caglar 2000; Srivastava 1996a, b; Mausner and Srivastava 1993; Srivastava and Dadachova 2001; Cuaron et al. 2009; Tolmachev et al. 2004; Unak et al. 2002; Stanciu 2012; Srivastava and Dadachova 2001; Das and Pillai 2013). A number of metallic radionuclides have been combined with key targeting macromolecules, which include whole antibodies, antibody fragments, small peptides, peptidomimetics, or nonpeptide receptor ligands, and have been studied for their potential use in tumor therapy. The use of metallic radionuclides is attractive and offers the convenience of designing a broad spectrum of exotic radiopharmaceuticals by modifying the coordination environment which surrounds the metal. These advances have thus led to considerable fascinating research and innovative strategies for treating disseminated human malignancies and various other disorders.

In principle, to achieve desired therapeutic effects, the radionuclide chosen should exhibit the necessary physical, chemical, and biological properties. A wide range of radionuclides based on their physical half-lives, energy of particle emission, type of particle emission and specific activity, etc., are available which can be used for the treatment, control, and palliation of many disseminated diseases. Although a summary is not provided here, subsequent chapters provide detailed information describing the properties of key therapeutic radioisotopes of current interest (see Chaps. 3, 4, 5, and 6). The chronology includes selection of a radionuclide with apparent optimal properties for a specific application with subsequent development of methods for routine production, processing, and purification.

A variety of therapeutic radionuclides are now regularly commercially produced as well as at many nuclear science research centers, utilizing research reactors and accelerators. In view of the tremendous prospects associated with the production of therapeutic radionuclide, a number of excellent review articles have been published (Cutler et al. 2013; Ruth et al. 1989, Volkert et al. 1991; Ehrhardt et al. 1998; Karenlin and Toporov 1998; IAEA 2012; Knapp et al. 1998; Mausner et al. 1988; Qaim 2012; Neves et al. 2002, 2005; Qaim and Coenen 2005; Karelin et al. 2000; Troutner 1987; Yeong et al. 2014; Zhuikov 2014). The rate at which interest and production methods are developing for a variety of radionuclides appears to be increasing. In order to sustain and broaden the scope and promote further

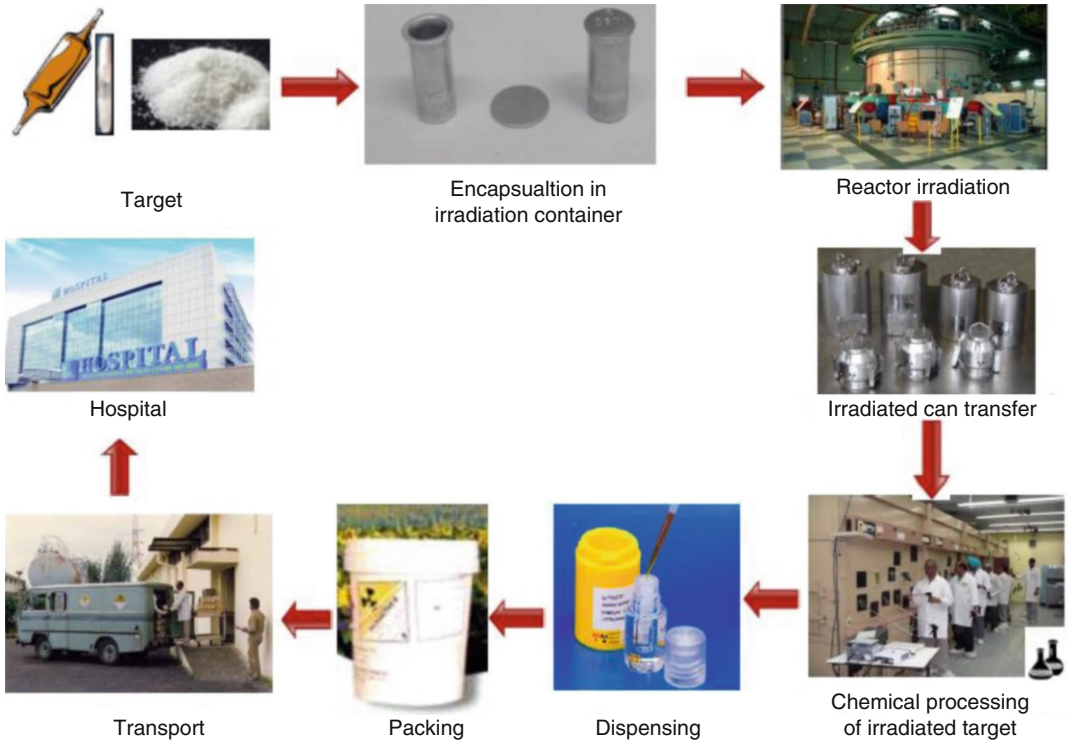

Fig. 2.1 Various steps of the therapeutic radionuclide production cycle

development of radionuclide therapy, radionuclide production and processing strategies need a vision for sustained future growth. Taking account of the progress made in therapeutic radionuclide production, it is timely to provide up-to-date information for current and expected activities in this field. The goal of this chapter is to present a comprehensive overview of production technologies and separation methodologies for several radionuclides of current interest and for those which have considerable potential for future applications in radionuclide therapy.

2.2 Criteria for Selection of Therapeutic Radionuclides

The success of radionuclide therapy in the nuclear medicine arena is dependent on the selection of appropriate radionuclides (Volkert and Hoffman 1999; Srivastava 1996a; Volkert et al. 1991). Although numerous radionuclides have potential applications in radionuclide therapy, only a very few possess favorable nuclear, physical, and biological characteristics which would identify them as practical for clinical use. The ultimate choice is based on several factors described in the following sections.

2.2.1 Particle Emission

Radionuclides which are suitable for radionuclide therapy owing to their high linear energy transfer (LET) to deliver localized cytotoxic ionizing radiation include those which decay by beta-particle emission (β^-), alpha-particle emission (α), and radionuclides that decay by electron capture (EC) and internal conversion (IC), leading to the emission of Auger and Coster–Kronig (C–K) electrons. The choice of a particular radionuclide is strongly dependent on the LET value and tissue range of emissions. Each type of particle emitted by the radionuclide has a different range, effective distance (see Fig. 2.1, Chap. 12), and relative biological effectiveness (RBE). The size of the tumor or the tissue mass to be

Table 2.1 General characteristics of therapeutic radionuclides

Decay	Particles (#)[a]	$E_{(min)}$–$E_{(max)}$	Range	LET (KeV/μm)
α^{++}-particle	He nuclei (1)	5–9 MeV[b]	40–100 μm	~80
β^{-}-particle	Energetic electrons (1)	50–2300 keV[c]	0.05–12 mm	~0.2
EC/IC	Nonenergetic electrons (5–30)	eV–keV[b]	2–500 nm	~4–26

[a]Number of particles emitted per decaying atom
[b]Monoenergetic
[c]Average (>1 % intensity); continuous distribution of energy

treated should be matched with the appropriate effective radiation range. Radionuclides emitting beta particles are effective for large tumors owing to their large millimeter range and cross fire. Since the range of α–particles is confined to 50–100 μm, they are effective for small tumors and micrometastases. Radionuclides that emit Auger and C–K electrons are effective for only single cells when they across the cell membrane. Nuclear targeting to induce irreversible DNA damage is the goal for Auger therapy, although the established efficacy of some radiopharmaceuticals labeled with Auger emitters such as ^{111}In-octreotate, which do not reach the cell nucleus, has not yet been elucidated (Table 2.1).

2.2.2 Tissue Treatment Morphology

The nature of the particle emission required largely depends on the size of the tumor or tissue treatment site, tissue distribution pharmacokinetics of the tracer, and other factors which are important to maximize therapeutic effectiveness.

2.2.3 Radionuclide Half-Life

The radionuclide physical half-life should be well matched with the in vivo biolocalization and clearance properties of the radiolabeled compound. If the half-life is too short, radionuclide depletion resulting from radioactive decay could occur before the radioisotope reaches and has sufficient residence time at the targeted site. Conversely, a long treatment site residence time could cause unnecessary radiation dose to normal tissues. A physical half-life of 1–14 days is often felt to be the optimal half-life range. In light of the explicit need to prepare site-specific radiolabeled compounds of high specific activity to target low-capacity systems such as receptors or antigens, the specific activity of the radionuclide should be high, and for this reason, no-carrier-added (NCA) radionuclides are preferable for these applications.

2.2.4 Radionuclide Decay Products

Ideally, the daughter radionuclide decay product should be stable (nonradioactive) or decay with low-energy emissions and have a short half-life.

2.2.5 Radionuclide Purity

The availability of radionuclides with the highest standard of purity (radionuclidic, radiochemical, elemental, and chemical) is essential for clinical applications for radionuclide therapy. These high purity requirements necessitate the use of nuclear reactions as well as chemical separation and purification schemes that result in products with high radionuclidic purity. To this end, enriched stable target nuclides are most often desirable to preclude ancillary activation of other isotopes in target.

2.2.6 Gamma Emissions

Emission of gamma rays in useful abundance and with optimal energy is usually very advantageous to permit quantification of targeted uptake and biokinetics to allow low-dose imaging, especially during staging, for dosimetry estimates and for monitoring response to therapy. Although gamma radiation

with low abundance is useful for imaging purposes, high abundance as well as high-energy gamma radiation results in poor images and contributes significantly to the whole-body radiation burden of the patient under treatment without significantly increasing the radiation damage to the target tissue.

2.2.7 Radiolabeling Chemistry

The radionuclide chemical properties should permit the opportunity for introduction into a wide range of targeting molecules.

2.2.8 Economic Factors

For projection of widespread and cost-effective dependable availability, the commercial production of the required activity levels of radionuclides with high specific activity and purity is an important aspect for radiopharmaceutical development, and for these reasons, the production of radionuclides is discussed in detail in Chaps. 5, 6, 7, and 8.

Although only a limited number of radionuclides that satisfy the above eight criteria have been found useful in designing therapeutic radiopharmaceuticals, emerging interest is focused on a number of promising radionuclides that may have future importance for radionuclide therapy. The issue of their current and future availability for radionuclide therapy studies warrants continued investigation. A wide range of radionuclides of different radiation emission characteristics, radiobiological effectiveness, and range of action have been used in the treatment of different diseases. The radionuclidic physical and nuclear characteristics must be appropriately matched with the therapeutic application of interest, or the disease under treatment, as discussed below.

2.3 Beta-Particle-Emitting Radionuclides

Radionuclides that decay by β^--particle emission have maximum kinetic energies of 0.3–2.3 MeV with corresponding ranges of ~0.5–12 mm in soft tissue (Fig. 2.1, Chap. 12). Such long penetration range precludes the need for cellular internalization and can be effectively targeted at or near to the cell membrane. The range of β^--particles, as compared to cell diameter, permits β^--particles to traverse several cells (10–1000), a useful therapeutic property that has been termed "crossfire," which ensures sufficient dose delivery to each cell in a large tissue mass. Depending on the size and location of the tissue site for dose delivery, the choice of the β^--emitter may be different. Although β^--particle-emitting radionuclides are effective for medium to large size tumors (Chaps. 9 and 10), for instance, they are less effective in treating smaller metastatic tumors owing to deposition of a larger fraction of the particle energy outside the tumor volume. On the other hand, when the tumor is large in comparison to the range of β^--particle, most of the energy is deposited within the tumor. Various other important clinical applications of β^--emitting radioisotopes are described for bone pain palliation (Chap. 12), nonmelanoma skin cancer therapy (Chap. 13), treatment of arthritis (synovectomy, Chap. 14), and arterial restenosis therapy (Chap. 15).

2.4 Alpha-Particle-Emitting Radionuclides

In contrast, the large positively charged α-particles have soft tissue path lengths (50–80 μm) which are much shorter than β^--particles and characterized by much high linear energy transfer (LET) (~100 keV/μm). The short path length provides a high degree of tumoricidal activity while sparing surrounding normal tissues. Because the high LET of α-particles leads to a high frequency of double-stranded DNA breaks, much of this damage is thus irreparable and accounts for the high kill rate of α-emitting radioisotopes. This property makes them effective in killing cancer cells that are in a hypoxic as well as normoxic tumor cell environments. Their cytotoxic potency is over 100 times greater than that of β^--emitters and, on an atom-by-atom or molecule-by-molecule basis, they are among the most cytotoxic compounds in existence with

fewer than five DNA hits required to kill a cell. The cytotoxicity of α-particles has been reported to be independent of both dose rate and oxygenation status of the cells (Hall 1994). The α-particle emitters are more compatible for use in treatment of tumors with small diameters and where their localization within the tumor is more spatially homogeneous as described in Chaps. 3 and 4.

2.5 Low-Energy Electron Emitters

The majority of low-energy Auger electrons emitted during radioactive decay traverse very short distances in biological tissue generally within a few nm. These short distances result in a highly localized energy deposition in the immediate site of the decaying radionuclide. In order to realize the full potential of Auger electron emitters in radionuclide therapy, it is expected necessary to target the radionuclides target cell nuclear DNA. Most interest in Auger emitters focuses on their potential unique application for cancer therapy, but the clinical use is in its infancy (Chap. 4). The short range of Auger electrons necessitates new and efficient chemical radiopharmaceutical radiolabeling and targeting strategies. However, because of the very short range in order to achieve uniform distribution of absorbed dose, all tumor cells must be targeted. Consequently, targeting approaches more sophisticated than simple radiopharmaceutical cellular internalization are warranted. In contrast to α- and β^--radiation, Auger electron emitters exhibit low cellular toxicity during transit in blood or bone marrow.

The selection of the optimal combination of type and energy of particle emission is largely determined by the size of the lesion or tumor to be treated, delivery site, nature of the tumor (homogeneous or heterogeneous), and required radiation dose. The cytotoxic dose requirement is dependent on the radiation sensitivity of the tissue, type of particle emission (α-particles, β^--particles, or Auger electrons), emitted particle energy, the tumor size, and location. The effectiveness of radionuclide therapy depends largely on the concentration of radionuclide in the tumor for a long duration. Thus, the radiopharmaceutical used for therapy should have fast tumor uptake, high tumor-to-background ratio, prolonged tumor residence time, and fast renal clearance. The aim is thus to reduce the radiation burden to normal nontarget organs, such as the kidney, liver and bone marrow. The major therapeutic radionuclides used in radionuclide therapy for different diseases are summarized and discussed in subsequent Chapters. In order to deliver an effective radiation dose, high target to nontarget ratios must be attained, which includes use of either in ionic species (i.e. thyroid) or by the use of carrier molecules/targeting biomolecules. Therefore, the design and selection of carrier molecules is very important for the development of a clinically useful therapeutic agent. The major therapeutic radiopharmaceuticals based on their chemical forms required for various applications are listed in Table 2.2.

2.6 Radionuclide Production

Production of radionuclides is described in detail in Chap. 5, 6, 7, and 8. The availability of therapeutic radionuclides is the initial major issue in planning the preparation and development of therapeutic radiopharmaceuticals and is also the cornerstone of the success as well as sustainable growth of radionuclide therapy. Production of therapeutic radionuclides involves use of various nuclear reactions conducted by neutron irradiation in a nuclear reactor or from charged particle bombardment in cyclotrons and accelerators. Depending on the production route, either no-carrier-added (NCA) or carrier-added (CA) radionuclides are obtained. The reactor offers large volume for irradiation, simultaneous irradiation of several samples, economy of production, and possibility to produce a wide variety of radioisotopes. The accelerator-produced isotopes relatively constitute a smaller percentage of total use. The accelerators are generally used to produce those isotopes which cannot be produced by reactor or which have unique properties. Because of their in vivo application, strict compliance

Table 2.2 Radiation characteristics of key diagnostic radionuclides with potential applications for Auger electron therapy

Radionuclide	$T_{1/2}$	Auger electrons/decay	IC electrons/decay	Auger energy/decay (keV)	IC energy/decay (keV)	Total energy/decay (keV)	Auger energy in % of total energy/decay	IC energy in % of total energy/decay
^{67}Ga	78 h	4.7	0.3	6.3	28.1	201.6	3.1	13.9
^{99m}Tc	6 h	4.0	1.1	0.9	15.4	142.6	0.6	10.8
^{111}In	67 h	14.7	0.2	6.8	25.9	419.2	1.6	6.2
^{123}I	13 h	14.9	0.2	7.4	20.2	200.4	3.7	10.1
^{125}I	59.4 days	24.9	0.9	12.2	7.2	61.4	19.9	11.8
^{201}Tl	73 h	36.9	1.1	15.3	30.2	138.5	11.0	21.8

IC internal conversion

with the production and quality control protocols of every radionuclide used in therapy has to be ascertained. The chemical, radiochemical, and radionuclidic purity of radionuclides are stringently regulated to meet the stipulated purity standards set forth by various regulatory bodies. Figure 2.1 depicts the various steps of the therapeutic radionuclide production cycle.

2.6.1 Targets for Irradiation

One of the important requirements for radionuclide involves preparation of the targets which are used for either neutron or charged particle activation. In order to maintain a sustainable availability of target material of required purity, advanced procurement is essential in order to ensure the security of the supply for therapeutic radionuclides. Target selection for reactor irradiation is based on number of considerations.

- *Target Material Costs* – Cost-effective availability of target materials is essential to insure affordability of the radionuclide.
- *Chemical Form of Target Material* – The chemical form of the targets must remain stable under the irradiation conditions and should enable easy post irradiation processing and recovery. Usually targets in metallic forms or oxides are preferred.
- *Physical Form of Target Material* – The physical form and geometry of the target material should be compatible for reactor/accelerator irradiation.
- *Target Purity* – The purity of the targets must be ensured to minimize coproduction of unwanted radionuclides.
- *Target Material Recycling* – While the use of enriched target materials constitutes a positive step to augment the radionuclide production yield as well as specific activity, recycling of the enriched target is usually essential, wherever feasible, to minimize radionuclide costs.

In light of the perceived need to maintain the safety of the reactor or accelerator production facility, it is mandatory to calculate the effects of reactivity effects and nuclear heating of the high levels of radioactivity produced in the target. Such practice is useful and in fact mandatory for the safe handling and transport of the irradiated materials as well. For neutron irradiation, the most preferred targets are metals or inorganic salts usually oxide, carbonate, nitrates, sulfates, etc., but not halides. When the sample size for irradiation is large, one must often pay particular attention to self- shielding, such as that encountered during reactor production of ^{188}W (see Chap. 5).

For accelerator production (Chap. 6), considerable efforts are required for target preparation for charged particle irradiations (IAEA 2009; Ruth 2013). The chemical and mechanical designs of the targets are crucial issues owing to the high rate of energy loss of charged particles as they progress through all materials. In general, irradiations are performed in an evacuated chamber, and thus irradiation of liquid and gases targets are more involved but usually surmountable. The target materials used for accelerator production should possess favorable thermal properties such as high melting point or high boiling point and good heat transfer coefficients. It is necessary to provide a cooling system to dissipate the heat energy deposited in the target material during irradiation. Additionally, the target used should have adequate corrosion and radiation resistance. Solid targets in the form of thin foils or deposits on thin backing material of thickness ~0.1–5 mg/cm^2 are generally preferred, but depend, of course on the rate of energy loss of the projectile particles passing through the target material. Various methods have been developed for the preparation of accelerator targets including evaporation, vacuum deposition, electrospraying, electrodeposition, and molecular plating, and a detailed discussion is beyond the scope of this discourse.

In contrast, the common route to obtain ^{223}Ra of current interest for bone pain palliation (Chaps. 8 and 13) is isolation from aging samples of natural uranium (i.e., decay product of ^{235}U). The activity levels of ^{223}Ra that can be obtained through this route are low and therefore inadequate to meet increasing therapeutic demands, requiring the alternative production of ^{223}Ra of

neutron irradiation of ^{226}Ra in a nuclear reactor. This method of production relies upon multiple successive neutron captures on ^{226}Ra requiring the use of high flux reactors, such as the High Flux Isotope Reactor (HFIR) at ORNL (Mirzadeh 1998). This production strategy involves reactor irradiation of ^{226}Ra, followed by chemical isolation of the ^{227}Ac product ($T_{½}$ = 21.8 years), which decays to ^{227}Th ($T_{½}$ = 18.7 days) and then to ^{223}Ra. The separation of pure ^{223}Ra from the irradiated target is a complex process which requires development and use of elaborate radiochemical separation and purification procedures as well as for radioactive waste handling.

2.6.2 Production of Therapeutic Radionuclides

Each radionuclide has unique properties and requires a specific and efficient production process as well as effective methods for isolation and purification from the irradiated target. Production of radionuclides requires a thorough understanding of the relevant nuclear reactions and decay schemes and processing methods rely upon an intimate knowledge of aqueous solution chemistry. A brief overview of production viability of currently used and promising therapeutic radionuclide is provided in this section with the production classified according to the mode of decay.

2.6.3 Auger Electron-Emitting Radionuclides

Interest in the therapeutic use internal radionuclide therapy using Auger electrons has increased over the last several years. Some radionuclides which have established applications in diagnostic nuclear medicine in fact exhibit significant Auger emissions. These include gallium-67 (^{67}Ga), indium-111 (^{111}In), iodine-123 (^{123}I), iodine-125 ^{125}I, technetium-99m (^{99m}Tc), and thallium-210 (^{201}Tl), which have in fact been discussed for specific therapeutic applications. Auger electron-emitting radionuclides have potential for the therapy of small cancers because of their high level of cytotoxicity, low-energy, high LET, and short-range biological effectiveness. In order to realize their therapeutic potential, Auger electron-emitting radionuclides are generally strongly dependent on their close proximity to DNA. Furthermore, many Auger electron emitters also emit γ-radiation, and this property makes Auger-emitting radionuclides an attractive option as therapeutic and diagnostic agents in the molecular imaging and management of tumors. Radiation properties of representative therapeutic radionuclides for Auger electron therapy are depicted in Table 2.2 (Buchegger et al. 2006). The therapeutic use of Auger emitters in both experimental models and in clinical applications is discussed in Chap. 4.

2.6.4 Alpha-Particle-Emitting Radionuclides

In contrast to β^--emitters, the shorter range and higher LET of α-particles allow the delivery of radiation in a highly localized manner and permit for more efficient and selective killing of individual cells of small-volume tumor. Early studies in cell culture have demonstrated that human cancer cells can be killed even after being hit by only a few alpha particles (Akabani et al. 2006) and that unlike other types of radiation, where oxygen is necessary for free radicals to be generated, efficient cancer cell elimination can be achieved even in an hypoxic environment. Although the conceptual advantages of alpha particles have been realized for some time, routine clinical use of these promising targeted radiotherapeutics has only just recently been accomplished with the introduction of ^{223}Ra (Xolfigo®) for treatment of bone pain from prostate cancer refractory to hormone therapy (Chap. 11). Other discussion of other α-emitting radionuclides is confined in Chap. 3 to those which exhibit potential for therapeutic applications and for which preliminary investigations have been reported in humans or animal models. Currently, interest in potential clinical application of α-particles for therapy has primarily focused on actinium-225 (^{225}Ac), astatine-211 (^{211}At), bismuth-212 (^{212}Bi), bismuth-213 (^{213}Bi),

Table 2.3 Characteristics of α-emitting radionuclides considered for radionuclide therapy

Radionuclide	E_{av} (MeV)	Particle(s) emitted	Half-life
^{211}At	6.79	1α	7.2 h
^{212}Bi	6.0	1α, 1β	60.6 min
^{213}Bi	8.32	1α, 2β	46 min
^{223}Ra	5.64	4α, 2β	11.43 days
^{225}Ac	6.83	4α, 2β	10 days

and radium-223 (^{223}Ra) (Allen 2008; Brechbiel 2007; Huclier-Markai et al. 2012; Lindegren and Frost 2011; Kim and Brechbiel 2012; McDevitt et al. 1998; Mulford et al. 2005; Nilsson et al. 2005; Pohlman et al. 2006; Vaidyanathan and Zalutsky 2011) (Table 2.3).

References

Akabani G, Carlin S, Welsh P, Zalutsky MR. In vitro cytotoxicity of 211At-labeled trastuzumab in human breast cancer cell lines: effect of specific activity and HER2 receptor heterogeneity on survival fraction. Nucl Med Biol. 2006;33(3):333–47.

Allen BJ. Clinical trials of targeted alpha therapy for cancer. Rev Rec Clin Trials. 2008;3:185–91.

Brechbiel MW. Targeted alpha-therapy: past, present, future? Dalton Trans. 2007;43:4918–28.

Britton KE. Towards the goal of cancer-specific imaging and therapy. Nucl Med Commun. 1997;18(11): 992–1007.

Buchegger F, Perillo-Adamer F, Dupertuis YM, et al. Auger radiation targeted into DNA: a therapy perspective. Eur J Nucl Med Mol Imaging. 2006;33(11):1352–63.

Chatal J-F, Hoefnagel CA. Radionuclide therapy. Lancet. 1999;354:931–5.

Cuaron JJ, Hirsch JA, Medich DC, et al. A proposed methodology to select radioisotopes for use in radionuclide therapy. AJNR Am J Neuroradiol. 2009;10: 1824–9.

Cutler CS, Hennkens HM, Sisay N, et al. Radiometals for combined imaging and therapy. Chem Rev. 2013;113: 858–83.

Das T, Pillai MRA. Options to meet the future global demand of radionuclides for radionuclide therapy. Nucl Med Biol. 2013;40(1):23–32.

Ehrhardt GJ, Ketring AR, Ayers LM. Reactor-produced radionuclides at the University of Missouri Research Reactor. Appl Radiat Isot. 1998;49:295–7.

Ercan MT, Caglar M. Therapeutic radiopharmaceuticals. Curr Pharm Des. 2000;6:1085–121.

Hall EJ. Radiobiology for the radiologist. 4th ed. Philadelphia: JB Lippincott Company; 1994.

Heeg MJ, Jurisson S. The role of inorganic chemistry in the development of radiometal agents for cancer therapy. Acc Chem Res. 1999;32:1053–60.

Hoefnagel CA. Radionuclide therapy revisited. Eur J Nucl Med. 1991;18:408.

Huclier-Markai S, Alliot C, Varmenot N, et al. Alpha-emitters for immuno-therapy: a review of recent developments from chemistry to clinics. Curr Top Med Chem. 2012;12(23):2642–54.

International Atomic Energy Agency (IAEA). Cyclotron produced radionuclides: physical characteristics and production methods. Technical report series 468. Vienna: IAEA; 2009.

International Atomic Energy Agency (IAEA). Nuclear data for production of therapeutic radionuclides. Technical report series 473. Vienna: IAEA; 2012.

Joensuu H, Tenhunen M. Physical and biological targeting of radiotherapy. Acta Oncol Suppl. 1999;13:75–83.

Karelin YA, Efimov VN, Filimonov VT, et al. Radionuclide production using a fast flux reactor. Appl Radiat Isot. 2000;53:825–7.

Karenlin YA, Toporov YG. RIAR reactor produced radionuclides. Appl Radiat Isot. 1998;49:299–304.

Kim YS, Brechbiel M. An overview of targeted alpha therapy. Tumour Biol. 2012;33(3):573–90.

Knapp Jr FF (R), Mirzadeh S, Beets AL. Reactor-produced radioisotopes from ORNL for bone pain palliation. Appl Radiat Isot. 1998;49:309–15.

Lindegren S, Frost SH. Pretargeted radioimmunotherapy with α-particle emitting radionuclides. Curr Radiopharm. 2011;4(3):248–60.

Mausner LF, Srivastava SC. Selection of radionuclides for radioimmuno- therapy. Med Phys. 1993;20:503–9.

Mausner LF, Kolsky KL, Joshi V, et al. Radionuclide development at BNL for nuclear medicine therapy. Appl Radiat Isot. 1988;49:285–94.

McDevitt MR, Sgouros G, Finn RD, et al. Radioimmunotherapy with alpha-emitting nuclides. Eur J Nucl Med. 1998;25:1341–51.

McDougall IR. Systemic radiation therapy with unsealed radionuclides. Semin Radiat Oncol. 2000;10(2):94–102.

McEwan AJB. Unsealed source therapy of painful bone metastases: an update. Semin Nucl Med. 1997;27: 165–82.

Mirzadeh S. Generator-produced alpha-emitters. Appl Radiat Isot. 1998;49:345–9.

Mulford DA, Scheinberg DA, Jurcic JG. The promise of targeted {alpha}-particle therapy. J Nucl Med. 2005; 46:199S–204.

Neves M, Kling A, Lambrecht RM. Radionuclide production for therapeutic radiopharmaceuticals. Appl Radiat Isot. 2002;57:657–64.

Neves M, Kling A, Oliveira A. Radionuclides used for therapy and suggestion for new candidates. J Radioanal Nucl Chem. 2005;266(3):377–84.

Nilsson S, Larsen RH, Fossa SD et al. First clinical experience with α-emitting radium-223 in the treatment of skeletal metastases, Clin Cancer Res 2005;11: 4451–59

O'Donoghue JA, Bardibs M, Wheldon TE. Relationships between tumor size and curability for uniformly targeted therapy with beta-emitting radionuclides. J Nucl Med. 1995;36:1902–9.

Pohlman B, Sweetenham J, Macklis RM. Review of clinical radioimmunotherapy. Expert Rev Antican. Ther. 2006;6(3):445–61.

Qaim SM. The present and future of medical radionuclide production. Radiochim Acta. 2012;100:635–51.

Qaim SM, Coenen HH. Produktion pharmazeutisch relevanter. Radionuk Pharm Unser Zeit. 2005;34:460–6 (German).

Ruth TJ. Accelerator production of medical radionuclides: a review. Nucl Phys News. 2013;23:30–3.

Ruth TJ, Pate BD, Robertson D, et al. Radionuclide production for biosciences. Nucl Med Biol. 1989;16:323–36.

Serafini AN. Current status of systemic intravenous radiopharmaceuticals for the treatment of painful metastatic bone diseases. Int J Radiat Oncol Biol Phys. 1994; 30:1187–94.

Spencer RP, Seevers RH, Friedman AM, editors. Radionuclides in therapy. Boca Raton: CRC Press; 1987.

Srivastava SC. Therapeutic radionuclides: making the right choice. In: Mather SJ, editor. Current directions in radiopharmaceutical research and development. Dordrecht: Kluwer Academic Publishers; 1996a. p. 63–79.

Srivastava SC. Criteria for the selection of radionuclides for targeting nuclear antigens for cancer radioimmunotherapy. Cancer Biother Radiopharm. 1996b;11:43–50.

Srivastava SC, Dadachova E. Recent advances in radionuclide therapy. Semin Nucl Med. 2001;31(4):330–41.

Stanciu AE. Radionuclide targeted therapy of cancer. Rev Roum Chim. 2012;57(1):5–13.

Stöcklin G, Qaim SM, Rösch F. The impact of radioactivity on medicine. Radiochim Acta. 1995;70/71:249.

Tolmachev V, Carlsson J, Lundqvist H. A limiting factor for the progress of radionuclide-based cancer diagnostics and therapy – availability of suitable radionuclides. Acta Oncol. 2004;43(3):264–7.

Troutner DE. Chemical and physical properties of radionuclides. Int J Radiat Appl Instrum B Nucl Med Biol. 1987;14(3):171–6.

Unak P, Enginar H, Biber FZ, Lambrecht FY, Aslani MA, Ozkilic H. A correlative study between 99mTc-EST-CPTA and 99mTc-MIBI in rats. Appl Radiat Isot. 2002;57(5):733-42.

Vaidyanathan G, Zalutsky MR. Applications of ^{211}At and ^{223}Ra in targeted alpha-particle radiotherapy. Curr Radiopharm. 2011;4:283–94.

Volkert WA, Hoffman TJ. Therapeutic radiopharmaceuticals. Chem Rev. 1999;99:2269–92.

Volkert WA, Goeckeler WF, Ehrhardt GJ, et al. Therapeutic radionuclides: production and decay property considerations. J NucI Med. 1991;32:174–85.

Yeong C-H, Cheng M-H, Ng K-H. Therapeutic radionuclides in nuclear medicine: current and future prospects. J Zhejiang Univ Sci B. 2014;15(10):845–63.

Zhuikov BL. Production of medical radionuclides in Russia: status and future—a review. Appl Radiat Isot. 2014;84:48–56.

Alpha Radionuclide Therapy

3

3.1 Introduction

Alpha radionuclide therapy has a history starting with the anticipation of medical uses of radium which led to establishing several commercial facilities in the USA for large-scale production of radium (Metzenbaum 1905; Schales 1978; Macklis 1993). In 1913 Frederick Proescher published the first paper which described injection of radium for therapy of various diseases (Proescher 1913). The realization that failing health of both Pierre and Marie Curie had resulted from radiation exposure received during unprotected work with radioactive materials and the failure of early attempts to use naturally occurring radioactive materials for systemic therapy led to a major setback for the field of radionuclide therapy. Although use of radium sources for brachytherapy of cancer continued for a short time, this technology was replaced with other radioisotopes.

Over the years, systemic alpha radionuclide therapy remained essentially dormant, with the treatment of the inflammatory disease *ankylosing spondylitis* with ^{224}Ra as one exception (Bertrand et al. 1978). Although this application is apparently no longer practiced, renewed interest in the use of alpha-emitting radioisotopes was later exemplified by studies with both ^{212}Bi, the decay product of ^{212}Pb, and artificially produced ^{211}At (Zalutsky and Vaidyanathan 2000; Sgouros et al. 1998). Many other investigators then initiated studies on the development of radiopharmaceuticals using both naturally occurring and artificially produced alpha emitters (Brechbiel 2007; Nicolini and Mazzi 1999; Mulford et al. 2005). Most of the radioisotopes selected for investigation belong to one of the radioactive series of uranium, thorium, actinium, or artificially produced neptunium series (^{232}U and ^{233}U decay chains). Intermediate radioisotopes in the decay chains which have suitable physical half-life values for therapy have been selected for development of target specific radiopharmaceuticals, which include ^{225}Ac, ^{212}Bi, ^{213}Bi, ^{227}Th, and several other key examples which are subsequently discussed. A major challenge for use of alpha-emitting radioisotopes is that most decay to radioactive daughter products, which requires containing the decay products within the target. In the last decades, ^{213}Bi emerged as the first alpha-emitting radioisotope to be used in modern human clinical trials in 1997 (Jurcic et al. 2002), and in more recent years, ^{223}Ra constitutes the first systemic targeted alpha emitter approved by regulatory agencies for human use (*vide infra*).

The development and clinical use of Xofigo® ($^{223}RaCl_3$, originally designated as Alpharadin®) is discussed in detail in Chap. 12 and represents the first alpha therapy agent which has completed Phase I/II/III clinical trials and has been subsequently approved by the US Food and Drug Administration (FDA) and regulatory bodies in other countries for the routine treatment of metastatic bone pain in hormone-resistant prostate cancer patients (Parker et al. 2013).

F.F. (Russ) Knapp, A. Dash, *Radiopharmaceuticals for Therapy*, DOI 10.1007/978-81-322-2607-9_3

3.2 Alpha Particles

Alpha particles are emitted by the decay of heavy radionuclides and are doubly charged energetic particles consisting of two protons and two neutrons (Fig. 3.1). After energy loss during travel through the medium, adsorption of two electrons then forms the helium nuclei. In a similar fashion, alpha particles can be produced by stripping two electrons from helium atoms and acceleration to high energy. The latter process is used to generate a beam of high-energy alpha particles in particle accelerators such as use of a cyclotron. The energies of the alpha particles obtained from the decay of radionuclides are in the range of 2–10 MeV, whereas alpha particles of up to a few hundreds of million electron volts (MeV) can be obtained by using an appropriately designed particle accelerator.

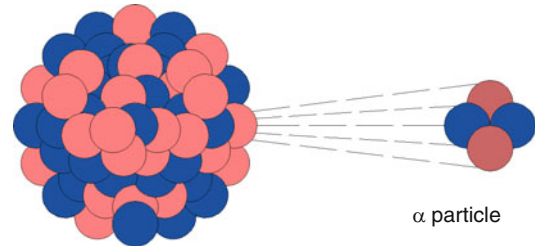

Fig. 3.1 Representation of the emission of an alpha particle via decay of a heavy radionuclide

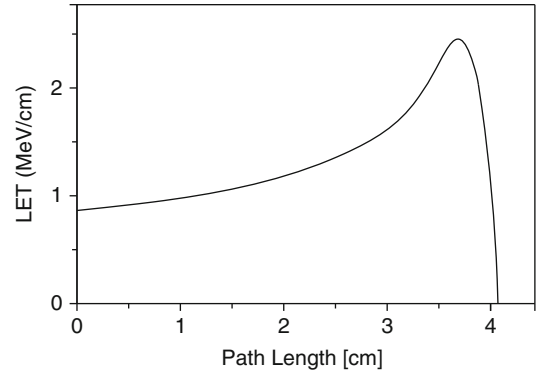

Fig. 3.2 Bragg curve representing the loss of energy and path length of an alpha particle in air

3.2.1 Energy Dissipation of Alpha Particles in a Medium

Energy is lost from alpha particles as they pass through a medium resulting from a series of primary collisions with the negatively charged electrons of the atoms in the medium. These interactions result in ionization and excitation of the atoms in the medium. The energy lost by the moving alpha particles increases with de-acceleration. The loss of energy of a typical alpha particle in air is shown in Fig. 3.2, which is called the Bragg curve.

3.2.2 Linear Energy Transfer (LET)

The linear energy transfer (LET) is the measure of the energy transferred to the medium through which ionizing radiation passes. The LET term is used to quantify the effect of ionizing radiation within the medium such as a biological specimen. LET is expressed in energy lost per unit distance travelled (i.e., MeV/cm, Fig. 3.2). For practical purposes, LET of alpha particles is expressed in the more realistic keV/μm unit. The energy lost is directly related to the density of the medium traversed by the alpha particle. The alpha particles lose energy within a short distance of travel through aqueous medium (soft tissue), for example, usually in a few centimeters in air (Fig. 3.2). Biological systems have much higher density as compared to air. In biological soft tissue, for example, the complete energy of an alpha particle is dissipated within a very short path length, which is often less than 100 μm (i.e., only a few cell diameters). Figure 3.3 illustrates the estimated path lengths of two alpha particles with different energies in a biological system.

The alpha particle LET is inversely related to energy, where higher energy alpha particles lose less energy within a given path length or they have lower LET and vice versa. For example, the LET of 5.750 MeV alpha particles is ~80 keV/m, whereas the path length is ~47 μm. The LET of 8.375 MeV alpha particle is ~60 keV/μm which have a path length of ~85 μm (12–15). The majority of the alpha particle energy loss occurs at the end of the path and at that moment the LET of the alpha particle increases to 200–250 keV/μm. All

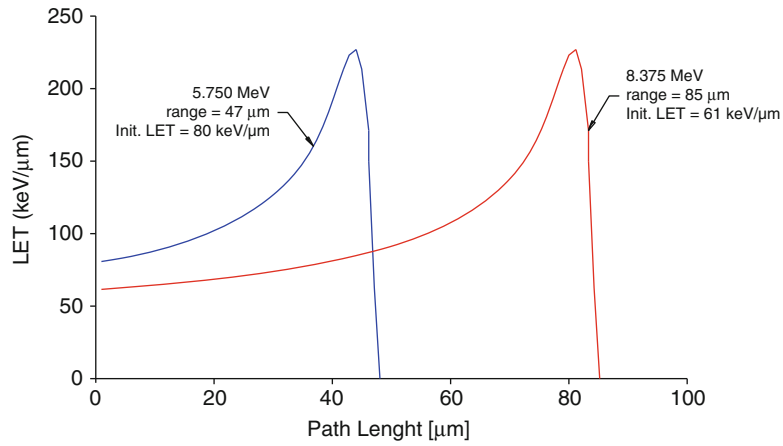

Fig. 3.3 Linear energy transfer (*LET*) of two different alpha particles in a biological system

alpha particles irrespective of the initial energy will have identical LET at endpoint. Hence, the LET of alpha particles of different energies are quoted as the initial loss of energy per unit volume. As the naturally occurring alpha particles have energy values in the 4–8 MeV range, the average range of alpha particles in soft tissues is ~50–80 µm. A comparison between the short path length of energy deposition from alpha particle decay and β^- decay is illustrated in Fig. 12.1. The advantages of high-LET radiation over low-LET radiation are the favorable dose distribution between tumor cells and normal cells and less dependence on tumor hypoxia, dose rate, and cell cycle position (Barendsen et al. 1966; Pouget and Mather 2001; Wang et al 2009). At the same time, the biological effects in the cells are more severe after high-LET radiation, resulting in high RBE.

3.2.3 Relative Biological Effectiveness (RBE)

The biological damage caused by ionizing radiations is expressed as the relative biological effectiveness (RBE), which relates to the biological damage of a radiation of interest compared with a reference radiation, usually 250 keV X-rays or the gamma rays emitted by ^{60}Co (1.33 and 1.17 MeV). RBE is used as a multiplicative term to adjust the estimated absorbed dose so that it reflects the likelihood or severity of a biological effect. If the biological endpoint is stochastic such as cancer induction, then the RBE is approximately 20. In targeted therapy the relevant biological endpoint is not carcinogenesis but rather efficacy or toxicity. Such therapeutic endpoints are deterministic and the measure associated with them is not probability of occurrence (i.e., risk) but severity of toxicity or level of response. The RBE for such endpoints is in the range of 3–7. Among nuclear radiations, the RBE of alpha particles is the highest followed by β-particles and gamma rays. Owing to the high concentrated dose deposited along the track and short range in tissues on the order of cellular dimensions, alpha particles have a high probability of inducing damage to DNA, making them quite cytotoxic. By contrast radiation-induced cellular inactivation for low-LET radiation requires the accumulation of sublethal damage, achieved only at much higher dose. This specific radiation quality of alpha particles, characterized by localized spatial distribution of the imparted energy and high density of ionization per unit path length, causes direct DNA damage rather than indirect free radical-mediated DNA damage. Toxicity originates from the increased frequency of clustered DNA double-strand breaks observed with high-LET radiation (Azure et al. 1994; Goodhead 1994; Howell et al. 1997). The higher the RBE value, the greater the damages encountered from radiation for the same absorbed energy (Azure et al. 1994; Schwarz et al. 1998; Zalutsky and Narula 1988) (Fig. 3.4).

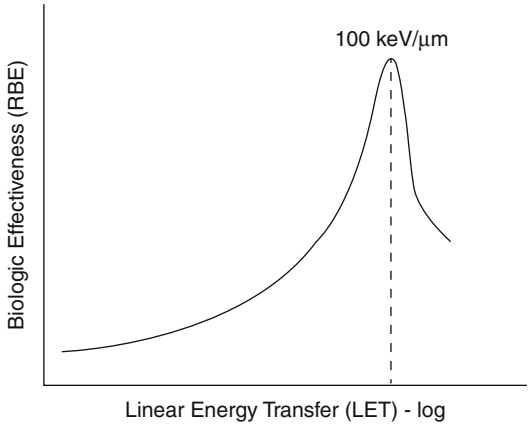

Fig. 3.4 RBE values as a function LET illustrating the much higher RBE values for alpha-emitting radioisotopes

The cytotoxicity of α particles has been shown as independent of both dose rate and oxygenation status of the cells (Hall 1994). In addition to directly damaging DNA, alpha particles have been demonstrated to cause chromosomal instability even in the descendants of non-irradiated stem cells in the vicinity of irradiated cells. This "bystander effect" reflects the potential for interaction between irradiated and non-irradiated cells in the production of genetic damage (Lorimore et al. 1998). The spatial distribution of alpha-particle sources and the geometry of the cells (thickness, diameter of the cell nucleus, distribution of DNA) have to be considered as important parameters in order to correlate the absorbed dose distribution with the observed biological response for the tissue of interest (tumor and/or critical organs).

3.2.4 Interaction of Alpha Particles in a Biological System

The dimensions and size of human cells are quite variable; however, the average cell diameter of most common cells is the order of 10–100 μm. Hence, most alpha particles lose their complete energy within 2–10 cell diameters. Since the total energy of alpha particle is dissipated in a small volume of cells, the damage caused to biological systems by an alpha particle-emitting radionuclide decaying in the vicinity of human cells is very high. In radiation biology, the effect of radiation is measured by multiplying the absorbed dose with a term called the quality factor (QF) or radiation weighing factor (W_R). The W_R of the alpha particles is 20. Hence, alpha-emitting radionuclides cause very high radiation damage once they are inside a living system. As per the International Atomic Energy Agency (IAEA) classification, alpha-emitting radionuclides are listed in Group 1, which means they have the highest toxicity and hence the maximum permissible body burden (MPBB) is the lowest (IAEA 1963).

3.2.5 Basis of Alpha Radionuclide Therapy

Alpha particles cause primary and secondary ionizations to atoms with which they interact and create several ions and excited molecules within cells. The net result of this intracellular turbulence is intermolecular bond biomolecule cleavage. Such events can occur with cytoplasm and all intracellular components as well as the cell nucleus. The desirable feature of alpha radiotherapy is the ability of the decaying alpha particle to cause intramolecular DNA bond cleavage within targeted cancer cells. The DNA molecule is double stranded and cleavage can occur in one or both the strands. The cartoon in Fig. 3.5 depicts the traverse of an alpha particle through a double-stranded DNA molecule and the resultant DNA fragments.

The DNA molecule has inherent ability to repair single-strand damage; however, the repair of a scission in double-stranded DNA to its original form is generally not possible. This damage is the intended therapeutic effect to sterilize cells which can then no longer divide. Repair of double-stranded scission of the DNA molecule can lead to gene mutation, which is an undesirable yet very uncommon outcome of controlled radiation exposure. There is an estimated 20–40 % probability that an α particle interacting with the DNA molecule can ensure breakage of the double strand leading to eventual cell death. In contrast, ⁻ radionuclide therapy requires several β^- decays ("hits") to take place in the vicinity

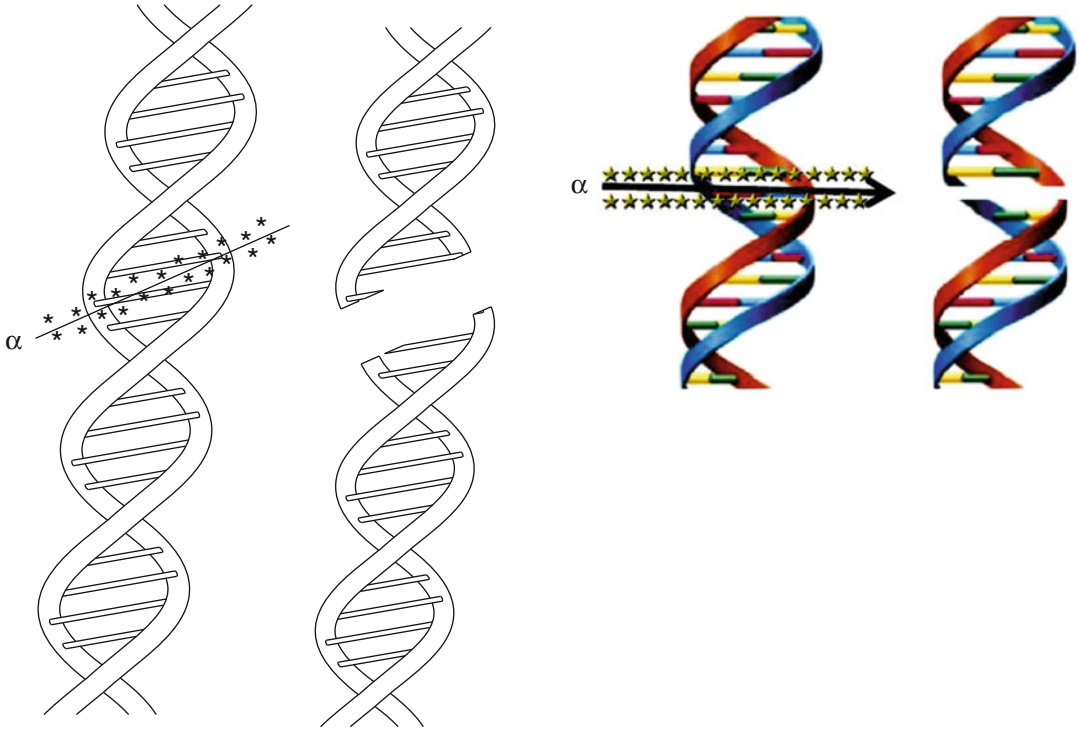

Fig. 3.5 Cartoon showing the passage of an alpha particle through the double-stranded DNA molecule and the resultant double-strand break fragments

of the cell to ensure cell killing (Wessels and Rogus 1984; Humm and Cobb 1990). However, alpha decay must occur in close proximity to the target cell because of the very short path length. In β^- radionuclide therapy, the much longer soft tissue penetration (Fig. 12.1) always irradiation of many cells in addition to the targeted cell because of the "cross-fire" effect to induce non-target cell death. For this reason, an essential condition for ensuring α therapy efficacy is the high degree of accuracy required to deliver the radiation dose to the target cells and at the same time to spare adjacent healthy cells. In the same context, β^- emitting radionuclides are generally more desirable for therapy of solid tumors.

3.2.6 Dosimetry

For α-particle emitters, accurate dosimetry calculations are required. In light of the perceived need to estimate the dose distribution, detailed knowledge of the activity distribution as a function of time at the cellular and subcellular levels as well as an accurate representation of the geometry is a necessity (Sgouros et al. 2011; Chouin and Bardies 2011). Efforts to use clinical scintigraphic imaging turned out to be futile owing to the requirement of spatial resolution of the order of several mm, which is two orders of magnitude greater than the microscopic scale at which one dose is deposited with alpha particles (Allen 2011). Owing to the important stochastic variations in the energy deposited in cell nuclei, macroscopic dosimetry approaches become less relevant and microscopic approaches are required. In this premise, the fundamental quantities required for microdosimetry are specific energy (energy per unit mass) and linear energy (energy per unit path length through the target) which can be used for the calculation adopting analytical methods (convolution via Fourier transforms) or Monte Carlo simulation methods (Bardiès 2000). In this context of long half-lives, the distribution

of both the parent and all daughters must take into account while performing dosimetry calculations (Koch et al 1999). Absorbed dose calculations for alpha-particle emitters can be routinely performed using the dosimetry formalism described in the Medical Internal Radiation Dose (MIRD) Committee Pamphlet 21 (Bolch et al. 2009) with the guidance provided in MIRD Pamphlet 22 (Sgouros et al. 2010).

3.3 Alpha-Particle-Emitting Radionuclides for Radiotherapy

There are over 100 radionuclides categorized in the Chart of Nuclides which decay by α particle emission, of which only a few are practical for radionuclide therapeutic applications. The main reasons for this restricted number of alpha emitters which are investigated include the inability for production in adequate activity levels for therapy and/or unfavorable physical half-lives. Table 3.1 summarizes the physical characteristics of a number of alpha-emitting radionuclides which are of interest for RT. With the exception of artificially produced ^{211}At and ^{149}Tb, all others are emitted from the decay chains of long-lived actinide elements. Most of these radioisotopes of interest are present in radioactive equilibria with their long-lived radioactive parents. For example, the decay product of the thorium series (Fig. 3.6) contains alpha-particle-emitting ^{224}Ra ($t_{1/2}$ 3.66 days) and ^{212}Bi ($t_{1/2}$ 60.55 min), which are both of great current interest for radionuclide therapy. Since the parent and daughter in each case are in secular equilibrium (Chap. 7), their respective activity levels will be equal to the activities of the long-lived parent radionuclides.

Alpha radionuclide therapy is generally preferred for special applications, which include situations targeting isolated cancer cells circulating in the lymphatic and vascular systems, the regression of metastatic cancer cell clusters, and for disrupting the vasculature of solid tumors. Radionuclides of current or potential use for alpha radionuclide therapy and short summaries of preclinical and clinical studies are discussed in the following sections of this chapter.

3.3.1 Astatine-211

Astatine-211 is an artificially produced alpha radionuclide with a half-life of 7.2 h and which decays via a branched pathway to stable lead as shown in Fig. 3.7. Electron capture (EC) decay (58.3 %) of ^{211}At leads to the production of ^{211}Po

Table 3.1 Examples of key alpha-emitting radionuclides useful for alpha radionuclide therapy

Radionuclide	Half-life	Daughter	[a]Energy of particles (keV)	Energy of β^- particles	Energy of rays, KeV
Actinium-225	10.0 days	^{221}Fr	5935 (100 %)		86 keV
Astatine-211	7.21 h	^{207}Bi ^{211}Po	5870 (41.7 %) 7450 (58.2 %)	786 keV (58.2 %)	
Bismuth-213	45.59 min	^{213}Po	5869 (93 %)	1427 (64.5 %) 986 (30.4 %)	440 (26.1 %)
Bismuth-212	60.55 min	^{208}Tl (35.94 %) ^{212}Po (64.06)	6089 (27.1 %) 6050 (69.9 %)	2254 (55.4 %)	
Radium-223	11.435 days	^{219}Fr	6559 (100 %)	Nil	269 (13.7)
Radium-224	3.66 days	^{220}Rn	5685 (100 %)	Nil	241 (4.1 %)
Terbium-149	4.118 h	^{145}Eu (17 %) ^{149}Gd (83 %)	3967 (17 %)	2432 (31.5 %)	853 (15.45 %) 817 (11.6 %)
Thorium-227	18.72 days	^{223}Ra	6038 (100 %)	Nil	256 (7 %) 236 (11.5 %)

[a]Alpha energy values of only the first daughter is indicated in the table. The percent given in brackets is the alpha yield of the first emission only

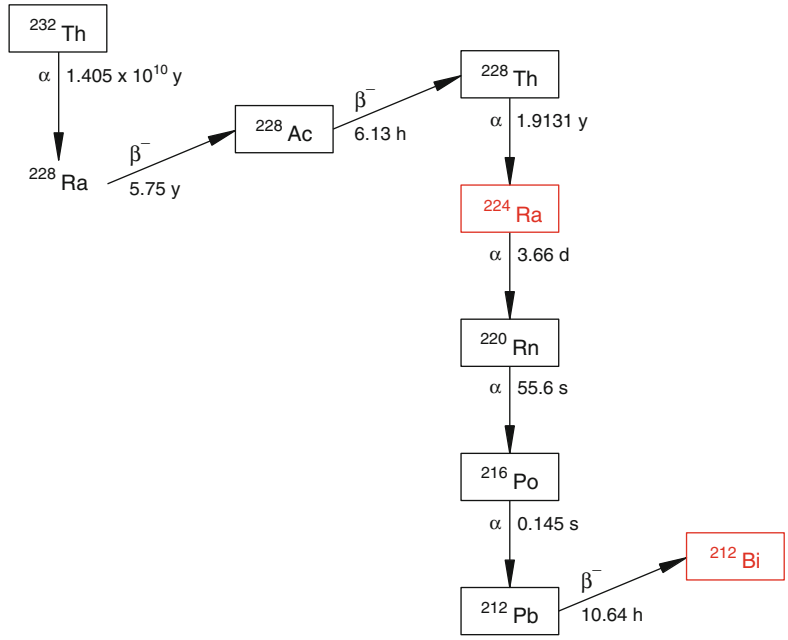

Fig. 3.6 The decay chain of the naturally occurring thorium (^{232}Th) series. The therapeutic radionuclides ^{224}Ra and ^{212}Bi are part of the ^{232}Th series

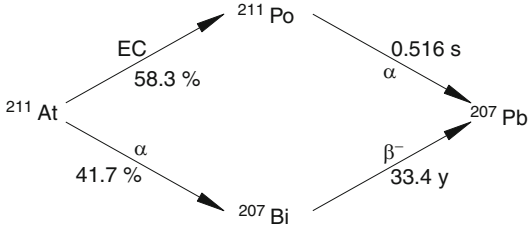

Fig. 3.7 Nuclear decay scheme of ^{211}At showing the two branched chains leading to its decay to ^{207}Pb

($t_{1/2}$ 0.516 s) which decays by emission of an alpha particle (7.45 MeV, 100 %) to stable ^{207}Pb. The second branch (41.7 %) decays to ^{207}Bi via emission of an alpha particle (5.87 MeV, 100 %). Although long lived ($t_{1/2}$ 33.4 years), the ^{207}Bi will not contribute to any radiation dose during therapy. Through these two branching routes, each of the decaying ^{211}At atoms contributes to the production of one alpha particle per decay. In addition, decay of ^{211}At emits β^-particles (58.3 %, β_{max} 786 keV). The soft tissue ranges of the two alpha particles are ~55 μm and ~80 μm with a mean initial LET of ~100 keV/μm (Fig. 3.8). The electron capture decay of ^{211}At to ^{211}Po (58 %) emits 77–92 KeV K X-rays of polonium which are suitable for scintigraphic imaging.

3.3.1.1 Production of ^{211}At

Astatine-211 is produced by alpha-particle bombardment on ^{209}Bi targets by the ^{209}Bi(α,2n)^{211}At reaction (IAEA 2009; Schwarz et al. 1998; Henriksen et al. 2001; Lebeda et al. 2005). Bismuth is mononuclidic and ^{209}Bi is present in 100 % abundance. The nuclear reaction cross section approaches a value of one barn at 28 MeV (Fig. 3.8). The thick target yield of ^{211}At is reported to be between 30 and 40 mCi/μA.h at 28–29.5 MeV (IAEA 2009). For this reason high activity levels of ^{211}At can be produced by use of a suitable solid target for irradiation in cyclotrons having α beams of 30 MeV and a beam current in the range of a few hundred μA. Dry distillation at 650 °C releases volatile ^{211}At, which can be removed by use of a carrier gas. The distilled ^{211}At is trapped in polyether ether ketone (PEEK) tubing maintained at −77 °C with a mixture of ethanol and ice. The trapped ^{211}At is then recovered by using organic solvents (Zalutsky and Pruszynski 2011).

Astatine-210 will also be coproduced during production of ^{211}At through the competing ^{209}Bi(α,3n)^{210}At reaction. The decay product of ^{210}At, ^{210}Po, has a half-life of 138 days, decays by alpha emission, and localizes in the bone marrow.

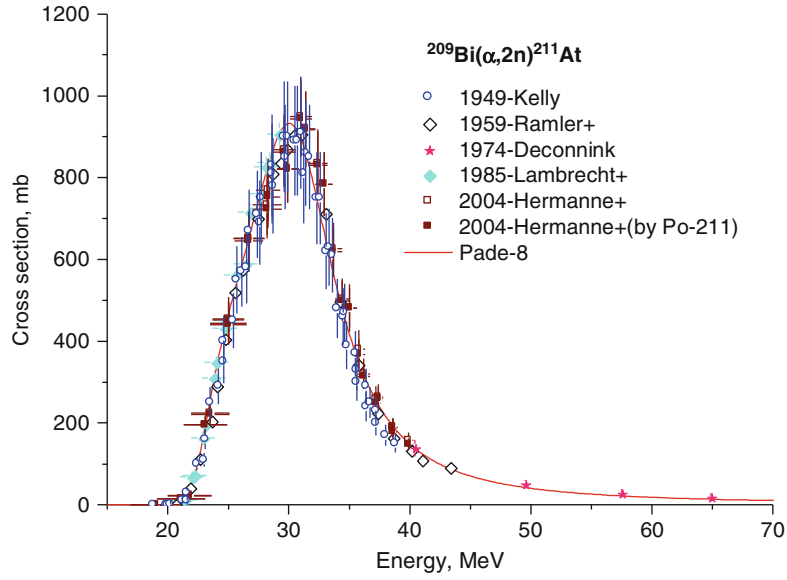

Fig. 3.8 Excitation function of $^{209}Bi(\alpha,2n)^{211}At$

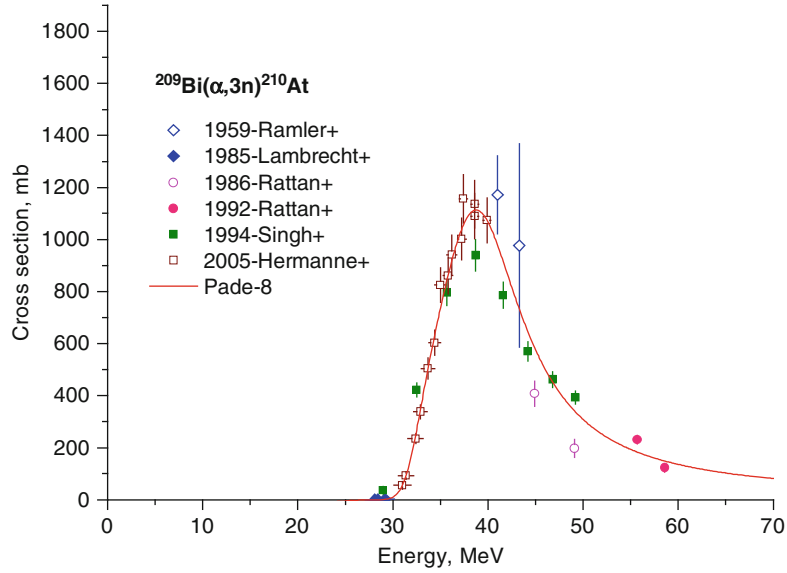

Fig. 3.9 Excitation function of $^{209}Bi(\alpha,3n)^{210}At$

Hence, ^{210}At is an undesirable radionuclidic impurity. The cross section for the production of ^{210}At is practically absent below 30 MeV (Fig. 3.9), and hence the beam energy is maintained below 30 MeV during target bombardment.

3.3.1.2 Astatine Chemistry

Astatine is the last member of the halogen family and hence the least electronegative in the series and thus exhibits some metallic properties. Astatine does not exist in any stable isotopic form, and unfortunately, the chemistry of At cannot be elucidated by chemical synthesis and characterization of nonradioactive compounds in the usual manner. The carbon–halogen bond strength decreases in higher homologues, and hence the carbon–astatine bond is the weakest, resulting in vulnerability of astatine compounds to deastatination. Astatine-211-labeled aromatic compounds are usually synthesized by exchange halogenation

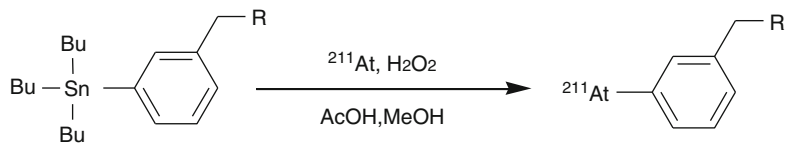

Fig. 3.10 Electrophilic astatodemetallation of organostannanes

or by electrophilic substitution on aromatic rings. Low specific activity is a serious limitation with exchange labeling. Electrophilic substitution of ^{211}At to the phenolic ring has been demonstrated; however, the carbon–astatine bonds formed with such activated aryl rings are labile, leading to poor in vivo stability of the products. Electrophilic astatodemetallation of organometallic derivatives, preferably organostannanes, is used for preparation of stable ^{211}At tracers (Fig. 3.10).

Utilizing the metallic properties of astatine, radiolabeling of antibodies using DTPA complex of ^{211}At has also been reported (Ning et al. 1998). The anionic character of astatine has been used to attach the ^{211}At anion to soft metal cations such as mercury, rhodium, and iridium complexed with bifunctional chelating agents. Since it is a halogen anion, any free astatide (^{211}At$^-$) has a tendency to be localized in the thyroid, spleen, bone marrow, stomach, and lungs (Visser et al. 1981). Hence, ^{211}At-labeled radiopharmaceuticals must exhibit high chemical stability in vivo, to avoid unwanted radiation dose to the above organs, especially to the thyroid.

3.3.1.3 Astatine-211 Radiopharmaceuticals

Astatine-211 has been extensively evaluated for alpha RT therapy in animal models especially and a comprehensive description of this work is described in a review article (Vaidyanathan and Zalutsky 2008). A brief description of preclinical studies with the various ^{211}At-labeled agents follows.

Astatide (^{211}At$^-$)

Like iodide, astatide (At$^-$) is taken up by the thyroid tissue mediated through the sodium iodide symporter (NIS), which is a membrane protein expressed on the basolateral surface of the thyroid epithelial cells. For this reason ^{211}At$^-$ could potentially be used for the treatment of cancers of thyroid origin; however, the consequences of targeting to sites such as the thyroid would have to be evaluated. The potential of NIS-mediated uptake of ^{131}I for non-thyroid cancer through gene incorporation has been proposed which could also be extended to astatine. The short half-life of ^{211}At as compared to ^{131}I is an advantage since the efflux of activity from the tumor is generally rapid and does not match the long half-life of ^{131}I ($t_{1/2}$ 8.02 days). An evaluation of the long-term effect of [^{211}At]astatide in NIS-induced tumor-bearing mice showed complete irradiation of the tumor in 3 months (Petrich et al. 2006; Brown and Carpenter 1991; Lundh et al. 2006; Carlin et al. 2003).

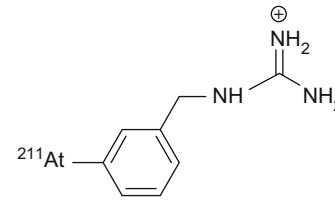

Fig. 3.11 *Meta*-[^{211}At]astatobenzyl guanidine (MABG)

^{211}At-MIBG

Many neuroendocrine tumors (NETs) overexpress the neurotransmitter norepinephrine, and the metaiodobenzylguanidine (MIBG) functional analog is also taken up by such cancer cells. Radioiodinated (^{123}I, ^{124}I, and ^{131}I) MIBG has been used for diagnosis and therapy of NETs (Bomanji et al. 2003). The ^{211}At-labeled analog *meta*-[^{211}At]astatobenzyl guanidine (MABG) (Fig. 3.11) was synthesized and studied for treatment of neuroendocrine tumors in animal models. The radioactivity levels required were 400–1000-fold lower with MABG as compared to MIBG to create the same biological effect in in vitro studies (Vaidyanathan et al. 1994).

^{211}At-Bisphosphonates

Bisphosphonates are pharmaceutically applied for the stimulation of osteoblastic activity for the

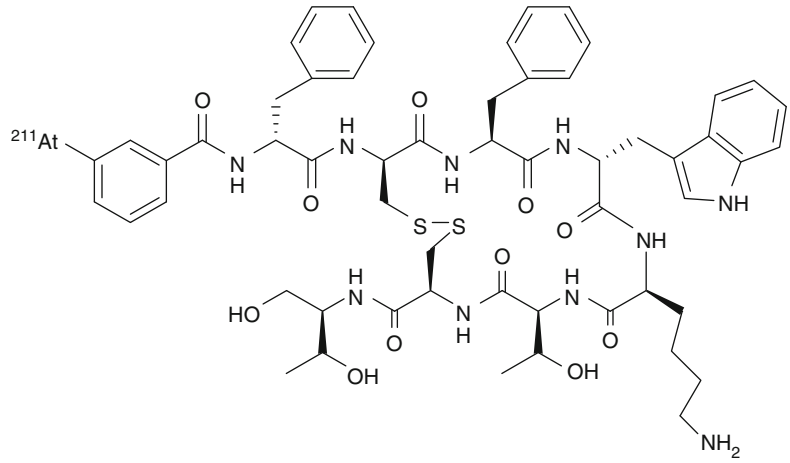

Fig. 3.12 ^{211}At-labeled octreotide (TOC)

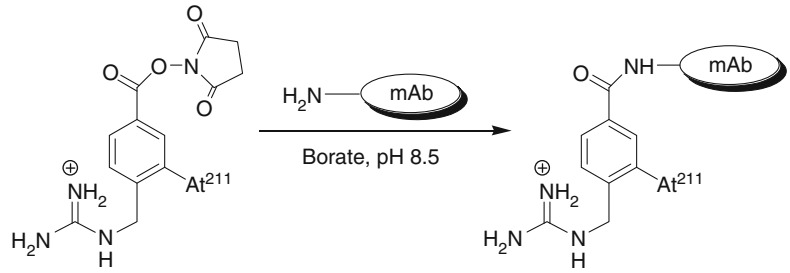

Fig. 3.13 Radiolabeling of monoclonal antibody with ^{211}At using N-succinimidyl 3-[^{211}At]astato benzoate

skeleton, and analogs radiolabeled with β−-emitting radionuclides are widely used for clinical palliation of metastatic bone pain (see Chap. 12). The ^{211}At-labeled analog of pamidronate, a commercially available bisphosphonate, was developed for the treatment of osseous cancers. The bisphosphonate was labeled using an ^{211}At intermediate which was conjugated to the bisphosphonate in 60–80 % chemical yield (Murud et al. 1999a, b). High bone uptake in normal mice was demonstrated and dosimetric studies indicated much lower bone marrow dose as compared to the β$^-$-emitter-based radiopharmaceuticals available for the same purpose.

^{211}At-Peptides

The 7.2-h half-life of ^{211}At is compatible for used for preparation and use of radiolabeled peptides for targeted therapy. Somatostatin analogs, octreotide and octreotate (see Chap. 10), have been labeled with ^{211}At using astatodemetallation using a tin moiety (Fig. 3.12). The resultant peptides showed in vitro uptake in SSTR2 receptor bearing cell lines but evidently have not been further evaluated (Vaidyanathan et al. 2000, 2004).

Clinical Studies with ^{211}At-Antibodies

The 7.2-h half-life of ^{211}At is too short for the preparation of radioimmunotherapeutic agents since the in vivo biokinetics and cellular uptake of monoclonal antibodies are very slow. Antibody fragments and genetically engineered antibody molecules are better suited for radiolabeling with ^{211}At, as their uptake by the tumor is more rapid. Astatination of antibodies and fragments by electrophilic substitution to the phenolic rings of the tyrosine moieties is possible, however, with poor stability. Conjugation of astatinated intermediates N-succinimidyl 3-[^{211}At]astato benzoate (SAB) and N-succinimidyl 4-[^{211}At]astato benzoate (PAB) yields products having better stability (Fig. 3.13) (Zalutsky and Narula 1988; Hauck et al. 1998).

In a phase 1 clinical study, the chimeric antitenacin monoclonal antibody 81C6 (ch81C6) radiolabeled with ^{211}At using an SAB conjugate was administered to the surgically created

resection cavity (SIRC) of 18 patients suffering from recurrent malignant glioma. Serial γ-camera imaging and blood sampling showed that >95 % of the activity remained in the SIRC even after 24 h. None of the patients experienced dose-limiting toxicity when dose of 71–347 MBq was used. This study provided proof of concept for regional targeted radiotherapy with ^{211}At-labeled molecules and remains the only clinical study thus far reported (Zalutsky et al. 2008).

The major difficulty for use of ^{211}At is the limited number of cyclotrons which have the required alpha-particle beams with energies of 25–30 MeV which are capable of producing adequate activity levels of ^{211}At. The short physical (7.2 h) half-life also constrains the radiochemical processing of irradiated targets, preparation, purification and quality control of the radiopharmaceuticals, and transportation of the product to user sites. The chemistry of ^{211}At is still not well defined, which leads to poor radiolabeling yields which in turn requires much higher activity levels of ^{211}At for radiopharmaceutical preparation. Due to the high-energy deposition of α particles, ^{211}At-labeledradiotracers also undergo high radiolytic damage on storage and hence require purification prior to administration. All the above are unfavorable factors in a clinical setting interested in large-scale routine radionuclide therapy with ^{211}At. Despite dedicated efforts and the publication of many research papers, ^{211}At is yet to demonstrate its place as a radionuclide for therapy.

3.3.2 Terbium-149

The ^{149}Tb radiolanthanide has a half-life of 4.1 h and decays by alpha emission as well as electron capture and β^+ emission. The decay scheme of ^{149}Tb is shown in Fig. 3.14. Alpha decay is only 17 % and the ^{145}Eu ($t_{1/2}$ 5.93 days) decay product decays through two consecutive electron captures to ^{145}Pm ($t_{1/2}$ 17.7 years). In the second route, ^{149}Tb decays to ^{149}Gd by the EC (76 %) or β^+ (7 %) modes. The ^{149}Gd is also long-lived ($t_{1/2}$ 9.5 days) which by EC decays to long-lived ^{149}Sm. The pharmacokinetics of ^{149}Tb-labeled antibodies can be determined by either SPECT or PET since it emits both X-rays due to electron capture as well as annihilation photons from β^+ decay.

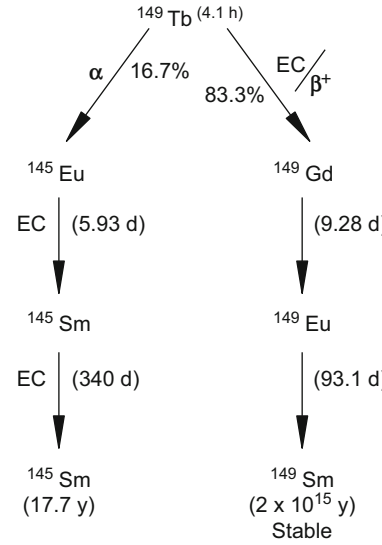

Fig. 3.14 Decay scheme of ^{149}Tb

Terbium-149 is produced in a particle accelerator either using heavy ions or protons. The suggested routes are Nd(^{12}C,5n)^{149}Dy → ^{149}Tb [108 MeV heavy ion ^{12}C] or ^{152}Gd(p,4n)^{149}Tb (Beyer et al. 2002). Both production routes require high-energy particles and the reaction cross sections are only moderate. Since it is a radiolanthanide available in the +3 state, ^{149}Te can be complexed with chelating agents such as DOTA or DTPA and conjugated to proteins, peptides, or antibodies. In one preclinical study with ^{149}Tb-labeled rituximab, which is specific to anti CD 20 antigen, this agent showed high efficiency elimination of leukemia in "skid" mice (Beyer et al. 2004). The major difficulty in development of ^{149}Tb radiopharmaceuticals is the requirement for high-energy cyclotrons. The short 4.12-h half-life is unfortunately not long enough for radiochemical separation of the radionuclide and for preparation of radiopharmaceuticals.

3.3.3 Actinium-225

Actinium-225 is the decay product of ^{229}Th belonging to the artificially produced protactinium series (Fig. 3.15). Both the ^{237}Np ($t_{1/2}$ 2.14×10^6 years) and ^{233}U ($t_{1/2}$ 1.6×10^5 years) parent radionuclides are not naturally occurring

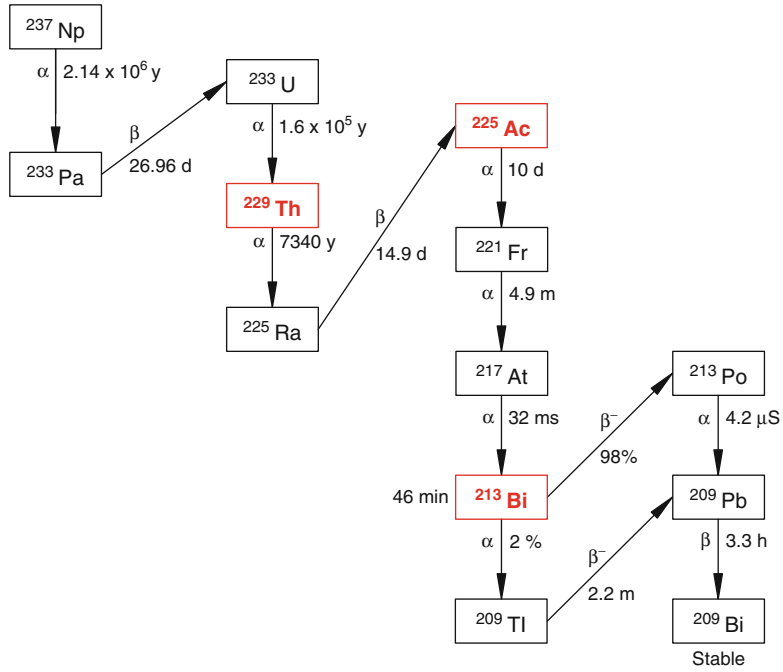

Fig. 3.15 Decay series of the artificially produced ^{237}Np/^{233}U series. ^{225}Ra, ^{225}Ac, and ^{213}Bi are the alpha-emitting radionuclides suitable for therapy in this series

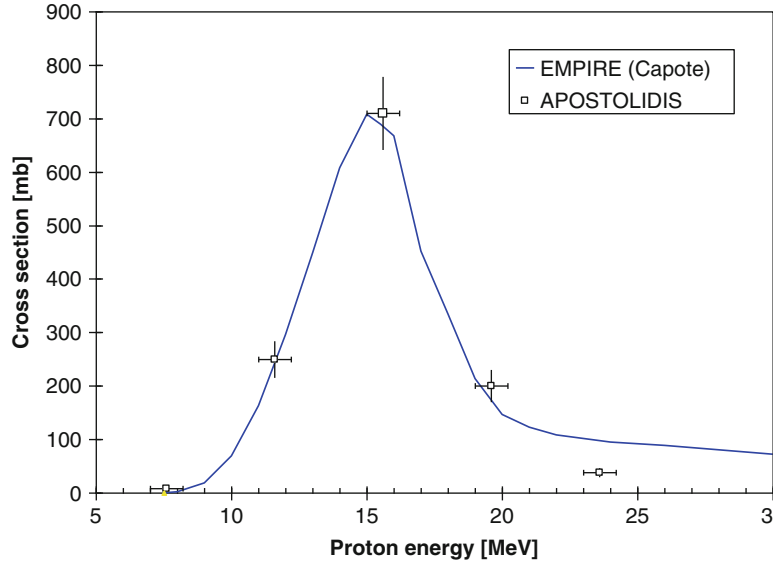

Fig. 3.16 Excitation function of ^{226}Ra(p,2n)^{225}Ac

and have been produced as by-products of the weapons program. Both these radioisotopes have very long half-lives and there are available in only limited amounts. Small quantities of ^{229}Th ($t_{1/2}$ 7880 years) could be isolated from the existing stock of ^{237}Np or ^{233}U which have only limited availability. Isolation of small quantities of ^{225}Ac from a mixture of ^{228}Th, ^{229}Th, and ^{232}Th is reported (Boll et al. 2005).

Actinium-225 can also be prepared by irradiating ^{226}Ra with a proton beam in a cyclotron by the ^{226}Ra(p,2n)^{225}Ac nuclear reaction (IAEA 2009; Apostolidis et al. 2005). The nuclear reaction cross section is 700 mb peaking at 15 MeV (Fig. 3.16). Although ^{226}Ra is available in nature, it is radioactive and hence there are challenges for target preparation, irradiation, post-irradiation handling, and recovery.

3.3.3.1 ^{225}Ac Decay Scheme

Actinium-225 exhibits a very complex decay scheme involving several radioactive isotopes (Fig. 3.17) which include ^{213}Bi ($t_{1/2}$ 46 min), generated through the intermediate ^{221}Fr ($t_{1/2}$ 4.9 min) and ^{217}At ($t_{1/2}$ 32 ms) daughter products. Once delivered to the target site, ^{225}Ac emits three alpha particles during its decay to ^{213}Bi ($t_{1/2}$ 46 min). Bismuth-213 decays with emission of an alpha particle and two β^- particles before it reaches stable ^{209}Bi.

The energy values for the four alpha particles emitted during complete decay of ^{225}Ac to ^{209}Bi are 5.75 MeV (^{225}Ac to ^{221}Fr), 6.297 (^{221}Fr to ^{217}At), 7.065 (^{217}At to ^{213}Bi), and 8.375 MeV (^{213}Po to ^{209}Pb). The average soft tissue ranges of the four alpha particles are 47 μm, 54 μm, 64 μm, and 85 μm, respectively (Fig. 3.18). The LET of the α particles are 80 keV/μm, 75 keV/μm, 64 keV/μm, and 61 keV/μm, respectively (Miederer et al 2008).

The decay of ^{225}Ac also results in emission of two β^- particles, and this cascade of both alpha and β^- particle emission from the decay of ^{225}Ac is highly toxic to cells even in very low activity levels. The long ^{225}Ac half-life (10 days) also contributes to a very high cumulative dose from a given level of radioactivity. Therefore, ^{225}Ac-labeled radiopharmaceuticals are theoretically very attractive, but in practice, a challenge is to avoid the release of the radionuclide decay species form the ^{225}Ac-radiopharmaceutical targeting sites. Accumulation of escaping daughter radionuclides in other organs and the undesirable biokinetics of the daughter radionuclides can be very toxic to normal nontargeted cells.

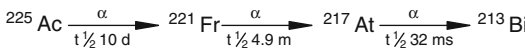

Fig. 3.17 Decay scheme of ^{225}Ac

3.3.3.2 Preclinical Studies with ^{225}Ac

There are few reports of human application of ^{225}Ac, but several reports describe the use ^{225}Ac-labeled monoclonal antibodies in mice. In most of the studies, DTPA or DOTA derivatives are used for conjugating ^{225}Ac with the targeting molecules (Essler et al. 2012; Chappell et al. 2000). In one of the successful animal studies, complete regression of the growth of implanted breast cancer cells was achieved in a mouse model. A single administration of 400 nCi of ^{225}Ac-labeled *anti*-rat HER-2/neu monoclonal antibody, using the bifunctional chelating agent, p-NCS-Bn-DOTA, led to killing of breast cancer cells in about 67 % of HER-2/neu transgenic mice, leading to long-term survival (Song et al. 2009). However, biodistribution studies showed the presence of the daughter products ^{221}Fr and ^{213}Bi in kidneys.

In another preclinical trial, a 12 coordination site chelator, 1,4,7,10,13,16-hexaazacyclohexadecane-N, N′, N″, N‴, N⁗, N⁗′-hexaacetic acid

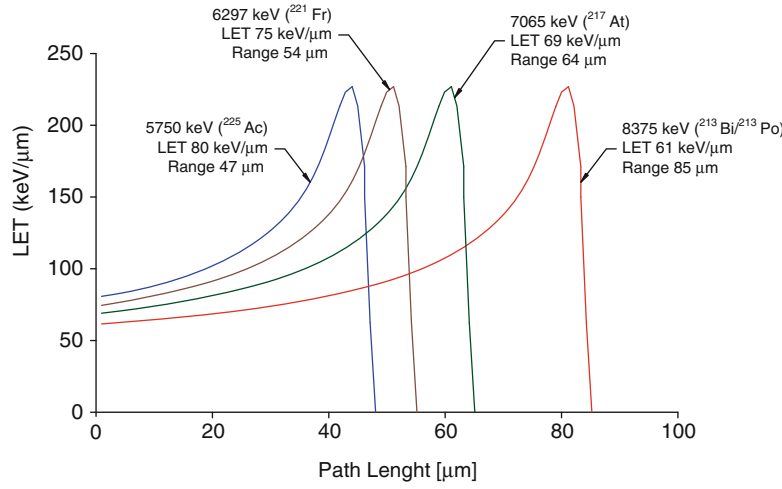

Fig. 3.18 Linear energy transfer of the different alpha particles emitted by decaying ^{225}Ac

(HEHA) (Fig. 3.19), was used as a chelating agent for radiolabeling the Mab 201B monoclonal antibody, which binds to murine thrombomodulin (Kennel et al. 2000, 1999; Kennel and Mirzadeh 1998). Vascular targeting radioimmunotherapy was evaluated to determine the efficacy of treatment using the labeled antibody in mouse lungs growing EMT-6 tumor colonies. The mice were injected with 0.5 μCi and showed only residual lung tumor but much longer survival as compared to control mice. Animals injected with 1 μCi showed better cure as compared to the set of animals treated with 0.5 μCi but had reduced survival due to high radiation toxicity. No window of therapeutic dose could be estimated from these limited studies.

3.3.4 Bismuth-213

In contrast to interest in ^{225}Ac and other alpha-emitting radionuclides, highly purified ^{213}Bi ($t_{1/2}$ 46 min) is available from the ^{225}Ac/^{213}Bi generator from decay of ^{225}Ac (Kennel et al. 1999; Friesen et al. 2013). The decay scheme for ^{213}Bi is shown in Fig. 3.20. The 97.91% branching decay of ^{213}Bi to ^{213}Po predominates. The radioactive ^{213}Po ($t_{1/2}$ 4.2 μs) intermediate is very short-lived and yields an alpha particle with an energy of 8.375 MeV having a range of 85 μm and initial LET of 61 keV/μm (Sgouros et al. 2010).

The ^{209}Pb ($t_{1/2}$ 3.253 h) decay product is sufficiently long-lived to migrate from the ^{213}Bi-agent targeting site, but since it is a β⁻-emitter (Eβ⁻ = 1427 keV), the radiation dose contribution to nontarget organs will be less as compared to the dose from the original radiopharmaceutical. The decay of ^{213}Bi also results in the emission of 440 keV (26.1 %) gamma rays which are important for imaging.

The availability and cost of the ^{225}Ac/^{213}Bi generator are major deterrents, however, for possible widespread clinical use of ^{213}Bi. The relatively short 10.0-day half-life of ^{225}Ac with the consequent requirement for regular generator replacement at short intervals have resulted thus far in the very high cost for use of ^{213}Bi. Despite the short 46 min half-life of ^{213}Bi, there are a number of reports describing its use for antibody radiolabeling and in vivo uptake studies in animal models as well as in vitro cell line investigations. Most importantly, in one ongoing clinical trial, the ^{213}Bi-labeled humanized anti-CD33 antibody lintuzumab (HuM195) which targets myeloid leukemia cells is under study in patients (Friesen et al. 2013; Jurcic 2013). In a phase I/II trial, 31 patients each received ^{213}Bi-lintuzumab at activity levels between 18.5 and 46.25 MBq/kg (Rosenblat et al. 2010). The maximum tolerated dose (MTD) was 37 (1 mCi/kg) as determined by myelosuppression lasting > 35 days. Significant reduction in marrow blasts was seen at all dose levels. The median response duration in patients was 6 months (ranging from 2 to 12 months), and treatment-related deaths occurred in 2 of 21 patients

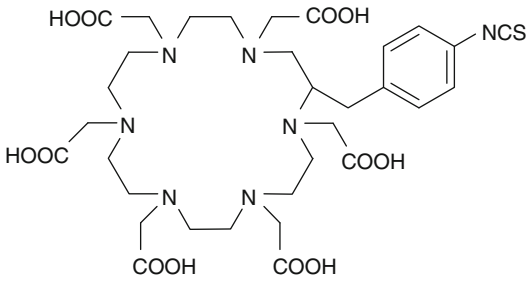

Fig. 3.19 The bifunctional chelating agent 1,4,7,10,13,16-hexaazacyclohexadecane-*N*,*N*',*N*'',*N*''', *N*'''', *N*''''-hexaacetic acid (HEHA)

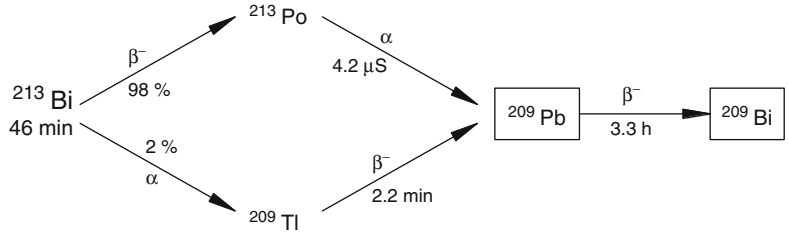

Fig. 3.20 Decay scheme of ^{213}Bi

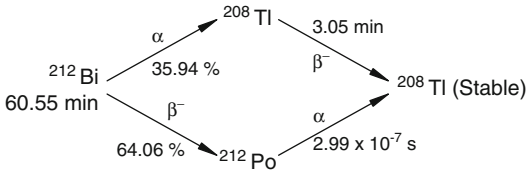

Fig. 3.21 Decay scheme of ^{212}Bi

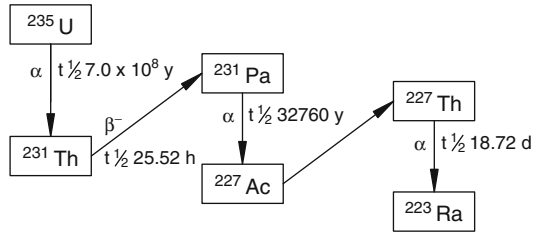

Fig. 3.22 Decay scheme of ^{235}U leading to the production of ^{223}Ra

(10 %) who received the maximum tolerated dose (MTD). These are very positive results in a patient with blood-borne leukemia cells which can be rapidly targeted using this technology.

3.3.5 Bismuth-212

Bismuth-212 ($t_{1/2}$ 60.55 min) is the daughter product of ^{232}Th decay series. Naturally occurring ^{232}Th ($t_{1/2}$ 1.405×10^{10} years) is widely available in nature and contains ^{224}Ra ($t_{1/2}$ 3.66 days) which is in transient equilibrium with ^{212}Pb ($t_{1/2}$ 10.64 h). Lead-212 can be separated from ^{224}Ra and can be used for the preparation of a ^{212}Pb/^{212}Bi generator from which pure ^{212}Bi can be separated for therapy (Atcher et al. 1988). The decay scheme of ^{212}Bi is shown in Fig. 3.21 and has two independent branching paths to ^{208}Tl (35.94 %) and ^{212}Po (64.06 %). Decay by beta-particle emission of ^{212}Bi leads to ^{212}Po ($t_{1/2}$ 3.053 min), which decays to stable ^{208}Pb by emission of an α particle. In the second mode, α emission of ^{212}Bi leads to ^{208}Tl ($t_{1/2}$ 3.053 min) which by β⁻ emission decays to ^{208}Pb. The half-lives of the ^{212}Po ($t_{1/2}$ 0.3 ms) and ^{208}Tl ($t_{1/2}$ 3.1 m) decay products are too short for escape of the daughter products from the targeted site. The 6207 keV (35.94 %) and 6050 keV (64.06 %) alpha energies are very close and hence have nearly the same effective range and LET. Bismuth-212 decay also results in the emission of high-energy β⁻ particles (2254 keV, 55.4 %). The one ^{208}Tl daughter product also emits imageable gamma photons (583 keV and 510 keV). There are also very high energy 2614 keV (99 %) gamma photons emitted from decay of ^{208}Tl which require shielding for non-patient personnel protection. Antibody radiolabeling of ^{212}Bi through diethylenetriaminepentaacetic acid (DTPA)-based BFCA has been reported (Metting et al. 1992; Montavon et al. 2012), and there is still interest in the use of this alpha emitter for targeted therapy.

3.3.6 Radium-223

Radium-223 ($t_{1/2}$ 11.43 days) belongs to the actinium series and is the decay product of the naturally occurring ^{235}U (Fig. 3.22). It can be isolated from ^{227}Ac ($t_{1/2}$ 21.773 y) which is a daughter product from decay of naturally occurring ^{235}U. Radium-223 decays to ^{211}Pb ($t_{1/2}$ 36.1 min) through emission of three alpha particles (Fig. 3.23). Lead-211 decays to ^{211}Bi ($t_{1/2}$ 2.14 min) by β⁻ emission which in turn decays to stable ^{207}Pb by emission of a β⁻ and an alpha particle through two independent branched decay modes. However, the decay through ^{207}Tl is predominant (99.7 %).

Radium-223 is one of the longest-lived alpha-emitting radionuclides considered for therapy and as $^{223}RaCl_2$ (Alpharadin; Algeta, Oslo, Norway) entered phase III clinical trials in symptomatic prostate cancer patients having bone metastasis (Parker et al. 2013). Now approved for routine clinical use as Xofigo® (Bayer), it represents the first alpha emitter which has been commercialized and recently introduced (see Chap. 12) for routine palliative treatment of bone pain in patients with castration-resistant prostate cancer. Among the various daughter products, ^{211}Pb ($t_{1/2}$ 36.1 min) and ^{211}Bi ($t_{1/2}$ 2.14 min) pose the potential challenges because of migration from the target. The other daughter

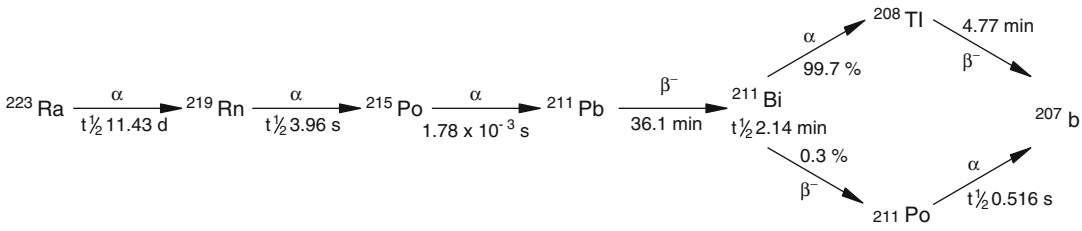

Fig. 3.23 Decay scheme of ^{223}Ra

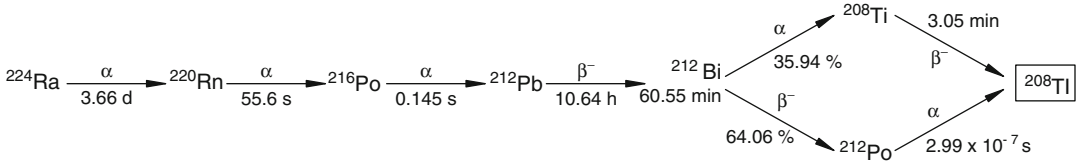

Fig. 3.24 Decay scheme of ^{224}Ra

products are evidently contained within the metastatic target sites since the half-life is too short. Xofigo® is generally administered by intravenous injection on a monthly basis for 4–6 months and generally shows effective pain relief.

3.3.7 Radium-224

Radium-224 belongs to the thorium series. Radium-224 decays to ^{212}Pb ($t_{1/2}$ 10.64 h) by emitting three alpha particles within a short life span. ^{224}Ra decays to ^{212}Pb by emission of 3 alpha particles (Fig. 3.24). The ^{212}Pb/^{212}Bi generator discussed earlier (Chap. 7) is part of this decay scheme. A major problem of the use of ^{224}Ra is the presence of ^{212}Pb ($t_{1/2}$ 10.64 h) and ^{212}Bi ($t_{1/2}$ 60.55 min) which will migrate from the target. There are limited reports on the development of radiopharmaceuticals with ^{224}Ra or on their applications.

3.3.8 Thorium-227

Thorium-227 is a member of the uranium-235 series (Fig. 3.22) and decays with a half-life of 18.72 days to ^{223}Ac, with emission of gamma photons with energies of 236 KeV (11.2 %) and 50 keV (8.5 %), which can be used for scintigraphic imaging. Small quantities of ^{227}Th can be isolated from ^{235}U and production by neutron activation of ^{226}Ra [^{226}Ra(n,γ)^{227}Ra(β⁻ decay) ^{227}Ac)(β⁻ decay)^{227}Th] in a nuclear reactor has also been reported (Holden et al. 2014). Thorium-227 is of interest for development of therapeutic radiopharmaceuticals. The ^{223}Ra decay daughter described above and used for bone pain palliation and subsequent alpha-emitting daughters might be sequestered in the bone without causing major toxicity to other tissues. Low-dose-rate therapy using the ^{227}Th-labeled monoclonal antibody rituximab was demonstrated to kill lymphoma cells in nude mice bearing human B-lymphoma xenografts (Dahle et al. 2006). Biodistribution studies, normal tissue toxicity, and therapeutic efficacy of the ^{227}Th-trastuzumab monoclonal antibody targeted to HER2-expressing breast cancer xenografts in mice have been reported (Abbas et al. 2012). The tumor uptake reached peak levels of 34 % ID/g (4.6 kBq/g) 3 days after injection of 400 kBq/kg of ^{227}Th-trastuzumab. The ^{223}Ra daughter radionuclide accumulated in the bone and resulted in high absorbed radiation dose (2.9 Gy to tumor and 2.4 Gy to femur). Dose-dependent antitumor effects were observed for dosages of 200, 400, and 600 kBq/kg of ^{227}Th-trastuzumab. No effect was seen with a nonspecific labeled antibody (^{227}Th-rituximab). In the mice studies, ^{227}Th-trastuzumab therapy resulted in a dose-dependent inhibition of breast cancer xenograft growth (Heyerdahl et al. 2013; Abbas et al. 2011).

3.4 Summary: Future Prospects of Alpha Radionuclide Therapy

Alpha radionuclide therapy offers the possibility of delivering very high levels of radiation to targeted sites with relatively low activity levels due to the high alpha-particle LET. With the exception of ^{211}At and ^{149}Tb, the majority of alpha-emitting radionuclides proposed are part of a radioactive decay series. All the alpha-emitting radionuclides identified for alpha radionuclide therapy decay to radioactive daughter products which may exhibit a tendency for migration from the targeted cells to normal cells. However, there are a number of scientific studies demonstrating the utility of alpha radionuclide therapy. The success of targeted alpha therapy (TAT) in terms of therapeutic outcome is influenced by a number of crucial issues including the specificity of the antibody/targeting construct, the level of antigenic expression on the tumor cells, the potential loss of immunoreactivity of the antibody/targeting construct, the amount of unlabeled antibody/targeting construct after injection, the existence of diffusion barriers that hinder the penetration of the antibody/targeting construct into the tumors, the choice of radionuclide (half-life and path length), and the specific radioactivity. While potential of α-particle radiation therapy for the treatment of smaller tumor burdens, micrometastatic disease, and disseminated disease have been amply demonstrated with limited clinical experience, development and growth of this modality of treatment have been principally compromised by economics and limited supply issues. The widespread clinical application of this treatment modality will depend upon the following:

- Availability of therapeutic doses of α-emitting radionuclide at a reasonable cost
- Availability of suitable antibody and suitable linker moiety
- Successful long-term therapy devoid of associated complications such as marrow toxicity, renal damage, etc.
- Efficacy of α-therapy in bulky tumors in addition to minimal disease states and hematologic malignancies

The major impediment for the hopeful further advance of this technology is the limited radionuclide availability at affordable cost. The clinical use of alpha radionuclide therapy represents a very promising approach, especially for the management of cancer. With the introduction of ^{223}Ra for routine clinical use and other technical advances, rapid growth of alpha radionuclide therapy is expected, once the issue of availability and cost is resolved.

References

Abbas N, Heyerdahl H, Bruland OS, et al. Experimental α-particle radioimmunotherapy of breast cancer using ^{227}Th-labeled p-benzyl-DOTA-trastuzumab. EJNMI Research. 2011. http://link.springer.com/article/10.1186/2191-219X-1-18/fulltext.html.

Abbas N, Bruland ØS, Brevik EM, et al. Preclinical evaluation of ^{227}Th-labeled and ^{177}Lu-labeled trastuzumab in mice with HER-2-positive ovarian cancer xenografts. Nucl Med Commun. 2012;33:838–47.

Allen BJ. Future prospects for targeted alpha therapy. Curr Radiopharm. 2011;4(4):336–42.

Apostolidis C, Molinet R, McGinley J, et al. Cyclotron production of Ac-225 for targeted alpha therapy. Appl Radiat Isot. 2005;62:383–7.

Atcher RW, Friedman AM, Hines JJ. An improved generator for the production of ^{212}Pb and ^{212}Bi from Ra. Int J Rad Appl Instrum A. 1988;39:283–6.

Azure MT, Archer RD, Sastry KSR, et al. Biological effect of lead-212 localized in the nucleus of mammalian cells: role of recoil energy in the radiotoxicity of internal alpha-particle emitters biological effect of lead-212 localized in the nucleus of mammalian cells: role of recoil energy in the radiotoxicity of internal alpha-particle emitters. Radiat Res. 1994;140:276–83.

Bardiès M. Dosimetry and microdosimetry of targeted radiotherapy. Curr Pharm Des. 2000;6:1469–502.

Barendsen GW, Koot CJ, Van Kersen GR, et al. The effect of oxygen on impairment of the proliferative capacity of human cells in culture by ionizing radiations of different LET. Int J Radiat Biol Relat Stud Phys Chem Med. 1966;10:317–27.

Bertrand A, Legras B, Martin J. Use of radium-224 in the treatment of ankylosing spondylitis and rheumatoid synovitis. Health Phys. 1978;35:57–60.

Beyer GJ, Comor J, Dakovic M, et al. Production routes of the alpha emitting ^{149}Tb for medical application. Radiochim Acta. 2002;90:247–52.

Beyer GJ, Miederer M, Vranjes-Duric S, et al. Targeted alpha therapy in vivo: direct evidence for single cancer cell kill using ^{149}Tb-rituximab. Eur J Nucl Med Mol Imaging. 2004;31:547–54.

Bolch WE, Eckerman KF, Sgouros G, et al. MIRD pamphlet No. 21: a generalized schema for radiopharmaceutical dosimetry-standardization of nomenclature. J Nucl Med. 2009;50:477–84.

Boll RA, Malkemus D, Mirzadeh S. Production of actinium-225 for alpha particle mediated radioimmunotherapy. Appl Radiat Isot. 2005;62:667–79.

Bomanji JB, Wong W, Gaze MN, Cassoni A, Waddington W, Solano J, Ell PJ. Treatment of neuroendocrine tumours in adults with ^{131}I-MIBG therapy. Clin Oncol. 2003;15:193–8.

Brechbiel MW. Targeted alpha-therapy: past, present, future? Dalton Trans. 2007;2(43):4918–28.

Brown I, Carpenter RN. At a-particle radiotherapy for undifferentiated thyroid cancer. Acta Radiol Suppl. 1991;376:174–5.

Carlin S, Akabani G, Zalutsky MR. In vitro cytotoxicity of (^{211}At)-astatide and (^{131})I-iodide to glioma tumor cells expressing the sodium/iodide symporter. J Nucl Med. 2003;44:1827.

Chappell LL, Deal KA, Dadachova E, et al. Synthesis, conjugation, and radiolabeling of a novel bifunctional chelating agent for ^{225}Ac radioimmunotherapy applications. Bioconjug Chem. 2000;11:510–9.

Chouin N, Bardies M. Alpha-particle microdosimetry. Curr Radiopharm. 2011;4(3):266–80.

Dahle J, Borrebaek J, Melhus KB, et al. Initial evaluation of (^{227})Th-p-benzyl-DOTA-rituximab for low-dose rate alpha-particle radioimmunotherapy. Nucl Med Biol. 2006;33:271–9.

Essler M, Gartner FC, Neff F, et al. Therapeutic efficacy and toxicity of ^{225}Ac-labelled vs. ^{213}Bi-labelled tumour-homing peptides in a preclinical mouse model of peritoneal carcinomatosis. Eur J Nucl Med Mol Imaging. 2012;39:602–12.

Friesen C, Roscher M, Hormann I, et al. Anti-CD33-antibodies labelled with the alpha emitter Bismuth-213 kill CD33-positive acute myeloid leukaemia cells specifically by activation of caspases and break radio- and chemoresistance by inhibition of the anti-apoptotic proteins X-linked inhibitor of apoptosis protein and B-cell lymphoma-extra large. Eur J Cancer. 2013; 49:2542–54.

Goodhead DT. Initial events in the cellular effects of ionizing radiations: clustered damage in DNA. Int J Radiat Biol. 1994;65:7–17.

Hall EJ. Radiobiology for the radiologist. 4th ed. Philadelphia: JB Lippincott Company; 1994.

Hauck ML, Larsen RH, Welsh PC, et al. Cytotoxicity of a-particle emitting 211At-labeled antibody in tumor spheroids: no effect of hyperthermia. Br J Cancer. 1998;77:753.

Henriksen G, Messelt S, Olsen E, Larsen RH. Optimization of cyclotron production parameters for the ^{209}Bi(α,2n)^{211}At reaction related to biomedical use of ^{211}At. Appl Radiat Isot. 2001;54:829–34.

Heyerdahl H, Abbas N, Sponheim K, et al. Targeted alpha therapy with ^{227}Th-trastuzumab of intraperitoneal ovarian cancer in nude mice. Curr Radiopharm. 2013;6(2):106–16.

Holden CS, Schenter RE. Production of actinium-227 and thorium-228 from radium-226 to supply alpha-emitting isotopes radium-223, thorium-227, radium-224, bismuth-212. 2014.US 20140226774. http://www.google.com/patents/US20140226774.

Howell RW, Goddu SM, Narra VR, et al. Radiotoxicity of gadolinium-148 and radium-223 in mouse testes: relative biological effectiveness of alpha-particle emitters in vivo. Radiat Res. 1997;147:342–8.

Humm JL, Cobb LM. Nonuniformity of tumor dose in radioimmunotherapy. J Nucl Med. 1990;31:75–83.

IAEA Technical Report SeriEs 15. A basic toxicity classification of radionuclides. 1963. http://www.iaea.org/inis/collection/NCLCollectionStore/_Public/24/072/24072024.pdf.

IAEA Technical Report Series 468. Cyclotron produced radioisotopes: physical characteristics and production methods. 2009. http://www-pub.iaea.org/MTCD/publications/PDF/trs468_web.pdf.

Jurcic JG. Targeted alpha-particle immunotherapy with bismuth-213 and actinium-225 for acute myeloid leukemia. J Postgrad Med Edu Res. 2013;47(1):14–7.

Jurcic JG, Larson SM, Sgouros G, et al. Targeted alpha particle immunotherapy for myeloid leukemia. Blood. 2002;100:1233–9.

Kennel SJ, Mirzadeh S. Vascular targeted radioimmunotherapy with ^{213}Bi – an alpha-particle emitter. Nucl Med Biol. 1998;25:241–6.

Kennel SJ, Boll R, Stabin M, et al. Radioimmunotherapy of micrometastases in lung with vascular targeted ^{213}Bi. Br J Cancer. 1999;80:175–84.

Kennel SJ, Chappell LL, Dadachova K, et al. Evaluation of ^{225}Ac for vascular targeted radioimmunotherapy of lung tumors. Cancer Biother Radiopharm. 2000;15: 235–44.

Koch L, Apostolidis C, Janssens W, et al. Production of Ac-225 and application of the Bi-213 daughter in cancer therapy. Czech J Phys. 1999;49:817–22.

Lebeda O, Jiran R, Rális J, et al. A new internal target system for production of ^{211}At on the cyclotron U-120M. Appl Radiat Isot. 2005;63:49–53.

Lorimore SA, Kadhim MA, Pocock DA, et al. Chromosomal instability in the descendants of unirradiated surviving cells after alpha-particle irradiation. Proc Natl Acad Sci U S A. 1998;95:5730–3.

Lundh C, Lindencrona U, Schmitt A, et al. Biodistribution of free 211At and 125I- in nude mice bearing tumors derived from anaplastic thyroid carcinoma cell lines. Cancer Biother Radiopharm. 2006;21:591–600.

Macklis RM. The great radium scandal. Sci Am. 1993;269:94–9.

Metting NF, Palayoor ST, Macklis RM. Induction of mutations by bismuth-212 alpha particles at two genetic loci in human B-lymphoblasts. Radiat Res. 1992;132:339–45.

Metzenbaum M. Radium: Its value in the treatment of lupus, rodent ulcer, and epithelioma, with reports of cases. Int Clin (JB Lippincott). 1905;4(14):21–31.

Miederer M, Scheinberg DA, McDevitt MR. Realizing the potential of the Actinium-225 radionuclide generator

in targeted alpha-particle therapy applications. Adv Drug Deliv Rev. 2008;60(12):1371–82.

Montavon G, Le Du A, Champion J, et al. DTPA complexation of bismuth in human blood serum. Dalton Tran. 2012;41(28):8615–23.

Mulford D, Scheinberg DA, Jurcic JG. The promise of targeted α-particle therapy. J Nucl Med. 2005;46(1): 199S–204.

Murud KM, Larsen RH, Bruland OS, Hoff P. Influence of pretreatment with 3-amino-1-hydroxypropylidene-1,1-bisphosphonate (APB) on organ uptake of 211At and I-labeled amidobisphosphonates in mice. Nucl Med Biol. 1999a;26:791–4.

Murud KM, Larsen RH, Hoff P, et al. Synthesis, purification, and in vitro stability of 211At- and 125I-labeled amidobisphosphonates. Nucl Med Biol. 1999b;26: 397–403.

Nicolini M, Mazzi U. Therapeutic potential of alpha-emitters: chemistry to biology to clinical applications. Padova: SGE Editorali; 1999.

Ning L, Jiannan J, Shangwu M, et al. Preparation and preliminary evaluation of astatine-211 labeled IgG via DTPA anhydride. J Radiol Nucl Chem. 1998;227: 187–90.

Parker C, Nilsson S, Heinrich D, et al. Alpha emitter radium-223 and survival in metastatic prostate cancer. N Engl J Med. 2013;369:213–23.

Petrich T, Quintanilla-Martinez L, Korkmaz Z, et al. Effective cancer therapy with the alpha-particle emitter [^{211}At]astatine in a mouse model of genetically modified sodium/iodide symporter-expressing tumors. Clin Cancer Res. 2006;15(12):1342–8.

Pouget JP, Mather SJ. General aspects of the cellular response to low- and high-LET radiation. Eur J Nucl Med. 2001;28:541–61.

Proescher F. The intravenous injection of soluble radium salts in men. Radium. 1913;1:9–10.

Rosenblat TL, McDevitt MR, Mulford DA, et al. Sequential cytarabine and alpha-particle immunotherapy with bismuth-213-lintuzumab (HuM195) for acute myeloid leukemia. Clin Cancer Res. 2010;16:5303–11.

Schales F. Brief history of Ra-224 usage in radiotherapy and radiobiology. Health Phys. 1978;35:25–32.

Schwarz UP, Plascjak P, Beitzel MP, et al. Preparation of ^{211}At labeled humanized anti-tac using ^{211}At produced in disposable internal and external bismuth targets. Nucl Med Biol. 1998;25:89–93.

Sgouros G, Finn RD, Humm JL. Radioimmunotherapy with alpha-emitting nuclides. Eur J Nucl Med. 1998;25(9):1341–51.

Sgouros G, Roeske JC, McDevitt MR, et al. SNM MIRD Committee, Bolch WE, Brill AB, Fisher DR, Howell RW, Meredith RF, Sgouros G, Wessels BW, Zanzonico PB. MIRD Pamphlet No. 22 (abridged): radiobiology and dosimetry of alpha-particle emitters for targeted radionuclide therapy. J Nucl Med. 2010;51:311–28.

Sgouros G, Hobbs RF, Song H. Modelling and dosimetry for alpha-particle therapy. Curr Radiopharm. 2011;4(3):261–5.

Song H, Hobbs RF, Vajravelu R, et al. Radioimmunotherapy of breast cancer metastases with alpha-particle emitter ^{225}Ac: comparing efficacy with ^{213}Bi and ^{90}Y. Cancer Res. 2009;69:8941–8.

Vaidyanathan G, Zalutsky MR. Astatine radiopharmaceuticals: prospects and problems. Curr Radiopharm. 2008;1:177–96.

Vaidyanathan G, Strickland DK, Zalutsky MR. Meta-[^{211}At] astatobenzylguanidine: further evaluation of a potential therapeutic agent. Int J Cancer. 1994;15(57):908–13.

Vaidyanathan G, Affleck D, Welsh P, et al. Radioiodination and astatination of octreotide by conjugation labelling. Nucl Med Biol. 2000;27:329–37.

Vaidyanathan G, Boskovitz A, Shankar S, et al. Radioiodine and 211At-labeled guanidinomethyl halobenzoyl octreotate conjugates: potential peptide radiotherapeutics for somatostatin receptor-positive cancers. Peptides. 2004;25(12):2087–97.

Visser GWM, Diemer EL, Vo CM, et al. The biological behaviour of some organic astatine compounds in rats. Int J Appl Radiat Isot. 1981;32:913–7.

Wang H, Liu S, Zhang P, Zhang S, Naidu M, Wang Y. S-phase cells are more sensitive to high-linear energy transfer radiation. Int J Radiat Oncol Biol Phys. 2009;74:1236–41.

Wessels BW, Rogus RD. Radionuclide selection and model absorbed dose calculations for radiolabeled tumor associated antigens. Med Phys. 1984;11:638–45.

Zalutsky MR, Narula AS. Astatination of proteins using an N-succinimidyl tri-n-butylstannyl benzoate intermediate. Int J Rad Appl Instrum A. 1988;39:227–32.

Zalutsky MR, Pruszynski M. Astatine-211 Production and availability. Curr Radiopharm. 2011;4:177–85.

Zalutsky MR, Vaidyanathan G. Astatine-211-labeled radiotherapeutics: an emerging approach to targeted alpha-particle radiotherapy. Curr Pharm Des. 2000;6(14):1433–55.

Zalutsky MR, Reardon DA, Akabani G, et al. Clinical experience with α-particle–emitting ^{211}At: treatment of recurrent brain tumor patients with ^{211}At-labeled chimeric antitenascin monoclonal antibody 81C6. J Nucl Med. 2008;49:30–8.

Auger Electron-Based Radionuclide Therapy

4

4.1 Introduction: Cancer Treatment with Radioisotopes

The potential use of Auger emitters for cancer therapy is important, since these radioisotopes decay with emission of Auger electrons which deposit very high energy over very short distances. In this manner, the use of selected Auger emitters conceptually represents an important alternative to the use of alpha-emitting and beta-emitting radioisotopes for cancer therapy. Interest in the use of Auger-emitting radioisotopes for cancer therapy is continually increasing partly because of the development of complementary targeting technologies for cell-specific delivery. However, an important which must also be addressed is the availability of the required Auger emitters.

The common treatment of cancerous tumors that cannot be surgically removed usually involves chemotherapy and external beam irradiation. When access is possible, sealed radioactive sources administered by a radiation oncologist ("brachytherapy") is another major treatment option. An additional approach employs the use of radiopharmaceutical agents labeled with unsealed radioactive sources ("radiopharmaceuticals") as discussed earlier in Chap. 1. In this technology for cancer therapy, for instance, therapeutic radioisotopes are attached to targeting molecules designed for site-specific tumor cell binding. These agents are injected intravenously and thus act as carriers for targeting of the therapeutic radioisotopes to cancer cells. The use of therapeutic radioisotopes in this manner can minimize many of the side effects encountered with many traditional treatment methods. This unique opportunity for site-specific targeting of cancer cells for therapy represents a major clinical weapon for the treatment of cancer. Specifically targeted antibodies for treatment of non-Hodgkin lymphoma cancer radiolabeled with the yttrium-90 (Zevalin®) and iodine-131 (Bexxar®) beta-emitting radioisotopes had been approved as the first agents for routine clinical use by the US Food and Drug Administration (FDA).

4.2 Particle Emission

The identification of the type of radiation or radioisotope best suited for treatment of a neoplasia is dependent upon a number of factors, which include the type of cancer, its staging, the size of the treatment area, the depth of radiation penetration required, and the location of the cellular sites for binding of the radioactive targeting agents. Traditionally, the use of high-energy beta-particle-emitting radioisotopes such as ^{90}Y, for instance, has permitted deep penetration (millimeters) into solid tumors and utilization of the effects of "cross fire" for the irradiation of target cells which may be even millimeters distant from the binding site (Table 4.1). The use of high penetration permits energy deposition to kill cells to

F.F. (Russ) Knapp, A. Dash, *Radiopharmaceuticals for Therapy*, DOI 10.1007/978-81-322-2607-9_4

Table 4.1 Comparison of relative maximal soft tissue penetration and energy deposition of high-energy beta particles, alpha particles, and Auger electrons used in cancer therapy

Type of particle emission	Example of radioisotope	Energy of emission	Approximate soft tissue penetration
Beta particle (β)	Yttrium-90	2 MeV	10 mm
Alpha particle (α)	Bismuth-213	8 MeV	4–5 cell diameters
Auger electron (AE)	Indium-111	<eV	Confined within single cell

which the targeting molecule may not bind (i.e., "cross fire"), but normal cells can also receive damaging levels of radiation. This can often be important because of the cellular heterogeneity of solid tumors, where normal cells and cancer cells are intermingled. However, at least theoretically, the possible therapeutic use of Auger emitters has at least theoretically many advantages in comparison to beta- and alpha-emitting radioisotopes (Behr et al. 2000; Humm et al. 1994; Sastry 1992).

4.3 The Auger Process

When radionuclides decay by electron capture (EC), e.g., ^{55}Fe, or by internal conversion (IC), e.g., ^{195m}Pt, a vacancy is created in the inner atomic shell of the residual atom. Subsequently, the excited atom undergoes a series of radiative and non-radiative transitions until the ground state of the atom is reached. Radiative transitions predominate for K-shell vacancies and result in the emission of a characteristic X-ray (see Fig. 4.1). Although there are a variety of non-radiative transitions, the most common are the Auger, Coster–Kronig (CK), and super Coster–Kronig (super CK) transitions as shown in Fig. 4.1. Non-radiative transitions are highly probable when the vacancy lies beyond the L-shell. In an Auger transition, an initial electron vacancy in a lower shell is filled by an electron from a higher shell and another electron is ejected from a higher shell. While CK transitions are similar, the electron that fills the vacancy originates from the same shell and the ejected electron is from a higher shell. In super CK transitions, the initial vacancy and the two electrons are all in the same shell. Radiative transitions move the electron vacancy to a higher shell with no change in the number of vacancies; with nonradiative transitions, the number of vacancies increases by one. As the innermost vacancy percolates towards the valence shell, a cascade phenomenon develops with corresponding vacancy multiplication and emission of numerous low-energy electrons, collectively referred to as Auger electrons. Most of the electrons have very low energies (less than a few hundred eV), intermediate values of linear energy transfer (10–25 keV μm^{-1}), and extremely short ranges (several nm) in biological matter. Since this electron cascade process is completed with ~10–15 s, the region in the immediate vicinity of the atom is showered with Auger electrons and, as a consequence, very high local energy densities are realized. It is this intense and localized energy deposition which we wish to exploit as an approach for cancer therapy.

4.4 Cell Killing with Auger Electron Emitters

In contrast to the use of high-energy beta particles, the high linear energy transfer (LET) alpha particles and Auger electrons have significantly lower soft tissue penetration (Table 4.1) and thus deposit all their energy in much shorter distances (microns or less). For this reason, the necessity of specific cancer cell targeting is much more important. If most of the tumor cells are accessible, carrier molecules labeled with alpha- and Auger electron-emitting radioisotopes can thus be targeted for transport within the target tumor cells or ideally to the target cell nucleus. In this manner, the limited range of these high LET emissions can be effectively used for cell killing. In this context, the optimal therapeutic approach for cancer therapy using unsealed radioactive sources which target tumor cells is the use of low LET beta-emitting radioisotopes for the treatment

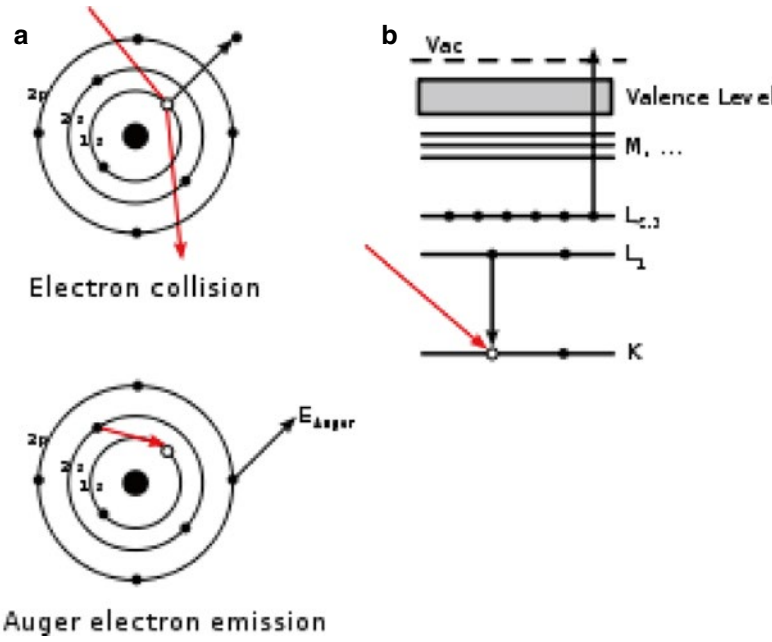

Fig. 4.1 Representation of the Auger cascade process

of the large (primary) tumor masses combined with the use of high LET (alpha or Auger) radioisotopes for therapy of small, cellular cluster metastatic sites. As an example, only recently, the internalization of peptides which specifically bind to receptors on cancer cells has been established, thus providing an effective targeting tool for delivery of these high LET radioisotopes. A commercially available octreotide analog, "Octreoscan" (^{111}In-Pentetreotide; Phe-D-octreotide), is used for somatostatin receptor scintigraph for the detection and localization of primary tumors and metastatic spread which are often missed by conventional imaging modalities (Krenning et al. 1996). Such octreotide analogs are known to internalized within the cell after binding to receptors expressed on the cell surface, and moreover, the therapeutic efficacy of In-111-Pentreotide has been demonstrated in high-dose studies, demonstrating the therapeutic effectiveness of intracellular Auger electron emission in both animal tumors models (de Jong et al. 1998) and in human tumors in vivo (Krenning et al. 1996), since ^{111}In decays with the emission of 34 KeV Auger electrons (Average Energy). It is important to note in this context that ^{111}In-labeled octreotate does not localize in the cell nucleus but remains in the cytoplasmic compartment after internalization. This observation would indicate that cytoplasmic targeting of radiopharmaceuticals labeled with Auger emitters can be therapeutically effective and that nuclear targeting is always not the key. However, ^{111}In may be impractical for routine clinical therapy because of its limited availability and very high production costs (Fig. 4.2).

This observation of the successful intracellular targeting of radiolabeled peptide is an important observation, and the use of Auger-emitting radioisotopes could thus be an attractive future widespread approach for tumor therapy. The ability to target radiolabeled peptides or other molecules to the cell interior suggests the important use of Auger electron-emitting radioisotopes for therapy. Just as clinical applications of alpha-emitting radioisotopes (Chap. 3) such as ^{225}Ac, ^{213}Bi, and ^{223}Ra have been demonstrated for the specific application for localized sterilization of small clusters of cancer cells, the next stage of development would be the expected use of Auger electron emitters for targeting of single cells to augment the use of lower LET radioisotopes and other strategies for cancer therapy.

An understanding of the transport of low-energy electrons in soft tissue is also an important

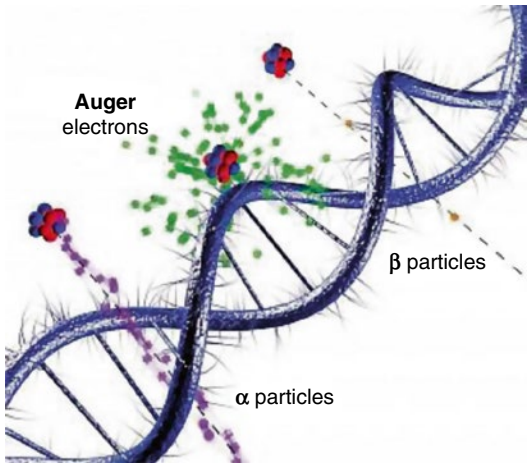

Fig. 4.2 Illustration of the relative interaction of Auger electrons with the double helix of the DNA molecule, in comparison with alpha (α) and beta (β) particles (Taken from Web site of, Department of Nuclear Physics Research School of Physics & Engineering ANU College of Physical & Mathematical Sciences)

issue for dose planning, safety concerns, and relating targeting with therapy response. There is broad interest from dosimetric, therapeutic, and clinical perspectives regarding the use of Auger-emitting radioisotopes coupled to specific cellular/nuclear targeting vectors for cancer therapy. The highest radiobiological effectiveness (RBE) results when Auger emitters are incorporated into the highly radiosensitive cell nucleus (Daghighian et al. 1996). Results of studies with the Auger electron-emitting radioisotope ^{125}I clearly demonstrate the severe radiotoxicity when a ^{125}I-labeled nucleic acid precursor (e.g., 5-^{125}I-iododeoxyuridine, a thymidine analog) is incorporated into the DNA of proliferating cells (Kassis et al. 1987). These studies have demonstrated the important potential for the use of Auger electron emitters for the treatment of cancer. However, while the use of the ^{125}I continues to be of importance for basic studies, this radioisotope is impractical for clinical use. There are thus a limited number of Auger emitters which can be practically produced and have the appropriate decay and chemical properties. As summarized in Table 4.2, only a few Auger emitters are probably of practical importance for clinical applications, and examples can be either reactor or accelerator produced. Two key reactor-produced Auger emitters of current interest are platinum-195*m* (^{195m}Pt) and rhodium-103*m* (^{103m}Rh). The number of Auger electrons emitted per each radioactive disintegration (*Ne/Nt*) is very high for ^{195m}Pt. The high auger yield from decay of ^{103m}Rh coupled with its carrier-free availability from a generator system and its well-known chelate chemistry—required for attachment to cancer cell targeting molecules—make this a key candidate for further studies. As the case for all targeted radiopharmaceuticals, a key challenge is the effective high-specific-activity radiolabeling required for targeting molecules to evaluate the potential effectiveness of such agents.

4.5 The Importance of Auger Electron-Emitting Radionuclides for Cancer Therapy

It is well recognized that the use of Auger-emitting radioisotopes is expected to be a new advance for cancer therapy, using peptides and other tumor cell targeting agents which are labeled with Auger-emitting radioisotopes. The development of new cancer therapeutic approaches using Auger emitters would be expected to be of enormous benefit to the population of patients who require this therapy. Over 1.2 million patients were diagnosed with cancers in 1999 (US Department of Human Health Services 2000). Approximately 50 % of these patients are projected to receive radiation therapy (American Cancer Society 1996). In addition to these therapeutic treatments, an estimated 10–12 million nuclear medicine imaging and therapy procedures are performed annually in the USA (Society of Nuclear Medicine 2000). A key issue which is required is the development and optimization of production and processing technologies to provide sufficient activity levels of candidate Auger-emitting radioisotopes for cell-targeted ablation therapy and development of required dosimetry models for calculation of localized dose delivery. There are really only a few practical examples

Table 4.2 Key examples of radioisotopes emitting secondary electrons that have potential applications for intracellular auger therapy

Radionuclide	production	Half-life	Emission	keV	<e> (keV)	Ne/Nt	Eγ (Iγ) keV (%)	Daughter radioisotope
^{103}Ru	R	39.4 days	*β*	763	41.7	NA	497 (86.4)	^{103m}Rh (56.1 m)
^{103}Pd	R, A	17.0 days	*EC*	546	42.5	NA	357 (0.02)	^{103m}Rh (56.1 m)
^{103m}Rh	R	56.1 m	*IT*	43	37.5	5.71	40 (0.07)	^{103}Rh (stable)
^{111}In	A	2.8 days	*EC*	850	33.9	7.2	171.3 (90.2) 254.4 (94.0)	^{111}Cd (stable)
^{123}I	A	13.2 h	*EC*	1200	27.6	13.7	159 (83.3)	^{123}Te (1.3×10^{13} years)
^{125}I	R	60.3 days	*EC*	178	17.9	22.9	35 (6.7)	^{125}Te (stable)
^{161}Ho	A	2.48 h	*EC*	25.7	…			^{161}Dy (stable)
^{193m}Pt	R	4.33 days	*IT*	150	130	21.8	135 (0.11)	^{193}Pt (50 years)
^{195m}Pt	R	4.02	*IT*	260	175	35.9	99 (11.4)	^{195}Pt(stable)
^{193m}Hg	A	1.73 days	*IT* (54 %) *EC* (46 %)	176 1520	139.6	NA	262 (32.4) 560 (7.5)	^{195}Hg (9.5 h)
^{195}Hg	A	9.5 h	*EC*	1520	61.3	NA	780 (7.0)	^{195}Ag (185 days)
^{197m}Hg	A	23.8 h	*IT* (93 %) *EC* (7 %)	299 600	214	NA	140 (34)	^{197}Hg (2.67 days)
^{197}Hg	A	2.67 days	*EC*	600	57	NA	191 (0.61)	^{197}Au (stable)

Secondary electrons refer to both Auger and conversion electrons; primary emissions = 100 %, unless noted
Q decay energy, <*e*> average electron energy, *Eγ (Iγ)* photon energy, *Ne/Nt* number of electrons emitted per disintegration, *R* reactor-produced, *A* accelerator produced, *NA* data not available

of Auger-emitting radioisotopes which would be expected to be clinically relevant using unsealed targeted radiopharmaceutical sources.

4.6 Key Auger Emitters

4.6.1 Iodine-125

The production and use of ^{125}I for a variety of clinical applications used primarily in brachytherapy sources for treatment of cancer of the eye, prostate, breast, etc., has been widely published. In the context of sealed sources, ^{125}I continues to play a key role for therapy. The production and processing of ^{125}I has also been widely reviewed in the literature. However, Auger emitter is generally not suited for use for traditional therapeutic targeting with unsealed radiopharmaceuticals. Nonetheless, many of the radionuclidic and therapeutic strategies which have been studied and postulated over the last decades for Auger-emitting radioisotopes have been developed using ^{125}I (Makrigiorgos et al. 1990a, b; Adelstein and Kassis 1987). The reactor production of ^{125}I is described in detail in Chap. 5.

4.6.2 Platinum-195m

As a key example because of its potent Auger yield, ^{195m}Pt is of widespread interest for biokinetic and metabolic studies of important platinum-based antitumor drugs and evaluation as a therapeutic radioisotope for Auger electron therapy. Several reactor production pathways have been evaluated (Mirzadeh et al. 1997), and reactor production by the traditional "direct" ^{194}Pt(n,γ)^{195m}Pt route produces only low specific activity ^{195m}Pt (~1 mCi/mg), and accelerator production results in only very low yields, but an "indirect" production method by the ^{194}Ir(n,γ)^{195m}Ir(β$^-\rightarrow$)^{195m}Pt may be amendable to provide much higher specific activity ^{195m}Pt from decay of reactor-produced iridium-195*m* (^{195m}Ir) with

estimated values of 50–100 mCi/mg. There continues to be interest in the potential use of ^{195m}Pt as a tracer for studies of the biokinetics and mechanism of action of important such as the widely clinically used cis-dichlorodiammineplatinum(II) ("cis-platinum"—"cis-DDP"), carboplatinum, and other platinum-based antitumor agents. The use of ^{195m}Pt for both biokinetic studies of platinum-based antitumor agents and for possible intracellular therapy, however, requires much higher specific activity than is currently available (~1 mCi/mg).

The estimated energy deposited from Auger electrons emitted from ^{195m}Pt in a 5 nm diameter spheroid is 2000 eV, while similar values are only 1000 and 450 eV for ^{125}I and ^{111}In, two other Auger electron emitters which are of interest for Auger therapy (Mariani et al. 2000). Platinum-195m has been widely discussed for potential cancer therapy if sufficient activity would be available with the required specific activity (Willins and Sgouros 1995; Mariani et al. 2000) if the appropriate carrier/targeting vectors were available for intracellular and presumably intranuclear targeting.

The expected importance of the potential use of ^{195m}Pt for Auger therapy has been described by Mariani, et al. (2000) since ^{195m}Pt exhibits the highest Auger electron yield and the energy levels which are deposited per decay in a 5-nm sphere are much higher than most other Auger emitters which may be useful for therapeutic applications. However, high activity levels of high-specific-activity ^{195m}Pt are not yet available, and the traditional and well established "direct" production of ^{195m}Pt by neutron irradiation of enriched ^{194}Pt by the ^{194}Pt(n,γ)^{195m}Pt provides ^{195m}Pt, even at very high thermal neutron flux (Hoeschele et al. 1979; Hoeschele 1980; Hoeschele et al. 1982), with specific activity values ≈<1 mCi/mg Pt, which are far too low for any practical used for human targeted therapy. An alternative ^{195}Pt(n,n',γ)^{195m}Pt "inelastic" route has also been evaluated to potentially provide higher specific activity, and although the yield from the (n, n′) neutron scattering reaction is higher than for the (n, γ) route, the relative specific activity gain increases only by a factor of about 1.4. The availability of much higher specific activity ^{195m}Pt is important; the expected usefulness of ^{195m}Pt-labeled agents can be assessed of for Auger therapy.

Production of higher specific activity (>100 μCi/μg) of ^{195m}Pt involves the ^{194}Ir(n,γ)^{195m}Ir(β$^-$ →)^{195m}Pt irradiation route and subsequent processing and separation from reactor-irradiated enriched iridium-193 (^{193}Ir) targets. Elution from an AG-50 W column with a mixture of HCl/thiourea (0.1–1.0 M HCl/0.1–0.2 M thiourea) effectively removes iridium, and platinum can then be eluted with the HCl solution without thiourea. This approach offers for the first time the availability of no-carrier-added ^{195m}Pt radioisotope in the 50–100 μCi/μg range for high-specific-activity radiolabeling of targeted-internalized peptides and evaluation as an important therapeutic Auger-emitting radioisotope for tumor therapy. Methods for accelerator production of carrier-free ^{195m}Pt have been unsuccessful (L. Mausner, *personal communication*).

The principal source of high LET Auger electrons from the decay of ^{195m}Pt are from the 99.9 % conversion of the 135 keV γ-rays, which follow the metastable decay of ^{195m}Pt, which results in very high radiotoxicity. The dose imparted by a number of Auger emitters has recently been examined and ^{195m}Pt delivers a significantly higher dose rate when this Auger electron emitter is internalized within the cell than with ^{123}I, ^{125}I, and ^{131}I (Daghighian et al. 1996; Willins and Sgouros 1995). The properties of several key Auger electron emitters are summarized in Table 4.2, and no-carrier-added ^{195m}Pt and ^{103m}Rh are available via decay of reactor-produced ^{195m}Ir and ^{103}Ru, respectively.

4.6.3 Rhodium-103m

Rhodium-103m (^{103m}Rh, $t_{1/2}$ 56 m) is another attractive Auger emitter, if rapid in vivo targeting is possible, and can be conveniently extracted with carbon tetrachloride on a batch basis from reactor-produced ^{103}Ru ($t_{1/2}$ 45 days) (Epperson et al. 1976; Wenzel and Wu 1987; Szucs et al.

2009; van Rooyen et al. 2008). Rhodium-103*m* is of interest for use in radioimmunotherapy due to its attractive decay properties (See Table 4.2 and Chap. 7) and availability from the proposed ^{103}Ru/^{103m}Rh generator system. The availability of ^{103m}Rh from a long-lived generator is of interest as another alternative strategy to provide an Auger emitter on demand for potential therapeutic applications. The ruthenium-103/rhodium-103m (^{103}Ru/^{103m}Rh) radionuclide generator system provides carrier-free ^{103m}Rh for Auger therapy and has been briefly described in the literature (Skarnemark et al. 2009). Other investigators have also identified ^{103m}Rh as a key Auger emitter for targeted radiotherapy (Bernhardt et al. 2001). The 40 keV isomeric decay energy is totally converted in the electronic shells of the stable ^{103}Rh daughter with no measurable γ-rays and results in a "shower" of low-energy electrons and X-rays. The ^{103m}Rh decays from the ^{103}Ru via ^{103}Pd ($t_{1/2}$ 17 days) and the use of reactor-produced ^{103}Pd has been suggested as much more efficient than use of ^{235}U fission to obtain ^{103}Ru for use in the ^{103}Ru/^{103m}Rh generator to obtain ^{103m}Rh for potential therapy (Skarnemark et al. 2009). Despite the promising therapeutic properties of ^{103m}Rh and its proposed availability from a radionuclide generator system, studies on the availability and use of this Auger emitter have evidently not been further pursued. Details of the availability of rhodium-103m from the ^{103}Rh/^{103m}Rh generator system are described in Chap. 7.

4.6.4 Holmium-161

As discussed earlier, there are only a few Auger electron emitters which appear, at least at the current time, to be practical for therapeutic use, primarily because of availability and chemical and radiochemical properties. Since it is a lanthanide, holmium-161 (^{161}Ho) is another example which has been discussed in the recent literature (Uusijaervi et al. 2006; Bernhardt et al. 2001). One production route involves bombardment of dysprosium foil by 11.6 MeV protons. Although the separation and chemistry were not described in detail, the authors suggest that clinically useful quantities of the nuclide are easily produced with a medical cyclotron.

4.7 Dosimetry

The biological effects of Auger electron-emitting radionuclides can be as severe as those of alpha-emitting radionuclides of noted high LET. The dense shower of short-range Auger electrons is released by radionuclides which decay by electron capture (EC) or internal conversion. These Auger electrons can result in severe biological damage that is highly dependent on the location of the decay site within the cell. Various in vitro and in vivo radiobiological studies with Auger emitters have demonstrated that the radiological risk associated with internal exposure to Auger electron emitters may have been underestimated and therefore may require reappraisal (Howell et al. 1991; Gaulden 1983; Hendee 1983; Rao et al. 1983; Pomplun et al. 1987; Makrigiorgos et al. 1990a, b; Adelstein et al. 1986). In addition, Auger electron emitters may serve as precision radiobiological tools to elucidate the primary radiosensitive targets in the cell (Rao et al. 1990; Yasui and Hofer 1986; Yasui et al. 1985; Narra et al. 1994; Hofer et al. 1992). Furthermore, radiolabeled compounds that target DNA are expected be very useful for cancer therapy when Auger emitters are employed (Behr et al. 2000). Although some effort has thus been expended to improve the calculations of the absorbed dose quantity, neither the International Commission on Radiological Protection (ICRP) nor the Medical Internal Radiation Dose (MIRD) Committee of the Society of Nuclear Medicine have yet addressed the Auger electron cascade. The components of any dose calculation, regardless of the spatial dimension of the problem, include the radiation spectra of the radionuclide, the energy loss characteristics of the emitted radiations, and the biological uptake and clearance patters of the radiochemical. The physical half-life of the radionuclide, characteristics of the emitted radiations, and interaction properties of the radiation with matter are the physical information required for dosimetry calculation, whereas the

Table 4.3 Expected Auger electrons per nuclear transformation

Radioisotope	*N*(/nt)
Rhodium-103*m*	5.71
Indium-111	7.20
Iodine-123	13.7
Iodine-125	22.9
Neodymium-149	0.967
Osmium-191	7.91
Platinum-193*m*	21.8
Platinum-195*m*	35.9

biological information required is the biokinetic data.

4.7.1 Electron Transport Evaluation and Dosimetry Assessment

Although not yet well understood, an understanding of the mechanisms of how electrons are transported is of fundamental importance for assessing the potential efficacy of using Auger therapy for cancer treatment. Modeling of the electron transport process on multiprocessor platforms in order to achieve high parallel efficiency is a significant computational challenge. Existing computer models such as the Monte Carlo N-Particle Program (MCNP) are generally used for analysis for dose calculations. However, opportunities exist to extend the MCNP energy thresholds as low as 1 keV, which is required for Auger emitters, since this energy range is not yet adequately modeled, which need production of electron cross-section data in this low-energy range. Some of the questions which must be assessed include the energy deposition and expected biological consequences for localization of the Auger emitters of interest on the cell surface, homogeneously within the cell cytoplasm, on the nuclear membrane, or homogeneously distributed within the nucleus (Table 4.3).

4.7.2 Auger Electron Spectra

In view of the importance of Auger electrons in causing biological damage, a number of early efforts have been made to calculate the Auger electron spectra for radionuclides decaying by EC and IC. ORNL's EDISTR code (Dillman 1980) has been used by the MIRD Committee (Weber et al. 1989) and the ICRP (1983) in publications of the radiation spectra for radionuclides. These compilations include Auger electron yields and energies. Although the theoretical Auger electron spectra presented EDISTR provide useful input into the dosimetry evaluation, these publications had not addressed the N- and O-shell Auger electrons which have a significant contribution to high local energy deposition in the immediate vicinity of the decay site. Realizing this inadequacy, as well as the increasing interest in therapeutic application of Auger emitters, investigators (Endo et al. 2003) had initiated an effort to extend EDISTR's treatment of Auger cascades. In addition, updates on electron-binding energies contained in the Evaluated Atomic Data Library (Cullen et al. 1997), and adoption of the methods of the computer code RELAX (Cullen 1992) in the calculations of the atomic spectra have been reported.

4.7.3 Energy Loss by Auger Electrons

A variety of techniques have been employed for determining the energy deposited in target regions by low-energy Auger electrons. For dimension ranging from nanometers to micrometers, some investigators (Sastry et al. 1988; Howell et al. 1991) have used the electron-range relations for unit density matter of (Cole 1969) which is based on a fit to experimental data for electron energies ranging from 20 eV to 2 MeV as defined by the formula $E(R) = 5.9(R + 0.007)^{0.565} + 0.00413R^{1.33} - 0.367$, where E is the electron energy in keV and R is the electron range in μm in unit-density matter. Differentiation of this equation results in the stopping power relationship for the electrons $dE/dR = 3.33(R + 0.007)^{-0.435} + 0.0055R^{0.33}$. Howell et al. have noted that the fit is poor for energies less than 0.4 keV and suggest the use of the following expression for electron energies between 0.06 and 0.4 keV:

$$\frac{dE}{dR} = 29.5 - 666.67R \tag{4.1}$$

For electrons less than 0.06 keV, the following expression is recommended:

$$\frac{dE}{dR} = 10.5 + 1126R - 9.252\times10^{5}R^{2} + 2.593\times10^{8}R^{3} + 4.964\times10^{10}R^{4} \tag{4.2}$$

These expressions may be appropriately used to compute the absorbed dose to various target volumes. The absorbed dose as a function of distance R, $D(R)$, from the point source, is given by Eq. 4.3, where ρ is the density of the matter:

$$D(R) = \frac{1}{4\pi R^{2}\rho}\frac{dE}{dR} \tag{4.3}$$

An alternative approach to obtain the energy deposition for Auger electrons is to use Monte Carlo track-structure calculations which model the entire stochastic process of electron interactions with matter. There are currently several electron track-structure codes which follow electron slowing down processes to energy of 10 eV and below (Paretske 1987; Terriisol et al. 1978; Zaider et al. 1983; Wright et al. 1990). These codes enable the user to monitor the spatial coordinates of each interaction, together with the energy deposition at each interaction. However, the more practical energy loss expressions above have been shown by Ssatry et al. (1988) to provide reasonably accurate estimate of the average energy deposited by Auger emitters even down to nanometers volumes.

4.7.4 Dosimetry Issues

The highly localized energy deposition in the immediate vicinity of the decay site raises questions as to how the absorbed dose should be calculated for Auger electrons, and there are a number of issues which must be resolved before the hopeful use of Auger emitters can move into the clinical arena. These include an evaluation of how important the differences are in various calculated Auger electron spectra and if the modifications implemented in the updated EDISTR code are adequate. In addition, the adequacy of calculations of the expected energies and intensities of the Auger electrons must be assessed if a full stochastic simulation of the atomic de-excitation is required. Finally, it must be determined if the applicable target volumes be known to enable a meaningful relationship between absorbed dose and the radiotoxicity of internal Auger emitters.

4.8 Summary

In spite of the tremendous interest and extensive experimental and theoretical efforts to understand the Auger process and the biological effects of these emissions with a few Auger-emitting radioisotopes, primarily with ^{125}I, these radioisotopes have not yet entered the routine clinical arena. It is to note that although the basis of the intense biological effectiveness is focused on the direct radiation and irreversible DNA damage, the therapeutic effect of the ^{111}In Auger emitter by administration of ^{111}In octreotide peptide has been widely described, in spite of the nontargeting of the nucleus with this agent. It would appear that there also exist some indirect "bystander"-type effects which may explain at least some of the therapeutic effects of Auger emitters which are not yet fully understood.

References

Adelstein S, Kassis AI. Radiobiological implications of the macroscopic distribution of energy from radionuclides. Nucl Med Biol. 1987;14:165.

Adelstein SJ, Kassis AI, Sastry KSR. Cellular vs. organ approaches to dose estimates. In: Schlafke-Stellson AT, Watson EE, editors. Proceedings of fourth international radiopharmaceutical dosimetry symposium. Springfield: NTS; 1986.

American Cancer Society. 1996. http://www.cancer.org/.

Behr TM, Behe M, Lohr M, et al. Therapeutic advantages of Auger electron- over β-emitting radionuclides or radioiodine when conjugated to internalizing antibodies. Eur J Nucl Med. 2000;27:753–65.

Bernhardt P, Forssell-Aronsson E, Jacobsson L, et al. Low-energy electron emitters for targeted radiotherapy of small tumours. Acta Oncol. 2001;40(5):602–8.

Cole A. Absorption of 20 eV to 50,000 eV electron beams in air and plastic. Radiat Res. 1969;38:7–33.

Cullen DE. Program RELAX: a code designed to calculate atomic relaxation spectra of x-rays and electrons. UCRL-ID-110438. 1992.

Cullen DE, Hubbell JH, Kissel L. EPDL97: the evaluated photon date library'97 version. UCRL-50400, vol. 6 (Rev. 5). 1997.

Daghighian F, Barendswaard E, Welt S, et al. Enhancement of radiation dose to the nucleus by vesicular internalization of ^{125}I-A33 Mab. J Nucl Med. 1996;37:1052.

de Jong M, Breeman WA, Bakker WH, et al. Comparison of ^{111}In-labeled somatostatin analogues for tumor scintigraphy and radionuclide therapy. Cancer Res. 1998; 58:437–41.

Dillman LT. EDISTR- A computer program to obtain a nuclear decay data base for radiation dosimetry. ORNL-TM-6689. 1980.

Endo A, Yamaguchi Y, Eckerman KF. Development and assessment of new radioactive decay database used for dosimetry calculation. Radiat Prot Dosimetry. 2003; 105(1-4):565–9.

Epperson CE, Landolt RR, Kessler WV. Solvent-solvent extraction of rhodium-103m from ruthenium-103 employing a sulfate-carbon tetrachloride medium. Anal Chem. 1976;48(7):979–81.

Gaulden ME. Biological dosimetry of radionuclides and radiation hazards. J Nucl Med. 1983;24(2):160–4.

Hendee WR. Particulate radiations emitted during electron capture and isomeric transitions. J Nucl Med. 1983;24(12):1192–3.

Hoeschele JD. Correlations of Physico-Chemical and Biological Properties with *In Vivo* Biodistribution Data for Platinum-195*m*-Labeled Chloroammineplatinum(II) Complexes. In: Martell AE, editor. Inorganic Chemistry in Biology and Medicine. ACS symposium series, vol. 140. American Chemical Society; 1980. p. 181–208.

Hoeschele JD, Butler TA, Roberts JA. Microscale Synthesis and Biodistribution of Pt-195-Labeled *Cis-Dichlorodiammineplatinum*(II), *Cis*-DDP. In: Proceedings, Radiopharmaceuticals II: Second International Symposium on radiopharmaceuticals, Society of Nuclear Medicine. American Chemical Society; 1979. p. 173–82.

Hoeschele JD, Butler TA, Roberts JA, Guyer CE. Analysis and refinement of the microsysnthesis of the ^{195m}Pt *cis-DDP*. Radiochim Acta. 1982;31:27.

Hofer KG, van Loon N, Schneiderman MH, et al. The paradoxical nature of DNA damage and cell death induced by ^{125}I decay. Radiat Res. 1992;130:121–4.

Howell RW, Rao DV, Hou DY, et al. The question of relative biological effectiveness and quality factor for Auger emitters incorporated into proliferating mammalian cells. Radiat Res. 1991;128:282–92.

Humm JL, Howell RW, Rao DV. Dosimetry of Auger-electron-emitting radionuclides: Report No. 3 of AAPM Nuclear Medicine Task Group No. 6. Med Phys. 1994;21:1901–15.

ICRP. Radionuclide transformations, publication 38. International commission on radiological protection. Oxford: Pergamon; 1983.

Kassis AI, Sastry KS, Adelstein SJ. Kinetics of uptake, retention, and radiotoxicity of 125IUdR in mammalian cells: implications of localized energy deposition by Auger processes. Radiat Res. 1987;109(1): 78–89.

Krenning EP, Kooij PP, Pauwels S, et al. Somatostatin receptor: scintigraphy and radionuclide therapy. Digestion. 1996;57(Suppl 1):57–61.

Makrigiorgos GM, Adelstein SJ, Kassis AI. Cellular radiation dosimetry and its implications for estimation of radiation risks. Illustrative results with technetium 99m-labeled microspheres and macroaggregates. JAMA. 1990a;264:592–5.

Makrigiorgos G, Adelstein SJ, Kassis AI. Auger electron emitters: insights gained from in vitro experiments. Radiat Environ Biophys. 1990b;29:75–91.

Mariani G, Bodei L, Adelstein SJ, Kassis AI. Merging roles of radiometabolic therapy of tumors based on Auger electron emission. J Nucl Med. 2000;41: 1519–21.

Mirzadeh S, Alexander CW, Knapp Jr FF. Evaluation of neutron inelastic scattering, [n, n′], for production of high spin 117mSn, 119mSn and 195mPt isotopes. Appl Radiat Isot. 1997;48:441–6.

Narra VR, Howell RW, Sastry KSR, et al. Auger electron emitters as tools for elucidating the location of the primary radiosensitive targets. Radiat Prot Dosimetry. 1994;52:229–32.

Paretzke HG. Quantitative mathematical models in radiation biology. In: Freeman GR, editor. Kinetics of inhomogeneous processes. New York: Wiley; 1987. p. 89–170.

Pomplun E, Boox J, Dydejczyk A, Feinendegen LE. A microdosimetric interpretation of the radiobiological effectiveness of I-125 and the problem of quality factor. Radiat Environ Biophys. 1987;26:181–8.

Rao DV, Govelitz GF, Sastry KSR. Radiotoxicity of thallium-201 in mouse testes: Inadequacy of conventional dosimetry. J Nucl Med. 1983;24:145–53.

Rao DV, Narra VR, Howell RW, Sastry KSR. Biological consequence of nuclear versus cytoplasmic decay of I-125: cysteamine as a radioprotector against Auger cascades in vivo. Radiat Res. 1990;124:188–93.

Sastry KSR. Biological effects of the Auger emitter ^{125}I: A review. Report No. 1 of AAPM Nuclear Medicine Committee Task Group No. 6. Med Phys. 1992;19: 1361–70.

Sastry KSR, Howell RW, Rao DV, et al. Dosimetry of Auger-emitters: physical and phenomenological approaches. In: Baverstock KF, Charlton DE, editors. DNA damage by Auger emitters. London: Taylor and Francis; 1988. p. 27–8.

Skarnemark G, Odegaard-Jensen A, Nilsson J, et al. Production of ^{103m}Rh for cancer therapy. J Radioanal Nucl Chem. 2009;280(2):371–3.

SNM 2000 Annual Meeting: fusion is the theme as nuclear medicine enters the new century. J Nucl Med. 2000;41:13N–15N. Society of Nuclear Medicine: http://www.snmmi.org/.

Szucs Z, van Rooyen J, Zeevaart JR. Recoil effect on beta-decaying *in vivo* generators, interpreted for ^{103}Pd/^{103m}Rh. Appl Radiat Isot. 2009;67(7-8):1401–4.

Terriisol M, Patau JP, Eudaldo T. Application a la microd-dosimetrie et a la radiobiologie de la simulation due transport des electron de basse energie dans l'easu a l'etat liqide. In: Boox J, Ebert HG, Smith BGR, editors. Proceeding 6th symposium on microdosimetry. London: Harwood Academic; 1978. p. 179–81.

US Department of Human Health Services. 2000. US cancer death info: https://nccd.cdc.gov/uscs/.

Uusijärvi H, Bernhardt P, Rösch F, et al. Electron- and positron-emitting radiolanthanides for therapy: aspects of dosimetry and production. J Nucl Med. 2006;47(5):807–14.

van Rooyen J, Szucs Z, Rijn Zeevaart J. A possible in vivo generator ^{103}Pd/^{103}mRh-recoil considerations. Appl Radiat Isot. 2008;66(10):1346–9.

Weber DA, Eckerman KF, Dillman LT, Ryman JC. MIRD: radionuclide data and decay schemes. New York: Society of Nuclear Medicine; 1989.

Wenzel M, Wu YF. Separation of [Rh-103m]-rhodocene derivatives from the parent [^{103}Ru]ruthenocene derivatives and their organ distribution. Int J Rad Appl Instrum A. 1987;38(1):67–9 (German).

Willins JD, Sgouros G. Modeling analysis of platinum-195m for targeting individual blood-borne cells in adjuvant radiotherapy. J Nucl Med. 1995;36:315–9.

Wright HA, Hamm RN, Turner JE, et al. Calculation of physical and chemical reactions with DNA in aqueous solution from Auger cascades. Radiat Prot Dosimetry. 1990;31:59–62.

Yasui LS, Hofer KG. Role of mitochondrial DNA in cell death induced by I-125 decay. Int J Radiat Biol. 1986;49:601–10.

Yasui LS, Hofer KG, Warters RL. Inhomogeneity of the nucleus to ^{124}IUdR cytotoxicity. Radiat Res. 1985;102:109–18.

Zaider M, Brenner DJ, Wilson WE. Application of track structure calculations to radiobiology, 1. Monte Carlo simulation of proton tracks. Radiat Res. 1983;95:231–47.

Part II

Production, Processing and Availability of Therapeutic Radioisotopes

Reactor-Produced Therapeutic Radionuclides

5

5.1 Introduction

Since most therapeutic radioisotopes used in nuclear medicine, oncology, and interventional therapeutic methods are neutron rich and often decay by beta-particle emission, they are thus generally produced in research reactors (Manual, IAEA 2003) by various reactions as shown in Fig. 5.1.

5.2 Reactor Production of Radionuclides

The neutron flux associated with nuclear fission in a reactor can be used to activate stable nuclides for radionuclide production. The target material is generally sealed in specially designed irradiation capsules which are usually pneumatically or hydraulically placed within the reactor core. These targets do not interfere with uranium fission reactions (Theobald 2011); during irradiation, the fission neutrons interact with the target material to form compound nuclei which decay via various paths producing the radioactive products.

5.3 Calculation of Production Yield

When a target is irradiated in a reactor, a nuclear reaction occurs, leading to production of isotope. The activation per second is represented by

$$\frac{dN}{dt} = N_o \sigma_{act} \phi \tag{5.1}$$

where $N_o \rightarrow$ total no. of atoms present in target
$\sigma_{act} \rightarrow$ activation cross section (cm^2)
$\phi \rightarrow$ neutron flux ($neutrons.cm^{-2}.sec^{-1}$)

This equation considers the neutron flux to be isotropic, and in the case where neutrons are not monoenergetic and a velocity distribution exists, then the average neutron flux value is considered and the neutron cross-section values are modified as required. Since the product radioisotope decays with a specific physical own half-life value, the net growth rate of radioactive product atoms can be expressed as

$$\frac{dN}{dt} = N_o \sigma_{act} \phi - \lambda N \tag{5.2}$$

where, $\lambda \rightarrow$ Decay constant (sec^{-1}) of the isotope produced

$$\text{or} \quad \frac{dN}{dt} + \lambda N = N_o \sigma_{act} \phi.$$

$$\text{or} \quad \text{activity} = \lambda N = N_o \sigma_{act} \phi \left(1 - e^{-\lambda t}\right) \tag{5.3}$$

If A is the mass number of the target element under irradiation, then expression of the above equation in Curies then becomes

F.F. (Russ) Knapp, A. Dash, *Radiopharmaceuticals for Therapy*, DOI 10.1007/978-81-322-2607-9_5

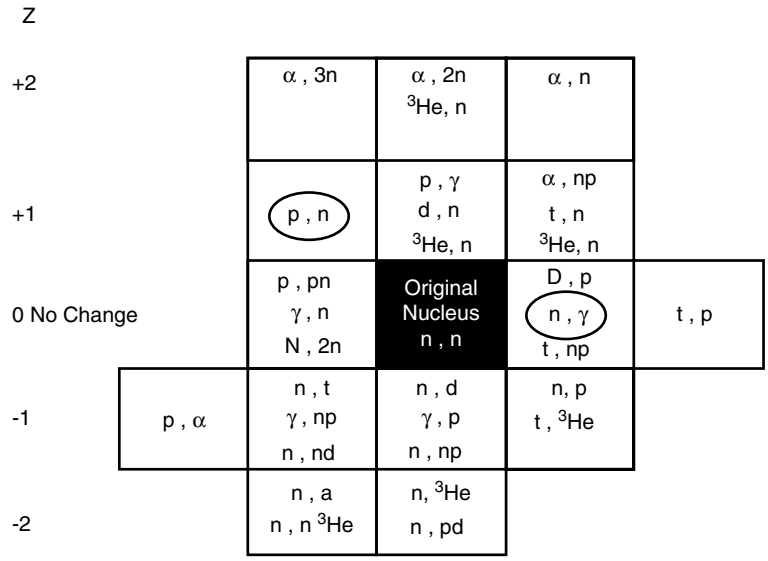

Fig. 5.1 Examples of particle-based pathways for radioisotope production

$$\text{Specific activity S'} = \frac{6.023\times10^{23}\times\sigma_{act}\phi}{A\times.3.7\times10^{10}\left(1-e^{-0.693t/T^{1/2}}\right)}\ \text{Ci/g} \tag{5.4}$$

where $\sigma_{act} \rightarrow$ activation 'cross section (barn × 10^{-24})

$\phi \rightarrow$ neutron flux (neutrons-cm^{-2}-sec^{-1})

$T_{½} \rightarrow$ half-life 'of the product nucleus (sec)

$t \rightarrow$ time of irradiation (sec)

When $t \gg T_{½}$, the production tends to saturate.

$$\text{Specific activity '}S_{sat}\text{'} = \frac{0.6\times\sigma_{act}\phi}{A\times3.7\times10^{10}}\ \text{Ci/g} \tag{5.5}$$

The above equation clearly shows that growth of activity in a target under irradiation is exponential in nature and reaches a saturation value limited by the reactor neutron flux. In practice, the activity induced in the target under irradiation will be less than the activity calculated using the above equation, due to several factors which include the following:

- Target self-shielding effect in the target
- Reactor power variation
- Flux depression due to adjacent samples in the reactor
- Target burnup over time
- Destruction of the product nucleus due to subsequent neutron capture

When correction for target burnup and destruction of target atoms is considered, Eq. (5.2) becomes

$$\frac{dN}{dt} = N\ \sigma_{abs}\phi - \lambda N_t - N_t\sigma_{abs}\phi \tag{5.6}$$

where $\sigma_{abs} \rightarrow$ absorption cross section (cm^2) of the target atom causing burnup,

$$N = N_o e^{-\sigma_{abs}\phi t}$$

N_t is the number of product atoms at time t,

$\sigma'_{act} \rightarrow$ activation cross section in barn

The above equation can then be expressed as

$$\lambda\ N_t + e^{t_c} + N_t\sigma_{abs}\phi = N_o e^{-\sigma_{abs}\phi t}\sigma_{act}\phi$$

$$\text{or}\quad \frac{dN}{dt} + N_t\left(\lambda + \sigma_{abs}\phi\right) = N_o e^{-\sigma_{abs}\phi t}\sigma_{act}\phi \tag{5.7}$$

If $C = \lambda + \sigma_{abs}\phi$ and $K = \sigma_{abs}\phi$, Eq. (5.7) becomes

$$\frac{dN}{dt} + N_t C = N_o e^{-Kt}\sigma_{abs}\phi \tag{5.8}$$

By integration and application of suitable conditions, this equation becomes

$$N_t = \frac{N_o \sigma_{act} \phi}{C - K}\left(e^{-Kt} - e^{-Ct}\right) \quad (5.9)$$

By further substituting of the factor, $N_o = \frac{6.023 \times 10^{23}}{A}$ where $A \rightarrow$ atomic weight of the target atom and λN expressing the activity produced in the target, the specific activity (S) of the isotope produced will be

$$S = \frac{0.6 \times \sigma_{act} \phi \lambda}{A(C - K)}\left(e^{-Kt} - e^{-Ct}\right) \quad (5.10)$$

$$\text{or} \quad S = \frac{0.6 \times \sigma_{act} \phi \lambda}{A\lambda}\left(e^{-Kt} - e^{-Ct}\right) \quad (5.11)$$

From this equation the value of time t at which the specific activity will be maximum which could be obtained can be established by equating $dS/dt = 0$

$$\text{i.e.} \quad -K e^{-Kt} - \left(-C e^{-ct}\right) = 0$$

$$\text{or} \quad C e^{-ct} = K e^{-Kt} \quad (5.12)$$

$$\text{or} \quad t = \frac{\log\left(\frac{\lambda + \sigma_{abs}}{\sigma_{abs}}\right)}{\lambda}$$

Since the target material is cooled after irradiation to allow the decay of the activated container material—which primarily consists of aluminum, i.e., ^{28}Al and other ultra-short-lived isotopes produced—a correction factor for the cooling period (t_c) is thus introduced:

$$S = \frac{0.6 \times \sigma_{act} \phi \lambda}{A\lambda}\left(e^{-Kt} - e^{-Ct}\right)e^{-\lambda t_c} \quad (5.13)$$

The factors which determine radionuclide production parameters in a reactor include:

- The energy of the neutrons and the neutron flux
- The characteristics and quantity of the target material
- The activation cross section for the desired nuclear reaction

Radionuclides are produced by a variety of mechanisms described below, based on different incident neutron–particle reactions as summarized in Fig. 5.1 with the target nucleus.

5.4 Direct (n, γ) Activation (Radiative Route)

The most common nuclear reaction used for reactor production of radionuclides consists of the radiative capture of thermal or epithermal neutrons by target nuclei followed by emission of prompt γ rays (Mausner et al. 1998). The activity levels produced at half saturation are related to Eq. (5.3), and by this route, the target is not entirely transformed, which results in the presence of considerable residual target atoms, or carrier, in the desired radioactive product. However, at higher neutron flux values, higher-specific-activity final products can often be produced, containing lower levels of target atoms. Thus, specific activity is a function of neutron flux and higher-specific-activity products can thus be obtained for high (n, γ) cross-section values and the target is irradiated at high neutron flux. An inherent potential disadvantage of this method is that impurities in the target will also undergo neutron activation, resulting in transformation into both radioactive and stable isotope impurities present in the desired product. For this reason, the use of target materials with very high chemical purity target is generally an essential requirement. In addition to high chemical purity, isotopically enriched targets are often also necessary in order to increase the specific activity as well as radionuclidic purity of the produced radionuclide. While production of no-carrier-added (NCA) radionuclides is not possible using the (n, γ) reaction, high-specific-activity products can be attained if the neutron capture cross sections are very high. Table 5.1 summarizes the characteristics of a variety of therapeutic radionuclides of current interest which are produced by the (n, γ) activation route.

5.5 Neutron Activation Followed by β⁻ Decay (n, γ → β⁻)

In this production mode, the target initially undergoes the (n, γ) reaction to produce an intermediate short-lived radioisotope, which on decay by beta

Table 5.1 Key examples of therapeutic radionuclides produced by the (n, γ) radiative route

Target	Product	Half-life (days)
Erbium-168	Erbium-169	9.4
Gold-197	Gold-198	2.7
Holmium-165	Holmium-166	1.1
Lutetium-176	Lutetium-177	6.68
Palladium-108	Palladium-109	0.57
Phosphorous-31	Phosphorous-32	14.3
Rhenium-185	Rhenium-186	3.72
Rhenium-187	Rhenium-188	0.7
Samarium-152	Samarium-153	2.0
Tin-116	Tin-117 m	13.6

emission produces the radionuclide of interest. The (n, γ) reaction does not directly populate the final product but represents a precursor that decays by beta decay which leads to the final product. In this case, the desired product can generally be separated from the initial product and is thus obtained with very high SA, often carrier-free. The optimum irradiation period required to attain maximum production yield depends on the half-life of the parent radionuclide. In this case, since the product radionuclide is chemically different from the original target (i.e., Z changes), the availability of efficient chemical processing is a prerequisite for obtaining the desired radionuclide. Radionuclides produced by this route are particularly attractive as they are generally NCA and will have SA values approaching the theoretical specific activity value. Typical examples of a few therapeutic radionuclides that can be produced in reactor by the (n, γ)→β⁻ route are shown in Table 5.2. In some cases, the β⁻-decay product resulting from decay of the initial radioactive product can then subsequently capture a neutron to form the desired radioactive product, such as for production of ^{166}Dy from neutron irradiation of enriched ^{164}Dy.

5.6 The (n,p) Production Reaction

In some cases the absorption of neutron leads to emission of a proton as outgoing particle (Fig. 5.1), referred to as the (n,p) reaction. With the lower-energy thermal neutrons, the cross-section values for this reaction are quite low. Such reactions are more probable with fast neutrons having energy values above the threshold energy which is mostly between 2 and 6 MeV. While radionuclides produced by (n,p) reactions are available in NCA form, this route of production suffers from low yields since the fast flux component of neutrons in a reactor is only a fraction of the total neutron flux and fast flux component is low in many research reactors. Also in this case, the product nuclei require chemical separation from the large macroscopic levels of target atoms. Table 5.3 lists several important therapeutic radioisotopes produced by the (n,p) reaction.

Several key therapeutic radioisotopes of current or potential interest can be reactor-produced and primarily include beta-emitting radioisotopes, although some Auger electron emitters and alpha emitters can also be produced in research reactors. The following sections summarize details of the production and chemical purification of several key examples.

5.7 Beta-Particle-Emitting Radionuclides

5.7.1 Arsenic-77

Arsenic-77 ($T_{1/2}$ = 1.6 d) is a promising medium-range β⁻-emitting radionuclide ($E_{\beta max}$ = 0.7 MeV) for in vivo radionuclide therapy owing to its favorable nuclear decay characteristics (Neves et al. 2002), decaying by 100 % via electron emission to stable ^{77}Se. The emission of low-energy gamma photons [239 keV (1.6 %), 520 keV (0.5 %)] allows imaging for evaluation of in vivo radiopharmaceutical localization and pharmacokinetics (Jennewein et al. 2006). The 1.6-d half-life of ^{77}As is compatible with the pharmacokinetics of several targeting biomolecules, including monoclonal antibodies (MAbs) (Emran and Phillips 1991) and is amenable for radiochemical synthetic procedures which may require several hours. The chemistry for effective labeling of biologically relevant molecules

Table 5.2 Examples of key therapeutic radionuclide produced by the (n, γ) → β⁻ route

Target	Intermediate radionuclide	Product radionuclide	Half-life (days)
Dysprosium-164	Dysprosium-166 $^{164}Dy(n,\gamma)^{165}Dy(n,\gamma)^{166}Dy$	Holmium-166	1.1
Gemanium-76	Gemanium-77	Arsenic-77	1.6
Neodymium-148	Neodymium-149	Promehtium-149	2.21
Palladium-110	Palladium-111 m	Silver-111	7.45
Platinum-198	Platinum-199	Gold-199	3.14
Ruthenium-104	Ruthenium-105	Rhodium-105	1.47
Tellurium-130	Tellurium-131	Iodine-131	8.02
Ytterbium-176	Ytterbium-177	Lutetium-177	6.7
Xenon-124	Xenon-25	Iodine-125	60

Table 5.3 Examples of therapeutic radionuclides produced by the (n,p) reaction

Target nuclide	Product radionuclide	Half-life (days)
Sulfur-32	Phosphorus-32	14.28
Sulfur-33	Phosphorous-33	25.3
Titanium-47	Scandium-47	3.35
Yttrium-89	Strontium-89	50.52
Mercury-199	Gold-199	3.15
Zinc-67	Copper-67	2.58

with arsenic radioisotopes is slowly evolving (Leonard 1991; Emran 1984; Hosain et al. 1982; Jennewein et al. 2003a, b; Zhu et al. 1997; Mirzadeh and Lambrecht 1996). Arsenic forms stable covalent bonds with carbon and sulfur and can substitute phosphorus in certain compounds with minimal alteration of the biological activity of the parent molecules. In addition, the potential use of ^{77}As for endoradiotherapeutic radiopharmaceuticals has also been proposed (Maki and Murakami 1974).

Reactor production of ^{77}As involves the $^{nat}Ge(n,\gamma)^{77}Ge \xrightarrow{\beta}{}^{77}As$ reaction, where GeO_2 or Ge metal targets of natural abundance are irradiated to undergo (n,γ) activation to produce ^{77}Ge (Table 5.2), which subsequently decays by β⁻ emission ($t_{½}$ = 11.3 h) to yield ^{77}As (Jennewein et al. 2005; Maki and Murakami 1974). Natural Ge is a mixture of five isotopes, ^{70}Ge, ^{72}Ge, ^{73}Ge, ^{74}Ge, and ^{76}Ge, with relative abundances of 21.23 %, 27.66 %, 7.72 %, 35.94 %, and 7.45 %, respectively (Jennewein et al. 2006). Neutron irradiation of this isotopic mixture results produces a mixture containing ^{71m}Ge, ^{71}Ge,^{70}Ga,^{72}Ga,^{73}Ga, ^{74}Ga, ^{75m}Ge,^{75}Ge, ^{76}Ga, ^{77m}Ge,^{77}Ge, ^{69m}Zn, ^{69}Zn,^{71m}Zn, ^{71}Zn, and ^{73}Zn (Erdtmann 1976). With the exception of ^{71}Ge ($T_{½}$ = 11.2 d), the other activated Ge radionuclides are short-lived. The production of radioactive Ga and Zn radioisotopes is negligible owing to the very low neutron cross sections. On the other hand, 24 % of the ^{77m}Ge produced ($t_{½}$ = 54 s) rapidly decays to ^{77}Ge ($t_{½}$ = 11.3 h), while the remainder disintegrates directly to ^{77}As ($t_{½}$ = 38.7 h) by β⁻ decay, which finally decays to stable ^{77}Se. During target cooling, most of the short-lived radionuclides decay, which not only facilitates the in-growth of ^{77}As to maximum levels but also reduces the radiation dose to a considerable extent.

The production, purification, and application of ^{77}As has been an active area of research in nuclear medicine and radiochemistry communities and ^{77}As can be cyclotron-/accelerator-produced by the deuteron-induced reaction on enriched ^{76}Ge targets by the ^{76}Ge(d,n) ^{77}As reaction, but this route has not been studied in detail (Jennewein et al. 2005). For processing, ^{77}As can be separated from cyclotron- or reactor-irradiated germanium or germanium oxide targets by methods involving distillation, coprecipitation, solvent extraction, thin layer chromatography, etc. (Jennewein et al. 2005; Maki and Murakami 1974; Chattopadhayay et al. 2007; Bokhari et al. 2009; Mirzadeh and Lambrecht 1996). Four successful preparative-scale separations of ^{77}As from Ge for clinical applications have been reported in the literature (Jennewein et al. 2005; Chattopadhayay et al. 2007; Bokhari et al. 2009; Chakravarty et al. 2011). One method is based on

the formation of soluble GeF_6^{-2} in concentrated hydrofluoric acid and conversion of As to AsI_3 by the addition of KI, followed by separation using a polystyrene-based solid-phase extraction system (Jeenewien et al. 2005). The method reported by Chattopadhayay et al. (2007) involves precipitation of GeO_2 followed by centrifugation or filtration and subsequent purification using six cycles of solvent extraction (twice with CCl_4 and four times with benzene). In an alternative approach, the target is initially dissolved in aqua regia, followed by removal of excess acid by evaporation, reconstitution of the feed in basic media, and passage of the solution through a hydrous zirconium oxide (HZO) column (Bokhari et al. 2009). The Ge is quantitatively retained on HZO, while ^{77}As is present in the effluent. The method adapted by BARC (Chakravarty et al. 2011) consists of a two-step ion-exchange procedure using a polymer-embedded nanocrystalline titania sorbent. The first step involves removal of the bulk Ge from ^{77}As and the second step involves purification and concentration.

5.7.2 Copper-67

Copper-67 ($T_{1/2}$=2.6 d) is a medium-energy β^- emitter with an energy of 0.6 MeV_{max} (141 keV average), with strong gamma emissions at 91.266 (7 %), 93.31 (16 %), and 184.57 keV (48.7 %) (Junde et al. 2005). Because of the degree of soft tissue penetration, the medium-energy β^- particle permits efficient use of ^{67}Cu for effective irradiation and sterilization of cells in solid tumors up to 4 mm in diameter. The range of the ^{67}Cu beta particle in tissue is of the same order as a cell diameter (Qaim 2001). The chemistry of copper is suitable for labeling purposes and precludes the concentrate in sensitive body tissues such as the bone marrow. The 2.6-d half-life is suitable for imaging slow in vivo pharmacokinetics with agents such as monoclonal antibodies and other carrier molecules without appreciable decay loss (DeNardo et al. 1999). The presence of relatively low-energy gamma photos can be effectively detected with Anger cameras [(184 keV 948.7 %), 93.3 (16.1 %)] and is useful for imaging studies (Shen et al. 1996). In vivo, ^{67}Cu in the inorganic form has favorable short-term retention, and both ^{67}Cu and its stable ^{67}Zn decay product are nontoxic since Cu and Zn are essential trace nutrients (Blower et al. 1996). Copper is not a skeletal or organ seeker and ^{67}Cu has a biological half-life of the same order as its radiological half-life (Johnson et al. 1992; Linder and Hazegh-Azam 1996).

Unfortunately ^{67}Cu cannot be effectively produced in a research reactor in sufficient activity levels to make this route practical. Reactor production of ^{67}Cu via the $^{67}Zn(n, p)^{67}Cu$ reaction has been reported by bombarding ^{67}Zn with neutrons in high-flux reactors having a high epithermal neutron component; however, the cross-section values are low (Mausner et al. 1998; Johnsen et al. 2015). Production of ^{67}Cu can be much more effectively carried out following using accelerator-based pathways (Katabuchi et al. 2008; Medvedev et al. 2012; Smith et al. 2012; Szelecsényi et al. 2009) and the cyclotron production of ^{67}Cu and different nuclear reactions are discussed and summarized in Table 6.2 in Chap. 6.

5.7.3 Erbium-169

Erbium-169 ($T_{1/2}$=9.4 d) emits beta particle ([$E_{\beta(max)}$=351 keV (55 %), 342 (45 %)]) with an average soft tissue range of 0.3 mm and is used in targeted therapy as a soft β^--emitting radionuclide, primarily for synovectomy of small joints as described in Chap. 14. Production of ^{169}Er can be conveniently carried out through neutron capture of stable ^{168}Er by the $^{168}Er(n, \gamma)^{169}Er$ reaction. Naturally occurring erbium is composed of six stable isotopes, which include ^{162}Er (0.14 %), ^{164}Er (1.61 %),^{166}Er (33.6 %), ^{167}Er (22.95 %),^{168}Er (26.8 %), and ^{170}Er (14.9 %). Neutron irradiation of ^{nat}Er not only leads to the coproduction of ^{165}Er and ^{171}Er as impurities but also produces low-SA ^{169}Er. In order to circumvent such drawbacks, isotopically enriched ^{168}Er targets are generally used for ^{168}Er production. Owing to the poor neutron capture cross section of this process (σ=1.95 barn), however, the activation product obtained is in only low specific activity.

Reactor production and electrochemical purification of ^{169}Er for vivo therapeutic applications have been reported (Chakravarty et al. 2014). Despite having useful radiation emission characteristics, poor specific activity is thus a major impediment that restricts the use of ^{169}Er for radiosynovectomy. However, use of ^{169}Er for the labeling of tumor receptor or antigen-targeting vectors is precluded because of the requirement for much higher specific activities for these applications. ^{169}Er is the most preferred choice for RSV of digital joints such as metacarpophalangeal metatarsophalangeal and digital interphalangeal joints (Karavida and Notopoulos 2010). Erbium-169-labeled silicate/citrate colloid is widely used as in the treatment of refractory painful arthritis (Gumpel et al. 1979; Bouvier et al. 1983; Kahan et al. 2004). Low volumes containing 0.5–1 mCi (20–40 Mbq) with a maximum of 20 mCi (750 Mbq) per administration are used for this application.

5.7.4 Gold-198

Gold-198 ($T_{1/2}$ = 2.7 d) has been of interest for many years and decays with emission a β^- particle with a maximum energy of 0.96 MeV (99 %) suitable for therapeutic applications. However, the high abundance of high-energy gamma photons (412 keV) (95.6 %) can be a significant disadvantage. Because of the unique properties of gold nanoparticles, in recent years there has been interest in designing and developing ^{198}Au nanoparticles for tumor therapy applications (Chanda et al. 2010). The ^{198}Au is reactor-produced by direct (n,γ) activation by the ^{197}Au(n, γ)^{198}Au reaction which has a very high thermal neutron cross section (σ 26,500 barn). The target used is either gold foil or metal and the neutron-irradiated target is dissolved in aqua regia (3:1 HCl/HNO_3) and partially evaporated to yield $HAuCl_4$ in dilute HCl (normally 0.05 M). In order to insure the product is free from trace radionuclide impurities, the $AuCl_4^-$ is extracted into organic solvents such as chloroform, dichloromethane, or ethyl acetate as its tetrabutyl ammonium salt, TBA ($AuCl_4$).

5.7.5 Gold-199

Gold-199 [$T_{1/2}$ = 3.14 d] also decays by emission of β^- particles ($E_{\beta(max)}$ = 452 keV (6.5 %), 293 keV (72 %), 244 keV (21.5 %)) and gamma photons [($E\gamma$ = 494 keV (97 %), 158 keV (36.9 %)]. Although the high gamma abundance is a disadvantage, interest in the potential use of ^{199}Au for therapeutic applications has persisted. Radiolabeling of gold clusters containing 11 gold atoms site selectively to monoclonal antibodies has been reported (Hainfeld 1987; Vaughan and Varley 1988; Hainfeld 1988; Hainfeld et al. 1990). Production of ^{199}Au is performed by an indirect method, involving neutron capture of ^{198}Pt followed by β^- decay of the ^{199}Pt ($T_{1/2}$ = 30.80 m) to generate ^{199}Au (Table 5.1). The reaction cross section is moderate with a value of 3.6 barn.

The use of natural platinum leads to the concomitant production of ^{193}Pt and ^{197}Pt which results in the production of inactive ^{197}Au, thereby decreasing the ^{199}Au SA. Use of enriched targets is thus necessary to avoid handling high activity levels arising from decay of other Pt radionuclides. The indirect method of production leads to the production of NCA ^{199}Au and the radiochemical separation procedure are well described in the literature (Kolsky and Mausner 1993; Bonardi et al. 2001; Das et al. 1999). Since the ^{199}Au is available NCA, this radionuclide is of interest for radiolabeling peptides and antibodies. However, stabilization of gold by chelation is a challenging task, due to the inertness of this metal.

5.7.6 Holmium-166

Holmium-166 ($T_{1/2}$ = 26.83 h) emits β^- particles with a maximum energy of 1.85 MeV [$E_{\beta(max)}$ = 1854 keV (50.0 %), 1774 keV (48.7 %)] and γ rays with energies of 80.6 (6.2 %) and 1379 keV (1.13 %). The 80 keV photon is within the optimal energy range for effective gamma camera imaging. The two β^- emissions have mean soft tissue penetration range of 4 mm and a maximum range of 8.7 mm in soft tissues (Marque et al. 2005; Nijsen et al. 1999). Holmium-166 is an excellent

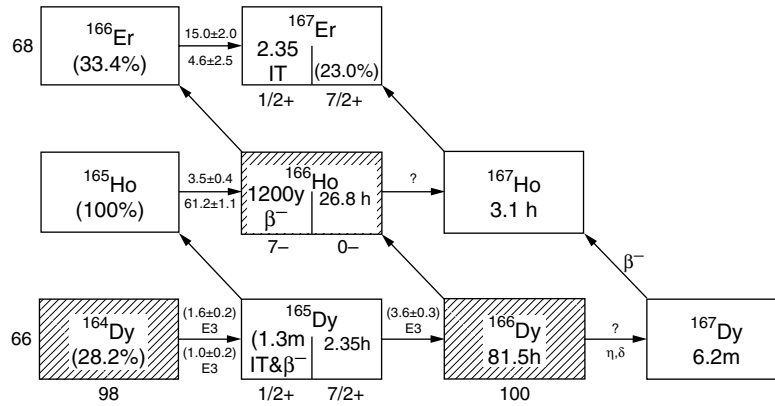

Fig. 5.2 Reactor production of ^{166}Ho

radionuclide suited for in vivo therapeutic applications (Dadachova et al. 1997; Hong et al. 2002, 2004; Chakraborty et al. 2001; Chakraborty et al. 2006b; Majali et al. 2001, 2002; Das et al. 2009a, b), although the relatively short half-life may often limit distribution of ^{166}Ho-labeled radiopharmaceuticals to within only short proximity to the production site. Although ^{166}Dy/^{166}Ho radionuclide generator prototypes have been described, these systems are not yet further developed or practical for routine clinical use (see Chap. 7). The most widely utilized ^{166}Ho radiopharmaceutical which has been described for therapy rather than palliation of bone cancer is ^{166}Ho-DOTMP (DOTMP = 1,4,7,10-tetraazacyclododecane-1,4,7,10-tetramethylene-phosphonic acid; Fig. 11.12, Chap. 11), which targets multiple myeloma, a cancer of the plasma white blood cells, that is presented in the bone marrow of these patients (Breits et al. 2006; Rajendren et al. 2002). Utility of ^{166}Ho-EDTMP for bone pain palliation has also been explored (Appelbaum et al. 1992; Bahrami-Samani et al. 2010; Sohaib et al. 2011).

For the treatment of unresectable liver cancer (see Chap. 11), several ^{166}Ho-labeled agents are in various stages of evaluation and include the percutaneous administration of the ^{166}Ho–chitosan complex (PHI) (Rajendren et al. 2002), the ^{166}Ho–oxine–lipiodol complex (Das et al. 2009a, b) and ^{166}Ho–polylactic acid microspheres (Nijsen et al. 1999).

Holmium-166 can be produced by direct neutron irradiation of ^{165}Ho, which is 100 % abundant (Table 5.1) and from decay of reactor produced ^{166}Dy (Fig. 5.2). Since the thermal neutron activation cross section is 66 barn, relatively high activity levels of ^{166}Ho can be produced, but with only moderate specific activity, because only a very small portion (~0.31 %) of target atoms are actually converted to ^{166}Ho at saturation yields (Fig. 5.3).

Although the modest SA of the ^{166}Ho produced by direct (n,γ) activation is not useful for radiolabeling receptor-specific biomolecules, these ^{166}Ho SA values are sufficient for several applications where much higher radiopharmaceutical masses can be administered, which include bone marrow ablation, therapy of hepatocellular carcinoma, and radiosynovectomy. For targeting low populations of binding sites such as receptor binding, the use of NCA ^{166}Ho is required, and the availability of NCA ^{166}Ho from a ^{166}Dy/^{166}Ho generator would be expected to be of interest for these applications. Potential of ^{166}Dy/^{166}Ho in vivo generator system for therapeutic use have also been explored (Ferro-Flores et al. 2003; 2004). Production of ^{166}Ho through hot atom reactions has also been explored (Nassan et al. 2011; Zeisler and Weber 1998).

For such applications, NCA ^{166}Ho can be produced via an indirect route (Table 5.2) in which an enriched ^{164}Dy target undergoes two sequential neutron captures (2n, γ) to provide ^{166}Dy that subsequently decays by β⁻ emission to the desired ^{166}Ho product by the $^{164}\mathrm{Gy}(2n,\gamma)^{166}\mathrm{Gy}\xrightarrow{\beta^-}{}^{166}\mathrm{Ho}$ route.

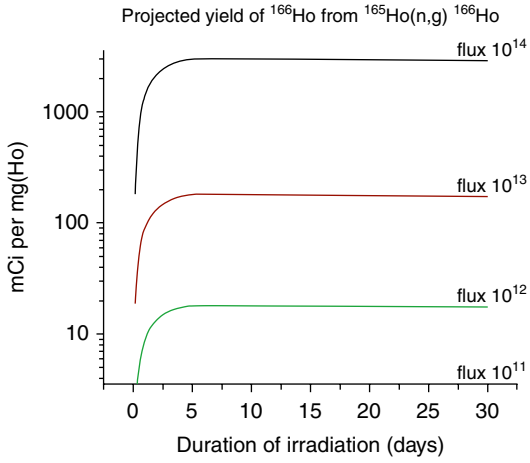

Fig. 5.3 Theoretical production yields of ^{166}Ho from irradiation of ^{165}Ho as a function of thermal neutron flux

This method necessitates availability of efficient methods to perform chemical separation of microscopic levels of ^{166}Ho from macroscopic amounts of ^{166}Dy. The initial neutron capture cross-section values are effectively 2731 barn thermal and 932 barn epithermal to form ^{165}Dy with a half-life of 2.33 h. Although the half-life of this intermediate radionuclide is relatively short, ^{165}Dy has thermal and epithermal neutron capture cross sections of 3600 and 22,000 barn, respectively, and thus a significant percentage of ^{165}Dy atoms undergo second neutron capture reaction to form ^{166}Dy. One milligram of enriched ^{164}Dy irradiated over 155 h at a thermal flux of 4×10^{14} neutrons cm^{-2} s^{-1} thermal and an epithermal flux of 1.6×10^{13} neutrons cm^{-2} s^{-1} at the MURR has been shown to produce close to the theoretical yield of 1.2 Ci of ^{166}Dy (Ma et al. 1996). Similar production studies at the ORNL HFIR have demonstrated production of ^{166}Dy and separation of ^{166}Ho (Dadchova et al. 1994; 1995; Lahiri et al. 2004). Efforts for separation of NCA ^{166}Ho from ^{166}Dy are described in Chap. 6.

5.7.7 Iodine-131

Iodine-131 ($T_{1/2}$ = 8.02 d) has been widely used for therapy for many years and has many advantages and has traditionally represented one of the most important and most widely used reactor-produced radionuclides (Ambade et al. 2015). Decay involves emission of medium-energy beta particles [$E_{\beta(max)}$ = 606 keV (89.9 %), 333 (7.27)] and gamma rays [$E\gamma$ = 364 keV (81.2 %), 636 (7.27 %)]. The 8.02-day half-life is long enough for uptake and incorporation of radioiodine into thyroglobulin by the follicular thyroid cells, which has been the primary treatment of thyroid cancer. The medium-energy beta particle has a mean path length of about 1 mm in soft issue and is well suited for the treatment of small tumors such as follicular cell carcinoma. The emission of gamma radiation—although of high energy—facilitates imaging, which permits the uptake and localization of low activity levels of ^{131}I to be assessed prior to administration of therapeutic doses. Ready availability of ^{131}I in liquid form at affordable cost permits straightforward dispensing and oral administration. The high-energy gamma radiation of ^{131}I can result in poor images and contributes significantly to the whole-body patient radiation burden without significantly increasing the radiation damage to the target tissue. This factor also adds to the radiation dose to staff and relatives, necessitating in most countries the admission and isolation of patients undergoing radioiodine therapy.

Iodide anions are localized in thyroid cells by active transport and directly incorporated into thyroglobulin from which the thyroid hormones are released. Iodine-131 for the treatment of thyroid disease is utilized for hyperthyroidism or well-differentiated thyroid carcinoma indications. There is also a large and growing body of evidence to support effective clinical use of ^{131}I for management of well-differentiated thyroid cancers (Ambrosetti et al. 2009; Pitoia and Cavallo 2012; Pagano et al. 2004; Reynolds and Robbins 1997; Giovanella 2011). Apart from its utility in the management of thyroid disorder, ^{131}I-MIBG (m-iodobenzylguanidine) is widely used for the treatment of neuroendocrine-originating tumors (Castellani et al. 2000; Bomanji et al. 2003; Gedik et al. 2008; Ezzidin et al. 2012), while ^{131}I-Tositumomab (anti CD20 antibody, Bexaar®) is a registered radiopharmaceutical for the treatment of non-Hodgkin's lymphoma (Tomblyn 2012; Lewington 2005; Dewaraja et al. 2010; Tsai et al. 2004; Kern 2000). The comparatively long half-life of ^{131}I

provides logistical advantage for the radiochemical production and processing/dispensing/shipment of ^{131}I radiopharmaceuticals.

Production of ^{131}I on a large scale can be performed either from ^{235}U(n,f)^{131}I (Siri and Mondino 2005; Nazari et al. 2001; Al-Janabi and Kadem 1990; Tabasi et al. 2005; Wojdowska 2010; Khalafi et al. 2005; Ahmad et al. 1982) or from the $^{130}\mathrm{Te}(n,\gamma)^{131}\mathrm{Te}\xrightarrow{\beta^-}{}^{131}\mathrm{I}$ nuclear reactions (Shikata and Amano 1973; Payamara 2011; Chattopadhyay and Saha-Das 2010; El-Absy et al. 2010; Constan 1958; El-Azony et al. 2004; Al-Janabi and Kadem 1990; Elom Achoribo et al. 2012; Alanis and Navarrete 1999; Sorantin and Bildstein 1965). Although the ^{235}U fission route provides HSA ^{131}I, this production method is of limited use because of the requirements for availability of an elaborate complex radiochemical processing technology, sophisticated equipment, a reliably well-trained workforce, and management of high levels of radioactive waste. The production of fission ^{131}I can be sustained only by countries pursuing fission ^{99}Mo production where ^{131}I could be produced as a by-product. Due to the inherent complexities in the production of fission ^{131}I, alternative production technologies using neutron activation of ^{130}Te is widely practiced. The natural abundances of tellurium isotopes and their corresponding thermal neutron (n, γ) cross-section values are summarized in Table 5.4.

Reactor production of ^{131}I is generally via irradiation of ^{130}Te via the ^{130}Te(n, γ)^{131}Te ($t_{½}$ = 25 min) and ^{130}Te(n, γ)^{131m}Te ($t_{½}$ = 30 h) nuclear reactions, which have thermal-neutron capture cross sections of 0.2 and 0.04 barn, respectively, and the three decay branches are shown in Figs. 5.4 and 5.5.

Use of natural tellurium target also results in the production of ^{127}I and ^{129}I as depicted in Table 5.5.

^{127}I is inactive, whereas ^{129}I is long-lived with a half-life of 1.57×10^{7} years. The activity levels of ^{129}I formed are very low, due to the long half-life; however, the number of atoms of iodine (^{127}I and ^{129}I) at the end of bombardment (EOB) constitutes about 80 % of the total iodine atoms. Thus the isotopic abundance of ^{131}I will not exceed 20 % at EOB and continues to reduce with progressive decay of ^{131}I. Separation of ^{131}I from irradiated Te is usually carried out following dry and wet chemical distillation method following the reported procedures (Ambade et al. 2015; Ahmad et al. 1982; Beyer and Pimentel-Gonzales 2000). However, dry distillation is preferred due to the significantly lower levels of radioactive liquid waste which are generated, the more rapid processing, and the ability to obtain high radioactive concentrations of the final ^{131}I product.

Table 5.4 Isotopic abundance of natural tellurium

Tellurium isotope	% Abundance	Nuclear reaction	Thermal neutron cross sections (σ) in barn (b)
^{120}Te	0.089	^{120}Te(n, γ)^{121}Te	2.0
		^{120}Te(n, γ)^{121m}Te	0.34
^{122}Te	2.46	^{122}Te(n, γ)^{123m}Te	1.1
^{124}Te	4.61	^{124}Te(n, γ)^{125m}Te	0.04
^{126}Te	18.71	^{126}Te(n, γ)^{127}Te	0.9
		^{126}Te(n, γ)^{127m}Te	0.135
^{128}Te	31.7	^{128}Te(n, γ)^{129}Te	0.14
		^{128}Te(n, γ)^{129m}Te	0.015
^{130}Te	33.8	^{130}Te(n, γ)^{131}Te	0.2
		^{130}Te(n, γ)^{131m}Te	0.04

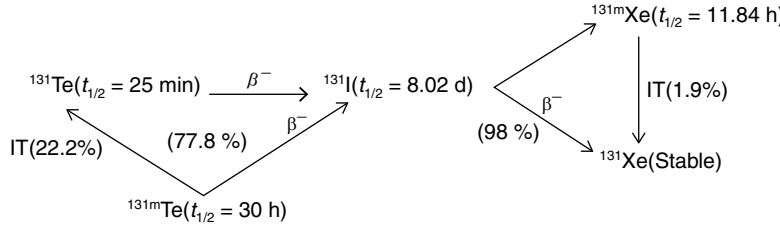

Fig. 5.4 Decay scheme of neutron-irradiated ^{131}Te

5.7.8 Lutetium-177

Lutetium-177 ($T_{1/2}$ = 6.65 d) represents therapeutic radioisotopes of rapidly increasing importance which decays with emission of low- to medium-energy β^- emission [$E_{\beta(max)}$ = 497 keV (78.6 %), 385 keV (9.1 %)] and photon emissions [$E\gamma$ = 208 keV (11.0 %), 113 keV (6.4 %)] which permit gamma camera imaging and which can be used as a 3+ lanthanide for facile radiolabeling chemistry. Lutetium-177 is also a very attractive theranostic radionuclide which can be used in diagnostic/therapeutic pairing and exhibits a soft tissue penetration range of several millimeters.

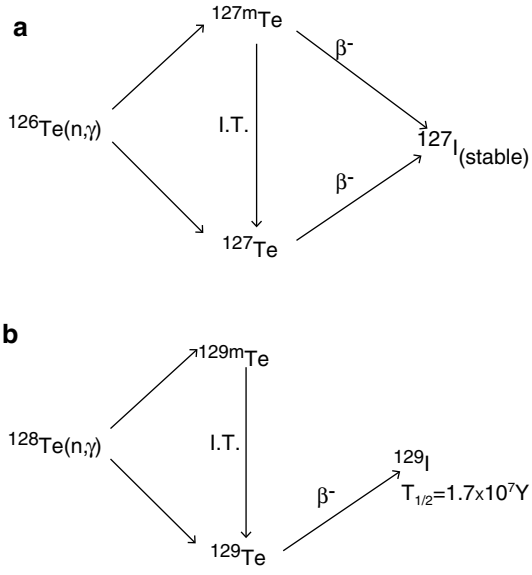

Fig. 5.5 Activation reactions and decay mode of (**a**) ^{126}Te and (**b**) ^{128}Te formed during the neutron irradiation of natural TeO_2

The use of ^{177}Lu-labeled peptides and for other applications is described in Chap. 10. The 6.65-day half-life is long enough for preparation of targeted biomolecules which have short or long biological half-lives and allows the products to be distributed for use at clinics distant to the production site. The gamma rays emitted by ^{177}Lu permit imaging of the uptake and biodistribution of the agent both before and during therapy administration. The principal applications of ^{177}Lu currently include treatment of neuroendocrine tumors (Kam et al. 2012; Gulenchyn et al. 2012; Esser et al. 2006), especially for bone pain palliation of metastatic cancer (Bodei et al. 2011; Delpassand et al. 2014; Kwekkeboom et al. 2008; Swärd et al. 2010; van Essen et al. 2010; Zaknun et al. 2013; Chakraborty et al. 2008a, c; Mathe et al. 2010; Liu et al. 2012; Das et al. 2002; Chakraborty et al. 2008a, b, c; Bryan et al. 2009), radiation synovectomy (Chakraborty et al. 2006a, b, c; Abbasi et al. 2011), and non-Hodgkin's lymphoma (Goldenberg and Sharkey 2006; Michel et al. 2005), and treatment of ovarian (Alvarez et al. 1997) and liver cancer (Chakraborty et al. 2008a, b, c) have also been studied.

Two alternative production routes are available for reactor production of ^{177}Lu (Fig. 5.6) which include the "direct" neutron activation of highly enriched ^{176}Lu targets by the ^{176}Lu (n, γ)^{177}Lu reaction, which can provide relatively high SA ^{177}Lu in medium- to high-flux research reactors due to the high thermal neutron cross section (Chakraborty et al. 2014; Dash et al. 2015a, b). The "indirect" route is based on neutron irradiation of enriched ytterbium targets by the ^{176}Yb(n, γ)^{177}Yb$\rightarrow\beta^-$ route to NCA ^{177}Lu.

Table 5.5 Other isotopes produced during the neutron irradiation of natural tellurium

Tellurium isotope in target	% Abundance	Isotope produced	$T_{½}$	Disintegration products
^{120}Te	0.089	^{121}Te	154 days	^{121}Te → ^{121}Sb(stable)
		^{121m}Te	16.8 days	
^{122}Te	2.46	^{123m}Te	119.7 days	^{123}Te (stable)
^{124}Te	4.61	^{125m}Te	57.4 days	^{125}Te (stable)
^{126}Te	18.71	^{127}Te	109 days	^{127}Te → ^{127}I (stable)
		^{127m}Te	9.35 h	
^{128}Te	31.7	^{129}Te	33.6 days	^{129}Te → ^{129}I (1.7×10^7 years)
		^{129m}Te	69.6 min.	

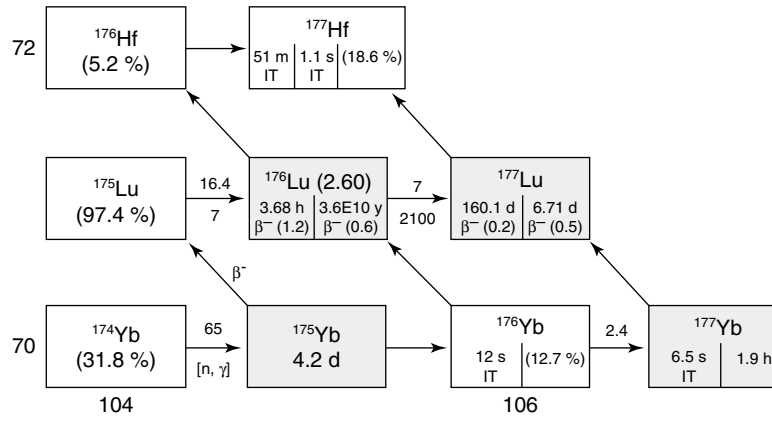

Fig. 5.6 Reactor production of ^{177}Lu

The radiochemical processing from the "direct" route involves simple dissolution of the irradiated targets, whereas purification of HSA ^{177}Lu from the "indirect" route involves more elaborate radiochemical processing to separate the microscopic levels of NCA ^{177}Lu from macroscopic ytterbium targets and other radionuclides.

In contrast to production of many radionuclides by the (n, γ) route (see Table 5.1), the direct neutron activation method of ^{177}Lu production is attractive because of the high thermal neutron capture cross-section value for ^{176}Lu ($\sigma = 2090$ b). In fact, this is the highest cross section encountered among all the therapeutic radionuclides of current interest reactor-produced by the (n, γ) route. It is possible to produce ^{177}Lu of specific activity of 740–1110 GBq/mg (20–30 Ci/mg) in medium-flux reactors using isotopically enriched ^{176}Lu in which only 20 − 30 % of the ^{176}Lu atoms are being converted to ^{177}Lu. The specific activity of ^{177}Lu can be augmented to 1850–2405 GBq/mg (50–65 Ci/mg) by irradiation in high-flux reactors such as the high-flux isotope reactor (HFIR) at Oak Ridge National Laboratory (ORNL) and at the SM3 reactor in Dimitrovgrad, Russian Federation. Experimental setup for radiochemical processing of irradiated lutetium target by the (n, γ) route is shown in Fig. 5.7.

The direct (n, γ) ^{177}Lu production route also leads to the co-production of low levels of the long-lived ^{177m}Lu impurity which has a half-life of 160 days. Although the presence of low activity levels of the ^{177m}Lu isomer is not expected to increase the patient radiation burden (Breeman et al. 2003), the presence of this long-lived radiocontaminate in radioactive waste may pose an issue in some countries (Bakker et al. 2006). For this reason, a careful optimization of the time of irradiation may be essential to obtain the highest SA and to also minimize ^{177m}Lu contamination levels (Chakraborty et al. 2014; Dash et al. 2015a, b; Pillai et al. 2003). While the use of isotopically enriched ^{176}Lu is a prerequisite for providing ^{177}Lu of adequate SA by the "direct" route amenable for radiolabeling peptides and antibodies, use of natural Lu targets is adequate to obtain ^{177}Lu of moderate SA adequate for preparation of several radiopharmaceuticals where high SA is not required for therapeutic application such as bone pain palliation, synovectomy, etc. Use of natural targets (see Table 5.6) does not pose any challenges with respect to radionuclidic impurity.

During irradiation of ^{nat}Lu, some of the ^{175}Lu atoms are transmuted to ^{176}Lu atoms during neutron irradiation which are subsequently transformed to ^{176}Lu, which enhances the contribution of ^{177}Lu due to double-neutron activation cross section (Fig. 5.8). The contribution of ^{175}Lu to ^{177}Lu production is higher in high-flux reactors since the ^{177}Lu formed from ^{175}Lu will be proportional to the square of the neutron flux (σ^2). The tremendous prospects associated with the (n, γ) method of ^{177}Lu production have thus witnessed extensive activity directed toward the establishment of production strategies using a wide spectrum of reactors of varying neutron flux (Mikolajczak et al. 2004; Nir-El 2004; Dvorakova et al. 2008; Zhernosekov et al. 2008; Chinol et al. 2010).

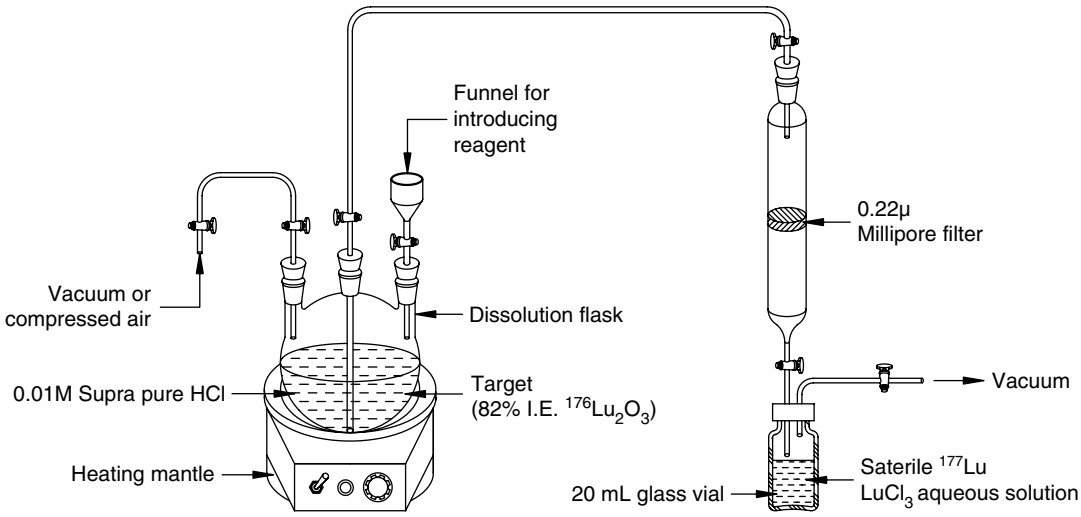

Fig. 5.7 Experimental setup for radiochemical processing of irradiated Lu_2O_3 target

Table 5.6 Neutron activation products of natural lutetium and ytterbium targets along with the nuclear decay characteristics of the product radionuclides

Element	Target isotope	% Abundance	σ (barn)	Activation product	Mode of decay	$T_{1/2}$	Decay product
Lu	^{175}Lu	97.41	16.7	^{176m}Lu	β⁻, γ	3.66 h	^{176}Hf
			6.6	^{176}Lu	β⁻, γ	4×10^{10} y	^{176}Hf
	^{176}Lu	2.59	2.8	^{177m}Lu	β⁻, γ & IT	160.4 d	^{177}Hf (78.6 %) ^{177}Lu (21.4 %)
			2090	^{177}Lu	β⁻, γ	6.65 d	^{177}Hf
Yb	^{168}Yb	0.13	2300	^{169}Yb	EC	32.02 d	^{169}Tm
	^{170}Yb	3.04	9.9	^{171}Yb	Stable		
	^{171}Yb	14.28	58.3	^{172}Yb	Stable		
	^{172}Yb	21.83	1.3	^{173}Yb	Stable		
	^{173}Yb	16.13	15.5	^{174}Yb	Stable		
	^{174}Yb	31.83	63	^{175}Yb	β⁻, γ	4.18 d	^{175}Lu
	^{176}Yb	12.76	2.85	^{177}Yb	β⁻, γ	1.9 h	^{177}Lu

In order to obtain NCA ^{177}Lu, several investigators have described radiochemical separation of NCA ^{177}Lu following neutron irradiation of macroscopic ytterbium targets (Mirzadeh et al. 2004; So et al. 2008; Morcos et al. 2008; Horwitz et al. 2005; Hashimoto et al. 2003; Lebedev et al. 2000; Lahiri et al. 1998; Bilewics et al. 2009; Kumric et al. 2006; Chakraborty et al. 2008b; Knapp et al. 2005; Dash et al. 2015a, b). In this method, an isotopically enriched ^{176}Yb target undergoes (n, γ) transmutation to produce ^{177}Yb which subsequently decays by β⁻-emission ($T_{½}$ = 1.9 h) to yield ^{177}Lu by the $^{176}\mathrm{Yb}(\mathrm{n},\gamma)^{177}\mathrm{Yb}\xrightarrow{\beta^-}{}^{177}\mathrm{Lu}$ process. The prospects associated with this route of ^{177}Lu production along with the challenge associated with the separation of chemically similar neighboring lanthanides have thus led to a considerable research and innovative detection strategies. At least four successful preparative-scale separations of ^{177}Lu from Yb for clinical applications have been reported in the literature (Lebedev et al. 2000; Bilewicz et al. 2009; Mirzadeh et al. 2004; Chakravarty et al. 2010). The method reported by

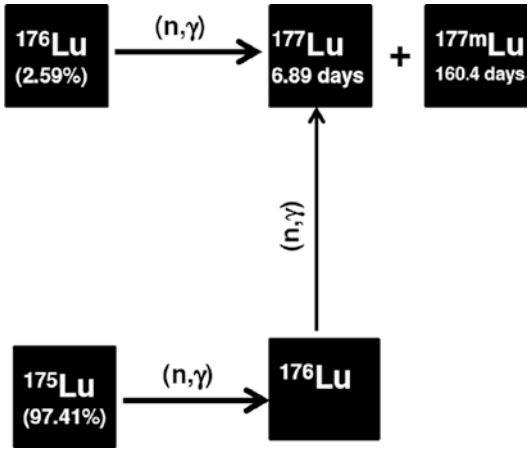

Fig. 5.8 Production of ^{177}Lu using natural Lu

Lebedev et al. is based on the selective extraction of Yb by sodium amalgam from Cl^-/CH_3COO^- electrolytes taking advantage of the higher solubility of metallic Yb than Lu in mercury. This rather complex and time-consuming process involves eight cementation cycles. The separated ^{177}Lu is reported to contain 10 μg Yb(III) from 200 mg of neutron-irradiated Yb_2O_3 and must be subjected to an ion exchange process for purification. Subsequently, Bilewicz et al. (2009) have reported a method based on the reduction of Yb(III) to Yb(II) with sodium amalgam followed by selective precipitation of Yb(II) as the sulfate. The ^{177}Lu solution obtained after the precipitation step contained 1 mg Yb(III) from 50 mg of neutron-irradiated Yb_2O_3 and was hence subjected to purification by an ion exchange process. The method described by Knapp and co-workers consists of a chromatographic extraction method containing LN resin comprised di(2-ethylhexyl) orthophosphoric acid (HDEHP) in which both Lu and Yb can be loaded. The column was eluted with 2 M HCl and the initial elution ^{170}Tm detected prior to Yb elution was presumed to be formed by neutron activation of the low levels of stable ^{169}Tm impurity present in the enriched ^{176}Yb target material. After the removal of ^{170}Tm and Yb, ^{177}Lu was then eluted with 6 M HCl. The specific activity of ^{177}Lu obtained by this method was estimated to be 3.7 TBq (100 Ci)/mg (i.e., 91 % of the 110 Ci/mg theoretical value).

The EXC technique was further exploited Horwitz and co-workers (Horwitz et al. 2005) and was found to be successful for the separation of NCA ^{177}Lu from a 300 mg irradiated ytterbium target. The whole separation process can be broadly divided in to three steps: (1) front-end target removal step, (2) primary separation step, and (3) secondary separation step. While the goals of each separation step differ, it basically consists of separation of Yb and Lu using the LN2 resin followed by concentration and acid adjustment of the Lu-rich eluate using Amberchrom® CG-71 resin. In another independent study, a multi-column solid-phase extraction (SPE) chromatography technique using di-(2-ethylhexyl) orthophosphoric acid (HDEHP)-impregnated OASIS-HLB sorbent-based SPE resins (OASIS-HDEHP) was used (Le et al. 2008a, b). The method was successful for the isolation of several hundred mCi of NCA ^{177}Lu using 50 mg Yb target irradiated in a medium neutron flux nuclear reactor ($\phi = 5.10^{13}$ n/cm^2/sec).

An alternative method (Fig. 5.9) reported by Chakravarty et al. (Chakravarty et al. 2010) consists of an electro-amalgamation approach in which a two-cycle electrolysis procedure was adopted for separation of 18.5 GBq (500 mCi) of ^{177}Lu from $^{169\text{-}177}$Yb/^{177}Lu mixture in lithium citrate medium. In the first step, the bulk of Yb target is removed, and in the second step, tracer quantities of Yb present in the ^{177}Lu are removed to obtain NCA grade ^{177}Lu.

5.7.9 Phosphorous-32

Phosphorous-32 ($T_{1/2} = 14.26$ d) is the first radionuclide used in therapeutic applications more than 50 years ago for the palliation of skeletal pain from bone metastases. Phosporus-32 is a pure β^- emitter with a maximum energy of 1.71 MeV and the mean and the maximum particle range in soft tissue are 3 and 8 mm, respectively. The traditional clinical application of ^{32}P has been of the treatment of polycythemia vera and leukemia (Najean and Rain 1997; Tefferi and Silverstein 1998; Meuret et al. 1975; Najean et al. 1996; Tefferi 2012). Phosphorus-32 was first produced in the cyclotron at the University of California in Berkeley, by

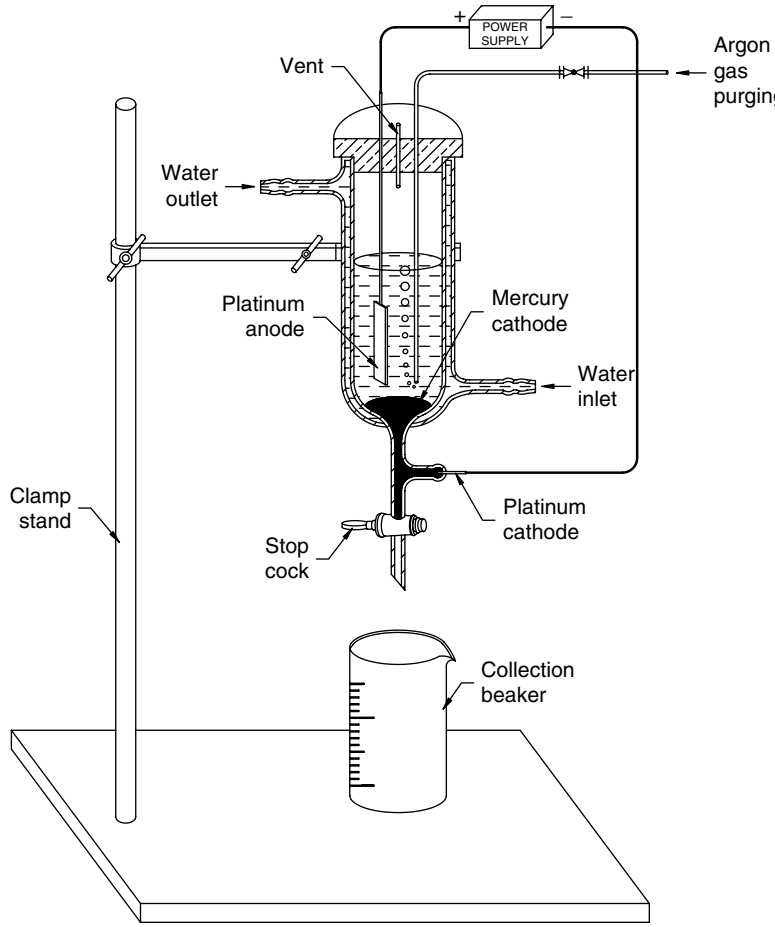

Fig. 5.9 Schematic diagram of the electrochemical setup used for the production of ^{177}Lu using the electro-amalgamation approach

E. Lawrence in 1936 by irradiating red phosphorus by the ^{31}P(d,p)^{32}P [$\sigma = 0.18 \times 10^{-27}$cm^2] nuclear reaction (Lawrence and Cooksey 1936). Subsequently, when the first nuclear reactor (Graphite Reactor) became available at the Oak Ridge National Laboratory, production shifted to the reactor route, since ^{32}P can be readily produced by either the ^{32}S(n,p)^{32}P or ^{31}P(n, γ)^{32}P nuclear reactions. Only relatively low SA ^{32}P can be produced by the neutron irradiation of ^{31}P (100 % abundance, $\sigma = 0.172$ barn) by the ^{31}P(n, γ)^{32}P route but could be used for the preparation of formulations for bone pain palliation (Vimalnath et al. 2013; 2014a, b). This production route requires only very simple chemical treatment after neutron irradiation, but the low SA restricts the useful therapeutic applications of ^{32}P produced by this method.

For these reasons, ^{32}P obtained by separation from the sulfur target irradiated in a fast neutron flux by the ^{32}S(n,p)^{32}P reaction ($\sigma = 0.068$b barn for fast neutrons) is currently used for the majority of research and clinical therapeutic applications. The ^{32}S(n,p)^{32}P nuclear reaction involves ejection of a charged particle which must overcome the Coulomb barrier and this reaction is thus favored with fast neutrons. However, the cross section of the ^{32}S(n,p)^{32}P reaction is only 0.068 barn for fast neutrons, and therefore, several hundred grams of sulfur are required for irradiation in order to provide a few hundred mCi of the ^{32}P product. Even though the cross-section values for the ^{32}S(n,p)^{32}P nuclear reaction are much lower than for the ^{31}P(n, γ)^{32}P route, the irradiation of ^{32}S targets is still of interest and utility because of the production of higher-SA ^{32}P. The isotopic composition of ^{nat}S consists of ^{32}S (95.02 %), ^{33}S (0.75 %), ^{34}S (4.21 %), and ^{36}S (0.02 %). It is imperative to

Table 5.7 Radionuclides produced by irradiation of natural sulfur with thermal and fast neutrons

Isotope of S	Isotopic abundance (%)	Activation products formed			
		Fast neutrons irradiation		Thermal neutrons irradiation	
		Nuclear reaction	Half-life	Nuclear reaction	Half-life
^{32}S	95.02	$^{32}S(n,p)^{32}P$	14.26 d	$^{32}S(n, \gamma)^{33}S$	Stable
^{33}S	0.75	$^{33}S(n,p)^{33}P$	25.3 d	$^{33}S(n, \gamma)^{34}S$	Stable
^{34}S	4.21	$^{34}S(n,p)^{34}P$	14.4 s	$^{34}S(n, \gamma)^{35}S$	87.2 d
^{36}S	0.02	$^{36}S(n,p)^{36}P$	5.9 s	$^{36}S(n, \gamma)^{37}S$	5.05 m

consider all the radionuclides produced both by thermal and fast neutrons when sulfur undergoes reactor irradiation; Table 5.7 summarizes the nuclear reactions which occur when natural sulfur undergoes irradiation with thermal and fast neutrons in a nuclear reactor.

From an analysis of the possible radionuclides formed by neutron irradiation of natural sulfur, only ^{35}S ($T_{1/2} = 87.2$ d) and ^{33}P ($T_{1/2} = 25.3$ d) are of concern and could be radiochemical impurities of the final ^{32}P product ($T_{1/2} = 14.28$ d). The ^{35}S levels contaminating the desired ^{32}P product are of concern, since they will be carried through the chemical separation process. The contribution of the longer-lived ^{33}P is a point of concern since separation from ^{32}P is not possible by traditional methods and it is not feasible to reduce the ^{33}P levels by cooling because of the longer half-life than ^{32}P. It has been experimentally observed that the ^{32}P and ^{33}P activity ratio produced in the same irradiation conditions is about 7000, because of the much lower isotopic abundance and low fast neutron cross section of the ^{33}S target as well as longer half-life of ^{33}P.

The bulk separation of only a few micrograms of ^{32}P from the bulk of ^{32}S must be conducted, and the ^{32}P SA obtained can be reduced by introduction of inactive phosphorous impurities during radiochemical processing. Due to the low neutron capture reaction cross section, significant large target irradiation volumes are required in the reactor for long periods of time in order to produce ^{32}P. The separation and purification of ^{32}P from irradiated S is usually carried out following wet chemical extraction and dry distillation methods. The wet extraction method consists of dissolution of irradiated powdered sulfur in boiling water in the presence of strong and weak acids to extract the phosphorus nuclide from the sulfur target using 2-octanol (Samsahl 1958; Razbash et al. 1991). One of the major impediments of this wet chemical extraction method is the dependence of extraction yield on the target sulfur particle size which is significantly decreased when the target is melted or solidified due to the exothermal heat generated during neutron irradiation. Additionally, the use of mineral acid is a major deterrent since its use introduces impurities and leaves solid waste behind which not only complicates the extraction process but also requires additional purification steps to achieve the required high chemical and radiochemical purity. The requirement of multistage processes results in poor recovery yields. Because of these drawbacks, the wet chemical extraction method is not often used for ^{32}P production.

The most widely used methods for the separation of ^{32}P from neutron-irradiated sulfur thus involve distillation methods, for instance, at 500 ° C in a nitrogen atmosphere in order to preclude the possibility of fire. Vacuum distillation of sulfur at 180–200 °C, which is lower than the sulfur ignition point, is conducted under a pressure of 1–10 mmHg (Gharemano et al. 1983; Yeh 1962). The distillation method has the advantage that high-purity products can be obtained since no reagents are added during the separation of ^{32}P from neutron-irradiated sulfur. The distillation method usually consists of a vacuum system, gas-feeding apparatus, and distillation assembly (Arrol 1953), in which pressure and temperature are optimally controlled (Gharemano et al. 1983; Yeh 1962; Arrol 1953; Alanis and Navarrete 2007; Karelin et al. 2000). Experimental setup for the radiochemical processing of irradiated elemental sulfur target is shown in Fig. 5.10.

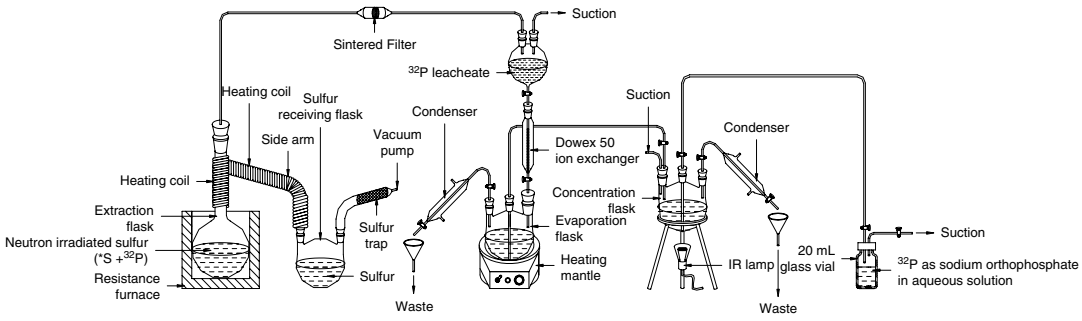

Fig. 5.10 Experimental setup for the radiochemical processing of irradiated elemental sulfur target

5.7.10 Praseodymium-143

Praseodymium-143 ($T_{1/2}$ = 13.57 d) is a long-lived medium-energy pure β⁻-emitting [$E_{\beta(max)}$ = 934 keV (100 %)] radionuclide useful for therapy. Although reactor production of ^{143}Pr can be performed by the ^{141}Pr(n, γ)^{142}Pr(n, γ)^{143}Pr double-neutron capture process, from this method the activated product consists of a ^{142}Pr and ^{143}Pr mixture, the proportion of which will depend on the irradiation duration and length of the post-irradiation decay period. For this reason, the indirect $^{142}\mathrm{Ce}(\mathrm{n},\gamma)^{143}\mathrm{Ce}\xrightarrow{\beta^-}{}^{143}\mathrm{Pr}$ reactor production route is preferred. A target cooling period of a few days is required to insure decay of the short-lived ^{143}Ce ($T_{½}$ = 33.04 h), which decays to ^{143}Pr. This production route provides NCA ^{143}Pr with high radionuclidic purity. Naturally occurring Ce is composed of ^{136}Ce (0.185 %), ^{138}Ce (0.251 %), ^{140}Ce (88.45 %), and ^{142}Ce (11.114 %). Neutron activation of natural CeO_2 would therefore lead to the formation of ^{143}Ce along with ^{139}Ce, ^{141}Ce, and ^{143}Ce as radionuclidic impurities. In order to reduce the radioactive burden from the irradiated target, use of enriched ^{142}Ce target is mandatory. The reaction cross section has a moderate value of 0.95 barn, which, coupled with the long half-life, not only necessitates long irradiation periods but also requires a high neutron flux irradiation to produce sufficient activity levels of ^{143}Pr (Vimalnath et al. 2005).

In a typical procedure, the irradiated $^{142}CeO_2$ target is dissolved in a mixture of 10 mL, conc. nitric acid and 1 mL 30 % H_2O_2, by gentle warming. The resultant clear solution is evaporated to near dryness and reconstituted in 50 mL of 1 M $NaBrO_3$ solution and the reaction vessel placed in a hot water bath maintained at 80 °C for about 10 min. After cooling over an ice bath, 2–10 mL saturated solution of HIO_3 is added with constant stirring to precipitate cerium as ceric iodate. The reaction mixture is then filtered through a sintered filter (G-2) wherein the precipitated ceric iodate is retained. The filtrate containing ^{143}Pr is evaporated to near dryness and reconstituted in minimum volume of 0.1 M HCI (Bakht and Sadeghi 2011).

5.7.11 Promethium-149

Promethium-149 ($T_{1/2}$ = 2.21 d) also emits moderate-energy β⁻ particles (1.07 MeV (95.9 %)) and a gamma ray with an energy of 286 keV (2.8 %) which can be readily imaged. Potential use of ^{149}Pm for radiotherapy has been studied (Hu et al. 2002; Mohsin et al. 2006; Lewis et al. 2004; Miller et al. 2005; Li et al. 2003). Since there are stable isotopes of Pm, direct neutron activation of targets is precluded. An alternative reactor production route involves the $^{148}\mathrm{Nd}(\mathrm{n},\gamma)^{149}\mathrm{Nd}\xrightarrow{\beta^-}{}^{149}\mathrm{Pm}$ reaction followed. The ^{149}Pm is then formed by β⁻ decay of the short-lived ^{149}Nd ($T_{½}$ = 1.73 h). Naturally occurring neodymium contains a mixture of the following seven stable isotopes: ^{142}Nd (27.2 %), ^{143}N (12.2 %), ^{144}Nd (23.8 %), ^{145}Nd (8.3 %), ^{146}Nd (17.2 %), ^{148}Nd (5.7 %), and ^{150}Nd (5.6 %). Because of the moderate thermal neutron cross section (2.5 barn) for the ^{148}Nd(n, γ)^{149}Nd

reaction, use of enriched ^{148}Nd is necessary to preclude contamination of ^{149}Nd with ^{147}Nd ($T_{1/2}$ = 10.98 d) produced by the ^{146}Nd(n, γ)^{147}Nd reaction (σ = 1.4 barn). Separation of ^{147}Nd in the irradiated target does not pose a problem since Nb can be effectively eliminated during the chemical separation steps, but the presence of Nb radioisotopes can significantly contribute radiation dose. The 1.73-h half-life of ^{149}Nd allows radiochemical processing of the irradiated target in less than 24 h EOB.

Promethium-149 can be chemically separated from neodymium following the reported solid-phase extraction procedure (Ketring et al. 2003). The separation is based on solid-phase extraction using a commercially available Ln Spec resin (50–100 μm) available from Eichrome, Inc., which is comprised of a solution of di(2-ethylhexyl)orthophosphoric acid (HDEHP) (40 % by weight) loaded onto the inert polymeric absorbent (60 % by weight) Amberchrom™ CG-71. The irradiated ^{148}Nd is dissolved in 0.15 N HCl and loaded onto a glass column containing 2 g of resin onto which both ^{148}Nd and ^{149}Pm are adsorbed. The ^{148}Nd is eluted at 0.5 M nitric acid followed by stripping of ^{149}Pm in 5 M nitric acid. The ^{149}Pm fractions are evaporated to dryness and redissolved in the desired solution, typically dilute HCl.

5.7.12 Rhenium-186

Rhenium-186 ($T_{1/2}$ = 90.64 h) is also a valuable reactor-produced therapeutic radionuclide which emits β^- particles with energies of 1069 keV (80 %), 932 keV (21.5 %), and 581 keV (5.8) and a gamma photon useful for imaging (137 keV, 8.6 %). The β^- particles have a range of 4.5 mm in soft tissue (Maxon et al. 1990) and ^{186}Re is an attractive radionuclide which was early evaluated for bone pain palliation. Rhenium-186 in the form of hydroxyethylidene diphosphonate (^{186}Re-HEDP) complex was thus developed as a bone-seeking radiopharmaceutical for use in patients with skeletal metastases (Lam et al. 2004; Minutoli et al. 2006; Kucuk et al. 2000; de Klerk et al. 1997). The relatively long physical half-life provides logistic advantages for transportation to users. The use of ^{186}Re for bone pain palliation is described in Chap. 12 and other applications and other chapters.

Rhenium-186 can be both reactor- and accelerator-produced. In a research reactor, ^{186}Re is produced by direct neutron activation of metallic rhenium-enriched ^{185}Re by the ^{185}Re(n, γ)^{186}Re nuclear reaction. Due to the relatively large nuclear reaction cross section (114 barn), the yield of ^{186}Re is high and the SA is moderate. Owing to the high epithermal neutron cross section for ^{185}Re (1632 barn), however, the activity obtained is usually higher depending upon the neutron energy spectrum of the reactor. Because of straightforward production and subsequent processing, this method is widely followed (Lewington 1996; Vucina and Han 2003; Sheybani et al. 2010).

The use of the Szilard–Chalmers process has also been reported as an alternative ^{186}Re production strategy, which provides ^{186}Re with higher SA (Zhang et al. 2000). This classical approach involves synthesis of the $ReN(S_2CNEt_2)_2$ rhenium complex and irradiation with thermal neutrons (neutron flux: 10^{12} n/s/cm^2) for 1 h. The recoiled radioactive rhenium atoms are separated by dissolving the irradiated rhenium compound from the target in dichloromethane solution and then stripping with an aqueous solution. The product is exclusively in perrhenate form with a SA of 0.72 GBq/mg Re (19.5 mCi/mg Re). Using a similar method developed by investigators at the Missouri University Research Reactor (MURR), the target usually consists of thin-film and powdered ^{185}Re in the form of metal or oxide with rhenium in a lower, relatively reduced oxidation state, which was irradiated with neutrons in the presence of an oxidizing medium sufficient to form a product nuclide in the higher oxidized state of perrhenate, ReO_4^-. Oxidation of the non-bombarded target nuclides is minimized by irradiating under vacuum, controlling the amount of oxidizing agent present, and cooling the target during irradiation. The ^{186}Re product nuclide is recovered by dissolving the perrhenate in a non-oxidizing solvent such as water or saline (Jia et al. 1999). This method reportedly produced ^{186}Re with an SA adequate for radioimmunotherapy and other nuclear therapeutic applications. Although

these approaches are interesting and yield high-SA ^{186}Re, the production yields are very low and would not be expected to be useful for providing the high ^{186}Re activity levels required for clinical applications. As an alternative, high activity levels of NCA ^{186}Re can be produced by accelerator methods as described in Chap. 6.

5.7.13 Rhenium-188

Rhenium-188 ($T_{1/2}$ = 16.9 h) is one of the most useful radionuclides for therapy and emits β⁻ particles (2.12 MeV, 71.1 % and 1.965 MeV, 25.6 %) and gamma photons (155 keV, 15.1 %) which are useful for imaging. The clinical efficacy of ^{188}Re has demonstrated for a broad range of therapeutic applications (Pillai et al. 2012; Jeong and Knapp 2008; Knapp et al. 1997; Lambert et al. 2009; Jeong and Chung 2003; Lambert and de Klerk 2006; Iznaga-Escobar 2001; Frier 2004; Dash et al. 2015a, b). The high beta energy results in a mean soft tissue range of ~3.5 mm. Relatively high-SA ^{188}Re can be directly produced by irradiation of enriched ^{187}Re by the ^{187}Re(n,γ)^{188}Re reaction, and NCA ^{188}Re is obtained by elution of the ^{188}W/^{188}Re generator fabricated from reactor-produced ^{188}W (Fig. 5.11). The development, operation, and use of the ^{188}W/^{188}Re generator system are described in Chap. 7, and the development of ^{188}Re-labeled radiopharmaceuticals and clinical applications are also discussed in several subsequent chapters.

Table 5.8 summarizes the nuclear constants available from literature for radionuclides involved in the ^{188}W production chain. In order to optimize the specific activity of ^{188}W, the prospect of irradiating the target at the highest available thermal neutron flux is necessary. Since the production yield for a successive double-neutron capture process is a function of the square of the neutron flux (ϕ), increasing the flux by only one order of magnitude will double the ^{188}W activity produced.

Reactor irradiation of ^{nat}Re yields a mixture of ^{186}Re and ^{188}Re (Vanderheyden et al. 1992); the proportion of each radioisotope depends on the irradiation duration and post-bombardment decay (Kothari et al. 1999). Radionuclidically pure ^{188}Re can be prepared by irradiating highly enriched ^{187}Re target in research reactors. The corresponding nuclear reaction cross section is 72 barn. The (n, γ) method of production using enriched ^{187}Re target leads to carrier-added (CA) ^{188}Re, and the specific activity is adequate for many applications, including preparation of ^{188}Re-phosphonates for bone pain palliation, synovectomy, agents for therapy of hepatocellular carcinoma, and for intravascular radionuclide

Table 5.8 Nuclear constants for radionuclides in the ^{188}W production chain

Nuclide	Decay constant, λ (s^{-1})	Cross section, σ (b)	Values for resonance integral, I (b)
^{186}W	–	37.9	485
^{187}W	8.09×10^{-6}	64.0	2760; 10
^{188}W	1.16×10^{-7}	12	0;50 000; 1.4
^{187}Re	—	76.4	300
^{188}Re	1.13×10^{-5}	<2	—

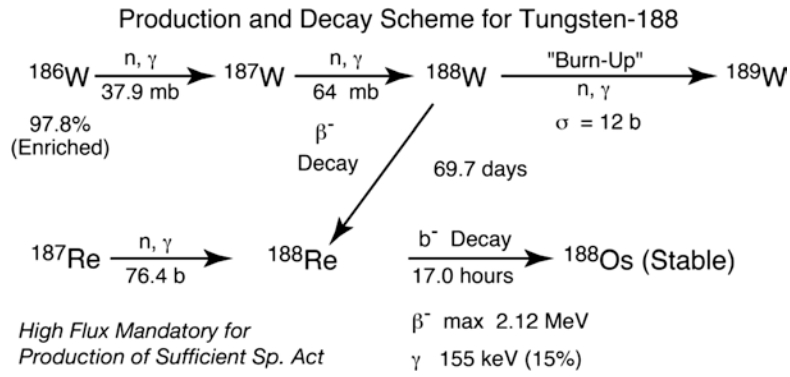

Fig. 5.11 Availability of ^{188}Re from reactor irradiation of ^{187}Re and from the ^{188}W/^{188}Re generator system

therapy (IVRT). However, preparation of other selected radiopharmaceuticals requires higher SA for radiolabeling of molecules such as peptides and antibodies which seek low-density targets such as receptors and tumor antigens which have a limited expression on tumor cells. In this context, the availability of generator-eluted ^{188}Re is an important capability to provide NCA ^{188}Re which would be suitable for preparation of radiopharmaceuticals useful for all applications.

Availability of ^{188}Re from a ^{188}W/^{188}Re generator is important since this capability provides a long-term source for NCA ^{188}Re for clinical applications on an on-demand basis. Access to ^{188}W is not available from accelerators and the parent radionuclide can only be practically produced by a double-neutron capture process with low neutron absorption cross-section values [^{186}W(n, γ)^{187}W ($\sigma = 37.9 \pm 0.6$ barn); ^{187}W(n, γ)^{188}W ($\sigma = 64 \pm 10$ barn)], using enriched ^{186}W targets. Since cross-section values are relatively low (~10^{-24} cm^2), the production yields are low even when very high flux research reactors are used (Dash et al. 2015a, b; Mirzadeh et al. 1992). Similarly, the neutron flux is a very important factor since production yields for the double-neutron capture process are a function of the square of the neutron flux (ϕ). Increasing the flux by only one order make thus result in production of two orders of magnitude higher activity level amounts of ^{188}W. For this reason, research reactors having thermal neutron flux values $> 5 \times 10^{14}$ n.cm^{-2}.sec^{-1} are only suitable for the ^{188}W production. The natural abundance of ^{186}W is 28.6 % and enriched targets are essential for the production of ^{188}W sufficient for generator use. By using enriched ^{186}W targets, the specific activity of ^{188}W is correspondingly augmented. Owing to a rather long physical ^{188}W half-life of 69 days, relatively long irradiation periods are required even for the production of ^{188}W of modest SA, even using high-flux reactors (Knapp et al. 1994; Pillai et al. 2012; Dash et al. 2015a, b). A specific activity of up to 185 GBq(5 Ci)/g can be obtained by using enriched targets and following an irradiation cycle of about 20–24 days at 10^{15} n.cm^{-2}.sec^{-1}. The current status of reactor production and processing of ^{188}W is summarized as a chapter of a recent book published by the International Atomic Energy Agency (IAEA) (Knapp et al. 2010; Dash et al. 2015a, b). As described in this detailed publication, ^{188}W having sufficiently high SA (>1 Ci/g W) suitable for the fabrication of ^{188}W/^{188}Re generators can be accomplished in only a limited number of the research reactors, the SM Reactor, RIAR, Dimitrovgrad, Russian Federation; the ORNL HFIR, USA; and the BR2 Reactor, Belgium. Enriched ^{186}W in metal as well as oxide form is used for irradiation. At ORNL, 97 % enriched ^{186}W as the oxide sealed in quartz tubes enclosed in aluminum capsules is irradiated for one or two cycles of 23–24 days each at a neutron flux of about 2.5×10^{15} n.cm^{-2}.s^{-1} (Callahan et al. 1992). The production yields (Fig. 5.12) are substantially lower than the calculated values using reported cross-section values for the different nuclear reactions. The loss of ^{188}W due to neutron burnup, ^{188}W(n, γ)^{189}W ($\sigma = 12$ barn), is one of the factors contributing to reduced production yields of ^{188}W (Mirzadeh et al. 1997). Sodium tungstate solution required for subsequent treatment for generator loading is prepared by dissolving irradiated tungsten oxide target in sodium hydroxide solution with moderate heating.

5.7.14 Rhodium-105

Rhodium-105 ($T_{1/2} = 35.4$ h) is a moderate-energy β$^-$-emitting radionuclide (0.566 and 0.248 MeV) which also emits low abundant γ rays at 319.2 (20 %) and 306 (5 %) keV. The β$^-$ particles have a maximum range in soft tissue ~ 0.89 mm and the weighted average β$^-$ energy of ^{105}Rh is similar to that of ^{131}I. The moderate-energy β$^-$ particles may be useful for treating small tumors (d ~ 1–2 mm) and the gamma ray emissions allow in vivo tracking. The 35.4-h half-life of ^{105}Rh is sufficient for the synthesis and shipment of potential radiopharmaceuticals. Rhodium exhibits high ligand stability with a number of bifunctional chelate moieties and forms kinetically inert complexes which are expected to be very stable in vivo (John et al. 1989). The nuclear properties of ^{105}Rh resemble properties exhibited by ^{67}Cu,

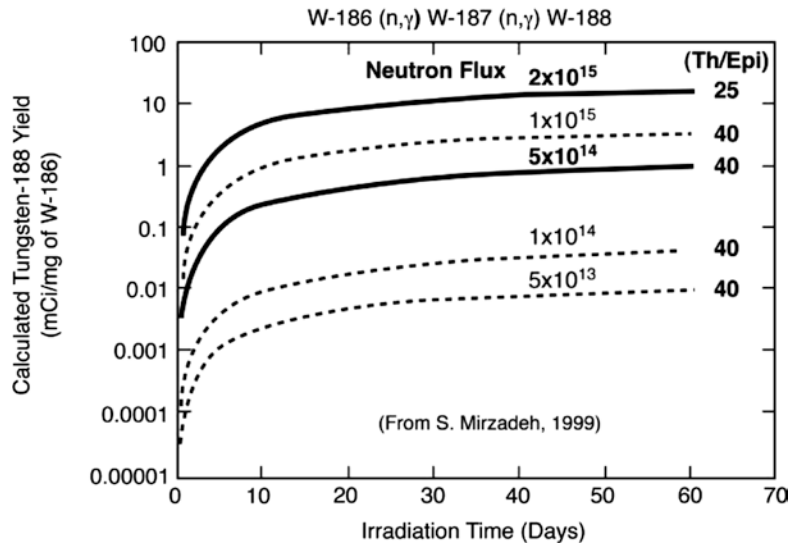

Fig. 5.12 Calculated reactor production yields of ^{188}W based on thermal neutron flux

which is a relatively difficult radionuclide to produce. The therapeutic potential of ^{105}Rh has been avidly studied (Pillai et al. 1990a, b, c; Lo et al. 1990; Li et al. 1997; Jurission et al. 1997; Ando et al. 2000; Brooks et al. 1999; Venkatesh et al. 1996; Goswami et al. 1999).

The potential of ^{105}Rh as a therapeutic radionuclide was first explored when high-specific-activity ^{105}Rh was produced using an enriched ^{104}Ru target via the indirect $^{104}\mathrm{Ru}(\mathrm{n},\gamma)^{105}\mathrm{Ru}\xrightarrow{\beta^-}{}^{105}\mathrm{Rh}$ reactor production route (Grazman and Troutner 1988). In this method an enriched ^{104}Ru target is irradiated with thermal neutrons in a reactor which undergo (n, γ) reaction to produce ^{105}Ru, which undergoes β⁻ decay with 4.4-h half-life to ^{105}Rh. Chemical separation is performed by treating the target with sodium hypochlorite in which Ru is oxidized to form RuO_4. The reaction mixture is distilled to collect RuO_4 in an HCl trap, maintaining ^{105}Rh in the +3 oxidation state. The ^{105}Rh remaining in the container is then heated to dryness and reconstituted with dilute HCl to provide an $RhCl_3$ solution (Jia et al. 2000). An alternative method consists of dissolution of the irradiated target in a mixture of KIO_4 and KOH in the presence of water (Unni and Pillai 2002). Solvent extraction with CCI_4 removes Ru followed by solvent extraction with tributyl phosphate (TBP) to remove traces of the ^{192}Ir impurity which is formed through activation of iridium impurities in the target. Production of NCA ^{105}Rh by the Szilard–Chalmers process using ruthenium acetylacetonate has also been reported but with limited success (Wong et al. 1989).

5.7.15 Samarium-153

Samarium-153 ($T_{1/2}$=46.27 h) decays by emission of β⁻ particles with a maximum energy of 0.8 MeV [$E_{\beta(\max)}$=808 keV(17.5 %), 705 keV (49.6 %), and 635 keV (32.2 %)] with an average soft tissue range of 0.3 mm. Emission of imageable γ rays with photon energies of 103 keV (28.3 %) and 70 keV (5.25 %) can be used for monitoring distribution as well as dosimetric estimations. Samarium-153 is one of the most widely preferred radionuclides for bone pain palliation (see Chap. 12), and commercially available ^{153}Sm-EDTMP (Quadramet®) is an approved clinical product in many countries. Many investigators feel that the medium-energy beta emissions of ^{153}Sm have an advantage compared to the much higher energy β⁻ particles emitted by ^{89}Sr and ^{32}P for bone pain palliation due to lower bone marrow toxicity. The overall gamma photon abundance is about 35 %, which is rather high, however, and generally a potential disadvantage for a therapeutic radionuclide.

Samarium-153 is reactor-produced by irradiation of enriched ^{152}Sm targets by the ^{152}Sm(n,γ)^{153}Sm nuclear reaction. Either Sm oxide or nitrate is used as a target material and the irradiated targets are dissolved in dilute hydrochloric acid. Owing to the large thermal neutron capture cross section of the ^{152}Sm(n,γ)^{153}Sm reaction (206 barn), ^{153}Sm can be produced in high activity levels with a specific activity of about 222 GBq/mg (6 Ci/mg) when irradiated at a flux of 1.2×10^{14} N cm^{-2} s^{-1} for approximately 155 h (Cutler et al. 2013). Natural samarium can also be used for the production of ^{153}Sm, and the product SA will still be sufficient for the preparation of low-SA radiopharmaceuticals used for bone pain palliation and synovectomy. However, use of natural targets will provide long-lived radionuclidic impurities, which include ^{145}Sm ($T_{1/2}=345$ days), ^{151}Sm ($T_{1/2}=90$ years), and ^{155}Eu ($T_{1/2}=4.76$ years), although some investigators feel that the radionuclidic impurity burden will not be high enough to preclude the use of the product for therapeutic applications (Ramamoorthy et al. 2002). Ion exchange chromatography can be used to separate ^{153}Sm from Eu radionuclides produced during the reactor irradiation process (Islami-Rad et al. 2011). The specific activity of ^{153}Sm produced is not sufficient, however, for use of ^{153}Sm for peptide or antibody labeling. Samarium-153 can also be used for radiation synovectomy of medium-sized joints, as described in Chap. 12. One major disadvantage for therapeutic use of ^{153}Sm is the rather short half-life ($T_{1/2}=46.28$ h) which may introduce constraints for the widespread use of ^{153}Sm-labeled radiopharmaceuticals.

5.7.16 Scandium-47

Scandium-47 ($T_{1/2}=3.35$ d) emits moderate-energy β$^-$ particle [$E_{\beta(max)}=441$ keV (68 %), 600 keV (32 %)] and imageable γ rays (159 keV, 68 %) and is a promising radionuclide for targeted radionuclide therapy. Scandium as the 3+ cation has favorable chemistry for chelation and attachment to various molecular targeting agents. This radionuclide is of interest for the preparation of specific therapeutic agents based on peptides/antibodies. There are two strategies for reactor production of carrier-free ^{47}Sc which include the ^{47}Ti(n,p)^{47}Sc reaction or the indirect radiative thermal neutron capture/β$^-$ decay ^{46}Ca(n, γ)^{47}Ca ($T_{½}=4.54$ d)$\beta^- \rightarrow {}^{47}$Sc route (Mausner et al. 1993). Since ^{47}Sc production using ^{47}Ti targets requires the ejection of a charged particle overcoming the Coulomb barrier, this reaction is favored with fast neutrons $En > 1$ MeV.

Production of ^{47}Sc following the $^{46}\mathrm{Ca}(\mathrm{n},\gamma)^{47}\mathrm{Ca} \xrightarrow{\beta^-} {}^{47}\mathrm{Sc}$ route is performed by reactor irradiation of an enriched ^{46}Ca target (natural abundance 0.004 %). The thermal neutron cross-section σ for the ^{46}Ca(n, γ)^{47}Ca reaction is only 0.74 barn. The advantage of this process includes the wide-scale availability of reactors with sufficiently high thermal neutron flux and the potential subsequent use of the ^{47}Ca/^{47}Sc generator system to provide ^{47}Sc. The principal impediment for use of ^{46}Ca targets is the exorbitant price of only 30 % enriched ^{46}Ca which is available. The enriched target must also be recovered and recycled in order to make the process cost-effective.

Although the production of ^{47}Sc by the ^{47}Ti(n,p)^{47}Sc route also requires an enriched target, the cost of highly enriched $^{47}TiO_2$ is much lower compared to ^{46}Ca. This route of production has also been extensively studied by several investigators (Mausner et al. 1998; Kolsky et al. 1998b; Pietrelli et al. 1992) but requires availability of a research reactor having a high fast neutron flux to obtain ^{47}Sc in practical quantities due to the low neutron cross section. Chemical processing of the irradiated TiO_2 target involves initial dissolution in hot sulfuric acid, evaporation, and then dissolution in water containing 0.3 % hydrogen peroxide to oxidize Ti to the Ti^{+4} state. This solution is then loaded onto a large cation exchange column in which the Ti is eluted with 1.0 and 2.0 N HCl. The ^{47}Sc is subsequently eluted with a mixture of 4.0 N HCl + 0.1 N HF, which is then evaporated to near dryness with 300 μL each of aqua regia followed twice by conc. HCl and finally by

30 % H_2O_2. The residue is then dissolved in water and loaded onto a second column to remove any final trace Ti target material and other trace metal impurities. The ^{47}Sc is finally eluted and evaporated (Kolsky et al. 1998a, b). In order to recover the enriched target material, the HCl fractions containing Ti from the cation exchange columns are combined and heated to boiling. The Ti is precipitated by pH adjustment to ~8 with NH_4OH and the solution is then filtered and the filtrate heated for 1 h at 400 °C for conversion to TiO_2 (Peitrelli et al. 1992).

Separation of Sc from processed Ti targets can also be accomplished using a solvent extraction technique. In this approach, Cupferron is added as an aqueous solution (100 mg/mL) and the Ti(IV) is then extracted as the cupferrate with 100 % chloroform. The extraction is rapid and requires only a 3 min contact period for complete equilibration. In order to obtain 98 % of Sc, five successive extraction steps are required and the ^{47}Sc remaining in the post-extraction solution is further purified by ion exchange (Pietrelli et al. 1992). The ^{47}Sc can also be adsorbed on a Dowex 50 cation exchange column and then eluted with 0.25 M ammonium acetate. Cyclotron production of ^{47}Sc has also reported via the ^{48}Ti(p,2n)^{47}Sc pathway using TiO_2 targets (98.5 % ^{48}Ti) with proton energies in the $48 < E_p < 150$ MeV region but with limited success (Mausner et al. 1998; Srivastava and Dadachova 2001; Kolsky et al. 1998a, b; DeNardo et al. 1999).

5.7.17 Silver-111

Silver-111 ($T_{1/2}$ 7.45 d) is a medium-energy β^--emitting therapeutic radionuclide which decays by β^- emission [$E_{\beta(max)} = 1036$ keV (92 %), 694 keV (7.1 %)] with associated gamma photons [$E\gamma = 342$ keV(6.7 %)]. Because of the favorable nuclear properties, ^{111}Ag may is of interest as a potential radionuclide for radiosynovectomy and radioimmunotherapy (Chattopadhyay et al. 2008). Naturally occurring Ag is composed of the ^{107}Ag (51.83 %) and ^{109}Ag(48.16 %) stable isotopes. Production of ^{111}Ag using natural Ag targets following the (n,γ) route is precluded owing to the formation of various other contaminating radioisotopes of Ag. The preferred reactor production of NCA ^{111}Ag involves irradiation of enriched ^{110}Pd with thermal neutrons by the ^{110}Pd(n,γ)^{111}Pd route followed by subsequent ^{111}Pd ($T_{1/2} = 23.4$ min) decay to ^{111}Ag. Because of the low-reaction ^{110}Pd thermal neutron cross section (0.226 barn) and long ^{111}Ag physical half-life, the use of enriched ^{110}Pd targets and irradiation at high thermal neutron flux is required. Use of the enriched target also eliminates production of ^{109}Pd ($T_{1/2} = 13.7$ h) by the ^{108}Pd(n,γ)^{109}Pd reaction ($\sigma = 8.55$ barn).

In the first step of a liquid–liquid extraction method for the separation of ^{111}Ag from irradiated natural palladium, the ^{111}Ag is extracted almost quantitatively, together with a small amount of palladium, from an aqueous solution into toluene by complexation with triphenylphosphine (Alberto et al. 1992). The ^{111}Ag is subsequently re-extracted selectively into a buffer solution. An ion exchange process has also been developed for the separation of NCA ^{111}Ag from neutron-irradiated natural palladium (Khalid et al. 2000). This method consists of loading the irradiated target in 0.01 M HCl on an ion exchange column containing alumina on which both Pd and ^{111}Ag are quantitatively retained. Palladium is removed by eluting with 0.1 M HCl and then ^{111}Ag is eluted with 4 M HCl. The potential therapeutic use of the medium-energy β^- particles emitted from ^{111}Ag may be a good strategy also because of the advantageous for imaging emission of low-abundance 342 keV photon (7.0 %). However, gold is a noble element and thus the chemistry for complexation of ^{111}Ag will be difficult and the complexes formed are expected to have limited stability.

5.7.18 Strontium-89

Strontium-89 ($T_{1/2} = 50.5$ d) is a pure beta emitter with a maximum β^- particle energy of 1.46 MeV. The maximum and average ranges in soft tissue are approximately 6.7 and 2.4 mm, respectively. Strontium-89 is one of the most commonly used radionuclides for treatment of bone pain palliation arising from skeletal metastasis which was first demonstrated in

1942 (Pecher 1942) and later subsequently corroborated by several researchers (Firusian and Schmidt 1973). Storntium-89 chloride was the first radionuclide approved by the US Food and Drug Administration (FDA) in 1993 for its routine application for treatment of bone pain palliation arising from skeletal metastasis (Pons et al. 1997; Robinson et al. 1995; Baranauskas et al. 2006; Crawford et al. 1994; Soffen et al. 1997; Jager et al. 2000). Strontium(II) is a biochemical analog of calcium (Group 2) and has the same biological transport mechanism. Following intravenous administration in chloride form, approximately 50 % of ^{89}Sr is localized in the bone, primarily in pain-generating regions of osteoblastic metastases (see Chap. 12). The maximum range in the bone of the high-energy β^- particles arising from ^{89}Sr decay does not exceed 7 mm, so the radiation effects are confined to the small area of the skeleton with minimum radiation burden on the marrow and nearby soft tissues. Since Sr is incorporated into the bone mineral structure, metabolism and release from the skeleton do not occur and ^{89}Sr remains localized for more than 100 days. About 80 % of ^{89}Sr is excreted through the kidneys and 20 % through the gastrointestinal system. The ^{89}Sr renal plasma clearance rate ranges from 4.1 to 12.8 % per day. The amount of ^{89}Sr taken up by the bone depends on and directly parallels the degree of osteoblastic metastatic bone involvement (Breen et al. 1992).

The two major ^{89}Sr production methods (Abalin et al. 2002) consists of neutron activation of enriched ^{88}Sr target following the ^{88}Sr(n, γ)^{89}Sr reaction and irradiation of ^{88}Sr targets by ^{89}Y(n,p)^{89}Sr reaction (Fig. 5.13).

Production of ^{89}Sr by irradiation of enriched ^{88}Sr targets is a simple production route performed in thermal neutron reactors and precludes any chemical separation but provides only low-SA ^{89}Sr, although almost no radioactive waste is generated. Natural strontium consists of stable ^{84}Sr (0.56 %), ^{86}Sr (9.9 %), ^{87}Sr (7.0 %), and ^{88}Sr (82.6 %) isotopes. Although the natural isotopic abundance of ^{88}Sr is very high (82.6 %), use of natural strontium target is precluded, owing to the formation of the long-lived/unwanted ^{85}Sr contaminant by the ^{84}Sr(n, γ)^{85}Sr reaction.

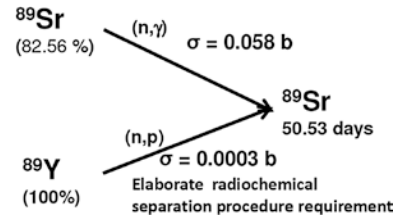

Fig. 5.13 Reactor production of ^{89}Sr

Schematic flowchart for the production ^{89}Sr following (n, γ) route is shown in Fig. 5.14.

In order to circumvent the co-production of undesirable levels of ^{85}Sr, highly enriched targets containing ^{88}Sr (>99.9 %) are used. The significantly low thermal neutron capture cross section (0.058 barn) for the ^{88}Sr(n, γ)^{89}Sr reaction, however, constitutes a major challenge that results in relatively low production yields of low-SA ^{89}Sr even when the irradiation is performed in a very high flux reactor, which in turn restricts the productivity of this method. The average activity obtained at Maria reactor (calculated at the activation end) is about 110 mCi (4.0 GBq)/g of Sr and that obtained at SM3 reactor (calculated at the activation end) is about 900 mCi (33 GBq) per target, i.e., 0.15–0.2 Ci (5.5–7.4 GBq)/g of strontium.

The second method in which high-specific-activity ^{89}Sr is obtained consists of the threshold reaction in fast-flux reactors with emission of charged particles based on the ^{89}Y(n,p)^{89}Sr reaction (Zvonarev et al. 1997; Karelin et al. 2000; Yu et al. 2003; Spahn et al. 2004; Mirz 1968). While this strategy permits use of natural ^{nat}Y (100 % abundance), such a pathway necessitates irradiation in the neutron flux of a nuclear reactor with a fast neutron spectrum and a radiochemical processing step for extraction of ^{89}Sr from the reaction mixture. One of the major impediments of this route is the low cross section of the (n,p) reaction on ^{89}Y, which is less than 0.0003 barn for fission spectrum. Production of ^{89}Sr by ^{89}Y(n,p)^{89}Sr is schematically show in Fig. 5.15. The technical issues associated with the separation of microscopic levels of ^{89}Sr from the macroscopic levels of the ^{89}Y target represent a challenging task. While the indirect ^{177}Lu production method resides at the interface between

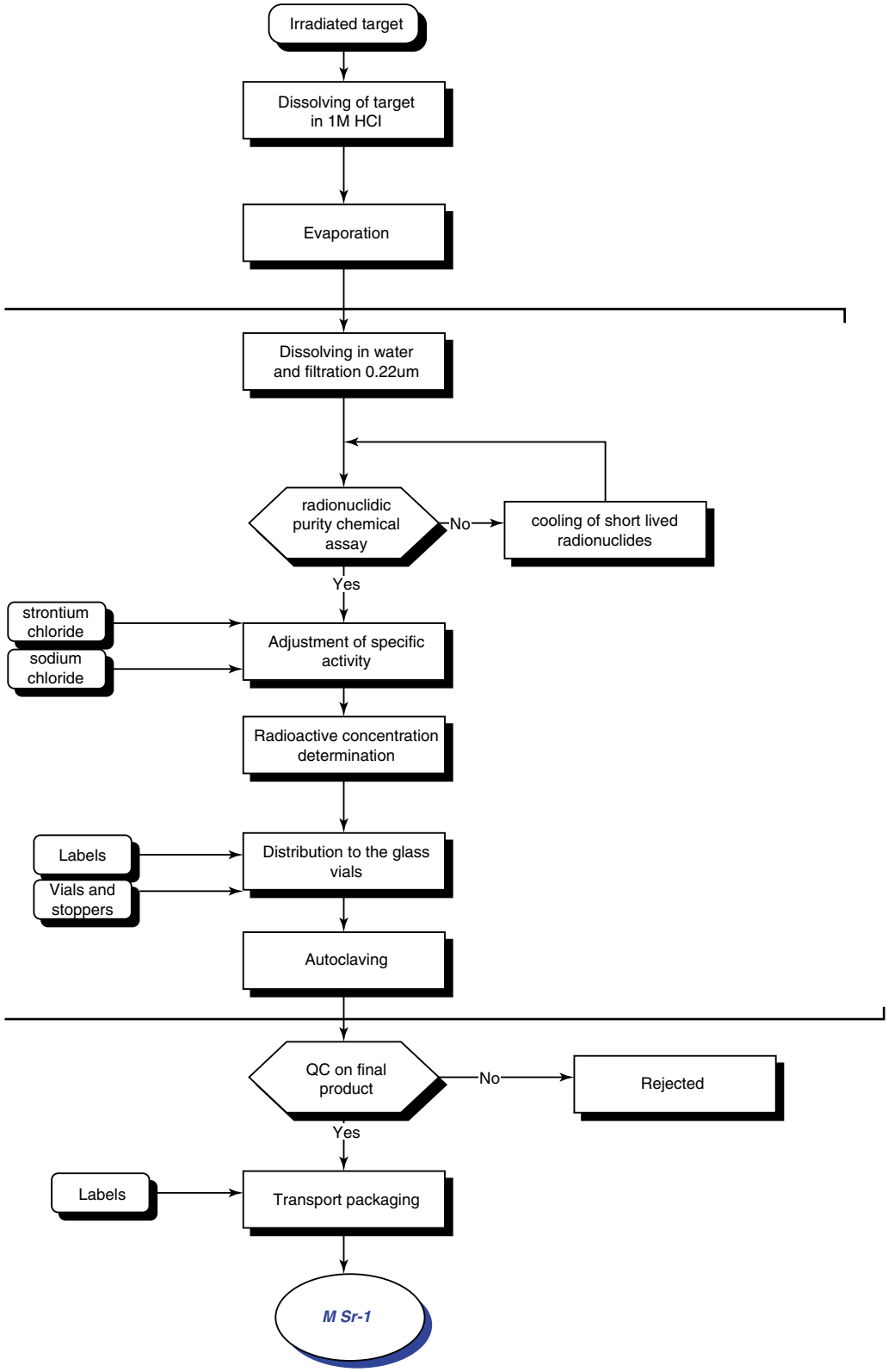

Fig. 5.14 Schematic flowchart for the processing of ^{89}Sr following (n,γ) route

many disciplines, the inherent determinant for the success of this production route lies on the selection of an appropriate Yb/Lu radiochemical separation.

In order to increase production yields of ^{89}Sr using this approach, neutron irradiation is conducted in reactors with a fast neutron spectrum. Thus, the low ^{89}Sr production yields and the necessity of using reactors which have fast neutron spectra are the major roadblocks for the potential success of this method. Although this thus appears to be a useful approach for ^{89}Sr production, unfortunately only few fast-flux reactors are available.

In order to mitigate these limitations, a new method for ^{89}Sr production using a solution reactor has been developed (Abalin et al. 2002; Yu et al. 2007) which is based on the decay of the gaseous ^{89}Kr radionuclide to ^{89}Sr. The ^{89}Kr produced as a result of the nuclear transformation of products in the $^{89}Se \rightarrow {}^{89}Br \rightarrow {}^{89}Kr \rightarrow {}^{89}Rb \rightarrow {}^{89}Sr$ decay chain of elements with mass 89. The reported method essentially consists of a solution nuclear reactor (Yu et al. 2007) in which inert gaseous fission fragments are produced and migrate to the free volume above the solution surface. The inert gaseous fission fragments are collected and allowed to decay for an appropriate time period and ^{89}Sr can then be separated. In this method, the ^{89}Kr production cross section is almost 500 times greater than for the neutron capture reaction. This new technology produces almost no radioactive waste with the advantage of high ^{89}Sr productivity.

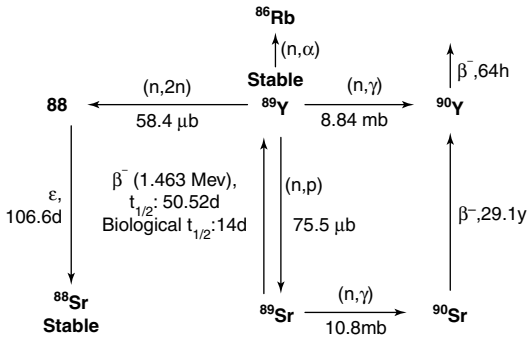

Fig. 5.15 Production of ^{89}Sr by the $^{89}Y(n,p)^{89}Sr$ route

5.7.19 Terbium-161

Terbium-161 ($T_{1/2}$ = 6.9 days) emits low-energy β^- particles [$E_{\beta(max)}$ = 593 keV (10.0 %), 567 keV (10.0 %), 518 keV (66.0 %), 461 keV (26.0 %)] with an average energy of 0.154 MeV and also gamma photons in low abundance [$E\gamma$ = 74 keV (9.8 %), 49 keV (14.8 %)]. The radionuclidic characteristics of ^{161}Tb are similar to ^{177}Lu; however, this radioisotope is also a good candidate for therapeutic applications. In addition, ^{161}Tb decays by conversion with the emission of Auger electrons. These conversion and Auger electrons have energy values between 3 and 50 keV and constitute 27 % of the beta energy which provides much higher local radiation dose density due to the shorter range in soft tissue (0.5–30 µm). For these reasons, ^{161}Tb provides a higher electron-to-photon dose ratio than ^{177}Lu. Due to the relatively short range of the β^- particles in soft tissue and consequently more localized radiation damage, ^{161}Tb can provide very high cytotoxicity and potentially therefore a greater therapeutic effect. The 3+ cation chemistry of terbium is similar to lutetium and is therefore compatible with existing radiolabeling techniques. The physical and chemical characteristics of ^{161}Tb provide the scope for improving existing radiolabeling chemistry, for therapeutic efficiency in terms of targeting strategies, and for the development of useful new radiopharmaceuticals. Although ^{161}Tb can be reactor-produced by double-neutron capture on natural terbium by the $^{159}Tb(2n, 2\gamma)^{161}Tb$ reaction, the SA available from this route is low since contamination of the ^{161}Tb with long-lived ^{160}Tb ($t_{½}$ = 72.3 days) cannot be avoided (Fig. 5.16).

The alternative reactor production route is via the $^{160}Gd\,(n,\gamma)^{161}Gd \xrightarrow{\beta^-} {}^{161}Tb$ reaction, which provides NCA ^{161}Tb (Fig. 5.17) (Lehenberger et al. 2011). This is the preferred ^{161}Tb reactor-based production route but must be carefully assessed because of the complexities of competing reactions and consequence for reduction of ^{161}Tb SA. The ^{161}Gd formed is short-lived

($T_{½}$ = 3.66 min) and essentially has decayed at the end of irradiation, providing radionuclidically pure ^{161}Tb. Radionuclide formed from the neutron activation of Gd target is shown in Fig. 5.17.

Use of highly enriched ^{159}Gd target material is absolutely necessary for ^{161}Tb production by this route, since activation of the following seven stable isotopes present in naturally occurring Gd as well as decay products will significantly reduce the SA of the desired ^{161}Tb: ^{152}Gd (0.20 %), ^{154}Gd (2.15 %), ^{155}Gd (14.73 %), ^{156}Gd (20.47 %), ^{157}Gd (15.68 %), ^{158}Gd (24.87 %), and ^{160}Gd (21.90 %), in which ^{160}Gd contributes only 21.9 %. Because of significant levels of ^{158}Gd (24.87 %), use of natural Gd for neutron irradiation leads to formation of stable ^{159}Tb as resulting from the $^{158}\mathrm{Gd}\,(\mathrm{n},\gamma)^{159}\mathrm{Gd}\xrightarrow{\beta^-}{}^{159}\mathrm{Tb}$ (stable) (σ = 2.3 barn) nuclear reaction. Presence of stable ^{159}Tb in the irradiated target will decrease the ^{161}Tb SA which is produced. Additionally, natural Gd is a neutron poison since it contains 15.68 % of ^{157}Gd with a very high thermal neutron cross section of 254,000 barn, leading to the production of ^{158}Gd by neutron capture. The ^{158}Gd thus formed will also undergo neutron capture to form ^{159}Tb as discussed above, leading to further reduction in ^{161}Tb SA. The activation of ^{159}Tb also leads to the accumulation of the relatively long-lived beta and photon emitter ^{160}Tb (T½ = 72.3 d), formed via the ^{159}Tb (n, γ)^{160}Tb reaction, which will also represent a radionuclidic impurity in the final product. For the above reasons, use of enriched ^{160}Gd is viewed as the necessary for the preparation of ^{161}Tb. Variation of specific activity of 161 Tb as a function of time when irradiated at a neutron flux of 10^{14} cm^{-2} s^{-1} is shown in Fig. 5.18. It is seen that theoretical specific activity of 161 Tb obtained is118.2 Ci/mg and 14 days irradiation period produce ~100 Ci/mg.

The decay of ^{161}Tb leads to the formation of stable ^{161}Dy which will also interfere in the complexation behavior of the final product. In order

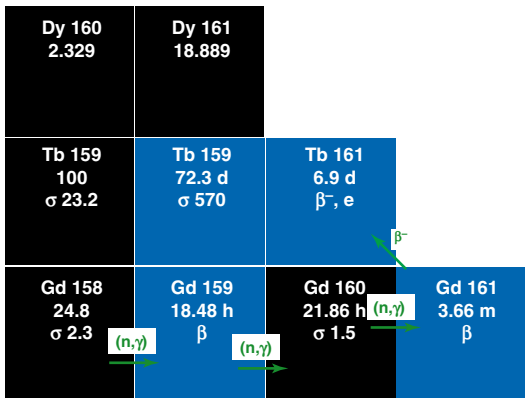

Fig. 5.16 Cutout from the chart of nuclides showing the production of ^{161}Tb

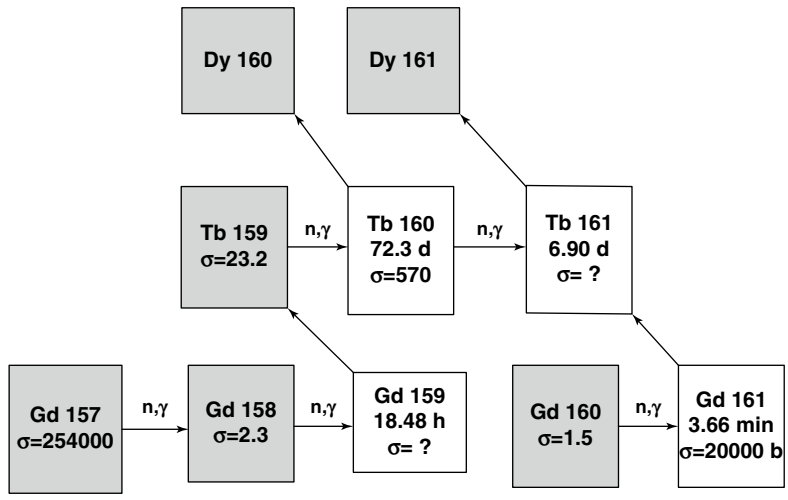

Fig. 5.17 Neutron activation of Gd target

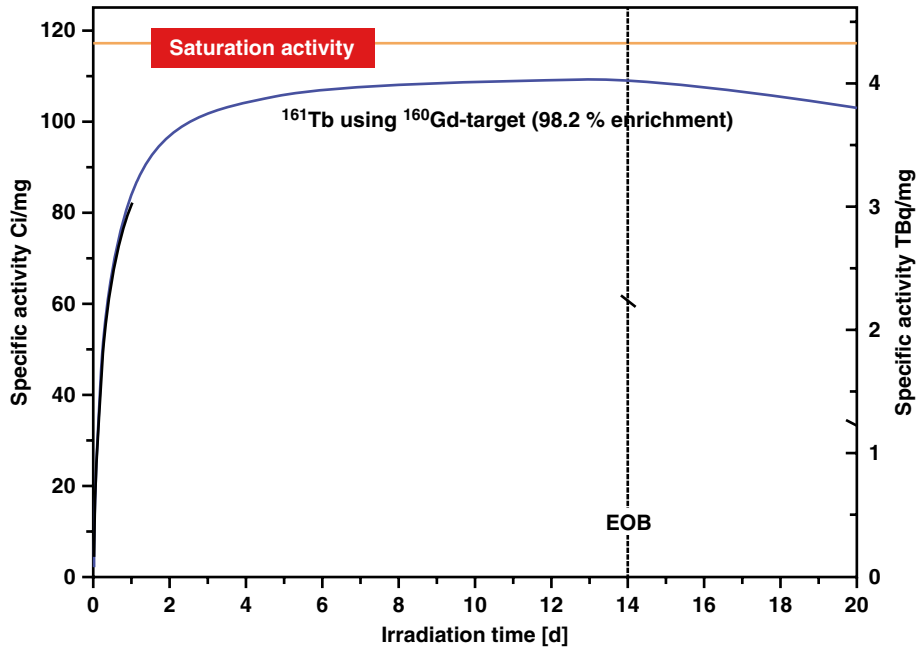

Fig. 5.18 Specific activity of ^{161}Tb as a function of time using neutron flux of 10^{14} cm^{-2} s^{-1}

to produce adequate activity levels of ^{161}Tb, the enriched ^{160}Gd target is irradiated, followed by an elaborate radiochemical process for the separation of ^{161}Tb from ^{60}Gd and ^{161}Dy. One process consists of dissolution of the irradiated material in 2–3 mL of a 0.05 M NH_4Cl solution (pH 3) followed by loading the resulting solution on a chromatographic column containing cation exchange resin Aminex A6 (Lehenberger et al. 2011). Separations are performed by isocratic elution of the column with 0.13 M α-hydroxyisobutyric acid (α-HIBA) at pH 4.5. The first elution peak containing Dy is discarded and the radioactive peak eluted corresponds to ^{161}Tb. The ^{161}Tb fractions collected are mixed with 1 M HCl solution adjusted the pH to ~1 and subjected to purification by loading the solution on a small secondary column filled with a Bio-Rad AG 50 W-X8 (200–400 mesh) cation exchanger in H^+ form. The column is washed with 5 mL of 1 M HCl solution and ^{161}Tb is finally eluted with 5 mL of 4 M HCl. The ^{161}Tb in HCl solution is evaporated to dryness and reconstituted with 0.04 M HCl suitable for radiolabeling reactions (de Jong et al. 1995).

5.7.20 Thulium-170

Thulium-170 ($T½ = 128.4$ d) is another radionuclidic which has properties suitable for therapeutic use and decays to stable ^{170}Yb by emission of β^- particles [$E_{\beta(max)} = 968$ keV] and emission of a gamma photon [$E\gamma = 84$ keV (3.26 %)] suitable for imaging and dosimetry. The yield (3.26 %) and energy (84 keV) of the gamma photon are well within the range for safe use in humans. The ^{170}Tm is produced in sufficient quantities by the ^{169}Tm(n, γ)^{170}Tm reaction by thermal neutron bombardment on natural Tm (mononuclidic, 100 % ^{169}Tm). The high thermal neutron capture cross section of $\sigma = 109$ barn for ^{169}Tm (Danon et al. 1998) and resonance integral $\sigma_{RI} = 1548$ barn (Van der Linden et al. 1974) present the possibility for reactor production of high activity levels of ^{170}Tm with sufficient SA using medium-flux research reactors. The potential use of this radionuclide for development of a bone pain palliative radiopharmaceutical has been explored (Das et al. 2009a, b, c; Simindokht 2010).

5.7.21 Tin-117 m

Tin-117 m ($T_{1/2}$ = 13.6 d) decays by isomeric transition with the emission of 3 three major monoenergetic conversion electrons with energies of 127, 129, and 152 keV, in 65 %, 12 %, and 26 % abundance, respectively. These electrons have high LET with discrete penetration ranges of between 0.22 (127 keV) and 0.29 mm (152 keV) in water. Emission of a gamma photon with the optimal energy of 159 keV also allows gamma camera imaging. Tin-117 m have been proposed for therapeutic applications which includes the use of ^{117m}Sn-DTPA for palliative treatment of bone pain from of metastatic disease (see Chap. 12) and for treatment of other inflammatory conditions such as active atherosclerotic disease (Srivastava 2012). For bone pain palliation, the minimal tissue penetration is felt by some investigators to be an important characteristic of ^{117m}Sn which results in reduced myelosuppression and greatly reduced radiation dose to normal organs compared with the use of high-energy β^--emitting radioisotopes for this application (Krishnamurthy et al. 1997; Bishayee et al. 2000; Swailem et al. 1998; Srivastava et al. 1998; Srivastava and Dadachova 2001; Srivastava 2004; 2007). In addition, ^{117m}Sn has also been proposed for other therapeutic applications, which include radiation synovectomy, radioimmunotherapy, and cardiovascular applications (Srivastava 2010; 2006; Ermolaev et al. 2009). The relatively longer 13.6-day half-life also provides sufficient time to prepare and distribute the ^{117m}Sn-labeled radiopharmaceuticals to sites distant from the production facility.

Reactor production is possible by either the radiative ^{116}Sn(n, γ)^{117m}Sn (Fukushima et al. 1963; Knapp et al. 1998; Mausner et al. 1992; Mirzadeh et al. 2011; Ponsard et al. 2009; Toporov et al. 2005; Yano et al. 1973) or inelastic ^{117}Sn(n n',γ)^{117m}Sn pathways (Mirzadeh et al. 1997). The low (6 ± 2 mbarn) cross section (~2 mCi/mg) for the neutron capture reaction emerged as the major deterrent that does not permit production of high-specific-activity ^{117m}Sn and provides only low-SA ^{117m}Sn. The neutron elastic scattering route is the threshold production strategy which occurs with fast neutrons (En > 0.1 MeV) (Mirzadeh et al. 2011). For reactor production using a fast neutrons flux, production of ^{117m}Sn has been reported using the SM reactor at the Research Institute of Atomic Reactors (RIAR) in Dimitrovgrad, Russia, where fast neutron fluxes up to 2×10^{15} cm^{-2}s^{-1} are available. Because of the poor reaction cross section of this reaction, several successive irradiation cycles using 92 % enriched ^{117}Sn target are required to obtain the highest SA. This had been the preferred route which provided the highest SA ^{117m}Sn until alternative accelerator production strategies had been recently developed as described in Chap. 6.

5.7.22 Ytterbium-175

Yttribium-175 ($T_{½}$ = 4.2 d) is another promising radionuclide for radiotherapy and decays by emission of β^- particles with a maximum energy of 480 keV (86.5 %) to stable ^{175}Lu. In addition, gamma photons with energies of 113 keV (1.9 %), 282 keV (3.1 %), and 396 keV (6.5 %) are also emitted. The abundance values for gamma photons emitted from ^{175}Yb are lower compared to the gamma emissions from other radiolanthanides used in nuclear medicine such as ^{153}Sm, ^{177}Lu, and ^{166}Ho. Therefore, the expected potential patient radiation dose burden arising from the ^{175}Yb gamma emission is expected to be relatively insignificant. The comparatively longer half-life of ^{175}Yb provides logistic advantages which can be considered as an important merit, particularly for those countries with limited radioisotope production facilities. The therapeutic utility of ^{175}Yb is being explored by several groups (Chakraborty et al. 2002; 2006a, b, c; Mathew et al. 2004; Safarzadeh et al. 2012). Ytterbium-175 with specific activity adequately high for many targeted radiotherapeutic applications can be produced by using natural ytterbium targets. The isotopic composition of natural Yb is summarized in Table 5.9.

Table 5.9 Isotopic composition of natural Yb

Isotope	% Natural abundance	σ (barn) for (n, γ) reaction	Products
^{168}Yb	0.14	2300	$^{169}\mathrm{Yb} \xrightarrow[T_{1/2}=32\mathrm{d}]{\mathrm{EC}} {}^{169}\mathrm{Tm}_{(\mathrm{stable})}$
^{170}Yb	3.11	10	^{171}Yb (stable)
^{171}Yb	14.43	53	^{172}Yb (stable)
^{172}Yb	21.87	1	^{173}Yb (stable)
^{173}Yb	16.22	17	^{174}Yb (stable)
^{174}Yb	31.59	69	^{175}Yb (β^-, $T_{1/2}$=4.2 d)
^{176}Yb	12.62	2.4	$^{177}\mathrm{Yb} \xrightarrow[T_{1/2}=6.17\mathrm{h}]{\beta^-} {}^{177}\mathrm{Lu}$

The simplified ^{175}Yb production scheme is

$$^{174}\mathrm{Yb}(\mathrm{n},\gamma)^{175}\mathrm{Yb} \xrightarrow[T_{1/2}=4.2d]{\beta^-} {}^{175}\mathrm{Lu}_{(\mathrm{stable})} \quad (\sigma = 69\ \mathrm{b}).$$

Reactions leading to the formation of radionuclidic impurities from thermal neutron bombardment on natural ytterbium target include

$$^{168}\mathrm{Yb}\ (\mathrm{n},\gamma)^{169}\mathrm{Yb} \xrightarrow[T_{1/2}=32\mathrm{d}]{\mathrm{EC}} {}^{169}\mathrm{Tm}_{(\mathrm{stable})},$$
$$\sigma = 2300\ \mathrm{b}$$

$$^{176}\mathrm{Yb}(\mathrm{n},\gamma)^{177}\mathrm{Yb} \xrightarrow[T_{1/2}=1.9\mathrm{d}]{\beta^-} {}^{177}\mathrm{Lu} \xrightarrow[T_{1/2}=6.17h]{\beta^-} {}^{177}\mathrm{Hf}_{(\mathrm{stable})},$$
$$\sigma = 2.4\ \mathrm{b}$$

Of the two possible radionuclidic impurities, ^{169}Yb ($T_{1/2}$=32 d) decays by electron capture process (100 % K electron capture) followed by the emission of Auger electrons of low yield (Firestone and Shirley 1995). It is thus envisaged that the presence of low activity levels of ^{169}Yb would not be expected to impose significant limitations for the in vivo application of ^{175}Yb. On the other hand, the presence of ^{169}Yb could also be useful in extended studies of the pharmacological characteristics of the ^{175}Yb-labeled radiopharmaceuticals in biological systems. One major impediment may be the co-production of significant activity levels of ^{177}Lu (half-life 6.7 days) as the major radionuclidic impurity. Although an electro-amalgamation approach has been reported to obtain radionuclidically pure ^{175}Yb by the separation from ^{175}Lu (Chakraborty et al. 2008b), it remains to be seen that such an approach is practical and cost-effective.

5.7.23 Yttrium-90

Yttrium-90 ($T_{1/2}$=64.1 h) is a pure β^--particle-emitting radionuclide with well-established applications in targeted therapy. There are several advantages for use of ^{90}Y as a therapeutic radionuclide, since it exhibits a suitable physical half-life (~64 h) and decays to the stable ^{90}Zr daughter product by emission of high-energy ($E_{\beta\max}$ 2.28 MeV) β^- particles. Yttrium exhibits relatively simple ion chemistry since the suitability of the Y^{+3} metal is well established for forming complexes with a variety of chelating agents. The availability of ^{90}Y and applications have been broadly described in the literature (Walker 1964; IAEA Report 2009; Montaña et al. 2012). The clinical use of ^{90}Y has been reported in detail for use in radiation for synovectomy (see Chap. 14) (Kampen et al. 2007; Miszczyk et al. 2007; Taylor et al. 1997; Asavatanabodee et al. 1997; Winfield and Gumpel 1979), for treatment of hepatocellular carcinoma (see Chap. 11) (Sato 2011; Kan et al. 2012; Lau et al. 2011), for peptide receptor radionuclide therapy (see Chap. 10) (Dumont et al. 2015; Villard et al. 2012; Nisa et al. 2011; Teunnissen et al. 2006), and for therapy of non-Hodgkin's lymphoma (Hagenbeek 2003; Dillman 2006; Emmanouilides 2009; Zinzani et al. 2008; Gisselbrecht et al. 2007; Chapuy et al. 2007; Cheung et al. 2006; Weigert et al. 2006; Cheson 2005; Micallef 2004). In 2002, ibritumomab tiuxetan (Zevalin®) was approved by the US FDA for radioimmunotherapy of patients with relapsed or refractory low-grade, follicular, or CD20+ transformed B-cell NHL and rituximab-refractory follicular NHL (Morschhauser et al. 2008, 2013; Weigert et al. 2006; Ibatici et al. 2014; Provencio et al. 2014).

Yttrium-90 can be directly produced by neutron activation of ^{89}Y in a nuclear reactor, and since yttrium is mononuclidic, there is no requirement for use of an enriched isotope for target fabrication. The radionuclidic purity of this directly activated product is generally very high. However, depending on the reactor epithermal flux, detectable levels of ^{89}Sr can be detected and are generated by the (n,p) reaction. The (n,γ) reactor production yields of ^{90}Y of low SA, result from the low ^{89}Y neutron absorption cross section (0.001 barn) (IAEA 2010). Yttrium-90 of moderate SA can only be produced by ^{89}Y target irradiation of the target in high-flux reactors. However, NCA ^{90}Y is required for the preparation of labeled antibodies and peptides used for targeted therapy (IAEA 2010) and can be alternatively reactor-produced by the $^{90}Zr(n,p)^{90}Y$ reaction using 100 % enriched ^{90}Zr target and a fast neutron flux of ~7.5×10^{13} cm^{-2} s^{-1} (Abassi et al. 2006). Although this method obviously holds promise as a viable approach, there are several issues related to the long-term availability and cost of enriched ^{90}Zr. In addition, the requirement for a fast neutron flux, the R&D associated with target design, and the need for separation of ^{90}Y and ^{90}Zr recycling are important issues which must be addressed. The activity levels of ^{90}Y produced by this route will also be limited.

Separation of ^{90}Y in NCA form from ^{90}Sr by use of a radionuclide generator system is the most appealing process to obtain large amounts of ^{90}Y (see Chap. 7). Strontium-90 is a major ^{235}U fission product with a fission yield of 5.93 % and can be isolated from aqueous nuclear fuel reprocessing of high-level liquid waste (HLLW) solutions (IAEA 2010; Wester et al. 2003; Ramanujam et al. 2000; Beard and Moore 1969; Bray 1961; Orth et al. 1994; Horwitz et al. 1991; Lumetta et al. 1993; Lange et al. 1957). The ^{90}Sr purity requirements for medical applications are very high, and extensive quality controls are essential. The separation of NCA ^{90}Y from ^{90}Sr has been a challenging task owing to the necessity of maintaining ^{90}Sr contamination levels as low as possible in ^{90}Y preparations for therapeutic applications; since ^{90}Sr localizes in the skeleton and because of its long physical half-life, it has a very low maximum permissible body burden of 74 kBq (2 μCi) over patient lifetime (National Bureau of Standards Handbook 1963). A variety of $^{90}Y/^{90}Sr$ separation approaches have thus been extensively evaluated for isolation of very high chemical and radiochemically pure ^{90}Y from ^{90}Sr, which include precipitation, solvent extraction, ion exchange chromatography, extraction chromatography, electrophoresis, membrane-based separation, electrodeposition, etc. (IAEA Report 2009; Montaña et al. 2012; Chakravarty et al. 2012a, b, Castillo et al. 2010). A review of $^{90}Sr/^{90}Y$ generator separation technologies (see Chap. 7) which have been explored indicates that the automated electrochemical $^{90}Sr/^{90}Y$ generator recently described (Chakravarty et al. 2012a, b; Kamadhenu 2010) may offer efficient adaption for use in centralized radiopharmacies to provide routine availability of ^{90}Y having the necessary quality and quantity over a sustained period (estimated as >10 years). Ensuring successful utilization of ^{90}Y for targeted therapy demands quantitative estimation of Bq levels of ^{90}Sr impurity in GBq quantities of ^{90}Y and should be within the pharmacopeia-established limit. The reported EPC concept (Pandey et al. 2008) which combines chelate-based extraction with partition chromatography is attractive as it would exploit the ability of 2-ethyl hexyl-2-ethylhexyl phosphonic acid (KSM-17) for real time QC. A key challenge for QC analysis of potential ^{90}Sr levels in the ^{90}Y product is the lack of emitted photons from decay of these two radioisotopes. For this reason, other strategies must be adopted.

5.8 Auger Electron-Emitting Radioisotopes

In addition to primarily beta-emitting radionuclide, several Auger electron-emitting radionuclides which deposit very high energy during short path length decay in biological soft tissue (Chap. 4) are also primarily be reactor-produced.

5.8.1 Iodine-125

Iodine-125 ($T_{1/2}$ = 60 d) decays by electron capture and emission of photons with energies of 35.5-keV γ-ray, a 31.1-keV Kβ X-ray (26 %), and a 27.4 keV Kα X-ray (113 %) with an average photon energy of ~ 28.5 keV. A number of Auger electrons are also emitted, and the use of ^{125}I to probe the properties of Auger electron emitters for targeted therapy has been a major area of research (see Chap. 4). Despite being neutron deficient, ^{125}I is a unique radioisotope for which large-scale reactor production is possible. While a paper describing the use of the stable XeF_2 solid xenon target has been reported (Kiss et al. 1969), the general ^{125}I production route is through the neutron irradiation of ^{124}Xe gas to form ^{125}Xe followed by decay to form ^{125}I (Harper et al. 1963). The isotopic compositions of the nine stable isotopes of xenon are depicted in Table 5.10 and both natural Xe and enriched ^{124}Xe have been used for ^{125}I production.

Table 5.10 Isotopic composition of different isotopes of natural xenon

Xe Isotopes	% Abundance
^{124}Xe	0.095
^{126}Xe	0.089
^{128}Xe	1.91
^{129}Xe	26.4
^{130}Xe	4.07
^{131}Xe	21.2
^{132}Xe	26.9
^{134}Xe	10.4
^{136}Xe	8.86

Different isotopes formed during the neutron irradiation of natural xenon are depicted in Fig. 5.19. Although the isotopic abundance of ^{124}Xe in natural targets (0.096 %) is an inherent disadvantage, relatively high neutron adsorption cross section of ^{124}Xe (σ_{th} = 128 ± 15 barn and resonance activation integral of 3600 ± 500 barn) is highly attractive because of which reasonable yields of the final product can be obtained. While using a natural Xe target, the radioactivity levels of co-produced radionuclide impurities could be viewed as disadvantages, but their contributions can be marginalized if the length of irradiation and the time of cooling of the target after irradiation are chosen prudently (Martinho et al. 1984). A facile approach for the production of ^{125}I from the neutron-irradiated natural Xe target using wet chemical distillation method is described by Joshi et al. (Joshi et al. 2012). Neutron irradiation of enriched ^{124}Xe target followed by the dry-distillation route is the preferred method commonly pursued by the commercial manufacturer (Boussoufi et al. 2008; Hassal 1997).

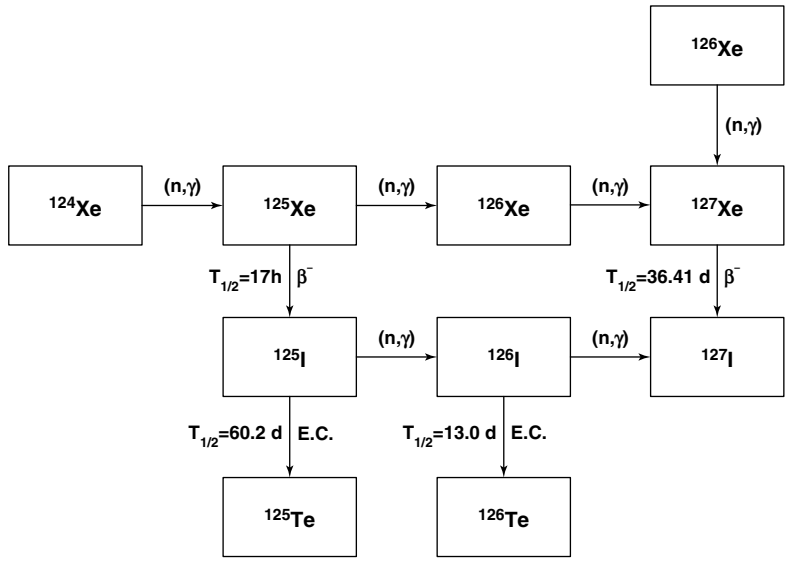

Fig. 5.19 Neutron irradiation of enriched ^{124}Xe

5.9 Summary

Research reactors continue to play a crucial and absolutely necessary role for the production of a large variety of radioisotopes for medical applications. Especially for most therapeutic applications, where beta-particle decay is required, neutron-rich radionuclides require strong neutron sources for their production. The IAEA (Manual 2003) maintains a database which currently documents the operation of about 256 research reactors worldwide (i.e., distinctly different species than power reactors). Many of these reactors have sufficient thermal neutron flux and irradiating facilities available for medical radioisotope production. Nearly without exception, the costs of reactors licensing, construction, and operation have been always been subsidized by national/federal governments. With the recent episodes of seriously reduced availability of fission-produced ^{99}Mo, and thus ^{99m}Tc required from the ^{99}Mo/^{99m}Tc generator systems (Dash et al. 2015a, b), the availability and costs of reactor irradiation services are being reassessed, to implement new cost models moving away from the traditional subsidies. It is thus crucially important that scientific investigators working in the radioisotope production and radiopharmaceutical development and manufacturing communities in association with their commercial and clinical partners are aware and support the continued, updating, and optimized operation of these facilities.

References

Abbasi I, Ishfaq M, Sohaib M. Preparation and preclinical study of ^{177}Lu-labelled hydroxyapatite for application in radiation synovectomy of small joints. Q J Nucl Med Mol Imaging. 2011;55:458–68.

Abbasi IA, Zaidi JH, Arif M, Waheed S, Subhani MS. Measurement of fission neutron spectrum averaged cross sections of some threshold reactions on zirconium: production possibility of no-carrier-added ^{90}Y in a nuclear reactor. Radiochim Acta. 2006;94:381–4.

Abalin S, Vereschagin Y, Grigoriev G, et al. Method of strontium-89 Radioisotope production. United States Patent US 6,456,680; 2002.

Ahmad S, Mannan A, Ahmad I, Qureshi IH. Radiochemical separation of ^{99}Mo, 99mTc and ^{131}I from irradiated uranium. Int J Appl Radiat Isot. 1982;33:469–72.

Alanis J, Navarrete M. Optimal parameters to produce ^{131}I by neutron irradiation and melting of sintered tellurium dioxide. Nucl Inst Meth Phys Res A. 1999; 422:10–5.

Alanis J, Navarrete M. Industrial production and purification of ^{32}P by sulfur irradiation with partially moderated neutron fluxes and target melting. J Radioanal Nucl Chem. 2007;273:659–62.

Alberto R, Bläuenstein P, Novak-Hofer I, et al. An improved method for the separation of ^{111}Ag from irradiated natural palladium. Int J Radiat Appl Inst A Appl Radiat Isot. 1992;43:869–72.

Al-Janabi MAA, Kadem AHM. Radiochemical separation of ^{131}I from irradiated natural uranium and tellurium dioxide by solvent extraction using dibenzo-18-crown-6. Int J Radiat Appl Inst A. 1990; 41:787–8.

Alvarez RD, Partridge EE, Khazaeli MB, et al. Intraperitoneal radioimmunotherapy of ovarian cancer with ^{177}Lu-CC49: a phase I/II study. Gynecol Oncol. 1997;65:94–101.

Ambade RN, Shinde SN, Khan MSA, et al. Development of a dry distillation technology for the production of ^{131}I using medium flux reactor for radiopharmaceutical applications. J Radioanal Nucl Chem. 2015;303: 451–67.

Ambrosetti MC, Colato C, Dardano A, Monzani F, Ferdeghini M. Radioiodine ablation: when and how. Q J Nucl Med Mol Imaging. 2009;53(5):473–81.

Ando A, Ando I, Tonami N, et al. Production of ^{105}Rh-EDTMP and its bone accumulation. Appl Radiat Isot. 2000;52:211–5.

Appelbaum FR, Brown PA, Sandmaier BM, et al. Specific marrow ablation before marrow transplantation using an aminophosphonic acid conjugate ^{166}Ho-EDTMP. Blood. 1992;80:1608–13.

Arrol WJ. Apparatus for large scale production of phosphorus-32. Nucleonics. 1953;11:26–8.

Asavatanabodee P, Sholter D, Davis P. Yttrium-90 radiochemical synovectomy in chronic knee synovitis: a one year retrospective review of 133 treatment interventions. J Rheumato. 1997;24(4):639–42.

Bahrami-Samani A, Bagheri R, Jalilian AR, et al. Production, quality control and pharmacokinetic studies of Ho-EDTMP for therapeutic applications. Sci Pharm. 2010;78:423–33.

Bakht MK, Sadeghi M. Internal radiotherapy techniques using radiolanthanide praseodymium-142: a review of production routes, brachytherapy, unsealed source therapy. Ann Nucl Med. 2011;25:529–35.

Bakker WH, Breeman WA, Kwekkeboom DJ, et al. Practical aspects of peptide receptor radionuclide therapy with [^{177}Lu][DOTA^0, Tyr^3]octreotate. Q J Nucl Med Mol Imaging. 2006;50:265–71.

Baranauskas Z, Valuckas K, Aleknavicius E, et al. Use of strontium-89 in the analgesic treatment of cancer patients with bone metastases. Medicina (Kaunas). 2006;42:11–4.

Beard SJ, Moore RL. Large-scale recovery and purification of fission products. In: Stevenson CE, Mason EA, Gresky AT, editors. Progress in nuclear energy (series

III), process chemistry, vol. 4. London: Pergamon Press; 1969. p. 645.
Beyer G-J, Pimentel-Gonzales G. Physicochemical and radiochemical aspects of separation of radioiodine from TeO-targets. Radiochim Acta. 2000;88:175–8.
Bilewicz A, Zuchowska K, Bartos B. Separation of Yb as $YbSO_4$ from ^{176}Yb target for production of ^{177}Lu via the $^{176}Yb(n, \gamma)^{177}Yb \rightarrow {}^{177}Lu$ process. J Radioanal Nucl Chem. 2009;280:167–9.
Bishayee S, Rao DV, Srivastava SC, et al. Marrow-sparing effects of Sn-117m (4+)DTPA for radionuclide therapy of cancer in bone. J Nuc Med. 2000;41:2043–50.
Blower PJ, Lewis JS, Zweit J. Copper radionuclides and radiopharmaceuticals in nuclear medicine. Nucl Med Biol. 1996;23:957–80.
Bodei L, Cremonesi M, Grana CM, et al. Peptide receptor radionuclide therapy with ^{177}Lu-DOTATATE: the IEO phase I-II study. Eur J Nucl Med Mol Imaging. 2011;38:2125–35.
Bokhari TH, Ahmad M, Khan IU. Separation of no-carrier-added arsenic-77 from neutron irradiated germanium. Radiochim Acta. 2009;97:503–6.
Bomanji JB, Wong W, Gaze MN, Cassoni A, Waddington W, Solano J, Ell PJ. Treatment of neuroendocrine tumours in adults with ^{131}I-MIBG therapy. Clin Oncol (R Coll Radiol). 2003;15:193–8.
Bonardi M, Gallorini M, Groppi F, et al. N.C.A. Gold-199: a radionuclide suitable for both spect and radionuclide therapy: production yield, radiochemical separation, radionuclidic purity and specific activity. J Label Compd Radiopharm. 2001;44:S767–9.
Boussoufi M, Flocchini R G, Lagunas-Solar MC, et al. Development of a large-scale Iodine-125 production at UC Davis's MNRC, Proc of ANS embedded topical meeting "Isotopes for Medicine and Industry" in Anaheim, 9–12 June 2008. p. 905–6. (Retrieved from: http://escholarship.org/uc/item/2zs5039m).
Bouvier M, Bouysset M, Bonvoisin B, et al. Erbium-169 synoviortheses and infiltrations of triamcinolone hexacetonide in metatarsophalangeal arthritis of chronic inflammatory rheumatism. Rev Rhum Mal Osteoarti. 1983;50:267–71.
Bray LA. The recovery and purification of multi-kilocurie quantities of fission product strontium by cation exchange, Rep. HW-70998. Richland: Hanford Atomic Products Operation; 1961.
Bryan JN, Bommarito D, Kim DY, et al. Comparison of systemic toxicities of ^{177}Lu-DOTMP and ^{153}Sm-EDTMP administered intravenously at equivalent skeletal doses to normal dogs. J Nucl Med Technol. 2009;37:45–52.
Breeman WA, de Jong M, Visser TJ, et al. Optimising conditions for radiolabelling of DOTA-peptides with ^{90}Y, ^{111}In and ^{177}Lu at high specific activities. Eur J Nucl Med Mol Imaging. 2003;30:917–20.
Breen SL, Powe JE, Porter AT. Dose estimation in strontium-89 radiotherapy of metastatic prostatic carcinoma. J Nucl Med. 1992;33:1316–23.
Breitz HB, Wendt RE, Stabin MS, et al. ^{166}Ho-DOTMP radiation-absorbed dose estimation for skeletal targeted radiotherapy. J Nucl Med. 2006;47:534–42.
Brooks RC, Carnochan P, Vollano JF, et al. Metal complexes of bleomycin: evaluation of [Rh-105]-bleomycin for use in targeted radiotherapy. Nucl Med Biol. 1999;26:421–30.
Callahan AP, Mirzadeh S, Knapp Jr FF. Large-scale production of tungsten-188. Radioact Radiochem. 1992;3:46–8.
Castillo AX, Pérez-Malo M, Isaac-Olivé K, et al. Production of large quantities of ^{90}Y by ion-exchange chromatography using an organic resin and a chelating agent. Nucl Med Biol. 2010;37:935–42.
Castellani MR, Chiti A, Seregni E, Bombardieri E. Role of ^{131}I-metaiodobenzylguanidine (MIBG) in the treatment of neuroendocrine tumours. Experience of the National Cancer Institute of Milan. Q J Nucl Med. 2000;44:77–87.
Chakraborty S, Das T, Banerjee S, et al. Preparation and preliminary biological evaluation of a ^{166}Ho labeled polyazamacrocycle for possible use as an intravascular brachytherapy (IVBT) agent. Appl Radiat Isot. 2006a;64:462–9.
Chakraborty S, Unni PR, Banerjee S, et al. Potential ^{166}Ho radiopharmaceuticals for intravascular radiation therapy (IVRT)-I: [(166)Ho] holmium labeled ethylene dicysteine. Nucl Med Biol. 2001;28:309–17.
Chakraborty S, Das T, Banerjee S, et al. ^{177}Lu-EDTMP: a viable bone pain palliative in skeletal metastasis. Cancer Biother Radiopharm. 2008a;23:202–13.
Chakraborty S, Das T, Banerjee S, et al. Preparation and preliminary biological evaluation of ^{177}Lu-labelled hydroxyapatite as a promising agent for radiation synovectomy of small joints. Nucl Med Commun. 2006b;27:661–8.
Chakraborty S, Das T, Sarma HD, Venkatesh M, Banerjee S. Preparation and preliminary studies on ^{177}Lu-labeled hydroxyapatite particles for possible use in the therapy of liver cancer. Nucl Med Biol. 2008b;35:589–97.
Chakraborty S, Vimalnath KV, Lohar SP, et al. On the practical aspects of large-scale production of ^{177}Lu for peptide receptor radionuclide therapy using direct neutron activation of ^{176}Lu in a medium flux research reactor: the Indian experience. J Radioanal Nucl Chem. 2014;302:233–43.
Chakraborty S, Das T, Sarma HD, et al. Comparative studies of ^{177}Lu-EDTMP and ^{177}Lu-DOTMP as potential agents for palliative radiotherapy of bone metastasis. Appl Radiat Isot. 2008c;66:1196–205.
Chakraborty S, Unni PR, Venkatesh M, Pillai MRA. Feasibility study for production of ^{175}Yb: a promising therapeutic radionuclide. Appl Radiat Isot. 2002;57:295–301.
Chakraborty S, Das T, Banerjee S, et al. ^{175}Yb-labeled hydroxyapatite: a potential agent for use in radiation synovectomy of small joints. Nucl Med Biol. 2006c;33:585–91.
Chakravarty R, Chakraborty S, Chirayil V, Dash A. Reactor production and electrochemical purification of ^{169}Er: a potential step forward for its utilization in in vivo therapeutic applications. Nucl Med Biol. 2014;41:163–70.
Chakravarty R, Das T, Dash A, Venkatesh M. An electro-amalgamation approach to isolate no-carrier-added

^{177}Lu from neutron irradiated Yb for biomedical applications. Nucl Med Biol. 2010;37:811–20.
Chakravarty R, Dash A, Pillai MRA. Availability of yttrium-90 from strontium-90: a nuclear medicine perspective. Cancer Biother Radiopharm. 2012a;27:621–41.
Chakravarty R, Ram R, Jagdeesan KC, et al. Polymer embedded nanocrystalline titania: a new generation sorbent for the separation of ^{77}As from Ge for biomedical applications. Chromatographia. 2011;74:531–40.
Chakravarty R, Das T, Venkatesh M, Dash A. An electroamalgamation approach to produce ^{175}Yb suitable for radiopharmaceutical applications. Radiochim Acta. 2012b;100:255–61.
Chanda AN, Kan P, Watkinson LD, et al. Radioactive gold nanoparticles in cancer therapy: therapeutic efficacy studies of GA-198AuNP nanoconstruct in prostate tumor-bearing mice. Nanomedicine. 2010;6:201–9.
Chapuy B, Hohloch K, Trümper L. Yttrium 90 ibritumomab tiuxetan (Zevalin): a new bullet in the fight against malignant lymphoma? Biotechnol J. 2007;2: 1435–43.
Chattopadhyay S, Pal S, Vimalnath KV, Das MK. A versatile technique for radiochemical separation of medically useful no-carrier-added (nca) radioarsenic from irradiated germanium oxide targets. Appl Radiat Isot. 2007;65:1202–7.
Chattopadhyay S, Vimalnath KV, Saha S, et al. Preparation and evaluation of a new radiopharmaceutical for radiosynovectomy,^{111}Ag-labelled hydroxyapatite (HA) particles. Appl Radiat Isot. 2008;66:334–9.
Chattopadhyay S, Saha-Das S. Recovery of ^{131}I from alkaline solution of n-irradiated tellurium target using a tiny Dowex-1 column. Appl Radiat Isot. 2010;68:1967–9.
Cheson BD. The role of radioimmunotherapy with yttrium-90 ibritumomab tiuxetan in the treatment of non-Hodgkin lymphoma. BioDrugs. 2005;19:309–22.
Cheung MC, Haynes AE, Stevens A, et al. Yttrium 90 ibritumomab tiuxetan in lymphoma. Leuk Lymphoma. 2006;47:967–77.
Chinol M, Cutler CS, Papi S, et al. Production of GMP-compliant lutetium-177: radiochemical precursor for targeted cancer therapy. Nucl Med Biol. 2010;37:717.
Constan R. Production de ^{131}I sans porteur a partir d'acide tellurique. J Inorg Nucl Chem. 1958;7:133–9.
Crawford ED, Kozlowski JM, Debruyne FM, et al. The use of strontium 89 for palliation of pain from bone metastases associated with hormone-refractory prostate cancer. Urology. 1994;44:481–5.
Cutler CS, Hennkens HM, Sisay N, et al. Radiometals for combined imaging and therapy. Chem Rev. 2013; 113:858–83.
Cyclotron produced radionuclides: physical characteristics and production. Technical reports series no. 468. Vienna: An International Atomic Energy Agency (IAEA) publication; 2009.
Dadachova E, Mirzadeh S, Lambrecht RM, et al. Separation of carrier-free Holmium-166 from neutron-irradiated dysprosium targets. Anal Chem. 1994; 66:4272–7.
Dadachova E, Mirzadeh S, Lambrecht RM, et al. Separation of carrier-free^{166} Ho from Dy_2O_3targets by partition chromatography and electrophoresis. J Radioanal Nucl Chem. 1995;199:115–23.
Dadachova E, Mirzadeh S, Smith SV, et al. Radiolabeling antibodies with holmium-166. Appl Radiat Isot. 1997;48:477–81.
Das NR, Banerjee K, Chatterjee K, Lahiri S. Separation of carrier-free 199Au as a β-decay product of 199Pt. Appl Radiat Isot. 1999;50:643–7.
Das T, Chakraborty S, Sarma HD, et al. ^{166}Ho-labeled hydroxyapatite particles: a possible agent for liver cancer therapy. Cancer Biother Radiopharm. 2009a; 24:7–14.
Das T, Chakraborty S, Sarma HD, et al. Preparation of ^{166}Ho-oxine-lipiodol and its preliminary bioevaluation for the potential application in therapy of liver cancer. Nucl Med Commun. 2009b;30:362–7.
Das T, Chakraborty S, Unni PR, et al. ^{177}Lu-labeled cyclic polyaminophosphonates as potential agents for bone pain palliation. Appl Radiat Isot. 2002;57:177–84.
Das T, Chakraborty S, Sarma HD, et al. ^{170}Tm-EDTMP: a potential cost-effective alternative to $^{89}SrCl_2$ for bone pain palliation. Nucl Med Biol. 2009c;36:561–8.
Dash A, Pillai MR, Knapp Jr FF. Production of ^{177}Lu for targeted radionuclide therapy: available options. Nucl Med Mol Imaging. 2015a;49:85–107.
Dash A, Chakravarty R, Knapp FF (R), Pillai MR. Indirect production of No Carrier Added (NCA) ^{177}Lu from Irradiation of Enriched ^{176}Yb: options for Ytterbium/Lutetium separation. Curr Radiopharm. 2015b;8(2):107–18.
Danon Y, Werner CJ, Youk G, et al. Neutron total cross-section measurements and resonance parameter analysis of holmium, thulium, and erbium from 0.001 to 20eV. Nucl Sci Eng. 1998;128:61–9.
de Jong M, Breeman WA, Bernard BF, et al. Evaluation in vitro and in rats of ^{161}Tb-DTPA-octreotide, a somatostatin analogue with potential for intraoperative scanning and radiotherapy. Eur J Nucl Med. 1995;22:608–16.
De Klerk JM, Zonnenberg BA, Blijham GH, et al. Treatment of metastatic bone pain using the bone seeking radiopharmaceutical Re-186-HEDP. Anticancer Res. 1997;17:1773–7.
Delpassand ES, Samarghandi A, Zamanian S, et al. Peptide receptor radionuclide therapy with ^{177}Lu-DOTATATE for patients with somatostatin receptor-expressing neuroendocrine tumors: the first US phase 2 experience. Pancreas. 2014;43:518–25.
DeNardo SJ, DeNardo GL, Kukis DL, Shen S, Kroger LA, DeNardo DA, Goldstein DS, Mirick GR, Salako QA, Mausner LF, Srivastava SC, Meares CF. ^{67}Cu-21T-BAT-Lym-1 pharmacokinetics, radiation dosimetry, toxicity and tumor regression in patients with lymphoma. J Nucl Med. 1999;40:302–9.
Dewaraja YK, Schipper MJ, Roberson PL, et al. ^{131}I-tositumomab radioimmunotherapy: initial tumor dose–response results using 3-dimensional dosimetry including radiobiologic modeling. J Nucl Med. 2010;51:1155–62.

Dillman RO. Radioimmunotherapy of B-cell lymphoma with radiolabelled anti-CD20 monoclonal antibodies. Clin Exp Med. 2006;6:1–12.

Dumont RA, Seiler D, Marincek N, et al. Survival after somatostatin based radiopeptide therapy with ^{90}Y-DOTATOC vs. ^{90}Y-DOTATOC plus ^{177}Lu-DOTATOC in metastasized gastrinoma. Am J Nucl Med Mol Imaging. 2015;5:46–55.

Dvorakova Z, Henkelmann R, Lin X, Türler A, Gerstenberg H. Production of ^{177}Lu at the new research reactor FRM-II: irradiation yield of ^{176}Lu(n, gamma)^{177}Lu. Appl Radiat Isot. 2008;66:147–51.

El-Absy MA, El-Garhy MA, El-Amir MA, Fasih TW, El-Shaha MF. Separation and purification of ^{131}I from neutron irradiated tellurium dioxide targets by wet-distillation method. Sep Purif Technol. 2010;71:1–12.

El-Azony KM, Mohty AA, Salah M. Separation and purification of ^{131}I from tellurium material using ion exchange for preparing tetra-butyl ammonium iodide ^{131}I. Appl Radiat Isot. 2004;61:1185–8.

Elom Achoribo AS, Akaho EH, Nyarko BJ, Osae Shiloh KD, Odame Duodu G, Gibrilla A. Feasibility study for production of I-131 radioisotope using MNSR research reactor. Appl Radiat Isot. 2012;70:76–80.

Emran A, Hosain F, Spencer RP, Kolstad KS. Synthesis and biodistribution of radioarsenic labeled dimethylarsinothiols: derivatives of penicillamine and mercaptoethanol. Int J Nucl Med Biol. 1984;11:259–61.

Emran AM, Phillips DR. Biomedical use of arsenic radioisotopes new trends in radiopharmaceutical synthesis. In: New trends in radiopharmaceutical synthesis, quality assurance, and regulatory control. New York: Plenum Press; 1991. p. 153–68.

Emmanouilides C. Review of Y-ibritumomab tiuxetan as first-line consolidation radio-immunotherapy for B-cell follicular non-Hodgkin's lymphoma. Cancer Manag Res. 2009;1:131–6.

Ermolaev SV, Zhuikov BL, Kokhanyuk VM, et al. Production of no-carrier added Tin-117m from proton irradiated antimony. J Radioanal Chem. 2009;280:319–24.

Erdtmann G. Neutron activation tables. Weinheim: Verlag Chemie; 1976.

Esser JP, Krenning EP, Teunissen JJ, et al. Comparison of [177Lu-DOTA(0), Tyr(3)]octreotate and [177Lu-DOTA(0), Tyr(3)]octreotide: which peptide is preferable for PRRT? Eur J Nucl Med Mol Imaging. 2006;33:1346–51.

Ezziddin S, Sabet A, Ko YD, et al. Repeated Radionuclide therapy in metastatic paraganglioma leading to the highest reported cumulative activity of ^{131}I-MIBG. Radiat Oncol. 2012;7:8.

Ferro-Flores G, Hernández-Oviedo O, Arteaga de Murphy C, et al. ^{166}Dy/^{166}Ho hydroxide macroaggregates: an *in vivo* generator system for radiation synovectomy. Appl Radiat Isot. 2004;61:1227–33.

Ferro-Flores G, Arteaga de Murphy C, Pedraza-López M, et al. Labeling of biotin with ^{166}Dy/^{166}Ho as a stable *in vivo* generator system. Int J Pharm. 2003;255:129–38.

Firusian N, Schmidt CG. Radioactive strontium for treatment incurable pain in skeletal neoplasm. Dtsch Med Wochenschr. 1973;98:2347–51.

Firestone RB, Shirley VS. Table of isotopes, vol. 2. 8th ed. New York: Wiley; 1995.

Frier M. Rhenium-188 and copper-67 radiopharmaceuticals for the treatment of bladder cancer. Mini Rev Med Chem. 2004;4:61–8.

Fukushima S, Hayashi S, Kume S, et al. The production of high specific activities of tin. Bull Chem Soc Japan. 1963;36(10):1225–8.

Gedik GK, Hoefnagel CA, Bais E, Olmos RA. ^{131}I-MIBG therapy in metastatic phaeochromocytoma and paraganglioma. Eur J Nucl Med Mol Imaging. 2008;35:725–33.

Gharemano AR, Najafi R, Nejad V, et al. Preparation of ortho-phosphoric acid/H3 32P O4/for application in medicine and agriculture in iran. Radiochem Radioanal Lett. 1983;58:49–53.

Giovanella L. Thyroglobulin-guided ^{131}I ablation in low-risk differentiated thyroid carcinoma: is the yardstick accurate enough? Head Neck. 2011;33:1379–80.

Gisselbrecht C, Bethge W, Duarte RF, et al. Current status and future perspectives for yttrium-90(^{90}Y)-ibritumomab tiuxetan in stem cell transplantation for non-Hodgkin's lymphoma. Bone Marrow Transplant. 2007;40:1007.

Goldenberg DM, Sharkey RM. Advances in cancer therapy with radiolabeled monoclonal antibodies. QJ Nucl Med Mol Imaging. 2006;50:248–64.

Goswami N, Nef W, Alberto R, et al. Rhodium-105 tetrathioether complexes: radiochemistry and initial biological evaluation. Nucl Med Biol. 1999;26:951–7.

Grazman B, Troutner DE. ^{105}Rh as a potential radiotherapeutic agent. Int J Rad Appl Instrum A. 1988;39:257–60.

Gulenchyn KY, Yao X, Asa SL, Singh S, Law C. Radionuclide therapy in neuroendocrine tumours: a systematic review. Clin Oncol (R Coll Radiol). 2012;24:294–308.

Gumpel JM, Matthews SA, Fisher M. Synoviorthesis with erbium-169: a double-blind controlled comparison of erbium-169 with corticosteroid. Ann Rheum Dis. 1979;38:341–3.

Hainfeld JF. A small gold-conjugated antibody label: Improved resolution for electron microscopy. Science. 1987;236:450–3.

Hainfeld JF. Gold cluster-labelled antibodies. Nature. 1988;333:281–2.

Hainfeld JF, Foley CJ, Srivastava SC, et al. Radioactive gold cluster immunoconjugates:potential agents for cancer therapy. Int J Rad Appl Instrum B. 1990;17:287–94.

Hagenbeek A. Radioimmunotherapy for NHL: experience of Y-ibritumomab tiuxetan in clinical practice. Leuk Lymphoma. 2003;44:S37–47.

Harper PV, Siements WD, Lathrop KA, et al. Production and use of Iodine 125. J Nucl Med. 1963;4:277–89.

Hashimoto K, Matsuoka H, Uchida S. Production of no-carrier-added ^{177}Lu via the ^{176}Yb(n, γ)^{177}Yb$\rightarrow$^{177}Lu process. J Radioanal Nucl Chem. 2003;255:575–9.

Hassal SB. Method and apparatus for production of radioactive iodine. U.S. Patent No. 5633900. 27 May 1997.

Hong YD, Park KB, Jang BS, et al. Holmium-166-DTPA as a liquid source for endovascular brachytherapy. Nucl Med Biol. 2002;29:833–9.

Hong YD, Choi SJ, Choi SM, Jang BS. The availability of contrast media in the application of Holmium-166-DTPA for vascular brachytherapy. Nucl Med Biol. 2004;31:225–30.

Horwitz EP, Mc Alister DR, Bond AH, Barrans RE, Williamson JM. A process for the separation of ^{177}Lu from neutron irradiated ^{176}Yb targets. Appl Radiat Isot. 2005;63:23–36.

Horwitz EP, Dietz ML, Fisher DE. SREX: A new process for the extraction and recovery of strontium from acidic nuclear waste streams. Solv Extr Ion Exch. 1991;9:1–25.

Hosain F, Emran A, Spencer RP, Clampitt KS. Synthesis of radioarsenic labeled dimethylchloroarsine for derivation of a new group of radiopharmaceuticals. Int J Appl Radiat Isot. 1982;33:1477–8.

Hu F, Cutler CS, Hoffman T, et al. Pm-149 DOTA bombesin analogs for potential radiotherapy. In vivo comparison with Sm-153 and Lu-177 labeled DO3A-amide-betaAla-BBN(7–14)NH(2). Nucl Med Biol. 2002;29:423–30.

Ibatici A, Pica GM, Nati S, et al. Safety and efficacy of ^{90}Yttrium-ibritumomab-tiuxetan for untreated follicular lymphoma patients. An Italian cooperative study. Br J Haematol. 2014;164:710–6.

International Atomic Energy Agency (IAEA). Production of long lived parent radionuclides for generators: ^{68}Ge, ^{82}Sr, ^{90}Sr and ^{188}W, IAEA radioisotopes and radiopharmaceuticals series, vol. 2. Vienna: International Atomic Energy Agency (IAEA); 2010.

Islami-Rad SZ, Shamsaei M, Gholipour-Peyvandi R, et al. Reactor production and purification of ^{153}Sm radioisotope via ^{nat}Sm target irradiation. Radiochemistry. 2011;53:642–5.

Iznaga-Escobar N. Direct radiolabeling of monoclonal antibodies with rhenium-188 for radioimmunotherapy of solid tumors-a review of radiolabeling characteristics, quality control and in vitro stability studies. Appl Radiat Isot. 2001;54:399–406.

Jager PL, Kooistra A, Piers DA. Treatment with radioactive ^{89}strontium for patients with bone metastases from prostate cancer. BJU Int. 2000;86:929–34.

Jennewein M, Schirrmacher R, Maus S, et al. Macroscopic synthesis of arsenoorganic precursors and first no-carrier-added radioarsenic labelling. J Lab Comp Radiopharm. 2003;46:42.

Jennewein M, Qaim SM, Hermanne A, et al. A new method for radiochemical separation of arsenic from irradiated germanium oxide. Appl Radiat Isot. 2005;63:343–51.

Jennewein M, Hermanne A, Mason RP, et al. A new method for the labelling of proteins with radioactive arsenic isotopes, Nuclear Instruments and Methods in Physics Research Section A: Accelerators, Spectrometers, Detectors and Associated Equipment, Volume 569, Issue 2, Proceedings of the 3rd International Conference on Imaging Technologies in Biomedical Sciences – Innovation in Nuclear and Radiological Imaging: from Basic Research to Clinical Application, 20 Dec 2006. p. 512–7.

Johnsen AM, Heidrich BJ, Durrant CB, et al. Reactor production of ^{64} Cu and ^{67} Cu using enriched zinc target material. J Radioanal Nucl Chem. 2015;305:61–71.

Jia W, Ehrhardt GJ. Production of ^{186}Re, ^{188}Re and other radionuclides via inorganic Szilard-chalmers process, United States Patent No. 5,862,193 dt. 01/19/1999; 1999.

Jia BW, Ma D, Volkert EW, et al. Production of No-Carrier-Added ^{105}Rh from Neutron Irradiated Ruthenium Target. Platinum Metals Rev. 2000;44:50–5.

Jeong JM, Knapp Jr FF. Use of the Oak Ridge National Laboratory tungsten-188/rhenium-188 generator for preparation of the rhenium-188 HDD/lipiodol complex for trans-arterial liver cancer therapy. Semin Nucl Med. 2008;38:S19–29.

Jeong JM, Chung JK. Therapy with ^{188}Re-labeled radiopharmaceuticals: an overview of promising results from initial clinical trials. Cancer Biother Radiopharm. 2003;18:707–17.

Joshi PV, Jagadeesan KC, Manolkar RB, et al. Production of ^{125}I from neutron irradiation of natural Xe gas and a wet distillation process for radiopharmaceutical applications. Ind Eng Chem Res. 2012;51:8575–82.

John CS, Pillai MRA, Lo JM, et al. Labeling of proteins with ^{105}Rh. Appl Radiat Isot. 1989;40:701–5.

Johnson PE, Milne DB, Lykken GI. Effects of age and sex on copper absorption, biological half-life, and status in humans. A J Clin Nutr. 1992;56:917–25.

Junde H, Xialong H, Tuli JK. Nucl Data Sheets. 106, 159 (2005). Data extracted from the ENSDF database, (April 1, 2005) National Nuclear Data Base. Brookhaven National Laboratory, USA; 2005.

Jurisson SS, Ketring AR, Volkert WA. Rhodium-105 complexes as potential radiotherapeutic agents. Transit Met Chem. 1997;22:315–7.

Kahan A, Mödder G, Menkes CJ, et al. ^{169}Erbium-citrate synoviorthesis after failure of local corticosteroid injections to treat rheumatoid arthritis-affected finger joints. Clin Exp Rheumatol. 2004;22:722–6.

Kam BLR, Teunissen JJM, Krenning EP, et al. Lutetium-labelled peptides for therapy of neuroendocrine tumours. Eur J Nucl Med Mol Imaging. 2012; 39:103–12.

Kamadhenu Electrochemical ^{90}Sr/^{90}Y generator. Model KA 01 operating manual. Isotope Technologies Dresden, Germany; 2010.

Kampen WU, Voth M, Pinkert J, Krause A. Therapeutic status of radiosynoviorthesis of the knee with yttrium [^{90}Y] colloid in rheumatoid arthritis and related indications. Rheumatology (Oxford). 2007;46:16–24.

Kan RW, Tsang SH, Poon RT, et al. Update on yttrium-90-based radio-embolization for treatment of hepatocellular carcinoma. ANZ J Surg. 2012;82:505–9.

Karelin Ye A, Efimov VN, Filimonov VT, Kuznetsov RA, Revyakin YL, Andreev OI, Zhemkov IY, Bukh VG, Lebedev VM, Spiridonov Ye N. Radionuclide production using a fast flux reactor. Appl Radiat Isot. 2000;53:825–7.

Katabuchi T, Watanabe S, Ishioka NS, et al. Production of ^{67}Cu via the ^{68}Zn(p,2p)^{67}Cu reaction and recovery of ^{68}Zn target. J Radioanal Nucl Chem. 2008;277:467–70.

Karavida N, Notopoulos A. Radiation Synovectomy: an effective alternative treatment for inflamed small joints. Hippokratia. 2010;14:22–7.

Khalafi H, Nazari K, Ghannadi-Maragheh M. Investigation of efficient 131I production from natural uranium at Tehran research reactor. Ann Nucl Energy. 2005;32:729–40.

Khalid M, Mushtaq A, Iqbal MZ. Separation of ^{111}Ag from neutron irradiated natural palladium using alumina as an adsorbent. Appl Radiat Isot. 2000;52:19–22.

Kern W. ^{131}I tositumomab: a viewpoint by Wolfgang Kern. Bio Drugs. 2000;14:203–4.

Ketring AR, Ehrhardt GJ, Embree MF, et al. Production and supply of high specific activity radioisotopes for radiotherapy applications. Alasbimn. Article N° AJ19-2. 2003. http://www.alasbimnjournal.cl/revistas/19/ketring.html.

Kiss I, Gróz P, Révész A, Sipos T. Production of ^{125}I from pile-irradiated xenon difluoride. J Inorg Nucl Chem. 1969;31:1225–7.

Kolsky KL, Joshi V, Mausner LF, Srivastava SC. Radiochemical purification of no-carrier-added scandium-47 for radioimmunotherapy. Appl Radiat Isot. 1998a;49:1541–9.

Knapp Jr FF, Callahan AP, Beets AL, et al. Processing of reactor-produced ^{188}W for fabrication of clinical scale alumina based ^{188}W/^{188}Re Generators. Appl Radiat Isot. 1994;45:1123–8.

Knapp FF, Mirzadeh S, Beets AL, et al. Reactor-produced radioisotopes from ORNL for bone pain palliation. Appl Radiat Isot. 1998;49(4):309–15.

Knapp Jr FF (R), Beets AL, Guhlke S. Development of the alumina-based tungsten-188/Rhenium-188 generator and use of Rhenium-188-labeled radiopharmaceuticals for cancer treatment. Antican Res. 1997;17:1783–96.

Knapp Jr FF, Mirzadeh S, Beets AL, Du M. Production of therapeutic radioisotopes in the ORNL High Flux Isotope Reactor (HFIR) for applications in nuclear medicine, oncology and interventional cardiology. J Radioanal Nucl Chem. 2005;263:503–9.

Knapp Jr FF, Mirzadeh S, Garland M, et al. Reactor production and processing of ^{188}W. In Production of long lived parent radionuclides for generators. ^{68}Ge, ^{82}Sr, ^{90}Sr and ^{188}W. IAEA; 2010. p. 79–109. http://www-pub.iaea.org/MTCD/publications/PubDetails.asp?pubId=8268.

Kolsky KL, Mausner LF. Production of no-carrier-added ^{199}Au for gold cluster-labelled antibodies. Appl Radiat Isot. 1993;44:553–60.

Kolsky KL, Joshi V, Mausner LF, et al. Radiochemical purification of no-carrier-added Scandium-47 for radioimmunotherapy. Appl Radiat Isot. 1998b;49:1541–9.

Kothari K, Pillai MR, Unni PR, et al. Preparation, stability studies and pharmacological behaviour of [^{186}Re]Re-HEDP. Appl Radiat Isot. 1999;51:51–8.

Kozempel PJ, Abbas K, Simonelli F, et al. Preparation of ^{67}Cu via deuteron irradiation of ^{70}Zn. Radiochim Acta. 2012;100:419–23.

Krishnamurthy GT, Swailem FM, Srivastava SC, et al. Tin-117m(4+)DTPA: pharmacokinetics and imaging characteristics in patients with metastatic bone pain. J Nucl Med. 1997;38:230–7.

Kumric K, Trtic-Petrovic T, Koumarianou E, et al. Supported liquid membrane extraction of ^{177}Lu(III) with DEHPA and its application for the purification of ^{177}Lu-DOTA-lanreotide. Sep Purif Technol. 2006;51:310–7.

Küçük NO, Ibiş E, Aras G, et al. Palliative analgesic effect of Re-186 HEDP in various cancer patients with bone metastases. Ann Nucl Med. 2000;14:239–45.

Kwekkeboom DJ, de Herder WW, Kam BL, et al. Treatment with the radiolabeled somatostatin analog [177 Lu-DOTA0, Tyr3]octreotate: toxicity, efficacy, and survival. J Clin Oncol. 2008;26:2124–30.

Lahiri S, Volkers KJ, Wierczinski B. Production of 166Ho through 164Dy(n, gamma)165Dy(n, gamma)166Dy(beta-)166Ho and separation of 166Ho. Appl Radiat Isot. 2004;61:1157–61.

Lahiri S, Nayak D, Nandy M, Das NR. Separation of carrier free lutetium produced in proton activated ytterbium with HDEHP. Appl Radiat Isot. 1998;49:911–3.

Lam MG, de Klerk JM, van Rijk PP. ^{186}Re-HEDP for metastatic bone pain in breast cancer patients. Eur J Nucl Med Mol Imaging. 2004;31:S162–70.

Lambert B, Bacher K, Defreyne L. Rhenium-188 based radiopharmaceuticals for treatment of liver tumours. Q J Nucl Med Mol Imaging. 2009;53:305–10.

Lambert B, de Klerk JM. Clinical applications of ^{188}Re-labelled radiopharmaceuticals for radionuclide therapy. Nucl Med Commun. 2006;27:223–9.

Lange G, Herrmann G, Strassmann F. Preparation of strontium-90 free yttrium-90 by electrolysis(Die darstellung von strontium-90-freiem yttrium-90 durch elektrolyse). J Inorg Nucl Chem. 1957;4:146–54.

Lau WY, Lai EC, Leung TW. Current role of selective internal irradiation with yttrium-90 microspheres in the management of hepatocellular carcinoma: a systematic review. Int J Radiat Oncol Biol Phys. 2011;81:460–7.

Lawrence EO, Cooksey D. On the apparatus for the multiple acceleration of light ions to high speeds. Phys Rev. 1936;50:1131–40.

Le VS, Morcos N, Zaw M, et al. Alternative chromatographic processes for no-carrier added ^{177}Lu radioisotope separation, Part I. Multi-column chromatographic

process for clinically applicable. J Radioanal Nucl Chem. 2008a;277(3):663–73.

Le VS, Morcos N, Zaw M. Alternative chromatographic processes for no-carrier added ^{177}Lu radioisotope separation. Part II. J Radioanal Nucl Chem. 2008b; 277(3):675–83.

Lebedev NA, Novgorodov AF, Misiak R, et al. Radiochemical separation of no-carrier-added 177Lu as produced via the 176Yb(n, γ)177Yb → 177Lu process. Appl Radiat Isot. 2000;53:421–5.

Lehenberger S, Barkhausen C, Cohrsb S, et al. The low-energy β − and electron emitter ^{161}Tb as an alternative to ^{177}Lu for targeted radionuclide therapy. Nucl Med Biol. 2011;38:917–24.

Leonard A. Metals and their compounds in the environment: occurrence, analysis, and biological relevance. Weinheim/New York/Basel/Cambridge: VCH; 1991. p. 751.

Lewis MR, Zhang J, Jia F, et al. Biological comparison of ^{149}Pm-, ^{166}Ho-, and ^{177}Lu-DOTA-biotin pretargeted by CC49 scFv-streptavidin fusion protein in xenograft-bearing nude mice. Nucl Med Biol. 2004; 31:213–23.

Lewington V. Development of ^{131}I-tositumomab. Semin Oncol. 2005;32:S50–6.

Lewington VJ. Cancer therapy using bone seeking isotopes. Phys Med Biol. 1996;41:2027–42.

Li N, Struttman M, Higginbotham C, Grall AJ, et al. Biodistribution of model ^{105}Rh-labeled tetradentate thiamacrocycles in rats. Nucl Med Biol. 1997;24(1): 85–92.

Li WP, Smith CJ, Cutler CS. Aminocarboxylate complexes and octreotide complexes with no carrier added ^{177}Lu, ^{166}Ho and ^{149}Pm. Nucl Med Biol. 2003;30:241–51.

Linder MC, Hazegh-Azam M. Copper biochemistry and molecular biology. Am J Clin Nutr. 1996;63: 797S–811.

Liu C, Brasic JR, Liu X, et al. Timing and optimized acquisition parameters for the whole-body imaging of ^{177}Lu-EDTMP toward performing bone palliation treatment. Nucl Med Commun. 2012;33:90–6.

Lo JM, Pillai MR, John CS, Troutner DE. Labeling of human serum albumin with ^{105}Rh-cysteine complexes. Int J Rad Appl Instrum A. 1990;41:63–7.

Lumetta GJ, Wester DW, Morrey JR, et al. Preliminary evaluation of chromatographic techniques for the separation of radionuclides from high level radioactive waste. Solv Extr Ion Exch. 1993;11:663–82.

Ma D, Ketring AR, Ehrhardt GJ, Jia W. Production of radiolanthanides and radiotherapy research at MURR. J Radioanal Nuc Chem. 1996;206:119–26.

Majali MA, Saxena SK, Joshi SH, et al. Potential ^{166}Ho radiopharmaceuticals for endovascular radionuclide therapy. II. Preparation and evaluation of ^{166}Ho-DTPA. Nucl Med Commun. 2001;22:97–103.

Majali MA, Debnath MC, Saxena SK, Joshi SH. Preparation and evaluation of [^{166}Ho] holmium-dimethyl diethylenetriaminepentaaceticacid (DMDTPA) as potential radiopharmaceutical for endovascular radiation therapy (EVRT). Appl Radiat Isot. 2002;56:863–9.

Maki Y, Murakami Y. The separation of arsenic-77 in a carrier-free state from the parent nuclide germanium-77 by a thin-layer chromatographic method. J Radioanal Chem. 1974;22:5–12.

Manual for reactor produced radioisotopes. Printed by the International Atomic Energy Agency (IAEA) in Austria, ISBN 92-0-101103-2, ISSN 1011–4289, © IAEA; 2003.

Marques F, Paulo A, Campello MP, et al. Radiopharmaceuticals for targeted radiotherapy. Rad Prot Dos. 2005;116:601–4.

Martinho E, Neves MA, Freitas MC. ^{125}I production: neutron irradiation planning. In J Appl Radiat Isotope. 1984;35:933–8.

Mathew B, Chakraborty S, Das T, et al. ^{175}Yb labeled polyaminophosphonates as potential agents for bone pain palliation. Appl Radiat Isot. 2004;60:635–42.

Máthé D, Balogh L, Polyák A, et al. Multispecies animal investigation on biodistribution, pharmacokinetics and toxicity of ^{177}Lu-EDTMP, a potential bone pain palliation agent. Nucl Med Biol. 2010;37:215–26.

Mausner LF, Kolsky KL, Mease RC, et al. Production and evaluation of Sc-47 for radioimmunotherapy. J Label Compds Radiopharm. 1993;32:388–90.

Mausner LF, Kolsky KL, Joshi V, Srivastava SC. Radionuclide development at BNL for nuclear medicine therapy. Appl Radiat Isot. 1998;49:285–94.

Mausner LF, Mirzadeh S, Srivastava SC. Improved specific activity of reactor produced ^{117m}Sn with the Szilard-Chalmers process. Int J Radiat Appl Instrum Appl Radiat Iso. 1992;43:1117–22.

Maxon HR, Schroder LE, Thomas SR, et al. Rhenium-186 HEDP for treatment of painful osseous metastases: initial clinical experience in 20 patients with hormone-resistant prostate cancer. Radiology. 1990;176:155–9.

Medvedev DG, Mausner LF, Meinken GE, et al. Development of a large scale production of ^{67}Cu from ^{68}Zn at the high energy proton accelerator: Closing the ^{68}Zn cycle. Appl Radiat Isot. 2012;70:423–9.

Meuret G, Hoffmann G, Gmelin R. ^{32}P-therapy in polycythemia vera. Klin Wochenschr. 1975;53:519–21.

Michel RB, Andrews PM, Rosario AV, et al. ^{177}Lu-antibody conjugates for single-cell kill of B-lymphoma cells in vitro and for therapy of micrometastases *in vivo*. Nucl Med Biol. 2005;32:269–78.

Mikolajczak R, Parus JL, Pawlak D, et al. Reactor produced ^{177}Lu of specific activity and purity suitable for medical applications. J Radioanal Nucl Chem. 2004;257:53–7.

Miller WH, Hartmann-Siantar C, Fisher D, et al. Evaluation of beta-absorbed fractions in a mouse model for ^{90}Y, ^{188}Re, ^{166}Ho, ^{149}Pm, ^{64}Cu, and ^{177}Lu-radionuclides. Cancer Biother Radiopharm. 2005;20:436–49.

Minutoli F, Herberg A, Spadaro P, et al. [^{186}Re]HEDP in the palliation of painful bone metastases from cancers

other than prostate and breast. Q J Nucl Med Mol Imaging. 2006;50(4):355–62.
Micallef IN. Ongoing trials with yttrium 90-labeled ibritumomab tiuxetan in patients with non-Hodgkin's lymphoma. Clin Lymphoma. 2004;5:S27–32.
Mirz MY. A new method for the carrier-free production of ^{90}Y from ^{90}Sr/^{90}Y mixture and ^{89}Sr from neutron-irradiated Y_2O_3. Anal Chim Acta. 1968;40:229–33.
Mirzadeh S, Knapp Jr FF, Callahan AP. Production of tungsten-188 and osmium-194 in a nuclear reactor for new clinical generators. In: Qaim SM, editor. Proceedings of the international conference on nuclear data for science and technology. New York: Springer; 1992. p. 595–7.
Mirzadeh S, Lambrecht RM. Radiochemistry of germanium. J Radioanal Nuc Chem. 1996;202:7–102.
Mirzadeh S, Knapp Jr FF, Lambrecht RM. Burn-up cross section of ^{188}W. Radiochim Acta. 1997;77:99–102.
Mirzadeh S, Du M, Beets AL. Knapp Jr FF (Russ). Method for preparing high specific activity ^{177}Lu. United States Patent 6716353dt; 2004. 04 June 2004.
Mirzadeh S, Mausner LF, Garland MA. Reactor-produced medical radionuclides. In: Vértes A, Nagy S, Klencsár Z, Lovas RG, Rösch F, editors. Handbook of nuclear chemistry. Mexico: Playa del Carmen. 2012; ISBN: 978-0-7354-1127-2.
Miszczyk L, Wozniak G, Jochymek B, et al. Effectiveness evaluation of knee joint ^{90}Y radiosynovectomy. Przegl Lek. 2007;64:450–3.
Mohsin H, Jia F, Sivaguru G, et al. Radiolanthanide-labeled monoclonal antibody CC49 for radioimmunotherapy of cancer: biological comparison of DOTA conjugates and ^{149}Pm, ^{166}Ho, and ^{177}Lu. Bioconjug Chem. 2006;17:485–92.
Montaña RL, González IH, Ramirez AA, Garaboldi L, Chinol M. Yttrium-90 – current status, expected availability and applications of a high beta energy emitter. Curr Radiopharm. 2012;5:253–63.
Morcos N, Zaw M, Pellegrini P, et al. Alternative chromatographic processes for no-carrier added ^{177}Lu radioisotope separation Part II. The conventional column chromatographic separation combined with HPLC for high purity. J Radioanal Nucl Chem. 2008;277:675–83.
Morschhauser F, Radford J, Van Hoof A. Phase III trial of consolidation therapy with yttrium-90-ibritumomab tiuxetan compared with no additional therapy after first remission in advanced follicular lymphoma. J Clin Oncol. 2008;26:5156–64.
Morschhauser F, Radford J, Van Hoof A, et al. ^{90}Yttrium-ibritumomab tiuxetan consolidation of first remission in advanced-stage follicular non-Hodgkin lymphoma: updated results after a median follow-up of 7.3 years from the International, Randomized, Phase III First-LineIndolent trial. J Clin Oncol. 2013;31:1977–83.
Najean Y, Rain JD. Treatment of polycythemia vera: use of ^{32}P alone or in combination with maintenance therapy using hydroxyurea in 461 patients greater than 65 years of age. The French Polycythemia Study Group. Blood. 1997;89:2319–27.
Najean Y, Rain JD, Dresch C, et al. Risk of leukaemia, carcinoma, and myelofibrosis in 32P- or chemotherapy-treated patients with polycythaemia vera: a prospective analysis of 682 cases. The French Cooperative Group for the Study of Polycythaemias. Leuk Lymphoma. 1996;1:111–9.
National Bureau of Standards Handbook (Maximum permissible body burden and maximum permissible concentrations of radionuclides in air and water for occupational exposure), vol 69. Washington, DC: US Government Printing Office; 1963, p. 38.
Nassan L, Achkar B, Yassine T. Production of ^{166}Ho and ^{153}Sm using hot atom reactions in neutron irradiated tris(cyclopentadienyl) compounds. Nukleonika. 2011;56(4):263–7.
Nazari K, Ghannadi-Maragheh M, Shamsaii M, Khalafi H. A new method for separation of ^{131}I, produced by irradiation of natural uranium. Appl Radiat Isot. 2001;55:605–8.
Neves M, Kling A, Lambrecht RM. Radionuclide production for therapeutic radio-pharmaceuticals. Appl Radiat Isot. 2002;57:657–64.
Nijsen JFW, Zonnenberg BA, Woittiez JRW, et al. Holmium-166 poly lactic acid microspheres applicable for intra-arterial radionuclide therapy of hepatic malignancies: effects of preparation and neutron activation techniques. Eur J Nucl Med. 1999;26:699–704.
Nir-El Y. Production of ^{177}Lu by neutron activation of ^{176}Lu. J Radioanal Nucl Chem. 2004;262:563–7.
Nisa L, Savelli G, Giubbini R. Yttrium-90 DOTATOC therapy in GEP-NET and other SST2 expressing tumors: a selected review. Ann Nucl Med. 2011;25:75–85.
Orth RJ, Kurath DE. Review and assessment of technologies for the separation of strontium from alkaline and acidic media, Rep. PNL-9053. Richland: Pacific Northwest National Laboratory; 1994.
Pagano L, Klain M, Pulcrano M, et al. Follow-up of differentiated thyroid carcinoma. Minerva Endocrinol. 2004;29:161–74.
Pandey U, Dhami PS, Jagesia P, et al. A novel extraction paper chromatography (EPC) technique for the radionuclidic purity evaluation of ^{90}Y for clinical use. Anal Chem. 2008;80:801–80.
Payamara J. Production of iodine-131using dry distillation method. J Chem Pharm Res. 2011;3:375–80.
Pecher C. Biological investigations with radioactive calcium and strontium: preliminary report on the use of radioactive strontium in the treatment of bone cancer. Univ Calif Publ Pharmacol. 1942;2:1117–49.
Pietrelli L, Mausner LF, Kolsky KL. Separation of carrier free 47Sc from titanium targets. J Radioanal Nucl Chem. 1992;157:335–45.
Pitoia F, Cavallo A. Thyroid cancer. In search of individualized treatment. Medicina (B Aires). 2012;72:503–13.
Pons F, Herranz R, Garcia A, et al. Strontium-89 for palliation of pain from bone metastases in patients with prostate and breast cancer. Eur J Nucl Med. 1997;24:1210–4.

Pillai MR, Lo JM, John CS, Troutner DE. Labeling of proteins using [Rh]Rh-4-(p-aminobenzyl)-diethylenetriamine. Int J Rad Appl Instrum B. 1990a;17:419–26.

Pillai MR, John CS, Troutner DE. Labeling of human IgG with rhodium-105 using a new pentadentate bifunctional ligand. Bioconjug Chem. 1990b;1:191–7.

Pillai MR, Lo JM, Troutner DE. Labeling of hematoporphyrin with ^{105}Rh and binding studies with human gamma globulin. Int J Rad Appl Instrum A. 1990c;41:69–73.

Pillai MR, Dash A, Knapp Jr FF. Rhenium-188: availability from the ^{188}W/^{188}Re generator and status of current applications. Curr Radiopharm. 2012;3:228–43.

Pillai MR, Chakraborty S, Das T, Venkatesh M, Ramamoorthy N. Production logistics of ^{177}Lu for radionuclide therapy. Appl Radiat Isot. 2003; 59(2–3):109–18.

Ponsard B, Srivastava SC, Mausner LF, Knapp FF, Garland MA, Mirzadeh S. Production of Sn-117m in the BR2 high-flux reactor. Appl Radiat Isot. 2009;67(7–8):1158–61.

Provencio M, Cruz Mora MÁ, Gómez-Codina J, et al. Consolidation treatment with Yttrium-90 ibritumomab tiuxetan after new induction regimen in patients with intermediate- and high-risk follicular lymphoma according to the follicular lymphoma international prognostic index: a multicenter, prospective phase II trial of the Spanish Lymphoma Oncology Group. Leuk Lymphoma. 2014;55:51–5.

Qaim SM. Therapeutic radionuclides and nuclear data. Radiochim Acta. 2001;89:297–302.

Rajendran JG, Eary JF, Bensinger W, et al. High-dose ^{166}Ho-DOTMP in myeloablative treatment of multiple myeloma: pharmacokinetics, biodistribution, and absorbed dose estimation. J Nucl Med. 2002;43:1383–90.

Ramamoorthy N, Saraswathy P, Das MK, Mehra KS, Ananthakrishnan M. Production logistics and radionuclidic purity aspects of ^{153}Sm for radionuclide therapy. Nucl Med Commun. 2002;23:83–9.

Ramanujam A, Dhami PS, Chitnis RR, Achuthan PV, Kannan R, Gopaiakrishnan V, Batu K. Separation of strontium-90 from PUREX high level waste and development of ^{90}Sr/^{90}Y generator. BARC report 2000/E/009. BARC India; 2000.

Razbash AA, Nerozin NA, Panarin MV et al. Winning ^{32}P in the BR-10 Reactor. Atomnaya Ehnergiya(Soviet Atomic Energy). 1991;70:333–35. Available at: http://link.springer.com/article/10.1007%2FBF01138230?LI=true#.

Reynolds JC, Robbins J. The changing role of radioiodine in the management of differentiated thyroid cancer. Semin Nucl Med. 1997;27:152–64.

Robinson RG, Preston DF, Schiefelbein M, et al. Strontium 89 therapy for the palliation of pain due to osseous metastases. JAMA. 1995;274:420–4.

Safarzadeh L, Ghannadi-Maragheh M, Anvari A, et al. Production, radiolabeling and biodistribution studies of ^{175}Yb-DOTMP as bone pain palliation. Iran J Pharm Sci. 2012;8(2):135–41.

Samsahl K. The Jener method for the extraction of pure ^{32}P from neutron-irradiated sulphur. Atompraxis. 1958;4:14–7.

Sato KT. Yttrium-90 radioembolization for the treatment of primary and metastatic liver tumors. Semin Roentgenol. 2011;46:159–65.

Shen S, DeNardo GL, DeNardo SJ, et al. Dosimetric evaluation of Copper-64 in copper-67-2IT-BAT-Lym-1 for radioimmunotherapy. J Nucl Med. 1996;37:146–50.

Sheybani S, Pourbeygi H, Tavakoli YH, Keyvani M. Production and evaluation of ^{186}Re radionuclide in the Tehran Research reactor for therapeutic applications. J Nucl Sci Tech. 2010;2:58–62.

Shikata E, Amano H. Dry-distillation of iodine-131 from several tellurium compounds. J Nucl Sci Technol. 1973;10:80–8.

Simindokht SA, Bahrami-Samani A, Jalilian AR, Ghannadi-Maragheh M. Production, quality control and biodistribiotion studies of 170Tm-DOTA-NHS-Cetuximab Iranian. J Nucl Med. 2010;18:18.

Siri S, Mondino AV. Production of fission ^{131}I. J Radioanal Nucl Chem. 2005;266:317–24.

Smith NA, Bowers DL, Ehst DA. The production, separation, and use of ^{67}Cu for radioimmunotherapy: a review. Appl Radiat Isot. 2012;70:2377–83.

So LV, Morcos N, Zaw M, Pellegrini P, Greguric I. Alternative chromatographic processes for no-carrier added ^{177}Lu radioisotope separation, part I. Multi-column chromatographic process for clinically applicable. J Radioanal Nucl Chem. 2008;277:663–73.

Soffen EM, Greenberg A, Baumann J, et al. The role of strontium-89 systemic radiotherapy in the management of osseous metastases from prostate cancer. Tech Urol. 1997;3:76–80.

Sohaib M, Ahmad M, Jehangir M, et al. Ethylene diamine tetramethylene phosphonic acid labeled with various $\beta(^-)$-emitting radiometals: labeling optimization and animal biodistribution. Cancer Biother Radiopharm. 2011;26:159–64.

Sorantin H, Bildstein H. Rapid preparation of carrier free I-131 from neutron-irradiated telluric acid. J Inorg Nucl Chem. 1965;27:521–6.

Spahn I, Coenen HH, Qaim SM. Enhanced production possibility of the therapeutic radionuclides 64Cu,67Cu and 89Sr via (n, p) reactions induced by fast spectral neutrons. Radiochim Acta. 2004;92:183–6.

Srivastava SC, Atkins HL, Krishnamurthy GT, et al. Treatment of metastatic bone pain with tin-117m(4+) DTPA: a phase II clinical study. Clin Cancer Res. 1998;4:61–8.

Srivastava SC, Dadachova E. Recent advances in radionuclide therapy. Semin Nucl Med. 2001;31:330–41.

Srivastava SC. Treatment of bone and joint pain with electron emitting radiopharmaceuticals. Ind J Nucl Med. 2004;19:89–97.

Srivastava SC. Radionuclide therapy with high-LET electron emitters: therapeutic applications of conversion electron emitter tin-117m. In: Mazzi U, Editoriali SG, editors. Technetium, rhenium, and other metals in chem-

istry and nuclear medicine. Padova: SG Editoriali; 2006. p. 553–68.
Srivastava SC. The role of electron-emitting radiopharmaceuticals in the palliative treatment of metastatic bone pain and for radiosynovectomy: applications of conversion electron emitter tin-117m. Brazil Arch Biol Technol. 2007;50:49–62.
Srivastava SC. Theragnostic radiometals: getting closer to personalized medicine. In: Mazzi U et al., editors. Technetium and other radiometals in chemistry and nuclear medicine. Padova: SG Editoriali; 2010. p. 553–68.
Srivastava SC. Paving the way to personalized medicine: production of some promising theragnostic radionuclides at Brookhaven national laboratory. Sem Nucl Med. 2012;42:151–63.
Swailem FM, Krishnamurthy GT, Srivastava SC, et al. *In vivo* tissue uptake and retention of Sn-117m (4+) DTPA in a human subject with metastatic bone pain and in normal mice. Nucl Med Biol. 1998;25: 279–87.
Swärd C, Bernhardt P, Ahlman H, et al. [^{177}Lu-DOTA 0-Tyr 3]-octreotate treatment in patients with disseminated gastroenteropancreatic neuroendocrine tumors: the value of measuring absorbed dose to the kidney. World J Surg. 2010;34:1368–72.
Szelecsényi F, Steyn GF, Dolley SG, et al. Investigation of the ^{68}Zn(p,2p)^{67}Cu nuclear reaction: new measurements up to 40 MeV and compilation up to 100 MeV. Nucl Instr Meth Phys Res B. 2009;267:1877–81.
Tabasi M, Ghannadi-Maragheh M, Shamsai M, Khanchi AR. Separation of ^{133}Xe from ^{99}Mo, ^{131}I and uranium, and removal of impurities using gas chromatography. J Radioanal Nucl Chem. 2005;264:679–86.
Taylor WJ, Corkill MM, Rajapaske CN. A retrospective review of yttrium-90 synovectomy in the treatment of knee arthritis. Br J Rheumatol. 1997;36:1100–5.
Tefferi A. Polycythemia vera and essential thrombocythemia: update on diagnosis, risk stratification, and management. Am J Hematol. 2012;87:285–93.
Tefferi A, Silverstein MN. Treatment of polycythaemia vera and essential thrombocythaemia. Baillieres Clin Haematol. 1998;11:769–85.
Teunissen JJ, Kwekkeboom DJ, Krenning EP. Staging and treatment of differentiated thyroid carcinoma with radiolabeled somatostatin analogs. Trends Endocrinol Metab. 2006;17:19–25.
Theobald T, editor. Sampson's textbook of radiopharmacy. 4th ed. London: Pharmaceutcial Press; 2011.
Tomblyn M. Radioimmunotherapy for B-cell non-hodgkin lymphomas. Cancer Control. 2012;19:196–203.
Toporov YG, Andreyev OI, Akhetov FZ, et al. Reactor production of high specific activity Tin-117m at RIAR. Proceeding of 5th Conference on Isotopes Brusels, Belgium, 25–29 Apr 2005. p. 47–53.
Tsai DE, Maillard I, Downs LH, et al. Use of iodine ^{131}I-tositumomab radioimmunotherapy in a patient with Waldenstrom's macroglobulinemia. Leuk Lymphoma. 2004;45:591–5.
Unni PR, Pillai MRA. Production and radiochemical separation of rhodium-105 for radiopharmaceutical applications. Radiochim Acta. 2002;90:363–9.
Van Essen M, Krenning EP, Kam BL, et al. Salvage therapy with ^{177}Lu-octreotate in patients with bronchial and gastroenteropancreatic neuroendocrine tumors. J Nucl Med. 2010;51:383–90.
Vanderheyden JE, Su F, Ehrhardt GJ. Soluble irradiation targets and methods for the production of radiorhenium United States Patent 5,145,636; 1992.
Van der Linden R, De Corte F, Hoste J. A compilation of infinite dilution resonance integrals-II. J Radioanal Chem. 1974;20:695–706.
Vaughan AT, Varley NR. Antibodies labeled with ^{199}Au: potential of ^{199}Au for radioimmunotherapy. Nucl Med Biol. 1988;15:293–7.
Venkatesh M, Goswami N, Volkert WA, et al. A Rh-105 complex of tetrathiacyclohexadecane diol with potential for formulating bifunctional chelates. Nucl Med Biol. 1996;23:33–40.
Villard L, Romer A, Marincek N, et al. Cohort study of somatostatin-based radiopeptide therapy with [(^{90}) Y-DOTA]-TOC versus [(90)Y-DOTA]-TOC plus [(^{177}) Lu-DOTA]-TOC in neuroendocrine cancers. J Clin Oncol. 2012;30:1100–6.
Vimalnath KV, Das MK, Venkatesh M, et al. Prospects and problems in the production of ^{143}Pr for radionuclide therapy applications. Radiochim Acta. 2005;93: 419–26.
Vimalnath KV, Shetty P, Chakraborty S, et al. Practicality of production of ^{32}P by direct neutron activation for its utilization in bone pain palliation as $Na_3[^{32}P]PO_4$. Cancer Biother Radiopharm. 2013;28:423–8.
Vimalnath KV, Shetty P, Rajeswari PA, et al. Reactor production of 32 P for medical applications: an assessment of 32S(n, p)32 P and 31P(n, γ)32P methods. J Radioanal Nucl Chem. 2014a;301:555–65.
Vimalnath KV, Shetty P, Lohar SP, et al. Aspects of yield and specific activity of (n, γ) produced 177Lu used in targeted radionuclide therapy. J Radioanal Nucl Chem. 2014b;302:809–12.
Vucina J, Han R. Production and therapeutic use of rhenium-186,188-the future of radionuclides. Med Pregl. 2003;56(7–8):362–5.
Walker LA. Radioactive yttrium-90; a review of its properties, biological behaviour and clinical uses. Acta Radiol Ther Phys Biol. 1964;2:302–14.
Wojdowska W. Studies on separation and purification of ^{99}Mo from nat-U, ^{131}Iand ^{103}Ru. Nucl Med Biol. 2010;37:715.
Weigert O, Illidge T, Hiddemann W, Dreyling M. Recommendations for the use of yttrium-90 ibritumomab tiuxetan in malignant lymphoma. Cancer. 2006;107:686–95.
Wester DW, Steele RT, Rinehart DE, DesChane JR, Carson KJ, Rapko BM, Tenforde TS. Large-scale purification of ^{90}Sr from nuclear waste materials for production of ^{90}Y, a therapeutic medical radioisotope. Appl Radiat Isot. 2003;59:35–41.

Winfield J, Gumpel JM. An evaluation of repeat intra-articular injections of yttrium-90 colloids in persistent synovitis of the knee. Ann Rheum Dis. 1979; 38:145–7.

Wong YK, Ketring AR, Lo JM, Troutner DE. Production of ^{105}Rh by the szilard-chalmers process with ruthenium acetylacetonate. J Label Compd Radiopharm. 1989;26(1–12):179–81.

Yano Y, Chu P, Anger HO. Tin—117m: production, chemistry and evaluation as a bone scanning agent. Int J Radiat Appl Instrum Appl Radiat Isot. 1973;24: 319–25.

Yeh H. Preparation of carrier free phosphorus by neutron irradiation. Ho Tzu K'o Hsueh (Taiwan). 1962;3: 33–7.

Yu DC, Meister JD, Abalin SS, Ball RM, Grigoriev GY, Khvostionov VE, Markovskij DV, Nordyke HW, Pavshook VA. An interleaved approach to production of 99Mo and 89Sr medical radioisotopes. J Radioanal Nucl Chem. 2003;257:59–63.

Yu DC, Khvostionov VE, Markovskij DV, Pavshook VA, Ponomarev-Stepnoy NN, Udovenko AN, Shatrov AV, Vereschagin YI, Rice J, Tome LA. Production of ^{89}Sr in solution reactor. Appl Radiat Isot. 2007;65:1087–94.

Zaknun JJ, Bodei L, Mueller-Brand J, et al. The joint IAEA, EANM, and SNMMI practical guidance on peptide receptor radionuclide therapy(PRRNT) in neuroendocrine tumours. Eur J Nucl Med Mol Imaging. 2013;40:800–16.

Zhang Z, Wang X, Wu Y, et al. Preparation of 186Re and 188Re with high specific activity by the Szilard–Chalmers effect. J Label Compd Radiopharm. 2000;43:55–64.

Zeisler SK, Weber K. Szilard-Chalmers effect in holmium complexes. J Radioanal Nucl Chem. 1998;227: 105–9.

Zhernosekov KP, Perego RC, Dvorakova Z, et al. Target burn-up corrected specific activity of ^{177}Lu produced via ^{176}Lu(n, gamma) ^{177}Lu nuclear reactions. Appl Radiat Isot. 2008;66(9):1218–20.

Zhu J, Koken MH, Quignon F, et al. Arsenic-induced PML targeting onto nuclear bodies: implications for the treatment of acute promyelocytic leukemia. Proc Natl Acad Sci U S A. 1997;94:3978–83.

Zinzani PL, d'Amore F, Bombardieri E, et al. Consensus conference: implementing treatment recommendations on yttrium-90 immunotherapy in clinical practice – report of a European workshop. Eur J Cancer. 2008;44:366–73.

Zvonarev AV, Matveenko IP, Pavlovich VB. ^{89}Sr production in fast reactors. Atomic Energy. 1997;82: 394–7.

Accelerator-Produced Therapeutic Radionuclides

6

6.1 Introduction

Cyclotrons are generally used for the preparation of neutron-deficient radionuclides, which decay mostly by β^+ emission or electron capture (EC), which are used for diagnostic applications (IAEA 2009). However, these production facilities are also sometimes used for the production of therapeutic α emitting and β —emitting radionuclides. In some instances, Auger- and Conversion electron-emitting (CE) therapeutic radioisotopes are also reactor-produced, but in general, the large majority of radioisotopes used for therapy are reactor-produced. Because of the power requirements, operational costs, and in general focused operations, cyclotron production of radionuclides is generally more expensive compared with those produced by reactor irradiation. With reactors, the general operation is not affected by target insertion and radiation, and usually many different experiments and irradiations are concurrently conducted. However, higher specific activities (SA) are generally available from the accelerator production routes, and no-carrier-added products (NCA) can often be obtained because the atomic number, Z, usually changes (Fig. 6.1).

As summarized in Table 6.1, a variety of accelerator-produced radioisotopes are of current interest for targeted therapy.

6.2 Accelerators for Radionuclide Production

The use of accelerators for production of medical radionuclides requires the delivery of charged particle beams which have two primary characteristics, since they must both have sufficient energy to induce the desired nuclear reaction and sufficient beam current to provide practical product yields. The basic characteristics of a medical cyclotron, for instance, include an ion source for ion production, an acceleration chamber for ion acceleration, a magnet to contain the ions on a circular path, and finally a stripper to "extract" the ions from the accelerator and direct on the target (Fig. 6.2). The extracted beam can be appropriately tuned to focus on a target or a few targets in separated beam stops simultaneously, since the beam can be focused within the accelerator itself or can be focused on a target station which is located exterior to the accelerator. The targets can consist of a solid, liquid, or gas (IAEA 2009).

When an energetic-charged particle passes through any material, there is a definite probability to interact with nucleus of atoms along its path. The particle may be scattered off the nucleus or, if the energy is high enough when collision occurs, may combine to form a compound nucleus which will then decompose through one of the several possible pathways, leading to the formation of the product radionuclide. Another important and often challenging requirement is

F.F. (Russ) Knapp, A. Dash, *Radiopharmaceuticals for Therapy*, DOI 10.1007/978-81-322-2607-9_6

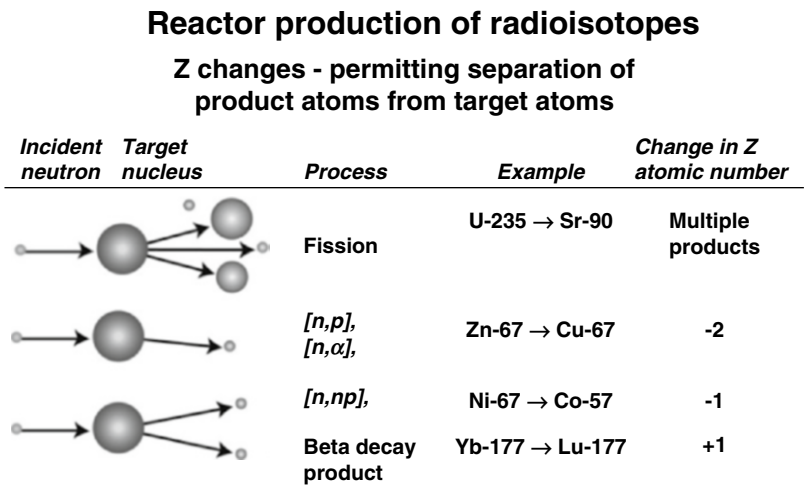

Fig. 6.1 Examples of particle reactions where Z changes and radioisotopic products can be separated from target atoms by traditional methods

Table 6.1 Key examples of accelerator-produced therapeutic radionuclides

Product Nuclide	Principle emission Type	Half-Life	Key examples Production route
Actinium-225	Alpha	10 days	Thorium
Astatine-211	Alpha	7.21 h	
Copper-67	Beta	2.58 days	$^{nat}Zn/^{68}Zn(p,2p)^{67}Cu$ $^{70}Zn(p,\alpha)^{67}Cu$
Gallium-67	Auger	3.26 days	$^{68}Zn(p,2n)^{67}Cu$ $^{64}Zn(d,2n)^{67}Cu$ $^{65}Cu(\alpha,2n)^{67}Cu$
Indium-111	Auger	2.8 days	$^{111}Cd(p,n)^{111}In$ $^{112}Cd(p,2n)^{111}In$
Radium-223	Alpha	11.4 days	Thorium
Rhenium-186	Beta	3.78 days	$^{186}W(p,n)^{186}Re$ $^{186}W(d,2n)^{186}Re$
Tin-117 m	CE	13.6 days	$^{nat}Sb(p,xn)^{117m}Sn$

the availability of efficient chemical methods for separation of the microscopic levels of the radionuclide products from the macroscopic target levels, which in turn must often be recovered for recycling for subsequent irradiation.

6.2.1 Calculation of Production Yield

The rate of radionuclide production is dependent on a number of factors, including the magnitude of the reaction cross section (i.e., probability of capture) as a function of energy; the incident particle energy; the thickness of the target in atoms per cm^2, which will determine the exit particle energy; and the flux of incoming particles. In the simplest case, where the cross section is assumed to be constant, the rate of production is given by the equation:

$$R = n_T I \sigma \tag{6.1}$$

where:

R is the number of nuclei formed per second.
n_T is the target thickness in nuclei/cm^2.
I is the incident particle flux per second and is related to the beam current.
σ is the reaction cross section, or probability of interaction, expressed in cm^2 and is a function of energy.

The cross section is always a function of energy, and hence Eq. (6.1) becomes modified as:

$$R = n_T I \int_{E_i}^{E_f} \frac{\sigma(E)}{dE / dX} dE \tag{6.2}$$

E is the energy of the incident particles.
x is the distance travelled by the particle.
$\int_{E_i}^{E_f}$ is the integral from the initial energy to the final energy of the incident particle along its path.

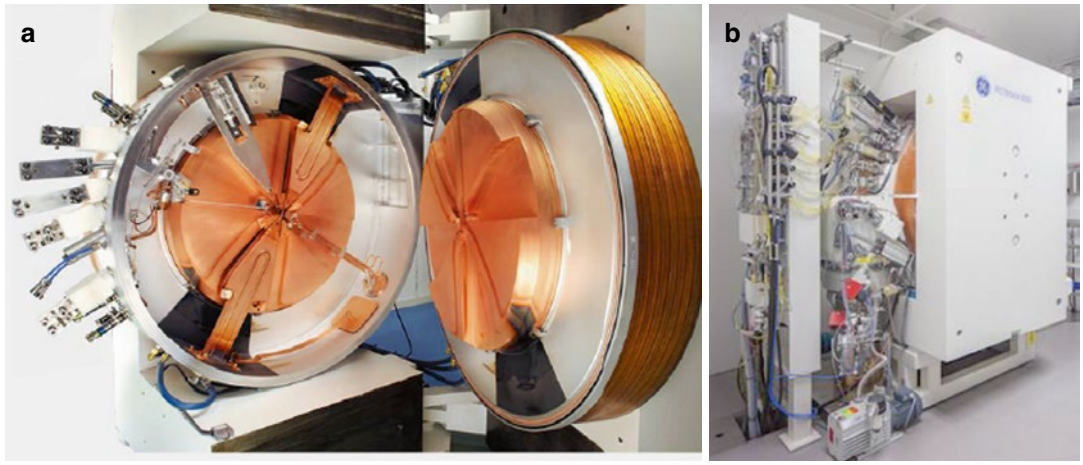

Fig. 6.2 Medical cyclotron, (**a**) internal view. (**b**) Medical cyclotron at RMC, India

As the charged particles passes through the target material, energy is lost due to interactions with the target electrons which is represented in the above equation by the term dE/dx (also called the "stopping power").Returning to the expression for the cross section, it is evident that n_T is given by the following expression:

$$n_T = \frac{\rho x}{A_\Gamma}\zeta \tag{6.3}$$

where:

n_T is the target thickness in nuclei/cm^2.
ρ is the density in g/cm^3.
x is the distance the particle travels through the material.
ζ is Avogadro's number.
A_T is the atomic weight of the target material in grams.

If the target material is a compound rather than a pure element, then the number of nuclei per unit area is given by the following expression:

$$N_G = \frac{F_A C \zeta}{A_A} \tag{6.4}$$

where:
N_G is the number of target nuclei per gram.
F_A is the fractional isotopic abundance.
C is the concentration by weight.
A_A is the atomic mass number of nucleus A.

The above equations illustrate that it is not always possible to eliminate the radionuclidic impurities in the product during radionuclide production using cyclotrons. This occurs even when using the highest isotopic target enrichment and the most precise energy selection, resulting from incident particle energy depletion with initiation of secondary nuclear reactions which is increased with higher-energy incident particles.

6.2.2 Saturation Factor

Radionuclide product decay begins as soon as they have formed, which leads to the following expression, where the overall rate of production becomes:

$$-\frac{dN}{dt} = n_T I \int_{E_f}^{E_o} \frac{\sigma(E)}{dE/dX} dE - \lambda N \tag{6.5}$$

where:
λ is the decay constant and is equal to ln $2/T_{½}$.
t is the irradiation time in seconds.
N is the number of radioactive nuclei in the target.

The term dE/dx in the above expression is often referred to as the total stopping power. At a particular energy E, it can be represented as $S_T(E)$ in units of MeV · cm^2 · g^{-1} and is given by the following expression:

$$S_T(E) = \frac{dE}{dX} \tag{6.6}$$

where:
dE is the differential loss in energy.
dx is the differential distance travelled by the particle.

The loss of energy, dE, in MeV of the particle is then given by:

$$dE = S_T(E)\rho dx \tag{6.7}$$

where ρ is the density of the material in units of g/cm^3, and the thickness of the target? ρdx (in g/cm^2) can be expressed as a function of dE:

$$\rho dx = \frac{dE}{S_T(E)} \tag{6.8}$$

If this equation is integrated to include the stopping power to account for energy loss during the transit of the particle through the target material and assuming that the beam current is the same as the particle flux (which is true only for particles with a charge of +1), then the yield of a nuclear reaction is given by:

$$Y_{EOB} = \frac{N_A I}{A_T}\left(1 - e^{-\lambda t}\right)\int_{E_F}^{E_i} \sigma_T(E)\frac{dE}{S_T(E)} \tag{6.9}$$

The radionuclide production rate is of course affected by the radioactive decay of the resulting radionuclide product. For short-lived nuclides, the competing reaction rates, production, and decay will achieve equilibrium at sufficiently long bombardment times since the rate of decay is proportional to the number of radionuclide present. The $(1 - e^{-\lambda t})$ term is often referred to as the saturation factor and accounts for the competition of the production of nuclei due to the particle reaction and the radioactive decay of the nuclei that have been produced. For an infinitely long irradiation, the saturation factor $(1 - e^{-\lambda t})$ tends to the value 1.

6.3 Key Accelerator-Produced Therapeutic Radionuclides

6.3.1 Actinum-225 and Radium-223

The accelerator production route which involves irradiation of natural ^{232}Th targets with medium-energy protons (Fig. 6.3) appears to be an attractive route in terms of yield and cost-effectiveness.

Actinium-225 is of great interest for therapy as well as a generator parent for the availability of ^{213}Bi (Apostolidis et al 2005; Miederer et al 2008; Scheinberg and McDevitt 2011). The scope of availing ^{225}Ac as well as ^{213}Bi for ^{229}Th is schematically depicted in Fig. 6.4.

Chemical isolation of Ra from irradiated metallic Th was performed by a gas-chemical method (Zhuikov et al. 2011). For ^{225}Ac and ^{223}Ra processing following irradiation of ^{nat}Th targets using 800 MeV protons, solvent extraction with ethyl acetate has been used (Weidner et al. 2012). A method for purification of ^{225}Ac from irradiated ^{226}Ra-targets consisting of a first extraction chromatography for separating ^{225}Ac from ^{226}Ra and other Ra-isotopes and a second extraction chromatography for separating ^{225}Ac from ^{210}Po and ^{210}Pb has been reported. The finally purified ^{225}Ac can be used in the preparation of radiopharmaceuticals (Turlera et al. 2013). This separation scheme is shown in Figs. 6.5 and 6.6.

Radium-223 has recently emerged as a key agent for bone pain palliation in castration-resistant metastatic cancer from prostate cancer and is discussed in detail in Chap. 12. An ^{227}Ac/^{223}Ra extraction generator based on selective extraction of ^{223}Ra from a solution of chlorinated cobalt dicarbollide and polyethylene glycol in a polar diluent from a solution of

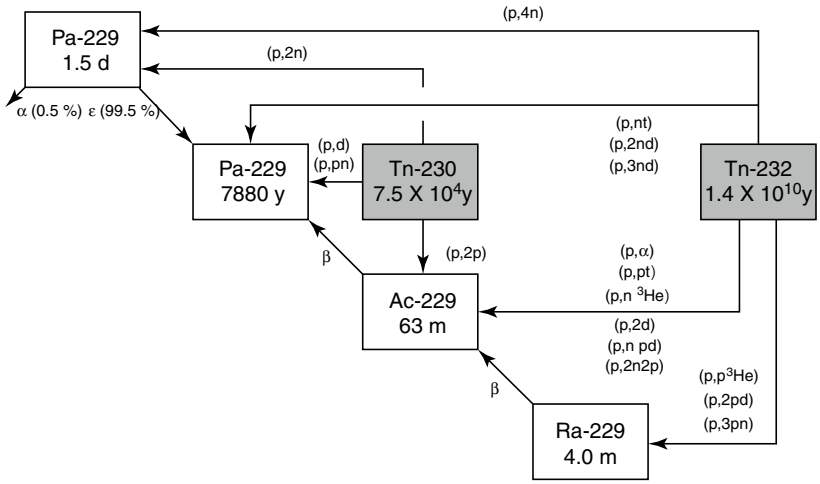

Fig. 6.3 Proton-induced reactions for the production of ^{229}Th

a mineral acid and a complexing agent has been proposed. Radium is stripped to any appropriate aqueous solution on adding TBP into the extractant (Weidner et al. 2012). A number of additional radiochemical separations approaches for the isolation of ^{223}Ra from ^{227}Th have been reported (Henricksen et al. 2001; Horowitz and Bond 2003; Boll et al. 2005; Kirby 1969). While the isolation of high purity ^{223}Ra and ^{227}Th from ^{227}Ac chemically appears to be straightforward, it is mechanically complex due to intense alpha and gamma radiation which produces reactive species (solvated electrons, hydroperoxide ions, atomic hydrogen, and free hydroxyl) that can cause the radiation damage to the ion exchangers and solvents and interfere with radiochemical separations.

6.3.2 Astatine-211

The radiotherapeutic potential of α-emitting ^{211}As ($T_{1/2}$ = 7.21 h) (see Chap. 3) has been recognized for over 30 years (Smit et al. 1973). Astatine in a halogen and the branched pathway for ^{211}As decay is illustrated in Fig. 6.7. The 7.2 h half-life is sufficient to permit multistep synthetic procedures and is also sufficiently long to accommodate for the pharmacokinetics of a wide variety of potential cell-specific targeting agents. The halogen chemistry of astatine is diverse and permits radiolabeling of a wide range of molecules. It is possible to exploit both its metallic characteristics (Milesz et al. 1989; Yordanov et al. 2000) and its halogen properties for the synthesis of ^{211}At-labeled molecules. Astatine-211 decays either directly by α-decay to ^{207}Bi (42 %), followed by EC decay to stable ^{207}Pb, or by EC decay to ^{211}Po (58 %), followed by α-emission to stable ^{207}Pb. The α particles have a range of only 55–80 μm in biological soft tissue, which represents only a few cell diameters. The high mean LET value of about 100 keV/μm is close to the optimum value for a high RBE to maximize the lethal damage (Zalutsky and Bigner 1996). The ^{211}Po daughter emits 77–92-keV X-rays that provide a valuable means for tissue tracking ^{211}At by SPECT imaging (Johnson et al. 1995). With regard to radiation protection issues, ^{211}As is easy to handle, since α particles represent more than 99 % of the radiation energy (Larsen et al. 1999).

Spallation reactions can be useful for ^{211}At production either directly or indirectly through the decay of ^{211}Rn, but the required high particle energies between 160 and 660 MeV and limited beam intensity, in addition to the extensive required separation procedures, emerged as major impediments for the use of this strategy for routine production required to meet expected clinical demands (Kirby 1985). Currently, the

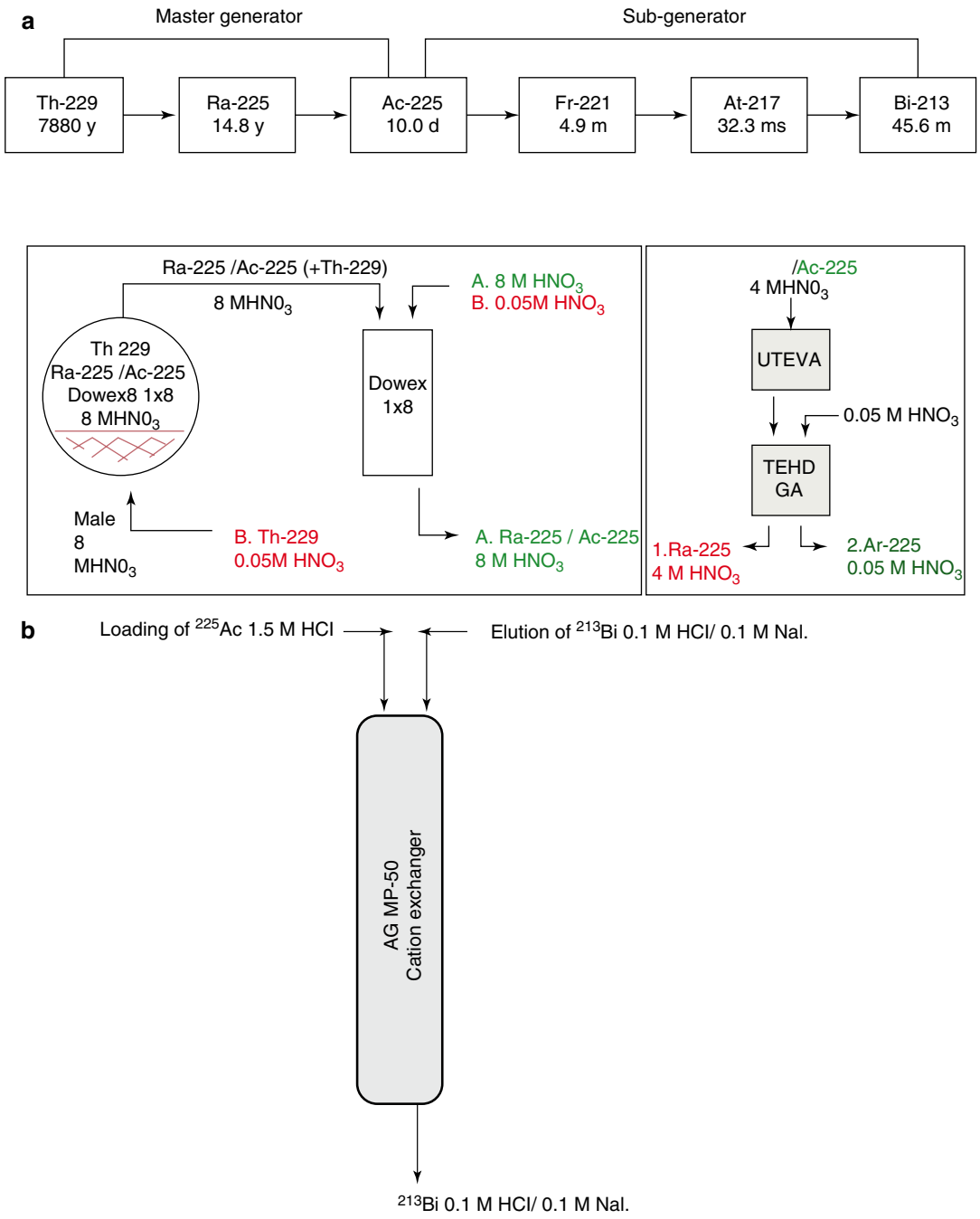

Fig. 6.4 Availability of ^{225}Ac as well as ^{213}Bi from ^{229Th}. (**a**) Master ^{229}Th/^{225}Ac generator, (**b**) sub ^{225}Ac/^{213}Bi generator

most commonly used method for producing ^{211}At is the bombardment of natural bismuth, usually in metallic form, with α particles (Zalutsky and Pruszynski 2011). Although the use of natural bismuth constitutes an ideal target material in terms of cost-effectiveness and precludes the need for chemical recovery for its subsequent use, its poor thermal conductivity (7.97 $W \cdot K^{-1} \cdot m^{-1}$) and low melting point (272 °C) necessitates adequate target cooling at high current production runs.

The purity of ^{211}At required for research and clinical studies is influenced by the radiochemical procedures adapted for the recovery of ^{211}At from the bismuth cyclotron target. Although a variety of methods have been reported for ^{211}At recovery (Eberle 1985), the most common method involves dry distillation or acid treatment of the target followed by solvent extraction. The most commonly utilized approach for separating ^{211}At from bismuth cyclotron targets is dry distillation at a temperature range of 650–800 °C for 30 min using a flow of carrier gas such as nitrogen (Lidegren 2001) or argon (Zalutsky 1996) in a quartz vessel. After volatilization from the cyclotron target, ^{211}At can be trapped using silica columns (Friedman et al. 1977), bubbler traps (Lindgren 2001), and capillary tubing cryotraps (Lambrecht and Mirzadeh 1985). The solvent extraction procedure consists of dissolution of target using concentrated HNO_3 followed by extraction of ^{211}At into either butyl or isopropyl ether (Yordanov et al. 2004). Another approach reported is based on dissolution of the Bi_2O_3 target in concentrated perchloric acid followed by solid–liquid extraction employing thiosemicarbazide incorporated onto Amberlite IRC-50 resin (Roy et al. 2004).

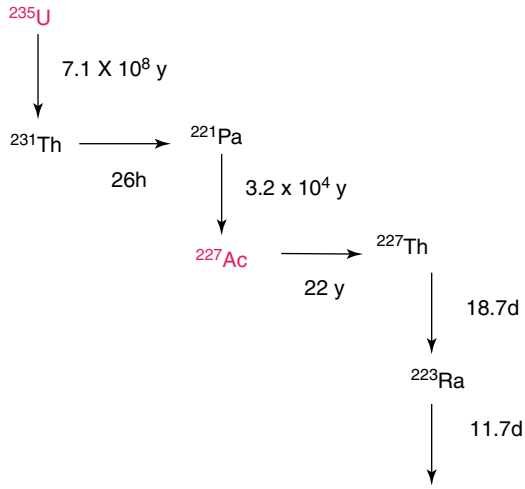

Fig. 6.5 Decay scheme for ^{223}Ra

6.3.3 Copper-67

The production yields of ^{67}Cu in a nuclear reactor by the ^{67}Zn(p,n)^{67}Cu reaction (*vide ante*) are low because of a low neutron capture cross section, even when high-energy neutrons are available. Accelerator production is the preferred approach to obtain both the high specific activity and high activity levels of ^{67}Cu which are required for

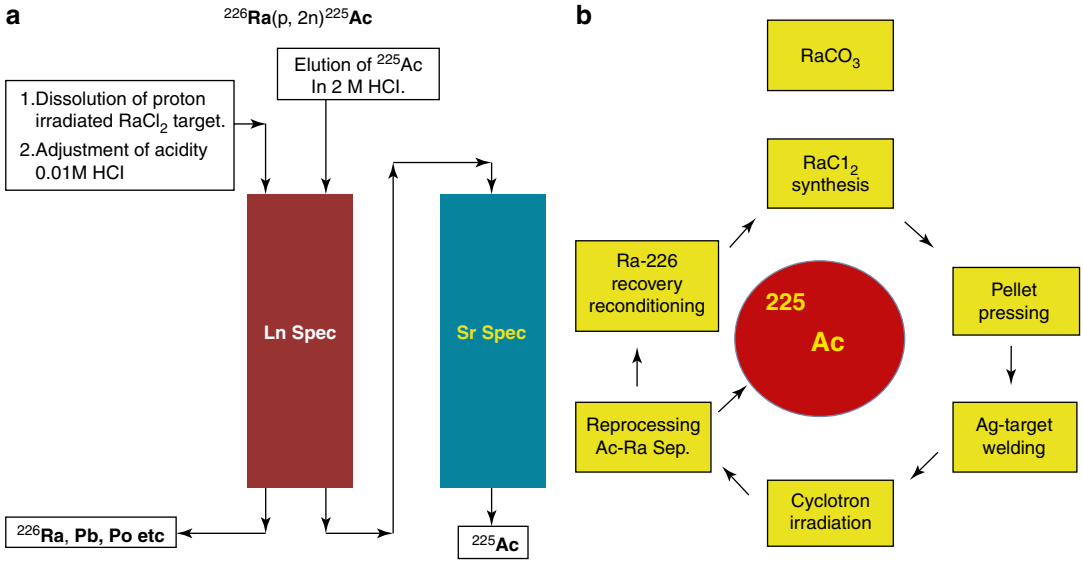

Fig. 6.6 Production and separation of ^{225}Ac by proton irradiation of ^{226}Ra target

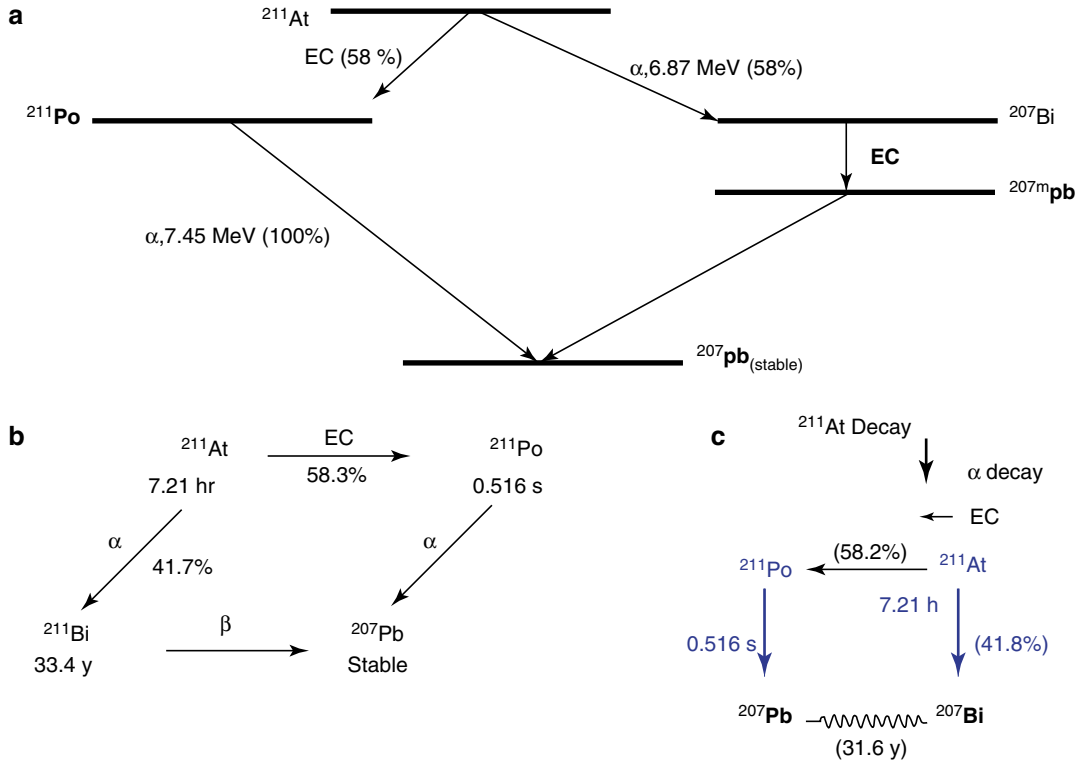

Fig. 6.7 Simplified decay scheme of ^{211}At

Table 6.2 Principal nuclear reactions for ^{67}Cu production

Particle	Nuclear reaction	Cross section (σ) in mb
p	^{68}Zn(p,2p)^{67}Cu	*6* (E_p=30…85 MeV) *24.8* (E_p=130…425 MeV)
	^{70}Zn(p,α)^{67}Cu	*15* (E_p=16 MeV)
α	^{64}Ni(α,p)^{67}Cu	*34* ($E_α$=22 MeV)
n	^{67}Zn(n,p)^{67}Cu	*1.07*
e→γ (photonuclear reaction)	^{68}Zn(γ,p)^{67}Cu	*11* ($E_γ$=22 MeV)

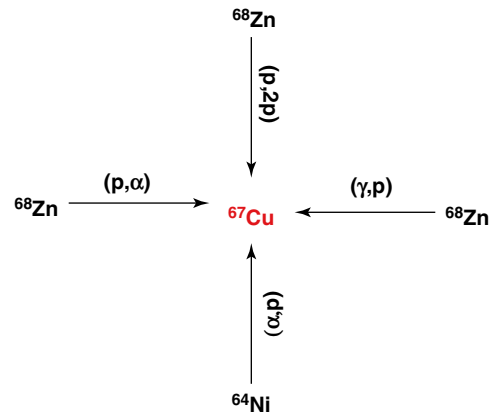

Fig. 6.8 Summary of key cyclotron production routes for ^{67}Cu

clinical applications, and several particle reactions have been evaluated (Table. 6.2) as shown in Fig. 6.3. Because of broad interest in the availability of ^{67}Cu, a wide variety of production and processing methods have been evaluated as described in the following sections. However, in spite of this effort, very few ^{67}Cu-labeled radiopharmaceuticals have been developed and evaluated in clinical trials (Fig. 6.8).

Cyclotron production of ^{67}Cu is performed by irradiating ^{nat}Zn or enriched ^{68}Zn with protons or α particles, and the most typical production route of

^{67}Cu has been the high-energy proton irradiation of natural zinc targets particles (Schwarzbach et al. 1995; Dasgupta et al. 1991; Mirzadeh et al. 1986). Copper-67 has been produced in the United States with high-energy accelerators at the Brookhaven (BNL) and Los Alamos (LANL) National Laboratories. Since 1994, the Center for Radiopharmaceutical Science at the Paul Scherrer Institute (PSI) in Switzerland has undertaken the production of ^{67}Cu with a 72-MeV accelerator to meet their own requirement (Knogler et al. 2007). The ^{68}Zn(p,2p)^{67}Cu nuclear reaction produces ^{67}Cu of low yields and requires an efficient separation procedures to remove radioactive contaminants, which include ^{62}Zn, ^{67}Ga, ^{65}Zn, ^{55}Co, ^{58}Co, and ^{57}Ni.

The ^{70}Zn(p,α)^{67}Cu reaction using 30-MeV alpha particles is promising owing to the production of minimal impurity levels and the accessibility of this reaction. Of the several options tabulated, the photonuclear reaction cross section is by an order of magnitude higher than the corresponding value for the (n,p) path. The photonuclear ^{68}Zn(n,p)^{67}Cu method is also attractive in view of a relatively low cost of electron accelerators and their low running expenses in comparison with heavy particle accelerators. In this method, linear accelerators generating 30–60 MeV electrons were allowed to focus on a convertor plate such as tungsten or tantalum to produce photons with a similar energy range (Starovoitova et al. 2014). One of the major hurdles of this method of production using natural zinc target is the coproduction of ^{63}Zn and ^{65}Zn which decay to stable copper, thereby reducing the ^{67}Cu-specific activity. The ^{66}Zn(γ,d)^{64}Cu side reaction is also problematic and leads to production of the ^{64}Cu ($T_{1/2}$ 1 = 12.7 h) radionuclide impurity, which can be reduced by allowing sufficient cooling time. The use of enriched targets is preferred in most of the production schemes summarized in Table 6.2 in order to achieve higher levels radionuclidic purity.

Because of methods which are well established for copper chemistry, several separation processes described below have been evaluated for purification of cyclotron-produced ^{67}Cu, which are based on differences in the physical and chemical properties of Zn and Cu. These strategies involve initial removal of the bulk zinc matrix followed by a secondary ion-exchange step as a final cleanup procedure.

6.3.3.1 Ion Exchange

A number multistep sequential ion-exchange chromatographic techniques using a variety of ion-exchange resins such as dithizone-impregnated resin, Bio-Rad AG-1 MP-1, Dowex-1, Bio-Rad AG-5OW, and Chelex-100 have been used to separate ^{64}Cu from irradiated Zn (Mausner et al. 1998; Dolley et al. 2006; Jamriska et al. 1995; Mushtaq et al. 1990; Shikata 1964; Yagi and Kondo 1978; Katabuchi et al. 2008; Polak et al. 1986; Schwarzbach et al. 1995). The method used at BNL for the production, chemical separation, and purification of ^{67}Cu obtained by the (n,p) path uses zinc oxide targets (Mausner et al. 1998). The target used for reactor irradiation consists of a 40-g pressed pellet of ZnO as well as enriched ^{67}ZnO powder in a quartz ampoule. After irradiation, the target is cooled, dissolved in concentrated HCl, evaporated to dryness, and reconstituted with 0.5-M sodium acetate buffer maintained at pH 3.27. The solution is then passed through a chromatographic column containing Chelex-100 (100–200 mesh), where the ^{67}Cu remains adsorbed and the bulk of the Zn passes through the column. After washing the column with 0.001 N HC1, Cu is eluted with 12 N HCl. Gallium and Fe are separated from Cu by passing this solution through a chromatographic column containing a cation exchange resin (Bio-Rad AG50W-X8, 100–200 mesh), where the impurities are adsorbed. The column is then washed with 10 N HCI. For final purification, the washing and the effluents are collected, and the combined fractions are loaded onto a chromatographic column containing an anion exchange column (Bio-Rad AGI-X8, 100–200 mesh). A 4.5 N HC1 rinse removes any Co isotopes which are collected and discarded as radioactive waste, and the ^{67}Cu is finally eluted with 3 N HCl. In order to perform radiolabeling, the ^{67}Cu solution is evaporated to dryness and reconstituted with 0.1 N HCl (Mausner et al. 1998).

6.3.3.2 Electrodeposition

The use of an electrolytic technique is another strategy for processing and recovery of ^{67}Cu (Mirzadeh et al. 1986). After irradiation, the target is dissolved in 10 mL of a 10:1 mixture of conc. HCI and conc. HNO_3. Following evaporation to near dryness the residue dissolved in 1 M H_2SO_4. The volume of solution is adjusted with1 M H_2SO_4 to maintain an ~ 2 M concentration of Zn^{2+}. The solution is then transferred to the electrolysis cell provided with a rotating Pt electrode. Under a constant potential of 2.1 V for 2 h, Cu is electroplated on the rotating (~1500 rpm) Pt electrode. The original electrolyte is removed and replaced with a second electrolyte (20 mL of 0.1 M ZnSO, and 1 M H_2SO_4,) without disconnecting the circuit. The polarities of the circuit are reversed and electrolysis is carried out for 5–10 min to dissolve the Cu from the Pt electrode. The electrolysis is repeated to electrodeposit Cu back onto the Pt cathode for an additional 2 h. Finally, the Pt cathode is removed and immersed in 2 mL of 3-M HNO_3 to recover the ^{67}Cu. For final purification, the solution containing ^{67}Cu is evaporated to near dryness, reconstituted with 1 mL of 1.8-M HCI and passed through an anion exchange column (MP-I, 100–200 mesh, 3×40 mm, prewashed with 1.8 M HCI) wherein all anionic impurities get trapped. The column is then washed with an additional 4 mL of 1.8 M HCI. The eluates are combined, and the total volume is adjusted to 5 mL with the addition of water (Mirzadeh et al. 1986),

6.3.3.3 Liquid–Liquid Extraction

The most commonly used procedure for recovery of ^{67}Cu by liquid–liquid extraction (Dasgupta et al. 1991; Stoll et al. 2002) consists of a primary extraction using 0.01 % dithizone in CCI_4 contacting a 0.5 M HCI layer containing the dissolved target. This solvent extraction is repeated four times to obtain the ^{67}Cu of desired purity. The ^{67}Cu is then back extracted from the organic fraction with 7.2 M HCI and H_2O_2. The aqueous back extracted layers are combined and contacted with isopropyl ether to remove Ga. Finally, the solution is passed through an anion exchange column to remove Ni, Mn, Cr, and Co isotopes.

6.3.3.4 Sublimation

This method exploits the low sublimation temperature and pressure of Zn compared to Cu (Mausner et al. 1998). Typically, the irradiated zinc target is placed in a sublimation assembly and heated at a temperature of ~800 °C in which zinc sublimes leaving the copper behind. Final purification is performed using ion-exchange chromatographic technique.

6.3.4 Gallium-67

Gallium-67 ($T_{1/2}$ = 3.26 d) decays by 100 % by electron capture and emits γ radiation with energies of 93.3 keV (37 %), 184.6 keV(20.4 %), and 300.2 keV(16.6 %). In addition to its use for diagnostic applications, interest in the effectiveness of Auger emissions from ^{67}Ga for some specific therapeutic applications has also been reported. Gallium-67 can be reactor-produced (Chap. 5), and the most common ^{67}Ga cyclotron production methods include (Fig. 6.9) proton irradiation of isotopically enriched ^{68}Zn targets by the ^{68}Zn(p,2n)^{67}Ga nuclear reaction (Little and Lagunas-Solar 1983). Deuteron irradiation has also been reported on isotopically enriched ^{67}Zn targets by the ^{67}Zn(d,2n)^{67}Ga nuclear reaction (Gul 2001) and α-particle irradiation by the ^{64}Zn(α,n)^{67}Ga or ^{65}Cu(α,2n)^{67}Ga reaction has been reported (Naidoo and Van der Walt 2001; Martin and Osso 2013).

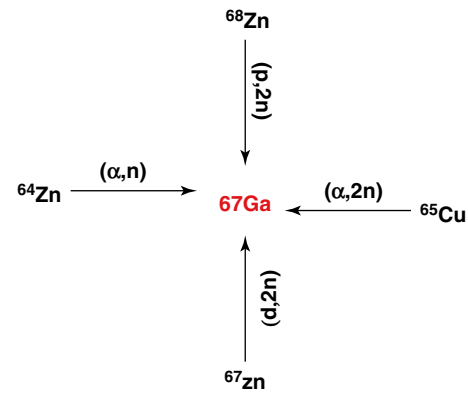

Fig. 6.9 Cyclotron methods for production of ^{67}Ga

Separation of pure gallium radioisotopes produced by cyclotrons—and also produced in nuclear reactors—from the target material and target holder (Zn and Cu, respectively) can be achieved by ion exchange (Aardaneh and Shirazi 2005; El-Azony et al. 2003; Massaoud et al. 2008). Recovery of gallium from aqueous solutions is commonly achieved by chemical precipitation (Sadeghi and Mokhtari 2010), complexation (Dumortier et al. 2005) and ion exchange (Massaoud et al. 2008). Each of these separation techniques of course has its merits and limitations for practical application. The radiochemical processing followed for the separation of ^{67}Ga available from the ^{68}Zn(p,2n)^{67}Ga reaction involves dissolution of the irradiated target in 10 M HCl with subsequent passage of the solution through a cation exchange resin (AG 50 W,H^+ form, mesh 200–400) which is preconditioned with 9 M HCl (Jalilian et al. 2009). The column is washed with 9 M HCl and ^{67}Ga eluted with 6 M HCl solution. The ^{67}Ga obtained from this column is purified by passing through an anion exchange column (AG1X8 Clform,100–200 mesh) pretreated with 6 M HCl where in ^{67}Ga is adsorbed. The ^{67}Ga is then eluted as $^{67}GaCl_3$ using 2 M HCl.

6.3.5 Indium-111

Indium-111 ($T_{1/2}$ = 2.8 d) decays by electron capture (EC 100 %) with emission of γ rays of 173 and 247 keV (89 % and 95 % abundance, respectively). As discussed earlier, these gamma emissions are accompanied by total internal conversions of about 10 % and 6 % (see Chap. 4), respectively. Therapeutic interest in ^{111}In has resulted from the use of ^{111}In-labeled peptides for targeted therapy, utilizing the Auger electrons (see Chap. 9). Commercial production involves irradiation of natural cadmium targets with energetic protons according to the ^{111}Cd(p,n)^{111}In or ^{112}Cd(p,2n)^{111}In reactions, and both remain the most widely used ^{111}In production methods (Zaitseva et al. 1990). When production of ^{111}In is carried out by bombarding Cd targets with protons, the ^{111}In activity at the end of bombardment (EOB) contains radionuclidic contaminates which include ^{109}In ($t_{½}$ = 4.3 h), ^{110m}In($t_{½}$ = 4.9 h), and ^{114m}In ($t_{½}$ = 4.9d). The first two radionuclides of indium have relatively short half-lives and hence cooling for 24 h after EOB is required to significantly reduce the levels of these contaminates (Lahiri et al. 2013).

Radiochemical separation of ^{111}In from the irradiated target can be performed using a wide variety of techniques such as coprecipitation with $Fe(OH)_3$ (Neirincks 1971), ion exchange (Das et al. 1996; Das et al. 1997), extraction chromatography (Levin et al. 1974; Sharma and Smith 1981; Horwitz et al. 1997), thermochromatography (Novgorodov et al. 1984; Schomakher et al. 1988), use of cation exchange resin (Das et al. 1997; Brown and Beets 1972; Nelson and Michelson 1966; Chattopadhyay et al. 1997), coprecipitation with $La(OH)_3$ (Filoosofov et al. 2001), liquid–liquid extraction using Cyanex923 (Guptna et al. 2004), liquid–liquid distribution of ion associates of tetrabromoindate (III) with quaternary ammonium counter ions (Yamamoto and Matsumoto 1977), using organophosphorus compounds as extractants (Rajeh and Subramanian 1994), extraction chromatography using liquid anion exchanger (Horwitz et al. 1995), and solid phase extraction (Horwitz and Dietz 1990; Horwitz et al. 1991; Inoue et al. 1994). Each of these techniques has its own advantages and disadvantages. Liquid–liquid extraction (LLE) (Zheng et al. 1993; Paiva 2001; Horwitz et al. 1993) and ion-exchange chromatography (IEC) are widely used for radiochemical separation of ^{111}In (Das et al. 1997; Rajeh and Subramainan 1994; Horwitz et al. 1995; 1991; Horwitz et al. 1997; Ham 1995).

6.3.6 Rhenium-186

Although ^{186}Re is often reactor-produced, when HSA is required, accelerator production is arising as the preferred production route because of the unique capability of NCA production. High activity levels of NCA ^{186}Re can be produced using cyclotrons (Shigeat et al. 1996; Zhang et al. 1999) by the ^{186}W(p,n)^{186}Re and ^{186}W(d,2n)^{186}Re nuclear reactions. However, because of the low

cross section for the $^{186}W(p,n)^{186}Re$ reaction, production of high activity levels of ^{186}Re using low-energy cyclotrons is a difficult proposition. On the other hand, the $^{186}W(d,2n)^{186}Re$ reaction is more favorable due to the larger cross section (Zhang et al. 2001). The measurement of ^{186}Re production yields by this approach has shown that it is more effective to use a deuteron beam (12.8 MeV) rather than the proton beam (16.5 MeV) for production. In this method the ^{186}W metal target was used dissolved in 30 % H_2O_2 and 1 M NaOH after irradiation with heating. After concentration to near dryness, it was reconstituted with a HCl solution, the pH of which was adjusted to 3–4 and loaded on an acid alumina column. The ^{186}Re was then eluted from the column with saline.

6.4 Tin-117 m

In addition to the expected benefits of AE for therapy, the benefits of conversion electrons (CE) have also been widely recognized and ^{117m}Sn represents one key example. The production of NCA ^{117m}Sn can be carried out in an accelerator using a number of possible nuclear reactions (Ermolaev et al. 2009). Using the $^{115m}In(\alpha,pn)^{117m}Sn$ reaction over the energy range of 45–20 MeV, a relatively pure product can be obtained, however, in very small yields. Natural antimony can be used to produce ^{117m}Sn following the $^{nat}Sb(p,xn)^{117m}Sn$ reaction over the energy range of 38–60 MeV (Mausner et al. 1998). This process, with a cross section of 5 mb, was found enough to produce therapeutic quantities of ^{117m}Sn with high specific activity. Subsequently, the method was upgraded to undertake larger-scale production of NCA ^{117m}Sn with high purity and high specific activity, using targets based on natural or enriched Sb. The thick targets of Sb or Sb–Ti intermetallic compounds are used for irradiation. Chemical recovery of ^{117m}Sn was carried out by solvent extraction with dibutyl ether followed by chromatographic purification on silica gel column. Using these methods, the production of ^{117m}Sn with specific activity of about ~1000 Ci/g with high radionuclidic purity is reported (Ermolaev et al. 2009).

6.5 Summary

Particle accelerators, and in particular cyclotrons, continue to play an integral role for the production of a variety of neutron-deficient therapeutic radioisotopes. The prominent role played by the cyclotrons for the production of therapeutic radionuclides dictates that a holistic consideration should be given to all governing factors while selecting a method. Coalescing the target preparation, cyclotron irradiation of target, and radiochemical separation science is the art of radionuclide production. Persistent efforts are on to uncover new ways to improve the production yields and minimize radioactive contaminants. While the use of enriched target material constitutes a successful paradigm to obtain high-specific-activity radionuclide of interest and good radiopurity, it is necessary to recycle the expensive enriched target material to defray the target cost over many production runs. The interest and availability of alpha-emitting radioisotopes is rapidly increasing, and it is also expected that a variety of other accelerator-produced therapeutic radioisotopes will continue to be evaluated for their potential role for therapy.

References

Aardaneh K, Shirazi B. Rapid separation of radiogallium from Zn and Cu targets using anion exchange technique. J Radioanal Nucl Chem. 2005;265:4.

Apostolidis C, Molinet R, Rasmussen G, Morgenstern A. Production of Ac-225 from Th-229 for targeted alpha therapy. Anal Chem. 2005;77:6288–91.

Boll RA, Malkemus D, Mirzadeh S. Production of actinium- 225 for alpha particle mediated radioimmunotherapy. Appl Radiat Isot. 2005;62:667–79.

Brown LC, Beets AL. Cyclotron production of carrier free indium-111. Int J Appl Radiat Isot. 1972;23:57–63.

Chattopadhyay S, Das MK, Sarkar BR, Ramamoorty N. Radiochemical separation of high purity ^{111}In from cadmium, copper, aluminium and traces of iron: use of a cation exchange resin with hydrobromic acid and hydrobromic acid. Appl Radiat Isot. 1997;48(8):1063–7.

Das SK, Guin R, Saha SK. Carrier-free separation of ^{111}In from a silver matrix. Appl Radiat Isot. 1996;47(3):293–6.

Das MK, Chattopadhayay S, Sarkar BR, Ramamoorthy N. A cation exchange method for separation of ^{111}In from inactive silver, copper, traces of iron and radioactive gallium and zinc isotopes. Appl Radiat Isot. 1997;48(1):11–4.

Dasgupta AK, Mausner LF, Srivastava SC. A new separation procedure for 67Cu from proton irradiated Zn. Appl Radiat Isot. 1991;42:371–6.

Dolley SG, Walt TN, Steyn GFE, Szelecseny F, Kovacs Z. The production and isolation of Cu-64 and Cu-67 from zinc target material and other radionuclides. Czech J Phys. 2006;56:D539–44.

Dumortier R, Weber ME, Vera JH. Removal and recovery of gallium from aqueous solutions by complexation with sodium di-(n-octyl) phosphinate. Hydrometallurgy. 2005;76:207–15.

Eberle SH. Gmelin handbook of inorganic chemistry – astatine. 8th ed. Berlin: Springer; 1985. p. 183–209.

El-Azony KM, Ferieg K, Saleh ZA. Direct separation of ^{67}Ga citrate from zinc and copper target materials by anion exchange. Appl Radiat Isot. 2003;59:329.

Ermolaev SV, Zhuikov BL, Kokhanyuk V, Srivastava SC. Production of carrier-added Tin-117m from proton irradiated antimony. J Radioanal Chem. 2009;280: 319–24.

Filoosofov DV, Lebedev NA, Novogrodov A, et al. Production, concentration and deep purification of ^{111}In radiochemicals. J Appl Radiat Isot. 2001;55:293–329.

Friedman AM, Zalutsky MR, Wung W, et al. Preparation of a biologically stable and immunogenically competent astatinated protein. Int J Nucl Med Biol. 1977;4:219–24.

Gul K. Calculations for the excitation functions of 3–26 MeV proton reactions on ^{66}Zn, ^{67}Zn and ^{68}Zn. Appl Radiat Isot. 2001;54:311–8.

Guptna B, Deep A, Malik P. Liquid-Liquid extraction and recovery of Indium using Cyanex 923. Anal Chim Acta. 2004;513:463–71.

Ham GJ. Determination of actinides in environmental materials using extraction chromatography. Scien Tot Environ. 1995;173/174:19–22.

Henricksen G, Hoff P, Alstad J, Larsen RH. ^{223}Ra for endoradiotherapeutic applications prepared from an immobilized ^{227}Ac/^{227}Th source. Radiochim Acta. 2001;89:661–6.

Horowitz EE, Bond AH. Purification of radionuclides for nuclear medicine: the multicolumn selectivity inversion generator concept. Czech J Phys. 2003;53:A713–6.

Horwitz EP, Dietz ML. Concentration and separation of actinides from urine using a supported bifunctinal organophosphorus extractant. Anal Chim Acta. 1990;238:263–71.

Horwitz EP, Dietz ML, Fisher DE. Separation and pre concentration of strontium from biological, environmental, and nuclear waste samples by extraction chromatography using a crown ether. Anal Chem. 1991;63(5):522–5.

Horwitz EP, Chiarizia R, Dietz ML, et al. Separation and preconcentration of actinides from acidic media by extraction chromatography. Anal Chim Acta. 1993;281:361–72.

Horwitz EP, Dietz ML, Chiarizia R, et al. Separation and preconcentration of actinides by extraction chromatography using a supported liquid anion exchanger. Application to the characterization of high-level nuclear waste solutions. Anal Chim Acta. 1995;310:63–78.

Horwitz EP, Chiarizia R, Dietz ML, et al. DIPEX: a new extraction chromatographic material for the separation and Pre-concentration of actinides from aqueous solution. React Func Polym. 1997;33:25–36.

Inoue K, Yoshizuka K, Yamguchi S. Solvent extraction of indium 8 trialkylphosphine oxide from sulphuric acid solutions containing chloride. J Chem Engin Japan. 1994;27(6):737–40.

International Atomic Energy Agency (IAEA) Publication Technical Reports Series No. Cyclotron produced radionuclides: physical characteristics and production, 468. Vienna; 2009.

Jalilian AR, Yousefnia H, Garousi J, et al. The development of radiogallium-acetylacetonate bis(thiosemicarbazone) complex for tumour imaging. Nucl Med Rev. 2009;12(2):65–71.

Jamriska DJ, Taylor WA, Ott MA, et al. Activation rates and chemical recovery of ^{67}Cu produced with low energy proton irradiation of enriched Zn targets. J RadioanaLl ucL Chem. 1995;195:263–70.

Johnson EL, Turkington TG, Jaszczak RJ, et al. Quantitation of ^{211}At in small volumes for evaluation of targeted radiotherapy in animal models. Nucl Med Biol. 1995;22:45–54.

Katabuchi T, Watanabe S, Ishioka N, et al. Production of Cu-67 via the Zn-68(p,2p)Cu-67 reaction and recovery of Zn-68 target. J Radioanal Nucl Chem. 2008;277:467–70.

Kirby HW. Residue adsorption – III: mutual separation of ^{227}Ac, ^{227}Th and ^{223}Ra. J Inorg Nucl Chem. 1969;31:3375–85.

Kirby HK. Gmelin handbook of inorganic chemistry – astatine. 8th ed. Berlin: Springer; 1985. p. 95–106.

Knogler K, Grünberg J, Zimmermann K, et al. Copper-67 radioimmunotherapy and growth inhibition by anti L1-cell adhesion molecule monoclonal antibodies in a therapy model of ovarian cancer metastasis. Clin Cancer Res. 2007;13:603–11.

Lahiri S, Maiti M, Ghosh K. Production and separation of ^{111}In: an important radionuclide in life sciences: a mini review. J Radioanal Nucl Chem. 2013;297: 309–18.

Lambrecht RM, Mirzadeh S. Cyclotron isotopes and radiopharmaceuticals – XXXV. Astatine-211. Int J Appl Radiat Isotop. 1985;36:443–50.

Larsen RH, Murud KM, Akabani G, et al. ^{211}At- and ^{131}I-labeled bisphosphonates with high *in vivo* stability and bone accumulation. J Nucl Med. 1999;40:1197–203.

Levin VI, Kozlova MD, Malinin AB, et al. The production of carrier-free indium. Int J Appl Radiat Isot. 1974; 25:286–8.

Lindegren S, Back T, Jensen H. Dry-distillation of astatine-211 from irradiated bismuth targets: a time-saving procedure with high recovery yields. Appl Radiat Isot. 2001;55:157–60.

Little FE, Lagunas-Solar MC. Cyclotron production of ^{67}Ga. Cross sections and thick-target yields for the ^{67}Zn (p, n) and ^{68}Zn (p,2n) reactions. Int J Appl Radiat Isot. 1983;34(3):631–7.

Martins ADA, Osso Jr JA. Thermal diffusion of ^{67}Ga from irradiated Zn targets. Appl Radiat Isot. 2013;82:279–82.

Massaoud AA, Hanafi HA, Siyam T, Saleh ZA, Ali FA. Separation of Ga(III) from Cu(II), Ni(II) and Zn(II) in aqueous solution using synthetic polymeric resins. Cent Eur J Chem. 2008;6(1):39–45.

Mausner LF, Kolsk KL, Joshi V, Srivastava SC. Radionuclide development at BNL for nuclear medicine therapy. Appl Radiat Isot. 1998;49:285–94.

Miederer M, Scheinberg DA, McDevitt MR. Realizing the potential of the Actinium-225 radionuclide generator in targeted alpha particle therapy applications. Adv Drug Deliv Rev. 2008;60: 1371–82.

Milesz S, Norseev YV, Szücs Z, Vasáros L. Characterization of DTPA complexes and conjugated antibodies of astatine. J Radioanal Nucl Chem Lett. 1989;137:365–72.

Mirzadeh S, Mausner LF, Srivastava SC. Production of no carrier-added Cu-67. Appl Radiat Isot. 1986; 37:29–36.

Mushtaq A, Karim H, Khan M. Production of no-carrier-added ^{64}Cu and ^{67}Cu in a reactor. J. RadioanaL Nucl Chem. 1990;141:261–9.

Naidoo C, Van der Walt TN. Cyclotron production of ^{67}Ga (III) with a tandem ^{nat}Ge–^{nat}Zn target. Appl Radiat Isot. 2001;54:915–9.

Neirincks RD. The separation of cyclotron-produced ^{111}In from a silver matrix, radio. Chem Radioanal Lett. 1971;4(2):153–5.

Nelson F, Michelson DC. Ion-exchange procedures ix Cation exchange in HBr solutions. J Chromatogr. 1966;25:414.

Novgorodov AF, Beyer GJ, Zelinski A, et al. Simple method for high temperature release of ^{111}In from silver. J I N R (Dubna). 1984;6(84):609.

Paiva AP. Recovery of indium from aqueous solutions by solvent extraction. Sep Sci Technol. 2001;36(7): 1395–419.

Polak P, Geradts J, Van der Vlist R, Lindner L. Photonuclear production of ^{67}Cu from ZnO Targets. Radiochim Acta. 1986;40:169–74.

Rajeh N, Subramainan MS. Extractive separation and determination of thallium and indium by liquid scintillation counting. Analyst. 1994;119:2071–4.

Roy K, Basu S, Ramaswami A, Nayak D, Lahiri S. Incorporation of thiosemicarbazide in Amberlite IRC-50 for separation of astatine from α-irradiated bismuth oxide. Appl Radiat Isotop. 2004;60: 793–9.

Sadeghi M, Mokhtari L. Rapid separation of ^{67,68}Ga from ^{68}Zn target using precipitation technique. J Radioanal Nucl Chem. 2010;284:471–3.

Scheinberg DA, McDevitt MR. Actinium-225 in targeted alpha-particle therapeutic applications. Curr Radiopharm. 2011;4:306–20.

Schomakher K, Schwratzbach R, Beyer G-J, Novogorodov AF. A further simplified method for the separation of ^{111}In from Silver targets by thermo chromatography. Appl Radiat Isot. 1988;39(6):483–5.

Schwarzbach R, Zimmermann K, Blaeuenstein P, et al. Development of a simple and selective separation of ^{67}Cu from irradiated zinc for use in antibody labelling: a comparison of methods. Appl Radiat Iso. 1995;46:329–36.

Sharma HL, Smith A. The short-lived radioisotope production program at Manchester. J Radioanal Chem. 1981;64(1, 2):249–55.

Shigeta N, Matsuoka H, Osa A, Koizumi M, Izumo M, Kobayashi K, Hashimoto K, Sekine T, Lambrecht RM. Production method of no-carrier-added ^{186}Re, J Radioanal Nucl Chem. 1996;205:85–92.

Shikata E. Research of radioisotope production with fast neutrons. vi. preparation of Cu-67. J Nucl Sci Technol (Tokyo, Jpn). 1964;1:177–80.

Smit JA, Myburgh JA, Neirinckx RD. Specific inactivation of sensitized lymphocytes *in vitro* using antigens labelled with astatine-211. Clin Exp Immunol. 1973;14:107–16.

Starovoitova VN, Tchelidze L, Wells DP. Production of medical radioisotopes with linear accelerators. Appl Radiat Isot. 2014;85:39–44.

Stoll T, Kastleiner S, Shubin YN, Coenen HH, Qaim SM. Excitation functions of proton induced reactions on 68Zn from threshold up to 71 MeV, with specific reference to the production of 67Cu. Radiochim Acta. 2002;90:309–13.

Turlera A, Huenges E, Henkelmann R, et al. Method for purification of ^{225}Ac from irradiated ^{226}Ra-targets. United States Patent No. US 2013/0266475 A1, 10 Oct 2013.

Weidner JW, Mashnik SG, John KD, et al. ^{225}Ac and ^{223}Ra production via 800 MeV proton irradiation of natural thorium targets. Appl Radiat Isot. 2012;70:2590–5.

Yagi M, Kondo K. Preparation of carrier-free 67Cu by the 68Zn(g, p) reaction. Int J Appl Radiat Isot. 1978; 29:757–9.

Yamamoto K, Matsumoto A. Liquid-Liquid distribution of ion associates of tetrabromoindate (III) with quaternarymoniun counter ions. Talanta. 1977;44: 2145–50.

Yordanov AT, Deal K, Garmestani K, Kobayashi H, et al. Synthesis and biodistribution study of a new ^{211}At-calix[4]arene complex. J Label Compd Radiopharm. 2000;43:1219–25.

Yordanov AT, Pozzi O, Carlin S, et al. Wet harvesting of no-carrier-added 211At from an irradiated 209Bi target for radiopharmaceutical applications. J Radioanalyt Nucl Chem. 2004;262:593–9.

Zaitseva NG, Knotek O, Kowalew A, et al. Excitation functions and yields for 111In production using. 113,114, natCd(p, xn)111In reaction with 65 MeV protons. Appl Radiat Isot. 1990;41:177–83.

Zalutsky MR, Bigner DD. Radioimmunotherapy with alpha-particle emitting radioimmunoconjugates. Acta Oncol. 1996;35:373–9.

Zalutsky MR, Pruszynski M. Astatine-211 – production and availability. Curr Radiopharm. 2011;4(3):177–85.

Zhang X, Lp W, Fang K, He W, Sheng R, Ying D, Hu W. Excitation functions for $^{nat}W(p, xn)^{181-186}Re$ reactions and production of no-carrier-added. ^{186}Re via $^{186}W(p, n)^{186}Re$ reaction. Radiochim Acta. 1999;86: 11–6.

Zhang X, Li Q, Li W, Sheng R, Shen S. Production of no-carrier-added ^{186}Re via deuteron induced reactions on isotopically enriched ^{186}W. Appl Radiat Isot. 2001;54: 89–92.

Zheng WI, Sipes IG, Carter DE. Determination of parts-per-billion concentrations of indium in biological materials by electrothermal atomic absorption spectrometry following Ion pair extraction. Anal Chem. 1993;65:2174–6.

Zhuikov BL, Kalmykov SN, Ermolaev SV, et al. Production of ^{225}Ac and ^{223}Ra by irradiation of Th with accelerated protons. Radiochem. 2011;53(1): 73–80.

7 Radionuclide Generator Systems Represent Convenient Production Systems to Provide Therapeutic Radionuclides

7.1 Introduction

Radionuclide generators represent important in-house production systems which can provide daughter radioisotopes generated by parent decay on-demand without the need for local access to an accelerator or research reactor. The ^{99}Mo/^{99m}Tc generator represents the most important example and provides NCA ^{99m}Tc without which the success of diagnostic nuclear medicine could not have been possible. It is estimated that ^{99m}Tc is used in over 30 million studies annually on an international basis. The in-house or central radiopharmacy use of radionuclide generators has many advantages, since their use represents a cost-effective strategy for obtaining the desired daughter radionuclide on demand and also ensures availability of the daughter radionuclides in high specific activity and usually in no-carrier-added form. The most widely used technology for fabrication of radionuclide generators for clinical applications is the column chromatography system. However, in recent years enormous interest has developed for use of other novel separation techniques to provide therapeutic radionuclides. Among many other requirements, such as those relating to establishment of chemical, radiochemical, and radionuclidic purity of the daughter radionuclide, radionuclide generators intended for clinical applications must be manufactured and operated under conditions of good manufacturing practice (GMP) guidelines since these products represent active pharmaceutical ingredients (APIs) which will be incorporated into radiopharmaceutical products prepared for human use.

In addition to a variety of other radionuclide generator systems which provide diagnostic radioisotopes (Osso and Knapp 2011; Roesch and Knapp 2011; Knapp and Mirzaeh 1994; Knapp and Butler 1984; Mirzadeh and Knapp 1996; Chakravarty and Dash 2013; Knapp et al. 2014), radionuclide generator systems also represent important resources to provide a variety of therapeutic radioisotopes for applications in nuclear medicine, oncology, and interventional specialties (Table 7.1). Many parent–daughter pairs have been evaluated as radionuclide generator systems (Roesch and Knapp 2011; Dash and Chakravarty 2014a, b; Knapp et al. 2014; Pillai et al. 2012). While only a few therapeutic generators are currently used in routine clinical practice, several others show great promise for further development and potential widespread clinical use. An important requirement for radionuclide generator systems for routine clinical use is a long half-life of the parent radionuclide, which provides logistics for production, transportation, and reduced injection dose costs because of long useful shelf lives. A variety of radionuclide generators which provide daughter radionuclides which are used and have been proposed for therapeutic applications are summarized in Table 7.1. The most widely used radionuclide generators for therapeutic applications include β-emitting daughters from the ^{188}W/^{188}Re and ^{90}Sr/^{90}Y

F.F. (Russ) Knapp, A. Dash, *Radiopharmaceuticals for Therapy*, DOI 10.1007/978-81-322-2607-9_7

Table 7.1 Key examples of radionuclide generators providing therapeutic radioisotopes

Generator system	Main production route of parent radionuclide	Parent radionuclide		Daughter radionuclide	
		$T_{½}$	Main decay mode	$T_{½}$	Main decay mode
$^{225}Ac/^{213}Bi$	Decay chain	10.0 days	α	45.6 min	β^-, α
$^{227}Ac/^{223}Ra$	Reactor decay chain	21.7 years	β^-, then α through ^{227}Th	11.4 days	α
$^{166}Dy/^{166}Ho$	Reactor	3.40 days	β^-	1.12 days	β^-
$^{194}Os/^{194}Ir$	Reactor	6.0 years	β^-	19.15 h	γ, β^-
$^{212}Pb/^{212}Bi$	^{228}Th ($T_{½}$ = 1.913 a) through ^{224}Ra	10.4 h	β^-	60.55 months	α
$^{226}Ra/^{222}Rn$	Decay chain	1.6×10^3 years	α	3.83 days	α
$^{90}Sr/^{90}Y$	Reactor (fission product)	28.5 years	β^-	2.67 days	β^-
$^{188}W/^{188}Re$	Reactor	69.4 days	β^-	16.98 h	β^-

generator systems and alpha-emitting radioisotopes obtained from the $^{225}Ac/^{213}Bi$ and $^{227}Ac/^{223}Ra$ generator systems.

Radionuclide generators provide therapeutic radionuclides which can decay by emission of beta particles, Auger electrons, low-energy photons, and alpha particles and are thus useful for a variety of therapeutic applications in nuclear medicine, oncology, and other clinical specialties. During the last decade, there has been a tremendous increase in the development and use of new therapeutic radiopharmaceuticals radiolabeled with radionuclides which are available from radionuclide generator systems (Pillai et al. 2012; Knapp et al. 2014; Chakravarty et al. 2008; Miederer et al. 2008; Scheinberg and McDevitt 2011; Zalutsky and Pozzi 2004). The availability of generator-derived therapeutic radionuclides is necessary for the development and testing and commercialization of agents with potential for endoradiotherapy (ERT) and has stimulated the development of an increasing spectrum of therapeutic tracers. Interest and the importance of the availability of therapeutic radionuclides available from generator systems have developed from the availability of several fully automated operations of many generators, coupled with parallel success in the development of therapeutic targeting agents, such as antibodies, peptides, and other agents. Applications of these generator-derived therapeutic radioisotopes include cancer therapy, synovectomy for the treatment of synovitis, and more recently therapy of skin cancer and inhibition of arterial restenosis after angioplasty of the coronary and peripheral vessels. A key example is the recent approval by the US Food and Drug Administration (FDA) for the use of the ^{90}Y-labeled murine anti-CD20 antibody "Zevalin" (ibritumomab tiuxetan) for the treatment of patients with low-grade, follicular or transformed non-Hodgkin's lymphoma. This agent is the first antibody radiolabeled with a generator-derived therapeutic radionuclide and represents the first of a variety of expected new therapeutic radiopharmaceuticals for oncologic applications.

7.2 Production of Parent Radionuclides

The production of the parent radioisotopes required for generator fabrication is an important issue. Production requires the availability of research reactors and various types of accelerators, as described in Chap. 5 and 6. Most therapeutic radionuclides currently in clinical use are neutron rich and characterized by beta decay and available from reactor production (Chap. 5), since neutron capture by the target nuclide forms a radioactive or unstable product which decays by beta emission. Key examples of therapeutic radionuclides obtained from

reactor-produced parent radionuclides include holmium-166 (^{166}Ho), from the dysprosium-166 (^{166}Dy)/^{166}Ho generator, and rhenium-188 (^{188}Re), from the tungsten-188 (^{188}W)/^{188}Re generator. Several generator parent radionuclides are produced during nuclear fission and include ^{90}Sr, isolated from fission products as the parent for the ^{90}Sr/^{90}Y generator. Recovery of radioactive parents from "extinct" radioactive decay processes represents another strategy to obtain generator parents. Thorium-229 ($T_{½}$ = 7340 years) is an important source to obtain ^{225}Ac as the parent of the ^{225}Ac/^{213}Bi generator system. The ^{211}At α-emitter is also of interest for targeted alpha therapy and can be obtained by the decay of 14.6 h ^{211}Rn (Vachtel et al. 1976; Visser et al. 1979; Mirzadeh and Lambrecht 1980), although usually accelerator-produced by the ^{209}Bi(α,2n) route.

7.3 Decay and In-Growth Principles

The relationships between parent radioisotope decay, daughter in-growth, and timing of daughter elution have been widely discussed and described in the literature (Roesch and Knapp 2011; Osso and Knapp 2011). The decay and growth of radionuclides are described by exponential equations which were originally formulated by Rutherford and Soddy (Rutherford and Soddy 1902) and the widely used Bateman equations (Bateman 1910) which were later developed to relate decay and in-growth of the naturally occurring actinium, uranium, and thorium series. As described in the following equations, at any time t, the activity A of a radioisotope is related to the number of atoms N, where λ represents the radionuclide decay constant.

$$A = \lambda \cdot N \tag{7.1}$$

The radionuclide decay with time follows the exponential law:

$$N = N_0 \cdot e^{-\lambda t} \tag{7.2}$$

$$A = A_0 \cdot e^{-\lambda} \tag{7.3}$$

where N and A represent the number of atoms and activity at time t and N_0 and A_0 the quantities when $t = 0$, respectively. The time required to reduce the activity of the radionuclide to 50 % of its initial value is the half-life, $T_{1/2}$. This value is related to λ by the following equation:

$$T_{1/2} = \frac{\ln 2}{\lambda} = \frac{0.6935}{\lambda} \tag{7.4}$$

The daughter decay product radioisotope is generally denoted by subscript 2 and the parent radioisotope by subscript 1. The following equations then relate the decay of the parent and in-growth and decay of the daughter:

$$-\left(\frac{\partial N_1}{\partial t}\right) = \lambda_1 \cdot N_1 \tag{7.5}$$

$$N_1 = N_1^0 \cdot e^{-\lambda_1 t} \tag{7.6}$$

$$-\left(\frac{\partial N_2}{\partial t}\right) = \lambda_1 \cdot N_1 - \lambda_2 \cdot N_2 \tag{7.7}$$

$$\left(\frac{\partial N_2}{\partial t}\right) = \lambda_2 \cdot N_2 - \lambda_1 \cdot N_1^0 \cdot e^{-\lambda_1 t} \tag{7.8}$$

Solving the equations above and assuming that when $t = 0$, $N_2^0 = 0$ the equation can then be solved as

$$N_2 = \frac{\lambda_1}{\lambda_2 - \lambda_1} \cdot N_1^0 \left(e^{-\lambda_1 t} - e^{-\lambda_2 t}\right) \tag{7.9}$$

This equation can be simplified to

$$A_2 = \frac{\lambda_2}{\lambda_2 - \lambda_1} \cdot A_1^0 \left(e^{-\lambda_1 t} - e^{-\lambda_2 t}\right) \tag{7.10}$$

Use of this equation permits calculation of the daughter activity level at any time t when the initial parent activity level is known. This equation is used to estimate the daughter activity in-growth curves illustrated for a hypothetical parent–daughter pair in Fig. 7.1, where successive elutions and in-growth of the daughter radioisotope are illustrated.

There are three types of equilibria which can arise which are dependent on the relative parent–daughter physical half-lives. In the case of "transient equilibria," the parent half-live is longer

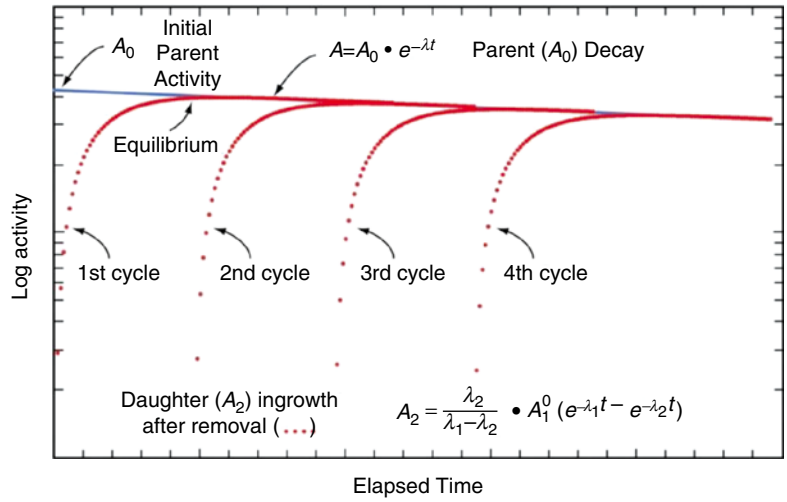

Fig. 7.1 Illustration of parent–daughter decay, daughter in-growth, and cycling of daughter by successive generator elutions (From Osso and Knapp 2011)

than the daughter half-life, i.e., $T_{1/2(1)} > T_{1/2(2)}$ or $\lambda_1 < \lambda_2$. Equation (7.9) can be simplified when $t \gg T_{1/2(2)}$, i.e., the decay time is much longer than the daughter half-life:

$$N_2 = \frac{\lambda_1}{\lambda_2 - \lambda_1} \cdot N_1^0 \left(e^{-\lambda_1 t}\right) = \frac{\lambda_1}{\lambda_2 - \lambda_1} N_1 \quad (7.11)$$

which can also be expressed as

$$\frac{A_1}{A_2} = 1 - \frac{\lambda_1}{\lambda_2} \quad (7.12)$$

After reaching equilibrium, the daughter decays with the half-life of the parent and the activity of the daughter will be higher than the parent activity. Alternatively, in the case of "secular equilibria," the parent half-life is much longer than the daughter half-life, and this is quite useful for the generator to serve as an in-house radioisotope production system, where the daughter can be successively repeatedly eluted over a long time period following sufficient in-growth between elutions. In this case, $T_{1/2(1)} >> T_{1/2(2)}$ or $\lambda_1 << \lambda_2$. For a typical radionuclide generator of this type which provided a short-lived therapeutic radioisotope from a radioactive pair at transient equilibrium, the ^{188}W ($T_{1/2} = 69$ days)/^{188}Re ($T_{1/2} = 16.9$ h) generator is an important example discussed in Sect. 7.6.1.2. In this case, when radioactive equilibrium is achieved, Eq. (7.9) can be simplified to

$$N_2 \cdot \lambda_2 = N_1 \cdot \lambda_1 \quad (7.13)$$

or

$$A_2 = A_1 \quad (7.14)$$

The relative growth and decay of the parent and daughter radionuclide pair is illustrated in Fig. 7.2a (transient equilibrium) and Fig. 7.2b for secular equilibrium.

Finally, in some cases, "no equilibrium" is achieved, and the half-life of the parent is shorter than the daughter half-life, i.e., $T_{1/2(1)} < T_{1/2(2)}$ or $\lambda_1 > \lambda_2$. This is an impractical situation to provide daughter radionuclides for clinical use, and there is no practical application, since the time (T_{max}) required to reach the maximum daughter activity level is

$$T_{max} = \frac{1}{\lambda_2 - \lambda_1} \ln \frac{\lambda_2}{\lambda_1} \quad (7.15)$$

For practical considerations, radionuclide generators are eluted at periodic intervals depending on the daughter activity requirements. Often the separation of the daughter from the parent may not occur at the time the daughter activity is at its maximum. Owing to the decrease of the parent radionuclide activity within the time between two elution steps, the radionuclide generator is expected to provide a reduced level of the daughter radionuclide activity by each subsequent elution as shown in Fig. 7.3.

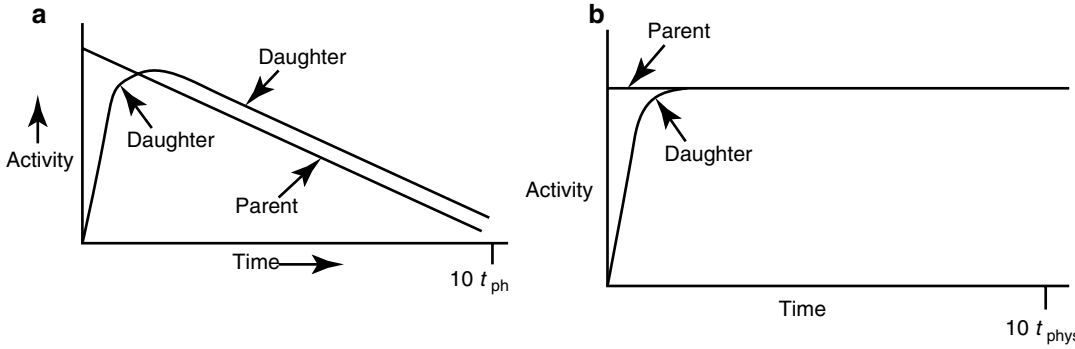

Fig. 7.2 Illustration of secular and transient equilibrium. (**a**) Transient equilibrium is a condition when the $t_{½(phys)}$ of the parent is approximately 10 times greater than the $t_{½(phys)}$ of the daughter. (**b**) Secular equilibrium is a condition when the $t_{½(phys)}$ of the parent is many times greater than the $t_{½(phys)}$ of the daughter(100–1000 times greater or more)

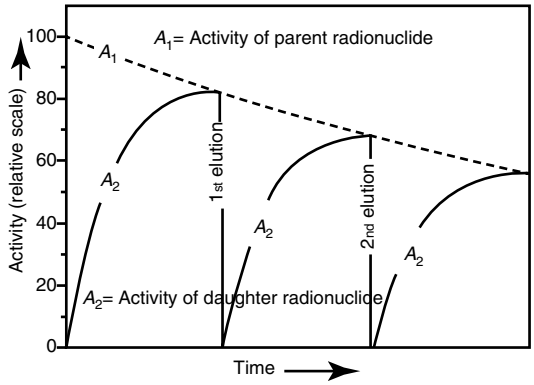

Fig. 7.3 Example of radionuclide daughter activity in-growth over repeated elutions. The radionuclide generator provides a reduced level of the daughter radionuclide activity by each subsequent elution

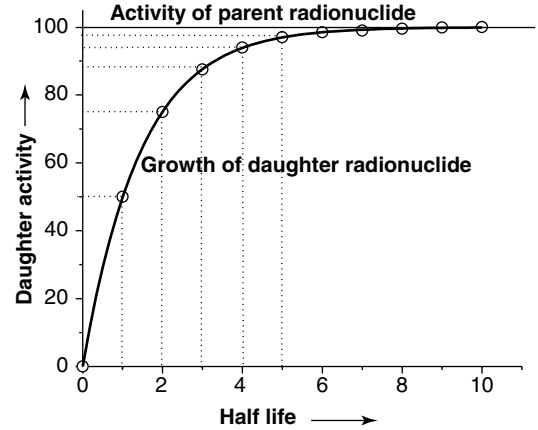

Fig. 7.4 The growth of daughter radionuclide in a pure parent fraction as a function of time. Depending upon the growth of the daughter radionuclide activity in the generator, different levels of the daughter radionuclide activity can be separated

When the daughter product is long-lived, periodic elution will take place prior to reaching the maximum equilibrium daughter activity levels and it is normal to use generators in this way. As an example, fifty percent daughter activity in-growth is detected in one half-life and 75 % in two half-lives, and the daughter activity reaches the activity of the parent radionuclide in 5–6 half-lives (Fig. 7.4).

The activity eluted from the generator typically follows a Gaussian distribution as shown in Fig. 7.5, with the maximum activity being eluted in the intermediate fractions. The eluent can also be "fractionated" by discarding those fractions with low activity if the activity concentration is a critical issue.

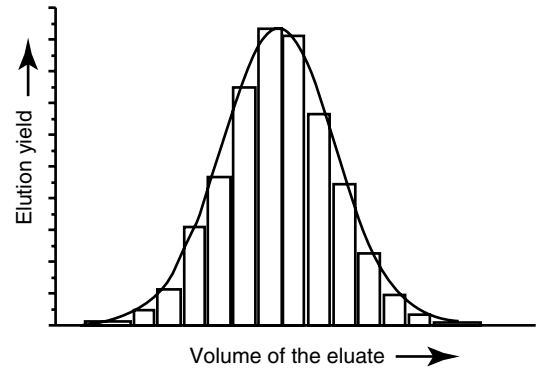

Fig. 7.5 Activity eluted from a generator which generally follows a Gaussian distribution

7.4 Radiochemical Separation of Therapeutic Radionuclides

Following reactor or cyclotron irradiation and discharge, the targets require subsequent radiochemical processing to obtain the desired radionuclide in high radionuclidic and radiochemical purity. In general, the radionuclides produced by reactor/accelerator activation are present in only microscopic levels and are diluted with target material and other radionuclidic impurities which are co-produced. In most cases the product radionuclide is chemically distinguishable from the target material, as illustrated in Fig. 7.6. It is necessary for the atomic number Z to change during the transmutation process for the product radionuclide to be available carrier-free from processing the irradiated target. This often occurs during accelerator production (Chap. 6), when a proton is added to the nucleus. In contrast, for most reactor-produced radioisotopes, the nuclear insertion of a neutron does not change the atomic number, resulting in the formation of product radioactive atoms which have the same Z as the target atoms. Since separation by the normally available methods is not possible, the product is diluted by the target atoms and thus is not available NCA. However, specific activity values for reactor-produced radioisotope vary greatly, depending on several factors, which include the neutron capture cross section, and if the product is formed by an alternative route such as beta decay of the initial radioactive product (Mirzadeh and Knapp 1996; Mausner et al. 1998). In addition, although higher epithermal neutron cross-section values are low and permit only low production yields, products formed by the (n,p) route can also be obtained in high specific activity following chemical processing. Since the product radionuclide of interest must be chemically separated from the target as well as from other radioactive and nonradioactive contaminants, however, the availability of appropriate radiochemical separation procedures is essential.

Radionuclide Production Yields in a cyclotron is given by the equation

$$I\left(1-e^{-\lambda_B \cdot t}\right)\cdot\frac{N_A\cdot\rho}{M}\cdot\int_{E_i}^{E_{th}}\frac{\sigma(E)}{(dE/dx)}dE$$

where I = beam current, N = number of atoms, λ_A = probability of transforming target atom A into B, and E = energy of the beam.

The term $\left(1-e^{\lambda t}\right)$ is known as activity build-up factor. Plot of this factor with half-life is shown in Figs. 7.7 and 7.8.

Conventional chemical separation technologies can generally be modified as required to isolate and concentrate radionuclides of interest. A variety of radiochemical separation procedures are employed to isolate the radionuclide of interest with the required purity. Each separation procedure has its own distinct advantages and disadvantages (Dash and Knapp

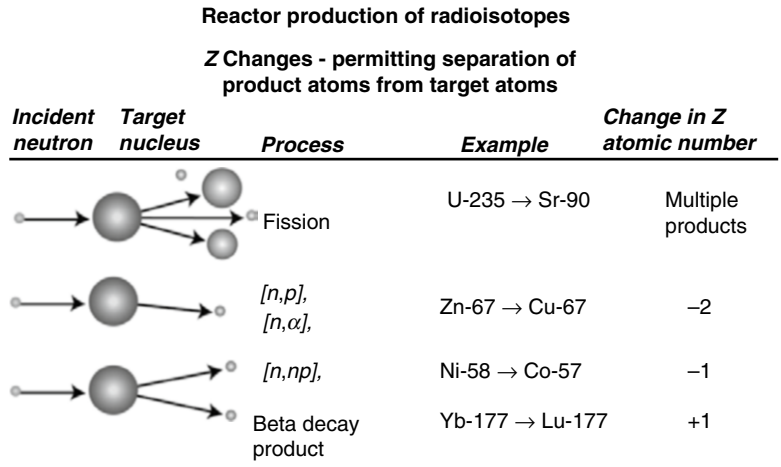

Fig. 7.6 Examples of production pathways from which carrier-free and carrier-added radioactive products can be obtained via reactor production when the Z changes

2015; Dash and Chakravarty 2014a, b; Dash et al. 2013), but since each radionuclide and its target have different chemistry, many options need to be evaluated. These methods can be adapted either alone or in different combinations with each other, depending upon the chemical nature of the target and radionuclide of interest to be separated with desirable purity and acceptable yield. Radiochemical separation of radionuclides presents a number of basic challenges owing to the often limited radiation stability of the conventional sorbents and solvents, extremely high selectivity and high purity requirements of the radionuclide to be separated. Some of the radiochemical separation procedures employed in radionuclide production are discussed below.

Fig. 7.7 Buildup of activity in a cyclotron

7.5 Methods for Parent–Daughter Separation

The methods available for separation of the parent and daughter chemical species which are amendable and practical for radionuclide generator development (Dash and Knapp 2015; Dash et al. 2013; Dash and Chakravarty 2014a, b) are extensive and include many well-known technologies described in the following sections. Several separation processes summarized in Table 7.2 are based on differences in physical and chemical properties that have been exploited.

7.5.1 Ion Exchange Column Chromatography

This is the most practical and widely used technology for radionuclide generator separations which relies on the reversible exchange of ions in solution with ions electrostatically bound to an insoluble support media based on their charge density and interaction between the ions and support media. This technology is usually performed in columns in which the insoluble stationary phase generally preferentially interacts with the particular charged ions (radioactive parent) to permit separation from the desired daughter radionuclide species. The radionuclide species uptake properties and chemical selectivity characteristics of a wide variety of ion exchange materials for a range of elements are available in

Reactor production of radioisotopes

No changes in *Z* - target and product atoms cannot be separated

Incident neutron	*Target nucleus*	*Process*	*Example*	*Change in Z atomic number*
		Radiative capture [n,γ]	Lu-176 → Lu-177	0
		Inelastic scattering [*n,n'*γ]	Sn-117 → Sn-117 m	0
		(n,2n)	Au-197 → Au-196	0

Fig. 7.8 Examples of key reactor routes for production of radioisotopes with no change in *Z*

Table 7.2 Examples of useful separation process that have been applied for radionuclide separation systems

Separation method	Physical/chemical property for parent–daughter separation	Basis
Column chromatography	Charge	Difference in adsorption on an adsorbent
Solvent extraction	Hydrophobicity	Difference in solubility in two phases
Sublimation	Vapor pressure	Difference in vapor pressure
Precipitation	Solubility	Difference in solubility product
Solid-phase column extraction	Hydrophobicity	Difference in affinity
Electrochemical	Standard electrode potential (E^o)	Difference in standard or formal electrode potential
Extraction chromatography	Specific chemical interaction	Difference in affinity of solutes dissolved in a liquid for an extractant immobilized in solid
Supported liquid membrane (SLM)	Chemical energy	Difference in solubility on the liquid membrane

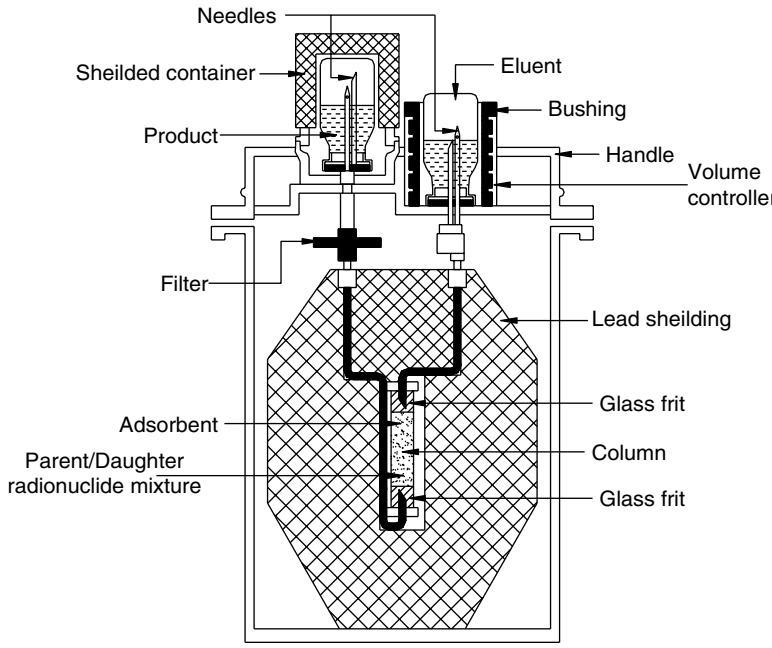

Fig. 7.9 Schematic diagram of a column chromatography generator housed in a lead-shielded container to provide daughter radionuclide. The column containing a bed of adsorbent binds the parent radionuclide and eluent from the inlet side is drawn through the column and into the outlet vial for daughter radionuclide collection

the literature. Using this information the radiochemical separation scheme for a given parent–daughter pair often be rationally designed. Ion exchange column chromatography currently developed has been refined to such a degree that this technology represents a highly selective and efficient technique that can separate closely related radionuclide from radionuclide mixtures. Table 7.1 summarizes the properties of typical radionuclide generators of current interest which provide therapeutic daughters. A schematic diagram of a generator housed in a lead-shielded container to provide the daughter radionuclide is shown in Fig. 7.9.

7.5.2 Solvent Extraction

The process of selective transfer of a component in a mixture of two or more components based on

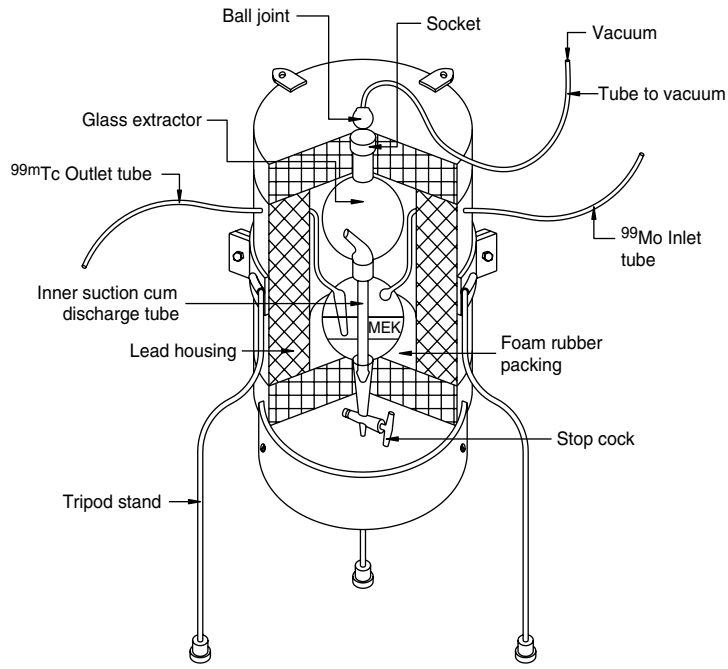

Fig. 7.10 Schematic diagram of the $^{99}Mo/^{99m}Tc$ MEK extraction generator. Methyl ethyl ketone (MEK) is introduced through the inlet tube into the container containing Na_2MoO_4 in 4M NaOH to extract ^{99m}Tc into the organic phase

the differences in solubility in two immiscible liquid phases is the basis of the solvent extraction technique. In this process two immiscible liquids—usually one aqueous and another organic—are vigorously shaken in an attempt to effectively disperse and efficiently contact with one another. In this manner, the radionuclide of interest which generally has higher organic solubility can migrate from the aqueous phase into the organic phase. Conventional liquid–liquid extraction in the classical version has seldom been used for the radiochemical separation of radionuclides because of the required use of expensive special-grade solvents. In addition, the issue of the difficulties in reaching complete extraction into the organic phase and the generation of organic liquid radioactive wastes are other factors. For the use of solvent extraction for radiochemical separation, extraction with solvent volumes as low as several milliliters and the use of special portable vessels under dynamic conditions are preferred, which places challenges on the widespread, high-activity use of this technology. However, one example in the diagnostic arena is the use of methyl ethyl ketone (MEK) for the effective extraction of NCA ^{99m}Tc from low-specific-activity ^{99}Mo (Anwar et al. 1968; Skuridin and Chibisov 2010; Zykov et al. 2001). Schematic diagram of the $^{99}Mo/^{99m}Tc$ MEK extraction generator is depicted in Fig. 7.10.

7.5.3 Distillation

Distillation is a separation technique in which differences in element vapor pressures or their compounds are exploited. This technology essentially takes advantage of the differences in the boiling points of the constituents to separate a desired radionuclide from a mixture. It is a useful separation tool if the radionuclide of interest is volatile or can be transformed into a volatile compound. Separation of radionuclide of interest from others is achieved by vaporization at the boiling point of the mixture and subsequent condensation of the vapor. This technique provides clean separations, provided that proper precautions are taken to avoid contamination of the distillate. Precautions are sometimes necessary to avoid loss of volatile radioactive substances during the dissolving of irradiated targets or during irradiation itself. This technology has been avidly

exploited for the separation of ^{99m}Tc from ^{99}Mo (Christian et al. 2000; Gerse et al. 1988; Zsinka 1987; Macháň et al. 1981). Operational principle of a ^{99}Mo/^{99m}Tc sublimation generator is illustrated in Fig. 7.11.

7.5.4 Precipitation

Precipitation is also a conventional separation technology in which the solubility of metal ions, salts, or complexes is exploited for the selective separation of one metal ion from the other. When the solubility limit of the solute in the solvent exceeds, the material appears as a precipitate and is separated from the other component(s). Effective separation of a radionuclide is accomplished by the judicious selection of the compound that forms the precipitate and the concentration of solutions used in the precipitate formation. Precipitation generally is followed by either centrifugation or filtration for the effective separation of the precipitate. The speed of separation is dictated by the nature of the precipitate (i.e., gelatinous, crystalline, amorphous, etc.), the sample size being processed, and other factors.

7.5.5 Extraction Chromatography

The possibility to incorporate an extractant or a solution of an extractant into an inert substrate is the genesis of the extraction chromatography (EXC). The concept of extraction chromatography separation seemed very attractive as it would exploit the selectivity of liquid–liquid extraction and at the same time offer the ease of operation of column-based separation system. Recent advances in ligand design, in particular the introduction of novel extractants capable of strong and selective complex formation with metal ion, have enhanced the scope of the technique (Dietz and Horwitz 2000; Jassin 2005).

7.5.6 Solid-Phase Column Extraction

An alternative to solvent extraction is the separation of metal ion by direct contact of the aqueous sample with a sorbent usually using column chromatographic technique. Desorption of metal ion of interest can be carried out by elution with a suitable solvent or solvent mixture. Optimal desorption of metal ion from the

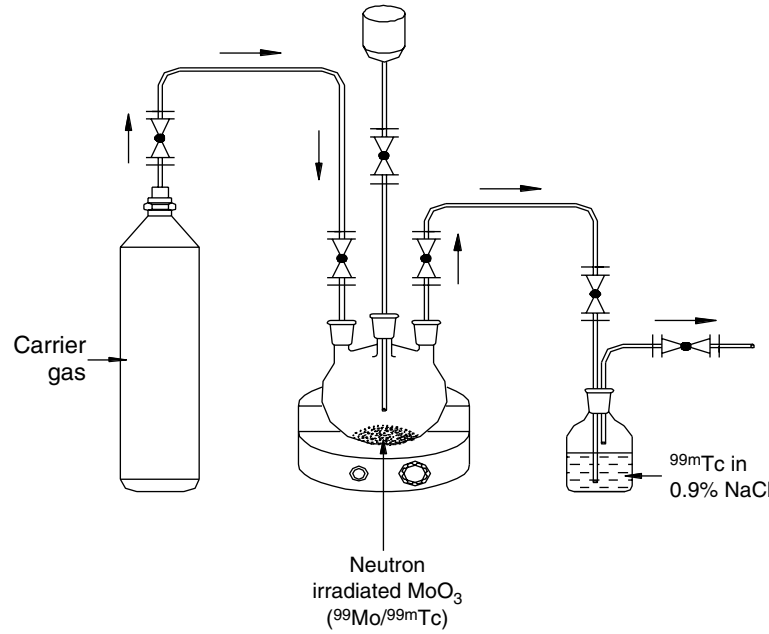

Fig. 7.11 Operational principle of a ^{99}Mo/^{99m}Tc sublimation generator. Carrier gas is allowed to pass through neutron-activated target and the separation of ^{99m}Tc is performed at sublimation temperature

column is determined by the selectivity (distribution coefficient) of the metal ions in the organic solvent/extractant. Utility of this technique has also tried for the development of ^{99}Mo/^{99m}Tc and ^{72}Se/^{72}As radionuclide generators (Braun et al. 1987; Jennewein et al. 2005; Chattopadhyay et al. 2008).

7.5.7 Electrochemical Separation

The strategy to exploit the differences in the standard metal ion reduction potential of is the basis to separate metal ions of interest from other species under the influence of an applied potential difference. A mixture of radionuclides having adequate difference in their formal potential values in an electrolytic medium can be mutually separated by selective electrodeposition of one radionuclide on an electrode surface under the application of the applied potential. Electrochemical strategy has been used for the development of ^{99}Mo/^{99m}Tc, ^{188}W/^{188}Re, and ^{90}Sr/^{90}Y generators (Dash and Chakravarty 2014a, b; Chakravarty et al. 2008, 2009, 2010a, b, c, 2012a, b). An electrochemical method based on the different reducibility of lanthanides and the ability to form amalgams has been utilized successively, for instance, for purification of ^{177}Lu (Chakravarty et al. 2010a, b, c). Under suitable conditions of electrolysis, the divalent lanthanide forming more easily the amalgam is preferentially transferred into the mercury electrode from other trivalent lanthanides. The amalgated lanthanide can again be transferred into solution by washing of mercury with dilute acid. Electrochemical separation is very specific and, therefore, can be successfully used in the presence of many other radionuclides. Schematic representation of electrochemical separation strategy is depicted in Fig. 7.12.

7.6 Key Examples of Therapeutic Radioisotopes Available from Radionuclide Generator Systems

As summarized in Table 7.1, several therapeutic radioisotopes of current interest are available from radionuclide generator systems. Although most of these systems provide beta-particle- or alpha-emitting radioisotopes, there are a very limited number of generator systems which

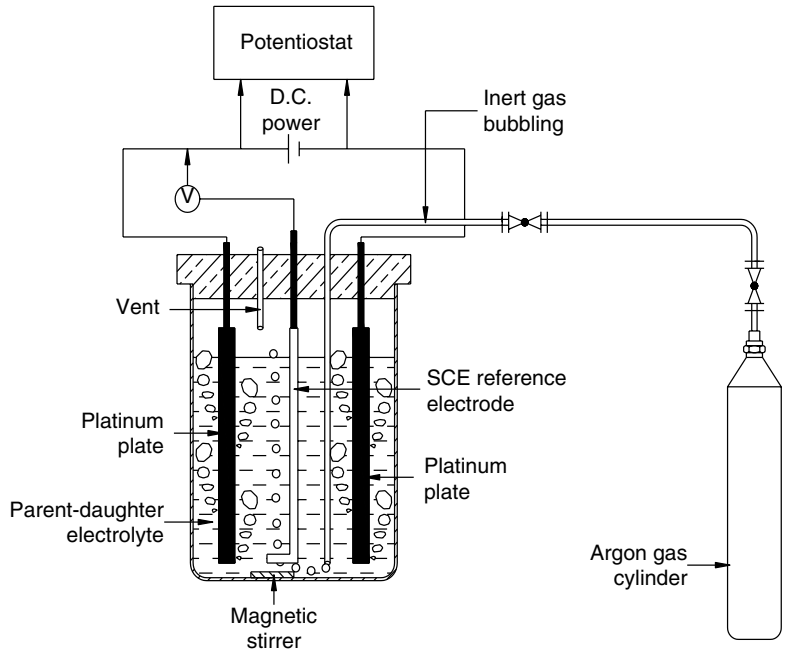

Fig. 7.12 Electrochemical separation strategy. Separation is primarily based on the selective electrodeposition of daughter radionuclide on a platinum cathode surface from an equilibrium mixture of parent–daughter radionuclide pair in an electrochemical cell under the influence of optimal applied potential. Electrodeposited daughter radionuclide is then stripped back into a 0.9 % saline solution

provide Auger electron-emitting daughter radioisotopes, and only the rhodium-103 (^{103}Rh)/ruthenium-103m (^{103m}Ru) is discussed.

7.6.1 Radionuclide Generator Systems Which Provide Beta-Emitting Radioisotopes

There a number of well-established radionuclide generator systems described in the literature which provide beta-particle-emitting daughter radioisotopes which have a broad established applications in nuclear medicine, oncology, and interventional applications

7.6.1.1 Dysprosium-166/Holmium-166 Generator

The^{166}Dy ($T_{½}$=3.4 days)/^{166}Ho ($T_{½}$=1.117 days) has been of interest for many years. Although ^{166}Ho can be produced with a specific activity of only 8–9 Ci mg^{-1} (~300 GBq mg^{-1}) ^{165}Ho by the ^{165}Ho(n,γ)^{166}Ho reaction even at saturation in a high thermal flux of $2.5 \cdot 10^{15}$ n cm^{-2} s^{-1}, no-carrier-added ^{166}Ho with a theoretical specific activity of about 700 Ci mg^{-1} (~26 TBq mg^{-1}) is obtained by decay of ^{166}Dy. The ^{166}Dy is reactor-produced by the ^{164}Dy(n,γ)^{165}Dy(n,γ)^{166}Dy reaction series. Separation of ^{166}Ho from ^{166}Dy has traditionally been a challenge. Although not a true generator system—since the ^{166}Dy parent is also recovered and requires column reloading for subsequent ^{166}Ho/^{166}Dy separations following adequate ^{166}Ho in-growth—a method has been described for successful ^{166}Ho/^{166}Dy separation which uses an HPLC reversed phase ion-exchange chromatographic method utilizing Dowex AG 50WX12 or Aminex A5 cation exchangers by elution with α-hydroxy-isobutyric acid (α-HIB) of 0.085 *M* at pH 4.3. This approach provides a Dy/Ho separation factor of approximately 10^3, with subsequent purification of the ^{166}Ho^{3+} by cation-exchange column chromatography after acid decomposition of the Ho-α-HIB complex (Dadachova et al. 1995a, b). More recently, an apparently simple and efficient method has described separation on the Eichrom Ln resin by elution with dilute nitric acid (Ketring et al. 2002).

Although ^{166}Ho has attractive radionuclidic properties as a lanthanide for various vector labeling and therapeutic strategies, it has not yet been widely used. Examples are studies of protein labeling with the CHX-B-DTPA ligand system (Dadachova et al. 1997). Animal studies demonstrated that no translocation of the ^{166}Ho daughter radionuclide occurred when the [^{166}Ho]DTPA complex was administered to rats (Smith et al. 1995). The results of these studies may suggest that the ^{166}Dy/^{166}Ho system may have some promise as an in vivo generator. Clinical applications which have been recently reported include radiation synovectomy with ^{166}Ho-ferric hydroxide (Ofluoglu et al. 2002), the use of [^{166}Ho]DTPA liquid-filled balloons for the inhibition of restenosis following coronary angioplasty (Hong et al. 2002), and the use of [^{166}Ho]DOTMP for myeloablative therapy of multiple myeloma (Rajendran et al. 2002). If the availability of no-carrier-added ^{166}Ho becomes a reality, use of this generator system may be a source for these and other applications.

7.6.1.2 Tungste-188/Rhenium-188 Generator

Rhenium-188 ($T_{1/2}$=16.9 h) is one of the useful radionuclides for therapy emitting β$^-$ particles (2.12 MeV, 71.1 % and 1.965 MeV, 25.6 %) and emits a gamma photon at 155 keV (15.1 % abundance), which can be readily imaged with gamma cameras, providing important information on biodistribution and excretion kinetics to assess targeting and dosimetry. Rhenium-188 is used for a host of therapeutic applications (Pillai et al. 2012; Jeong and Knapp 2008; Jeong and Chung 2003; Lambert and de Klerk 2006; Iznaga-Escobar 2001). The beta energies are on the higher side giving a mean range of ~3.5 mm in soft tissues. The 155 keV (14.9 %) gamma rays are suitable for imaging. The issues associated with reactor production of the ^{188}W parent are discussed in Chap. 5.

Extensive research on ^{188}W production and development of the ^{188}W/^{188}Re generator system was initiated at the Oak Ridge National Laboratory (ORNL) in the mid 1980s, focused on preparation of a ^{188}W/^{188}Re generator system

using acidic alumina matrix analogous to the widely used ^{99}Mo/^{99m}Tc generator (Knapp et al. 1991, 1993, 1997; Kamioki et al. 1994; Jeong and Knapp 2008). Owing to the limited sorption capacity of alumina (maximum 50 mg W/g) (Jeong and Knapp 2008; Pillai et al. 2012), ^{188}Re available from the alumina-based ^{188}W/^{188}Re generators is of low radioactivity concentration, if low-specific-activity ^{188}W is used. This in turn would require post-elution concentration of the ^{188}Re eluate (Lisic et al. 1992; Knapp et al. 1998; Guhlke 1998; Guhlke et al. 2000; Sarkar et al. 2009; Mushtaq et al. 2007; Chakravarty et al. 2010a, b, c). The tremendous prospects associated with the use of generator-produced ^{188}Re have led to development of automated systems for the concentration of ^{188}Re eluate (Jäckel et al. 2005; Wunderlich et al. 2008). Over the years, different approaches such as the gel generator, electrochemical generator, thermo-chromatographic generator, and chromatographic generator with high-capacity adsorbents and nanomaterial-based adsorbents have been explored (Dash and Knapp 2015) which in turn has opened the prospect of using ^{188}Re for therapy.

Rhenium-188 is currently of broad interest for the development of a wide variety of new therapeutic approaches for applications in nuclear medicine, oncology, and even interventional cardiology, because of the benefits, advantages, and significantly reduced expense of using ^{188}Re in comparison to many other therapeutic radionuclides (Knapp et al. 1997, 1998a, b). There is currently a large number of physician-sponsored clinical protocols in progress. Tungsten-188 is reactor-produced by double neutron capture of enriched ^{186}W by the ^{186}W(n,γ)^{187}W(n,γ)^{188}We route. Since the production yield is a function of the square of the thermal neutron flux, even at high thermal neutron flux ($>2 \cdot 10^{15}$ n cm^{-2} s^{-1}), ^{188}W is produced with only modest specific activity of 4–5 Ci g^{-1} (~180 GBq g^{-1}) per cycle (Knapp et al. 1994). This is due to the modest neutron capture cross sections and burnup of the ^{188}W product (Mirzadeh et al. 1997). Although the first prototype ^{188}W/^{188}Re generators were described as early as 1966 using zirconium oxide (Lewis 1966) and with aluminum oxide in 1972 (Mikheev et al. 1972), in spite of the excellent radionuclidic properties of ^{188}Re, there was no practical use of this therapeutic radionuclide until nearly 25 years later, when appropriate carrier molecules and targeting agents became available (Knapp et al. 1997, 1998a, b).

The ^{188}W/^{188}Re generator systems today are mainly based on separation chemistry similar to that used for the ^{99}Mo/^{99m}Tc generator which includes the adsorption of tungstic acid in the alumina-based generator (Mikheev et al. 1972; Callahan et al. 1989; Knapp et al. 1994). In addition to the adsorption column chromatographic separation on alumina, zirconium oxide (Dadachova et al. 1994) and gel-type generators have been reported. For batch separation of ^{188}Re, a thermochromatographic technique was described.

The adsorption-type generator is most practical, since it is easy to prepare and has long-term stability with high ^{188}Re yields and consistently low ^{188}W breakthrough. The availability of effective and inexpensive post-elution tandem column-based concentration systems (Guhlke et al. 2000; Knapp et al. 1997, 1998a) provides a useful method for ^{188}Re concentration to very high specific volumes (<1 mL total volume). There are presently a large number of physician-sponsored clinical trials in progress using the Oak Ridge National Laboratory (ORNL) alumina-based ^{188}W/^{188}Re generator system. ^{188}Re-labeled HEDP (Savio et al. 2001) and DMSA (Blower et al. 2000) have proven to be effective agents for the palliative relief of bone pain from skeletal metastases in patients with prostatic carcinoma and may represent a more cost-effective alternative to other radionuclides used for this application. In addition, the use of liquid-filled angioplasty balloons for the inhibition of hyperplastic restenosis after coronary balloon angioplasty using ^{188}Re-perrhenate (Hoeher et al. 2000; Kotzerke et al. 2000; Makkar et al. 2000; Schuelen et al. 2001; Kropp et al. 2002), ^{188}Re-MAG3 (Weinberger et al. 1999a, b; Park et al. 2001), and [^{188}Re]DTPA (Hong et al. 2002) have been published, and the use of the ^{188}Re-labeled anti-CD66 has also been reported (Nowak et al. 2001).

The use of the ^{188}Re-labeled anti-CD66 antibody (*anti*-NCA95) has been found to be a useful new method for marrow ablation using combinational preconditioning in leukemia patients (Bunjes 2002; Reske et al. 2001; Buchman et al. 2002). The use of the ^{188}W/^{188}Re generator in developing regions has been demonstrated to be of particular usefulness because of its cost-effectiveness, and multicenter trials supported by the International Atomic Energy Agency are in progress for restenosis therapy with ^{188}Re-perrhenate and for the treatment of liver cancer (Sundram et al. 2002) with ^{188}Re-labeled lipiodol analogs (Jeong et al. 2001). A ^{188}Re-labeled antibody has been used for treatment of bladder cancer (Murray et al. 2001), and the use of the ^{188}Re-labeled P2045 SSTR-targeting peptide for the treatment of lung cancer has also been reported (Bugai et al. 2002) and is now in clinical trials in the USA.

Several new generator prototypes for the separation of nca ^{188}Re from ^{188}W have been recently described and include use of a new high-capacity adsorbent consisting of synthetic alumina functionalized with sulfate moieties prepared from a sol-gel process (Lee et al. 2009). This material is reported to have a tungsten loading capacity of >450 mg/g, allowing preparation of a 3 Ci generator using only 1 g of adsorbent, which is a much higher loading capacity than reported for acid-washed alumina. Elution with 5 mL of saline at 1 mL/min results in ^{188}Re yields of 70–90 %. In this manner, a 1 Ci generator can provide ^{188}Re solutions with a specific volume of >200 mCi/mL saline. In addition, a simple electrochemical separation technique has been reported using platinum electrodes immersed in ^{188}W/^{188}Re equilibrium mixture by applying a constant 7 V potential difference at 80 °C for 60 min. The ^{188}Re is stripped as perrhenic acid from the platinum cathode with warm 0.1 N HCl (Chakravarty et al. 2009). Decay-corrected ^{188}Re yields of >70 % have been reported in preliminary studies using 30 mCi of ^{188}W. There are several examples of recent clinical applications with ^{188}Re which include use of the ORNL ^{188}W/^{188}Re generator for preparation of the HDD agent for liver cancer therapy (Jeong and Knapp 2008). Results of the recent multicenter clinical trial with this agent coordinated through the IAEA have demonstrated the efficacy of ^{188}Re-labeled HDD/Lipiodol for the transarterial palliative treatment in patients with non-resectable/non-transplantable liver tumors (Pandey et al. 2008). Further assessment of the initial use of ^{188}Re liquid-filled angioplasty balloons for the inhibition of hyperplasia following PCTA of the coronaries has now been demonstrated for the peripheral arteries (Wohlgemuth et al. 2008).

7.6.1.3 Strontium-90/Yttrium-90 Generator

Yttrium-90 ($T_{1/2}$ = 64.1 h) is a pure β^--particle-emitting radionuclide with well-established applications in targeted therapy. There are several advantages of ^{90}Y as a therapeutic radionuclide. It has a suitable physical half-life (~64 h) and decays to a stable daughter product ^{90}Zr by emission of high-energy (E_{max} 2.28 MeV) β^- particles. Yttrium has a relatively simple chemistry and its suitability for forming complexes with a variety of chelating agents is well established. The availability of ^{90}Y and their applications are well described in the literature (Walker et al. 1964; IAEA Report 2009; Montaña et al. 2012; Chakravarty et al. 2012a, b). Use of ^{90}Y in synovectomy (Kampen et al. 2007; Miszczyk et al. 2007; Taylor et al. 1997; Asavatanabodee et al. 1997; Winfield and Gumpel 1979), in the treatment of hepatocellular carcinoma (Sato 2011; Kan et al. 2012; Lau et al. 2011), peptide receptor radionuclide therapy (Cwikla et al. 2010; Marincek et al. 2013; Vinjamuri et al. 2013; Goffredo et al. 2011; Savelli and Giubbini 2011; Teunissen et al. 2006), and non-Hodgkin's lymphoma (Hagenbeek 2003; Dillman 2006; Emmanouilides 2009; Zinzani et al. 2008; Gisselbrecht et al. 2007; Chapuy et al. 2007; Cheung et al. 2006; Weigert et al. 2006; Cheson 2005; Micallef 2004) has been extensively studied. In 2002 ibritumomab tiuxetan (Zevalin®) was approved by the US FDA for radioimmunotherapy of patients with relapsed or refractory low-grade, follicular, or CD20+-transformed B-cell NHL and rituximab-refractory follicular NHL (Dillman 2006; Davies 2007; Bodet-Milin et al. 2013).

No-carrier-added (NCA) ^{90}Y is required for the preparation of labeled antibodies and peptides used for targeted therapy (Bodet-Milin et al. 2013) and can be produced in a nuclear reactor by pursuing the ^{90}Zr(n,p)^{90}Y reaction using 100 % enriched ^{90}Zr target and fast neutron flux of ~7.5×10^{13} cm^{-2} s^{-1} (Abbasi et al. 2006). Although this method obviously holds promise as a viable approach, several issues related to the long-term availability and cost of enriched ^{90}Zr, such as the requirement of fast neutron flux, R&D associated with target design, separation of ^{90}Y, and ^{90}Zr recycling, must be resolved. The amount of ^{90}Y produced by this route will also be limited. The most practical method to obtain high activity levels of NCA ^{90}Y in NCA is from decay of ^{90}Sr using the ^{90}Sr/^{90}Y radionuclide generator system (Chakravarty et al. 2012a, b; Montaña et al. 2012). Strontium-90 is one of the major fission products of ^{235}U with fission yield of 5.93 % and can be isolated from aqueous nuclear fuel reprocessing high-level liquid waste (HLLW) solutions (IAEA Report 2010; Wester et al. 2003; Ramanujam et al. 2000; Beard and Moore 1969; Bray 1961; Orth and Kurath 1994; Horwitz et al. 1991; Lumetta et al. 1993; Lange et al. 1957).

The radionuclidic and chemical purity requirements are very high for ^{90}Sr to provide medically useful ^{90}Y, and the use of extensive quality controls is essential. Ionic ^{90}Sr localizes in the skeleton, and because of its long half-life, the maximum permissible body burden of 74 kBq (2 μCi) over patient lifetime is very low. The separation of NCA ^{90}Y from ^{90}Sr thus represents a challenging task because of the necessity of maintaining ^{90}Sr contamination levels as low as possible in the ^{90}Y product used for therapeutic applications. A variety of approaches have thus been evaluated for separation of high-purity ^{90}Y from ^{90}Sr, which are based on precipitation, solvent extraction, ion-exchange chromatography, extraction chromatography, electrophoresis, membrane-based separation, electrodeposition, etc. (Walker 1964; IAEA Report 2009; Montaña et al. 2012). A review of the ^{90}Sr/^{90}Y generator technologies indicates that the automated electrochemical ^{90}Sr/^{90}Y generator described can be efficiently adapted in centralized radiopharmacy facilities (see Chap. 17) set up for an assured supply of ^{90}Y of required quality and quantity over a sustained period (>10 years) (Montaña et al. 2012; Isotope Technologies 2010). Ensuring successful utilization of ^{90}Y for targeted therapy demands quantitative estimation of Bq levels of ^{90}Sr impurity in GBq quantities of ^{90}Y and should be within the pharmacopeia-established limit. The reported EPC concept (Pandey et al. 2008) which combines chelate-based extraction with partition chromatography is attractive and exploits the ability of 2-ethyl hexyl-2-ethyl hexyl phosphonic acid (KSM-17) to selectively retain ^{90}Y at the point of spotting and at the same time offer the convenience of separating other impurities by partition chromatography.

Therapy of solid tumors with ^{90}Y is of interest because of the emission of a high-energy beta particle (E_{max} = 2.3 MeV) and its availability from the ^{90}Sr/^{90}Y generator system. The emission of the 2.3 MeV beta particle results in deep soft tissue is also important for the "cross-fire" effect for irradiation of unlabeled cells in the targeting territory (see Chaps. 8 and 9). A generator system described early which has been widely used for the separation of ^{90}Y from ^{90}Sr uses the strongly acidic Dowex exchange resin (Chinol and Hnatowich 1987). The ^{90}Sr/^{90}Y generators have been available for some years, but interest in the clinical use of ^{90}Y really blossomed with the availability of bifunctional chelating groups which strongly bind the Y^{3+} cation. In addition to tumor targeting, its use for radiation synovectomy of large synovial joints had also been pursued. As always where bone targeting of metallic cations is an issue, skeletal localization of free trivalent $^{90}Y^{+3}$ species must be avoided to preclude marrow suppression. The availability of DOTA and the CHX-substituted DTPA chelates provides an opportunity to use ^{90}Y in a predictably safe manner. The availability of the chelates in consort with vectors having very specific cellular targeting, such as the DOTATOC octreotide agent which binds with high specificity to the somatostatin receptors, provided important agents for the treatment of a wide variety of tumors. Because of the safety issues associated

with the use and handling of ^{90}Y and ^{90}Sr, these high-level generators are typically installed in a centralized processing area for preparation of the no-carrier-added ^{90}Y by batch solvent extraction techniques and distribution of the highly purified ^{90}Y product. One method (Bray and Wester 1996) involves freshly purified HDEHP extraction of ^{90}Y from a nitric acid solution of the purified ^{90}Sr/^{90}Y mixture. The final ^{90}Y/^{90}Sr activity ratio of the purified ^{90}Y is $<10^{-7}$ with a concentration of metal impurities of <10 ppm per Ci ^{90}Y.

There are a variety of methods available for the separation of ^{90}Y from ^{90}Sr including solvent extraction, ion exchange, and other radiochemical separation techniques which have been reviewed (Chuang and Lo 1996). Because of the importance high radiation resistance, generators based on inorganic ion exchange materials have been primarily evaluated (Hsieh et al. 1993; Bilewicz 1995; Chinol et al. 1997). The installation of the ^{90}Sr/^{90}Y generator in a hospital-based nuclear pharmacy is generally unusual, because of the potential dangers in handling ^{90}Sr. Preparations of both research-grade and sterile, pyrogen-free ^{90}Y for human studies are generally obtained from a central processing-approved GMP facility. The limited availability and high costs of the required very high chemically and radiochemically pure ^{90}Sr are two major issues. It could be as the use of ^{90}Y significantly expands that availability through tightly controlled central radiopharmacies may be envisioned in the future.

7.6.2 Radionuclide Generator Systems Which Provide Alpha-Emitting Radioisotopes

Interest in the use of alpha particle-emitting radioisotopes has increased exponentially over the last several years and there are several generator systems which provide alpha-emitting daughter radioisotopes. Various improvements, the development of new prototypes, and the implementation of automation are making these systems more readily available to provide the alpha-emitting daughter radioisotopes for various therapeutic applications.

7.6.2.1 Actinium-225/Bismuth-213 Generator

Actinium-225 ($T_{1/2}$ = 10.0 days) decays by α emission through 3 atoms, ^{221}Fr (half-life, 4.8 min), ^{217}At (half-life, 32.3 ms), and ^{213}Bi (half-life, 45.6 min), each of which also emits an α particle. Interest in the ^{225}Ac/^{213}Bi generator system has rapidly progressed, resulting from the promising effectiveness of alpha emitters for targeted therapy. Because of the very high linear energy transfer (LET) in the 50–90 μm range, α particles often have many advantages for more specialized therapy of microscopic or subclinical disease, such as for the treatment of micrometastatic disease (cf. Chap. 8 of this Volume). The attachment of α emitters to cellular-targeted carrier molecules such as antibodies or peptides is the most common approach. For this reason, interest in the ^{225}Ac/^{213}Bi generator system has rapidly increased in the last few years. The ^{225}Ac is generally obtained as a decay product of ^{229}Th which is extracted as a radioactive decay product of the ^{233}U, a member of the "extinct" ^{237}Np decay chain (Chap. 6). Production has also been proposed via accelerators, as an example, by the ^{226}Ra(p,2n)^{225}Ac reaction. The ^{229}Th can be obtained from processing of the ^{233}U stockpile, which had originally been produced in a proposed molten salt breeder reactor program at ORNL. From a complex series of ion exchange and extraction chromatographic steps for recycling of ^{229}Th(IV), the Ra(II) decay product is separated at optimal timing and the ^{225}Ac then separated. A variety of chromatographic-type ^{225}Ac/^{213}Bi generators has been described (Geerlings et al. 1993; Wu et al. 1997; Boll et al. 1997; Mirzadeh 1998; Hassfjell and Brechbiel 2001).

The ^{225}Ac in 1 M HNO_3 solution is available from ORNL and can be available investigators together with the required generator components for on-site generator loading, to minimize the effects of radiolysis. The AG 50W-X4 strong cation exchange resin is used with elution of the ^{213}Bi daughter with 0.15 M HI solution. A variety of other ^{225}Ac/^{213}Bi generator systems have been reported, one of which utilizes two successive Dowex 50W-X8 cation exchange columns

(Geerlings et al. 1993). In this system, ^{225}Ac is initially separated from $^{224/225}$Ra and ^{213}Bi separated from ^{225}Ac formed from radon decay. Using another strategy, the inorganic AC-resin ion exchanger is used for a generator where the ^{213}Bi is eluted with 1 M HCl in a continuous elution mode. Following dilution of the eluant to 0.2 M HCl, it is loaded on a second small AGMP-50 cation exchange resin and eluted with 0.1 M HI (Wu et al. 1997). McDevitt et al. (1999a) utilize a similar column for elution of ^{213}Bi which has been reported in several publications for treatment of acute myeloid leukemia (AML) (McDevitt et al. 1999b; Sgoruos et al. 1999; Jurciv et al. 2002). Other systems have also been developed and use a disk containing a thin film of the Anex (3 M Company) strong anion-exchange resin. As the ^{225}Ac solution is passed through the membrane, the ^{213}Bi is retained and then eluted with pH 5.5 solution of 0.05 M NaOAc. As discussed later in this section, in addition to its utilization in a generator system to provide ^{213}Bi for alpha-targeted therapy, there is also increasing interest (McDivitt et al. 2001) for direct use of the longer-lived ^{225}Ac parent for targeted therapy (i.e., $t_{1/2}$ 10 days vs. 45.6 min for ^{213}Bi). There would be the emission of a total of four alpha particles per decay so the use of ^{225}Ac would represent a type of in vivo generator (Chang et al. 2008; Miederer et al. 2008; Sofou et al. 2007; Antczak et al. 2006). The treatment of acute myelogenous leukemia (AML) is the current principal clinical application of ^{213}Bi (Jurcic and Rosenblat 2014; Pfost et al. 2009; Teiluf et al. 2015).

The availability of the required activity levels projected to be required for broader use of both ^{225}Ac and ^{213}Bi represents a significant challenge. Neutron irradiation of ^{232}Th provides ^{233}U, which α decays to ^{229}Th which subsequently α decays to ^{225}Ac. Strategies to produce ^{225}Ac from ^{226}Ra include multiple neutron captures by ^{226}Ra. The product is a mixture ^{227}Ac, ^{228}Th, and ^{229}Th, from which ^{229}Th is obtained in higher yield. Through careful radiochemical manipulations, the ^{225}Ac can be isolated by ion exchange separation methods using a titanium phosphate adsorbent. Accelerator production is also possible by the ^{226}Ra(p,2n)^{225}Ac proton-induced (18 MeV) reaction, with subsequent ^{225}Ac purification by Dowex-50 column chromatography. The photonuclear production of ^{227}Ac is also possible via the instantaneous $^{226}\mathrm{Ra}+\gamma \rightarrow {}^{225}\mathrm{Ra}+\mathrm{n}$ reaction. Following irradiation the ^{225}Ra is at the maximum activity level. Access to direct production of ^{225}Ac for ^{226}Ra is not possible, so ^{225}Ac is available from beta decay via $^{225}Ra\left(T_{1/2}=14.8\ days\right)\overset{\beta^-}{\rightarrow}{}^{225}Ac$.

Because of the emission of 4 alpha particles and the relatively long 10.0-d half-life, ^{225}Ac has been evaluated in mouse xenografts with several types of cancer cells and showed with greater cytotoxicity and prolongation of survival than ^{213}B. One continuing concern for the therapeutic use of ^{225}Ac is that the chelation binding energy is not strong enough to overcome the destruction 100 and 200 keV energy of the actinium ion alpha particle recoil. For this reason, the daughter radionuclides from ^{225}Ac decay may cause damage to normal nontargeted cells since they can diffuse from the targeted site. The ^{213}Bi daughter ($T_{1/2}=45.59$ min) from decay of ^{225}Ac decays with emission of an α particle [$E_\alpha=5869$ keV] and two β^- particles [$E_{\beta^-}=1427$ keV to stable ^{209}Bi] and a 440-keV photon emission which allows evaluation of detailed biodistribution, pharmacokinetic, and dosimetry studies. The ^{213}Bi is obtained from the ^{225}Ac/^{213}Bi generator in which ^{225}Ac is dispersed on a cation exchanger which prevents resin decomposition resulting from the very high radiation. The ^{213}Bi can be conjugated with targeting molecules, including mAbs, peptides, and other molecules to which the appropriate bifunctional chelating groups have been attached. The ^{225}Ac and the generators have been available from the Oak Ridge National Laboratory (USA) and also from the Institute for Transuranium Elements of Karlsruhe (Germany). As interest in the use of alpha emitters expands, and in particular the ^{225}Ac/^{213}Bi generator system, issues which must be addressed include the availability of sufficient ^{225}Ac at reasonable cost.

7.6.2.2 Actinium-227/Radium-223 Generator

Radium-223 ($t_{1/2}$ 11.7 days) has emerged as a promising new candidate for routine use for

palliative treatment of bone pain from tumor metastases to the skeleton, because of availability from decay of ^{227}Ac ($t_{1/2}$ 21.7 years), localization of ionic radium in the growing bone, and the high LET (Bruland et al. 2008; Nilsson et al. 2007). Radium-223 can be conveniently repeatedly obtained from separation from the ^{227}Ac parent. The ^{227}Ac is obtained from decay of ^{235}U and decays to ^{227}Ac through ^{227}Th or can be reactor-produced by neutron irradiation of ^{226}Ra (Larsen et al. 2007) or from alpha irradiation of protactinium-231 targets. The availability of beryllium/actinium neutron sources which are often used for well logging can provide a ready source of ^{227}Ac. The ^{227}Ac/^{227}Th is purified by traditional ion exchange methods, for example, by adsorption on 1 M HCl preconditioned P,P′-di(2-ethylhexyl)methanediphosphonic acid/silica (Dipex-2) extraction resin (Henriksen et al. 2001). The ^{223}Ra is initially eluted with 1 M HCl or HNO_3 and further purification of the ^{223}Ra is accomplished using a small AG 50W-X12 cation resin by elution with 1 M nitric acid. Although there are no practical complexing/chelating agents for ionic radium, the targeting of Ra^{2+} to the hydroxyl apatite in metabolically active bone allows the simple administration of radium chloride. In this manner, the generator can be eluted and the ^{223}Ra eluant evaporated then dissolved in saline/sodium citrate buffer and dispensed by sterile filtration. It is then ready for administration precluding any complex radiolabeling and purification procedures normally encountered for radiopharmaceutical administration.

Radium-223 ($T_{1/2}$ = 11.435 days) decays through a sequence involving four α emissions and two β^- emissions through the intermediary radioisotopes radon-219 (^{219}Rn, $T_{½}$ = 3.9 s), polonium-215 (^{215}Po, $T_{½}$ = 1.8 ms), lead-211 (^{211}Pb, $T_{½}$ = 36.1 min), bismuth-211 (^{211}Bi, $T_{½}$ = 2.1 min), and thallium-207 (^{207}Tl, $T_{½}$ = 4.8 min), a decay to stable lead-207 (^{207}Pb). More than 95 % of the energy released is accounted for by four distinct alpha particle emissions. Although the four α emissions are an advantage for therapy, there are challenges from the perspective of radiolabeling, since ^{219}Ra is a gas released from ^{223}Ra decay. The ^{219}Ra will be released in the circulation from the targeting site and could be toxic to normal tissues (Wick et al. 2008). As discussed later (Chap. 12), cationic $^{223}Ra^{+2}$ is a promising candidate for delivery of high-LET radiation to cancer cells adjacent to bone surfaces, since it is a congener of Ca^{+2} and binds strongly to hydroxyl apatite. Animal experiments have demonstrated death secondary to hemorrhage when ^{223}Ra is administered at high doses (>185 kBq/kg) to rats. However, at lower doses (60–110 kBq/kg), significant antitumor activity was exhibited in certain model systems and these dose levels were tolerated (Larsen et al. 2006). As discussed, ^{223}Ra is obtained in relatively high activity levels from natural decay in uranium mill tailings and also from the ^{227}Ac/^{223}Ra generator system (Soderquist et al. 2012; Boll et al. 2005).

In May 2013, the US Food and Drug Administration (FDA) approved the intravenous administration of ^{223}Ra dichloride as Xofigo® Injection (formerly known as Alpharadin; Bayer HealthCare Pharmaceuticals) for the treatment of patients with castration-resistant prostate cancer (CRPC) plus symptomatic bone metastases and no known visceral metastatic disease (US FDA 2013). A regimentation of 6 doses of ^{223}Ra (50 kBq, 1.35 mCi) IV per kilogram of body weight is the standard treatment protocol, administered at 4-week intervals. After IV injection, approximately 60 % of injected activity is rapidly targeted in the bone within 4 h, resulting in good palliative results. The use of ^{223}Ra for the treatment of advanced prostate cancer is rapidly evolving, providing patients with longer and better quality of life despite a diagnosis of castration-resistant disease (Renzulli et al. 2015; Mukherji et al. 2014; El-Amm and Aragon-Ching 2015; Vuong et al. 2014; Lien et al. 2015).

A recent and original approach described loading of ^{223}Ra into liposomes coated with folate-F(ab')2 to target tumor cells expressing the folate receptor (Henriksen et al. 2004). The common route to obtain ^{223}Ra is isolation from aged samples of natural uranium, since it is the decay product of ^{235}U. The activity levels of ^{223}Ra that could be obtained through this route are low and therefore inadequate to meet therapeutic requirements. The alternative source of ^{223}Ra is in a nuclear

reactor from neutron irradiation of ^{226}Ra by the ^{226}Ra(n,γ)^{227}Ra(β$^-$ →)^{227}Ac(β$^-$ →)^{227}Th(α→)^{223}Ra route. This production method relies upon neutron capture on ^{226}Ra and is conducted using high thermal neutron flux reactors, such as the High Flux Isotope Reactor (HFIR) at ORNL (Boll et al. 2005). Following reactor irradiation of ^{226}Ra, complex chemical isolation provides the "parent" ^{227}Ac ($T_{½}$ = 21.8 years), which decays to intermediary ^{227}Th ($T_{½}$ = 18.7 days) and then into ^{223}Ra. The separation of pure ^{223}Ra from the irradiated target is thus a very complex process requiring elaborate procedures of radiochemical separation and purification as well as for radioactive waste handling. The accelerator production route involving irradiation of natural ^{232}Th targets with medium-energy protons (Chap. 6) appears to be a potentially attractive route in terms of yield and cost-effectiveness. Chemical isolation of Ra from irradiated metallic Th can be accomplished by a gas-chemical method and by solvent extraction.

7.6.2.3 The Radium-224/Lead-212 Generator

Bismuth-212 (^{212}Bi, $T_{1/2}$ = 60.55 min) has been of interest for some time and is available from decay of ^{212}Pb. The traditional generator involves loading a cation exchange resin with ^{224}Ra with subsequent elution of the ^{212}Bi with HCl or HI (Atcher et al. 1988). This methodology requires replacement of the generator every 3–6 days because of the short 10.4 half-life of the ^{212}Pb parent. More recently a generator based on gaseous ^{222}Ra being released from ^{228}Th decay from thin films of Th barium stearate has been described (Hassfjell and Brechbiel 2001). This approach is based on the collection of gaseous ^{224}Ra in a trap containing an organic solvent such as methanol, hexane, or a methanol/hexane mixture, at temperatures lower than −72 °C. The ^{212}Pb decay product can be obtained in about 70 % yield and this system has the advantage of an indefinite shelf-life of the long-lived ^{228}Th ($T_{½}$ = 1.913 a) source.

Bismuth-212 decays through either ^{208}Th (36 %) or ^{212}Po (64 %) to stable ^{208}Pb. Both decay routes involve α particle emission (average energy of 7.8 MeV and path length in biological tissues from 40 to 100 μm) and β$^-$ emission. Thallium-208 is the daughter of ^{212}Bi and emits a very high energy 2.6-MeV gamma ray that necessitates heavy shielding in a clinical setting to minimize radiation exposure to personnel. The isolation of ^{212}Bi from the ^{228}Th decay chain on a large scale is probably impractical because of the short physical half-life. The activity levels of ^{212}Bi required for radiotherapy are generally available from a ^{224}Ra/^{212}Bi generator. Bismuth-212 can be eluted selectively from the ^{224}Ra generator in either the chloride form or as the tetraiodide complex. Following the adjustment of pH, the ^{212}Bi eluate is used for radiolabeling of mAbs, peptides, or other vectors conjugated with a suitable bifunctional chelating agent. One of the major impediments of this generator is the relatively short 3.6-day half-life of ^{224}Ra which requires frequent generator recharging with ^{224}Ra.

7.6.3 Radionuclide Generator Systems Which Provide Auger Electron-Emitting Radioisotopes

Interest in internal radionuclide therapy using Auger electrons has been increasing in recent years (see Chap. 4). Even some of the well-established diagnostic radionuclides used in nuclear medicine, such as gallium-67 (^{67}Ga), indium-111 (^{111}In), iodine-123 (^{123}I), ^{125}I, technetium-99m (^{99m}Tc), and thallium-201 (^{201}Tl), also decay with significant Auger electron emission and have therefore been discussed, and in some cases even evaluated, for therapeutic applications. Auger electron-emitting radionuclides have potential for the therapy of small-size cancers because of their high level of cytotoxicity, low energy, high linear energy transfer, and short-range biologic effectiveness. In order to realize their therapeutic potential, Auger electron-emitting radionuclides are strongly dependent on their close proximity to DNA. Furthermore, many Auger electron emitters also emit γ radiation, and this property makes Auger-emitting radionuclides an attractive option as therapeutic

Table 7.3 Radiation characteristics of potential radionuclides for Auger electron therapy

Radionuclide	$T_{1/2}$	Electrons per decay		keV values/decay			Percent of total energy per decay	
		A	IC	A	IC	Total	A	IC
^{67}Ga	78 h	4.7	0.3	6.3	28.1	201.6	3.1	13.9
^{99m}Tc	6 h	4.0	1.1	0.9	15.4	142.6	0.6	10.8
^{111}In	67 h	14.7	0.2	6.8	25.9	419.2	1.6	6.2
^{123}I	13 h	14.9	0.2	7.4	20.2	200.4	3.7	10.1
^{125}I	59.4 days	24.9	0.9	12.2	7.2	61.4	19.9	11.8
^{201}Tl	73 h	36.9	1.1	15.3	30.2	138.5	11.0	21.8

A Auger electron, *IC* internal conversion

and diagnostic agents in the molecular imaging and management of tumors. Radiation properties of representative therapeutic radionuclides for Auger electron therapy are depicted in Table 7.3.

Although there are limited examples, there are also radionuclide generator systems which can provide Auger-emitting daughter radioisotopes, and because of the potential importance and development of new technologies for single-cell targeting, the availability of these systems for potential focused therapeutic applications is expected to be of importance.

7.6.4 Ruthenium-103/Rhodium-103m Generator

Although few useful primary Auger-emitting radioisotopes are available from radionuclide generator systems, ^{103m}Rh is a key example of an Auger-emitting candidate which can be obtained from decay of reactor-produced ^{103}Ru (Fig. 7.13). Interest for use of ^{103m}Rh in radioimmunotherapy and other strategies for targeted therapy result from its attractive decay properties (see Tab. 7.1) and potential availability from a ^{103}Ru/^{103m}Rh generator system for targeted radiotherapy. The 40 keV isomeric decay energy is totally converted in the electronic shells of the stable ^{103}Rh daughter with no measurable γ rays and results in a "shower" of low-energy electrons and X-rays. Daily elution of equilibrium levels of ^{103m}Rh is possible from the ^{103}Ru/^{103m}Rh generator. Rhodium-103m is expected to exhibit high cytotoxicity resulting from its decay by highly converted isomeric transition and emission of Auger electrons. Availability of a ^{103}Ru/^{103m}Rh generator system would offer an opportunity to provide carrier-free ^{103m}Rh on a routine basis for assessment of its potential for Auger therapy. Either fission- or reactor-produced ^{103}Ru could be used for the generator system. Although the 3 % fission yield of ^{103}Ru from ^{235}U is quite high, fission products are not routinely available.

The availability of lower-specific-activity ^{103}Ru from reactor irradiation of enriched ^{102}Ru production with sufficient specific activity in many in research reactors on an international basis would be expected to be reliable routine source of ^{103}Ru for fabrication of the ^{103}Ru/^{103m}Rh generator system. Rhodium-103m can also be obtained by decay of ^{103}Pd (Fig. 7.13), and the use of the ^{103}Pd/^{103m}Rh in vivo generator has been proposed (Szucs et al. 2008), which may be suggest that a ^{103}Pd/^{103m}Rh generator for routine availability of ^{103m}Rh may be feasible. Development of a chromatographic-type ^{103}Ru/^{103m}Rh generator would be expected to provide ^{103m}Rh from separation of Rh from Ru compared to Rh from Pd. In addition, the very low 1.02 % natural abundance of ^{102}Pd, the high costs of enrichment for reactor production of ^{103}Pd, the high costs of accelerator production of ^{103}Pd from ^{103}Ru(p,n), and the shorter physical half-life of ^{103}Pd compared to ^{103}Ru are other issues.

The separation of Rh from Ru had been described some years ago by solvent extraction techniques (Chiu et al. 1978; Epperson et al. 1976), and these methods with carbon

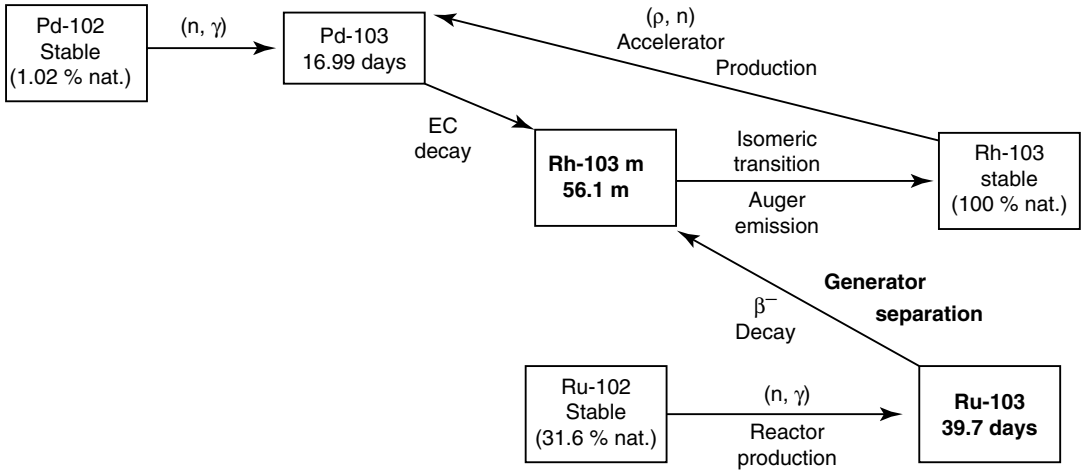

Fig. 7.13 Availability of ^{103m}Rh from reactor-produced long-lived ^{103}Ru from decay of ^{103}Pd

tetrachloride extraction for RuO_4 from Ru/Rh mixtures in HCl have served as the basis for the more recent interest in the availability of ^{103m}Rh. A recent solvent-extraction-type ^{103}Ru/^{103m}Rh generator has recently been reassessed (Bartos et al. 2007 and 2009; Skarnemark et al. 2009), which is based on the earlier extraction work (Epperson et al. 1976; Chiu et al. 1978), and other studies have used both fission- and reactor-produced Ru (Bartos et al. 2009). However, it may be impractical to utilize the batch liquid extraction/post processing of Rh from Ru to provide ^{103m}Rh since it would presumably require a central processing site and not accessible in most research centers. The chromatographic-type generator may be more accessible and thus more practical at most institutions to obtain ^{103m}Rh.

7.7 Summary

This chapter has described the extremely important role in the use of radionuclide generator systems essentially as in-house radioisotope production systems to provide a variety of therapeutic radioisotopes. This exiting radioisotope production paradigm continues to evolve with expected future improvements. Innovative separation strategies together with technology inventions have been the important driving forces that continue to catalyze the development of new radionuclide generator technologies. Although many of these generator systems are well established and reliable for use in hospital-based or centralized radiopharmacy centers (i.e., ^{225}Ac/^{213}Bi, ^{188}W/^{188}Re, etc.), others, such the ^{90}Sr/^{90}Y generator, are generally operated in commercially based centralized manufacturing facilities because of potential health hazards from possible parent contamination. Because these systems are by nature repeatedly used, the regulatory and GMP issues associated with their use are in some ways more challenging than for singe use kit-based agents, as described in Chap. 17. The regulatory nature of cGMP compliance of radionuclide generator requires a high degree of focus on product quality, system operation as well as validation, and production records. Regulators place a high value on accuracy and completeness of production records. Simplicity and user-friendliness are increasingly coming into their own as radionuclide generators destined to adapt themselves to users, rather than the reverse. In this context, automation of the separation procedure is not only viewed as a more simple proposition to implement GMP compliance but also effective in providing consistent product quality and improved productivity and offers consistent separation performance. In addition to reducing the radiation exposure to personnel, these systems diminish the probability of human errors and provide a log of the operations

performed. The use of automation also provides the scope of collecting complete production records commensurate with cGMP compliance. An important capability for routine, reliable operation is the recent widespread availability of PC-based automated elution and dispensing systems as discussed in Chap. 17.

References

Abbasi IA, Zaidi JH, Arif M, et al. Measurement of fission neutron spectrum averaged cross sections of some threshold reactions on zirconium: production possibility of no-carrier-added ^{90}Y in a nuclear reactor. Radiochim Acta. 2006;94:38.

Antczak C, Jaggi JS, Lefavre CV, Curico MJ, McDevitt MR, Scheinberg DA. Influence of the linker on the biodistribution and catabolism of actinium-225 self-immolative tumor-targeted isotope generators. Bioconjug Chem. 2006;17:1551–60.

Anwar M, Lathrop K, Rosskelly D, Harpen PV, Lathrop K, Rosselly D. Pertechnetate production from ^{99}Mo by liquid-liquid extraction. J Nucl Med. 1968;9:298–9.

Asavatanabodee P, Sholter D, Davis P. Yttrium-90 radiochemical synovectomy in chronic knee synovitis: a one year retrospective review of 133 treatment interventions. J Rheumatol. 1997;24(4):639–42.

Atcher RW, Friedman AM, Hines JJ. An improved generator for the production of 212Pb and 212Bi from 224Ra. Int J Rad Appl Instrum A. 1988;39:283–6.

Bartos B, Kowaslka E, Bilewicz A, Skarnemark G. ^{103}Ru/^{103}mRh generator. J Lab Cmpds Radiopharm. 2007;50:S94.

Bartos B, Kowaslka E, Bilewicz A, Skarnemark G. ^{103}Ru/^{103}mRh generator. J Radioanal Nucl Chem. 2009;279:655–7.

Bateman H. Solution of a system of differential equations occurring in the theory of radioactive transformations. Proc Cambridge Philos Soc. 1910;15:423–7.

Beard SJ, Moore RL. Large-scale recovery and purification of fission products. In: Stevenson CE, Mason EA, Gresky AT, editors. Progress in nuclear energy (series III), process chemistry, vol. 4. London: Pergamon Press; 1969. p. 645.

Bilewicz A. Separation of ^{90}Y from ^{90}Sr on crystalline antimonic acid. Radiochim Acta. 1995;69:137–40.

Blower PJ, Kettle AG, O'doherty MJO, Coakley AJ, Knapp Jr FF. (99 m)Tc(V)DMSA quantitatively predicts (188)Re(V)DMSA distribution in patients with prostate cancer metastatic to bone. Eur J Nucl Med. 2000;27:1405–9.

Bodet-Milin C, Ferrer L, Pallardy A, Eugène T, et al. Radioimmunotherapy of B-cell non-Hodgkin's lymphoma. Front Oncol. 2013;3:177.

Boll RA, Mirzadeh S, Kennel SJ. Optimization of radiolabeling of immunoproteins with ^{213}Bi. Radiochim Acta. 1997;79:145–9.

Boll RA, Malkemus D, Mirzadeh S. Production of actinium-225 for alpha particle mediated radioimmunotherapy. Appl Radiat Isot. 2005;62:667–79.

Braun T, Imura H, Suzuki N. Separation of ^{99m}Tc from parent ^{99}Mo by solid-phase column extraction as a simple option for a new ^{99m}Tc generator concept. J Radioanal Nucl Chem Letters. 1987;119:315–25.

Bray LA. The recovery and purification of multi-kilocurie quantities of fission product strontium by cation exchange, Rep. HW-70998, Hanford Atomic Products Operation, Richland, 1961.

Bray LA, Wester DW. Method of preparation of yttirum-90 from strontium-90. US Patent # 5,512,256, 30 Apr 1996.

Bruland OS, Jostein D, Olsen DR, Larsen RH. Targeted high-LET therapy of bone metastases. Chapter 10. In: Stigbrand T, et al., editor. Targeted radionuclide tumor therapy. Springer Netherlands; 2008. p. 181–184. ISBN 978-1-4020-8695-3 (hard cover); DOI: 10.1007/978-1-4020-8696-0.

Buchmann I, Bunjes D, Kotzerke J, Martin H, Glatting G, Seitz U, Rattat D, Buck A, Döhner H, Reske SN. Myeloablative radioimmunotherapy with Re-188-anti-CD66-antibody for conditioning of high-risk leukemia patients prior to stem cell transplantation: biodistribution, biokinetics and immediate toxicities. Cancer Biother Radiopharm. 2002;17:151–63.

Bugai JE, Bickel EM, Azure MT, Friebe M, Lister-James J, Dean RT, Dinkelborg LM. Radiotherapeutic efficacy of a SSTR-targeting peptide (^{188}Re-P2045) in a small cell lung cancer (SCLC) mouse model. J Nucl Med. 2002;43:123.

Bunjes D. 188Re-labeled anti-CD66 monoclonal antibody in stem cell transplantation for patients with high-risk acute myeloid leukemia. Leuk Lymphoma. 2002;43:2125–31.

Callahan AP, Rice DE, Knapp Jr FF. Rhenium-188 for therapeutic applications from an alumina-based tungsten-188/rhenium-188 generator. NucCompact. 1989;20:3–6.

Chakravarty R, Pandey U, Manolkar RB, et al. Development of an electrochemical ^{90}Sr-^{90}Y generator for separation of ^{90}Y suitable for targeted therapy. Nucl Med Biol. 2008;35:245–53.

Chakravarty R, Dash A, Kothari K, et al. A novel ^{188}W/^{188}Re electrochemical generator with potential for medical applications. Radiochim Acta. 2009;97:309–17.

Chakravarty R, Dash A, Venkatesh M. A novel electrochemical technique for the production of clinical grade ^{99m}Tc using (n, gamma)^{99}Mo. Nucl Med Biol. 2010a;37:21–8.

Chakravarty R, Dash A, Pillai MRA, Venkatesh M. Post-elution concentration of ^{188}Re by an electrochemical method. Appl Radiat Isot. 2010b;68:2302–5.

Chakravarty R, Das T, Dash A, Venkatesh M. An electro-amalgamation approach to isolate no-carrier-added ^{177}Lu from neutron irradiated Yb for biomedical applications. Nucl Med Biol. 2010c;37(7):811–20.

Chakravarty R, Dash A, Pillai MRA. Electrochemical separation is an attractive strategy for development of

radionuclide generators for medical applications. Curr Radiopharm. 2012a;5:271–87.
Chakravarty R, Dash A, Pillai MRA. Availability of yttrium-90 from strontium-90: a nuclear medicine perspective. Cancer Biother Radiopharm. 2012b;27: 621–41.
Chakravarty R, Dash A. Development of radionuclide generators for biomedical applications, Lambert Academic Publishing GmbH & Co. KG Heinrich-Böcking-Str. 6–8 66121, Saarbrücken, 2013.
Chang MY, Seideman J, Sofou S. Enhanced loading efficiency and retention of ^{225}Ac in rigid liposomes for potential targeted therapy of micrometastases. Bioconjug Chem. 2008;19:1274–82.
Chapuy B, Hohloch K, Trümper L. Yttrium 90 ibritumomab tiuxetan (Zevalin): a new bullet in the fight against malignant lymphoma? Biotechnol J. 2007;2: 1435–43.
Chattopadhyay S, Das SS, Das MK, Goomer NC. Recovery of 99mTc from Na2[99Mo]MoO4 solution obtained from reactor-produced (n, g) 99Mo using a tiny Dowex-1 column in tandem with a small alumina column. Appl Radiat Isot. 2008;66:1814–7.
Cheson BD. The role of radioimmunotherapy with yttrium-90 ibritumomab tiuxetan in the treatment of non-Hodgkin lymphoma. BioDrugs. 2005;19: 309–22.
Cheung MC, Haynes AE, Stevens A, et al. Yttrium 90 ibritumomab tiuxetan in lymphoma. Leuk Lymphoma. 2006;47:967–77.
Chinol M, Franceschini R, Paganelli G, Pecorale A, Paiano A. Simple production of Yttrium-90 in a chemical form suitable to clinical grade radioconjugates radioactive isotopes in clinical medicine and research. In: Bergmann H, Kroiss A, Sinzinger H, editors. Advances in pharmacological science. Badgastein: Birkhäuser Basel; 1997. p. 327–32. DOI: 10.1007/978-3-0348-7772-5; Softcover ISBN 978-3-0348-7774-9
Chinol M, Hnatowich DJ. Generator-produced yttrium-90 for radioimmunotherapy. J Nucl Med. 1987;28: 1465–70.
Chiu JH, Landolt RR, Kessler WV. Separation of rhodium-103 m from ruthenium-103 by solvent extraction. Anal Chem. 1978;50:670–1.
Christian JD, Pett DA, Kirkham RJ, Bennett RG. Advances in sublimation separation of technetium from low specific activity molybdenum-99. Ind Eng Chem Res. 2000;39(9):3157–68.
Chuang JT, Lo JG. Extraction chromatographic separation of carrier-free ^{90}Y from ^{90}Sr/^{90}Y generator by crown ether coated silica gels. J Radioanal Nucl Chem. 1996;204:83–93.
Cwikla JB, Sankowski A, Seklecka N, et al. Efficacy of radionuclide treatment DOTATATE Y-90 in patients with progressive metastatic gastroenteropancreatic neuroendocrine carcinomas (GEP-NETs): a phase II study. Ann Oncol. 2010;21:787–94.
Dadachova E, Mirzadeh S, Lambrecht RM, Hetherington E, Knapp Jr FF. Separation of carrier-free holmium-166 from neutron-irradiated dysprosium targets. Anal Chem. 1995a;66:4272–7.
Dadachova E, Mirzadeh S, Lambrecht RM, Hetherington EL, Knapp Jr FF. Separation of carrier-free ^{166}Ho from Dy2O3 targets by partition chromatography and electrophoresis. J Radioanal Nucl Chem Lett. 1995b;1999:115–23.
Dadachova E, Mirzadeh S, Smith SV, Knapp Jr FF, Hetherington EL. Radiolabeling antibodies with holmium-166. Appl Radiat Isot. 1997;48:477–81.
Dash A, Chakravarty R. Pivotal role of separation chemistry in the development of radionuclide generators to meet clinical demands. RSC Adv. 2014a;4:42779–803.
Dash A, Chakravarty R. Electrochemical separation: promises, opportunities, and challenges to develop next-generation radionuclide generators to meet clinical demands. Ind Eng Chem Res. 2014b;53: 3766–77.
Dash A, Knapp FF (Russ) Jr. An overview of radioisotope separation technologies for development of ^{188}W/^{188}Re radionuclide generators providing ^{188}Re to meet future research and clinical demands. RSC Adv. 2015;5: 39012–36.
Dash A, Knapp FF (Russ) Jr, Pillai MRA. ^{99}Mo/^{99m}Tc separation: an assessment of technology options. Nucl Med Biol. 2013;40(2):167–76.
Davies AJ. Radioimmunotherapy for B-cell lymphoma: Y^{90} ibritumomab tiuxetan and I^{131} tositumomab. Oncogene. 2007;26:3614–28.
Dietz ML, Horwitz EP. Applications of extraction chromatography in the development of radionuclide generator systems for nuclear medicine. Ind Eng Chem Res. 2000;39(9):3181–8.
Dillman RO. Radioimmunotherapy of B-cell lymphoma with radiolabelled anti-CD20 monoclonal antibodies. Clin Exp Me. 2006;6:1–12.
El-Amm J, Aragon-Ching JB. Radium-223 for the treatment of castration-resistant prostate cancer. Onco Targets Ther. 2015;8:1103–9.
Emmanouilides C. Review of Y-ibritumomab tiuxetan as first-line consolidation radio-immunotherapy for B-cell follicular non-Hodgkin's lymphoma. Cancer Manag Res. 2009;1:131–6.
Epperson CE, Landolt RR, Kessler WV. Solvent – solvent extraction of rhodium-103 m from ruthenium-103 employing a sulfate-carbon tetrachloride medium. Anal Chem. 1976;48:979–81.
Geerlings MW, Kaspersen FM, Apostolidis C, Van Der Hout R. The feasibility of 225Ac as a source of alpha-particles in radioimmunotherapy. Nucl Med Commun. 1993;14:121–5.
Gerse J, Kern J, Imre J, Zsinka L. Examination of a portable^{99}Mo/^{99m}Tc isotope generator: SUBLITECH. J Radioanal Nucl Che. 1988;128(1):71–9.
Gisselbrecht C, Bethge W, Duarte RF, et al. Current status and future perspectives for yttrium-90(^{90}) Y)-ibritumomab tiuxetan in stem cell transplantation for non-Hodgkin's lymphoma. Bone Marrow Transplant. 2007;40:1007.
Goffredo V, Paradiso A, Ranieri G, et al. Yttrium-90 (90Y) in the principal radionuclide therapies: an efficacy correlation between peptide receptor radionuclide therapy, radioimmunotherapy and transarterial

radioembolization therapy. Ten years of experience (1999–2009). Crit Rev Oncol Hematol. 2011;80(3): 393–410.

Guhlke S. Convenient concentration of ^{188}Re perrhenate or ^{99m}Tc pertechnetate eluates from ^{188}W/188Re or (n, γ) produced 99Mo/99mTc generators to high specific volumes. J Label Compd Radiopharm. 1998;40:294.

Guhlke S, Beets AL, Oetjen K, et al. Simple new method for effective concentration of ^{188}Re solutions from alumina-based ^{188}W-^{188}Re generator. J Nucl Med. 2000;41:1271–80.

Hagenbeek A. Radioimmunotherapy for NHL: experience of ^{90}Y-ibritumomab tiuxetan in clinical practice. Leuk Lymphoma. 2003;44:S37–47.

Hassfjell S, Brechbiel MW. The development of the alpha-particle emitting radionuclides 212Bi and 213Bi, and their decay chain related radionuclides, for therapeutic applications. Chem Rev. 2001;101:2019–36.

Henriksen G, Hoff P, Alstad J, Larsen RH. ^{223}Ra for endoradiotherapeutic applications prepared from an immobilized ^{227}Ac/^{227}Th source. Radiochim Acta. 2001;89: 661–6.

Henriksen G, Schoultz BW, Michaelsen TE, et al. Sterically stabilized liposomes as a carrier for alpha-emitting radium and actinium radionuclides. Nucl Med Biol. 2004;31:441–9.

Hoeher M, Woerle J, Wohlfrom M, Hanke H, Voisard R, Osterhaus HH, Kochs M, Reske SN, Hombach V, Kotzerke J. Intracoronary β-irradiation with a liquid ^{188}Re-filled balloon six-month results from a clinical safety and feasibility study. Circulation. 2000;101: 2355–60.

Hong YD, Park KB, Jang BS, Choi SJ, Choi SM, Kim YM. Holmium-166-DTPA as a liquid source for endovascular brachytherapy. Nucl Med Biol. 2002;29:833–9.

Horwitz EP, Dietz ML, Fisher DE. SREX: a new process for the extraction and recovery of strontium from acidic nuclear waste streams. Solv Extr Ion Exch. 1991;9:1.

Hsieh BT, Ting G, Hsieh HT, Shen LH. Preparation of carrier-free yttrium-90 for medical applications by solvent extraction chromatography. Appl Radiat Isot. 1993;44:1473–80.

Iznaga-Escobar N. Direct radiolabeling of monoclonal antibodies with rhenium-188 for radioimmunotherapy of solid tumors–a review of radiolabeling characteristics, quality control and in vitro stability studies. Appl Radiat Isot. 2001;54:399–406.

Jäckel B, Cripps R, Güntay S, Bruchertseifer H. Development of semi-automated system for preparation of (188)Re aqueous solutions of high and reproducible activity concentrations. Appl Radiat Isot. 2005;63:299–304.

Jassin LE. Radiochemical separation advancements using extraction chromatography: a review of recent Eichrom users' group workshop presentations with a focus on matrix interferences. J Radioanal Nucl Chem. 2005;163:93–6.

Jennewein M, Qaim SM, Kulkarni PV, et al. A no-carrier-added ^{72}Se/^{72}As radionuclide generator based on solid phase extraction. Radiochim Acta. 2005;93:579–83.

Jeong JM, Chung JK. Therapy with ^{188}Re-labeled radiopharmaceuticals: an overview of promising results from initial clinical trials. Cancer Biother Radiopharm. 2003;18:707–17.

Jeong JM, Kim YJ, Lee YS, et al. Lipiodol solution of a lipophilic agent, ^{188}Re-TDD, for the treatment of liver cancer. Nucl Med Biol. 2001;28:197–204.

Jeong JM, Knapp Jr FF. Use of the Oak Ridge National Laboratory tungsten-188/rhenium-188 generator for preparation of the rhenium-188 HDD/lipiodol complex for trans-arterial liver cancer therapy. Semin Nucl Med. 2008;38(2):S19–29.

Jurcic JG, Larson SM, Sgouros G, et al. Targeted alpha particle immunotherapy for myeloid leukemia. Blood. 2002;100:1233–9.

Jurcic JG, Rosenblat TL. Targeted alpha-particle immunotherapy for acute myeloid leukemia. Am Soc Clin Oncol Educ Book. 2014; e126-31. doi: 10.14694/EdBook_AM.2014.34.e126

Kamadhenu Electrochemical ^{90}Sr/^{90}Y generator, Model KA 01 Operating Manual. Isotope Technologies Dresden, 2010.

Kamioki H, Mirzadeh S, Lambrecht RM, et al. ^{188}W/^{188}Re generator for biomedical applications. Radiochim Acta. 1994;65:39–46.

Kampen WU, Voth M, Pinkert J, Krause A. Therapeutic status of radiosynoviorthesis of the knee with yttrium [^{90}Y] colloid in rheumatoid arthritis and related indications. Rheumatology (Oxford). 2007;46:16–24.

Kan RW, Tsang SH, Poon RT, Cheung TT. Update on yttrium-90-based radio-embolization for treatment of hepatocellular carcinoma. ANZ J Surg. 2012;82:505–9.

Ketring AR, Ehrhardt GJ, Embree MF, Bailey KD, Tyler TT, Gawenis JA, Jurisson SS, Englebrecht HP, Smith CJ, Cutler CS. Production and supply of high specific activity radioisotopes for radiotherapy applications. Revista Med Nucl Alasbimn J. 2002;5:1.

Knapp FF (Russ) Jr, Beets AL, Mirzadeh S, Guhlke S. Concentration of perrhenate and pertechnetate solutions. U.S. Patent No. 5,729,821. 1998.

Knapp FF (Russ) Jr, Beets AL, Mirzadeh S, Guhlke S. Use of a new tandem cation/anion exchange system with clinical-scale generator provides high specific volume solution of technicium-99m and rhenium-188. In: Proceedings, international trends in radiopharmaceuticals for diagnosis and therapy. Lisbon, Portugal, Mar 30–Apr 1998.

Knapp FF Jr, Butler TA, editor. Radionuclide generators: new systems for nuclear medicine applications. 241 ACS Symposium Series, American Chemical Society, United States, 1984.

Knapp Jr FF, Mirzaeh S. The continuing important role of radionuclide generator systems for nuclear medicine. Eur J Nucl Med. 1994;21:1151–65.

Knapp Jr FF, Lisic EJ, Mirzadeh S, et al. A new clinical prototype W-188/Re-188 generator to provide high levels of carrier-free Rhenium-188 for radioimmunotherapy. Eur J Nucl Med. 1991;18:538.

Knapp FF, Lisic EC, Mirzadeh S, Callahan AP. Tungsten-188/carrier-free rhenium-188 Perrhenic acid generator system. U.S. Patent No. 5,186,913; 1993.

Knapp Jr FF, Callahan AP, Beets AL, Mirzadeh S. Processing of reactor-produced ^{188}W for fabrication of clinical scale alumina based ^{188}W/^{188}Re Generators. Appl Radiat Isot. 1994;45:1123–8.

Knapp Jr FF, Beets AL, Guhlke S, et al. Availability of rhenium-188 from the alumina-based tungsten-188/rhenium-188 generator for preparation of rhenium-188-labeled radiopharmaceuticals for cancer treatment. Anticancer Res. 1997;17:1783–95.

Knapp Jr FF, Beets AL, Mirzadeh S, Guhlke S. Use of a new tandem cation/anion exchange system with clinical—scale generators provides high specific volume solutions of technetium-99m and rhenium-188, IAEA-ECDOC-1029. Vienna: IAEA; 1998. p. 419–25.

Knapp Jr FF, Pillai MRA, Osso Jr JA, Dash A. Re-emergence of the important role of radionuclide generators to provide diagnostic and therapeutic radionuclides to meet future research and clinical demands. J Radioanal Nucl Chem. 2014;302:1053–68.

Kotzerke J, Hanke J, Hocher M. Endovascular brachytherapy for the prevention of restenosis after angioplasty. Eur J Nucl Med. 2000;27:223–36.

Kropp J, Reynen K, Koeckeritz U, Wunderlich G, Schmeisser A, Strasse RH, Knapp Jr FF. Prevention of in-stent stenosis with liquid filled 188Re balloon: the Dresden in-stent restenosis trial (DIRRT). World J Nucl Med. 2002;1:S13.

Lambert B, de Klerk JM. Clinical applications of ^{188}Re-labelled radiopharmaceuticals for radionuclide therapy. Nucl Med Commun. 2006;27:223–9.

Lange G, Herrmann G, Strassmann F. Preparation of strontium-90 free yttrium-90 by electrolysis. J Inorg Nucl Chem. 1957;4:146.

Larsen RH, Saxtorph H, Skydsgaard M, et al. Radiotoxicity of the alpha-emitting bone-seeker 223Ra injected intravenously into mice: histology, clinical chemistry and hematology. Vivo. 2006;20(3):325–33.

Larsen SH, Borrebaek J, Dahle J, Melhus KB, Krogh MH, Valan MH, Bruland OS. Preparation of Th-227-labeled radioimmunoconjugates, assessment of serum stability and antigen binding ability. Cancer Biother Radiopharm. 2007;22:431–7.

Lau WY, Lai EC, Leung TW. Current role of selective internal irradiation with yttrium-90 microspheres in the management of hepatocellular carcinoma: a systematic review. Int J Radiat Oncol Biol Phys. 2011;81(2):460–7.

Lee JS, Lee J-S, Park U-J, Son K-J, Han H-S. One column operation for (90)Sr/(90)Y separation by using a functionalized-silica. Appl Radiat Isot. 2009;67:1332–5.

Lewis RE. Production of 70-day tungsten-188 and development of a 17 hour rhenium-188 radioisotope generator. J Nucl Med. 1966;7:804–5.

Lien LME, Tvedt B, Heinrich D. Treatment of castration-resistant prostate cancer and bone metastases with radium-223 dichloride. Int J Urol Nurs. 2015;9(1):3–13.

Lisic EC, Callahan AP, Mirzadeh S, Knapp Jr FF. The tandem tungsten-188/rhenium-188 Perrhenate/Perrhenic acid generator system. Radioact Radiochem. 1992;3:42–5.

Lumetta GJ, Wester DW, Morrey JR, Wagner MJ. Preliminary evaluation of chromatographic techniques for the separation of radionuclides from high level radioactive waste. Solv Extr Ion Exch. 1993;11:663.

Macháň V, Vilček S, Kalinčák M. Technetium-99m sublimation from molybdenum trioxide eutectic mixtures. J Inorg Nucl Chem. 1981;43:3063–6.

Makkar R, Whiting JA, Hidehiko H, Fishbien MC, Knapp Jr FF, Litvack F, Eigler NL. Effects of beta(−)-emitting (188)Re balloon in stented porcine coronary arteries: an angiographic, intravascular ultrasound, and histomorphometric study. Circulation. 2000;102:3117–23.

Marincek N, Jörg AC, Brunner P. Somatostatin-based radiotherapy with [^{90}Y-DOTA]-TOC in neuroendocrine tumors: long-term outcome of a phase I dose escalation study. J Transl Med. 2013;15:11–7.

Mausner LF, Kolsky KL, Joshi V, Srivastava SC. Radionuclide development at BNL for nuclear medicine therapy. Appl Radiat Isot. 1998;49(4):285–94.

McDevitt MR, Finn RD, Sgouros G, Ma D, Scheinberg DA. An 225Ac/213Bi generator system for therapeutic clinical applications: construction and operation. Appl Radiat Isot. 1999a;50:895–904.

McDevitt MR, Finn RD, Sgorous G, Ma D, Scheinberg DA. Preparation of alpha-emitting 213Bi-labeled antibody constructs for clinical use. J Nucl Med. 1999b;40:1722–7.

McDevitt MR, Ma D, Lai LT, Simon J, Borchardt P, Frank RK, Wu K, Pellegrini V, Curcio MJ, Miederer M, Bander NH, Scheinberg DA. Tumor therapy with targeted atomic nanogenerators. Science. 2001;294:1537–40.

Micallef IN. Ongoing trials with yttrium 90-labeled ibritumomab tiuxetan in patients with non-Hodgkin's lymphoma. Clin Lymphoma. 2004;5:S27–32.

Miederer M, Scheinberg DA, McDevitt MR. Realizing the potential of the Actinium-225 radionuclide generator in targeted alpha particle therapy applications. Adv Drug Deliv Rev. 2008;60:1371–82.

Mikheev NS, Popovich VS, Rumer IA, Volkova NC. Rhenium-188 generator. Isotopenpraxis. 1972;8:248–51.

Mirzadeh S, Knapp Jr FF. Biomedical radioisotope generator systems. J Radioanal Nucl Chem. 1996;203:471–88.

Mirzadeh S, Knapp Jr FF, Lambrecht RM. Burn-up cross section of ^{188}W. Radiochim Acta. 1997;77:99–110.

Mirzadeh S, Lambrecht RM. Excitation function for the 209Bi(7Li, 5n)211Rn nuclear reaction. Int J Appl Radiat Isot. 1980;31:351–5.

Miszczyk L, Wozniak G, Jochymek B, Spindel J, Wygoda Z. Effectiveness evaluation of knee joint ^{90}Y radiosynovectomy. Przegl Lek. 2007;64:450–3.

Mirzadeh S. Generator-produced alpha-emitters. Appl Radiat Isot. 1998;49:345–9.

Montaña RL, González IH, Ramirez AA, et al. Yttrium-90 – current status, expected availability and

applications of a high beta energy emitter. Curr Radiopha. 2012;5(3):253–6.

Mukherji D, Dika IE, Temraz S, Haidar M, Shamseddine A. Evolving treatment approaches for the management of metastatic castration-resistant prostate cancer – role of radium-223. Ther Clin Risk Mana. 2014;10:373–80.

Murray A, Simms MS, Scholfield DP, Vincent RM, Denton G, Bishop MC, Price MR, Perkins AC. Production and characterization of 188Re-C595 antibody for radioimmunotherapy of transitional cell bladder cancer. J Nucl Med. 2001;42:726–32.

Mushtaq A, Bukhari TH, Khan IU. Extraction of medically interesting ^{188}Re-perrhenate in methyl ethyl ketone for concentration purposes. Radiochimica Acta. 2007;95:535–53.

Nilsson S, Franzen L, Parker C, Tyrell C, Blom R, Tennevall J, Lenneras B, Petersson U, Johannessen DC, Sokail M, Pigott K, Yachnin J, Garkavij M, Strang P, Harmenberg J, Bolstad B, Bruland OS. Bone-targeted radium-223 in symptomatic, hormone-refractory prostate cancer: a randomised, multicentre, placebo-controlled phase II study. Lancet Oncol. 2007;8(7):587–94.

Nowak B, Meyer JMA, Goergen T, Fluehs D, Block S, Guenther RW, Howecker H, Buell U. Dosimetry of a ^{188}rhenium-labeled self-expanding stent for endovascular brachytherapy in peripheral arteries. Cardiovasc Radiat Med. 2001;2:246–63.

Ofluoglu S, Schwameis E, Zehetgruber H, Havlik E, Wanivenhaus A, Schweeger I, Weiss K, Sinzinger H, Pirich C. Radiation synovectomy with (166)Ho-ferric hydroxide: a first experience. J Nucl Med. 2002;43:1489–94.

Orth RJ, Kurath DE. Review and assessment of technologies for the separation of strontium from alkaline and acidic media, Rep. PNL-9053, Pacific Northwest National Laboratory, Richland, 1994.

Osso J, Knapp Jr FF. Invited, Chapter 21: Principles and operation of radionuclide generators. In: Sampson's textbook on radiopharmacy. 4th ed. London: Pharmaceutical Press; 2011. p. 339–64. ISBN 978 0 85369 789 3.

Pandey U, Dhami PS, Jagesia P, et al. A novel extraction paper chromatography (EPC) technique for the radionuclidic purity evaluation of ^{90}Y for clinical use. Anal Chem. 2008;80:801.

Park SW, Hong MK, Moon DH, Oh SJ, Lee CW, Kim JJ, Park SJ. Treatment of diffuse in-stent restenosis with rotational atherectomy followed by radiation therapy with a rhenium-188-mercaptoacetyltriglycine-filled balloon. J Am Coll Cardiol. 2001;38:631–7.

Pfost B, Seidl C, Autenrieth M, et al. Intravesical alpha-radioimmunotherapy with 213Bi-anti-EGFR-mAb defeats human bladder carcinoma in xenografted nude mice. J Nucl Med. 2009;50:1700–8.

Pillai MR, Dash A, Knapp Jr FF. Rhenium-188: availability from the ^{188}W/^{188}Re generator and status of current applications. Curr Radiopharm. 2012;5:228–43.

Production of long lived parent radionuclides for generators: ^{68}Ge, ^{82}Sr, ^{90}Sr and ^{188}W (2010) IAEA Radioisotopes and Radiopharmaceuticals Series No. 2. Vienna: IAEA.

Rajendran JG, Eary JF, Bensinger W, Durack LD, Vernon C, Fritzberg A. High-dose 166Ho-DOTMP in myeloablative treatment of multiple myeloma: pharmacokinetics, biodistribution, and absorbed dose estimation. J Nucl Med. 2002;43:1383–90.

Ramanujam A, Dhami PS, Chitnis RR, et al. Separation of strontium-90 from PUREX high level waste and development of ^{90}Sr/^{90}Y generator. BARC report 2000/E/009, BARC India, 2000.

Renzulli JF, Collins J, Mega A. Radium-223 dichloride: illustrating the benefits of a multidisciplinary approach for patients with metastatic castration-resistant prostate cancer. J Multidiscip Health. 2015;8:279–86.

Reske SN, Bunjes D, Buchmann I, Seitz U, Glatting G, Neumaier B, Kotzerke J, Buck A, Martin H, Döhner H, Bergmann L. Targeted bone marrow irradiation in the conditioning of high-risk leukaemia prior to stem cell transplantation. Eur J Nucl Med. 2001;28:807–15.

Roesch F, Knapp FF Jr. Chapter 4: Radionuclide generators. In: Vertes A, Klencsar NS, Roesch F, editors. Handbook of nuclear chemistry. Vol 4, 2nd ed. Dordrecht: Kluwer Academic Publishers; 2011. p. 1935–76. ISBN 978-1-4419-0720-2.

Rutherford E, Soddy F. The cause and nature of radioactivity. Philos Mag. 1902;4:370–96; Part II 4:569–85.

Sarkar SK, Venkatesh M, Ramamoorthy N. Evaluation of two methods for concentrating perrhenate (^{188}Re) eluates obtained from 188 W-188 Re generator. Appl Radiat Isot. 2009;67:234–9.

Sato KT. Yttrium-90 radioembolization for the treatment of primary and metastatic liver tumors. Semin Roentgenol. 2011;46:159–65.

Savelli G, Giubbini R. Yttrium-90 DOTATOC therapy in GEP-NET and other SST2 expressing tumors: a selected review. Ann Nucl Med. 2011;25:75–85.

Savio E, Gaudiano J, Robles AM, Balter H, Paolino A, Lo'pez A, Hermida JC, De Marco E, Martinez G, Osinaga E, Knapp Jr FF. Re-HEDP: pharmacokinetic characterization, clinical and dosimetric evaluation in osseous metastatic patients with two levels of radiopharmaceutical dose. BMC Nucl Med. 2001;1:2.

Scheinberg DA, McDevitt MR. Actinium-225 in targeted alpha-particle therapeutic applications. Curr Radiopharm. 2011;4:306–20.

Schuelen H, Eigler N, Whiting JS, Haubner R, Hausleiter J, Dirschinger J, Kastrati A, Schwaiger M, Schömig A. Usefulness of intracoronary brachytherapy for in-stent restenosis with a 188Re liquid-filled balloon. Am J Cardiol. 2001;87:463–6.

Sgouros G, Ballangrud AM, Jurcic JG, et al. Pharmacokinetics and dosimetry of an alpha-particle emitter labeled antibody: ^{213}Bi-HuM195 (anti-CD33) in patients with leukemia. J Nucl Med. 1999;40:1935–46.

Skarnemark G, Odegaard-Jense A, Nilsson J, Bartos B, Kowalska E, Bilewicz A, Bernhardt P. Production of ^{103m}Rh for cancer therapy. J Radioanalyt Nucl Chem. 2009;280:371–3.

Skuridin VS, Chibisov EV. Development of a small-size extractor for separation of the ^{99}Mo/^{99m}Tc couple. Radiochemistry. 2010;52(1):90–4.

Smith SV, Di Bartolo N, Mirzadeh S, Lambrecht RM, Knapp Jr FF, Hetherington EL. [166Dy]dysprosium/[166Ho]holmium in vivo generator. Appl Radiat Isot. 1995;46:759–64.

Soderquist CZ, McNamara BK, Fisher DR. Production of high-purity radium-223 from legacy actinium-beryllium neutron sources. Curr Radiopharm. 2012;5:244–52.

Sofou S, Kappel BJ, McDevitt MR, Scheinberg DA, Sgorous G. Enhanced retention of the alpha-particle-emitting daughters of Actinium-225 by liposome carriers. Bioconjug Chem. 2007;18:2061–7.

Sundram FX, Yu S, Somanesan S, Jeong JM, Bernal P, Osorio M, Esguerra R, Chau TCM, Long HD, Hoa NV, Huy NDS, Onkhuudai P, Lamjav T, Zanzonica P, Divgi C, Padhy AK, Martindale A, Saw MM, Rolland Y, Knapp Jr FF. Phase I study of transarterial rhenium-188 HDD lipiodol in treatment of inoperable primary hepatocellular carcinoma – a multicentre evaluation. World J Nucl Med. 2002;1:5–11.

Szucs Z, Van Rooyen J, Zeevaart JR. A possible in vivo generator 103Pd/103mRh – recoil considerations. Appl Radiat Isot. 2008;66:1346–9.

Taylor WJ, Corkill MM, Rajapaske CN. A retrospective review of yttrium-90 synovectomy in the treatment of knee arthritis. Br J Rheumatol. 1997;36:1100–5.

Teiluf K, Seidl C, Blechert B, et al. α-Radioimmunotherapy with ^{213}Bi-anti-CD38 immunoconjugates is effective in a mouse model of human multiple myeloma. Oncotarget. 2015;6(7):4692–703.

Teunissen JJ, Kwekkeboom DJ, Krenning EP. Staging and treatment of differentiated thyroid carcinoma with radiolabeled somatostatin analogs. Trends Endocrinol Metab. 2006;17:19–25.

Therapeutic Radionuclide Generators: ^{90}Sr/^{90}Y and ^{188}W/^{188}Re generators. IAEA Technical Report Series No. 470. Vienna: IAEA; 2009.

US Food and Drug Administration. Radium Ra 223 dichloride. Updated May 15 2013. www.fda.gov/Drugs/InformationOnDrugs/ApprovedDrugs/ucm352393.htm?source=govdelivery. Accessed 15 June 2014.

Vachtel VM, Vinel GV, Vylov T, Gromova II, Novgorodov AF, Norseev YV, Chumin VG, Khalkin VA. Gas-thermochromatographic method for astatine separation. Relative yield of astatine isotopes from uranium. Radiokhimiya. 1976;18:886.

Vinjamuri S, Gilbert TM, Banks M. Peptide receptor radionuclide therapy with ^{90}Y-DOTATATE/^{90}Y-DOTATOC in patients with progressive metastatic neuroendocrine tumours: assessment of response, survival and toxicity. Br J Cancer. 2013;108:1440–8.

Visser J, Brinkman GA, Bakker CNM. Production of astatine and radon isotopes by photospallation of ^{232}Th and ^{238}U. Int J Appl Radiat Isot. 1979;30:745–8.

Vuong W, Sartor O, Pal SK. Radium-223 in metastatic castration resistant prostate cancer. Asian J Androl. 2014;16:348–53.

Walker LA, Radioactive yttrium-90. A review of its properties, biological behaviour and clinical uses. Acta Radiol Ther Phys Biol. 1964;2:302–14.

Weigert O, Illidge T, Hiddemann W, Dreyling M. Recommendations for the use of yttrium-90 ibritumomab tiuxetan in malignant lymphoma. Cancer. 2006;107:686–95.

Weinberger J, Giedd KN, Simon AD, Marboe C, Knapp FF, Trichter F, Amols H. Radioactive beta-emitting solution-filled balloon treatment prevents porcine coronary restenosis. Cardiovasc Radiat Med. 1999a;1:252–6.

Weinberger J, Knapp Jr FF. Use of liquid-filled balloons for coronary irradiation. In: Waksman R, editor. Vascular brachytherapy. 2nd ed. Armonk: Futura Publishing; 1999b. p. 521–35. ISBN 0-87993-4131.

Wester DW, Steele RT, Rinehart DE, et al. Large-scale purification of ^{90}Sr from nuclear waste materials for production of ^{90}Y, a therapeutic medical radioisotope. Appl Radiat Iso. 2003;59:35–41.

Wick RR, Nekolla EA, Gaubitz M, Schulte TL. Increased risk of myeloid leukaemia in patients with ankylosing spondylitis following treatment with radium-224. Rheumatology (Oxford). 2008;47:855–9.

Winfield J, Gumpel JM. An evaluation of repeat intra-articular injections of yttrium-90 colloids in persistent synovitis of the knee. Ann Rheum Dis. 1979;38:145–7.

Wohlgemuth WA, Leissner G, Wengenmair H, Bohndorf K, Kirchhof K. Endovascular brachytherapy in the femoropopliteal segment using ^{192}Ir and ^{188}Re. Cardiovasc Intervent Radiol. 2008;31(4):698–708.

Wu C, Brechbiel MW, Gansow OA. An improved generator for the production of 213Bi from 225Ac. Radiochim Acta. 1997;79:141–4.

Wunderlich G, Hartmann H, Andreeff M, Kotzerke J. A semi-automated system for concentration of rhenium-188 for radiopharmaceutical applications. Appl Radiat Isot. 2008;66:1876–80.

Zalutsky MR, Pozzi OR. Radioimmunotherapy with alpha-particle emitting radionuclides. Q J Nucl Med Mol Imaging. 2004;48:289–96.

Zinzani PL, d'Amore F, Bombardieri E. Consensus conference: implementing treatment recommendations on yttrium-90 immunotherapy in clinical practice – report of a European workshop. Eur J Cancer. 2008;44:366–73.

Zsinka L. ^{99m}Tc sublimation generators. Radiochim Acta. 1987;41:91–6.

Zykov MP, Romanovskii VN, Wester DW, et al. Use of extraction generator for preparing a ^{99m}Tc radiopharmaceutical. Radiochemistry. 2001;43:297–300.

8 Availability of Alpha-Emitting Radioisotopes by Reactor and Accelerator Production and via Decay of Naturally Occurring Parents

8.1 Introduction

Because of the very high LET and opportunity to sterilize target cells without the potential irradiation and damage of nontarget adjacent cells which is encountered with the use of beta-emitting radioisotopes, interest in the use of alpha emitters, especially for oncology applications, has dramatically increased in the last decade. Very eloquent chemistry and innovation production strategies have provided access to adequate activity levels of many of these desired radioisotopes for the first time. Table 8.1 provides properties of representative radionuclides in various decay chains which provide alpha-emitting radioisotopes of interest for targeted alpha therapy (TAT) key information for key alpha-emitting radioisotopes of current and expected interest. Chapter 2 introduces and provides key examples of the biological strategies for targeting alpha emitters, and Chaps. 6 and 7 provide introduction to the use of both research reactors and accelerators for production of these species, and Chap. 7 discusses radionuclide generator systems which provide several alpha emitters of interest. This chapter is dedicated to a discussion of the processing and purification chemistry which are required to obtain these radioisotopes for subsequent radiolabeling and biological investigation.

8.2 Production and Processing of Alpha Emitters in the Thorium Series

8.2.1 Actinium-225

Actinium-225 ($T_{1/2} = 10.0$ days) can be obtained from decay of ^{229}Th (Fig. 8.1) and decays by emission of three alpha-particles through the ^{221}Fr (half-life, 4.8 min)/^{217} at (half-life, 32.3 ms)/^{213}Bi (half-life, 45.6 min) decay chain. There are several avenues to obtain ^{299}Th which include neutron irradiation of ^{232}Th which leads to ^{233}U, from which α-decay forms ^{229}Th, with subsequent α-decay to ^{225}Ac. Another strategy is reactor irradiation of ^{226}Ra, by multiple neutron captures and also provides ^{229Th} (see Chap. 3). Because of its very long 7340-year half-life, ^{229}Th represents a convenient source material to obtain ^{225}Ac on a regular basis by elution of the ^{229}Th/^{225}Ac generator. In addition, ^{225}Ac has been directly produced via 800 MeV high-energy irradiation of natural thorium (^{232}Th) targets (Zhuikov et al. 2012). Actinium-225 is being evaluated for in vivo therapeutic applications because of its useful half-life of 10 days and emission of multiple α-particles. In addition, the ^{225}Ac/^{213}Bi generator provides the short-lived (half-life 45 m in) ^{213}Bi alpha emitter which has been widely studied for targeted alpha therapy (see Chap. 3).

F.F. (Russ) Knapp, A. Dash, *Radiopharmaceuticals for Therapy*, DOI 10.1007/978-81-322-2607-9_8

Table 8.1 Radioactive properties of representative radionuclides in decay chains which provide alpha-emitting radioisotopes of interest for targeted alpha therapy (TAT)[a]

Radioisotope	Half-life	Decay mode	Radiation energy			Comment
			Alpha MeV	Beta MeV	Gamma keV	
Actinium radioisotopes						
Actinium-225	10 days	α	5.935 (100 %)		99.8	Parent of ^{213}Bi
Actinium-227	21.77 years	α	5.042 (1.38 %)	0.0449 (98.6 %)	100	Parent of ^{227}Th/^{223}Ra
Bismuth radioisotopes						
Bismuth-212	61 m	α, β^-	6.207 (35.9 %)	2.254 (64 %)	238, etc.	
Bismuth-213	45 m	α, β^-	5.982 (2.09 %)	1.427 (97.91 %)	440	
Lead radioisotopes						
Lead-212	10.6 h	β^-		0.574 (100 %)	0.15	Parent of ^{212}Bi
Radium radioisotopes						
Radium-223	11.43 days	α	5.979 (100 %)		269, etc.	$^{223}RaCl_2$ = Xofigo®
Radium-224	3.66 days	α	5.788 (100 %)		240, etc.	Parent of ^{212}P
Radium-226	1,600 years	α	4.870 (100 %)		186	Important target material
Thorium radioisotopes						
Thorium-227	18.65 days	α	6.146 (100 %)		236, etc.	Parent of ^{223}Ra
Thorium-228	1.912 years	α	5.520 (100 %)		216, etc.	Parent of ^{224}Ra
Thorium-229	7.34×10^3 years	α	5.187 (100 %)		193, etc.	Parent of ^{225}Ac
Thorium-232	1.405×10^{10} years	α	4.082 (100 %)		59	Parent of ^{228}Th, ^{224}Ra

[a]Data from Firestone and Ekstrom (2004)

There are several production strategies to provide ^{225}Ac from ^{226}Ra which include irradiation in a nuclear reactor where there is successive multiple neutron capture on ^{226}Ra. A mixture of ^{227}Ac, ^{228}Th, and ^{229}Th is produced (Boll et al. 1997), from which ^{229}Th can be directly obtained with a relatively high yield and ^{225}Ac can be isolated by ion exchange separation method using titanium phosphate adsorbent. Another promising production pathway is via the ^{226}Ra(p,2n)^{225}Ac proton-induced reaction using 18 MeV protons which requires repeated irradiation of ^{226}Ra. After production, ^{225}Ac requires purification on a Dowex-50 column (Geerlings et al. 1993) before use for radiolabeling or for fabrication of the ^{225}Ac/^{213}Bi generator. A more recent strategy involves the 200 MeV high-energy spallation of natural thorium targets (^{232}Th) (Weidner et al. 2012). The preliminary cross section data have suggested that multi-Curie activity levels of both ^{225}Ac and ^{223}Ra can be produced using accelerators available at both BNL and LANL. Other routes which have been proposed but evidently not yet evaluated include the use of alpha-particles for ^{229}Th production by the ^{226}Ra(^{3}He,γ)^{229}Th and ^{226}Ra(α,n)^{229}Th reactions (Mirzadeh and Garland 2010).

Production of ^{227}Ac is also possible by the $^{226}Ra + \gamma \rightarrow {}^{225}Ra + n$ photonuclear reaction. This reaction is virtually instantaneous, so that ^{225}Ra activity levels reach a maximum value after irradiation and will decrease slowly over time (Melville et al. 2006). Since there is no direct production avenue to provide ^{225}Ac from the irradiation of ^{226}Ra, the natural decay of ^{225}Ra is utilized where ^{225}Ra subsequently decays to ^{225}Ac

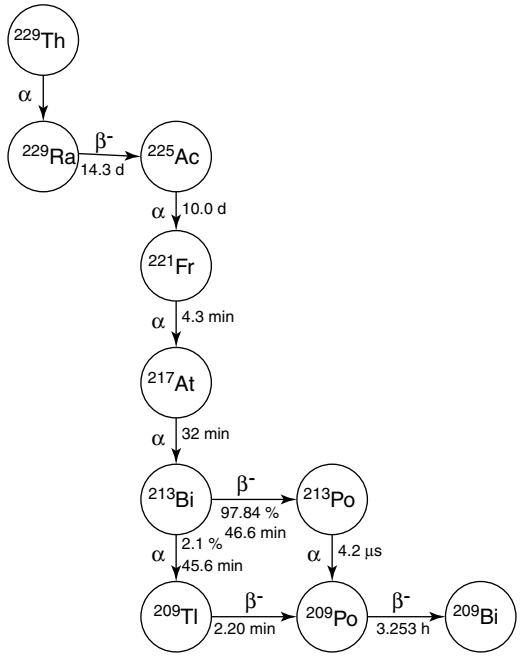

Fig. 8.1 The ^{225}Ac and ^{213}Bi decay chain. The ^{225}Ac is obtained as the decay product of ^{229}Th and decays by α-emission through ^{221}Fr, ^{217}At, and ^{213}Bi, each of which also emits an α-particle

by beta emission ($T_{1/2}$ = 14.8 days) by the ^{225}Ra $\xrightarrow{\beta}$ ^{225}Ac decay reaction.

The therapeutic use of the actinium alpha emitters provides greater cytotoxicity than use of ^{213}Bi-labeled agents since the ^{225}Ac 10.0 days half-life and emission of 4 alpha-particles from decay of ^{227}Ac, as demonstrated in the prolonged survival of mouse xenograft models for several types of experimental cancers (McDevitt et al. 2001). A major expected impediment of using ^{225}Ac for many therapeutic strategies is that the chelation binding energy is not strong enough to withstand the recoil energy released during alpha-particle emission of the actinium ion (between 100 and 200 keV). This energy usually release the ^{225}Ac from chelate stabilization sphere (Davis et al. 1999; Kennel and Mirzadeh 1998; Deal et al. 1999). In this manner, the ^{225}Ac daughter radionuclides are released from the localized site selectivity and diffuse away, causing cell damage in normal tissue (McDevitt et al. 1998; Schwartz et al. 2011). However, methods for stabilization of the ^{225}Ac to recoil release of decay products have been evaluated, and simple gold-coated nanoparticles have exhibited stability in animal studies (McLaughlin et al. 2013).

8.2.2 Actinium-227

Although not widely available, ^{227}Ac has emerged as an important radionuclide to provide the ^{227}Th and ^{223}Ra decay products, from the ^{227}Ac/^{227}Th/^{223}Ra generator system. In addition to availability from reactor irradiation of ^{226}Ra targets followed by complex radiochemical separation and purification, a more direct route involves isolation from used actinium-beryllium neutron generator sources (Soderquist et al. 2012). In this approach, following dissolution in sulfuric acid/nitric acid, an actinium fraction is separation from the soluble beryllium fraction by coprecipitation with thorium fluoride. Following anion exchange chromatography by elution with a water–methanol–nitric acid mixture, the actinium nitrate is obtained. Subsequent anion exchange column chromatography provides initial fractions of the ^{223}Ra with subsequent elution of the Ac/Th mixture for storage and reuse (Fig. 8.2).

8.2.3 Bismuth-212

Bismuth-212 ($T_{1/2}$ = 60.55 min) decays through either ^{208}Tl (36 %) or ^{212}Po (64 %) to stable ^{208}Pb (Fig. 8.3). Both decay routes involve α-particle emission with an average energy of 7.8 MeV and a path length in biological tissues from 40 to 100 μm and a β^--emission. Thallium-208 is the daughter radionuclide of ^{212}Bi and emits a 2.6-MeV gamma ray that necessitates heavy shielding in a clinical setting to minimize the radiation exposure to personnel, and for this and other reasons, research has been more focused on the use of ^{213}Bi.

Isolation of ^{212}Bi from the ^{228}Th decay chain is not a practical route because of its short 1.009 physical hour half-life. Alternatively, ^{212}B required for radiotherapy application is generally more conveniently available from a ^{224}Ra/^{212}Pb/^{212}Bi

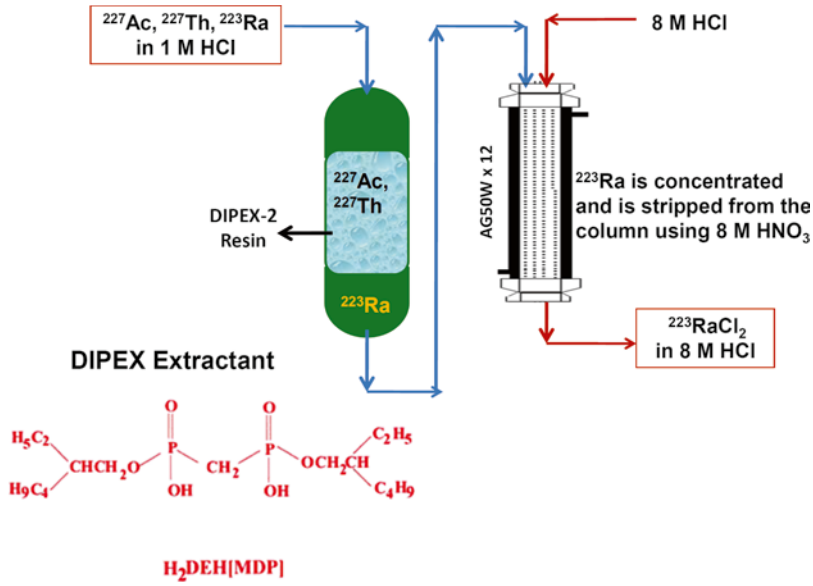

Fig. 8.2 Illustration of a generator system for isolation of ^{223}Ra from the ^{227}Ac/^{227}Th mixture

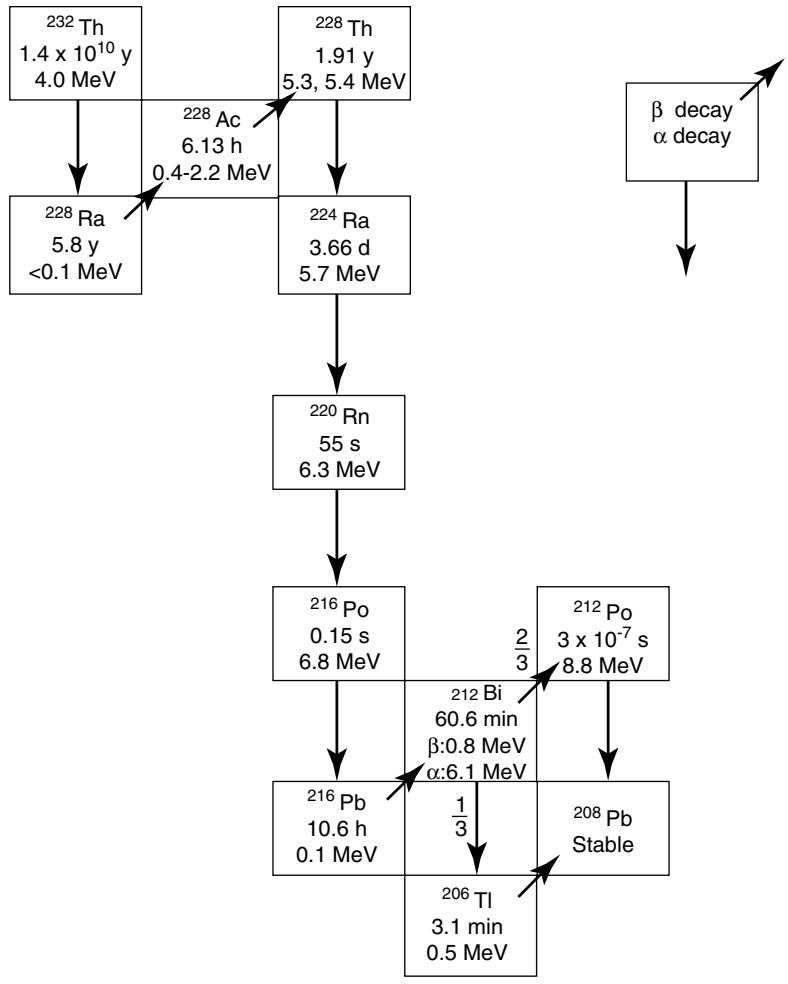

Fig. 8.3 Availability of ^{212}Bi from decay of ^{224}Ra

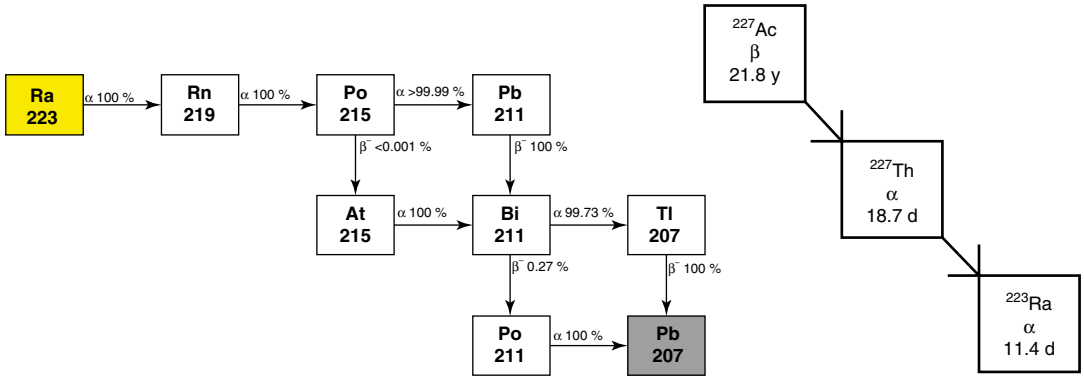

Fig. 8.4 Production and decay scheme for ^{223}Ra

generator system (Atcher et al. 1987, 1988), where it can be selectively eluted from ^{224}Ra in either the chloride form or as the tetraiodide complex (see Chap. 6). After pH adjustment, this material can be used to radiolabel monoclonal antibodies, peptides, or other targeting vectors conjugated with a suitable bifunctional chelating agent. Challenges for more widespread use of this generator system include the relatively short ^{224}Ra half-life ($T_{1/2}$ 3.6 days) which requires frequent generator recharging and the high-energy gamma emission (2.8 MeV, 99 %) from decay of ^{208}Tl ($T_{1/2}$ 3.05 m), which is formed during the ^{212}Bi/^{212}Po/^{208}Pb/^{208}Tl decay process.

8.2.4 Radium-223

Radium-223 ($T_{1/2}$ = 11.435 days) decays through the ^{219}Ra ($T_{½}$ = 3.9 s), ^{215}Po ($T_{½}$ = 1.8 ms), l^{211}Pb ($T_{½}$ = 36.1 min), ^{211}Bi ($T_{½}$ = 2.1 min), and ^{207}Tl ($T_{½}$ = 4.8 min) decay sequence (Fig. 8.4) that involves four α-emissions and two β⁻-emissions to stable ^{207}Pb. The emission of the four distinct alpha-particles accounts for more than 95 % of the released energy. While the availability of four α-emissions is an advantage from a therapeutic point of view, the complex decay scheme and α-particle emissions represent a drawback for preparation of targeted radiopharmaceuticals which will be unstable in vivo. The ^{219}Ra gaseous daughter radionuclide which is released from decay of ^{223}Ra can redistribute in the body and exhibit toxicity to normal tissues (Harrison et al. 1966; Howell et al. 1997). Because of inherent bone-seeking properties, cationic ^{223}Ra is a promising candidate for delivery of high-LET radiation to cancer cells on bone surfaces. Radium-223 can be obtained from uranium mill tailings in large quantities and more conveniently for clinical applications, from various ^{227}Ac/^{223}Ra generator systems (Boll et al. 1997; Guseva 2009). The ^{227}Ac is available by recovery from processed Be/Ac neutron sources. In addition, the production of ^{223}Ra by irradiation of natural ^{232}Th with medium-energy protons (90–135 MeV) has also been reported, and this approach is also a convenient strategy discussed earlier for ^{225}Ac production (Zhuikov et al. 2012). Beginning in 2012, this approach using 200-MeV protons has been used for ^{225}Ac production at BNL and LANL (Weidner et al. 2012).

Radium-223 chloride is a promising agent for bone pain palliation which is in advanced clinical trials (see Chap. 12). Radium-223 as ^{223}RaCl$_2$ (originally denoted as Alpharadin®; Algeta, Oslo, Norway) has completed phase III clinical evaluation and has received regulatory approval by the USA and by regulatory authorities in many other countries for routine use as a new therapeutic radiopharmaceutical (Xofigo®, Bayer) for the treatment of bone metastases in patients with hormone-refractory prostate cancer. One recent and original research approach has described the loading of ^{223}Ra into liposomes coated with folate-F(ab´)2 to target tumor cells expressing folate receptor (Henriksen et al. 2004). Since ^{223}Ra (see Chap. 3) is the decay product of ^{235}U,

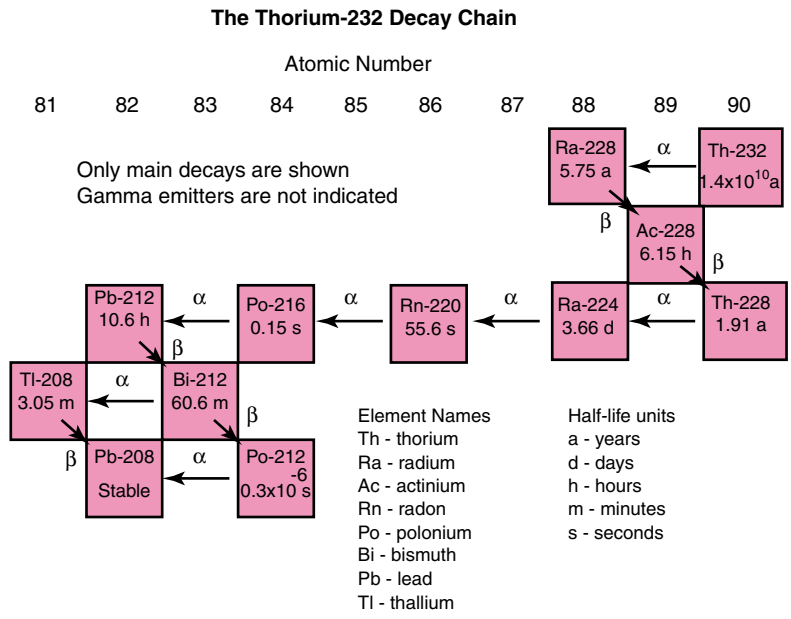

Fig. 8.5 ^{224}Ra is a member of the ^{232}Th decay series

one route to obtain ^{223}Ra is its isolation from aged samples of natural uranium. The activity levels of ^{223}Ra that can be obtained through this route are low and inadequate to meet therapeutic requirements. Another route to obtain ^{223}Ra is by neutron irradiation of ^{226}Ra in nuclear reactor. This method of production relies upon multiple neutron captures on ^{226}Ra and can be pursued at high flux reactors, such as the High Flux Isotope Reactor (HFIR) at the Oak Ridge National Laboratory (ORNL) (Van Geel et al. 1994). This method of production involves reactor irradiation of ^{226}Ra in a nuclear reactor followed by chemical isolation of the ^{227}Ac ($T_{½}$=21.8 years), which decays via ^{227}Th ($T_{½}$=18.7 days) to ^{223}Ra as described in detail in Chap. 3. The separation and purification of ^{223}Ra from the irradiated target is a complex process which requires elaborate procedures of radiochemical separation and purification as well as for radioactive waste handling. Animal experiments also demonstrated that ^{223}Ra administered at high activity doses (>185 kBq/kg) to rats exhibited significant antitumor activity in certain model systems and resulted in death secondary to hemorrhage but with lower doses (60–110 kBq/kg) was fairly tolerated (Howell et al. 1997; Durbin et al. 1958; Henriksen et al. 2004; Van Geel et al. 1994).

An attractive accelerator-based ^{223}Ra production route involves spallation by irradiation of natural ^{232}Th targets with medium-energy protons and provides ^{223}Ra in good yields and expected cost-effectiveness. Chemical isolation of Ra from the irradiated metallic Th was performed by a gas–chemical method (Zhuikov et al. 2012) or by solvent extraction with ethyl acetate (Weidner et al. 2012). An ^{227}Ac/^{223}Ra extraction generator based on selective extraction of ^{223}Ra from a solution of chlorinated cobalt dicarbollide and polyethylene glycol in a polar diluent from a solution of a mineral acid and a complexing agent has also been proposed. Radium is stripped to any appropriate aqueous solution on adding TBP into the extractant (Shishkin et al. 2011), and there are other studies also described in Chap. 8 (Soderquist et al. 2012).

8.2.5 Radium-224

Radium-224 has half-life of 3.64 days and is a decay product of ^{232}Th and decays via alpha, beta, and gamma emissions to ^{220}Rn, ^{216}Po, ^{212}Pb, ^{212}Bi, ^{212}Po, and ^{208}Th (Fig. 8.5). Thorium-232 is the most prevalent isotopic member of naturally occurring thorium and has a half-life of 1.405×10^{10} years.

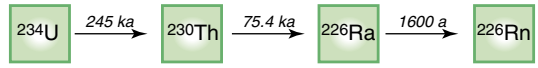

Fig. 8.6 Formation of ^{226}Ra from ^{234}U, its decay products, and examples of its subsequent pivotal target role for production of useful alpha-emitting radioisotopes

Originally denoted as "thorium X," ^{224}Ra had been widely used until the 1990s, primarily in Germany, administered as $RaCl_2$ (Drug AT 0103, or "224SpondylAT") for the palliative treatment of refractory Morbus Bechterew (Strumpell–Marie–Bechterew's disease or ankylosing spondylitis). The ^{224}Th had been the preferred therapy for this connective tissue inflammatory disease where other pain treatment options such as the use of analgesics and antiphlogistics had been unsuccessful. Since both radium and barium are members of IIA in the periodic table, radium radioisotopes are usually separated and purified based on well-established methods described for barium. The use of ^{224}Ra for this application is evidently no longer available, because of well-established side effects which overshadowed the palliative benefits. These unfortunate side effects from alpha radiation resulting from the direct intravenous administration of $^{224}RaCl_2$ are well documented in the literature and include cases of cataracts, dental resorption, growth retardation in children, lens opacification with impaired vision, myeloid leukemia, and osteosarcomas. The use of ^{224}Ra is thus now primarily focused on its use for the generator production of ^{212}Bi for targeted alpha therapy as described below.

8.2.6 Radium-226

Formed by decay of ^{234}U, the ^{226}Ra plays a pivotal role as a target for production of a variety of useful alpha-emitting radionuclides (Fig. 8.6).

8.2.7 Thorium-226

Because of its useful half-life of 30.6 minutes and emission of gamma photons (111, 131, and 242 keV), production of the ^{226}Th alpha emitter has also been evaluated by production of its carrier-free ^{230}U parent (half-life 20.8 days) via the ^{231}Pa(p,2n)^{230}Pa (β^- decay, $T_{1/2}$17.4 days)→^{230}U pathway (Morgenstern et al. 2008a, b).

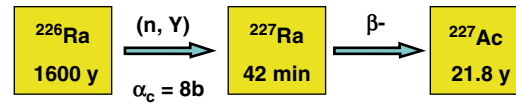

Fig. 8.7 Decay of ^{226}Ra to ^{227}Ac

8.2.8 Thorium-227

Actinium-227 (half-life 21.8 years) is formed by decay of ^{235}U (Fig. 8.7) and represents a convenient stock material which decays to the intermediary ^{227}Th (18.7 days) with subsequent alpha decay to ^{223}Ra (*vide ante*). The ^{227}Th is also of interest for targeted therapy.

8.3 Summary

Although fission product chemistry of the higher elements and their decay products have been the basis for modern radiochemistry and all the decay series and relationships have been well known for many years, the renewed interest reflects the rapidly growing interest and applications of alpha-emitting radioisotopes for therapy of different diseases. It is interesting to link the initial use of radium so many years with this new renaissance in the radiochemistry of alpha emitters. Some of the applications of alpha-emitting radioisotopes are discussed in other chapters (Chaps. 2, 3, 5, 6, 7, 12, and 16).

References

Atcher RW, Firedman AM, Hines J. Isotopic generator for bismuth-212 and lead-212 from radium, US Patent 4,663,129, May 5, 1987.

Atcher RW, Friedman AM, Hines JJ. An improved generator for the production of ^{212}Pb and ^{212}Bi from ^{224}Ra. Int J Radiat Appl Instrum A. 1988;39:283–6.

Boll RA, Mirzadeh S, Kennel SJ. Optimization of radiolabeling of immunoproteins with ^{225}Bi. Radiochimica Acta. 1997,79:145–9.

Davis IA, Glowienka KA, Boll RA, Deal KA, Brechbiel MW, Stabin M, Bochsler PN, Mirzadeh S, Kennel SJ. Comparison of ^{225}actinium chelates: tissue distribution and radiotoxicity. Nucl Med Biol. 1999;26(5):581–9.

Deal KA, Davis IA, Mirzadeh S, et al. Improved in vivo stability of actinium-225 macrocyclic complexes. J Med Chem. 1999;42(15):2988–92.

Durbin PW, Asling CW, Jeung N, et al. The metabolism and toxicity of radium-223 in rats. Berkeley: University of California Radiation Laboratory; 1958.

Firestone RB, Eksrom LP. Radioactive elements, version 2.1. LBNL, USA. http://ie.lbl.gov/toi/index.asp; 2004.

Geerlings MW, Kaspersen FM, Apostolidis C, et al. The feasibility of ^{225}Ac as a source of alpha-particles in radioimmunotherapy. Nucl Med Commun. 1993;14:121–5.

Guseva LI. A tandem generator system for production of ^{223}Ra and ^{211}Pb/^{211}Bi in DTPA solutions suitable for potential application in radiotherapy. J Radioanalyt Nucl Chem. 2009;281:577–83.

Harrison GE, Carr TE, Sutton A, et al. Plasma concentration and excretion of calcium-47, strontium-85, barium-133 and radium-223 following successive intravenous doses to a healthy man. Nature. 1966;209:526–7.

Henriksen G, Schoultz BW, Michaelsen TE, et al. Sterically stabilized liposomes as a carrier for alpha-emitting radium and actinium radionuclides. Nucl Med Biol. 2004;31:441–9.

Howell RW, Goddu SM, Narra VR, et al. Radiotoxicity of gadolinium-148 and radium-223 in mouse testes: relative biological effectiveness of alpha-particle emitters *in vivo*. Radiat Res. 1997;147:342–8.

Kennel SJ, Mirzadeh S. Vascular targeted radioimmunotherapy with ^{213}Bi–an alpha-particle emitter. Nucl Med Biol. 1998;25(3):241–6.

McDevitt MR, Sgouros G, Finn DR, et al. Radioimmunotherapy with alpha-emitting nuclides. Eur J Nucl Med. 1998;25(9):1341–51.

McDevitt MR, Ma D, Lai LT, et al. Tumor therapy with targeted atomic nanogenerators. Science. 2001;294 (5546):1537–40.

McLaughlin MF, Woodward J, Boll RA, et al. Gold coated lanthanide phosphate nanoparticles for targeted alpha therapy. PLoS One. 2013;8(1):e54531.

Melville G, Liu SF, Allen BJ. A theoretical model for the production of Ac-225 for cancer therapy by photon induced transmutation of Ra-226. J Appl Radiat Isot. 2006;64(9):979–88.

Mirzadeh S, Garland MA. US Patent 7,852,975 B2, issued Dec. 14, 2010. Production of thorium-229 using helium nuclei.

Morgenstern A, Apostolidis C, Bruchertseifer F, et al. Cross-section of the reaction ^{232}Th(p,3n)^{230}Pa for production of ^{230}U for targeted alpha therapy. Appl Radiat Isot. 2008a;66(10):1275–80.

Morgernstern A, Lebeda O, Strusa J, et al. Production of ^{230}U/^{226}Th for targeted alpha therapy via proton irradiation of ^{231}Pa. Anal Chem. 2008b;80(22):8763–70.

Schwartz J, Jaggi JS, O'Donoghue JA, et al. Renal uptake of bismuth-213 and its contribution to kidney radiation dose following administration of actinium-225-labeled antibody. Phys Med Biol. 2011;56(3): 721–33.

Shishkin DN, Krupitskii SV, Kuznetsov SA. Extraction generator of ^{223}Ra for nuclear medicine. Radiokhimiya. 2011;53(4):343–5.

Soderquist CZ, McNamara BK, Fisher DR. Production of high-purity radium-223 from legacy actinium-beryllium neutron sources. Curr Radiopharm. 2012; 5(3):244–52.

Van Geel JNC, Fuger JJ, Koch L. Method for producing actinium-225 and bismuth-213. United States Patent 5355394; 1994.

Weidner JW, Mashnik SG, John KD. ^{225}Ac and ^{223}Ra Production via 800 MeV proton irradiation of natural thorium targets. Appl Radiat Isot. 2012;70: 2590–5.

Zhuikov BL, Kalmykov SN, Ermolaev SV, et al. Production of ^{225}Ac and ^{223}Ra by irradiation of Th with accelerated protons. Radiochemistry. 2012;53(1): 73–80.

Part III

Therapeutic Radiopharmaceuticals for Cancer Therapy

Radioimmunotherapy (RIT) 9

9.1 Introduction

For the purposes of this discussion, radioisotopes are attached to antibodies for either diagnostic or therapeutic application. The use of antibodies radiolabeled with therapeutic radioisotopes is referred to as radioimmunotherapy (RIT). This technology has evolved from the spectacular advances and growth in the fields of molecular biology and biotechnological. The ability of an antibody to recognize the cognate target antigen with exquisite specificity is the genesis of RIT. In particular, the use of monoclonal antibodies (mAb) radiolabeled with therapeutic radionuclides directed against specific tumor antigens is a unique strategy for site-specific delivery of radiation directly to the tumor, and this represents the cornerstone for the success of RIT. In this context, the invention of hybridoma technology by Kohler and Milstein in 1975 merits special attention (Kohler and Milstein 1975). In 1984, they shared the Nobel Prize for Physiology and Medicine just 9 years after publishing their seminal paper on hybridoma technology. The pioneer research of Kohler and Milstein resulted for the first time in the production of rodent antibodies of single specificity (monoclonal antibodies), and this triggered the use of monoclonal antibodies as delivery vehicles for radionuclides for therapy. RIT combines the synergistic effects of both radiation and immunotherapy with manageable local and systemic side effects. The characteristic and complex interactions between the tumor, host, radionuclide, and the antigen–antibody complex determine the effectiveness of RIT.

9.2 Identification of Cell Surface Markers

The cluster of differentiation (CD) is a protocol used for the identification and investigation of cell surface molecules present on leukocytes. CD molecules can act in numerous ways, often acting as receptors or ligands (the molecule that activates a receptor) important to the cell. The CD nomenclature was proposed and established in the 1st International Workshop and Conference on Human Leukocyte Differentiation Antigens (HLDA) (Zola et al. 2005; Zola and Swart 2005). This system was intended for the classification of the many monoclonal antibodies (mAbs) generated by different laboratories around the world against epitopes on the surface molecules of leukocytes (white blood cells). Since then, its use has expanded to many other cell types, and more than 320 CD unique clusters and subclusters have been identified. The human leukocyte antigen (HLA) is expressed as cell surface molecules/antigens on various immune cells. Through flow cytometry, the CD markers or HLA molecules are identified using mAbs directed against a specific cell surface antigen. Under the current naming system, antigens that are well characterized are assigned an arbitrary number (e.g., CD1,

F.F. (Russ) Knapp, A. Dash, *Radiopharmaceuticals for Therapy*, DOI 10.1007/978-81-322-2607-9_9

CD2, etc.), whereas molecules that are recognized by just one monoclonal antibody are given the provisional designation "CDw." Physiologically, CD antigens do not belong in any particular class of molecules, with their functions ranging from cell surface receptions to adhesion molecules. Although initially used for just human leukocytes, the CD molecule naming convention has now been expanded to cover both other species (e.g., mouse) as well as other cell types. Human CD antigens are currently numbered up to CD363. Before discussing RIT in detail, it is helpful to provide a brief introductory discussion on antibodies, antigens, and lymphoma and their roles in RIT.

9.3 Antibodies

Antibodies are immune system-related proteins called immunoglobulins. A typical antibody molecule is made up of four polypeptide chains. The four chains are divided into two identical light chains and two identical heavy chains (Fig. 9.1). An antibody molecule is depicted as Y-shaped molecules with two identical antigen-binding sites at the ends of the arms of the Y. The light and heavy chains contribute to the antigen-binding sites to receptors or specific "antigens." Each antibody molecule can bind to two identical antigenic determinants. Where the arms meet, the stem of the Y is known as the hinge region. The hinge region allows segmental flexibility of the antibody molecule. The two antigen-binding ends (or amino-terminal ends) of the antibody molecule are called the Fab fragments (for fragment antigen binding), whereas the stem (or carboxyl-terminal end) of the Y is considered to be the Fc fragment (for fragment crystallizable). The Fc region of the antibody molecule is responsible for its biologic properties.

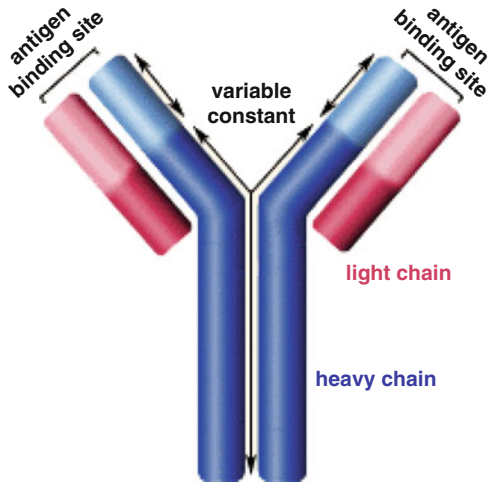

Fig. 9.1 Illustration of antibody structural components

The amino-terminal end of an antibody is called the variable, or V, region and the carboxyl-terminal end is called the constant, or C, region. The C region is about the same size as the V region in the light chain and three to four times larger than the V region in the heavy chain. The V regions of light and heavy chains form the antigen-binding sites. Light and heavy chains consist of repeating, similarly folded homology units or domains. The light chain has one V region (VL) domain and one C region (CL) domain, whereas the heavy chain has one V region (VH) and three or four C region (CH) domains. The most variable parts of the V regions are limited to several small hypervariable regions or complementarity-determining regions (CDRs). The light- and heavy-chain V regions contain three CDRs. The CDRs come together at the amino-terminal end of the antibody molecule to form the antigen-binding site, which determines specificity. The invariant regions of amino acids, between the CDRs, make up about 85 % of the V regions and are designated framework residues. The three functions which explain antibody chemical structure include binding versatility, binding specificity, and biological activity.

9.3.1 B Cells and T Cells

White blood cells (lymphocytes) play an important role in the immune response. While the production of lymphocytes is initiated in bone marrow, after maturation, these circulate through the blood and lymphatic vessels. Lymphocytes fall into the B-cell and the T-cell groups, and each cell is specific for a particular antigen which

resides in a receptor for antigen including the B-cell receptor (BCR) for antigen and the T-cell receptor (TCR), respectively. Both BCRs and TCRs are integral membrane proteins displayed on their surface and present in thousands of identical copies exposed at the cell surface, available even before the cell ever encounters an antigen and encoded by genes assembled by the recombination of segments of DNA. However, they differ in structure and the genes that encode them and the type of epitope to which they bind.

Different B cells carry different antibodies, and when a foreign organism invades through the bloodstream, it encounters B cells which express antibodies that can recognize one of the invading antigens. Subsequently, a concerted action follows involving T cells and cells which are called "phagocytes," where binding of the antigen to the B cell causes further rapid and repeated B-cell division. The resulting collection of daughter cells is called a "clone." The T cells provide several activities collectively referred to as "cellular immunity," which is an especially important capability of the body to fight against viruses and to assist B cells for antibody production. The T cells have surface membrane protein receptors which recognize and bind to specific antigens. However, this only occurs when the antigens are attached on cell surfaces. Once the T cells have bound to the antigen, they divide quickly and repeatedly to form an activated clone (Tosato et al. 1980).

9.3.2 Polyclonal and Monoclonal Antibodies

Polyclonal antibody mixtures contain different antibodies developed in the blood of immunized animals from different cell types. Polyclonal antibodies are a combination of immunoglobulin (IgG) molecules secreted against a specific antigen, each identifying a different epitope. As most antigens bear multiple epitopes, they can stimulate the proliferation and differentiation of a variety of B-cell clones. Thus, a heterogeneous pool of serum antibodies can be produced with specificity for particular epitope(s) of the antigen. Polyclonal antibodies recognize multiple epitopes on any one antigen, and the serum obtained will contain a heterogenous complex mixture of antibodies of different affinities. Polyclonals will recognize multiple epitopes on any one antigen and this process has several advantages which include high affinity, since polyclonals can assist in signal amplification from target protein with low expression level, since the target protein will bind more than one antibody molecule on the multiple epitopes. Polyclonal antibody mixtures react with multiple epitopes on the surface of the antigen and will thus be more tolerant of minor changes in the antigen, e.g., polymorphism, heterogeneity of glycosylation, or slight denaturation, than will monoclonal (homogenous) antibodies. Due to recognition of multiple epitopes, polyclonals can provide better results in IP/ChIP and will identify proteins of high homology to the immunogen protein or can be used to screen for the target protein in tissue samples from species other than that of the immunogen. This is because polyclonal antibodies are sometimes used when the nature of the antigen in an untested species is unknown. This capability also makes it important to check immunogen sequence for any cross-reactivity. Often, polyclonal antibodies are the preferred choice for detection of denatured proteins, since multiple epitopes generally provide more robust detection.

9.3.3 Monoclonal Antibodies (mAbs)

In contrast, monoclonal antibodies (mAbs or moAbs) are a mixture of homogenous antibody molecules with affinity towards a specific antigen as they are made by identical immune cells that are several copies of a same parent cell, often generated using a hybridoma by fusing a B cell with a single lineage of cells containing a definite antibody gene (Fig. 9.2).

The availability of mAb through hybridoma technology had revolutionized immunology and has had far reaching implications for a large number of technologies. Monoclonal antibodies have monovalent affinity and homogeneous, in that they bind to the same epitope which makes them effective in therapies. The mAb consists of

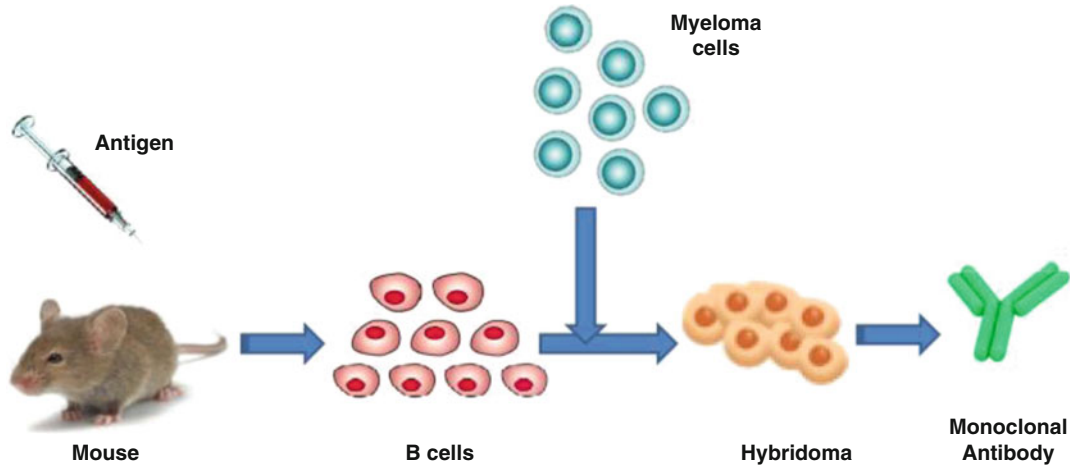

Fig. 9.2 Production of a monoclonal antibody through hybridoma fusion of a B-cell with a single lineage of cells

only one antibody subtype (e.g., IgG1, IgG2, IgG3) that has high specificity, i.e., detects only one epitope on the antigen. As they are more specifically detecting one target epitope, they are less likely to cross-react with other proteins. Compared to polyclonal antibodies, homogeneity of monoclonal antibodies is very high. Specificity of monoclonal antibodies makes them extremely efficient for binding of antigen within a mixture of related molecules. The mAbs are more vulnerable to the loss of epitope through chemical treatment of the antigen than polyclonal antibodies. The basic technique involved in making of monoclonal antibodies relies on fusion of B cells from an immunized mouse with a myeloma (tumor cell line) cell line and let the cells grow in a condition where unfused normal and tumor cells cannot survive. The cells that are fused and able to grow through this procedure are called as hybridomas. Table 9.1 illustrates the key differences between polyclonal and monoclonal antibodies.

Table 9.1 Key differences between polyclonal and monoclonal antibodies

Polyclonal antibodies	Monoclonal antibodies
Inexpensive to produce	Expensive to produce
Skills required are low	Training is required for the technology used
Time scale is short	Time scale is long for hybridomas
Produces large amounts of nonspecific antibodies	Can produce large amounts of specific antibodies
Recognizes multiple epitopes on any one antigen	Recognizes only one epitope on an antigen
Can have batch-to-batch variability	No or low batch-to-batch variability
	Once a hybridoma is made, it is a constant and renewable source

The success of RIT largely depends on the production of sufficient amounts of monoclonal antibodies which are required for therapy. Table 9.2 provides information for various key antibodies developed for RIT (Fig. 9.3).

The majority of early clinical studies using radioimmunoconjugates—where therapeutic radioisotopes are attached to antibodies discussed later in—failed to demonstrate a therapeutic impact because monoclonal antibodies of murine origin had been used which are immunogenic in humans and thus prevent repeated administration to patients. Additionally, most radioimmunotherapy approaches for the treatment of solid tumors have proven ineffective because the radiation dose delivered to neoplastic masses was insufficient to induce objective responses and cures. In more recent years, the limitation imposed by the use of monoclonal antibodies of murine origin has been circumvented by the availability and use of more refined chimeric, humanized, and fully

human antibodies that can be mass produced (Winter and Harris 1993). The use of techniques to humanize or chimarize monoclonal antibodies to decrease their murine components has been an important advance in this field. These molecules have a long vascular half-life and can interact with human complement or effector cells of the patient immune system. These molecules also behave in a manner similar to naturally occurring immunoglobulin and work along the lines of our normal antibody-based immune response as effective agents in treating patients with cancer (Dillman 2003). Table 9.3 provides information describing a variety of commercially available humanized or chimarized monoclonal antibodies and used in various clinical indications.

Table 9.2 Examples of antibodies developed for RIT

Antibody designation	Antigen designation	Type of antibody
Lym-1	HLA-DR10	Murine IgG2a
anti-B1	CD20	Murine IgG2a
2B8	CD20	Murine IgG1
C2B8	CD20	Chimeric IgG1
hLL2	CD22	Humanized IgG1
MB-1	CD37	Murine IgG1
Campath-1H	CD52	Humanized IgG

Abbreviations: *CD* acronym for the "cluster of designation", *IgG* immunoglobulin G

9.4 Antigens

An antigen is defined as "any foreign substance that elicits an immune response (e.g., the production of specific antibody molecules) when introduced into the tissues of a susceptible animal and is capable of combining with the specific antibodies formed." Antigens are generally of high molecular weight and are commonly proteins, carbohydrates, or polysaccharides, lipids, nucleic acids, or even small molecules like neurotransmitters which can act as antigens. These molecules elicit an immune response involving the production of specific antibody molecules when introduced into the tissues of a susceptible animal or human. The antigens are capable of combining with the specific antibodies which are formed. Specific antibodies can interact with

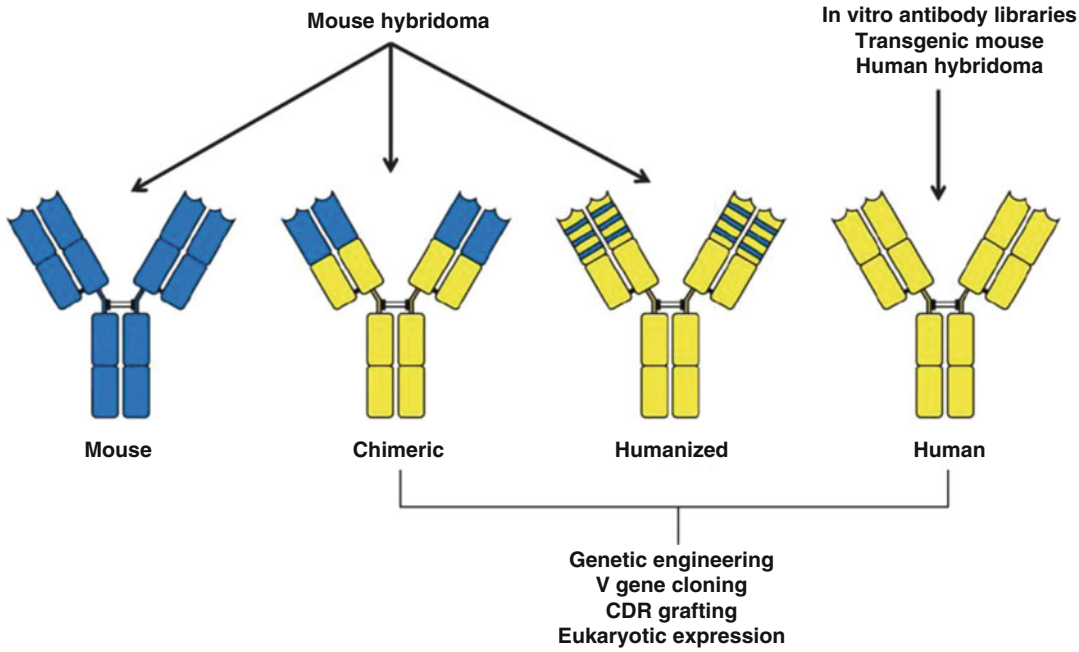

Fig. 9.3 Examples of antibody engineering strategies to obtain "humanized" antibodies

Table 9.3 Key examples of commercially available monoclonal antibodies

Monoclonal antibody	Target antigen	Clinical application
OKT3	CD3 antigens on T lymphocytes	Acute rejection of transplanted kidney, heart, and liver
Abciximab GP	IIb/IIIa on platelets	Antithrombotic applications
Rituximab	CD20 receptors on B lymphocytes	Non-Hodgkin's lymphoma
Daclizumab	Interleukin-2 receptors on activated T lymphocytes	Acute rejection of transplanted kidneys
Trastuzumab (Herceptin)	HER-2 growth factor receptors	Advanced breast carcinomas expressing HER-2 receptors
Infliximab	TNF (tumor necrosis factor)	Rheumatoid arthritis and Crohn's disease
Basiliximab	Interleukin-2 receptors on activated T lymphocytes	Acute rejection of transplanted kidney
Palivizumab	F protein of respiratory syncytial virus (RSV)	RSV infection in children
Gemtuzumab	CD33 antigen	Relapsed acute myeloid leukemia
Alemtuzumab	CD52 antigen on B and T lymphocytes	B-cell chronic lymphocytic leukemia
Cetuximab	EGFR (epidermal growth factor receptor)	Colorectal carcinoma and some other tumors

Abbreviations: *NHL* non-Hodgkin's lymphoma, *VEGF* vascular endothelial growth factor, *EGFR* epidermal growth factor receptor

only a small region of an antigen, and in the case of a polypeptide, this is generally about 5–12 amino acids. This region can be continuous or it can be distributed in different regions of a primary structure that are brought together because of the secondary or tertiary structure of the antigen. The antigen region which is recognized by an antibody is called an "epitope" and usually consists of one to six monosaccharides or 5–8 amino acid residues on the antigen surface. Because antigen molecules exist in space, the epitope recognized by an antibody may be dependent upon the presence of a specific three-dimensional antigenic conformation. This may be represented by a unique site formed by the interaction of two native protein loops or subunits. In addition, the epitope may correspond to a simple primary sequence region. The range of possible binding sites is enormous, with each potential binding site exhibiting its own structural properties derived from covalent bonds, ionic bonds, and hydrophilic and hydrophobic interactions. For efficient interaction to occur between the antigen and the antibody, the epitope must be readily available for binding. If the target molecule is denatured, e.g., through fixation, reduction, pH changes, or during preparation for gel electrophoresis, the epitope may be altered, and this may affect its ability to interact with an antibody. The epitope may be present in the antigen's native, cellular environment, or only exposed when denatured. In their natural form, they may be cytoplasmic (soluble), membrane associated, or secreted. The number, location, and size of the epitopes depend on how much of the antigen is presented during the antibody-making process.

There are a large variety of important characteristics of biologic antigens. The most striking feature of antigen–antibody interactions is the high specificity and affinity. It is accepted that almost all the antigens are identified by specific antibodies, but very few have the ability to stimulate the antibodies. Often, it is useful to illicit the formation of antibodies in response to small molecules of interest. However, in contrast to macromolecular molecules which can often illicit the formation of antibodies, small molecules cannot independently provoke an immune response and thus antibody formation. To overcome this, immunologists can attach several copies of small

molecules of interest, called "haptens," to a carrier protein prior to immunization. In this manner, the antibodies which are formed are specific to the hapten/carrier–protein complex. Each antibody binds to a particular part of the antigen called the antigenic determinant (or epitope), which is the specific site on an antigen to which the specific antibody binds. Epitopes are hence also called as antigenic determinants. The random structure on the antigenic molecule that are identified by the antibody as an antigenic binding site thus form the epitope of that antigen. The strength of the antibody–antigen binding is important, and the binding strength between an antigenic determinant in an antigen (epitope) and an antigen-binding site in an antibody (paratope) is referred to as the affinity. Different epitopes can be organized on a single protein molecule in such a manner that their spacing may affect the binding of antibody molecules in various ways. There are a variety of specific terms used in RIT which include the following.

9.4.1 Affinity

This term describes the strength of binding between one antibody-binding site and an antigenic determinant (epitope or hapten). It is the sum of the attractive and repulsive forces, which include van der Waals interactions, hydrogen bonds, salt bridges, and hydrophobic force, although the exact contribution of each of these factors depends on the particular antigen–antibody pair and the combining site of the antibody. The affinity is thus the equilibrium constant that describes the antigen–antibody reaction. The potency of the reaction between a specific antigenic determinant and its single combining site on the antibody determines its affinity. Most antibodies have a high affinity for their antigens.

9.4.2 Avidity

The strength with which a multivalent antibody binds a multivalent antigen is termed avidity, to differentiate it from the affinity of the bond between a single antigenic determinant and an individual combining site. The avidity of an antibody for its antigen is determined by the sum of all of the individual interactions taking place between individual antigen-binding sites of antibodies and determinants on the antigens. The avidity of an antibody for its antigen strongly depends on the affinities of the individual combining sites for the determinants on the antigens. It is controlled by three major factors: antibody epitope affinity, the valence of both the antigen and antibody, and the structural arrangement of the interacting parts. Avidity is more than the sum of the individual affinities.

9.4.3 Specificity

Specificity refers to the ability of an individual antibody-combining site to react with only one antigenic determinant or the ability of a population of antibody molecules to react with only one antigen. In general, there is a high degree of specificity in antigen–antibody reactions. Antibodies can distinguish differences in the primary structure of an antigen, isomeric forms of an antigen, and secondary and tertiary structure of an antigen.

9.4.4 Cross-Reactivity

This term refers to the ability of an individual antibody-combining site to react with more than one antigenic determinant or the ability of a population of antibody molecules to react with more than one antigen. Cross-reactions arise because the cross-reacting antigen shares an epitope in common with the immunizing antigen or because it has an epitope which is structurally similar to one on the immunizing antigen (multispecificity). Normally, antigen–antibody-binding site on antibodies is essentially flat and hence spacious so that they can attach large complexes or structures (Fig. 9.4).

9.5 Lymphomas

Lymphomas are malignancies of the lymphoid tissue and are broadly classified into Hodgkin's lymphoma (HD) and non-Hodgkin's

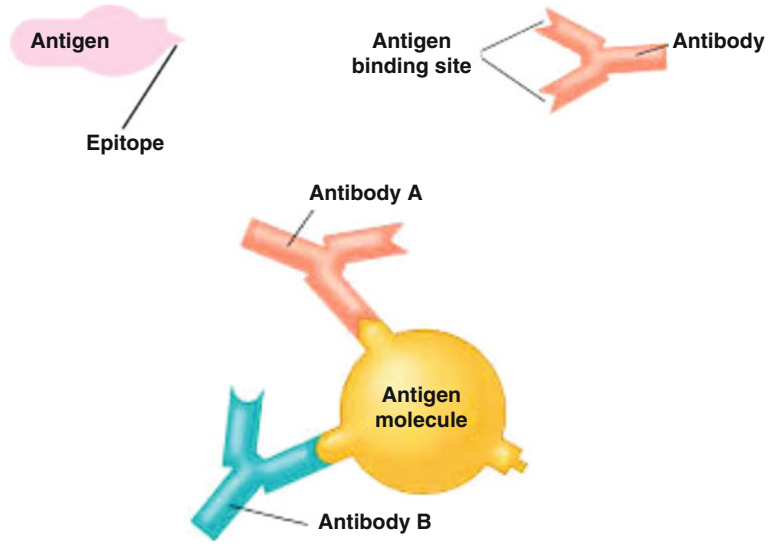

Fig. 9.4 Antibody–antigen binding depends on both specificity and avidity

lymphomas (NHL, 85 %). The hallmark of Hodgkin's lymphoma (HL) is the presence of large, mononucleated Hodgkin and multinucleated Reed/Sternberg cells. These cells represent the tumor cells, but usually comprise less than 1 % of the cellular infiltrate in the lymphoma tissue (Weiss et al. 1999). Due to the rarity of the Hodgkin and Reed/Sternberg (HRS) cells and their unusual phenotype, the origin of these cells from germinal center (GC) B cells in both the lymphocyte predominant (LP) and the classical subtype of HL has only recently been clarified (Küppers 2002). Only in very rare cases do the HRS cells of classical HL represent transformed T cells (Müschen et al. 2000; Seitz et al. 2000).

In contrast, non-Hodgkin's lymphomas are a heterogeneous group of lymphoreticular malignancies with a wide range of aggressiveness. The majority of NHL are B-cell lymphomas, with the follicular and diffuse large B-cell lymphomas constituting up to 50 % of NHL. NHL can also be classified as indolent (i.e., slow progression; 40 %) or aggressive lymphomas (60 %). B-cell CLL/small lymphocytic lymphoma, marginal zone lymphoma, lymphoplasmacytoid, and follicle center lymphoma constitute the indolent types, whereas diffuse large B-cell, mantle cell, Burkitt's, and precursor B-cell leukemia constitute the aggressive types. NHL accounts for 4 % of all malignancies and 4 % of all cancer-related deaths (Anand et al. 2008).

9.6 Radioimmunotherapy (RIT)

The preceding discussions represent the foundation required to describe the use of antibodies radiolabeled with therapeutic radioisotopes for RIT. Radioimmunotherapy (RIT) uses monoclonal antibodies as the vector for transport of the radioactivity to cancer cells (Chatal and Mahé 1998). Thus, the antibody–antigen-binding targeting mechanism and the radioisotope which decays by emission of ionizing radiation is the payload. The radiolabeled antibodies are directed against various antigens overexpressed on tumor cells or blood vessels formed during angiogenesis (Ahlskog et al. 2006; Carmeliet 2003; Folkman 1995). These radioimmunoconjugates exploit the exquisite targeting specificity of the humoral immune system to deliver lethal doses of cytotoxic radiation by the decaying radionuclides to the tumor. Although considered as one of the classic techniques, RIT has significantly progressed in the past decade due to several factors which include the large-scale availability of mAbs, humanization of mAbs,

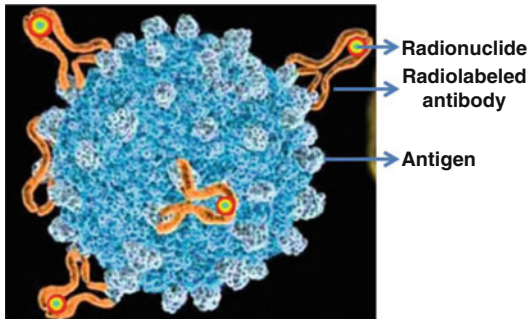

Fig. 9.5 Radiolabeled antibodies are targeted against various antigens which are overexpressed on the tumor cell surface

and development of new chelate molecules and novel-targeting techniques (Sharkey et al. 2003). This modality is primarily used for the treatment for hematopoietic malignancies which are very susceptible to radiation damage. Rapid targeting is effective for treatment of non-Hodgkin's lymphoma, which requires only low doses of radiation (~15 Gy) (Postema et al. 2001; Goldenberg 2001; Witzig 2001; White et al. 2000; Wiseman et al. 2001) (Fig. 9.5).

9.6.1 Advantages of RIT

The abundant and well-characterized cell surface antigens overexpressed on the cells in the case several major cancers offer the possibility of effective targeting in RIT. The ability to target specific antigens expressed on the surfaces of human cancer cells provides the prospect of using radiolabeled antibodies to guide the radionuclides to the tumor. In this sense, RIT provides a comprehensive route to the identification of tumor cells which generally overexpress antigens. Lymphomas are very sensitive to radiation in a dose-dependent fashion, and for this reason, they are ideal targets for RIT. The use of RIT offers the opportunity to attack not only the primary tumor cells but also lesions which are systemically metastasizing. The level of radiation that reaches the target—and thus the estimated radiation dose which will be delivered—can be accurately determined using pre-dose imaging techniques using low activity levels and therefore offers the possibility to administer higher radiation doses to the tumor site. In general, the levels of radiation to nontarget organs are predictable from imaging studies. The therapeutic effectiveness of RIT depends mainly on the radionuclide payload, rather than antibody-dependent cellular cytotoxicity and complement-dependent cytotoxicity (Kaminski et al. 1993; Trikha et al. 2002). Chapters 5, 6, and 7 describe the properties and production methods for these therapeutic radionuclides. Unlike unconjugated antibodies, radioimmunoconjugates can be effective when the host immune system is not fully functional, can destroy antigen-negative cells within tumors, and can overcome poor penetration of the antibody into tumors. The latter is possible with the use of appropriate radionuclide with required radiation penetration capability, as described in Chap. 2. This strategy thus offers the scope of treating patients who failed treatment with non-radiolabeled monoclonal antibodies. In this context, an important added advantage of radioimmunotherapy is the relevant "cross-fire effect." Since the radiation emitted from the radionuclides carried by the radioimmunoconjugate may be deposited in an area covering several cell diameters, poorly perfused or non-antigen-expressing cells within the tumor mass also could suffer the cytotoxic radiation effect (Fig. 9.6).

There are several instances when RIT is extremely valuable (Sautter-Bihl et al. 1996) and include residual micrometastatic lesions, residual tumor margins after surgical resection, tumors in the circulating blood including hematologic malignancy, and malignancies that present as free-floating cells.

9.6.2 Selection of Target Antigen

The choice of the target antigen plays a key role in determining the success of RIT. The antigen should be confined to the malignant cells for effective targeting and prevent a subpopulation of antigen-negative cells from proliferating, and for this reason, a favorable antigen expression profile is desirable for successful tumor targeting. To ensure specificity,

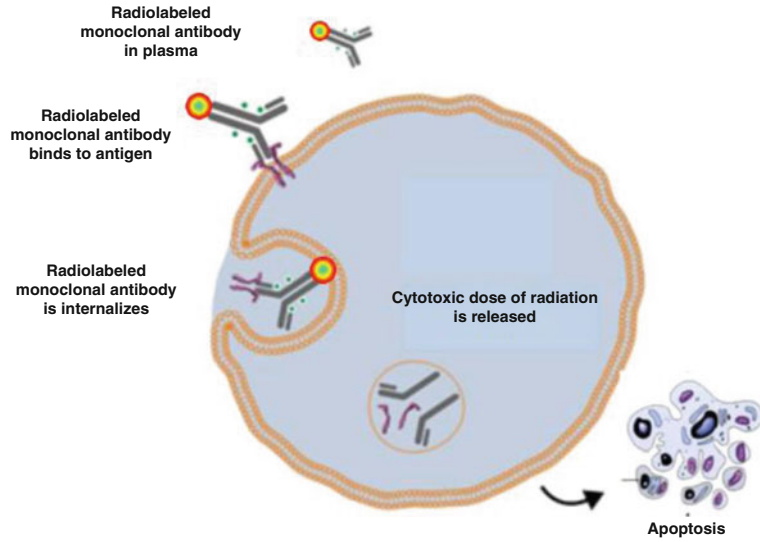

Fig. 9.6 Illustration of the primary mechanism of action of radiolabeled monoclonal antibodies for the targeted delivery of cytotoxic doses of radiation

the antigen must be overexpressed in target cells and have minimum presence in healthy cells. In terms of antigen location and binding stability, effective antibody-mediated cytotoxicity is achieved if the target antigen is not internalized or shed following antibody binding. In order to achieve effective therapy, a high density of antibody binding to the cell surface is essential, and of course antigens that shed from the cell surface and circulate in the peripheral blood at high concentration are not useful targets in these cases. Finally, the chosen antigen should not mutate in a way that would allow cancer cells to avoid destruction by the immune system. Based on the above criteria, a wide variety of antigens on cell surface have been considered as targets for a variety of tumors which fulfill such criteria to differing degrees (Caron et al. 1994; Goldenberg et al. 1981; Schlom et al. 1990) (Fig. 9.7).

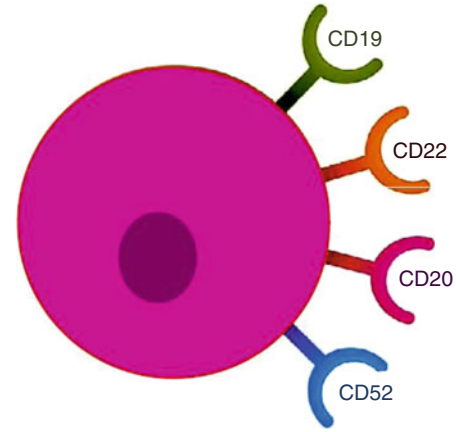

Fig. 9.7 Illustration of the expression of multiple cell surface epitopes

9.6.3 Antibody Selection

While RIT exists at the interphase of various disciplines, its success primarily depends on the selective accumulation of a cytotoxic radionuclide at the targeted site. The success of RIT therefore resides on the selection of the mAbs which must possess key features which include the ability to recognize target antigens with high affinity and specificity. The mAbs should also exhibit high binding affinity to the intended target, and binding should result in high tumor-to-background ratios. In order to be therapeutically useful, the radiolabeled antibody should have the ability to activate host effector functions such as complement-dependent cytotoxicity (CDC) and antibody-dependent cell cytotoxicity (ADCC). moAb binding of the radiolabeled antibody should induce apoptosis or inhibit survival signals in the targeted neoplastic cells. In

terms of the development of moAbs for therapy, monoclonal antibodies which are already approved for clinical immunotherapy applications are of course candidates for development of radioimmunotherapeutic conjugates, and this is indeed the strategy which has often progressed in the RIT field.

9.6.4 Selection of a Radionuclide for RIT

Selection of a radionuclide for RIT primarily focuses on the type of particle which is required, the energy of particulate emission, the physical half-life, and ability to be incorporated into the antibody either directly or through BFC agents. The choice of radionuclide (Chap. 2) is also influenced by the clinical disease, such as tumor size, physiological behavior, and tumor radiosensitivity. Radionuclides which decay with emission of beta radiation (β^-) are advantageous for RIT of solid tumors especially, owing to cost-effective availability and the "cross-fire" effect where surrounding cells not receiving sufficient antibody binding are also destroyed by radiation from adjacent targeted cells. A low abundance of low-energy gamma radiation emission is helpful for imaging and dosimetry. On the basis of in vitro cytotoxicity findings, in vivo studies, and upon theoretical dosimetry calculations, it is well established that α-emitting radionuclides (Chaps. 3 and 8) and Auger electron emitting radionuclides (Chap. 4) have the ability to treat even single tumor cells in the circulation, micrometastases, and, in certain cases, minimal residual disease (Humm 1987, 1996; Kozak et al. 1986; Zalutsky et al. 1996; Behr et al. 1998; Griffiths et al. 1999; Barendswaard et al. 2001). It has been suggested that shorter-range radionuclides are effective for the treatment of cancers, such as neoplastic meningitis and ovarian cancer (Goldsmith 2010). Characteristics of radionuclides with potential for use in radioimmunotherapy are discussed in detail in this chapter and in Chap. 10 and are summarized below in Table 9.4.

9.7 Treatment of Non-Hodgkin's B-Cell Lymphoma

As a key successful example of RIT in the clinical arena, as discussed earlier, lymphomas are malignancies of the lymphoid tissue which are broadly classified into Hodgkin's lymphoma (HD) and non-Hodgkin's lymphomas (NHL). Non-Hodgkin's lymphomas are a heterogenous group of lymphoreticular malignancies with a wide range of aggressiveness. The majority of NHL are B-cell lymphomas, with the follicular and diffused large B-cell lymphomas constituting up to 50 % of NHL (Azinovic et al. 2006). NHL provides an ideal candidate for RIT owing to its accessibility to the therapeutic antibodies as well as sensitivity to apoptosis, complement-dependent cytotoxicity (CDC), and antibody-dependent cellular cytotoxicity (ADCC)-mediated killing of cancer cells. The CD20 antigen is one of the many epitopes expressed on the mature B cells, making it a suitable target antigen for therapeutic radioactive monoclonal antibodies. CD20 is not present on stem cells and its expression does not vary at different stages of the cell cycle. Moreover, this antigen does not internalize or shed from the cell surface in response to antibody binding. By linking anti-CD20 monoclonal antibodies to an appropriate therapeutic radionuclide, disseminated disease sites can effectively be targeted (Schroff et al. 1985). Although several radionuclides have been considered for RIT, most attention has been focused on the use of iodine-131 (^{131}I) and yttrium-90 (^{90}Y). The relative advantages and disadvantages of these two radionuclides for RIT are listed in Table 9.5.

In 2002, ibritumomab tiuxetan (Zevalin®) radioimmunotherapy was approved by the US FDA for the treatment of patients with relapsed or refractory low-grade, follicular, or CD20+ transformed B-cell NHL and rituximab-refractory follicular NHL (Schroff et al. 1985). The antibody moiety of Zevalin®, ibritumomab, is a murine IgG1 kappa monoclonal antibody, targeting the same epitope on the CD20 antigen. Its chimeric counterpart is rituximab, a commercially available monoclonal antibody used for immunotherapy. Tiuxetan (1,4-methyl-benzyl

Table 9.4 Attractive radionuclides and their use in radioimmunotherapy

Key radionuclide examples	Half-life	Max range in soft tissue	Clinical use or animal model studies	Key features
β^--emitters				
^{90}Y	64.1 h	11.3 mm	^{90}Y-ibritumomab tiuxetan (Zevalin)	FDA approved for C20 positive non-Hodgkin's lymphoma
^{131}I	8.0 days	2.3 mm	^{131}I-tositumomab (Bexxar)	FDA approved for C20 positive non-Hodgkin's lymphoma
^{177}Lu	6.7 days	1.8 mm	^{177}Lu-LL1 antibody investigated in mice bearing B-cell lymphoma xenografts	Limited studies
α-emitters				
^{211}At	7.2 h	60 μm	^{211}At-Mov18 antibody investigated in mice-bearing human ovarian cancer	Limited availability
^{212}Bi	60.6 m	90 μm	^{212}Bi-B72.3 used in a murine model of human colon carcinoma	Short half-life may limit to locoregional applications
^{213}Bi	45.6 m	84 μm	^{213}Bi-HuM 195 in clinical trial for CD33 positive acute or chronic myeloid leukemia	Short half-life may limit to locoregional applications
Auger electron emitters				
^{125}I	60.2 days	<100 nm	^{125}I-A33 antibody used in phase I/II clinical trials in patients with advanced colon cancer	Long half-life may limit clinical utility
^{123}I	13.2 h	<100 nm	DNA-associated decay of ^{123}I shown to be effective at inducing DNA damage and cytotoxicity due to Auger component	Relatively high-energy γ-emission used for diagnostic imaging
^{111}In	8.0 days	<100 nm	^{111}In-anti HER2 antibodies shown to specifically induce cytotoxicity in human breast and ovarian cancer cell lines	Mainly used for imaging and dosimetry prior to therapeutic administration of Zevalin®

isothiocyanate diethylenetriamine pentaacetic acid, MX-DTPA), a modified chelator, is covalently bound to ibritumomab which allows chelating ^{111}In for imaging as well as ^{90}Y for therapy. In 2003, Bexxar®, a monoclonal antibody (tositumomab) labeled with ^{131}I, was approved by the US FDA for the treatment of CD20 positive, follicular NHL refractory to rituximab and has relapsed following chemotherapy. Tositumomab is a mouse monoclonal antibody and hence could result in HAMA response on repeated use. Iodine-131 is incorporated into antibodies by direct iodination of tyrosine residues. RIT with ^{131}I-tositumomab or ^{90}Y-ibritumomab tiuxetan has been reported to be an effective treatment option for patients with relapsed or refractory indolent B-cell NHL. Comparisons of their properties along with treatment details are elaborated in Table 9.6 (Michel et al. 2005; Goldenberg and Sharkey 2006). In a very insightful article, the diminished use of these agents in relation to the well-established patient benefit has even been reported in the main stream press (Berenson 2007).

Several other major cancers other than NHL are being targeted to be treated with radiolabeled monoclonal antibodies. Table 9.7 summarizes examples of many radiolabeled moAbs which have been used or RIT of cancer reported in this century (Kawashima 2014).

Table 9.5 Advantages and disadvantages of iodine-131 and yttrium-90 for RIT

Radionuclide	Advantages	Disadvantages
Iodine-131	Relatively inexpensive and readily available The gamma component makes it amenable to imaging using conventional gamma cameras	The long path length of the gamma component can result in increased exposure to hospital staff during treatment administration and follow-up Retention of radionuclide in the tumor is lower due to dehalogenation and release of the iodine from the targeted antibody ^{131}I that detaches from the antibody is typically taken up into the thyroid gland, and such accumulation could potentially lead to hypothyroidism as a late effect of treatment Large variability among patients in radionuclide excretion, thus requiring dosimetry for customized patient dosing
Yttrium-90	The beta emission from ^{90}Y has a longer path length than that of ^{131}I, which is advantageous in tumors with heterogeneous antibody distribution as it permits radiation to a larger area Since ^{90}Y has no gamma component, shielding of hospital personnel or using high patient doses are easily managed and do not require hospital stay after administration	Direct attachment to the antibody is not feasible; therefore, a bifunctional chelating agent is first attached to the antibody The lack of a gamma component requires bremsstrahlung imaging or the use of a surrogate radioisotope if an imaging component is desired. Typically, ^{111}In is used since binding to the targeting antibody conjugate is similar to that of ^{90}Y If freed from the chelated mAb, $^{90}Y^{+3}$ accumulates in bone, thereby increasing radiation to the marrow Requires on-site availability of a ^{90}Sr/^{90}Y generator. Relatively expensive and not widely available

9.8 Summary

Radioimmunotherapy (RIT) has emerged as one of the most promising therapeutic strategies for the treatment and management of hematologic malignancies and affords patients often with a high chance of achieving a potentially durable remission. Recent advances in radiochemistry, antibody technology, genetic engineering, and radiobiology provide important tools for RIT. An important RIT landmark was the FDA approval of radiolabeled anti-CD20 mAbs ^{90}Y-labeled ibritumomab tiuxetan (Zevalin®; Cell Therapeutics, Inc., Seattle, USA) and ^{131}I-labeled tositumomab (Bexxar®; GlaxoSmithKline LLC, Delaware, USA), although only Zevalin® is currently used in the USA for the treatment of relapsed or refractory low-grade B-cell non-Hodgkin's lymphoma and Bexxar® is evidently no longer available. In terms of use in the myeloablative setting, available data are encouraging, and phase III studies with Zevalin® are in progress. Although the exact role of such agents is still being established, newer radioimmunoconjugates are under development. Although dose-limiting toxicity of RIT is hematological, depending on bone marrow involvement and prior treatment, non-hematological toxicity is generally low. Reported studies are assessing innovative RIT protocols or new indications, in particular treatment in patients with aggressive lymphomas. High-dose treatment, RIT as consolidation after different therapeutic induction modalities, RIT in first-line treatment, or fractionated RIT showed promising results. RIT is coming of age at a time when molecular medicine is becoming a reality. New mAbs, in particular humanized mAbs, or combinations of naked and radiolabeled mAbs, by themselves, are finding their place in cancer therapy, as are small molecules that modulate a variety of processes, from cell surface receptor expression to intracellular enzyme activity. Personalized dosimetry protocols should be developed to determine injected activity.

Table 9.6 Comparison of Zevalin® and Bexxar®

Properties	Zevalin®	Bexxar®
Radioisotope	^{90}Y	^{131}I
Type of radiation	β^-	β^- and γ
Max beta energy (mean)	2.29 MeV (0.9 MeV)	0.6 MeV (0.19 MeV)
Path length in soft tissue	0.8 mm	5.3 mm
Isotope half-life	64 h	8 days
Source of radionuclide	$^{90}Sr/^{90}Y$ generator	Reactor production
Availability of radionuclide	Limited	Widely
Antibody	Murine IgG-1 kappa antibody to CD^{20+}	Murine IgG2a lambda antibody to CD^{20+}
Ease of labeling	More complex	Ease
Pre-infusion antibody	Chimeric (rituximab)	Murine (tositumomab)
Pre-infusion dose	250 mg of rituximab	450 mg of tositumomab
Tracer imaging	5 mCi of ^{111}In	5 mCi of ^{131}I
Clearance	Urinary	Urinary, more rapidly
Purpose of diagnostic scan using tracer	1–2 scans to visually assess distribution	3 scans to determine clearance and determine therapeutic dose
Therapeutic dose	0.4 mCi/kg (maximum of 32 mCi)	Dose to deliver 75 cGy to total body dose
Critical organ	Spleen, testes	Thyroid
Dose determination	Fixed based on weight and platelets (0.4 or 0.3 mCi/kg)	Clearance rate/dosimetry based to deliver 75 or 65 cGy total body dose
Pre-therapy preparation	Antihistamines/NSAID	Additional thyroid blocking
Hematological toxicity	Predominant toxicity	Predominant toxicity, less severe than Zevalin
Other unique toxicities	Dehalogenation in liver and effect on marrow	Hypothyroidism
Radiation precautions	Universal for 1 week	Additional precautions for gamma radiation
Therapy setting	Outpatient	Majority outpatient

Table 9.7 Examples of radiolabeled anticancer agents for RIT

Cancer	Target molecule	mAb	Radioisotope	Subject
Direct radiolabeling methods[a]				
Non-Hodgkin's lymphoma	CD20	Ibritumomab	Y-90	Human (in clinical use)
		Tositumomab	I-131	Human (in clinical use)
		Rituximab	I-131	Human (phase II)
	CD22	Epratuzumab	Y-90	Human (phase II)
Myeloid leukemia	CD33	Lintuzumab	Bi-213	Human (phase II)
Raji B lymphoma	CD74	L243	Ga-67	Cell
Colorectal cancer	Carcinoembryonic antigen (CEA)	cT84.66	Y-90	Human (phase I)
	A33 glycoprotein	huA33	At-211	Mouse xenograft model
Colorectal cancer (liver metastases)	CEA	F6 $F(ab')_2$	I-131	Human (phase II)
	CEA-related cell adhesion molecule	Labetuzumab	I-131	Human (phase II)
Gastrointestinal cancer	CEA	A5B7	I-131	Human (phase I)

(continued)

Table 9.7 (continued)

Cancer	Target molecule	mAb	Radioisotope	Subject
Breast cancer	HER-2	Trastuzumab	Y-90	Mouse xenograft model
			Pb-212	Human (phase I)
		NLS-trastuzumab	In-111	Cell
Ovarian cancer	Na-dependent phosphate transporter	MX35 $F(ab')_2$	At-211	Human (phase I)
Prostate cancer	MUC-1	m170	Y-90	Human (phase I)
		J591	Y-90	Human (phase I)
			Lu-177	Human (phase I)
			Bi-213	Mouse xenograft model
Multiple myeloma	CD138	Anti CD138 Ab	Bi-213	Mouse xenograft model
Indirect radiolabeling methods[a]				
Non-Hodgkin's lymphoma	CD20	TF4 (HSG)	Y-90	Mouse xenograft model
		1 $F5(scFv)_4$ (streptavidin)	Y-90	Mouse xenograft model
	CD20, CD22, HLA-DR	Corresponding Abs (streptavidin)	Y-90	Mouse xenograft model
Colon cancer	CEA	hBS14 (HSG)	Y-90	Mouse xenograft model
		MN14 (MORF)	Re-188	Mouse xenograft model
	Ep-CAM	NR-LU-10 (HSG)	Y-90	Human (phase II)
Gastrointestinal cancer	TAG-72	CC49-$(scFv)_4$ (streptavidin)	Y-90	Human (phase I)
Glioma	Tenascin	BC4 (biotin)	Y-90	Human (phase II)

[a]Direct radiolabeling refers to methods used to attach the radioisotope directly to the antibody macromolecule. For indirect radiolabeling, the radioisotope is attached to another chemical moiety which is attached to the antibody

References

Ahlskog J, Paganelli G, Neri D. Vascular tumor targeting. Q J Nucl Med Mol Imaging. 2006;50:296–309.

Anand P, Kunnumakara AB, Sundaram C. Cancer is a preventable disease that requires major lifestyle changes. Pharm Res. 2008;25(9):2097–116.

Azinovic I, DeNardo GL, Lamborn KR, et al. Survival benefit associated with human anti-mouse antibody (HAMA) in patients with B-cell malignancies. Cancer Immunol Immunother. 2006;55:1451–8.

Barendswaard EC, Humm JL, O'Donoghue JA. Therapeutic efficacy of ^{125}I- and ^{131}I-labeled monoclonal antibody A33 in a human colon cancer xenograft. J Nucl Med. 2001;42:1251–6.

Baxevanis CN, Perez SA, Papamichail M. Cancer immunotherapy. Crit Rev Clin Lab Sci. 2009;46(4):167–89.

Behr TM, Sgouros G, Vougiokas V, et al. Therapeutic efficacy and dose limiting toxicity of Auger-electron versus beta emitters in radioimmunotherapy with internalizing antibodies: evaluation of ^{125}I-versus ^{131}I-labeled CO17-1A in a human colorectal cancer model. Int J Cancer. 1998;76:738–48.

Berenson A. Market forces cited in lymphoma drugs' Disuse. New York Times, 14 Jul 2007.

Carmeliet P. Angiogenesis in health and disease. Nat Med. 2003;9:653–60.

Caron PC, Schwartz MA, Co MS. Murine and humanized constructs of monoclonal antibody M195 (anti-CD33) for the therapy of acute myelogenous leukemia. Cancer. 1994;73:1049–56.

Chatal JF, Mahé M. Therapeutic use of radiolabelled antibodies. In: Murray IPC, Ell PJ, editors. Nuclear medicine in clinical diagnosis and treatment. Edinburgh: Churchill Livingstone; 1998. p. 1101–14.

Dillman RD. Monoclonal antibody therapy. In: Oldman RK, editor. Principles of cancer biotherapy. 4th ed. Norwell: Kluwer Academic Publishers; 2003. p. 329–90.

Folkman J. Angiogenesis in cancer, vascular, rheumatoid and other disease. Nat Med. 1995;1:27–31.

Goldenberg DM. The role of radiolabeled antibodies in the treatment of non-Hodgkin's lymphoma: the

coming of age of radioimmunotherapy. Crit Rev Oncol Hematol. 2001;39:195–201.
Goldenberg DM, Sharkey RM. Advances in cancer therapy with radiolabeled monoclonal antibodies. Q J Nucl Med Mol Imaging. 2006;50:248–64.
Goldenberg DM, Gaffar SA, Bennett SJ, et al. Experimental radioimmunotherapy of a xenografted human colonic tumor (GW-39) producing carcinoembryonic antigen. Cancer Res. 1981;41:4354–60.
Goldsmith SJ. Radioimmunotherapy of lymphoma: Bexxar and Zevalin. Semin Nucl Med. 2010;40:122–35.
Griffiths GL, Govindan SV, Sgouros G, et al. Cytotoxicity with auger electron- emitting radionuclides delivered by antibodies. Int J Cancer. 1999;81:985–92.
Humm JL. A microdosimetric model of astatine-211 labeled antibodies for radioimmunotherapy. Int J Radiat Oncol Biol Phys. 1987;13:1767–73.
Humm JL. Problems and advances in the dosimetry of radionuclide targeted therapy. In: Bihl S, Luise M, Bihl H, Wannenmacher M, editors. Systemic radiotherapy with monoclonal antibodies, options and problems. Berlin/Heidelberg/Germany: Springer; 1996. p. 37–66.
Kaminski MS, Zasadny KR, Francis IR, et al. Radioimmunotherapy of B-cell lymphoma with [^{131}I]anti-B1 (anti-CD20) antibody. N Engl J Med. 1993;329:459–65.
Kawashima H. Radioimmunotherapy: a specific treatment protocol for cancer by cytotoxic radioisotopes conjugated to antibodies. Scientific World Journal. 2014;49:2061.
King J, Waxman J, Stauss H. Advances in tumour immunotherapy. QJM. 2008;101(9):675–83.
Kohler G, Milstein C. Continuous cultures of fused cells secreting antibody of predefined specificity. Nature. 1975;256:495–7.
Kozak RW, Atcher RW, Gansow OA. Bismuth-212-labeled anti-TAC monoclonal antibody: alpha-particle-emitting radionuclides as modalities for radioimmunotherapy. Proc Natl Acad Sci. 1986;83:474–8.
Krüger C, Greten TF, Korangy F. Immune based therapies in cancer. Histol Histopathol. 2007;22(6):687–96.
Küppers R. Molecular biology of Hodgkin's lymphoma. Adv Cancer Res. 2002;44:277–312.
Matzku S, Zöller M. Specific immunotherapy of cancer in elderly patients. Drugs Aging. 2001;18(9):639–64.
Michel RB, Andrews PM, Rosario AV, et al. ^{177}Lu-antibody conjugates for single-cell kill of B-lymphoma cells in vitro and for therapy of micrometastases in vivo. Nucl Med Biol. 2005;32:269–78.
Müschen M, Rajewsky K, Bräuninger A, et al. Rare occurrence of classical Hodgkin's disease as a T cell lymphoma. J Exp Med. 2000;191:387–94.
Postema EJ, Boerman OC, Oyen WJ, et al. Radioimmunotherapy of B-cell non-Hodgkin's lymphoma. Eur J Nucl Med. 2001;28:1725–35.
Sautter-Bihl ML, Herbold G, Bihl H. Minimal residual disease: a target for radioimmunotherapy with ^{131}I-labeled monoclonal antibodies? Some dosimetric considerations. Recent Results Cancer Res. 1996;141:67–75.
Schlom J, Colcher D, Siler K, et al. Tumor targeting with monoclonal antibody B72.3: experimental and clinical results. Cancer Treat Res. 1990;51:313–35.
Schroff RW, Foon KA, Beatty SM, et al. Human antimurine immunoglobulin responses in patients receiving MoAb therapy. Cancer Res. 1985;45:879–85.
Scott AM, Wolchok JD, Old LJ. Antibody therapy of cancer. Nat Rev Cancer. 2012;12:278–87.
Seitz V, Hummel M, Marafioti T, et al. Detection of clonal T-cell receptor gamma-chain gene rearrangements in Reed-Sternberg cells of classic Hodgkin disease. Blood. 2000;95:3020–4.
Sharkey RM, Brenner A, Burton J, et al. Radioimmunotherapy of non-Hodgkin's lymphoma with ^{90}Y-DOTA humanized anti-CD22 IgG (^{90}Y-Epratuzumab): do tumor targeting and dosimetry predict therapeutic response? J Nucl Med. 2003;44:2000–18.
Tosato G, Magrath IT, Koski IR, et al. B cell differentiation and immunoregulatory T cell function in human cord blood lymphocytes. J Clin Invest. 1980;66(2):383–8.
Trikha M, Yan L, Nakada MT. Monoclonal antibodies as therapeutics in oncology. Curr Opin Biotechnol. 2002;13:609–14.
Weiner LM, Surana R, Wang S. Monoclonal antibodies: versatile platforms for cancer immunotherapy. Nat Rev Immunol. 2010;10:317–27.
Weiss LM, Chan JKC, MacLennan K, et al. Pathology of classical Hodgkin's disease. In: Mauch PM, Armitage JO, Diehl V, Hoppe RT, Weiss LM, editors. Hodgkin's disease. Philadelphia: Lippincott Williams & Wilkins; 1999. p. 101–20.
White CA, Berlfein JR, Grillo-Lopez AJ. Antibody-targeted immunotherapy for treatment of non-Hodgkin's lymphoma. Curr Pharm Biotechnol. 2000;1:303–12.
Winter G, Harris WJ. Humanized antibodies. Trends Pharmacol Sci. 1993;14:139–43.
Wiseman GA, White CA, Sparks RB. Biodistribution and dosimetry results from a phase III prospectively randomized controlled trial of Zevalin radioimmunotherapy for low-grade, follicular, or transformed B-cell non-Hodgkin's lymphoma. Crit Rev Oncol Hematol. 2001;39:181–94.
Witzig TE. Radioimmunotherapy for patients with relapsed B-cell non- Hodgkin lymphoma. Cancer Chemother Pharmacol. 2001;48:91S–5.
Zalutsky MR, Schuster JM, Garg PK, et al. Two approaches for enhancing radioimmunotherapy: a emitters and hyperthermia. In: Bihl SML, Bihl H, Wannenmacher M, editors. Systemic radiotherapy with monoclonal antibodies, options and problems. Berlin/Heidelberg/Germany: Springer; 1996. p. 101–22.
Zola H, Swart B. The human leucocyte differentiation antigens (HLDA) workshops: the evolving role of antibodies in research, diagnosis and therapy. Cell Res. 2005;15:691–4.
Zola H, Swart B, Nicholson I, et al. CD molecules 2005: human cell differentiation molecules. Blood. 2005;106(9):3123–6.

Peptide Receptor Radionuclide Therapy (PRRT)

10

10.1 Introduction

Peptides are usually classified as containing less than 50 amino acid residues (~5500 Da) and consist of any combination of amino acids linked by peptide bonds. Many tumors overexpress specific cell-surface receptors which allow the development of therapeutic peptides which can target these cells for treatment of a wide variety of cancers. Among the different peptides used for tumor targeting, somatostatin analogs (SST) have attracted unprecedented attention as a treatment modality for patients with inoperable or metastasized endocrine gastroenteropancreatic (GEP) tumors (Okarvi 2004; Heppeler et al. 2000; Van Den Bossche and Van de Wiele 2004), discussed later in this chapter in Sect. 10.3.2. The breadth of research on targeted peptides is very broad and has, in particular, evolved into a key clinical specialty in nuclear medicine and oncology for targeted tumor therapy. Table 10.1 illustrates examples of a variety of radiolabeled peptides which have been evaluated for cancer cell targeting, many of which have entered the clinical arena.

10.2 Amino Acids, Peptides, and Proteins

10.2.1 Amino Acids

The role of amino acids (Fig. 10.1) in the evolution of biological diversity is well established, and these biomolecules play a pivotal role as building blocks for a vast array of molecular signaling, signal transduction, and recognition of transformation peptide and protein units. The ability of these molecules to perform as neurotransmitters offers a pool of precursors for neurotransmitters, for instance, exemplified by the adrenergic, dopaminergic, and serotonergic systems. When assembled into small peptides, amino acids can generate a variety of hormones, releasing factors, neurotransmitters, and neuromodulators. Larger constructs of amino acids comprise molecular recognition systems such as immunoglobulins and receptors. On the other hand, assembly into enzymes provides catalyzing nearly the entire spectrum of bioorganic reactions occurring in living systems.

F.F. (Russ) Knapp, A. Dash, *Radiopharmaceuticals for Therapy*, DOI 10.1007/978-81-322-2607-9_10

Table 10.1 Key examples of regulatory peptides and their receptors overexpressed on tumors

Peptide	Number of amino acid residues	Receptor types/subtypes	Tumor expression
α-MSH	13	α-MSH-R	Melanomas
Bombesin/GRP	14	BB1 (NMB-R), BB2 (GRP-R), BB3, BB4	Prostate, breast, pancreas, gastric, colorectal, small-cell lung cancer
CCK/gastrin	17 or 34	CCK1, CCK2	Medullary thyroid cancer, small-cell lung cancer, gastrointestinal stromal tumor, stromal ovarian cancer, astrocytomas
LHRH	10	LHRH-R	Prostate, breast cancer
Neurotensin	13	NTR1, NTR2, NTR3	Small-cell lung cancer, colon, exocrine ductal pancreatic cancer, Ewing sarcoma, meningioma, astrocytoma, breast, prostate cancer
RGD		αvβ3-integrin	Glioma, breast, prostate cancer
Somatostatin	14 or 28	SST1, SST2, SST3, SST4, SST5	Neuroendocrine tumors lymphoma, paraganglioma, carcinoids, breast, brain, renal, small-cell lung cancer, medullary thyroid cancer
Substance P	11	NK1, NK2, NK3	Glial tumors (glioblastoma, medullary thyroid cancer), pancreas, breast, small-cell lung cancer
VIP	28	VPAC1, VPAC2	Adenocarcinomas of breast, prostate, stomach, and liver; neuroendocrine tumors

GRP gastrin-releasing peptide, *VIP* vasoactive intestinal peptide, *CCK* cholecystokinin, *α-MSH* α-melanocyte-stimulating hormone, *LHRH* luteinizing hormone-releasing hormone

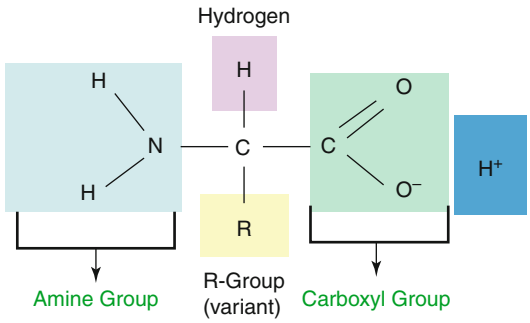

Fig. 10.1 Basic amino acid structure

10.2.2 Peptides and Proteins

Proteins are large macromolecules (Fig. 10.2) consisting of polymerized amino acid units connected by amide bonding and are essential to determine the structure as well as to perform most functions in living cells including structural components, enzyme catalysts, and other functions. There are about 20 different amino acids in nature which are assembled in chains of varying lengths to form proteins. The order of amino acids (primary structure) determines the structure and function of the protein. In contrast, peptides are much smaller molecules consisting of two or more amino acids linked together by amide (peptide) bonds in which the amino acid amine and carboxylic acid functional groups join together to form amide bonds of the peptide. Peptide thus consists of short- or medium-length-chain building blocks of amino acids. The size of peptides can roughly vary from molecules with only two amino acids to as many as 50.

The different amino acids and the order in which they are joined together by peptide bonds in a peptide or protein are referred to as the primary structure. In addition to dramatic differences in molecular size, proteins and peptides also differ in other ways, since proteins consist of only 20 different amino acids, while in peptides these 20 "protein" amino acids are found as well as other naturally available amino acids. Peptides are basically small proteins, having molecular weights less than 5,000 and do not possess a

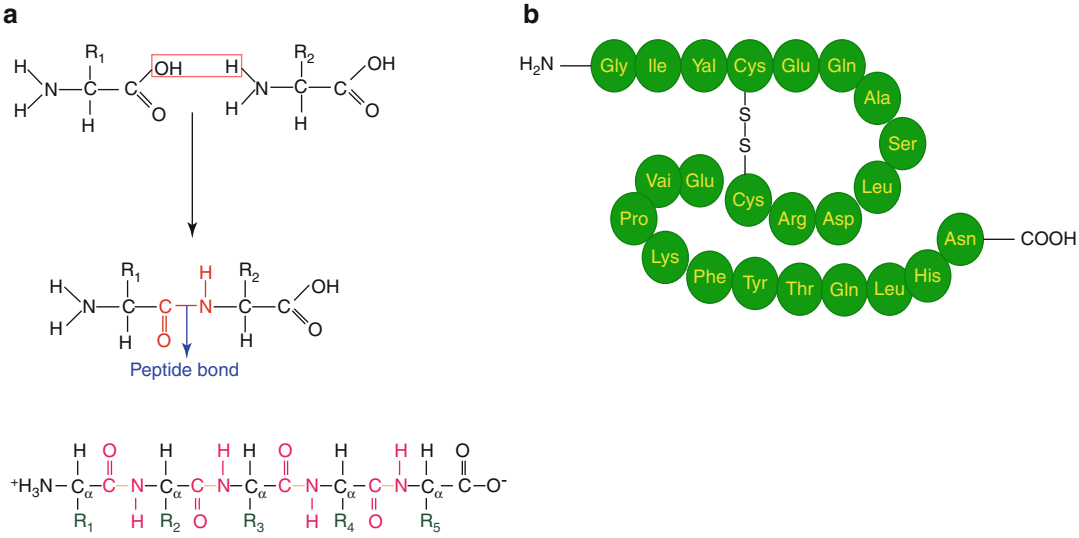

Fig. 10.2 (**a**) Condensation of amino acids to form the amide bond, and (**b**) primary polyamino protein structure illustrating disulfide bonding

well-defined three-dimensional (tertiary) structure. On the other hand, proteins are typically much larger, with folded chains which have biological significance. As a result of this difference in size, proteins and peptides are also different in the types of three-dimensional structures and functionalities that they possess. In contrast to proteins, peptides generally do not possess a well-defined three-dimensional (tertiary) structure. Peptides not only exist in natural form but also can be prepared synthetically.

10.2.3 Regulatory Peptides

Peptides regulate most physiological processes, acting at some sites as endocrine or paracrine signals and at others as neurotransmitters or growth factors. Peptides that are primarily synthesized in the brain, especially in neurons, are called "neuropeptides" and function either directly or indirectly to modulate synaptic activity. In addition, "neuropeptides" may also function as primary neurotransmitters. Peptides are found and have important biological significance throughout the body, which includes the gut, lymphatic tissue, endocrine system, and many other tissues. The heterogeneous peptide hormones produced by the gastrointestinal tract control digestion and are secreted from cells that line the lumen of the gut, which include the mucosa as well as in endocrine organs such as the pancreas. Gut hormones also regulate cell growth, but in some instances, well-recognized peptides such as substance P and pancreatic polypeptide are recognized as gut hormones, but their function is still uncertain. However, these peptides can be secreted by endocrine tumor cells and may be responsible for some systemic manifestations. In general terms, regulatory peptides represent a group of different families of molecules known to act on multiple targets in the human body at extremely low concentrations.

Biologically active peptides are the products of genes, and their targets are proteins or protein-coupled receptors. These naturally occurring peptides play a regulatory role in the body and generally mediate their function through specific binding to receptors, such as the transmembrane G-protein-coupled receptors. Peptide-receptor binding to this protein can activate or inhibit biological processes via different mechanisms, including activation of G-proteins, tyrosine kinases, or transcription processes. Importantly for therapeutic radiopharmaceutical targeting, many of these receptors have been shown to be

Table 10.2 Examples of key regulatory peptides in PRRT

Abbreviation	Name	Biological effects
α-MSH	α-Melanocyte-stimulating hormone	Melanogenesis
ANF	Atrial natriuretic factor	Natriuresis, vasodilation
AT	Angiotensin	Vasoconstriction
BN	Bombesin/gastrin-releasing peptide	Gut hormone release
BK	Bradykinin	Vasodilation, hypotension
CCK	Cholecystokinin	Gallbladder contraction, exocrine pancreatic secretion
CT	Calcitonin	Calcium homeostasis
GAL	Galanin	Gastrointestinal immotility
LHRH	Luteinizing hormone-releasing hormone	LH and FSH stimulation
NPY	Neuropeptide Y	Induction of food intake, inhibition of anxiety
NT	Neurotensin	Vasoconstriction, raise in vascular permeability
SEC	Secretin	Pancreatic $NaHCO_3$ secretion
SST	Somatostatin	Inhibition of hormone and exocrine secretion
SP	Substance P	Hypotension, salivary secretion
VP	Vasopressin	Vasoconstriction, antidiuresis
VIP	Vasoactive intestinal peptide	Vasodilation, water and electrolyte secretion in the gut

significantly overexpressed in certain diseases and especially in particular tumor types. The targeting of these overexpressed receptors in various tumors has thus generated tremendous interest in the development of specific peptides for diagnosis as well as therapy. A number of tumor receptors such as somatostatin (SST), integrin, gastrin-releasing peptide (GRP), cholecystokinin (CCK), R-melanocyte-stimulating hormone (R-MSH), and glucagon-like peptide-1 (GLP-1) receptors have been identified, and application of radioactive specific regulatory peptides targeted (Table 10.2) to these receptors for tumor receptor therapy is in various stages of development.

10.2.4 Peptides as Therapeutic Vectors

The ability to target specific receptors expressed on the surfaces of human cancer cells offers the scope of using radiolabeled peptides as transport vehicles to guide the radionuclides to the tissues expressing a particular receptor (Rufini et al. 2006). These receptors constitute useful molecular targets for the treatment of cancer owing to their location on the plasma membrane. Due to their low molecular weight, they show rapid diffusion into target tissue, and upon binding of the radioligand, the receptor–ligand complex is often internalized, allowing long retention of radioactivity in tumor cells. They also generally exhibit rapid vascular clearance from nontarget tissues, resulting in high tumor-to-background tissue ratios, which is a goal to minimize radioactive dose to nontarget tissues. In addition, peptides generally are non-immunogenic, so do not illicit any unwanted response. The most dramatic example of successfully targeting of cellular receptors with radiolabeled peptides (Fig. 10.3) is represented by somatostatin receptors, which are overexpressed in a majority of neuroendocrine tumors such as gastrointestinal and bronchial neuroendocrine tumors, pituitary adenomas, paragangliomas, pheochromocytomas, and neuroblastomas. Several key important regulatory peptides along with their receptors which are overexpressed on tumor cells are summarized in Table 10.1 (Okarvi 2004; Reubi et al. 2005). Since most of these peptides act through multiple peptide receptor subtypes, it is crucial that the peptide receptor subtype expressed by a given tumor corresponds to the subtype to which the radioligand used for PRRT binds with high affinity.

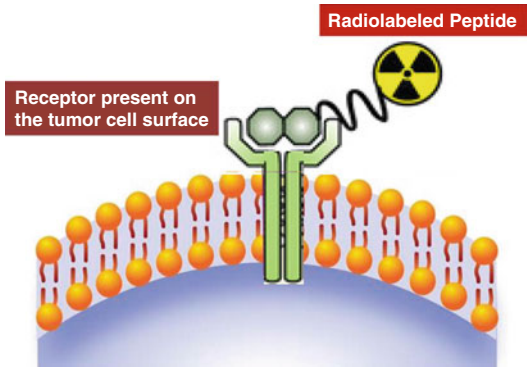

Fig. 10.3 Idealized illustration of radiolabeled peptide binding to a cell-surface receptor

10.2.5 Advantages of Peptides for Therapy

There are a variety of attractive properties for targeting small radiopeptides over other biologically active molecules for therapeutic applications (Reubi et al. 2005). The small size and low molecular weight of peptides facilitate rapid access to target tissue. Peptides are also easy to chemically synthesize using either an automated peptide synthesizer or by manual synthesis. Automated synthesis is used for rapid production of simple peptides, whereas manual synthesis is often more practical for time-consuming or difficult sequences and peptide modifications. High-specific-activity peptides can be prepared and used to minimize unwanted physiologic effects (i.e., eliciting physiological effects), and known sequences of amino acids can be modified to decrease their in vivo catabolic rate. Peptides also allow the possibility for radiolabeling with a variety of radionuclides by using both conventional and novel chelating moieties and also offer the feasibility of "kit" formulation as a practical strategy for the preparation of therapeutic agents. In addition, peptides are amenable to extensive chemical/molecular modifications to optimize their affinity for a particular receptor and to display a more specific biodistribution pattern. From a synthetic perspective, peptides have the ability to tolerate harsh conditions (pH, temperature, etc.) of chemical modifications and also the possibility for attachment of a chelating agent at the C- or N-terminus, as well to the free amine or carboxylic acid present on the peptide. Biologically, they have high affinity and specificity toward a wide range of target molecules. The specificity of the peptides toward G-protein-coupled receptors, which are overexpressed by cancer cells, identifies such peptides as ideal vectors for transportation of conjugated radionuclides to primary tumors and metastatic sites. Their small size and low molecular weight facilitate rapid penetration of peptides to target tissues, compared to the much larger proteins and antibodies. Another advantage usually displayed by peptides is the favorable pharmacokinetics characterized by high concentration in the target tissues and rapid clearance from the blood pool and nontarget tissues. In this context, elimination processes can be modified to accommodate a variety of possible routes of excretion or metabolism.

10.2.6 Limitations of Peptides for Therapy

Criteria for successful use of peptide tracers include high target specificity, high binding affinity, prolonged metabolic stability, and high target-to-nontarget background ratio. A short vascular half-life is a major road impediment for successful in vivo application of radiolabeled peptides because of susceptibility to degradation before reaching the intended target site. In order to circumvent such enzymatic destruction, most peptides can be synthetically modified. Considerable research efforts have been directed toward the development of metabolically stable peptides suitable for clinical use by the introduction of appropriate molecular modifications, such as the use of more stable D-amino acids instead of the naturally occurring L-amino acid isomer and the use of pseudopeptide bonds. In addition, the inclusion of amino alcohols and the insertion of unnatural amino acids or amino acid residues with modified side chains without compromising the receptor-binding affinity and biological activity of the peptide have been exceptionally successful (Okarvi 2004). Because of the ability of bioactive peptides to induce pharmacologic

effects even in trace amounts, the capability of preparing high-specific-activity (radioactivity per mass) peptides is an important requirement. Another strategy which has been successfully implemented is the use of antagonists (receptor binding but no physiological response) rather than agonist (receptor binding eliciting physiological response) peptide entities in order to diminish unwanted physiological effects. The loss of receptor-binding affinity and in vivo peptide metabolism resulting from coupling with a chelator and/or introduction of a radiolabel is another major challenge which can be associated with the use of small peptides. This issue can be effectively circumvented by site-directed radiolabeling that can be achieved by inserting a spacer group between the binding sequence and the chelating moiety (Okarvi 2004). One successful appealing approach is the cyclization of the peptide around a metal core which not only makes the peptide analogs resistant to chemical and proteolytic degradation in vivo but also greatly increases the target receptor affinity (Chen et al. 1999; Miao et al. 2007). Another issue often associated with the use of radiolabeled peptides is their high uptake and retention by the kidneys, which is a concern, particularly for radionuclide therapy because of the potential nephrotoxicity (Valkema et al. 2005; Imhof et al. 2011; Teunissen et al. 2005).

10.2.7 Development of Peptide-Based Radiopharmaceuticals

The synthesis of stable and well-defined peptides for use for targeted therapy is an important aspect of providing these tools for clinical application and involves a well-defined strategy and series of events (Okarvi 2004). It is initially essential to identify the enzyme or receptor molecular target (receptor) with relevance to human disease and identify for a potential tumor-specific peptide, either natural or synthetic. The endogenous ligand that displays high affinity for the corresponding receptor system must be identified, and the molecularly engineered synthesis of the peptide must be developed followed by attachment of a bifunctional chelating agent (BFCA) through a metabolic-resistant covalent bond. Adaptation of an appropriate radiolabeling procedure is required to permit high labeling efficiency to obtain a high-specific-activity product. It is crucial to choose a radiolabeling procedure that retains the receptor-binding affinity of the peptide. Screening by in vitro binding studies is often an important tool in this assessment. In vitro characterization includes studies such as binding of the radiopeptide with tumor cells, stability of chelated peptide in serum, receptor-binding affinity, internalization into the tumor cells, and dissociation from the tumor cells. These studies are critical for recognition of the potential peptide receptors and tumor types that are to be targeted with a specific peptide. Subsequent studies involve in vivo evaluation of the radiopeptide with respect to tumor-targeting properties using animal models. In order to assess the in vivo stability of the metal complex, evaluation in an appropriate animal model is necessary. After completion of these required preclinical and other tests, toxicological studies, and established radiopharmaceutical preparation, the radiopeptide is then assessed for efficacy in potential human studies involving only a small number of patients.

10.2.8 Preparation of Radiolabeled Peptides

Successful use of peptide-based targeted agents for targeted delivery of therapeutic radionuclides involves development of appropriate radiolabeling procedures. This requires suitable chelation chemistry for adequate sequestration of the radionuclide of interest, which usually is a metallic cation requiring appropriate chelation (i.e., $^{177}Lu^{+3}$, $^{90}Y^{+3}$, etc.). In this context, both the rate at which the metal complex forms and the rate of dissociation need to be considered. Cavity size of the bifunctional chelating agent (BFCA) should

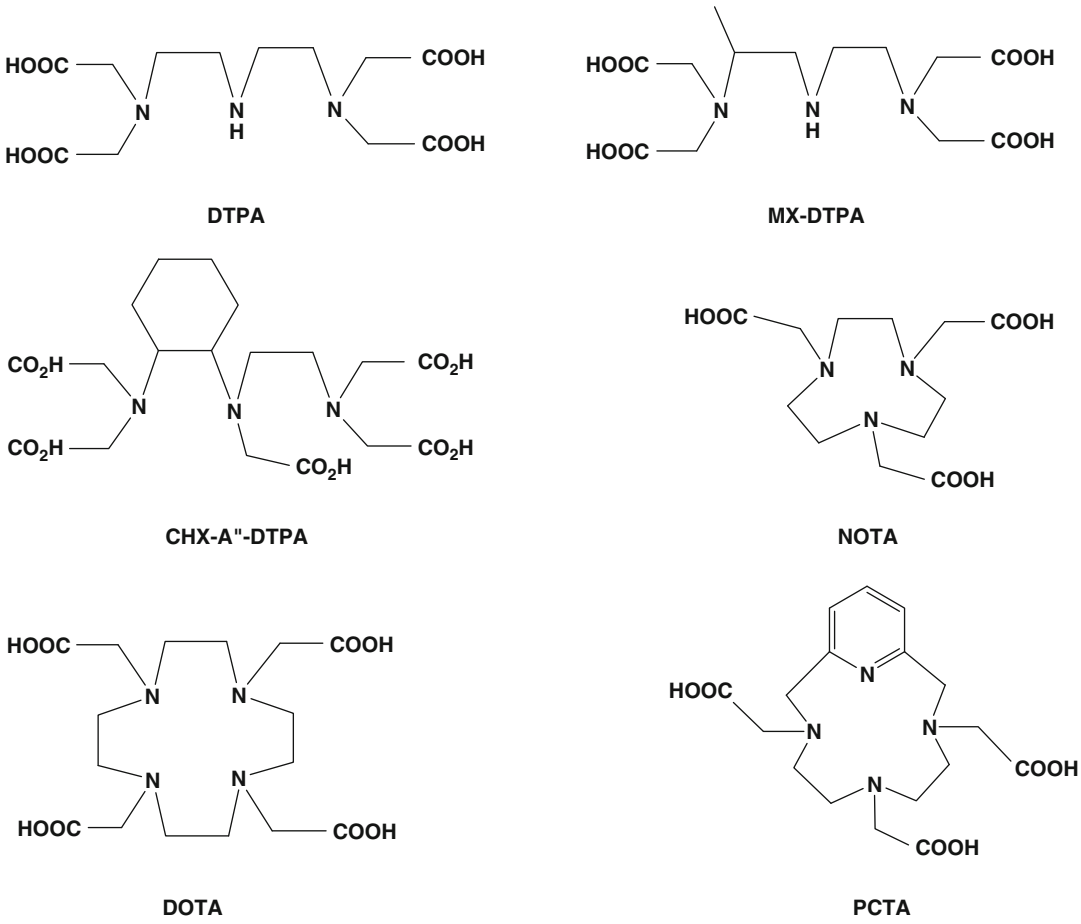

Fig. 10.4 Structures of typical acyclic and cyclic bifunctional chelating agents used for chelating radiometals

be compatible with the ionic radius of the radionuclide such that all of required donor groups can be properly aligned for optimal metal binding to provide high stability and limiting dissociation, i.e., thermodynamic stability and kinetic inertness. In recent years, a wide variety of BFCAs have been developed from well-established chelating agents, permitting rapid and convenient radiolabeling of peptides with different radionuclides. Structures of common acyclic and cyclic bifunctional chelating agents used for chelating radiometals in PRRT are shown in Fig. 10.4.

The major steps involved in the development of a peptide-based radiopharmaceutical are shown schematically in Scheme 10.1.

10.2.9 Radionuclides for Receptor-Mediated Peptide Therapy

Table 10.3 summarizes a number of important regulatory peptides and their analogs, which are of current interest for clinical PRRT application targeted to receptors overexpressed on tumors. As most of the peptides act through multiple peptide receptor subtypes, it is crucial that the peptide receptor subtype expressed by a given tumor corresponds to the subtype to which the radioligand used for PRRT binds with high affinity. The peptide analogs used as the targeting vector to deliver the radiation dose to the diseased site may function both as the receptor agonist or antagonist.

Scheme 10.1 Major steps involved in the development of a peptide-based radiopharmaceuticals

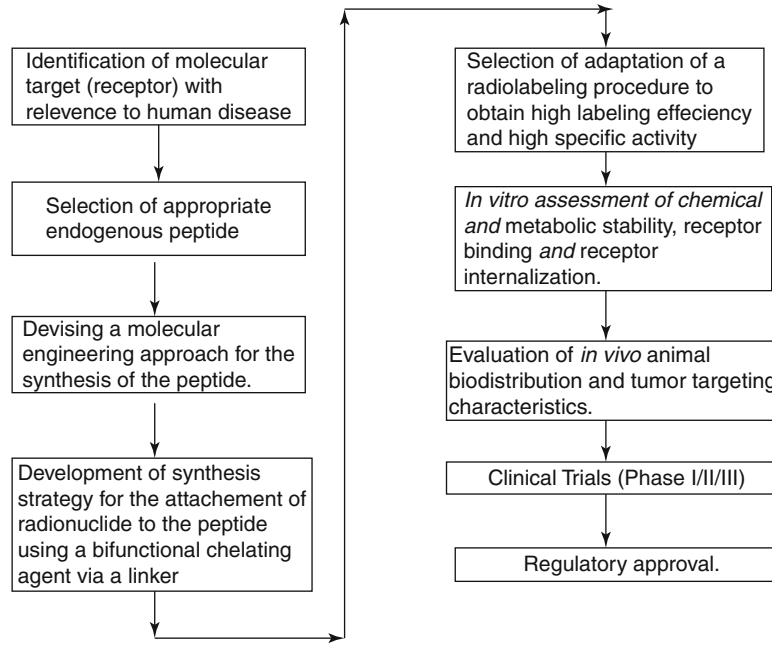

Table 10.3 Key regulatory peptides/analogs and their receptors overexpressed on tumors

Peptide	Number of amino acids	Receptor types/subtypes	Tumor expression
α-MSH	13	α-MSH-R	Melanomas
Bombesin	14	BB1 (NMB-R), BB2 (GRP-R), BB3, BB4	Prostate, breast, pancreas, gastric, colorectal, small-cell lung cancer
CCK	8, 33, 39, or 58	CCK1, CCK2	Medullary thyroid cancer, small-cell lung cancer, gastrointestinal stromal tumor, stromal ovarian cancer, astrocytomas
GRP	17 or 34	CCK2	
LHRH	10	LHRH-R	Prostate, breast cancer
Neurotensin	13	NTR1, NTR2, NTR3	Small-cell lung cancer, colon, exocrine ductal pancreatic cancer, Ewing sarcoma, meningioma, astrocytoma, breast, prostate cancer
RGD	3	Integrin $\alpha_v\beta_3$	Glioma, breast, colon, lung cancer
Somatostatin	14 or 28	SST1, SST2, SST3, SST4, SST5	Neuroendocrine tumors (NETs) such as GEP-NET, carcinoids, paraganglioma, breast, brain, renal, small-cell lung cancer, medullary thyroid cancer
	8		
Octreotide/octreotate			
Substance P	11	NK1, NK2, NK3	Glial tumors (glioblastoma, medullary thyroid cancer), pancreas, breast, small-cell lung cancer
VIP	28	VPAC1, VPAC2	Adenocarcinomas of breast, prostate, stomach, and liver; neuroendocrine tumors

GRP gastrin-releasing peptide, *VIP* vasoactive intestinal peptide, *CCK* cholecystokinin, *α-MSH* α-melanocyte-stimulating hormone, *LHRH* luteinizing hormone-releasing hormone, *RGD* arginine–glycine–aspartic acid

Table 10.4 Characteristics of some key radionuclides proposed for PRRT

Radionuclide	Half-life	Emissions	Mean energy (keV)	Maximum tissue penetration range of particle	Source
Indium-111	2.81 days	Conversion electrons	245	550 μm	Cyclotron
		Auger e	25	10 μm	
		γ-rays	171, 245		
Yttrium-90	2.67 days	β^--particles	934	12 mm	Generator
Lutetium-177	6.65 days	β^--particles	149	3 mm	Reactor
		γ-rays	208		
Copper-67	2.58 days	β^--particles	121	2–3 mm	Reactor/cyclotron
		γ-rays	184		
Scandium-47	3.42 days	β^--particles	143	3 mm	Reactor/cyclotron
		γ-rays	159		
Terbium-161	6.90 days	β^--particles	154	3 mm	Reactor
		γ-rays	75		
Actinium-225	10.0 days	α-, β^--particles, γ-rays	Decay series	–	Accelerator
					Reactor
Bismuth-213	46 min	α-, β^--particles, γ-rays	Decay series	–	Generator

An important feature of such agonists is that after binding to the receptor, the peptides or their radiolabeled analogs are internalized by receptor-mediated endocytosis, leading to an accumulation of the radioactive agonist within the tumor cell. On the other hand, peptide analogs, which function as receptor antagonists, have minimum or no internalization. Instead, once these agents bind to their cognate receptor, their function is blocked.

Although it has been one of the most popular therapeutic radioisotopes for the past several decades, use of ^{131}I in PRRT applications was not successful. Bakker et al. (1996) reported extensive radiolytic decomposition of octreotide after preparation of therapeutic dose of ^{131}I labeled octreotide for somatostatin receptor targeted therapy (Bakker et al. 1996), which was attributed to the radionuclidic decay properties. Yttrium-90 and ^{177}Lu are the most successfully used β^--emitting radionuclides, whereas the Auger electron-emitting radionuclide, ^{111}In, has also been evaluated, although with relatively less success for PRRT. Very recently, alpha particle emitters such as ^{213}Bi has been proposed for use (Norenberg et al. 2006; Cordier et al. 2010). The characteristics of the most commonly used radionuclides for PRRNT are summarized in Table 10.4.

10.3 Peptide Receptor Radionuclide Therapy (PRRT) for Neuroendocrine Tumors

Neuroendocrine tumors (NETs) represent a heterogeneous group of neoplasms which originate mainly from the gastroenteropancreatic tract (GEP NETs). The tumors include those arising from the endocrine cells within the respiratory and gastrointestinal tracts, known as "carcinoid" tumors. These tumors are classified as foregut, midgut, and hindgut, according to their presumed embryological origins. They are characterized by their endocrine metabolism and histological pattern. As opposed to other tumor entities, they range from well-differentiated, slow-growing tumors to poorly differentiated, highly invasive malignancies and may be functioning or non-functioning. NETs characteristically synthesize, store, and secrete a variety of peptides and neuroamines which may lead to clinical syndromes

such as the carcinoid syndrome, the Zollinger–Ellison syndrome, or the Verner–Morrison syndrome (ENETS Consensus Guidelines 2008; Modlin et al. 2008). However, most GEP NETs are clinically silent until late presentation with metastases. Features such as neuroamine uptake mechanisms and/or specific receptors at the cell membrane, such as somatostatin receptors (SSTRs), provide the scope for the identification, localization, and therapy of NETs (Oberg 2002, 2004). Of the five major subtypes of SSTR which bind the 14-amino-acid peptide somatostatin and its high-affinity 28-amino-acid precursor, $SSTR_2$ and $SSTR_5$, are the subtypes most commonly expressed in NETs. However, there is considerable variation in SSTR subtype expression among the different tumor types and among tumors of the same type (de Herder et al. 2003). The majority of NETs express SSTRs and appear as ideal targets and provide scope for treatment with somatostatin analog (SST analog)-derived radiopeptides (Krenning et al. 1999; de Herder et al. 2003). The extraordinary affinity of these peptides for SSTRs together with the internalization of the receptor–peptide complex facilitates retention of the radiopeptide in receptor-expressing tumors, and at the same time their relatively small size facilitates rapid blood clearance. Because of the necessity to ensure the stability of the radiolabeled molecule, the radioisotope is bound to a BFCA which is covalently attached to the peptide. Structures of several key common DOTA-coupled somatostatin analogs are depicted in Fig. 10.5.

Common DOTA-coupled, somatostatin-based radiopharmaceuticals are ^{90}Y-DOTA^0-Tyr3-octreotide (^{90}Y-DOTATOC), ^{90}Y-DOTA-lanreotide, and ^{177}Lu-DOTA-Tyr3-Thre8-octreotide (^{177}Lu-DOTATATE). The DOTATATE derivative exhibits the highest affinity to $SSTR_2$ and hence widely used as a vector for targeted therapy. On the other hand, DOTA-lanreotide possesses the lower affinity to $SSTR_2$ although demonstrating considerable $SSTR_5$ affinity (Krenning et al. 2005). Factors that determine the amount of uptake of radiolabeled SST analogs include stability of the radioligand, density of SSTR expression on the tumor, type of SSTRs expressed by the tumor, affinity of the radioligand for the SSTRs, efficiency of SSTR-mediated internalization, and the mass of the administered peptide. Several radiolabeled SST peptide analogs which are currently in clinical use for treatment of patients with SST receptor-expressing tumors are described below.

10.3.1 PRRT Studies with [^{111}In-DTPA] octreotide

Investigator in the mid- to late-1990s used [^{111}In- DTPA]octreotide for PRRT since this approved radiopharmaceutical was already in use for diagnostic imaging. Since ^{111}In is an Auger electron-emitting radionuclide, the goal was to increase the administered dose to assess possible therapeutic effects. While the use of high activity levels of [^{111}In-DTPA^0]octreotide in patients with metastasized neuroendocrine tumors was initially encouraging with regard to symptom relief, tumor size regression was unsatisfactory (Valkema et al. 2002; Anthony et al. 2002). The major impediments for expanded use of ^{111}In-coupled peptides are the small particle range of the particle and consequently short tissue penetration (~10 μm) and radiotoxicity (Kaltsas et al. 2005; Kwekkeboom et al. 2005).

Subsequently, the peptide-targeting moiety was modified by replacing the Phe3 amino acid residue with Tyr3 in the octapeptide sequence to increase hydrophilicity and to improve affinity for SST_2 as compared to octreotide. In addition, the DTPA chelator was replaced with DOTA to improve radionuclide chelator complex stability. Concurrently, the ^{111}In radionuclide has been replaced with more effective β^--emitting therapeutic radionuclides, such as ^{90}Y and ^{177}Lu. These radionuclides decay with emission of β^--particles with sufficient energy to cause cell damage with tissue penetration via the bystander effect for therapy of both small and large tumors (Otte et al. 1998).

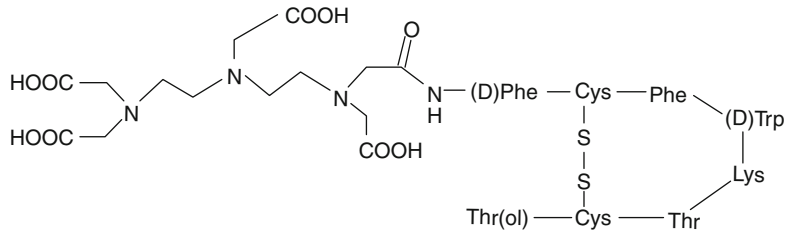

DTPA-Octreotide

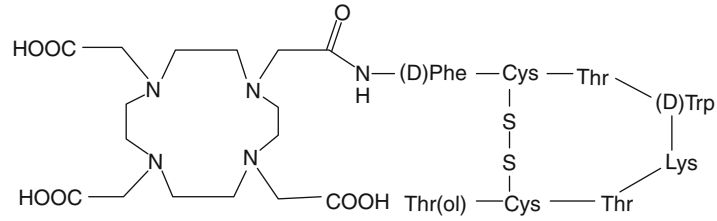

DOTA-TOC

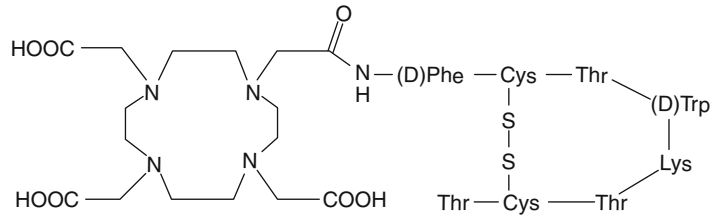

DOTA-TATE

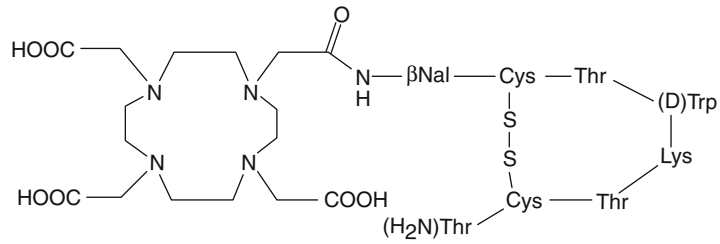

DOTA-LAN

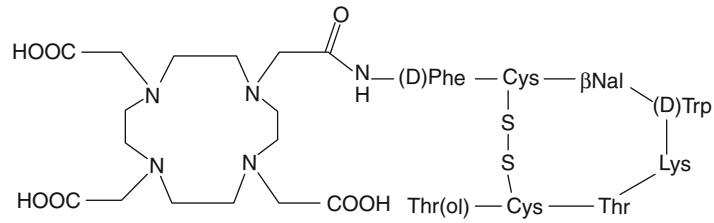

DOTA-NOC

Fig. 10.5 Structures of common DTPA/DOTA-coupled somatostatin analogs

10.3.2 Somatostatin Receptor Radiotherapy with [^{90}Y-DOTA^{0},Tyr^{3}] octreotide (^{90}Y-DOTATOC) and [^{90}Y-DOTA^{0},Tyr^{3}] octreotate (DOTATATE)

In an attempt to develop a more effective somatostatin (SST) analog for peptide receptor radionuclide therapy, the modified somatostatin analog [DOTA^{0},-Tyr^{3}]octreotide was used in the second generation of somatostatin receptor targeted radionuclide therapy to which DOTA rather than DTPA has been attached to the peptide as the chelator. Such analogs not only possess a higher affinity for somatostatin receptor subtype-2 but also provide a more stable binding of the intended beta-emitting radionuclide ^{90}Y. In clinical studies conducted at different institutions with this SST (^{90}Y-DOTATOC or OctreoTher; Fig. 10.6) peptide analog (Otte et al. 1998; Imhof et al. 2011; Waldherr et al. 2002; Bodei et al. 2004; Valkema et al. 2006), treatment outcome showed that ^{90}Y-DOTATOC is effective for complete or partial remissions (10–34 %) in patients with neuroendocrine tumors (NETs). These ranges were higher than those obtained with ^{111}In-DTPA^{0}-octreotide. In the light of explicit need to develop a more effective SST analog for peptide receptor radionuclide therapy, [DOTA^{0},Tyr3]octreotate (DOTATATE) has been developed by replacing the C-terminal threoninol moiety in DOTATOC with threonine. This at first glance rather minor molecular structural alteration was in fact shown to have a ninefold higher affinity for the $SSTR_2$ compared with DOTATOC in vitro (Reubli et al. 2000).

With a view to realize the clinical benefit of ^{90}Y-DOTATOC, the Basel group has used protocol with administration of a cumulative dose of 7.4 GBq/m^2 in two cycles and observed partial remission in 7–28 % of the patients and stable disease in 50 % up to 80 % (Otte et al. 1999; Waldherr et al. 2001). These authors have also observed that responses were higher in pancreatic endocrine tumors than in carcinoid tumors. Dosimetric and dose-escalating phase I studies of ^{90}Y-DOTATOC using doses up to 5.6 GBq per cycle with and without the administration of renal-protecting agents have been carried out in Milan, Italy (Chinol et al. 2002). Therapeutic responses were found to be partial remission in about 29 % of the patients. In a multicenter dose-escalating, phase I trial, 60 patients with ^{90}Y-DOTATOC received escalating doses of radioactivity without reaching the maximum tolerated single dose. In this study, the cumulative radiation dose to the kidneys was limited to 27 Gy and concomitant amino acid infusion was performed. Partial remission was obtained in 30 % and stable disease in 50 % (Valkema et al. 2006). In a large international multicenter trial, where ^{90}Y-edotreotide (DOTATOC) was administered of three cycles of 4.4 GBq in 90 patients, 75 % showed stable disease or response (Bushnell et al. 2010). Recently, response, survival, and long-term toxicity were evaluated after treatment with ^{90}Y DOTATOC in 1,109 NET patients.

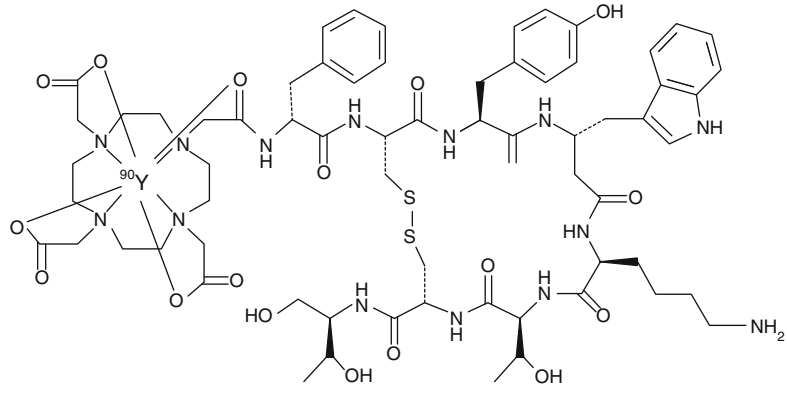

Fig. 10.6 Structure of the ^{90}Y-labeled DOTATOC peptide

Objective response was noted in 34 %, median survival 44.7 months overall, 12 % hematological grade 3/4 toxicity was found and 9 % grade 3/4 renal toxicity (Imhof et al. 2011).

10.3.3 Somatostatin Receptor Radiotherapy with [^{177}Lu-DOTA^{0},Tyr^{3}] octreotate (DOTATATE)

Lutetium-177, although relatively introduced as a radionuclide for targeted therapy, has already emerged as one of the important therapeutic radionuclides due to its more favorable radionuclidic characteristics as well as the relative ease for production with very high specific activity and in high activity levels in many research reactors. Targeted radionuclide therapy with ^{177}Lu-DOTATATE (Kwekkeboom et al. 2005, 2007; van Essen et al. 2007a, b) showed an overall response of 30–38 %, and a significantly high median overall survival of 48 months has been reported. It was observed that the quality of life improved significantly after treatment with ^{177}Lu-DOTATATE (Fig. 10.7).

As expected because of the different energies of β^--emissions and expected soft tissue penetration, animal experiments had revealed that ^{90}Y-labeled somatostatin analogs are more effective for treatment of larger tumors, whereas ^{177}Lu-labeled somatostatin analogs more effectively treat smaller tumors. In addition, their combination may be even more effective (Jong et al. 2002). In this context, the results of recent studies are important, where a cocktail of 50 % activity levels of ^{90}Y-DOTATATE + 50 % ^{177}Lu-DOTATATE in 25 patients were compared with a second group of 25 patients treated only with the ^{90}Y-DOTATATE agent (Kunikowska et al. 2011). The results of these studies demonstrated striking differences in overall survival and progressive disease in favor of the combination ^{90}Y+^{177}Lu therapy compared with the single-agent treatment. While the tandem therapy was reported to be more effective, there were no significant differences with respect to tumor response and progression-free survival.

It is pertinent to point out that high energy β^--particles (av. 2.3 MeV) are emitted by radioactive decay of the ^{90}Y radionuclide with good deposition of radioactivity in tumor cells and good cross fire throughout the tumor, with a moderate physical half-life leading to a high-dose rate. On the other hand, ^{177}Lu emits much lower energy β^--particles (av. 0.495 MeV) with a much shorter particle range in soft tissue. For this reason, the ^{177}Lu-labeled peptides are therefore better absorbed for treatment of smaller tumors and micrometastatic sites. For these reasons, the use of the (^{90}Y and ^{177}Lu) radionuclide mixture represents an ideal proposition for treatment of patients with heterogeneous tumors of variable sizes.

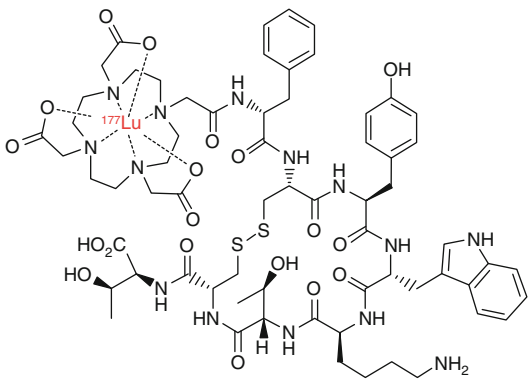

Fig. 10.7 Structure of ^{177}Lu-DOTATATE

10.4 Bombesin Peptide Analogs

Bombesin (BN) is a member of a family of brain-gut peptides, which play an important role in cancer, and is a 14-amino-acid peptide present in amphibian tissues, a homolog of the 27-amino acid mammalian gastrin-releasing peptide (GRP). GRP and bombesin differ by only one of the 10 carboxyl-terminal residues, and owing to their structural similarities, the biological activity of the two peptides is identical. GRP acts mainly in the central and enteric nervous systems and primarily responsible for the regulation of several physiological processes including thermoregulation, circadian rhythm, smooth muscle contraction, immune function, as well as

modulating the release of other peptide hormones (Bunnett 1994; Walsh 1994). Both BN and GRP exhibit high binding affinity to the human GRP receptor, which is overexpressed by a variety of cancers, including prostate, breast, gastrointestinal, and small-cell lung cancer (Gonzalez et al. 2008; Ohki-Hamazaki et al. 2005). Bombesin and GRP mediate their actions through membrane-bound, G-protein-coupled receptors, which include at least four different subtypes, namely, the neuromedin B (BB_1), GRP (BB_2), the BB_3, and the BB_4 receptor subtypes (Gonzalez et al. 2008; Ohki-Hamazaki et al. 2006). Among these, the GRP receptor (BB_2) is of particular interest since it overexpressed in a variety of tumors, including lung, breast, GI, brain, and prostate (Gonzalez et al. 2008; Ohki-Hamazaki et al. 2006), and is thus an attractive target for the detection and treatment of these cancers. Like other naturally occurring peptides, the naturally occurring BN peptide has a very short circulation half-life (<2 min). Radiolabeled BN-like peptides, which bind to BN/GRP receptors with high affinity and specificity, have emerged as an important option for site-directed radionuclide therapy. Various BN analogs based on their key amino acid sequence have been screened mostly by incorporating therapeutic radionuclides at the N-terminus of the peptide. One major impediment for the use of BN-like peptides is their tendency for liver and intestinal accumulation owing to high hepatobiliary clearance despite their hydrophilic nature (Mariani et al. 2006). The presence of GRP receptors in gastrointestinal tissues might be responsible to account for the high hepatobiliary clearance (Pansky et al. 2000). Several BN peptide analogs radiolabeled with ^{111}In and ^{177}Lu have been prepared and investigated for targeting of BN receptor-expressing tumors including prostate and breast cancer (Zhang et al. 2004, 2007; Maddalena et al. 2009; Smith 2003; Smith et al. 2003; Prasanphanich et al. 2007; de Visser et al. 2007). Based on the experimental data, it has been revealed that the GRP antagonist analogs are superior targeting agents to GRP receptor agonists, since they have fewer side effects compared to the corresponding agonists. Such observations indicate a paradigm shift in the field of PRRNT using BN-like peptides.

10.5 Vasoactive Intestinal Peptide (VIP) Analogs

The vasoactive intestinal peptide (VIP) is a 28-amino acid neuropeptide isolated from the small porcine intestine. It is an important immunomodulator which stimulates secretion of various hormones. In addition to its vasodilatory properties, VIP promotes growth and proliferation of normal and cancer cells mediated by cell-surface receptors (Okarvi 2004; Raderer et al. 2000). VIP receptors are found not only in the brain but ubiquitously in a majority of human cell membranes of normal intestinal and epithelial cells, which are overexpressed on various tumor cells, such as colonic adenocarcinomas, pancreatic carcinomas, and carcinoids. The actions of VIP are mediated by two $VPAC_1$ and $VPAC_2$ receptor subtypes. While each of these receptor subtypes exhibit different pharmacology and in vivo distribution patterns, they both have high affinity for VIP receptor subtypes (Igarashi et al. 2005). In most of these tissues, the VIP receptor subtype preferentially expressed is the $VPAC_1$ receptor, for instance, in hepatocytes, gastrointestinal mucosa, lobules and ducts of the breast, thyroid follicles, prostatic glands, urothelium of the bladder and ureter, and acini of the lung and pancreatic ducts. One of the impediments on the use of VIP is its pharmacological toxicity which necessitates an efficient purification step for the radiolabeled peptide prior to administration which is intended to reduce the administration dose to sub-pharmacologic levels. In vivo data using ^{123}I-VIP as a universal ligand targeting VPAC1 and VPAC2 are available as proof of concept that VIP receptor-positive tumors, specifically gastrointestinal cancers, can be targeted in vivo in selected patients (Virgolini et al. 1996; Hessenius et al. 2000). While the overexpression of VIP receptor on various tumor cells obviously holds promise as a treatment approach, the overexpression of VIP receptors on normal tissues,

particularly in the lungs, central nervous system, liver, and intestine, has limited the widespread therapeutic application of radiolabeled VIP analogs. For this reason, further efforts are required to assess the therapeutic potential of such VIP analogs.

10.6 Cholecystokinin (CCK)/ Gastrin Peptide Analogs

Cholecystokinin (CCK) and gastrin are structurally and functionally related peptide hormones that primarily function in the gastrointestinal tract and central nervous system. CCK and gastrin share an identical sequence of five amino acids at their biologically active C-terminal region. The biological action of these peptide hormones is mediated by CCK/gastrin receptors belonging to the superfamily of G-protein-coupled receptors. These receptors are distributed in a number of different tissues rather than as a selective expression of specific subtypes and exert their functions through interaction with two CCK2/gastrin and CCK1 receptors (Nock et al. 2005). The CCK-2/gastrin receptors are overexpressed in a high percentage (>90 %) on medullary thyroid cancers (MTC) and in other tumors of small-cell lung cancers, astrocytomas, stromal ovarian tumors, and gastroenteropancreatic cancers (Brans et al. 2006). Development of radiolabeled CCK/gastrin peptide analogs is beneficial for targeting the CCK/gastrin-expressing tumors in vivo. Recently, several radiolabeled CCK/gastrin peptide analogs have been prepared and evaluated for diagnostic imaging or radionuclide therapy of CCK/gastrin receptor-expressing tumors (Froberg et al. 2009; Laverman et al. 2011). One of the main limiting factors for the development of PRRT using CCK_2 receptors may be the high problematic kidney uptake with current CCK analogs (Behr and Behe 2002), which is an observation often detected with many radioactive peptide-targeting agents. In order to circumvent such a drawback, a new generation of CCK analogs has been designed which exhibit much less kidney uptake (Bernard et al. 2003)

10.7 Neurotensin Peptide Analogs

Neurotensin (NT) is a 13-amino acid peptide found in the brain and gut and has many growth regulatory functions. NT is a neurotransmitter and a local hormone and is also detected in the central nervous system and in peripheral tissues. Three NT receptor subtypes have been cloned to date, and overexpression of NT receptors has been found in many tumors. The biological effects of NT are mediated through the action of three different NTR_1, NTR_2, and NTR_3 receptors through the specific peptide interaction with cell-surface receptors (Tanaka et al. 1990). While NTR_1 and NTR_2 belong to the superfamily of G-protein-coupled receptors, NTR_3 is a single transmembrane domain receptor which is similar to sortilin, a protein involved in receptor sorting (Vincent et al. 1999). Overexpression of NTR1 has been found in several human cancers including Ewing sarcomas, meningiomas, astrocytomas, medulloblastomas, and pancreatic carcinomas (Brans et al. 2006). While the neurotensin peptide analogs hold promise as treatment options, the initial clinical findings are not very favorable due to the high nonspecific uptake of radioactivity in the intestinal region and in kidneys (Miao et al. 2007: Wei et al. 2007a, b; Cheng et al. 2007).

10.8 Glucagon-Like Peptide (GLP) Analogs

The glucagon-like peptide receptor (GLP-1R) is also a member of the G-protein-coupled receptor family and is secreted from L cells in the gastrointestinal tract. Glucagon is the principal counter-regulatory hormone that opposes insulin action leading to coordinate bi-hormonal control of glucose homeostasis. Glucagon also inhibits glycogen synthesis and glycolysis in the liver. The biological active molecule of GLP-1 consists of 31 amino acids, derived from a precursor 36-amino acid sequence. The multifaceted physiological actions of GLP-1 include stimulation of insulin gene expression, stimulation of insulin

secretion, trophic effects on the beta cells, inhibition of glucagon secretion, promotion of satiety, inhibition of food intake, and the reduction of gastric emptying, all of which contribute to normalizing elevated glucose levels (Drucker 2001; MacDonald et al. 2002). This receptor is primarily expressed β cells of pancreatic islets, the intestine, lung, kidney, breast, and brainstem. The GLP-1 receptors are overexpressed in most human insulinomas (de Jong et al. 1999), gastrinomas (Reubli et al. 1999), and pheochromocytomas (Korner et al. 2007). The GLP-1-receptor agonists, however, have a short half-life of less than 2 min in vivo due to degradation by the dipeptidyl peptidase-IV and tendency to rapidly degrade in blood (Meier and Nauck 2005; Hassan et al. 1999). However, GLP-l analogs, such as exendin-4 and exendin-3, have similar biological activity but longer in vivo half-lives. Exendin-4 and exendin-3 are two 39-amino acid natural peptides which are metabolically resistant and share nearly 50 % homology with the human GLP-1. These peptides differ by only two amino acid residues near the amino terminus. While the initial results are encouraging (Wicki et al. 2007; Wild et al. 2011; Pattou et al. 2010; Wild et al. 2008; Christ et al. 2009; Hubalewska-Dydejczyk et al. 2011; Sowa-Staszczak et al. 2011), no clinical studies using GLP-1-receptor-targeting analogs have yet been reported. High kidney retention of exendin-4 analogs could be the major impediment to realize the scope of using this analog for therapeutic purposes. Nevertheless, if the high kidney accumulation can be mitigated, the high GLP-1-receptor expression on tumors, in combination with the favorable in vivo characteristics of the recent exendin-4 analogs, may offer use of GLP-1 receptor-targeted PRRT as an attractive strategy.

GLP-2 is co-secreted together with GLP-1 from intestinal L cells in a 1:1 ratio. While GLP-1 elicits its main effects on the endocrine pancreas, the majority of GLP-2 action is observed directly in the gastrointestinal mucosa. In contrast to the widespread tissue distribution of the GLP-1R, GLP-2R expression is highly restricted, predominantly to the gastrointestinal tract. GLP-2 receptor transcripts have been detected in the stomach, small and large bowel, the brain, and the lung (Tang-Christensen et al. 2000; Yusta et al. 2000; Jain 1987). From the clinical perspective, PRRT with GLP analogs is still in its infancy (Table 10.4).

10.9 RGD Peptides for Targeting Integrin $\alpha_v\beta_3$ Expression

10.9.1 Angiogenesis

Angiogenesis is a physiological process involving the formation of new blood vessels from preexisting vessels. When the size of tumors attains approximately 2 mm^3, the increased interstitial pressure within the tumor appears to hinder the diffusion of metabolites and nutrients necessary for tumor growth. As a consequence, a state of cellular hypoxia initiates, inducing the sprouting of new blood vessels from the established vasculature to facilitate the supply of oxygen and nutrients to tumor cells to survive and proliferate (Jain 1987). Hypoxia increases cellular hypoxia-inducible factor (HIF) transcription, leading to upregulation of proangiogenic proteins such as vascular endothelial growth factor (VEGF), platelet-derived growth factor (PDGF), or tumor necrosis factor-α (TNF-α) (Carmeliet and Collen 2000) (Fig. 10.8).

The process of new blood vessel formation with the removal of pericytes from preexisting blood vessels results in degradation of the endothelial cell basement membrane and extracellular matrix which is regulated by the matrix metalloproteinases (MMPs). After this degradation, endothelial cells proliferate and migrate until they form unstable microvessels. Mesenchymal cells differentiate into pericytes, which allow the stability of new formatted vessels to establish blood flow. Such a progression of tumor from a nonangiogenic to an angiogenic phenotype is called the "angiogenic switch," which is triggered by signals such as metabolic stress (low pH, low oxygen pressure), mechanical stress, inflammatory response, and genetic mutations (Francavilla et al. 2009). These signals lead to increased expression of angiogenic proteins by

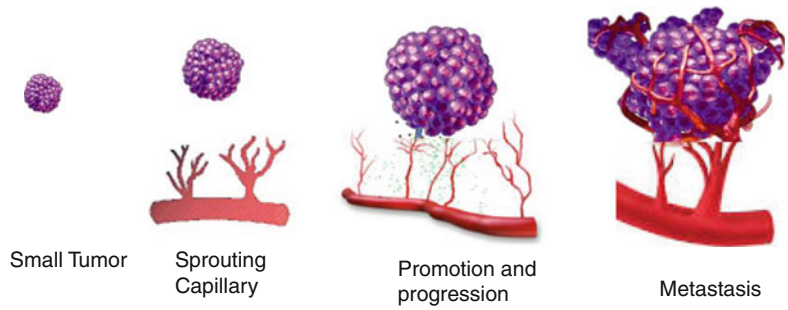

Fig. 10.8 Cartoon illustrating the progression of angiogenesis and tumor growth

tumor cells, such as VEGF. In addition, increased expression of angiogenic proteins by stromal cells is observed with decreased expression of angiogenic inhibitors such as thrombospondin-1 by tumor cells and stromal cells, which directly govern the angiogenic switch.

During the "dormancy state," which refers to prior to tumor angiogenesis, the tumor mass expands slowly, resulting in an asymptomatic and nonmetastatic state. However, after the angiogenic switch, the tumor mass expands rapidly and the process of tumor angiogenesis is associated with the participation of a range of adhesion molecules such as integrin, cadherin, selectin, and immunoglobulin families. Members of the integrin family play vital roles during various cancer stages such as malignant transformation, tumor growth and progression, invasion, and metastasis. Among cell adhesion molecules (CAM), integrins are cell adhesion receptors for extracellular matrix (ECM) proteins, immunoglobulin, growth factors, cytokines, and matrix-degrading proteases. Integrins are divalent cation-dependent heterodimeric membrane glycoproteins composed of non-covalently associated α- and β-subunits. Eighteen α-subunits and eight β-subunits can assemble into 24 different heterodimers. Each subunit is composed of an extracellular domain, a single transmembrane region, and a cytoplasmic region.

The combination of α- and β-subunits determines the ligand-binding specificity and signaling properties of a given integrin which can be classified based on their properties or based on their subunit composition (Avraamides et al. 2008). The cell–cell and cell–matrix adhesion processes through binding of integrins to their ligands play critical roles in physiological processes, including cell attachment, proliferation (Miyata et al. 2000; Hollenbeck et al. 2004; Zhou et al. 2004), bone remodeling (Horton 1995), and wound healing (Singh et al. 2004). Besides, integrins also contribute to pathological events such as thrombosis, atherosclerosis (Chao et al. 2004; Antonov et al. 2004), tumor invasion, angiogenesis and metastasis (Tsuji 2004; Guo and Giancotti 2004; Chung et al. 2004; Zheng et al. 1999), infection by pathogenic microorganisms (Zecchinon et al. 2004; Isberg and Van Nhieu 1995), and immune dysfunction. Therefore, integrins have been proposed as the molecular targets for the treatment of cancer (Reardon et al. 2008; Miller et al. 2000; Burke and DeNardo 2001; Tucker 2006; Gottschalk and Kessler 2002; Smith et al. 2003), thrombosis (Lal et al. 2009; Nissinen et al. 2010), and other diseases (Stefanelli et al. 2008; Hilden et al. 2006). The role of integrins has been reviewed extensively (Caswell et al. 2009; Bennett et al. 2009; Wegener and Campbell 2008).

The expression of β_3-integrins is mostly associated with the ability of tumors to metastasize. Tumor cells can migrate effectively on ECM substrates, and the multiple integrin functioning contributes to this process (Switala-Jelen et al. 2004). An array of integrins are involved in angiogenesis, among which, $\alpha_v\beta_3$ is most important owing to its strong involvement in the regulation of angiogenesis. The $\alpha_v\beta_3$-integrin, which binds to arginine–glycine–aspartic acid (RGD)-containing components of the interstitial matrix, is significantly upregulated on endothelia during angiogenesis but not on quiescent endothelium. In

breast cancer, overexpression of $\alpha_v\beta_3$-integrin is not only associated with bone metastasis but also induces increased tumor growth and invasion in response to osteopontin (Takayama et al. 2005; Furger et al. 2003). In glioblastoma, $\alpha_v\beta_3$-integrin is overexpressed at the invasive margins of the tumor (Sheldrak and Patterson 2009). In prostate carcinoma, $\alpha_v\beta_3$-integrin is expressed resulting in metastasis to bone because of an association between integrins and processes of attachment and migration involving laminin, fibronectin, and osteopontin (Sheldrak and Patterson 2009). In pancreatic tumor, the increased expression of $\alpha_v\beta_3$-integrin is associated with increased activation of MMP-2 and lymph node metastasis (Hosotani et al. 2002).

10.9.2 RGD Peptide-Based Radiotherapeutics Targeting Integrin $\alpha_v\beta_3$

The RGD sequence emerged as the basic module for a variety of molecules designed for the preferential binding to $\alpha v\beta_3$-integrin and other integrins (Temming et al. 2005). The RGD triple-peptide itself is limited for in vivo use because of its short circulation half-life. Conformational restriction by ring closure of the peptides and further chemical modification, such as the use of D-amino acids, like in the c(RGDfV) (with f standing for D-phenylalanine) analog, not only increases their $\alpha_v\beta_3$-binding affinity but also improves bioavailability (Eble and Haier 2006). While a series of radiolabeled cyclic RGD peptides and analogs have been intensively investigated for use in PET and SPECT imaging of integrin $\alpha_v\beta_3$-expression (Liu 2006; Chen 2006; Cai et al. 2008), only a few reports discuss the possibility therapeutic tumor targeting. One example is the reported receptor-binding characteristics of dimeric and multimeric RGD peptides would be better than that use of monomeric RGD peptide based upon polyvalency (Liu et al. 2006; Iten et al. 2007; Dijkgraaf et al. 2007). The receptor binding of one RGD peptide will significantly enhance the local concentration of the other RGD peptides in the vicinity of the receptor, which may lead to a more rapid rate of receptor binding or a slower rate of dissociation of the dimeric RGD probes. The dimeric or multimeric RGD peptides are reported to have integrin-binding affinity one order of magnitude higher than the monomeric analog. ^{90}Y-labeled multimeric RGD peptides possessing higher receptor affinity and longer tumor retention time are being studied for therapy animal models (Liu et al. 2009; Shi et al. 2008, 2009; Wang et al. 2009; Liu et al. 2010; Liu 2009; Yoshimoto et al. 2008). However, due to the lower tumor uptake of the RGD monomer, single-dose administration has not yet shown significant inhibition in tumor growth and the radionuclide therapeutic efficacy of the multiple dose administration was also generally limited. Further research and development is clearly required to assess the potential of this approach, since the translation of preclinical results from bench to bedside has been slow.

10.10 Summary

Radiolabeled peptides are poised to make a huge impact in the near future in the area of cancer treatment. The results of PRRNT with long-acting SST analogs indicate that this modality of therapy has its place in the treatment of patients with SSTR-positive NETs for size reduction, improvement of quality of life, and overall prognosis. The expression of other different classes of receptors, such as gastrin, bombesin, and $\alpha_v\beta_3$-integrin, constitutes the basis for new therapy applications with proper radiopeptides, in a multi-receptor targeting that could be possibly extended to cover other non-neuroendocrine tumors. With rapid advancement in genomic and proteomic research, it is possible to identify the presence of new peptide receptor types/subtypes for efficient tumor targeting for therapy. Along with existing radiolabeled peptides already developed for therapy, a number of peptide-based therapies are currently on clinical trials and are expected to yield positive results. Development of peptide-based therapy is fundamentally different from traditional drug development. A major

challenge is to harmonize the many different factors for development of more sensitive, specific, and stable peptide-based therapy strategies. The development and application of peptide therapy must move forward before this approach is well utilized for the treatment of cancer. Despite these challenges, it is important that interdisciplinary research at the interface of chemistry, molecular peptide biology, and detection technology can provide numerous unexplored possibilities.

References

Anthony LB, Woltering EA, Espanan GD, et al. Indium-111-pentetreotide prolongs survival in gastroenteropancreatic malignancies. Semin Nucl Med. 2002;32:123–32.

Antonov AS, Kolodgie FD, Munn DH, et al. Regulation of macrophage foam cell formation by αvβ3 integrin: potential role in human atherosclerosis. Am J Pathol. 2004;165:247–58.

Avraamides CJ, Garmy-Susini B, Varner JA. Integrins in angiogenesis and lymphangiogenesis. Nat Rev Cancer. 2008;8:604–17.

Bakker WH, Breeman WAP, van der Pluijm ME, et al. Iodine-131 labeled octreotide: not an option for somatostatin receptor therapy. Eur J Nucl Med. 1996;23:775.

Behr TM, Behe MP. Cholecystokinin-B/Gastrin receptor-targeting peptides for staging and therapy of medullary thyroid cancer and other cholecystokinin-B receptor-expressing malignancies. Semin Nucl Med. 2002;32:97–109.

Bennett JS, Berger BW, Billings PC. The structure and function of platelet integrins. J Thromb Haemost. 2009;7 Suppl 1:200–5.

Bernard BF, Béhé M, Breeman WAP, et al. Preclinical evaluation of minigastrin analogs for CCK-B receptor targeting. Cancer Biother Radiopharm. 2003;18:28.

Bodei L, Cremonesi M, Grana C, et al. Receptor radionuclide therapy with 90Y-[DOTA]0-Tyr3-octreotide (90Y-DOTATOC) in neuroendocrine tumours. Eur J Nucl Med Mol Imaging. 2004;31:1038–46.

Brans B, Linden O, Giammarile F, Tennvall J, Punt C. Clinical applications of newer radionuclide therapies. Eur J Cancer. 2006;42:994–1003.

Bunnett G. Gastrin-releasing peptide. In: Walsh JH, Dockray GJ, editors. Gut peptides: biochemistry and physiology. New York: Raven Press, Ltd; 1994. p. 423–45.

Burke PA, DeNardo SJ. Antiangiogenic agents and their promising potential in combined therapy. Crit Rev Oncol Hematol. 2001;39:155–71.

Bushnell Jr DL, O'Dorisio TM, O'Dorisio MS, et al. ^{90}Y-edotreotide for metastatic carcinoid refractory to octreotide. J Clin Oncol. 2010;28:1652–9.

Cai W, Niu G, Chen X. Imaging of integrins as biomarkers for tumor angiogenesis. Curr Pharm Des. 2008;14:2943–73.

Carmeliet P, Collen D. Transgenic mouse models in angiogenesis and cardiovascular disease. J Pathol. 2000;190(3):387–405.

Caswell PT, Vadrevu S, Norman JC. Integrins: masters and slaves of endocytic transport. Nat Rev Mol Cell Biol. 2009;10:843–53.

Chao JT, Meininger GA, Patterson JL, et al. Regulation of α7-integrin expression in vascular smooth muscle by injury-induced atherosclerosis. Am J Physiol Heart Circ Physiol. 2004;287:H381–9.

Chen X. Multimodality imaging of tumor integrin αvβ3 expression. Mini Rev Med Chem. 2006;6:227–34.

Chen JQ, Giblin MF, Wang N, et al. In vivo evaluation of 99mTc/188Re-labeled linear alpha-melanocyte stimulating hormone analogs for specific melanoma targeting. Nucl Med Biol. 1999;26:687–93.

Cheng Z, Zhang L, Graves E, et al. Small-animal PET of melanocortin 1 receptor expression using a 18F-labeled α-melanocyte-stimulating hormone analog. J Nucl Med. 2007;48:987–94.

Chinol M, Bodei L, Cremonesi M, Paganelli G. Receptor-mediated radiotherapy with Y-DOTA-DPhe-Tyroctreotide: the experience of the European Institute of Oncology Group. Semin Nucl Med. 2002;32:141–7.

Christ E, Wild D, Forrer F, et al. Glucagon-like peptide-1 receptor imaging for localization of insulinomas. J Clin Endocrinol Metab. 2009;94:4398–405.

Chung J, Yoon SO, Lipscomb EA, Mercurio AM. The Met receptor and α6β4 integrin can function independently to promote carcinoma invasion. J Biol Chem. 2004;279:32287–93.

Cordier D, Forrer F, Bruchertseifer F, et al. Targeted alpha-radionuclide therapy of functionally critically located gliomas with 213Bi-DOTA-[Thi8, Met(O2)11]-substance P: a pilot trial. Eur J Nucl Med Mol Imaging. 2010;37:1335–44.

de Herder WW, Hofland LJ, van der Lely AJ, Lamberts SW. Somatostatin receptors in gastroentero-pancreatic neuroendocrine tumours. Endocr Relat Cancer. 2003;10:451–8.

de Jong M, Breeman WA, Bernard BF, et al. Tumour uptake of the radiolabelled somatostatin analogue [DOTA0, TYR3]octreotide is dependent on the peptide amount. Eur J Nucl Med. 1999;26:693–8.

de Visser M, van Weerden WM, de Ridder CM, et al. Androgen-dependent expression of the gastrin-releasing peptide receptor in human prostate tumor xenografts. J Nucl Med. 2007;48:88–93.

Dijkgraaf I, Kruijtzer JA, Liu S, et al. Improved targeting of the αvβ3 integrin by multi-merisation of RGD peptides. Eur J Nucl Med Mol Imaging. 2007;34:267–73.

Drucker DJ. Minireview the glucagon-like peptides. Endocrinology. 2001;142:521–7.

Eble JA, Haier J. Integrins in cancer treatment. Curr Cancer Drug Targets. 2006;6:89–105.

ENETS Consensus Guidelines. In: de Herder WW, O'Toole D, Rindi G, Wiedenmann B, editors. ENETS consensus guidelines for the diagnosis and treatment of neuroendocrine gastrointestinal tumors Part 2 – Midgut and Hindgut Tumors. Neuroendocrinology Special Issue, vol. 87. Basel: Karger Medical and Scientific Publishers; 2008, No. 1. ISBN: 978-3-8055-8459-3;e-ISBN:978-3-8055-8460-9;DOI:10.1159/isbn.978-3-8055-8460.

Francavilla C, Maddaluno L, Cavallaro U. The functional role of cell adhesion molecules in tumor angiogenesis. Semin Cancer Biol. 2009;19:298–309.

Froberg AC, de Jong M, Nock BA, et al. Comparison of three radiolabelled peptide analogues for CCK-2 receptor scintigraphy in medullary thyroid carcinoma. Eur J Nucl Med Mol Imaging. 2009;36:1265–72.

Furger KA, Allan AL, Wilson SM, et al. Beta(3) integrin expression increases breast carcinoma cell responsiveness to the malignancy-enhancing effects of osteopontin. Mol Cancer Res. 2003;1:810–9.

Gonzalez N, Moody TW, Igarashi H, et al. Bombesin-related peptides and their receptors: recent advances in their role in physiology and disease states. Curr Opin Endocrinol Diabetes Obes. 2008;15:58–64.

Gottschalk KE, Kessler H. The structures of integrins and integrin-ligand complexes: Implications for drug design and signal transduction. Angew Chem Int Ed Engl. 2002;41:3767–74.

Guo W, Giancotti FG. Integrin signalling during tumour progression. Nat Rev Mol Cell Biol. 2004;5:816–26.

Hassan M, Eskilsson A, Nilsson C, et al. In vivo dynamic distribution of ^{131}I-glucagon-like peptide-1 (7-36) amide in the rat studied by gamma camera. Nucl Med Biol. 1999;26:413.

Heppeler A, Froidevaux S, Eberle AN, Maecke HR. Receptor targeting for tumor localisation and therapy with radiopeptides. Curr Med Chem. 2000;7:971–94.

Hessenius C, Bäder M, Meinhold H, et al. Vasoactive intestinal peptide receptor scintigraphy in patients with pancreatic adenocarcinomas or neuroendocrine tumors. Eur J Nucl Med. 2000;27:1684–93.

Hilden TJ, Nurmi SM, Fagerholm SC, Gahmberg CG. Interfering with leukocyte integrin activation-a novel concept in the development of anti-inflammatory drugs. Ann Med. 2006;38:503–11.

Hollenbeck ST, Itoh H, Louie O, et al. Type I collagen synergistically enhances PDGF-induced smooth muscle cell proliferation through pp60src-dependent crosstalk between the α2β1 integrin and PDGFβ receptor. Biochem Biophys Res Commun. 2004;325:328–37.

Horton MA. Interactions of connective tissue cells with the extracellular matrix. Bone. 1995;17:51S–3.

Hosotani R, Kawaguchi M, Masui T, et al. Expression of integrin alphaVbeta3 in pancreatic carcinoma: relation to MMP-2 activation and lymph node metastasis. Pancreas. 2002;25:e30–5.

Hubalewska-Dydejczyk A, Sowa-Staszczak A, Mikolajczak R, et al. ^{99m}Tc labeled GLP-1 scintigraphy with the use of [Lys40-(Ahx-HYNIC/EDDA) NH2]-Exendin-4 in the insulinoma localization. J Nucl Med. 2011;52 Suppl 1:561.

Igarashi H, Ito T, Mantey SA, Pradhan TK, et al. Development of simplified vasoactive intestinal peptide analogs with receptor selectivity and stability for human vasoactive intestinal pep-tide/pituitary adenylate cyclase-activating polypeptide receptors. J Pharmacol Exp Ther. 2005;315:370–81.

Imhof A, Brunner P, Marincek N, et al. Response, survival, and long-term toxicity after therapy with the radio-labeled somatostatin analogue [90Y-DOTA]-TOC in metastasized neuroendocrine cancers. J Clin Oncol. 2011;29:2416–23.

Isberg RR, Van Nhieu GT. The mechanism of phagocytic uptake promoted by invasin-integrin interaction. Trends Cell Biol. 1995;5:120–4.

Iten F, Muller B, Schindler C, et al. Response to [90Yttrium-DOTA]-TOC treatment is associated with long-term survival benefit in metastasized medullary thyroid cancer: a phase II clinical trial. Clin Cancer Res. 2007;13:6696–702.

Jain R. Transport of molecules in the tumor interstitium: a review. Cancer Res. 1987;47:3039–51.

Jong M, Valkema R, Jamar F, et al. Somatostatin receptor-targeted radionuclide therapy of tumors: preclinical and clinical findings. Semin Nucl Med. 2002;32(2):133–40.

Kaltsas GA, Papadogias D, Makras P, Grossman AB. Treatment of advanced neuroendocrine tumours with radiolabelled somatostatin analogues. Endocr Relat Cancer. 2005;2:683–99.

Korner M, Stockli M, Waser B, et al. GLP-1 receptor expression in human tumors and human normal tissues: potential for in vivo targeting. J Nucl Med. 2007;48:736.

Krenning EP, de Jong M, Kooij PP, et al. Radiolabelled somatostatin analogue(s) for peptide receptor scintigraphy and radionuclide therapy. Ann Oncol. 1999;10 Suppl 2:S23–9.

Krenning EP, Valkema R, Kwekkeboom DJ, et al. Molecular imaging as in vivo molecular pathology for gastroenteropancreatic neuroendocrine tumors: implications for follow-up after therapy. J Nucl Med. 2005;46 Suppl 1:76S–82.

Kunikowska J, Krolicki L, Hubalewska-Dydejczyk A. Clinical results of radionuclide therapy of neuroendocrine tumours with (90)Y-DOTATATE and tandem (^{90})Y/(^{177})Lu-DOTATATE: which is a better therapy option? Eur J Nucl Med Mol Imaging. 2011;38(10):1788–97.

Kwekkeboom DJ, Teunissen JJ, Bakker WH, et al. Radiolabeled somatostatin analog [177Lu-DOTA0, Tyr3]octreotate in patients with endocrine gastroentero-pancreatic tumors. J Clin Oncol. 2005; 23:2754–62.

Kwekkeboom DJ, Teunissen JJ, Kam BL, Valkema R, de Herder WW, Krenning EP. Treatment of patients who have endocrine gastroenteropancreatic tumors with radiolabeled somatostatin analogues. Hematol Oncol Clin North Am. 2007;21:561–73.

Lal H, Verma SK, Foster DM, et al. Integrins and proximal signaling mechanisms in cardiovascular disease. Front Biosci. 2009;14:2307–34.

Laverman P, Joosten L, Eek A, et al. Comparative biodistribution of 12 ^{111}In-labelled gastrin/CCK2 receptor-targeting peptides. Eur J Nucl Med Mol Imaging. 2011;38:1410–6.

Liu S. Radiolabeled multimeric cyclic RGD peptides as integrin αvβ3 targeted radiotracers for tumor imaging. Mol Pharm. 2006;3:472–87.

Liu S. Radiolabeled cyclic RGD peptides as integrin αvβ3-targeted radiotracers: maximizing binding affinity via bivalency. Bioconjug Chem. 2009;20:2199–213.

Liu Z, Liu S, Wang F, Liu S, Chen X. Noninvasive imaging of tumor integrin expression using 18F-labeled RGD dimer peptide with PEG4 linkers. Eur J Nucl Med Mol Imaging. 2009;36:1296–307.

Liu Z, Liu S, Niu G, Wang F, Liu S, Chen X. Optical imaging of integrin αvβ3 expression with near-infrared fluorescent RGD dimer with tetra(ethylene glycol) linkers. Mol Imaging. 2010;9:21–9.

MacDonald PE, El-Kholy W, Riedel MJ, et al. The multiple actions of GLP-1 on the process of glucose-stimulated insulin secretion. Diabetes. 2002;51 Suppl 3: S434–42.

Maddalena ME, Fox J, Chen J, et al. ^{177}Lu-AMBA biodistribution, radiotherapeutic efficacy, imaging, and autoradiography in prostate cancer models with low GRP-R expression. J Nucl Med. 2009;50:2017–24.

Mariani G, Erba PA, Signore A. Receptor-mediated tumor targeting with radiolabeled peptides: there is more to it than somatostatin analogs. J Nucl Med. 2006;47:1904–7.

Meier JJ, Nauck MA. Glucagon-like peptide 1 (GLP-1) in biology and pathology. Diabetes Metab Res Rev. 2005;21:91.

Miao Y, Benwell K, Quinn TP. ^{99m}Tc- and ^{111}In-labeled α-melanocyte-stimulating hormone peptides as imaging probes for primary and pulmonary metastatic melanoma detection. J Nucl Med. 2007;48:73–80.

Miller WH, Keenan RM, Willette RN, et al. Identification and in vivo efficacy of small-molecule antagonists of integrin αvβ3 (the vitronectin receptor). Drug Discov Today. 2000;5:397–408.

Miyata S, Koshikawa N, Yasumitsu H, et al. Trypsin stimulates integrin α5β1-dependent adhesion to fibronectin and proliferation of human gastric carcinoma cells through activation of proteinase-activated receptor-2. J Biol Chem. 2000;275:4592–8.

Modlin IM, Oberg K, Chung DC, et al. Gastroenteropancreatic neuroendocrine tumours. Lancet Oncol. 2008;9:61–72.

Nissinen L, Pentikäinen OT, Jouppila A, et al. A small-molecule inhibitor of integrin α2β1 introduces a new strategy for antithrombotic therapy. Thromb Haemost. 2010;103:387–97.

Nock BA, Maina T, Behe M, et al. CCK-2/gastrin receptor-targeted tumor imaging with 99mTc-labeled minigastrin analogs. J Nucl Med. 2005;46:1727–3176.

Norenberg JP, Krenning BJ, Konings IRHM, et al. 213Bi-[DOTA0, Tyr3]octreotide peptide receptor radionuclide therapy of pancreatic tumors in a preclinical animal model. Clin Cancer Res. 2006;12: 897–903.

Oberg K. Carcinoid tumors: molecular genetics, tumor biology, and update of diagnosis and treatment. Curr Opin Oncol. 2002;14:38–45.

Oberg K. Future aspects of somatostatin-receptor mediated therapy. Neuroendocrinology. 2004;80 Suppl 1:57–61.

Ohki-Hamazaki H, Iwabuchi M, Maekawa F. Development and function of bombesin-like peptides and their receptors. Int J Dev Biol. 2005;49:293–300.

Okarvi SM. Peptide-based radiopharmaceuticals: future tools for diagnostic imaging of cancers and other diseases. Med Res Rev. 2004;24:357–97.

Otte A, Mueller-Brand J, Dellas S, et al. Yttrium-90-labelled somatostatin-analogue for cancer treatment. Lancet. 1998;351:417.

Otte A, Herrmann R, Heppeler A, Behe M, Jermann E, Powell P, Maecke HR, Muller J. Yttrium-90 DOTATOC: first clinical results. Eur J Nucl Med. 1999;26:1439–47.

Pansky P, De Weerth A, Fasler-Kan E, et al. Gastrin releasing peptide-preferring bombesin receptors mediate growth of human renal cell carcinoma. J Am Soc Nephrol. 2000;11:1409–18.

Pattou F, Kerr-Conte J, Wild D. GLP-1-receptor scanning for imaging of human beta cells transplanted in muscle. N Engl J Med. 2010;363:1289–90.

Prasanphanich AF, Nanda PK, Rold TL, et al. [^{64}Cu-NOTA-8-Aoc-BBN(7-14)NH2] targeting vector for positron-emission tomography imaging of gastrin-releasing peptide receptor-expressing tissues. Proc Natl Acad Sci U S A. 2007;104:12462–7.

Raderer M, Kurtaran A, Leimer M, et al. Value of peptide receptor scintigraphy using 123I-vasoactive intestinal peptide and ^{111}In-DTPA-D-Phe1-octreotide in 194 carcinoid patients: Vienna University Experience, 1993 to 1998. J Clin Oncol. 2000;18:1331–6.

Reardon DA, Nabors LB, Stupp R. Cilengitide: an integrin-targeting arginine-glycine-aspartic acid peptide with promising activity for glioblastoma multiforme. Expert Opin Investig Drugs. 2008;17:1225–35.

Reubi JC, Macke HR, Krenning EP. Candidates for peptide receptor radiotherapy today and in the future. J Nucl Med. 2005;46 Suppl 1:67S–75.

Rufini V, Calcagni ML, Baum RP. Imaging of neuroendocrine tumors. Semin Nucl Med. 2006;36:228–47.

Sheldrak HM, Patterson LH. Function and antagonism of beta3 integrins in the development of cancer therapy. Curr Cancer Drug Targets. 2009;9:519–40.

Shi J, Wang L, Kim YS, et al. Improving tumor uptake and excretion kinetics of 99mTc-labeled cyclic arginine-glycine-aspartic (RGD) dimers with triglycine linkers. J Med Chem. 2008;51:7980–90.

Shi J, Kim YS, Zhai S, et al. Improving tumor uptake and pharmacokinetics of 64Cu-labeled cyclic RGD peptide dimers with Gly3 and PEG4 linkers. Bioconjug Chem. 2009;20:750–9.

Singh P, Reimer CL, Peters JH, et al. The spatial and temporal expression patterns of integrin α9β1 and one of its ligands, the EIIIA segment of fibronectin, in cutaneous wound healing. J Invest Dermatol. 2004;123: 1176–81.

Smith JW. Cilengitide Merck. Curr Opin Investig Drugs. 2003;4:741–5.

Smith CJ, Gali H, Sieckman GL, et al. Radiochemical investigations of 177Lu-DOTA-8-Aoc-BBN[7-14] NH2: an in vitro/in vivo assessment of the targeting ability of this new radio-pharmaceutical for PC-3 human prostate cancer cells. Nucl Med Biol. 2003;30:101–9.

Sowa-Staszczak A, Stefanska A, Pach D, et al. First clinical application of 99mTc labelled long-acting agonist of GLP-1 (Exendin-4) in endocrine diagnosis. Eur J Nucl Med Mol Imaging. 2011;38 Suppl 2:S206.

Stefanelli T, Malesci A, De La Rue SA, Danese S. Anti-adhesion molecule therapies in inflammatory bowel disease: touch and go. Autoimmun Rev. 2008;7: 364–9.

Switala-Jelen K, Dabrowska K, Opolski A, et al. The biological functions of beta3 integrins. Folia Biol (Praha). 2004;50:143–52.

Takayama S, Ishii S, Ikeda T, et al. The relationship between bone metastasis from human breast cancer and integrin alpha(v)beta3 expression. Anticancer Res. 2005;25:79–83.

Tanaka K, Masu M, Nakanishi S. Structure and functional expression of the cloned rat neurotensin receptor. Neuron. 1990;4:847–54.

Tang-Christensen M, Larsen PJ, Thulesen J, et al. The proglucagon-derived peptide, glucagon-like peptide-2, is a neurotransmitter involved in the regulation of food intake. Nat Med. 2000;6(7):802–7.

Temming K, Schiffelers RM, Molema G, Kok RJ. RGD based strategies for selective delivery of therapeutics and imaging agents to the tumour vasculature. Drug Resist Updat. 2005;8:381–402.

Teunissen JJ, Kwekkeboom DJ, de Jong M, et al. Endocrine tumours of the gastrointestinal tract. Peptide receptor radionuclide therapy. Best Pract Res Clin Gastroenterol. 2005;9:595–616.

Tsuji T. Physiological and pathological roles of α3β1 integrin. J Membr Biol. 2004;200:115–32.

Tucker GC. Integrins: molecular targets in cancer therapy. Curr Oncol Rep. 2006;8:96–103.

Valkema R, de Jong M, Bakker WH, et al. Phase I study of peptide receptor radionuclide therapy with [111In-DTPA0]Octreotide: The Rotterdam experience. Semin Nucl Med. 2002;32:110–22.

Valkema R, Pauwels SA, Kvols LK, et al. Long-term follow-up of renal function after peptide receptor radiation therapy with 90Y-DOTA0, Tyr3-octreotide and 177Lu-DOTA0, Tyr3-octreotate. J Nucl Med. 2005;46 Suppl 1:83S–91.

Valkema R, Pauwels S, Kvols LK, et al. Survival and response after peptide receptor radionuclide therapy with [90Y-DOTA0, Tyr3]octreotide in patients with advanced gastroentero-pancreatic neuroendocrine tumors. Semin Nucl Med. 2006;36:147–56.

Van Den Bossche B, Van de Wiele C. Receptor imaging in oncology by means of nuclear medicine: current status. J Clin Oncol. 2004;22:3593–607.

van Essen M, Krenning EP, De Jong M, et al. Peptide receptor radionuclide therapy with radiolabelled somatostatin analogues in patients with somatostatin receptor positive tumours. Acta Oncol. 2007a;46:723–34.

van Essen M, Krenning EP, Bakker WH, et al. Peptide receptor radionuclide therapy with 177Lu-octreotate in patients with foregut carcinoid tumours of bronchial, gastric and thymic origin. Eur J Nucl Med Mol Imaging. 2007b;34:1219–27.

Vincent JP, Mazella J, Kitabgi P. Neurotensin and neurotensin receptors. Trends Pharmacol Sci. 1999;20: 302–9.

Virgolini I, Raderer M, Kurtaran A, et al. ^{123}I-vasoactive intestinal peptide (VIP) receptor scanning: update of imaging results in patients with adenocarcinomas and endocrine tumors of the gastrointestinal tract. Nucl Med Biol. 1996;23:685–92.

Waldherr C, Pless M, Maecke HR, et al. The clinical value of [^{90}Y-DOTA]-D-Phe1-Tyr^{3}-octreotide (^{90}Y-DOTATOC) in the treatment of neuroendocrine tumours: a clinical phase II study. Ann Oncol. 2001;12:941–5.

Waldherr C, Pless M, Maecke HR, et al. Tumor response and clinical benefit in neuroendocrine tumors after 7.4 GBq 90Y-DOTATOC. J Nucl Med. 2002;43: 610–6.

Walsh JH. Gastrointestinal hormones. In: Johnson LR, editor. Physiology of the gastrointestinal tract. 3rd ed. New York: Raven Press, Ltd; 1994. p. 1–128.

Wang L, Shi J, Kim YS, et al. Improving tumor-targeting capability and pharmacokinetics of 99mTc-labeled cyclic RGD dimers with PEG4 linkers. Mol Pharm. 2009;6:231–45.

Wegener KL, Campbell ID. Transmembrane and cytoplasmic domains in integrin activation and protein-protein interactions (review). Mol Membr Biol. 2008;25:76–87.

Wei L, Butcher C, Miao Y, et al. Synthesis and biologic evaluation of 64Cu-labeled rhenium-cyclized α-MSH peptide analog using a cross-bridged cyclam chelator. J Nucl Med. 2007a;48:64–72.

Wei L, Miao Y, Gallazzi F, et al. Gallium-68-labeled DOTA-rhenium-cyclized α-melanocyte-stimulating hormone analog for imaging of malignant melanoma. Nucl Med Biol. 2007b;34:945–53.

Wicki A, Wild D, Storch D, et al. [Lys40(Ahx-DTPA-111In)NH2]-Exendin-4 is a highly efficient radiotherapeutic for glucagon-like peptide-1 receptor-targeted therapy for insulinoma. Clin Cancer Res. 2007;13: 3696–705.

Wild D, Macke H, Christ E, et al. Glucagon-like peptide 1-receptor scans to localize occult insulinomas. N Engl J Med. 2008;359:766–8.

Wild D, Christ E, Caplin ME, et al. Glucagon-like peptide-1 versus somatostatin receptor targeting reveals 2 distinct forms of malignant insulinomas. J Nucl Med. 2011;52:1073–8.

Yoshimoto M, Ogawa K, Washiyama K, et al. αvβ3 Integrin-targeting radionuclide therapy and imaging

with monomeric RGD peptide. Int J Cancer. 2008;123:709–71.

Yusta B, Huang L, Munroe D, et al. Enteroendocrine localization of GLP-2 receptor expression in humans and rodents. Gastroenterology. 2000;119(3):744–55.

Zecchinon L, Fett T, Baise E, Desmecht D. Characterization of the caprine (Capra hircus) beta-2 integrin CD18-encoding cDNA and identification of mutations potentially responsible for the ruminantspecific virulence of Mannheimia haemolytica. Mol Membr Biol. 2004;21:289–95.

Zhang H, Chen J, Waldherr C, et al. Synthesis and evaluation of bombesin derivatives on the basis of pan-bombesin peptides labeled with indium-111, lutetium-177, and yttrium-90 for targeting bombesin receptor-expressing tumors. Cancer Res. 2004;64:6707–15.

Zhang H, Schuhmacher J, Waser B, et al. DOTA-PESIN, a DOTA-conjugated bombesin derivative designed for the imaging and targeted radionuclide treatment of bombesin receptor-positive tumours. Eur J Nucl Med Mol Imaging. 2007;34:1198–208.

Zheng DQ, Woodard AS, Fornaro M, et al. Prostatic carcinoma cell migration via αvβ3 integrin is modulated by a focal adhesion kinase pathway. Cancer Res. 1999;59:655–1664.

Zhou X, Murphy FR, Gehdu N. Engagement of αvβ3 integrin regulates proliferation and apoptosis of hepatic stellate cells. J Biol Chem. 2004;20279:23996–4006.

Therapeutic Radiopharmaceuticals for Treatment of Primary and Metastatic Hepatic Cancer

11

11.1 Introduction

HCC represents the sixth most common malignancy worldwide and the third most common cause of cancer-related mortality causes estimated to result in half a million deaths annually (Parkin et al. 2005; Bosch et al. 2004; El-Serag et al. 1992). The most relevant risk factors for HCC include chronic hepatitis C (HCV) infection, hepatitis B (HBV) infection, alcoholic cirrhosis, and nonalcoholic fatty liver (steatohepatitis) (Deuffic et al. 1998). While local therapy by surgical resection with tumor-free margins (llovet et al. 2003) or liver transplantation (Bismuth and Majno 2000) represent potentially curative treatments, only one third of patients with HCC are suitable candidates for hepatic resection, due to either anatomic location of the lesion(s), lesion size, the number of lesions, concurrent nonmalignant liver disease, or insufficient hepatic reserve. Although another therapeutic option widely practiced for primary and secondary hepatic malignancies is systemic chemotherapy, it is confined to tumor response rates of less than 30 % (Vassiliou et al. 2007; Dawson et al. 2000). The use of external beam radiotherapy making use of intensity-modulated radiotherapy (IMRT) for the treatment of primary of metastatic liver tumors is often of limited use in patients with diffuse, multiple lesions, due to the low tolerance of normal liver parenchyma to radiation. The cytotoxic dose required to eradicate solid tumor is estimated to be ~70 Gy, which is far greater than the liver tolerance dose of 35 Gy that could be delivered to the whole liver by IMRT in 1.8 Gy/day fractions (Dawson et al. 2000; Kennedy et al. 2007). Therefore, palliative management has emerged as the mainstay of therapy for most patients with inoperable HCC (Cammà et al. 2002; Cabibbo et al. 2010). Given the limited efficacy of external beam radiotherapy approaches for the treatment of HCC, a number of techniques to deliver targeted tumor radiation by means of radiopharmaceuticals have thus been developed and evaluated.

Transarterial chemoembolization (TACE) is a locoregional therapy that involves the injection of chemotherapeutic agents, with or without lipiodol and embolic agents, into the branch of the hepatic artery that feeds the tumor. This regional therapy is widely used for unresectable HCC to achieve a higher local concentration of the agents with limited systemic toxicity (Geschwind 2002). In TACE of HCC, single-agent doxorubicin is most commonly used in Europe and Japan, while the combination of mitomycin C, doxorubicin, and cisplatin is more popular in the USA. Single or combination agents are typically emulsified in lipiodol, an oily contrast agent believed to increase intratumoral retention of the cytotoxic agent (Kennedy and Sangro 2014).

Radionuclide therapy for HCC thus appears to be an effective therapeutic option, for the treatment of large inoperable HCC, particularly with

F.F. (Russ) Knapp, A. Dash, *Radiopharmaceuticals for Therapy*, DOI 10.1007/978-81-322-2607-9_11

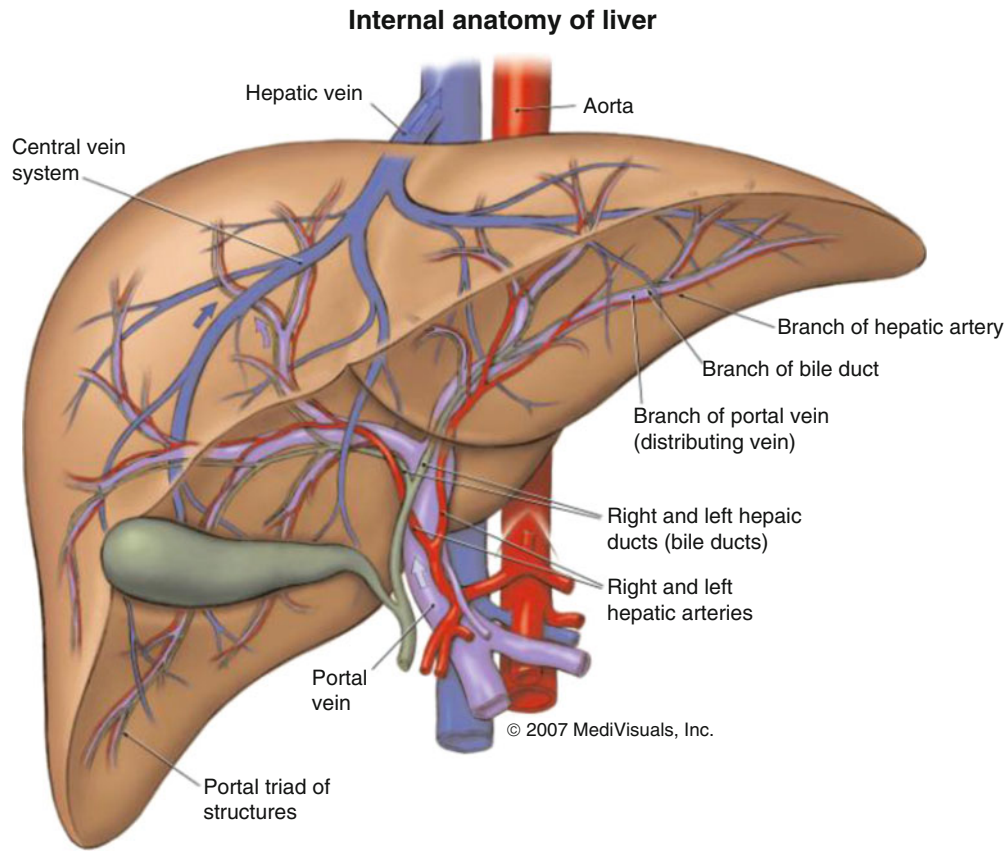

Fig. 11.1 Illustration of the hepatic blood supply

portal vein thrombosis and of small inoperable tumors unsuitable for any reason for percutaneous therapy embolization, with or without chemotherapeutic agents. This technology is also practiced as neoadjuvant therapy before hepatic transplantation to reduce the risk of recurrence in the graft or before hepatic resection to shrink the tumor size or as an adjuvant therapy after surgery or percutaneous ablative therapy to reduce the risk of recurrence. The selection of an appropriate treatment option for HCC is very patient specific/personalized and depends on careful assessment of tumor staging and assessment of the underlying liver disease. Strategies for delivery of radionuclide to the liver for the purpose and targeting the tumor can be accomplished by three distinct modalities. Direct intratumor implantation of the radionuclide is possible and parenteral injection of radiolabeled antibodies specific to HCC antigens (radioimmunotherapy) is also an option. The most appealing option for HCC treatment is trans-arterial radioisotope therapy (TART) involving direct administration of radionuclide through the hepatic artery directly into the tumor. The major blood supply to hepatocytes in the liver parenchyma is via the portal vein, and tumors are generally fed via the hepatic arterial supply (Fig. 11.1) which represents an accessible avenue to administer these radioactive agents.

11.2 Direct Intratumor Implantation

Direct introduction of the radionuclide into the target lesion tumor under ultrasonographic guidance is one of the procedures often used with varying success (Tian et al. 1996; Goh et al. 2007;

Kim et al. 2006). Major drawbacks of this modality is the growing concern regarding the leakage of radioactivity outside the tumor into the peritoneal cavity, difficulties in achieving a homogenous distribution of radioactivity over a large tumor mass, and difficulties in treating percutaneously inaccessible tumors.

11.3 Radioimmunotherapy

Radioimmunotherapy (RAIT) is another therapeutic approach for patients with HCC and a variety of antibodies such as anti-CEA antibodies and anti-AFP, and anti-ferritin labeled with ^{131}I or ^{90}Y have been widely evaluated for this purpose (Order et al. 1985, 1986, 1991; Fan et al. 1992; Liu et al. 1989; Tang et al. 1990; Abrams et al. 1998). Ferritin is both a normal tissue- and tumor-associated protein which acts as an immunosuppressant and as an iron storage protein. As a tumor-associated protein, it is related to virally induced tumors. As one example, the State Food and Drug Administration in the People's Republic of China (PRC) has approved ^{131}I-metuximab (Licartin, Chengdu Huasun Bio-Tech) as a therapeutic anti-HCC radioimmunological agent for the treatment of unresectable HCC. As another example, ^{131}I-metuximab is an iodine ^{131}I-labeled murine monoclonal antibody (mAb) HAb18 F(ab')$_2$ fragment against the HCC-associated antigen HAb18G/CD147. The mAb HAb18 (immunoglobulin G1) has been obtained by use of a cell suspension extracted from fresh human HCC tissues to immunize BALB/c mice and for hybridoma preparation. Its HAb18G/CD147 antigen was highly expressed on HCC cells and is a member of the CD147 family (Chen et al. 2006; Zhang et al. 2006; Zeng et al. 2002). Although some positive results have been reported, this form of treatment has several limitations which include the heterogeneity of tumor cells and not all the cells express the same antigen. In addition, there is poor localization of murine immunoglobulin in tumor tissue, probably resulting from the large variation of tumor vascularity and irregular penetration of antibodies into large tumors which contain a necrotic center. Bone marrow toxicity caused by the presence of radiolabeled antibodies in the peripheral circulation can also be encountered, and host reaction to the murine antibodies may lead to the potentially dangerous development of human anti-mouse antibodies (HAMA).

11.4 Trans-arterial Radioisotope Therapy (TART)

In contrast, trans-arterial radioisotope therapy is a promising technique that exploits the unique hepatic dual blood supply, involving both the portal vein and hepatic artery. In a normal functioning liver, the portal vein is responsible for supplying the majority of blood to the liver parenchyma (75–80 %), with the hepatic artery providing only 20–25 %. This balance is significantly altered in HCC where the hepatic artery solely provides perfusion to the tumor and liver parenchyma derives >75 % of its blood supply from the portal vein. HCCs are rich in vasculature and almost exclusively dependent on arterial blood supply. This anatomical configuration precisely provides the basis for the development of trans-arterial radioisotope therapy for the treatment of HCC. Radiolabeled microspheres with a diameter between 20 and 50 μm are selectively injected into the hepatic vessels supply tumors and selectively congregate in the hepatic end-arterioles, allowing localized delivery of therapeutic doses, while sparing the surrounding liver parenchyma (Ackerman et al. 1970). The goal of TART is to cause tumor necrosis and tumor control while preserving as much functional liver tissue as possible and so to prolong life. Thus, it is essentially a flow-directed mode of radionuclide treatment that is dependent on neoangiogenesis.

The advantages of TART include radioisotopic tumor-destroying effects of the radioisotope which are independent on the HCC cellular characteristics since it is not necessary for the radioisotope to actually be taken up by the tumor cells for the desired destructive irradiation of the adjacent tumor cells. Since the hepatic artery is usually not embolized during this procedure, it can be safely used in patients with compromised

liver function or portal vein thrombosis, which are usually observed in a large number of patients with locally advanced disease. The use of β-emitting therapeutic radioisotopes which also emit gamma photons, such as ^{131}I, ^{188}Re, ^{166}Ho, etc., makes external dosimetry possible which can help in individualizing patient treatment and thus help avoid or reduce side effects/toxicity and help achieve better tumor response by administering the tumoricidal dose (in cases of radioisotopes having gamma emissions). Also, prophylactic irradiation of apparently normal liver parenchyma can reduce the risk of recurrence (adjuvant/neoadjuvant role).

11.5 Selection of Radionuclide for TART

Therapeutic radioisotopes that can be used for the treatment of HCC should meet several criteria which include the emission of radioactive particles, and β^--emitting radionuclides have been of choice for this application because of their regional energy deposition and the wide selection of reactor-produced candidates (Chap. 5). The energy of beta radiation should be adequately intense to create a zone of high radiation exposure confined to the vicinity of the tumor while minimizing non-tumorous hepatic parenchymal exposure to tolerable levels. For these reasons, the use of high-energy β^- radiation with low mean free path is desirable. The physical half-life of the radionuclide is also an important issue and should be relatively short but effective in delivering a cytotoxic radiation dose to the tumor. It also is desirable to use radionuclides with high specific activity, but this is not a necessity and depends on the mass load of the particles. Higher-specific-activity radionuclides provide flexibility to bound desired amount of activity to the embolic particles. The chemical characteristic of the radionuclide should also permit efficient incorporation into a wide range of embolic particles. Finally, the detectable percentage of gamma emission for imaging is advantageous to assess targeting, residence time, and dosimetry to relate dose delivery with response.

11.6 Selection of Microspheres

Radiolabeled microspheres for intra-arterial therapy should (Harbert 1996) be mechanically strong enough to withstand the capillary force during their passage through the capillary network. Excellent chemical stability is also required to circumvent elution of the radiolabel, macrophage removal, or radiolysis to prevent bone marrow toxicity. Uniform particle size is necessary and the density of the particles should be greater than or equal to 1 to prevent settling or streaming. The procedure should be a simple and efficient method for radiolabeling, and the particles should of course be nontoxic, biocompatible, and preferably biodegradable.

11.7 Common Microsphere Materials

Given the scope of using TART for the treatment of HCC, several materials for fabrication of microspheres with a diameter between 20 and 50 μm have been developed and evaluated. Both glass, resins, albumin, and polymers are examples of materials which have been used. Selection of glass is primarily based on its resistant to radiation damage. It is also highly insoluble, nontoxic and spheres of uniform sizes can be readily prepared (Leung et al. 1994). It is possible to produce glass microspheres with negligible leaching (Ehrhardt and Day 1987). While these aspects are appealing, their high density and their nonbiodegradability have emerged as issues which have to be further evaluated (Ho et al. 1997; Mumper et al. 1991). The relatively high-density glass is one of the major barriers that increase the likelihood of intravascular settling (Turner et al. 1994). Resin-based microspheres are attractive for radioembolization as they are insoluble and nontoxic, with commercial availability of uniform sizes, and radionuclides are easily incorporated with high labeling yield. A broad range of commercially available resins such as Bio-Rex 70, Cellex-P, Chelex 100, Sephadex SP, and AG 50W-X8 have been used (Ho et al. 1998; Schubiger et al. 1991; Wang et al. 1998; Burton

et al. 1998). Another advantage is that the resin particles do not undergo degradation in vivo. Human serum albumin (HSA) has been widely used as these particles are biocompatible and biodegradable. Both ^{188}Re and ^{90}Y have been bound to HSA by suspending in sodium acetate buffer and incubated at room temperature (Lau et al. 1994). One of the major impediments of using HSA is the time-consuming labeling process and generally poor radiolabeling yields. Major advantages of polymer-based microspheres are their near-plasma density, biodegradability, and biocompatibility. The poly (L-lactic acid) (PLLA) microspheres have been extensively used for radioembolization of holmium-166 (^{166}Ho), yttrium-90 (^{90}Y), and rhenium-186/rhenium-188 (^{186}Re/^{188}Re) (Watanabe et al. 1999; Jay et al. 1998; Nijsen et al. 1999; O'Donnell and McGinity 1997; Mumper and Jay 1999).

11.8 Radionuclide Used for Treatment of HCC

In this modality, ^{131}I-labeled lipiodol, ^{90}Y microspheres, ^{166}Ho microspheres, and ^{188}Re-labeled lipiodol and microspheres are the radiopharmaceutical agents which have been extensively studied. Physical characteristics of these radionuclide are summarized in Table 11.1.

11.9 Radioisotopes for TART

11.9.1 Iodine-131-Lipiodol

Traditionally, ^{131}I was the first beta-emitting radioisotope which had been used and shown to have some efficacy for TART, and a large number of studies using ^{131}I lipiodol for the treatment of unresectable HCC have been reported (Kooijman et al. 2000; Raoul et al. 1994; Bhattacharya et al. 1995; Risse et al. 2000, 2006; Boucher et al. 2003, 2007; Kanhere et al. 2008; Chua et al. 2010). This agent is commercially available as Lipiocis® (CIS Bio International, Gif sur Yvette, France). Lipiodol is an iodinated ethyl ester of the naturally occurring fatty acids of poppy seed oil containing 38 % of iodine by weight which had been used earlier as a contrast medium for the X-ray detection of HCC which is sequestered and remains in these tumors for a longer period compared to normal liver or other tissues. The ^{131}I is chemically attached to the naturally occurring Lipiodol isomers. In order to preclude the toxicity of ^{131}I, it is essential to block the thyroid gland with perchlorate or Lugol's solution (iodide) before and after the treatment. The procedure involves a selective hepatic artery catheterization and injection of 2–3 mL of ^{131}I-lipiodol with an activity of 0.9–2.4 GBq in single or multiple administrations (Becker et al. 2008; Bretagne et al. 1998). The cumulative radiation doses delivered to tumors generally range from 10 to 260 Gy. The response of HCC and therapeutic outcome is very much dependent on the tumor size as well as the activity levels delivered for treatment. The required therapy activity for the intended tumor dose is calculated for a given tumor mass according to size. There is also a role for ^{131}I lipiodol as an effective therapy option therapy in patients with portal vein thrombosis (Raoul et al. 1994, 2009). One of the main limiting factors for broader use of ^{131}I-lipiodol is the requirement of long period for patient isolation because of the long 8.02-day half-life of ^{131}I. No significant tumor reduction is usually seen in single study treatment of liver metastases. In

Table 11.1 Characteristic of key radionuclides used for TART treatment of HCC

Radionuclide/production mode	Emission	Half-life (days)	Mean soft tissue penetration depth (mm)	Imaging possibility
^{166}Ho/Reactor	β^-, γ	1.2	1.23	Yes
^{131}I/Reactor	β^-, γ	8.04	0.4	Yes
^{188}Re/Reactor	β^-, γ	0.709	4.0	Yes
^{90}Y/Reactor	β^-	2.7	3.0	No

order to achieve optimum response, multiple sessions may be required. Some authors have expressed their concern about hypothyroidism (Toubeau et al. 2001).

11.9.2 ^{90}Y-Labeled Agents

Once ^{90}Y-microspheres became available, and then later when they emerged as approved clinical products, TART with two ^{90}Y-labeled agents emerged as the mainstream treatment modality. The two commercially available ^{90}Y-labeled products are TheraSphere® and SIR-Spheres®. The TheraSphere product consists of small glass particles (MDS Nordion, Ottawa, ON, Canada) and the SIR-Spheres microspheres are fabricated from resin (Sirtex Medical, Sydney, Australia). The TheraSphere® product consists of ^{90}Y embedded into non-biodegradable glass microspheres of 25 μm diameter and have been recently approved by the US Food and Drug Administration (FDA) for treatment of unresectable HCC. SIR-Spheres® consist of biocompatible resin-based microspheres containing ^{90}Y. SIR-Spheres use was granted approval for metastatic colorectal cancer in 2002 (Fig. 11.2). The characteristics of these two preparations are summarized in Table 11.2.

SIR-Spheres® are used for the treatment of unresectable metastatic liver tumors from primary colorectal cancer, with adjuvant intrahepatic artery chemotherapy of floxuridine. The indication for use of TheraSpheres® is for irradiation treatment or as a neoadjuvant to surgery or transplantation in patients with unresectable

Table 11.2 Comparison of commercially available ^{90}Y-microspheres used for treatment of HCC

Characteristics	SIR-Spheres®	TheraSphere®
Material	Resin	Glass
Particle size (μm)	20–60	20–30
Specific gravity	Low (<1.8)	High (>2)
Activity per sphere (Bq)	40–70	2,500
Maximum prescribed activity (GBq)	3	20
Average activity (GBq)	2	5
Average dose rate	1.8 μGy/h, with a maximum of 16 μGy/h	1.9 μGy/h, with a maximum of 12 μGy/h
Particles per administration	20–40 million	1–4 million
Regulatory approval	US FDA approval 1999 (colorectal)	US FDA approval 2002 (HCC)

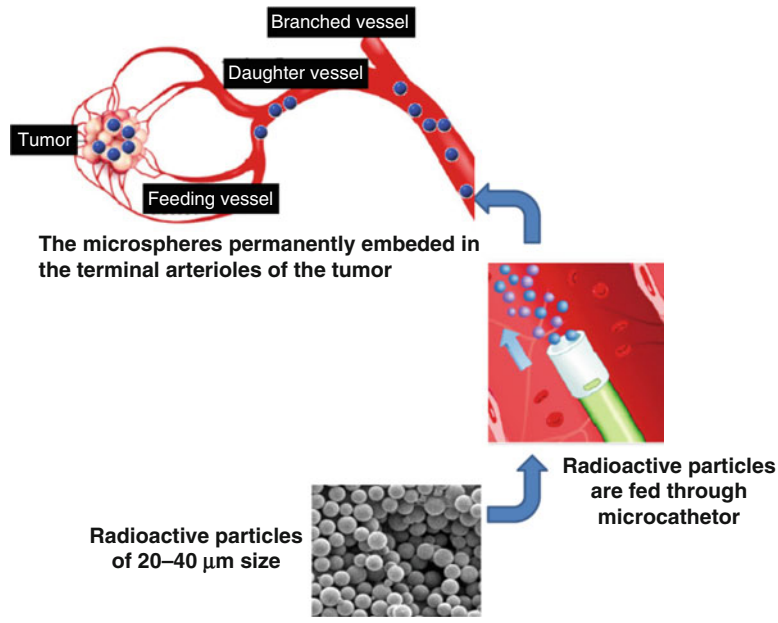

Fig. 11.2 Illustration of intra-arterial release of radioactive microspheres in a hepatic artery

hepatocellular carcinoma, who qualify for appropriate hepatic arterial catheter placement. Both glass and resin microspheres produce heterogeneous high-dose regions in the tumor. After injection, the microspheres deliver over 95 % of their total radioactive dose over a period of 2 weeks. Patients typically receive only two treatments to each lobe of the liver, given at approximately 2 months intervals. Detailed accounts of the recommended clinical procedures and patient indicators have been well studied (Murthy et al. 2005; Lau et al. 2004; Uthappa et al. 2011; Kennedy et al. 2012; Kao et al. 2012; Wang et al. 2010; Iñarrairaegui et al. 2010; Hendlisz et al. 2010; Deleporte et al. 2010; Salem and Thurston 2006). Use of these agents is considered as a safe and efficient treatment modality in salvage therapy of colorectal cancer metastatic to the liver and in unresectable HCC when selection criteria are applied strictly, particularly in terms of liver function tests. Treatments have been shown to have good clinical outcome and to increase survival and are approved as definitive therapy, as abridge to transplantation and as downstaging to surgery.

11.9.3 Rhenium-188 Lipiodol/ Microspheres

In addition to the routine use of the two commercially available ^{90}Y products, a large number of clinical trials have also been reported using ^{188}R-labeled products combined with Lipiodol for the TART application, because of the ready, in-house, on-demand availability of ^{188}Re from the ^{188}W/^{188}Re radionuclide generator system (Chap. 7). A number of embolic platforms of ^{188}Re such as glass microspheres (Chang and Lin 2007), human serum albumin microspheres (HSAM) (Wunderlich et al. 2005), poly-(L-LACTIDE) (PLA) microspheres (Saatchi and Hafeli 2009), and two Lipiodol complex agents have been studied for their possible use for tumor treatment in inoperable HCC (Andreana et al. 2012). Among these, ^{188}Re 4-hexadecyl-1, 2,9,9-tetramethyl-4,7-diaza-1,10-decanethiol (HDD)-labeled iodized oil (Fig. 11.3) has received maximum attention (Kumar et al. 2007; Sundram et al. 2004; Bernal et al. 2007, 2008; Lambert et al. 2004, 2005; Liepe et al. 2007). Rhenium-188 has obvious advantages over use of ^{131}I due to lower γ emission energy, greater β^- penetration, and reduced cost. In addition, the in-house availability of the ^{188}W/^{188}Re radionuclide generator for on-demand preparation of these therapeutic agents was also an important factor. These two lipophilic ^{188}Re-labeled agents (Fig. 11.3) have high miscibility with lipiodol. The resulting quantity of the ^{188}Re HDD iodized oil (lipiodol) administered is based on the radiation absorbed dose (RAD) to critical organs, which is calculated after trans-arterial administration of test dose of the radioconjugate (Kumar et al. 2007). The limited availability as well as the high cost of ^{188}W/^{188}Re generator emerged as the major road block toward its wide-scale applicability. The requirement of greater patient dose due to its shorter half-life is also an impediment. An *International Atomic Energy Agency* (IAEA)-sponsored multicenter study using intra-arterial ^{188}Re lipiodol for the treatment of inoperable HCC showed safety and efficacy of this radioconjugate Bernal et al. 2007, 2008).

While the use of ^{188}Re-HDD/Lipiodol solution constitute a successful exemplar for

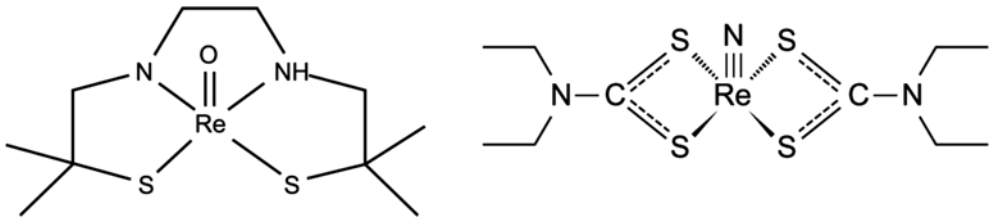

Fig. 11.3 Rhenium-188 lipophilic agents HDD (*left*) and DEDC (*right*) used for TART

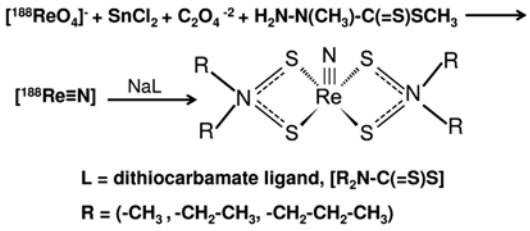

Fig. 11.4 Two-vial, freeze-dried kit formulation strategy

palliative treatment of hepatocellular carcinoma (HCC), requirement of a multi-step synthesis procedure with low labeling yield emerged as the major impediment and thus led to a development of new radiopharmaceuticals that may be produced with high yield. An efficient procedure for radiolabeling lipiodol with ^{188}Re using a two-vial, freeze-dried kit formulation based on the preliminary preparation of the highly lipophilic complex bis(diethyldithiocarbamato) nitrido [^{188}Re] rhenium (^{188}ReN-DEDC) followed by mixing of the complex with lipiodol was successively produced at the Institute of Isotopes in Budapest, Hungary. The preparation of the complex ^{188}ReN-DEDC involved mixing of $[^{188}ReO_4]^-$ with reagents in vial A and glacial acetic acid to yield the intermediate $[^{188}Re \equiv N]^{2+}$ core which was, then, converted into the final complex ^{188}ReN-DEDC by addition of the content of vial B to vial A (Boschi et al. 2004). The reaction scheme is shown in Fig. 11.4.

For ^{188}ReN-DEDC, labeling yields exceeding 95 %, have been reported.

A new class of complexes with perthiobenzoate and dithiobenzoate moieties [M $(PhCS_3)_2$ $(PhCS_2)$] nicknamed SSS, standing for "Super-Six sulphur" (because the metal core is coordinated by six sulphur atoms) was used to developed freeze-dried kits. ^{188}Re-SSS stands for ^{188}Re-$(PhCS_2)(PhCS_3)_2$. Interest on the use of this complexes lies due to the oxidation state + III of the metal which is more stable than + V, and they are, in addition, susceptible to bifunctional approach to design target-specific agents (Fig. 11.5) (Lepareur et al. 2005, Tisato et al. 2006).

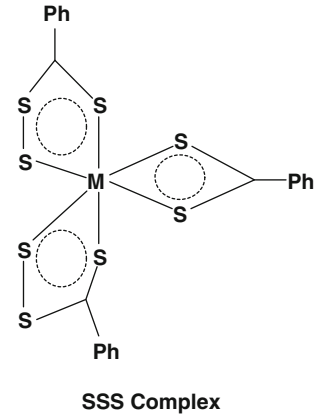

Fig. 11.5 The chemical structure of ^{188}Re-$(PhCS_2)$ $(PhCS_3)_2$

A kit formulation strategy consisting of 0.8 mg $SnCl_2 \cdot 2H_2O$ (dissolved in 0.1 mL HCl 1 M), 7.5 mg sodium gluconate, 30 mg ascorbic acid, and 40 mg potassium oxalate was used. This freeze-dried kit is reconstituted in 0.5 mL saline, and the perrhenate (0.5 mL of saline) is then added. After 15 min at room temperature, 20 mg of sodium dithiobenzoate is added, and the solution is heated for 30 min at 100 °C, to provide the ^{188}Re-SSS complex, as a precipitate. 2–3 mL of Lipiodol is added to the mixture, which is then centrifuged, and the phases are carefully collected. ^{188}Re-SSS/Lipiodol was obtained with >80 % yield (Garin et al. 2004). With a view to prepare therapeutic doses ^{188}Re-SSS/Lipiodol regularly and to preclude excessive radiation exposure to the operator, and particularly at the finger tips, the kit formulation was tuned, and reaction conditions were slightly modified. An optimized kit formulation strategy consisting of 4 mg $SnCl_2 \cdot 2H_2O$ (dissolved in 0.1 mL HCl 1 M), 30 mg sodium gluconate, 30 mg ascorbic acid, and 40 mg potassium oxalate was used. This kit was reconstituted in 0.5 mL saline, and the perrhenate (0.5 mL of saline) was then added. After 15 min at room temperature, 40 mg of sodium dithiobenzoate is added, and the solution is heated for 15 min at 100 °C, to provide the ^{188}Re-SSS complex, as a precipitate. Two to three milliliters of Lipiodol is added to the mixture, which is then

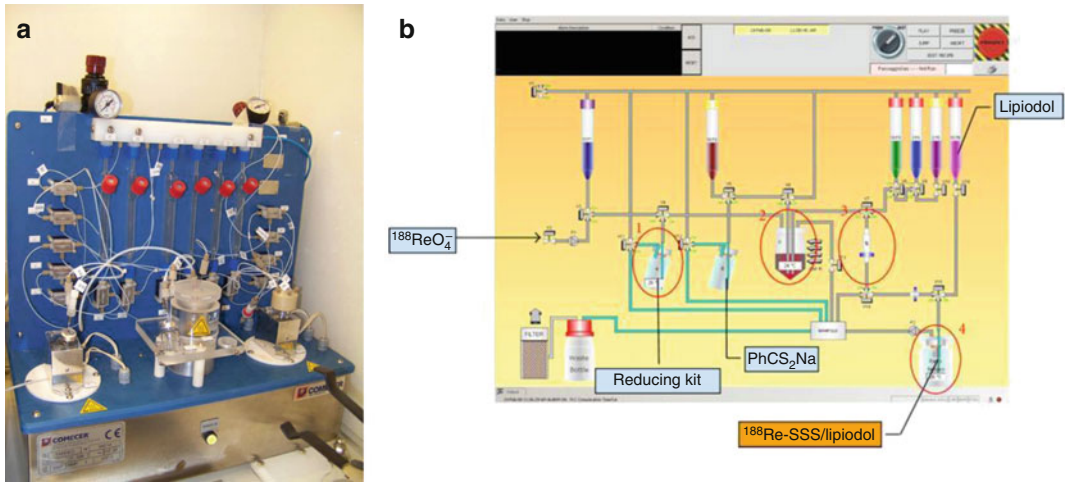

Fig. 11.6 (**a**) TADDEO module (COMECER, Castel Bolognese, Italy). (**b**) Flowchart of the TADDEO module for the preparation of ^{188}Re-SSS/Lipiodol

stirred with a vortex. After 10 min of centrifugation (2200 g), both phases are separated, and the lower phase (radiolabeled Lipiodol) is carefully recovered. ^{188}Re-SSS/Lipiodol is obtained with a 98.56 ± 1.2 % yield and a final RCP of 92.52 ± 2.3 % and is stable for at least 7 days. In the light of the implicit need to limit the radiation exposure to the personnel, as well as to have a reproducible synthesis, development of an automated procedure is not only an interesting proposition but also a necessity. The remote-controlled system employed is a TADDEO module (COMECER, Castel Bolognese, Italy) and is depicted in Fig. 11.6 (Lepareur et al. 2011). The main change was the substitution of the centrifugation step and the use of solid-phase extraction cartridges to purify the product. The final yield is somewhat lower than with manual preparation (%), due to the loss of activity in the tubing and the vessels.

11.9.4 Holmium-166

When complexed with poly (L-lactide) (PLA) (Vente et al. 2009; Smits et al. 2010) and the Chitosan embolic platform (Kim et al. 2006), ^{166}Ho has also been evaluated for the TART application. Chitosan is a unique substance derived from chitin from the shells of crustaceans and has the ability to dissolve in water under acidic conditions but forms a gel in basic environments. The use of holmium/chitosan complex propagated by Milican, Dong Wha Pharmaceutical Co., Seoul, Korea, was found to be effective in treating small HCCs (<3 cm in size) (Sohn et al. 2009); however the effectiveness for treatment of large size HCCs is still under evaluation (Sohn et al. 2009; Lee et al. 2011; Lee and Seong 2012).

11.10 Comparison of Properties of Radioisotopes Used for TART

A variety of options using a range of isotopes for this modality of treatment have been discussed and their comparative advantages and disadvantages have been indicated in Table 11.3 (Salem and Thurston 2006; Burrill et al. 2011). Each radionuclide as well as the embolic carrier has its unique set of benefits and limitations, but since every institution has different scientific and technical resources, each radionuclide would be expected to have a place.

Table 11.3 Radionuclide used for treatment of hepatocellular carcinoma (HCC)

Radionuclide	Advantages	Disadvantage
Iodine-131	Ready availability as required	Long half-life necessitates longer hospitalization for patient (~1 week)
	Accompanying γ emission facilitates post-procedural imaging	High γ energy may cause collateral damage to surrounding tissues
	High tumor/nontumor ratio	Short β^- range entails multiple sessions to achieve optimum response
	Offers possibility to treat patient with portal vein thrombosis owing to low embolic load	Shunting can cause lung fibrosis resulting in death in approximately 1 % of cases
	Precludes collateral arterial embolization prior to radioembolization	Although reduction in abdominal pain could be successfully achieved, there is marginal reduction in tumor size
	Easy preparation protocol	
	Ideal for postsurgical adjuvant therapy	
Yttrium-90	A high-energy pure β^- emitter, with a mean tissue penetration of 2.5 mm with to a maximum depth of 11 mm. This limited tissue penetration allows local high-dose radiation with less risk of radiation-induced hepatic necrosis	The absence of γ-ray emission component in ^{90}Y complicates dosimetric studies
	Offers scope for delivering of a higher liver tumor radiation dose compared with other radioisotopes currently used in this treatment modality	Kit formulation procedure is designed primarily for safety, however, can be somewhat cumbersome during administration
	Pure ^{90}Y radioactive species without mutant radioactive species	Unable to check for reflux or stasis during administration
	Treatment can be repeated or fractionated	
	Availability of easy to use kit formulation procedure	
	Extensively published clinical outcome literatures	
Rhenium-188	β^- and γ emission permits convenient post-procedural dosimetry	Requirement of greater patient dose required due to shorter half-life. A four- to fivefold higher ^{188}Re activity is required to obtain an equivalent absorbed dose compared to ^{90}Y
	Convenient site availability of ^{188}Re from the ^{188}W/^{188} Re generator	Unavailability of kit formulation procedure as well as limited availability of ^{188}W/^{188}Re generator
Holmium-166	Permits imaging using fluoroscopy owing to high X-ray attenuation	Lower energy and shorter half-life than ^{90}Y and therefore a lower absorbed dose requiring three times more radioactivity than ^{90}Y
	Paramagnetic characteristics could allow visualization by MRI	Requirement of supra-selective catheterization
	Biodegradability of the embolic matrix (both PLA and chitosan) is an added advantage	In order to avoid leaching, it is essential to perform serum alkalinization prior to therapy
		Low therapeutic index is a major deterrent
		Cumbersome microdosimetry protocol

11.11 Summary

Radionuclide therapy has been established to have an important role in the management of liver tumors and has the capability of improving survival and the quality of life of HCC patients. Radionuclide therapy of HCC with ^{90}Y-labeled microspheres has emerged as the promising technique, in which outpatient treatment can be administered in a day clinic setting, whereas

radiolabeled lipiodol treatment with ^{131}I or ^{188}Re requires additional radioprotective measures and a hospital stay of 2–7 days. This revolutionary approach capitalizes on the basic principles of tumor hypervascularity, concentrating radiation within that tumor, while at the same time minimizing the risks of non-target radiation. In light of the perceived need to minimize toxicity, it is of utmost importance to identify predictive variables for those patients who are most likely to develop toxicity and side effects after TART. Additional studies are warranted not only to improve our understanding of the relative perfusion of radioactive microspheres to tumor versus benign liver but also to develop ideal dosimetry techniques to optimize tumor kill while sparing the surrounding liver. Despite the unequivocal success of ^{90}Y-labeled microspheres, the requirement of two angiographic procedures per treatment session is one of the drawbacks that may offset the advantages. Despite the unambiguous success of the RIT and the progresses that has been achieved thus far, there is still a need to develop new, tailored radioimmunoconjugates to enhance tumor uptake and retention to identify novel agents for more efficient tumor targeting.

References

Abrams RA, Pajak TF, Haulk TL, et al. Survival results among patients with alpha-fetoprotein-positive, unresectable hepatocellular carcinoma: analysis of three sequential treatments of the RTOG and Johns Hopkins Oncology Center. Cancer J Sci A. 1998;4:178–84.

Ackerman NB, Lien WM, Kondi ES, et al. The blood supply of experimental liver metastases. I: the distribution of hepatic artery and portal vein blood to "small" and "large" tumors. Surgery. 1970;66:1067–72.

Andreana L, Isgrò G, Marelli L, et al. Treatment of hepatocellular carcinoma (HCC) by intra-arterial infusion of radioemitter compounds: trans-arterial radio-embolisation of HCC. Cancer Treat Rev. 2012;38(6):641–64.

Becker S, Laffont S, Vitry F, et al. Dosimetric evaluation and therapeutic response to internal radiation therapy of hepatocarcinomas using iodine-131-labelled lipiodol. Nucl Med Commun. 2008;29:815–25.

Bernal P, Raoul JL, Vidmar G, et al. Intra-arterial rhenium-188 lipiodol in the treatment of inoperable hepatocellular carcinoma: results of an IAEA-sponsored multination study. Int J Radiat Oncol Biol Phys. 2007;69(5):1448–55.

Bernal P, Raoul JL, Stare J, et al. International Atomic Energy Agency-sponsored multination study of intra-arterial rhenium-188-labeled lipiodol in the treatment of inoperable hepatocellular carcinoma: results with special emphasis on prognostic value of dosimetric study. Semin Nucl Med. 2008;38(2):S40–5.

Bhattacharya S, Novell JR, Dusheiko GM, et al. Epirubicin-Lipiodol chemotherapy versus 131iodine-Lipiodol radiotherapy in the treatment of unresectable hepatocellular carcinoma. Cancer. 1995;76(11):2202–10.

Bismuth H, Majno PE. Hepatobiliary surgery. J Hepatol. 2000;32 Suppl 1:208–24.

Bosch FX, Ribes J, Diaz M, Cleries R. Primary liver cancer: worldwide incidence and trends. Gastroenterology. 2004;127:S5–16.

Boschi A, Uccelli L, Duatti A, et al. A kit formulation for the preparation of ^{188}Re-lipiodol: preclinical studies and preliminary therapeutic evaluation in patients with unresectable hepatocellular carcinoma. Nucl Med Commun. 2004;25(7):691–9.

Boucher E, Corbinais S, Rolland Y, et al. Adjuvant intra-arterial injection of iodine-131-labeled lipiodol after resection of hepatocellular carcinoma. Hepatology. 2003;38(5):1237–41.

Boucher E, Garin E, Guylligomarc'h A, et al. Intra-arterial injection of iodine-131-labeled lipiodol for treatment of hepatocellular carcinoma. Radiother Oncol. 2007;82(1):76–82.

Bretagne JF, Raoul JL, Bourguet P, Duvauferrier R, Deugnier Y, et al. Hepatic artery injection of I-131-labelled lipiodol – part 2. Radiology. 1998;168: 547–50.

Burrill J, Hafeli U, Liu DM. Advances in radioembolization – embolics and isotopes. J Nucl Med Radiat Ther. 2011;2(1):107.

Burton MA, Gray BN, Klemp PF, et al. Selective internal radiation therapy: distribution of radiation in the liver. Eur J Cancer Clin Oncol. 1998;25:1487–91.

Cabibbo G, Enea M, Attanasio M, et al. A meta-analysis of survival rates of untreated patients in randomized clinical trials of hepatocellular carcinoma. Hepatology. 2010;51(4):1274–83.

Cammà C, Schepis F, Orlando A, et al. Transarterial chemoembolization for unresectable hepatocellular carcinoma. Metall Anal. 2002;224:47–54.

Chang MC, Lin W-Y. The effect of intratumoral injection of ^{188}Re-microspheres on the hematologic, hepatic and renal functions in the treatment of VX2 hepatic tumor: an animal study. Ann Nucl Med Sc. 2007;20:187–92.

Chen ZN, Mi L, Xu J, Song F, Zhang Q, Zhang Z, et al. Targeting radioimmunotherapy of hepatocellular carcinoma with iodine (131I)metuximab injection: clinical phase I/II trials. Int J Radiat Oncol Biol Phys. 2006;65(2):435–44.

Chua TC, Chu F, Butler SP, et al. Intra-arterial iodine-131-lipiodol for unresectable hepatocellular carcinoma. Cancer. 2010;116(17):4069–77.

Dawson LA, McGinn CJ, Normolle D. Escalated focal liver radiation and concurrent hepatic artery fluorodeoxyuridine for unresectable intrahepatic malignancies. J Clin Oncol. 2000;18:2210–8.

Deleporte A, Flamen P, Hendlisz A. State of the art: radiolabeled microspheres treatment for liver malignancies. Expert Opin Pharmacother. 2010;11(4):579–86.

Deuffic S, Poynard T, Buffat L, Valleron AJ. Trends in primary liver cancer. Lancet. 1998;351:214–5.

Ehrhardt GJ, Day DE. Therapeutic use of ^{90}Y microspheres. Nucl Med Biol. 1987;14:233–42.

El-Serag HB, Davila JA, Petersen NJ, et al. The continuing increase in the incidence of hepatocellular carcinoma in the United States: an update. Ann Intern Med. 1992;139(10):817–23.

Fan Z, Tang Z, Liu K, Zhou D, Lu J, Yuan A, et al. Radioiodinated anti-hepatocellular carcinoma (HCC) ferritin. J Cancer Res Clin Oncol. 1992;118:371–6.

Garin E, Denizot B, Noiret N, et al. Re 188-SSS lipiodol: radiolabelling and biodistribution following injection into the hepatic artery of rats bearing hepatoma. Nucl Med Commun. 2004;10:1007–13.

Geschwind JF. Chemoembolization for hepatocellular carcinoma: where does the truth lie? J Vasc Interv Radiol. 2002;13(10):991–4.

Goh AS, Chung AY, Lo RH, et al. A novel approach to brachytherapy in hepatocellular carcinoma using a phosphorous32 (32P) brachytherapy delivery device-a first-in man study. Int J Radiat Oncol Biol Phys. 2007;67:786–92.

Harbert JC. In: Harbert JC, Eckelman WC, Neumann RD, editors. Nuclear medicine: diagnosis and therapy. New York: Thieme Medical Publishers, Inc.; 1996. p. 1141–55.

Hendlisz A, Van den Eynde M, Peeters M, et al. Phase III trial comparing protracted intravenous fluorouracil infusion alone or with yttrium-90 resin microspheres radioembolization for liver-limited metastatic colorectal cancer refractory to standard chemotherapy. J Clin Oncol. 2010;28:3687–94.

Ho S, Lau WY, Leung TWT, et al. Clinical evaluation of the partition model for estimating radiation doses from yttrium-90 microspheres in the treatment of hepatic cancer. Eur J Nucl Med. 1997;24:293–8.

Ho S, Lau WY, Leung TWT, Johnson PJ. Internal radiation therapy for patients with primary or metastatic hepatic cancer. Cancer. 1998;83:1894–907.

Iñarrairaegui M, Thurston KG, Bilbao JI, et al. Radioembolization with use of yttrium-90 resin microspheres in patients with hepatocellular carcinoma and portal vein thrombosis. J Vasc Interv Radiol. 2010;21:1205–21.

Jay M, Khare SS, Mumper RS, Ryo UY. Microencapsulation of activable radiotherapeutic agents. Biol Syn Mem. 1998;292:293–300.

Kanhere HA, Leopardi LN, Fischer L, et al. Treatment of unresectable hepatocellular carcinoma with radiolabelled lipiodol. ANZ J Surg. 2008;78(5):371–6.

Kao YH, Hock TAE, Burgmans MC, et al. Image-guided personalized predictive dosimetry by artery-specific SPECT/CT partition modeling for safe and effective 90Yradioembolization. J Nucl Med. 2012;53(4):559–66.

Kennedy AS, Sangro B. Nonsurgical treatment for localized hepatocellular carcinoma. Curr Oncol Rep. 2014;16(3):373.

Kennedy A, Nag S, Salem R, et al. Recommendations for radioembolization of hepatic malignancies using yttrium-90 microsphere brachytherapy: a consensus panel report from the radioembolization brachytherapy oncology consortium. Int J Radiat Oncol Biol Phys. 2007;68(1):13–23.

Kennedy A, Coldwell D, Sangro B, et al. Radioembolization for the treatment of liver tumors: general principles. Am J Clin Oncol. 2012;35(1):91–9.

Kim JK, Han KH, Lee JT, et al. Long-term clinical outcome of phase IIb clinical trial of percutaneous injection with holmium-166/chitosan complex (Milican) for the treatment of small hepatocellular carcinoma. Clin Cancer Res. 2006;12(2):543–8.

Kooijman H, Nijsen JFW, Spek AL, van het Schip AD. Diaquatris(pentane-2,4-dionato-O, O')holmium(III) monohydrate and diaquatris(pentane-2,4-dionato-O, O')-holmium(III) 4-hydroxypentan-2-one solvate dihydrate. Acta Crystallogr. 2000;C56:156–8.

Kumar A, Srivastava DN, Chau TT, et al. Inoperable hepatocellular carcinoma: transarterial ^{188}Re HDD-labeled iodized oil for treatment – prospective multicenter clinical trial. Radiology. 2007;243(2):509–19.

Lambert B, Bacher K, Defreyne L. Rhenium-188 based radiopharmaceuticals for treatment of liver tumours. Q J Nucl Med Mol Imaging. 2004;53(3):305–10.

Lambert B, Bacher K, De Keukeleire K, et al. ^{188}Re-HDD/lipiodol for treatment of hepatocellular carcinoma: a feasibility study in patients with advanced cirrhosis. J Nucl Med. 2005;46(8):1326–32.

Lau WY, Leung WT, Ho S, et al. Treatment of inoperable hepatocellular carcinoma with intrahepatic arterial yttrium-90 microspheres: a phase I and II study. Br J Cancer. 1994;70:994–9.

Lau WY, Ho SK, Yu SC, et al. Salvage surgery following downstaging of unresectable hepatocellular carcinoma. Ann Surg. 2004;240:299–305.

Lee IJ, Seong J. The optimal selection of radiotherapy treatment for hepatocellular carcinoma. Gut Liver. 2012;6(2):139–48.

Lee IK, Seong J, Koom WS, et al. Selection of the optimal radiotherapy technique for locally advanced hepatocellular carcinoma. Jpn J Clin Oncol. 2011;41(7):882–9.

Lepareur N, Mévellec F, Noiret N, et al. Syntheses and reactivity of 'sulfur rich' Re(III) and Tc(III) complexes containing trithioperoxybenzoate, dithiobenzoate and dithiocarbamate ligands. Dalton Trans. 2005;17:2866–75.

Lepareur N, Ardisson V, Noiret N, et al. Automation of labelling of Lipiodol with high-activity generator-produced Re 188. Appl Radiat Isot. 2011;69(2):426–30.

Leung WT, Lau WY, Ho S, et al. Selective internal radiation therapy with intra-arterial iodine-131-Lipiodol in inoperable hepatocellular carcinoma. J Nucl Med. 1994;35(8):1313–8.

Liepe K, Brogsitter C, Leonhard J, et al. Feasibility of high activity rhenium-188-microsphere in hepatic radioembolization. Jpn J Clin Oncol. 2007;37(12): 942–50.

Liu KD, Tang ZY, Bao Y, et al. Radioimmunotherapy for hepatocellular carcinoma (HCC) using I-131-anti HCC isoferritin IgG: preliminary results of experimental and clinical studies. Int J Radiat Oncol Bioi Phys. 1989;16:319–23.

Llovet JM, Burroughs A, Bruix J. Hepatocellular carcinoma. Lancet. 2003;362:1907–17.

Mumper RJ, Jay M. Poly(L-lactic acid) microspheres containing neutron-activatable holmium-165: a study of the physical characteristics of microspheres before and after irradiation in a nuclear reactor. Pharm Res. 1999;9:149–54.

Mumper RJ, Ryo UY, Jay M. Neutron activated holmium-166-Poly(L-lactic acid) microspheres: a potential agent for the internal radiation therapy of hepatic tumours. J Nucl Med. 1991;32:2139–43.

Murthy R, Xiong H, Nunez R, et al. Yttrium 90 resin microspheres for the treatment of unresectable colorectal hepatic metastases after failure of multiple chemotherapy regimens: preliminary results. J Vasc Interv Radiol. 2005;16:937–45.

Nijsen JFW, Zonnenberg BA, Woittiez JRW, et al. Holmium-166 poly lactic acid microspheres applicable for intra-arterial radionuclide therapy of hepatic malignancies: effects of preparation and neutron activation techniques. Eur J Nucl Med. 1999;26:699–704.

O'Donnell PB, McGinity JW. Preparation of microspheres by solvent evaporation technique. Adv Drug Deliv Rev. 1997;28:25–42.

Order SE, Stillwagon GB, Klein JL, et al. Iodine-131 antiferritin, a new treatment modality in hepatoma: a radiation therapeutic oncology group study. J Clin Oncol. 1985;3:1573–82.

Order SE, Klein JL, Leichner PK, et al. 90-Yttrium antiferritin: a new therapeutic radiolabelled antibody. Int J Radiat Oncol Biol Phys. 1986;12:277–81.

Order S, Pajak T, Leibel S, et al. A randomized prospective trial comparing full dose chemotherapy to ^{131}I Antiferritin: an RTOG study. Int J Radiat Oncol Biol Phys. 1991;20:953–63.

Parkin DM, Bray F, Ferlay J, Pisani P. Global cancer statistics, 2002. CA Cancer J Clin. 2005;55(2):74–108.

Raoul JL, Guyader D, Bretagne JF, et al. Randomized controlled trial for hepatocellular carcinoma with portal vein thrombosis: intra-arterial iodine-131-iodized oil versus medical support. J Nucl Med. 1994;35(11):1782–7.

Raoul JL, Boucher E, Roland V, Garin E. 131-iodine Lipiodol therapy in hepatocellular carcinoma. Q J Nucl Med Mol Imaging. 2009;53(3):348–55.

Risse JH, Grunwald F, Kersjes W, et al. Intraarterial HCC therapy with I-131-Lipiodol. Cancer Biother Radiopharm. 2000;15(1):65–70.

Risse JH, Rabe C, Pauleit D, et al. Therapy of hepatocellular carcinoma with iodine-131-lipiodol. Results in a large German cohort. Nuklearmedizin. 2006;45(4):185–92.

Saatchi K, Hafeli UO. Radiolabeling of biodegradable polymeric microspheres with $[^{99m}Tc(CO)_3]^+$ and in ViWo biodistribution evaluation using Micro SPECT/CT imaging. Bioconjugate Chem. 2009;20:1 209–17.

Salem R, Thurston KG. Radioembolization with ^{90}Y microspheres: a state-of-the-art brachytherapy treatment for primary and secondary liver malignancies. Part 1: technical and methodological considerations. J Vasc Interv Radiol. 2006;17: 1251–78.

Schubiger PA, Beer H-F, Geiger L, et al. ^{90}Y-resin particles-animal experiments on pigs with regard to the introduction of superselective embolization therapy. Nucl Med Biol. 1991;18:305–11.

Smits ML, Nijsen JF, van den Bosch MA, Lam MG, Vente MA, et al. Holmium-166 radioembolization for the treatment of patients with liver metastases: design of the phase I HEPAR trial. J Exp Clin Cancer Res. 2010;29:70.

Sohn JH, Choi HJ, Lee JT, et al. Phase II study of transarterial holmium-166-chitosan complex treatment in patients with a single, large hepatocellular carcinoma. Oncol. 2009;76:1–9.

Sundram F, Chau TC, Onkhuudai P, et al. Preliminary results of transarterial rhenium-188 HDD lipiodol in the treatment of inoperable primary hepatocellular carcinoma. Eur J Nucl Med Mol Imaging. 2004;31(2):250–7.

Tang ZY, Liu KD, Bao YM, et al. Radioimmunotherapy in the multimodality treatment of hepatocellular carcinoma with reference to second-look resection. Cancer. 1990;65:211–5.

Tian JH, Xu BX, Zhang JM, et al. Ultrasound-guided internal radiotherapy using yttrium-90-glass microspheres for liver malignancies. J Nucl Med. 1996;37:958–63.

Tisato F, Porchia M, Bolzati C, et al. The preparation of substitution-inert ^{99}Tc metal-fragments: promising candidates for the design of new ^{99m}Tc radiopharmaceuticals. Coord Chem Rev. 2006;250:2034–45.

Toubeau M, Touzery C, Berriolo-Riedinger A, et al. ^{131}I thyroid uptake in patients treated with 131I-Lipiodol for hepatocellular carcinoma. Eur J Nucl Med. 2001;28(5):669–70.

Turner JH, Claringbold PG, Klemp PFB, et al. ^{166}Ho-microsphere liver radiotherapy: a preclinical SPECT dosimetry study in the pig. Nucl Med Commun. 1994;15:545–55.

Uthappa MC, Ravikumar R, Gupta A. Selective internal radiation therapy: ^{90}Y (yttrium) labeled microspheres

for liver malignancies (primary and metastatic). Indian J Cancer. 2011;48(1):18–23.

Vassiliou I, Arkadopoulos N, Theodosopoulos T, et al. Surgical approaches of resectable synchronous colorectal liver metastases: timing considerations. World J Gastroenterol. 2007;13:1431–4.

Vente MA, de Wit TC, van den Bosch MA, et al. Holmium-166 poly(L: -lactic acid) microsphere radioembolisation of the liver: technical aspects studied in a large animal model. Eur Radiol. 2009;20:862–9.

Wang S-J, Lin WY, Chen MN, et al. Intratumoral injection of rhenium-188 microspheres into an animal model of hepatoma. J Nucl Med. 1998;39:1752–7.

Wang SC, Bester L, Burnes JP, et al. Clinical care and technical recommendations for ^{90}Yttrium microsphere treatment of liver cancer. J Med Imaging Radiat Oncol. 2010;54(3):178–87.

Watanabe N, Oriuchi N, Endo K, et al. Yttrium- 90-labeled human macroaggregated albumin for internal radiotherapy: combined use with DTPA. Nuc Med Biol. 1999;26:847–51.

Wunderlich G, Drews A, Kotzerke J. A kit for labeling of [^{188}Re] human serum albumin microspheres for therapeutic use in nuclear medicine. Appl Radiat Isot. 2005;62(6):915–8.

Zeng ZC, Tang ZY, Yang BH, et al. Comparison between radioimmunotherapy and external beam radiation therapy for patients with hepatocellular carcinoma. Eur J Nucl Med Mol Imaging. 2002;29(12):1657–68.

Zhang Z, Bian H, Feng Q, Mi L, et al. Biodistribution and localization of iodine-131-labeled metuximab in patients with hepatocellular carcinoma. Cancer Biol Ther. 2006;5(3):318–22.

Part IV

Therapeutic Radiopharmaceuticals for Treatment of Chronic Disease

Therapeutic Radiopharmaceuticals for Bone Pain Palliation

12

12.1 Introduction

Bone pain from skeletal metastases resulting from many types of primary tumors is a common debilitating issue which greatly decreases the quality of life (Paes et al. 2011; D'angelo et al. 2012; Finlay et al. 2005; Gough et al. 2014; Jansen et al. 2010; Knapp and Baum 2012; Mantyh 2014; Ogawa et al. 2012; Paes et al. 2011). Such metastases result from tumor cells entering the circulation and lodging in the richly oxygenated bone marrow with subsequent proliferation into metastatic sites. Such bone pain resulting from skeletal metastases of primary tumors is often encountered in patients presenting with primary tumors of the prostate, breast, small cell lung, and other cancers (D'angelo et al. 2012; Gough et al. 2014; Lewington 1993; Mantyh 2014; Ogawa 2012; Jansen et al. 2010). The hallmarks are destruction of bone tissue, marrow crowding, fractures, and distinct localized chemical changes. Although not well understood, the sensation of bone pain generally results from stimulation of specialized nociceptor pain-sensitive nerve fibers that innervate bone tissue. These pain signals are relayed from the sensory neurons to the brain, creating the sensation of pain, which originates from both the periosteal pressure and from the bone marrow. Activation of nociceptors responsible for bone pain results from a variety of mechanisms which include the deterioration of surrounding tissue and bone destruction. This is a debilitating situation which can dramatically affect mobility and quality of life.

Patients with these skeletal metastases very often present with bone pain for which the traditional first-line treatment has been the use of opiates. Often teletherapy and also chemotherapy with bisphosphonates are also used, often in combination. These methods are often only partially effective and have their own drawbacks. Although whole-body or hemibody irradiation has been used, because of the effects of gastrointestinal damage, these approaches are not often used, especially for multiple metastases juxtaposed to the viscera. Localized irradiation is effective for localized sites such as limbs, where radiation damage to normal tissue is minimized and dose levels of 8 Gy are used with a prescription of up to 40 Gy for multiple sessions. The use of bisphosphonates is very common as one treatment option used alone or in combination for bone pain. While narcotics reduce the associated pain indirectly, the phosphonates act as a type of chemotherapy by inhibition and destruction of osteoclasts. Since these substances are not radioactive, no license or specialized facilities are required for their application.

12.2 Treatment of Metastatic Bone Pain with Therapeutic Radioisotopes

Since these strategies can have dramatic clinically relevant side effects, the use of therapeutic radioisotopes which localize at the metastatic

F.F. (Russ) Knapp, A. Dash, *Radiopharmaceuticals for Therapy*, DOI 10.1007/978-81-322-2607-9_12

sites and result in pain reduction is an attractive and effective alternative strategy generally with minimal side effects (Atkins et al. 1995; Bauman et al. 2005; Brady et al. 2013; D'angelo et al. 2012; Lewington 1993, 2005; Liepe et al. 2000a, b; Mantyh 2014; Morris and Scher 2003; Ogawa and Washiyama 2012; Paes and Serafini 2010; Paes et al. 2011; Robinson 1986; Silberstein 1993; Srivastava 2002). The first assessment of the use of a radioisotope for bone pain palliation was conducted by Charles Pecher, a Belgian physician working at the Lawrence Berkeley Laboratory as early as 1936, who produced ^{89}Sr in the cyclotron and then conducted many experiments using this tracer to assess calcium pharmacokinetics and metabolism. He first reported the clinical use of ^{89}Sr, which was the first report for use of a therapeutic radioisotope for the palliation of bone pain (Pecher 1942). Following his untimely suicidal death, this seminal scientific achievement was apparently forgotten by the medical community during the 1942–1993 period and not resurrected until the development and availability of Medastron®. However, sadly, no mention of his contributions for the use of ^{89}Sr for bone pain palliation has been included in the commercial product literature. Radiopharmaceuticals used for the palliation of painful bone metastases should exhibit several key criteria including high tumor-to-normal bone ratio, in vivo stability, low bone marrow toxicity, rapid clearance from normal bone and soft tissues, ability to predict biodistribution patterns based on bone scintigraphy, and ease of preparation.

Most radioactive phosphonates chemisorb to the bone while the rhenium-labeled agents also appear to form an oxide species [i.e., oxidation of Re(V) to Re(VII] and chelate release) which attaches to the bone surface. Although the exact mechanism of action is not fully understood, the radiation released is felt to evidently sterilize those cells which release growth substances such as cytokines which results in periosteal pressure and nerve stimulation which causes the pain. It is curious that some authors refer to killing of skeletal metastatic tumor cells as the mechanism of action of the use of radioisotopes for bone pain palliation, although tumor reduction is generally not observed. The mechanism of action results from sterilization of cells which release inflammatory substances which activate the nociceptors. Both osteoblastic (new bone formation) and osteolytic (osteoclast breakdown, resorption/bone destruction) lesions are present in skeletal metastases. It should be noted that the goal of such treatments is to palliate the pain to manageable levels and thus to dramatically improve the quality of life. Although these methods in general do not eradicate the tumor metastases, there are promising recent results that therapeutic effects are possible with multiple repeat dosing (*vide infra*). The key radioisotopes which have been used or which are being evaluated for bone pain palliation are summarized in Table 12.1.

Because of the importance of evaluating the use of alternative more effective methods with minimal side effects, the use of beta-emitting radionuclides which target these sites of increased bone metabolism was evaluated as early as the late 1940s with ^{89}Sr (Pecher 1942). Since strontium is categorized in Group IIA of the periodic chart and is a congener of calcium, the use of ^{89}Sr was a good choice and can be reactor-produced by the neutron irradiation of enriched ^{88}Sr (Davis et al. 2000). The use of ^{89}Sr slowly gained interest and was approved by the US Food and Drug Administration (FDA) in 1993 based on the work of Robinson and others (Lewington et al. 1991; Quilty et al. 1994; Robinson 1986; Robinson et al. 1987). Because of the special role which beta-emitting radioisotopes were expected to play for the treatment of bone pain palliation, in the intervening time period a number of other candidates—most notably ^{32}P (Silberstein 1993).

The phosphonates labeled with such radioisotopes concentrate in the bone as a function of the osteoblastic activity. Several ^{186}Re-labeled agents have been evaluated for both bone pain palliation (De Klerk et al. 1996; Maxon et al. 1991) and osteosarcoma therapy (Bruland et al. 1996), and ^{153}Sm agents (Singh et al. 1989; Turner et al. 1989) have also been developed.

Table 12.1 Properties of radioisotopes and agents for bone pain palliation

Radioisotope agent	Production mode[a]	Half-life	Particle emissions, E_{max}	~Soft tissue penetration, mm_{max}	Principle gammas
Commercially available bone pain palliation agents					
Samarium-153 "Quadramet®"	R	1.9 days	β, 0.81 MeV	4 mm	103 (28 %)
Strontium-89 "Metastron®"	R	50.5 days	β, 1.46 MeV	7 mm	910 (0.01 %)
Rhenium-186[b] (Sn)HEDP "Etidronate"	R/A	3.8 days	β, 1.07 MeV	5	137 (9 %)
Bone pain palliation agents reported in clinical trials					
Phosphorus-32 Orthophosphate	R/A	14.3 days	β, 1.71 MeV	8.5 mm	None
Yttrium-90 Citrate and bisphosphonate	R/F	2.7 days	B 2.27 MeV	12 mm	None
Iodine-131 "BPB3"	R				
Rhenium-188 (Sn)HEDP	R	0.7 days[c]	β, 2.12 MeV	10 mm	155 (15 %)
Lutetium-177 BPMAD/EDTMP DOTMP	R	6.7 days	β, 0.497 MeV		
Strontium-85	R	64 days	CE, 10–15 keV	10 mm	514 keV
Radium-223 Chloride "Xofigo®"	Decay	11.4 days	CE – α's 5.606 MeV 5.715 MeV		
Tin-117m DTPA	R, A	13.6 days	CE, 126, 129, 151 keV		158 keV
Thorium-227[d] EDTMP	18.7 days	18.7 days	α's 5.757, 5.977, 6.038 MeV		
Lead-212[e] DOTMP	10.2 h	10.2 days	CE 334 keV		234 keV

[a]*R* nuclear reactor, *A* accelerator
[b]Available in Europe by physician prescription through 2005
[c]Available from in-house $^{188}W/^{188}Re$ generator system—local approval in some countries
[d]Parent of radium-223
[e]Available from ^{224}Ra generator system

The radioisotopes are attached to the phosphonate-targeting agents which have been commercialized. More recently, several other beta-emitting radioisotopes—in particular ^{188}Re and ^{177}Lu—have entered clinical trials and have also shown promise for this type of application. Those agents which have been approved by the FDA (^{153}Sm-EDTMP and ^{89}Sr-chloride) provide a reported 40–95 % pain relief response beginning 1–4 weeks following initiation of therapy. Response can last up to 18 months, and in many patients the use of opiates and other analgesics is drastically reduced. Reversible marrow suppression is often observed as thrombocytopenia and neutropenia.

In addition, the use of radioisotopes which have very short range penetration such as ^{117m}Sn (conversion electron) and ^{223}Ra (alpha emission) are also being explored for this application. However, in spite of the benefits of the use of these effective radioisotopic methods, first-line clinical treatment for bone pain continues to focus on traditional

methods administered by oncologists, urologists, and radiologists, who have been trained in the use of these methods and who are often unaware of the benefits for referral for nuclear medicine therapy. In addition to benefits for palliation, the use of radioisotopes has also been shown in some studies to provide therapeutic effects.

The goal of this chapter is to describe the development and use of a variety skeletal metastatic site-specific radiopharmaceuticals for the palliative treatment of bone pain. One important point is that many of these radioisotopes for bone pain palliation are neutron-rich and CE-/beta-particle-emitting radioisotopes available from reactor production, as described in Chap. 2. This illustrates the further importance of research reactors for the availability of many radioisotopes which are used in both unsealed radiopharmaceutical source (nuclear medicine) and sealed source (radiation oncology/interventional radiology–cardiology) applications. Agents which are commercially available are briefly discussed since these radiopharmaceuticals are well documented in the literature. Agents which are currently under development and those in clinical trials are discussed in more detail.

Important practical issues for radioisotope choice include availability and costs and also the half-life and thus the dose rate for use in outpatient therapy, depth of particle penetration, and emission of gamma photons for imaging. Availability and costs revolve around the required production and processing (See Chaps. 5, 6, 7, and 8) and other practical and economic factors. The radioactive agents used for bone pain palliation generally consist of either simple radioactive ionic species such as ^{32}P (as the phosphate anion) and ^{89}Sr and ^{223}Ra, as the divalent M^{+2} cations. These species target the bone because of their periodic similarity to natural constituents. Other radioactive agents or carrier molecules used for bone targeting include phosphonates (−C-P-C-) to which the radioisotopes are chemically attached and include ^{153}Sm EDTMP, $^{186/188}Re$ HEDP, and ^{177}Lu-EDTMP.

12.3 Commercially Available Beta-Particle-Emitting Approved Agents for Bone Pain Palliation

12.3.1 Rhenium-186 HEDP

Substituted phosphonate (Fig. 12.1) complexes represent attractive carrier molecules for targeting therapeutic radioisotopes to skeletal regions of increased osteolytic metabolism. Rhenium is a Group VIIb transition metal, and the ^{186}Re hydroxyethylidene diphosphonate (HEDP) complex, as an example, was developed in the 1980s for bone pain palliation and, in contrast to the traditional use of ^{89}Sr, had the added advantage of gamma photon emission (Table 12.1) which permits evaluation of localization with gamma camera imaging. It was expected that clinical use of this agent would rapidly progress but only became available locally on a physician prescription basis in Europe and was never approved for broad routine use because of apparent regulatory issue.

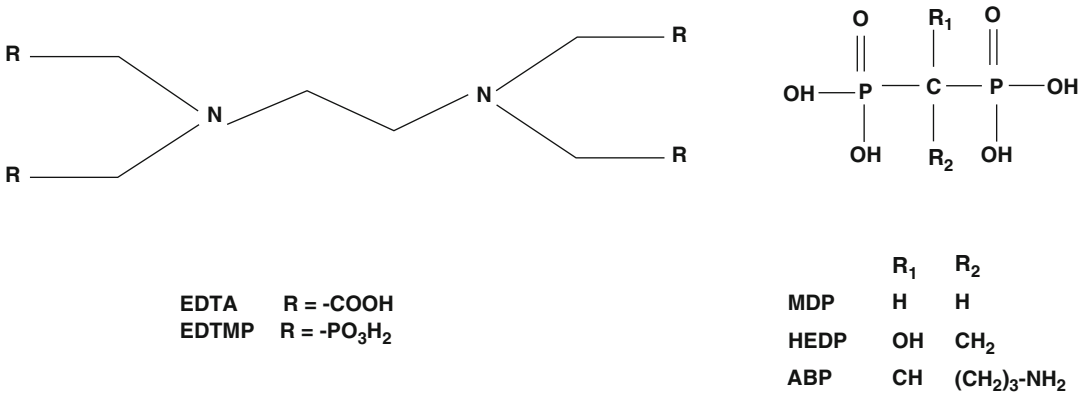

Fig. 12.1 Phosphonate carrier ligands for bone pain palliation agents

Although preparation of ^{186}Re-HEDP had been well established, the relatively low specific activity of reactor-produced ^{186}Re was a key requirement for preparation of the HEDP complex which was not initially realized. This was later established where only soft tissue uptake rather than skeletal localization was detected during evaluation of ^{188}Re HEDP prepared using very high specific activity no-carrier-added generator-produced ^{188}Re (Dash and Knapp 2015). In contrast, when carrier rhenium is added to similar levels encountered during the use of low specific activity ^{186}Re, the expected targeted skeletal localization is realized (Lam et al. 2008). In studies reported by Edler et al., the apparent reason for these observations is the unknown chemical structure of the Re(V)-HEDP species, which apparently consists of Re-Re bonds and is formulated as an oligomer (Elder et al. 1997). The authors used extended X-ray absorption fins structure (EXAFS) analysis to evaluate the species formed using nonradioactive rhenium and have formulated that the species formed in the presence of high levels of the stannous ion reductant probably represents a tetramer of rhenium atoms which are bridged by the HEDP ligands. This structure evidently also binds an equivalent number of tin atoms as well as additional HEDP ligands. Based on the levels of the stannous ion-reducing agent used, different species are apparently formed. When an excess of the stannous ion-reducing agent is used, the species formed appears to have the composition Li(x) $Re_4(OH)_2Sn_4HEDP_{12}$. Thus, ^{186}Re-HEDP and ^{188}Re HEDP described below are examples of agents which show specific targeted uptake but which have unknown chemical structures.

12.3.2 Samarium-153 EDTMP ("Quadramet®")

Samarium-153 is reactor-produced by the neutron irradiation of enriched ^{152}Sm targets (Sartor 2004) and is incorporated into the phosphonate entity, referred to as lexidronam (Fig. 12.2). With the emission of a moderate energy beta particle and an excellent half-life for outpatient applications, ^{153}Sm was evaluated as an alternative to ^{89}Sr for bone pain palliation (Bauman et al. 2005; Finlay et al. 2005; Silberstein 2005). Another advantage—which probably has not been fully appreciated until in more recent times—is the emission of a gamma photon, which permits the use of ^{153}Sm to monitor uptake/targeting, biokinetics, and evaluation of dose delivery in relation to therapeutic response. In the current developing era of "personalized medicine," the use of dual beta-/gamma-emitting radioisotopes for these and other therapeutic applications thus offers several advantages.

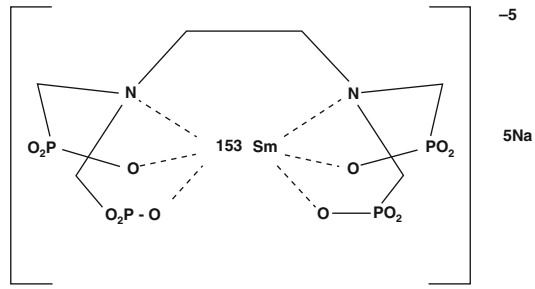

Fig. 12.2 Chemical structure of lexidronam

12.3.3 Stronium-89 Chloride

Since both strontium and calcium are members of Group IIA the use of ^{89}Sr as a surrogate of calcium was an early strategy which had been explored and ^{89}Sr is still used for bone pain palliation. The evaluation of ^{89}Sr as a targeted agent for bone pain palliation was initially reported in Germany in 1946. This agent was later approved in the US by the Food and Drug Administration (FDA) as "Metastron®" in 1993 and has since that time been a widely used agent for bone pain palliation.

12.4 Examples of Bone Pain Palliation Agents under Development and in Clinical Trials

In addition to the widespread use of the commercial regulatory-approved agents described above, in particular ^{153}Sm and ^{89}Sr, there are also several other palliative agents radiolabeled with

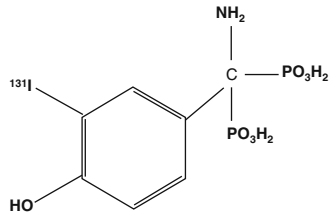

^{131}I-labeled α-amino-(4-hydroxybenzylidene)-disphosphonate (BPB3)

Fig. 12.3 Iodine-131-labeled benzylidene diphosphonate structures

beta-emitting radioisotopes described below which have shown promise for bone pain palliation and are being used in patient trials.

12.4.1 Iodine-131

Another diphosphonate option for bone pain palliation utilized ^{131}I, which is a readily available and well-established therapeutic radioisotope. Preparation and studies in a rat model were initially reported with the ^{131}I-labeled α-amino-(4-hydroxybenzylidene)-diphosphonate (BPB3) agent (Fig. 12.3) (Eisenhut 1984). Iodine-131 radiolabeling was performed in about 95 % yield with a BPB3 specific activity of about 50 mCi/mg by electrophilic aromatic substitution using the iodate anion in 1 N HCl. The biokinetics, dosimetry data, and pain response were reported in initial studies in 18 patients with skeletal metastases from prostate, breast, and other primary carcinomas receiving doses from 6–48 mCi of ^{131}I-BPB3 (Eisenhut et al. 1986a). In further studies, these authors then pursued evaluation of several structurally related radioiodinated benzylidenediphosphonates (BDP) with *alpha* and *para* position substitutions including -H, −OH, and -NH_2 (Eisenhut et al. 1987). The 4-methoxy- and 4-nitro-substituted diphosphonates were prepared by phosphorous acid treatment of the respective benzonitriles in the presence of phosphorus bromide (PBr_3). The 4-hydroxy and 4-nitro derivatives were then prepared by hydrolytic HBr cleavage and subsequent catalytic hydrogenation. Transformation of the 2-amino to the 2-hydroxy derivative was accomplished by treatment with sodium nitrate in HCl. The proposed structures of these derivatives were confirmed by chromatography, spectroscopy, and elemental analysis and were then radiolabeled with ^{131}I. Further studies of these BDP analogs were focused on the comparative biokinetics and bone uptake values in Sprague Dawley rats. Total-body retention measurements of α-amino-(3-[^{131}I]iodo-4-hydroxybenzylidene) diphosphonate analog revealed an effective half-life of the activity of 169 h. LD_{50} measurements in rats amounted to 64 mg/kg. In addition, autoradiographic analyses were performed in bone samples obtained from osteosarcomic SD rats following intravenous administration (Eisenhut et al. 1986b). Apparently, these agents have not been evaluated further and subsequent patient trials have not been reported.

12.4.2 Phosphorus-32

The bone is constructed of a complex hydroxyapatite matrix in which phosphorus plays an integral role. The use of beta-emitting ^{32}P as the phosphate had thus been an obvious candidate to evaluate for bone pain palliation since it mimicked the natural cation and has been cost-effectively available on a broad scale. In an IAEA-coordinated multicenter study (Fettich et al. 2003) to evaluate safety and efficacy of ^{32}P for palliation of bone pain due to bony metastases by comparing it to ^{89}Sr, or bone pain palliation, 93 cancer patients with osteoblastic bony metastases were included into the study of which 48 were treated by ^{89}Sr (150 MBq) and 45 by ^{32}P (450 MBq). The results of this study suggested that ^{32}P is slightly but not significantly less effective than ^{89}Sr for palliation of bone pain due to bony metastases. Although ^{32}P appears to be more toxic it is important to note that no toxic effects requiring specific treatment were seen in either group. This study inferred that ^{32}P was as safe as ^{89}Sr using doses up to 450 MBq (Fettich et al. 2001). The results of this study are expected to shed further light on the perspectives of ^{32}P for patients with painful skeletal metastases. In light of the cost-effective availability, widespread use of ^{32}P should be encouraged to reduce cost of

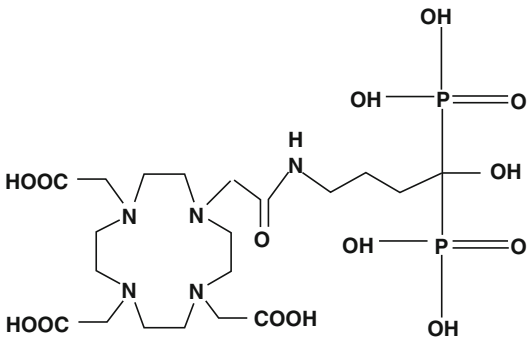

Fig. 12.4 DOTA conjugated 4-amino-1-hydroxybutylidene-1,1-bisphosphonate (DOTA-HBP)

medical care of patients with intractable bone pain due to cancer metastases, but further widespread use of ^{32}P for bone pain palliation has not been reported.

12.4.3 Yttrium-90-Labeled Citrate and EDTMP

Very early during the assessment of beta-emitting radioisotopes for bone pain palliation ^{90}Y had been evaluated as a high-energy beta particle-emitting radioisotope for this application as the citrate complex but had not been subsequently widely used. Renewed interest in the use of ^{90}Y, however, resulted in the commercial release of the Multibone® agent (EDTMP) in central Europe for radiolabeling with ^{153}Sm, ^{90}Y, ^{111}In, and ^{188}Re (Mitterhauser et al. 2004a, b). In this case, the strategy was to make available a common kit which could be used for radiolabeling with a variety of radionuclides. In the case of bone pain palliation, the use of beta emitters with different beta energies would permit the tailoring of irradiation of diagnosed metastases to minimize damage to normal tissue (Bouchet et al. 2000; Lewington 2005). The commercially available multibone EDTMP kit agent consists of EDTMP, $SnCl_2$, ascorbic acid, and glucose (Mitterhauser et al. 2004a, b). The ^{90}Y-DOTA conjugated 4-amino-1-hydroxybutylidene-1,1-bisphosphonate (^{90}Y-DOTA-HBP) (Fig. 12.4) has also been prepared and biodistribution studies compared with ^{90}Y-citrate in mice (Ogawa et al. 2009). The HBP analogs demonstrated much faster blood and most soft tissue clearance and higher bone accumulation. The advantage of further studies and potential human use of the HBP analogs is the very stable Y^{+3}-DOTA complex, which would not release free $^{90}Y^{+3}$ for targeting to normal bone.

12.5 New Radiolabeled Agents Being Developed for Bone Pain Palliation

In addition to the use of ^{186}Re, ^{153}Sm, and ^{90}Sr as the three major commercially available bone pain palliation agents, there are a variety of other beta-emitting radioisotopes which are being evaluated for bone pain palliation. The results from several clinical trials have been reported with several of these agents suggest their potential utility for further evaluation and potential routine clinical use.

12.5.1 Rhenium-188

Because of its availability from the $^{188}W/^{188}Re$ generator which has a useful shelf-life of several months (Dash and Knapp 2015), the use of ^{188}Re-HEDP offers many benefits. In addition to similarity to the established use of ^{186}Re-HEDP, the ^{188}Re-HEDP has been extensively evaluated on a clinical trial basis with extensive discussion in the literature. Within the basic science and clinical research communities, ^{188}Re-labeled bone pain palliation agents have by far seen the greatest progress.

12.5.1.1 Rhenium-188 (V) DMSA

Since both Tc and Re are transition metal members of Group VIIB of the periodic chart and have similar oxidation states and chemistry, many ^{188}Re-labeled radiopharmaceuticals are based on their ^{99m}Tc analogs. *Meso*-2,3-dimercaptosuccinic acid (DMSA) represents excellent ligand properties for formation of many different metal ions, including Tc and Re (Stanik et al. 2012). A trianionic Tc(III)-DMSA complex is prepared by acidic reduction of pertechnetate which has been

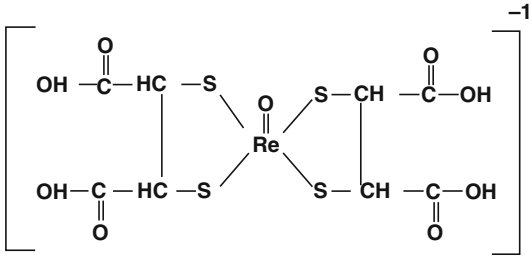

Fig. 12.5 Rhenium(V)-DMSA isomers

widely used for renal imaging. The ^{186}Re-DMSA agent was prepared using the standard kit and stannous ion reduction at 100 ° C (Bisunadan et al. 1991), and this agent demonstrated localization for imaging of medullary carcinoma thyroid cancer and a variety of other tumors. In contrast, carefully controlled stannic ion reduction of pertechnetate at high pH (sodium bicarbonate) reacts with DMSA to form the quite different stable mono-anionic Tc(V)-DMSA complex which showed good targeting to bone metastases (Lam et al. 1997) which was a prelude for the evaluation of the ^{188}Re congener for palliation.

These data led to the preparation and evaluation of the corresponding ^{188}Re-DMSA for evaluation for the palliative treatment of skeletal lesions. In this case a basic pH of the reaction mixture is not required, and a range of pH values form the single mono-anionic Re(V)-DSMA species (Fig. 12.5) which is prepared by stannous ion reduction of perrhenate in the presence of the commercially available DMSA kit by heating to 100 ° C (Singh et al. 1993).

The presence of these isomers was confirmed by X-ray diffraction (Singh et al. 1991). Evaluation in animal models with subsequent patient studies demonstrated the excellent targeting of this agent in skeletal metastases from prostate cancer (Blower et al. 1998). Since DMSA exists in the *meso* (R, S) and racemic (DL) isomers, the mono-anionic product consisting of three species were separated by subsequent careful HPLC chromatographic analyses. Preparation of ^{186}Re(V)DMSA requires a DMSA/$SnCl_2$/Re ratio of 10:5:1 at 100 °C for 30 min (Singh et al. 1993). The chemistry of Re(V)-DMSA has been discussed in detail (Blower and Prakash 1999). Evaluation of the individual ^{188}Re-labeled DMSA isomers showed only minor differences in skeletal uptake and thus established that isomer separation was not required for isolation of the most favorable isomer (Guhlke et al. 2009). Subsequent studies evaluated a new kit for preparation of the ^{188}Re(V)-DMSA (Pirmettis et al. 2001).

Initial biological studies with the kit-based preparation of ^{188}Re(V)-DMSA in animals and humans provided biodistribution, excretion, and dosimetry data on which further therapeutic studies could be based (Blower et al. 1998). Data from three patients who presented with skeletal metastases from primary prostate cancer showed and three with bronchus cancer with bone metises confirmed by standard skeletal imaging were imaged 3 and 24 h following administration of 370 MBq of the ^{188}Re-(V)-DMSA. Clearance of ^{188}Re was evaluated by blood and urine analyses. Normal bone uptake was similar to soft tissue and bone metastases demonstrated good targeting, with kidney uptake also observed. These preliminary findings then lead to subsequent detailed studies comparing the ^{99m}Tc and ^{188}Re congeners for comparison of the tumor/normal tissue and kidney/soft tissue ratios in a group of 10 prostate cancer patients with skeletal metastases and to determine if imaging with ^{99m}Tc-DMSA could predict the targeting and subsequent therapy of lesions with ^{188}Re-DMSA (Blower et al. 2000a, b, c). Imaging at 4 and 24 h after administration demonstrated a high linear correlation between the two agents. These data suggest that traditional tumor imaging could be used to estimate tumor and kidney radiation dose which would be delivered by the use of ^{188}Re(V)-DMSA for bone pain palliation. Although this agent showed great promise for broader evaluation of patients presenting with skeletal metastases of other tumors, this agent is not evidently being evaluated further.

12.5.1.2 Rhenium-188 HEDP

Because of the early success and expected broad clinical use of ^{186}Re-HEDP, ^{188}Re HEDP was further developed and evaluated as an attractive

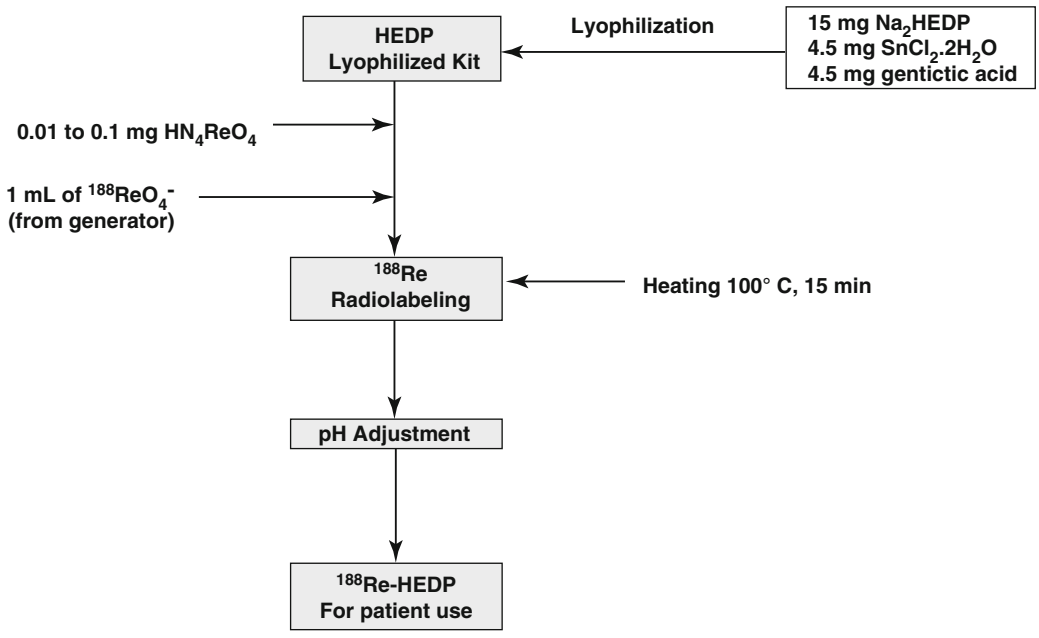

Scheme 12.1 Preparation scheme for ^{188}Re-HEDP

analog (Lambert and de Klerk 2006; Liepe et al. 1998, 1999a, b, c, 2000a, b, c, 2001, 2002, 2003a, b, c, d, e, 2005a, b, 2009; Lin et al. 1997; Palmedo et al. 1997, 1998a, b, 1999a, b, 2000, 2002, 2003a, b; Maxon et al. 1998; Orsini et al. 2012; Savio et al. 2001; Scheffler et al. 2003, Zhang et al. 2003). The ^{188}Re is available carrier-free from the ^{188}W/^{188}Re generator system (Hsieh et al. 1996; Pillai et al. 2012; Knapp 1998; Knapp et al. 1994, 1997, 1998, 2000, 2004; Jeong and Chung 2003; Dash and Knapp 2015). An extensive number of clinical trials with ^{188}Re-HEDP have been described and demonstrate the excellent and cost-effective use of this agent for treatment of skeletal bone pain. In addition, several "kit" formulations have been developed for routine radiopharmacy preparation of this agent (Schmaljohan et al. 2000; Verdera et al. 1996, 1997a, b; Lin et al. 1997), and a detailed typical kit formulation strategy is depicted in Scheme 12.1.

As described earlier, preparation of ^{188}Re-HEDP requires that the specific activity of the no-carrier-added ^{188}Re-perrhenate obtained by NaCl elution of the ^{188}W/^{188}Re generator system be significantly reduced by addition of carrier perrhenate (ammonium perrhenate) prior to stannic ion reduction in order to form the requisite oligomeric product which shows localization in skeletal metastases (Verdera et al. 1997a, b; Inoue et al. 1981). Preparation of ^{188}Re-HEDP using high specific activity ^{188}Re-perrhenate forms a product which only shows soft tissue uptake (Bordoloi et al. 2015). Autoradiographic studies of skeletal samples from rats administered with ^{188}Re-HEDP showed that the uptake of rhenium-188-HEDP in cortical bone was 33.5 % and in trabecular bones was 66.5 % after 4 h, 34.6 and 65.4 % after 24 h, and 35.9 and 64.1 % after 48 h, respectively. In bone metastases, an inhomogeneous distribution with a minimal and maximal tumor to non-tumor ratio of 3:1 and 14:1 after 4 h, 5:1 and 14:1 after 24 h, and 5:1 and 16:1 after 48 h was observed (Liepe et al. 2009), which probably has broad implications on the localization of other radiolabeled phosphonates and will provide some insight into the dosimetric considerations.

Rhenium-188-HEDP is generally prepared using 10 μmol of carrier Re, and drug composition may not only affect stability of the final drug product but may also influence bone affinity and

subsequent efficacy. Since there are no standardized preparation methods, however, a study by ter Hein and co-workers reported the first GMP preparation of ^{188}Re-HEDP production using stocks of sterile nonradioactive starting materials (ter Heine et al. 2014). On-site GMP production has the obvious advantage to allow rapid availability of this agent for treatment of patients who present with unmanageable pain. The production of GMP grade ^{188}Re-HEDP will allow application of this therapeutic radiopharmaceutical in routine clinical practice and for support of clinical studies.

A more recent study by the same authors evaluated bone uptake in mice as a function of Re carrier concentration. Since the exact stoichiometric requirements for carrier Re had not been defined, the influence of Re carrier concentration during the preparation of ^{188}Re-HEDP was investigated for the first time (Lange et al. 2015), by studying product radiochemical purity, in vitro affinity of the ^{188}Re-HEDP for hydroxyapatite (HA) affinity, and in vivo bone accumulation in mice. Both HA binding and bone uptake were influenced by carrier, and the relationship between changes in HA binding and carrier perrhenate concentration appeared to be related to radiochemical purity. However, the results of animal studies suggested than bone accumulation ^{188}Re-HEDP with adequate radiochemical purity and HA uptake did not necessarily predict acceptable biodistribution of ^{188}Re-HEDP.

12.5.1.3 Other Rhenium-186/188 (^{186}Re/^{188}Re) Analogs

In general, most Re(V) phosphonate complexes which have been prepared and evaluated show good stability and high skeletal targeting and low soft tissue uptake and must be evaluated further to develop any compelling justification that they would be superior to Re(V) HEDP. Other rhenium analogs which have been prepared and evaluated for bone uptake include the pharmacologic bone pain palliation agent, 1-hydroxy-3-aminopropylidenediphosphonate (APD; Fig. 12.6). In one study, the ^{186}Re-labeled phosphonate with ^{186}Re-ADP (Alyafei et al. 1999) was prepared by tin chloride reduction of ^{186}Re-perhenate in the presence of gentisic acid. Studies in normal mice 1–240 h post injection demonstrated high bone/blood ratios ranging from 25 to 189 over the evaluation period, with low soft tissue accumulation. In similar studies, generator-derived ^{188}Re-potassium perrhenate was reduced at acidic pH with tin fluoride in the presence of the ADP ligand to provide the ^{188}Re-ADP product which was subsequently evaluated in rats (Arteaga de Murphy et al. 2001). Biodistribution data and skeletal targeting were similar to ^{99m}Tc-ADP, suggesting to the authors that the ^{188}Re is a promising agent for further evaluation. Rhenium-188 has also been complexed in >95 % radiochemical yield with *N*,*N*,*N'*,*N'*-tetrakis-methylene phosphonic acid (EDTMP; Fig. 12.6) at low pH with stannous chloride (Oh et al. 2002) and compared with ^{188}Re-HEDP in Wistar male rat biodistribution studies. The data were similar for both agents, with rapid clearance and low soft tissue uptake and high bone uptake. With regard to complex structures, none of these agents were evaluated so the comparison with the complex oligomeric structure of Re(V)-HEDP is unknown.

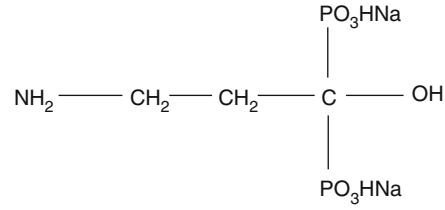

Fig. 12.6 Structure of sodium salt of ADP

As the phosphonate groups in $^{186/188}$Re-HEDP are used as both ligands for coordination and as carrier to HA in bone, there is a possibility that it may decrease the inherent affinity of HEDP for bone. In order to circumvent such possibilities, ^{186}Re-monoaminemonoamidedithiol (MAMA)- and ^{186}Re-mercaptoacetylglycylglycylglycine (MAG3)-conjugated bisphosphonate compounds (^{186}Re-MAMA-BP,^{186}Re-MAMA-HBP, and ^{186}Re-MAG3-HBP) have been developed (Ogawa et al. 2004, 2005, 2006). Their chemical structures have been illustrated in Fig. 12.7.

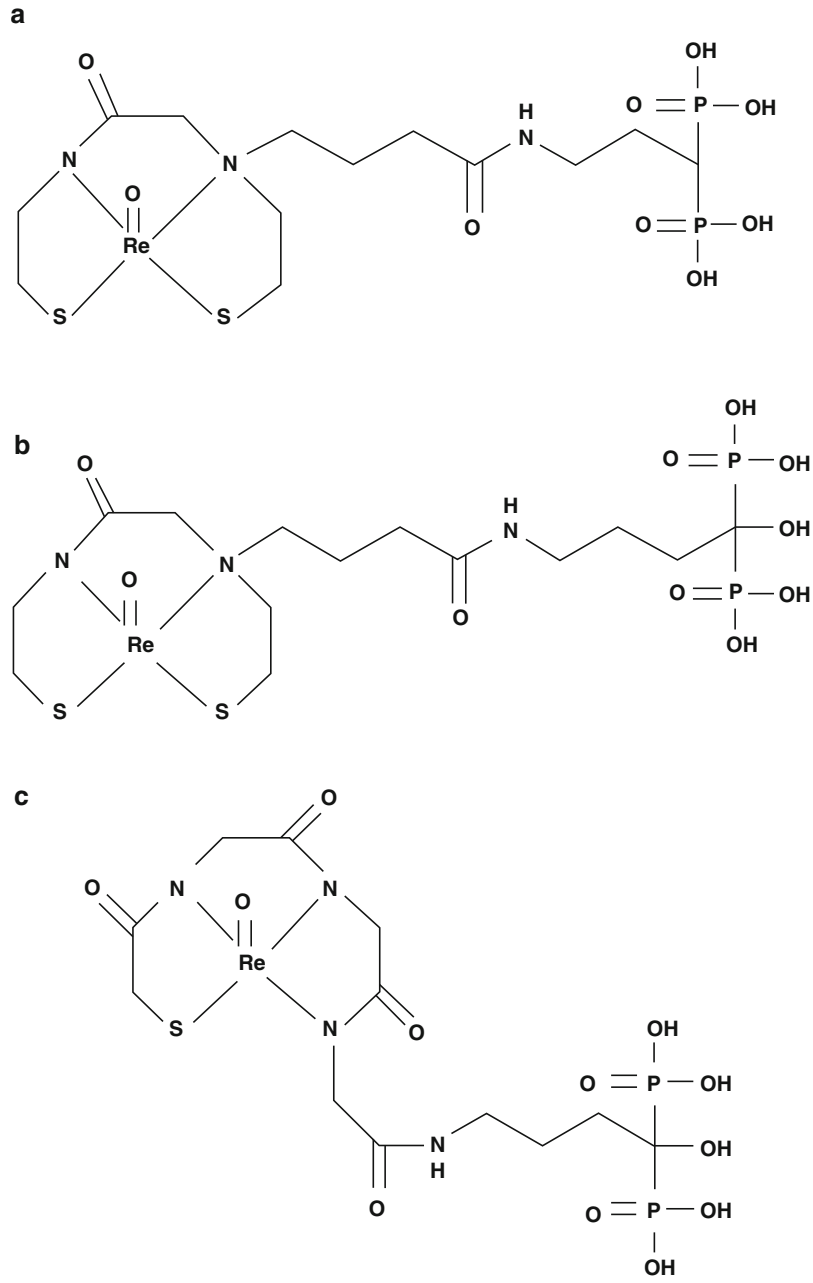

Fig. 12.7 Chemical structures of (**a**) ^{186}Re-MAMA-BP, (**b**) ^{186}Re-MAMA-HBP, (**c**) ^{186}Re-MAG3-HBP

On a similar theme Uehara et al. (2007) developed a tricarbonyl [^{186}Re][(cyclopentadienylcarbonyl amino)-acetic acid] rhenium complex ([^{186}Re]CpTR-Gly)-conjugated bisphosphonate [^{186}Re-CpTR-Gly-APD] which has been reported to have characteristics superior to those of ^{186}Re-HEDP, such as higher stability in plasma, a higher binding rate for HA, higher bone accumulation, and lower plasma protein binding. Subsequently De Rosales et al. (2010) have developed ^{188}Re(CO)$_3$-DPA-alendronate which showed higher stability in vitro compared with ^{188}Re-HEDP and superior biodistribution of radioactivity than ^{188}Re-HEDP. Chemical structures of [^{186}Re]CpTR-Gly-APD and ^{188}Re(CO)$_3$-DPA-alendronate are shown in Fig. 12.8.

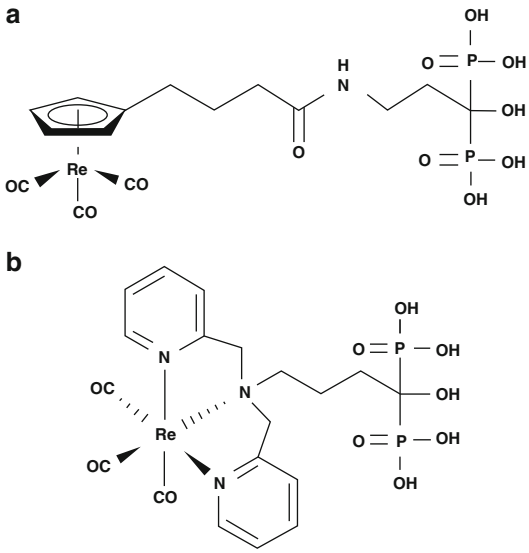

Fig. 12.8 Chemical structures of (**a**) [^{186}Re]CpTR-Gly-APD, and (**b**) ^{188}Re(CO)$_3$-DPA-alendronate

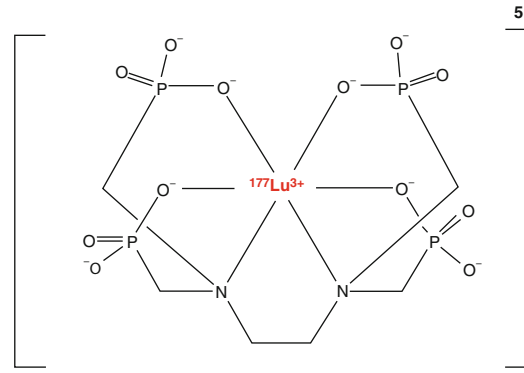

Fig. 12.9 ^{177}Lu-ethlyendiamminetetramethylenephosphonate (EDTMP).

12.5.2 Lutetium-177 Diphosphonates

More recently, several studies have described the use of ^{177}Lu-labeled phosphonate complexes for bone pain palliation. Lutetium-177 is a lanthanide (+3) therapeutic radioisotopes of great interest (Banerjee et al. 2015), since it can be reactor-produced even at moderate thermal neutron flux with very high specific activity (Dash et al. 2015). Ando et al. have reported for the first time the utility of ^{177}Lu-ethlyendiammine tetramethylene phosphonate (EDTMP; Fig. 12.9) (Ando et al. 1998). In one study, the *International Atomic Energy Agency (IAEA)* sponsored a multicenter trial evaluating the efficacy of ^{177}Lu-ethlyendi amminetetramethylenephosphonate (EDTMP) (Chopra 2011).

In addition, the ^{177}Lu-labeled (DOTMP) has also been evaluated. The ^{177}Lu-labeled (4-{[*bis*-(phosphonomethyl) carbamoyl} methyl}-7,10-*bis* (carboxymethyl)-1,4,7,10-tetraazacyclododec-1-yl)acetic acid (BPAMD; Fig. 12.10) has been developed as a new bone pain palliation agent (Fellner et al. 2010). The +3 DOTA is an excellent lanthanide-chelating moiety which has the specific advantages of very tightly binding +3 metal and allowing very facile nearly quantitative radiolabeling yields of lanthanides under mild conditions with the formation of a highly stable Lu complex. Initial human trials have demonstrated the excellent targeting of this agent in skeletal lesions (Fellner et al. 2010) and MIRD/OLINDA/EXM dosimetry estimates utilizing data from 8 patients with skeletal metastases from prostate cancer have also been recently reported (Schuchart et al. 2013; Yousefnia et al. 2015). These studies have demonstrated very rapid blood clearance whole-body biexponential clearance with a second half-life of 62 ± 19 h and a metastases site clearance of 57–162 h. In addition, the broad interest in the production and use of ^{177}Lu (Pillai and Knapp 2015)—currently focused on the use of therapeutic peptides such as ^{177}Lu-DOTATATE and DOTATOC—would suggest that the expected broad availability of pharmaceutical grade ^{177}Lu may catalyze further interest and broad use of ^{177}Lu-BPAMD.

Bisphosphonates containing an imidazole ring have higher affinity for bone mineral. In this context, the potential utility of zoledronic acid (ZOL) [2-(imidazole-1-yl)-hydroxy-ehtylidene-1,1-bisphosphonic acid] (Fig. 12.11), a bisphosphonate containing an imidazole ring and the most potent of the clinically tested compound, has been exploited (Majkowska et al. 2009; Rasheed et al. 2015). Hydroxyapatite adsorption experiments have shown that the binding values obtained with complexes of zoledronic acid labeled with ^{177}Lu is much higher than those of

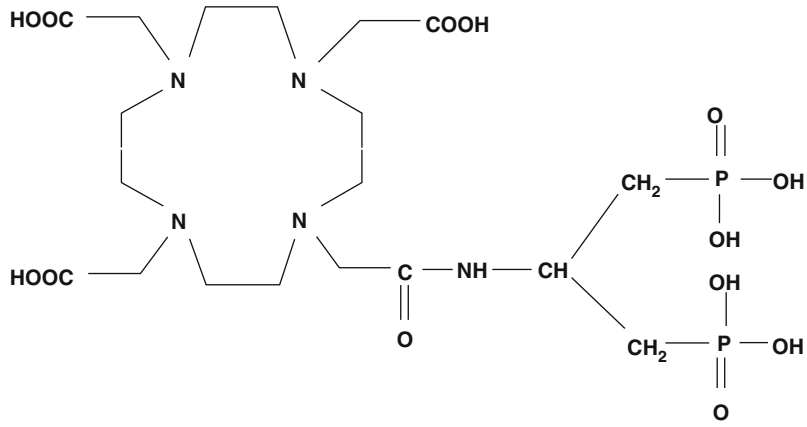

Fig. 12.10 Structure of (4-{[*bis*-(phosphonomethyl) carbamoyl}methyl}-7,10-*bis* (carboxymethyl)-1,4,7,10-tetraaza-cyclododec-1-yl)acetic acid (BPAMD)

bisphosphonates labeled with ^{153}Sm and ^{166}Ho (Majkowska et al. 2009).

The ^{177}Lu triethylenetetramine-hexamethylene phosphonic acid (^{177}Lu-TTHMP) analog (Fig. 12.12) has also been reported as a potent radiopharmaceutical for bone pain palliation (Zolghadri et al. 2015), although detailed clinical data on this agent are yet to appear in the literature.

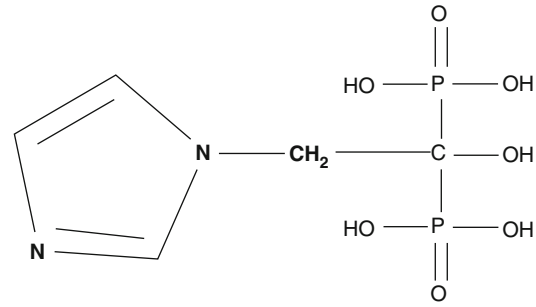

Fig. 12.11 Structure of zoledronic Acid

12.5.3 Samarium-153 and Holmium-166

Both ^{153}Sm and ^{166}Ho are reactor-produced and have promising radionuclidic properties for therapy (Table 12.1). Samarium-153 EDTMP (Fig. 12.13) has been prepared by adding 1.0 ml of ^{153}SmC13 (0.9 mg Sm) to 60 mg/1.5 ml EDTMP at pH 9 (molar ratio 1:23, Sm/EDTMP, w/w) and adjusting the pH of reaction mixture to 10–11 at 60–70 °C for 30 min. After incubation the pH was adjusted to 7.5–8 or through kit formulation strategy (Singh et al. 1989).

Modified phosphonate complexes which have been prepared and evaluated include N,N-dimethylenephosphonate-1-hydroxy-4--aminopropylidenediphosphonate (APDDMP) (Marques et al. 2006) and 13- and 14-membered macrocyclic ligands containing methylcarboxylate (TRITA and TETA) and methylphosphonate (TRITP and TETP) moieties (Fig. 12.14). Based on the results of in vitro hydroxyapatite binding and plasma stability studies and biodistribution studies in mice, the authors concluded that the ^{166}Ho-TRITP analog may be a useful candidate for further evaluation as a bone palliation agent and that ^{153}Sm/^{166}Ho-TRITP complexes may be useful agents for therapy. In another study, both ^{153}Sm and ^{166}Ho complexes of APDDMP were prepared and evaluated for skeletal targeting (Zeevart et al. 2001). The APDDMP was synthesized from the 1-hydroxy-3-aminopropylidenediphosphonate (ADP). Both ^{153}Sm- and ^{166}Ho-labeled APDDMP showed relatively low bone uptake.

12.5.4 Thulium-170

As an interesting radioisotopic alternative to the use of ^{89}Sr, ^{170}Th phosphonates have also been prepared and evaluated. The potential benefits of using ^{170}Tm include the good thermal neutron

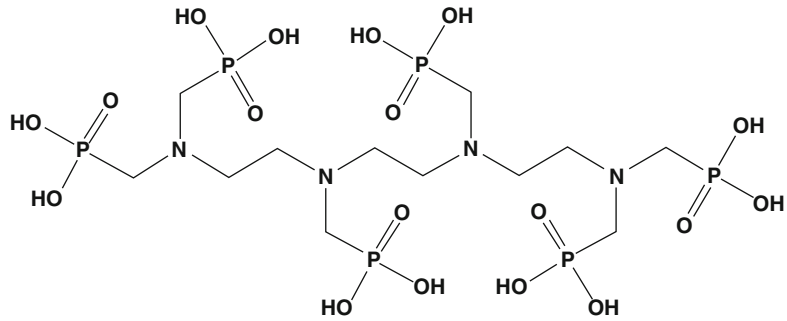

Fig. 12.12 Structure of TTHMP

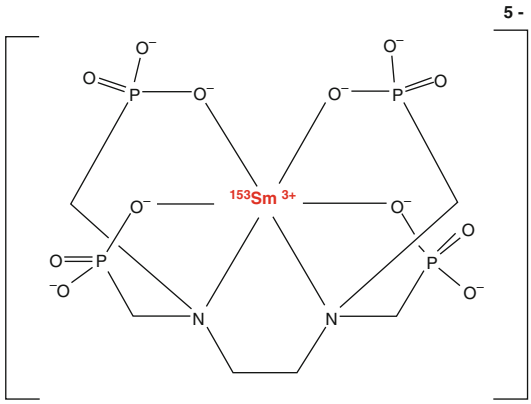

Fig. 12.13 ^{153}Sm-ethlyendiamminetetramethylenephosphonate (EDTMP)

cross section (109 barn) for the ^{169}Tm(n,γ)^{170}Tm reactor production pathway (Chap. 5) and that production and processing could be more cost-effective than for ^{89}Sr. More importantly, the emission of a photon with an energy of 84 keV (3.26 % abundance) permits gamma camera imaging, which could be expected to be an important capability as we move further into the era of personalized medicine. In this manner, targeted uptake and biokinetics could be monitored to correlate dosimetry with response. Thulium-170 has a half-life of 128.4 days and also decays with emission of a high-energy beta particle (β_{max} 0.968 MeV). In one study, natural Tm was irradiated and the ^{170}Tm obtained by the usual processing scenario (Das et al. 2009). The EDTMP complex was readily prepared in high yield with >99 % radiochemical purity at room temperature and evaluated in normal Wistar rats. Approximately 50–55 % of the administered activity was detected in the skeleton and low soft tissue uptake was observed with long-term 60-day skeletal retention. In a more recent study, natural high-purity $Tm_2(NO)_3$ targets (100 % ^{169}Tm) were used to produce the ^{170}Tm with a specific activity range of 10–15 mCi/mg and radionuclide purity >99.99 % during a 5-day irradiation period at a thermal neutron flux of $3–4 \times 10^{13}$ neutrons/cm^2/s (Shirvani-Arani et al. 2013). The EDTMP complex was prepared in high yield with an optimal ligand/metal ratio of approximately 20:1 and a pH range of 6–8 >99 % yield. The complex has an amazing stability after storage for 2 months at room temperature. Biodistribution studies in rats for periods of 2 h to 2 months demonstrated that ^{170}Tm-EDTMP rapidly locates in the skeleton after 2 h (2 % ID/g) with very low blood levels (<0.1 % ID/g). These combined data are promising, but the long half-life and very long skeletal retention similar to ^{89}Sr would indicate that titration of the effective dose and repeated dose administration would not be possible.

12.5.5 Ytterbium-175

Ytterbium-175 is one of radioisotopes that decay by emission of beta particles 470 keV maximum energy (86.5 %) to stable ^{175} Lu. The prominent gamma rays emitted from ^{175}Yb are 113.8 keV (1.88 %), 286 keV (3.01 %), and 396 keV (6.4 %). The prospect of using this radioisotope for bone pain palliation in enticing as the medium energy beta energy could be used for therapy and gamma-ray energies are suitable for imaging studies. The thermal neutron cross section of ^{174}Yb is 63.2 b which

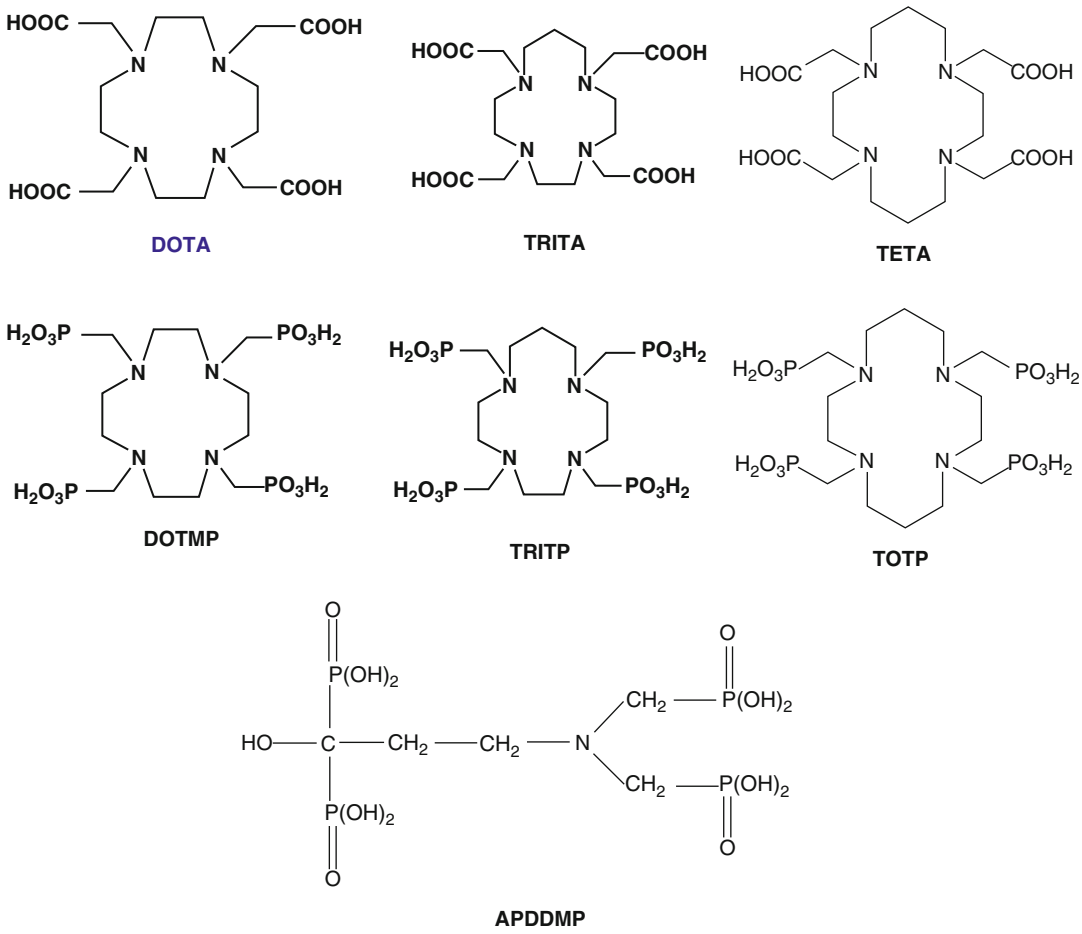

Fig. 12.14 Structures of methylcarboxylate and methylphosphonate complexes evaluated and APDDMP for preparation of new ^{153}Sm and ^{166}Ho bone-targeting agents

offers the scope to produce ^{175}Yb in moderate specific activity and good radionuclidic purity using natural Yb target in medium flux reactors. The relatively longer (compared to ^{153}Sm or ^{166}Ho) physical half-life of ^{175}Yb provides logistic advantages for facilitating supply to nuclear medicine centers far away from the reactors. Radiolabeling studies of ^{175}Yb with four polyaminomethylene phosphonic acid ligands, ethylenediamine tetramethylene phosphonic acid, propylenediamine tetramethylene phosphonic acid, triethylenetetramine hexamethylene phosphonic acid, and diethylenetriamine pentamethylene phosphonic acid have been reported (Mathew et al. 2004). Triethylenetetraminehexamethylene phosphonic acid (TTHMP), a multidentate polyaminopolyphosphonic acid ligand, has been explored for possible use in bone palliation (Safarzadeh 2014).

12.6 Bone Pain Palliation Agents Using Radioisotopes Which Have Minimal Soft Tissue Penetration

Although the spectrum of agents currently commercially available as approved agents used for bone pain palliation contain beta-emitting radioisotopes, several radioisotopes which decay by emission of particles which have limited soft

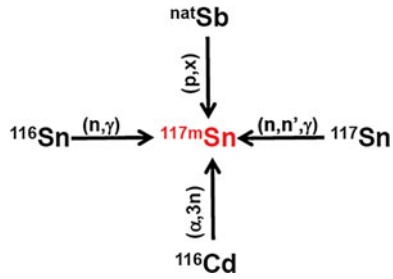

Fig. 12.15 Summary of reactor and accelerator production of ^{117m}Sn

tissue penetration are being actively investigated. Because of the potential marrow damage from high-energy beta-particle emissions, some investigators have focused on the use of radioisotopes which have very high LET and minimal soft tissue penetration as a strategy to spare the bone marrow.

12.6.1 Tin-117m (^{117m}Sn) DTPA

Tin-117m is a CE emitter, is both reactor- and accelerator-produced, and has a 13.6-day half-life and decays with emission of low-energy conversion electrons with principal energies of 0.126 MeV (64 %) and 0.152 MeV (26.1 %) (Table12.1) which have limited soft tissue penetration. Tin-117m can be produced in either a nuclear reactor or an accelerator, but the SA varies tremendously (Fig. 12.15). Reactor production is possible by either the radiative ^{116}Sn(n,γ)^{117m}Sn (Fukushima et al. 1963; Knapp et al. 1998; Mausner et al. 1992; Mirzadeh et al. 2011; Ponsard et al. 2009; Toporov et al. 2005; Yano et al. 1973) or inelastic ^{117}Sn(n n', γ)^{117m}Sn pathways (Mirzadeh et al. 1997). However, the specific activity via the reactor routes even at high thermal neutron flux is still <10–15 mCi/mg. Although the mass levels of Sn which result from preparation of ^{117m}Sn-DTPA may still not reach a toxic threshold, the evaluation of accelerator-based production strategies provides ^{117m}Sn for this and other targeted applications with much higher specific activity. Thus the production and efficient chemical processing of ^{117m}Sn accelerator targets is a key issue to make sufficient activity levels of HAS ^{117m}Sn available for use in bone pain palliation trials and for other therapeutic applications.

One alternative approach involves the use of high-energy fast protons for irradiation of natural antimony by the ^{nat}Sb(p,x)^{117m}Sn pathway (Kyu et al. 2010). Processing of the irradiated antimony targets and purification of the ^{117m}Sn present some challenges since the large macroscopic levels of the 2–3 g antimony targets contrast with the microscopic levels of the desired ^{117m}Sn product. Optimization resulted in *n*-butyl ether extraction of ^{117m}Sn from the target following dissolution in 10 M HCl. For separation of tin from the primary cadmium, indium, and tellurium impurities, sodium iodide addition formed an HI solution in which the impurities were soluble, and the resulting tin iodide (SnI_4) complex was readily extracted with benzoyl hydrocarbons. After three extractions and washing the combined ^{177m}Sn fractions with 6 M HCl, the ^{117m}Sn was then be obtained by extraction with 0.1 M NaOH or HCl. It was estimated by the authors that for high-activity-level production scale, the antimony target size could be increased to 50 g.

In another approach the production of high specific activity ^{117m}Sn by the ^{116}Cd(α, 3n)^{117m}Sn reaction has been demonstrated (Maslov et al. 2011). In this approach, the irradiated targets are dissolved in nitric acid, filtered, and the nitrates treated with HF to form the Cd and Sn fluorides. Subsequent successive HF chemical treatments and evaporation provided the concentrated product solution which was dissolved in 0.1 N HF and loaded onto a Dowex 1 × 8 (200–400 mesh) anion exchange column. The Cd was removed with 0.1 N HF and the ^{117m}Sn was then eluted with 3 M nitric acid. There was clean separation of the two peaks, and using a 13.16 mg/cm^2 ^{nat}CdO target, the estimated ^{117m}Sn production yield was 37.5 kBq/μAh and 410 kBq/μAh using a 95 % enriched ^{116}CdO target. The ^{117m}Sn was recovered in 98 % radiochemical yield with >99 % radionuclide purity with an estimated specific activity of 2.4 GBq/mg Sn, which is much higher than can be obtained from the reactor production routes. Because of the limited number of accelerators which are capable for accelerating alpha particles,

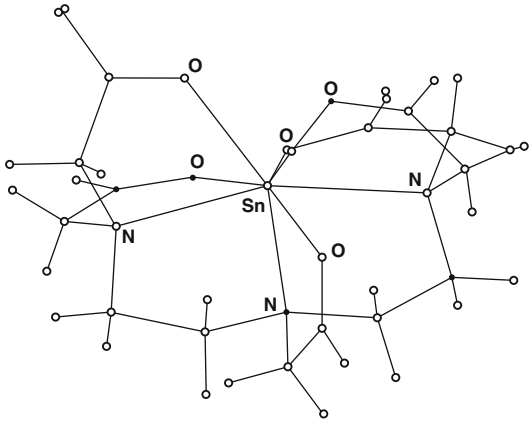

Fig. 12.16 Structure of the tin(IV) DTPA complex

however, this method would not be expected to be practical for routine availability of the high activity levels of the ^{117m}Sn which would be expected to be required for late-stage clinical trials or routine clinical use of ^{117m}Sn. The use of the proton reaction for routine production of ^{117m}Sn also has been further assessed and validated.

Studies in the literature have thus far only reported the use of reactor-produced ^{117m}Sn for the preparation of the Sn-DTPA used for clinical trials. Use of the ^{117m}Sn(+4)DTPA complex (Fig. 12.16) for bone pain palliation permits gamma camera imaging since ^{117m}Sn emits a gamma photon with an energy of 159 keV, again, an advantage for personalized medicine. This was first described as a candidate for skeletal localization and as a potential bone pain palliation agent in 1973 (Yano et al. 1973). This agent is ready prepared by the complexation of sodium DTPA with ^{117m}Sn(IV) in dilute HCl in an oxygen-free atmosphere. Animal studies demonstrated that the stannic form of Sn-DTPA [Sn-117m (4+) DTPA)] behaved much differently from the stannous form [Sn-117m (2+) DTPA]. It was not rapidly excreted into the urine, as expected, but taken up and retained almost exclusively into the bone (Srivastava et al. 1985). Further studies (Oster et al. 1995) showed that its behavior mimicked that of ^{99m}Tc MDP in certain pathological conditions. A pilot study in 15 patients indicated that pain palliation was achieved through administration of Sn-117m DTPA at 71–143 μCi/kg levels (Atkins et al. 1995). The first phase 1 activity escalation study conducted over the activity range of 66–573 MBq reported symptom benefit in 9 of 10 evaluable patients with no significant myelotoxicity (Atkins et al. 1993). A later phase I/II activity escalation study in 47 patients with painful bone metastases reported a 75 % overall pain response (range, 60–83 %), with complete pain relief in 30 % (Srivastava et al. 1998). There is no dose–response relationship and the onset of pain relief is also much earlier than that with the other agents described. At doses of ≥444 MBq (≥12 mCi) (per 70 kg body weight), pain palliation has been noted as early as 1 week after treatment (Srivastava et al. 1998).

The ^{117m}Sn is traditionally produced (Chap. 5) by the neutron irradiation of enriched ^{116}Sn in a nuclear reactor (Fukushima et al. 1963; Knapp et al. 1998; Mausner et al. 1992; Mirzadeh et al. 2011; Ponsard et al. 2009; Toporov et al. 2005; Yano et al. 1973). However, because of the relatively low thermal neutron cross section of 0.14 b, the ^{117m}Sn specific activity available by irradiation of ^{116}Sn (radiative route) or ^{117}Sn (inelastic route) even in high thermal neutron flux ($>1\times10^{15}$ neutrons/cm^2/s) reactors such as the *high-flux isotope reactor (HFIR)* at the Oak Ridge National Laboratory (ORNL) and the *SM3 reactor*, in Dimitrovgrad, Russia, results in production of ^{117m}Sn with only modest specific activity of 10–15 mCi/mg (Mirzadeh et al. 1997). At present, ^{117m}Sn is commercially available with reported specific activities of 20 Ci/g (~0.74 GBq/mg) at the end of bombardment (EOB).

Because of the requirement for higher specific activity and higher production yields/target at lower costs, the accelerator production of ^{117m}Sn has been more recently evaluated and reported. In this strategy, ^{nat}Sb targets have been irradiated by high-energy proton beams of 38–60 MeV (Ermolaev et al. 2007, 2009). Following chemical recovery of ^{117m}Sn by extraction of Sb with dibutyl ether and chromatographic purification on silica gel column, the ^{117m}Sn has been recovered with specific activity of 1000 mCi/mg in 50–100 mCi batch yields. It has not yet been reported if this is a cost-effective and practical ^{117m}Sn production route because of costs and

availability, but the availability of high specific activity ^{117m}Sn is expected to be important for other applications of this radioisotopes, such for therapy of coronary plaques (Srivastava et al. 2009). More recent large multicenter trials using ^{117m}Sn DTPA for bone pain palliation have not been reported, probably reflecting the status and progress of using the variety of beta-emitting radioisotopes discussed earlier.

12.6.2 Radium-223 Chloride

Another new strategy for bone pain palliation using radioisotopes which have very shallow soft tissue penetration is the use of alpha-emitting radioisotopes (Allen et al. 2004; Howell et al. 1997; Li et al. 2004; Polig et al. 1992). The prospect of using α-emitting radioisotopes as sources in metabolically concentrated radionuclide therapy against skeletal metastases is enticing because the short range of the α-particles could affect a reduction in bone marrow exposure. Among the radionuclide investigated as a bone-seeking agent, ^{212}Bi has attracted considerable attentions. While the use of ^{212}Bi-DOTMP showed a significant bone affinity, the short physical half-life of ^{212}Bi ($t_{½}$=60 min) and the substantial time requirement for ^{212}Bi-DOTMP to localize in the target tissue emerged as the major impediments that result in significant normal tissue exposure during the uptake and elimination phases (Hassfjell et al. 1997). Recent interest has evolved to use of ^{223}Ra chloride as a promising new strategy for bone pain palliation, with the supposition that the very short range of alpha particles in soft tissue would minimize damage to normal tissue (Brady et al. 2013; Harrison et al. 2013; Hoskin et al. 2014; McGann and Horton 2015; Turner and O'Sullivan 2014). The radionuclidic properties of ^{223}Ra are summarized in Table 12.2 and the decay scheme illustrated in Fig. 12.17.

Selection of ^{223}Ra is primarily based on its favorable decay chain and half-life (Nilsson et al. 2005). Radium-223 begins to decay almost instantaneously, reaching a final stable lead product over a 6-stage decay process. For each atom of ^{223}Ra, 4 alpha particles are released, representing 94 % of the total radiation energy emitted (Bruland et al. 2006). Radium is a member of Group IIA in the periodic table, and because of its similarity to calcium as a +2 metal, it mimics calcium in forming complexes with the bone mineral hydroxyapatite, which specifically targets bone metastases and thus requires no special chemical attachment to a bone-seeking carrier molecule (Den et al. 2014; Henriksen et al. 2003). Radium-223 preferentially targets in areas of new bone formation in close proximity to regions of bone metastases and deliver a highly localized density of ionizing radiation within the tumor

Table 12.2 Radionuclidic properties of ^{223}Ra

Half-life	Path length	Emission	Maximum energy (MeV)
11.43 days	60 μm (mean) 100 μm (maximum)	α (4)	5.78, 6.88, 7.53, 6.68
		β (2)	0.45, 0.49
		γ (5)	0.82, 0.154, 0.269, 0.351, 0.402

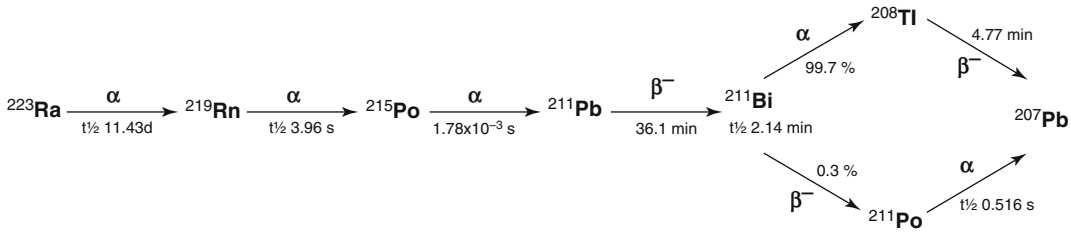

Fig. 12.17 Decay scheme of ^{223}Ra

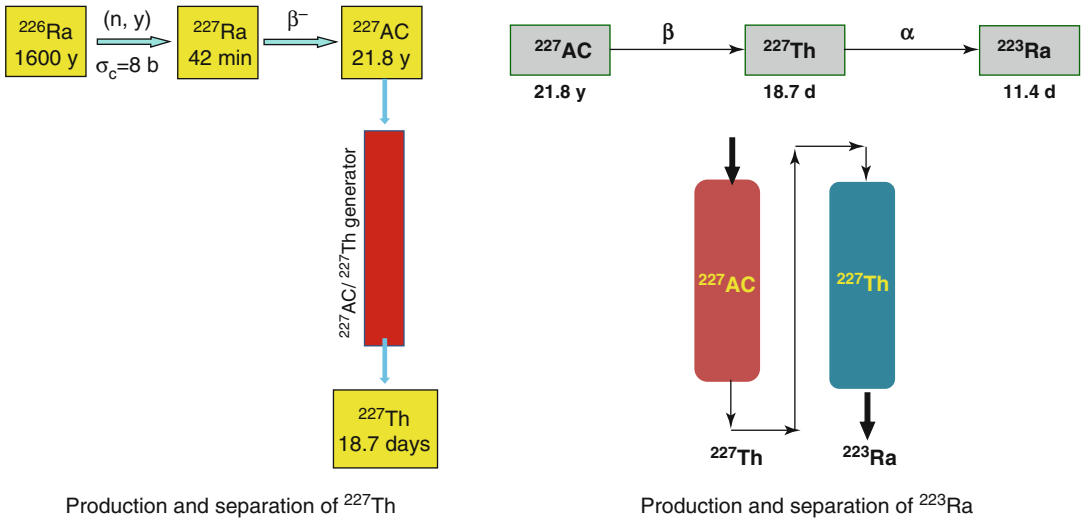

Fig. 12.18 Availability of ^{223}Ra and ^{227}Th from radioactive decay of ^{227}Ac

microenvironment, causing a significant amount of irreparable double-stranded DNA damage. This DNA damage triggers tumor cell death, thus eliciting greater cytotoxic effects on bone-metastatic tumor sites (Den et al. 2014; Jadvar and Quinn 2013).

The ^{223}Ra is available from decay of ^{227}Ac (21.770-year half-life) via the ^{227}Th intermediate (Fig. 12.18). Actinium-227 decays primarily via beta emission (46 keV) and also emits very low intensity energy alphas. Although ^{227}Ac is found only in trace amounts in uranium ore, it can be produced in milligram levels by neutron irradiation of ^{226}Ra and subsequent decay of the short-lived (42 min) ^{227}Ra activation product (Mirzadeh 1998). The intermediary ^{227}Th has also been evaluated for bone pain palliation (Henriksen et al. 2004; Washiyama et al. 2004). Actinium-227 is most often obtained by extraction from legacy actinium-beryllium neutron sources (Soderquist et al. 2012).

Early studies with radium-223 showed a promising clinical profile in patients with bone metastases, including no dose-limiting hematologic toxicity (Nilsson et al. 2005), in phase IA (25 patients) and phase IB (six patients). In a phase I study in men and women with bone metastases, all patients showed a reduction in alkaline phosphatase (ALP) levels, but the effect was more marked in men than in women (Nilsson et al. 2005), suggesting that ^{223}Ra may target osteoblastic lesions more effectively than osteolytic lesions (Bellmunt 2013). Therefore, the phase II studies focused on patients with metastatic CRPC. Randomized phase II studies included a saline control group (31 patients) and patients treated four times with ^{223}Ra at four-week intervals (33 patients) and a second saline group and patients treated with external beam therapy (31 patients) (Bruland et al. 2008). The data demonstrated the excellent lesion targeting of intravenously administered $^{223}RaCl_2$ with high antitumor activity and impressive increase in overall survival in a group of hormone refractory prostate cancer patients.

The pivotal phase III trial was the Alpharadin (i.e., initial designation of Xofigo®) in *symptomatic prostate cancer patients* (ALSYMPCA) study, a multicenter, randomized, double-blind study that enrolled 921 patients in more than 100 centers in 19 countries with metastatic, castration-resistant prostate cancer. Men in the trial were randomly assigned to receive either ^{223}Ra (six intravenous injections, one every 4 weeks) plus the best standard of care or a placebo plus the best standard of care. The trial's primary endpoint was overall survival (OS) with planned follow-up for 3 years. Secondary endpoints

included time to the first symptomatic skeletal event—such as a bone fracture, spinal cord compression, or the need for radiation to treat bone-related symptoms—and quality of life measures. The interim analysis showed a statistically significant benefit in favor of ^{223}Ra, so the study was prematurely terminated/unblinded and the placebo recipients were offered ^{223}Ra (Parker et al. 2013). In the final analysis, median OS was 14.9 months with ^{223}Ra versus 11.3 months with placebo (Parker et al. 2013). There was a 30 % reduction in the risk of death with radium-223 (HR = 0.70; 95 % CI, 0.58–0.83; $P < .001$), which was seen in all subgroups of patients. The significant clinical benefit of ^{223}Ra relative to placebo was also seen in all the major secondary endpoints, including time to first symptomatic skeletal event (median, 15.6 months vs. 9.8 months; HR = 0.66; 95 % CI, 0.52–0.83; $P < .001$) and time to an increase in ALP or PSA level. More ^{223}Ra patients experienced a meaningful improvement in overall quality of life. These data are very promising but probably indicate that the very limited soft tissue penetration would be expected to preclude deeper penetration, and thus irradiation for large lesions and would not exhibit potentially complete therapeutic effect. Based on the results of this clinical trial, the US Food and Drug Administration (FDA) approved Xofigo® (radium-223 dichloride) for the treatment of patients with castration-resistant prostate cancer (CRPC), symptomatic bone metastases, and no known visceral metastatic disease.

12.7 Soft Tissue Penetration and Efficacy of Radioisotopes for Bone Pain Palliation

In spite of the very rapid effective introduction and use of ^{223}Ra for treatment of bone pain in hormone-refractory patients with skeletal metastases from prostate cancer, there continues to be widespread debate and discussion concerning the consequences of marrow suppression using radioisotopes which emit particles which have deep soft tissue penetration such as ^{186}Re, ^{32}P, ^{90}Y, and ^{188}Re (Pandit-Taskar et al. 2004). The role of these agents is of course to treat the inflammatory site to reduce the pain associated with activation of nociceptors by the metastasis. In this regard, with the issue of costs and availability aside, this issue represents in some ways the impetus for support for use of CE- and alpha-emitting radioisotopes such as ^{117m}Sn and ^{223}Ra (Lewington 2005). However, at least in cases where the marrow has not been compromised, it is generally agreed that the transitory nadir for marrow suppression rebounds after a few weeks (Baker and Levin 1998). The other issue is the possibility of a therapeutic effect, which requires penetration into the tumor mass, i.e., beyond the inflammatory area. It could be that the use of bone pain palliation agents may evolve to a personalized approach, where the appropriate agent can be prescribed based on the metastatic progression. As an example, Fig. 12.19 illustrates the qualitative expected particle penetration comparing an alpha and beta emitter in a typical PET/CT image of a vertebral metastases. In this scenario, it would not be expected that alpha radiation would reach the center tumor mass and that bone pain palliation agents radiolabeled with high-energy beta emitters may have a greater chance to exhibit am actual therapeutic response in such a case.

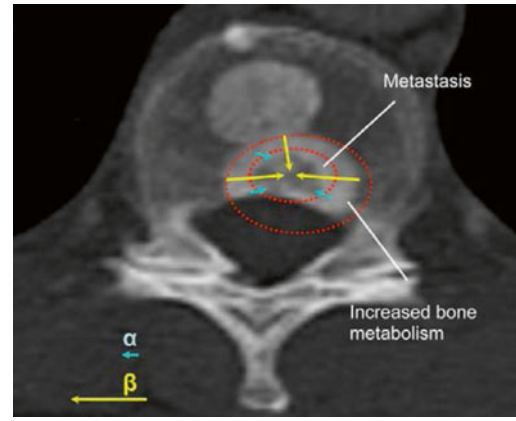

Fig. 12.19 Example of a bone metastasis comparing the expected range of beta and alpha particles deposited on the bone surface (Courtesy of Prof. Dr. H.-J. Biersack, Clinic for Nuclear Medicine, University Hospital, Bonn, Germany)

12.8 The Possibility of Therapeutic Effects on Bone Metastases with High Activity Doses of Agents Used for Bone Pain Palliation

In addition to the well-known and effective use of particle-emitting targeted radioisotopes for the palliation of pain associated with skeletal metastases, another goal for such therapies is the potential eradication of these metastatic lesions (Morris and Scher 2003). There is growing evidence that the repeat, multiple dosing of bone palliation agents radiolabeled with particle-emitting radioisotopes can have a therapeutic effect. Such results have been reported using ^{188}Re-HEDP (Palmedo et al. 1998b, 2000, 2003a, b; Biersack et al. 2011). In addition, similar studies conducted with multiple dosing with ^{153}Sm-EDTMP (Quadramet®) have provided similar results (Autio et al. 2013; Morris and Scher 2003).

In a phase II trial comparing the response rate in CRPC patients with bone metastases after 1 or 2 administrations of ^{188}Re-HEDP within 8 weeks, pain palliation was significantly higher and associated with >50 % PSA reduction in 39 % of the patients in the double-dose group compared with 7 % in the single-dose group, and the mean survival increased from 7 to 13 months in the double-dose cohort (Palmedo et al. 2003a, b). A retrospective analysis of these data of the same group showed, in a total number of 60 patients suffering from bone metastases of hormone-refractory prostate cancer, an improvement of the mean survival from 4.5 to 15.66 months, in the subgroup with multiple (3 and more) successive administrations of ^{188}Re-HEDP (Biersack et al. 2011). In another publication by the same group, it has been observed that pain control was significantly better in the repeated-therapy group (24 vs. 8 weeks (Sinzinger et al. 2011). It is pertinent to mentioned that the response of metastases already existing prior to the first therapy was significantly better than the response of those appearing during repeated therapy (Sinzinger et al. 2011).

In another study, 6 of 40 patients with metastatic breast cancer treated with ^{89}Sr for painful skeletal metastases received repeated ^{89}Sr administrations. Higher overall response rates (83 % versus 60 %) were recorded in the re-treatment subset by comparison with patients who had received a single treatment (Fuster et al. 2000). Prolonged response duration (3.08 ± 0.48 versus 5.33 ± 2.36 months) was observed in breast cancer patients receiving multiple ^{89}Sr administrations compared with patients who had received a single treatment (Kasalický and Kraská 1998).

Addition of cytotoxic chemotherapy to radionuclide treatment in patients with predominantly osteoblastic bone metastases ("chemosensitization") has emerged as another modality. In two randomized clinical trials in men with CRPC, significant prolongation of mean survival, improved quality and duration of pain reduction, and delayed pain in clinically silent metastases were observed in patients treated using ^{89}Sr/cisplatin compared with ^{89}Sr/placebo (Sciuto et al. 2002; Tu et al. 1997). Difference in hematological toxicity between the two groups was insignificant. In another randomized study by Tu et al., CRPC patients were pretreated with induction doxorubicin and vinblastine to receive further doxorubicin as monotherapy or doxorubicin with ^{89}Sr. A greater than 80 % PSA reduction was observed in 72 % of the subjects who had received doxorubicin with ^{89}Sr compared with 36 % of those who had received doxorubicin alone. The mean survival increased from 17 months in the monotherapy arm to 28 months in the combined treatment group (Tu et al. 2001). Early results indicate that high linear energy transfer (LET) therapeutic alpha-particle-emitting radionuclides exert a tumoricidal effect in skeletal metastases. Result of a randomized, placebo-controlled phase II study using fractionated ^{223}Ra in metastatic CRPC patients revealed significant reductions in bone alkaline phosphatase, delayed time to PSA progression (26 versus 8 weeks), and prolonged median overall survival (65.3 vs. 46.4 weeks) in the active treatment arm by comparison with the control group. The hematological toxicity was similar in both groups (Nilsson et al. 2007).

12.9 Summary

There are currently several approved radiopharmaceuticals available for treatment of painful skeletal metastases and continued interest and the development of new agents reflects the expected advancing importance for broader clinical use of these agents. These agents have a well-documented effectiveness in reducing the debilitating pain associated with skeletal metastases and offer an important option for patients, especially those who present with multiple metastatic sites which preclude the use of external irradiation. The improvement of quality of life is an important factor, even in end-stage patients. In spite of the effectiveness and expected increased availability, therapeutic radiopharmaceutical agents do not yet represent the first-line therapy for bone pain palliation. This issue probably reflects the training of oncologists and urologists in more traditional therapeutic options using opiate analgesics in these specialties, with ordering nuclear medicine techniques generally only as a last-line option. If patients were treated early in their disease progression with radiopharmaceutical agents, this may offer a better more effective option and such studies are required to determine how first-line use of these agents compares with the traditional therapeutic options for these patients. It is important that referring physicians are educated to the benefits for first-line therapy of such an effective bone pain palliation agent. Although late-stage therapy with this agent is important, it would be expected that early application would have many benefits in total therapy cost savings and reducing patient morbidity, and the possibility of providing therapeutic effects earlier in the disease process may be possible.

References

Allen BJ, Raja C, Rizvi S, et al. Targeted alpha therapy for cancer. Phys Med Biol. 2004;49:3703–12.

Alyafei S, Tomiyoshi K, Sarwar M, et al. Biodistribution studies of ^{186}Re complexes of 3-amino-1-hydroxypropyliene-1,1-bisphosphonic acid in mice. Nucl Med Commun. 1999;20:551–7.

Ando A, Ando I, Tonami N, et al. ^{177}Lu-EDTMP: a potential therapeutic bone agent. Nucl Med Commun. 1998;19(6):587–91.

Arteaga de Murphy C, Ferro-Flores G, Pedraza-Lopez M, et al. Labelling of Re-ABP with ^{188}Re for bone pain palliation. Appl Raiat Isot. 2001;54:435–42.

Atkins HL, Mausner LF, Srivastava SC, et al. Biodistribution of Sn-117m(4+)DTPA for palliative therapy of painful osseous metastases. Radiology. 1993;186:279–83.

Atkins HL, Mausner LF, Srivastava SC, et al. Tin-117m(4+)-DTPA for palliation of pain from osseous metastases: a pilot study. J Nucl Med. 1995;36:725–9.

Autio KA, Pandit-Taskar N, Carrasquillo JA, et al. Repetitively dosed docetaxel and ^{153}samarium-EDTMP as an antitumor strategy for metastatic castration-resistant prostate cancer. Cancer. 2013;119(17):3186–94.

Baker GR, Levin J. Transient thrombocytopenia produced by administration of macrophage colony-stimulating factor: investigations of the mechanism. Blood. 1998;91:89–99.

Banerjee S, Pillai MRA, Knapp Jr FF. Lutetium-177 therapeutic radiopharmaceuticals – linking chemistry, radiochemistry and practical applications. Chem Rev. 2015;115:2934–74.

Bauman G, Charette M, Reid R, Sathya J. Radiopharmaceuticals for the palliation of painful bone metastasis-a systemic review. Radiother Oncol. 2005;75(3):258–70.

Bellmunt J. Tackling the bone with alpha emitters in metastatic castration- resistant prostate cancer patients. Eur Urol. 2013;63(2):198–200.

Biersack HJ, Palmedo H, Andris A, et al. Repeated Re-188 HEDP therapy of hormone refractory bone metastases in prostate cancer. J Nucl Med. 2011;52:1721–6.

Bisunadan MM, Blower PJ, Clarke SEM, et al. Synthesis and characterization of [^{186}]Rhenium(V)dimercaptosuccinic acid: a possible tumour radiotherapy agent. Appl Radiat Isot. 1991;42:167–71.

Blower PJ, Prakash S. The chemistry of rhenium in nuclear medicine. In: Perspectives on bioinorganic chemistry. Connecticut: JAI Press, Inc; 1999. p. 91–143.

Blower PJ, Lam ASK, O'Doherty MJ, et al. Biodistribution and dosimetry of pentavlaent Rhenium-188-dimercaptosuccinic acid in patients with disseminated bone metastasis. Eur J Nucl Med. 1998;25:613–21.

Blower PJ, Kettle AG, O'Doherty MJO. ^{99m}Tc(V)DMSA quantitatively predicts ^{188}Re(V)DMSA distribution in patients with prostate cancer metastatic to bone. Eur J Nucl Med. 2000a;27:1405–9.

Blower PJ, Kettle AG, O'Doherty MJ, et al. ^{99m}Tc(V) DMSA quantitatively predicts ^{188}Re(V)DMSA distribution. In: 28th annual meeting, British Nuclear Medicine Society, Brighton, 10–12 Apr 2000b.

Blower PJ, Kettle AG, O'Doherty MJ, Knapp Jr FF. Quantitative prediction of ^{188}Re(V)DMSA distribution from ^{99m}Tc(V)DMSA scans for targeted radiotherapy planning. J Nucl Med. 2000c;41(Suppl):274P.

Bordoloi JK, Berry D, Khan IU, et al. Technetium-99m and rhenium-188 complexes with one and two pendant

bisphosphonate groups for imaging arterial calcification. Dalton Trans. 2015;44(11):4963–75.
Bouchet LG, Bolch WE, Goddu SM, et al. Considerations in the selection of radiopharmaceuticals for palliation. J Nucl Med. 2000;41(4):682–7.
Brady D, Parker CC, O'Sullivan JM. Bone-targeting radiopharmaceuticals including radium-223. Cancer J. 2013;19(1):71–8.
Bruland OS, Skretting A, Solheim OP, Aas M. Targeted radiotherapy of osteosarcoma using ^{153}Sm-EDTMP. A new promising approach. Acta Oncol. 1996;35: 381–4.
Bruland Ø, Nilsson S, Fisher DR, Larson RH. High-linear energy transfer irradiation targeted to skeletal metastases by the α-emitter ^{223}Ra: adjuvant or alternative to conventional modalities? Clin Cancer Res. 2006;12(20 Suppl):6250s–7.
Bruland OS, Jonasdottir TJ, Fisher DR, Larsen RH. Radium-223: from radiochemical development to clinical applications in targeted cancer therapy. Curr Radiopharm. 2008;1:103–208.
Chopra A. ^{177}Lu-labeled methylene diphosphonate. Molecular imaging and contrast agent database (MICAD) [internet]. Bethesda: National Center for Biotechnology Information (US); 2011. p. 2004–13.
D'angelo G, Sciuto R, Salvatori M, et al. Targeted "bone-seeking" radiopharmaceuticals for palliative treatment of bone metastases: a systematic review and meta-analysis. Q J Nucl Med Mol Imaging. 2012;56(6): 538–43.
Das T, Chakraborthy S, Sarma HD, et al. ^{170}Tm-EDTMP: a potential cost-effective alternative to $^{89}SrCl_2$ for bone pain palliation. Nucl Med Biol. 2009;36: 561–8.
Dash A, Knapp Jr FF. An overview of radioisotope separation technologies for development of ^{188}W/^{188}Re radionuclide generators providing ^{188}Re to meet future research and clinical demands. RSC Adv. 2015; 5:39012–3903.
Dash A, Pillai MRA, Knapp FF. Production of ^{177}Lu for targeted radionuclide therapy: available options. Nucl Med Mol Imaging. 2015;49:85–107.
Davis J, Cook ND, Pither RJ. Biologic mechanisms of $^{89}SrCl_2$ incorporation into type I collagen during bone mineralization. J Nucl Med. 2000;41:183–8.
De Klerk JM, van het Schip AD, Zonnenberg BA, et al. Phase 1 study of Rhenium-186-HEDP in patients with bone metastases originating from breast cancer. J Nucl Med. 1996;37:244–9.
De Rosales RTM, Finucane C, Foster J, et al. ^{188}Re(CO)-dipicolylamine-alendronate: a new bisphosphonate conjugate for the radiotherapy of bone metastases. Bioconj Chem. 2010;21:811–5.
Den RB, Doyle LA, Knudsen KE. Practical guide to the use of radium 223 dichloride. Can J Urol. 2014;21(2 Suppl 1):70–6.
Eisenhut M. Iodine-131-labeled diphosphonates for the palliative treatment of bone metastases: I. Organ distribution and kinetics of I-131 BDP3 in rats. J Nucl Med. 1984;25(12):1356–61.
Eisenhut M, Beberich R, Kimming B, et al. Iodine-131-labeled diphosphonates for the palliative treatment of bone metastases: II. Preliminary clinical results with iodine-131 BDP3. J Nucl Med. 1986a;27(8):1255–61.
Eisenhut M, Fritz P, Kimmig B, et al. Iodine-131-labeled diphosphonates for the palliative treatment of bone metastases: III. Considerations of interaction. Binding and adsorbed dose. Int J Rad Appl Instrum A. 1986b;37(8):741–7.
Eisenhut M, Barber J, Taylor DM. Iodine-131-labeled diphosphonates for the palliative treatment of bone metastases: IV. Syntheses of benzylidenephosphonates and their distribution in rats. Int J Rad App Instrumen A. 1987;38(7):535–40.
Elder RC, Yuan J, Helmer B, et al. Studies of the structure and composition of rhenium-1,1-hydroxyethylidenediphosphonate (HEDP) analogues of the radiotherapeutic agent (186)ReHEDP. Inorg Chem. 1997;36(14):3055–63.
Ermolaev SV, Zhuikov BL, Kokhanyuk VM, et al. Production yields of ^{117m}Sn from natural antimony target in proton energy range 145–35 MeV. J Label Compd Radiopharm. 2007;50:611–2.
Ermolaev SV, Zhuikov BL, Kokhanyuk AA. Production of no-carrier added tin-117m from proton irradiated antimony. J Radioanal Nucl Chem. 2009;280:319–24.
Fellner M, Baum R, Kubicek V, et al. ^{177}Lu-BPAMD – from bone imaging to therapy with a macrocycle-bisphosphonate ligand. J Nucl Med. 2010;51 Suppl 2:1164.
Fettich J, Nair G, Padhy AK, et al. Phosphorus-32 for bone pain palliation due to bone metastases, its safety and efficacy in patients with advanced cancer. Vienna: IAEA-TECDOC-1228; 2001. p. 193–8.
Fettich J, Padhy A, Nair N, et al. Comparative clinical efficacy and safety of phosphorus-32 and strontium-89 in the palliative treatment of metastatic bone pain: results of an IAEA coordinated research project. World J Nucl Med. 2003;2:226–31.
Finlay IG, Mason MD, Shelley M. Radioisotopes for palliation of metastatic bone cancer: a systematic review. Lancet Oncol. 2005;6:392–400.
Fukushima S, Hayashi S, Kume S, et al. The production of high specific activities of Tin. Bull Chem Soc Jpn. 1963;36(10):1225–8.
Fuster D, Herranz R, Vidal-Sicart S, et al. Usefulness of strontium-89 for bone pain palliation in metastatic breast cancer patients. Nucl Med Commun. 2000;21:623–62.
Gough N, Miah AB, Linch M. Nonsurgical oncological management of cancer pain. Curr Opin Support Palliat Care. 2014;8(2):102–11.
Guhlke S, Scheithauer S, Oetjen K, et al. ^{188}Re(V)-DMSA: *in-vitro* and *in-vivo* studies on the individual stereo isomers. Radiochim Acta. 2009;92:277–83.
Harrison MR, Wong TZ, Armstrong AJ, George DJ. Radium-223 chloride: a potential new treatment for castration-resistant prostate cancer patients with metastatic bone disease. Cancer Manag Res. 2013;5: 1–14.

Hassfjell SP, Bruland ØS, Hoff P. ^{212}Bi-DOTMP–an α particle emitting bone seeking agent for targeted radiotherapy. Nucl Med Biol. 1997;24:231–7.

Henriksen G, Fisher DR, Roeske JC, et al. Targeting of osseous sites with alpha-emitting ^{223}Ra: comparison with the beta-emitter ^{89}Sr in mice. J Nucl Med. 2003;44:252–9.

Henriksen G, Bruland OS, Larsen RH. Thorium and actinium polyphosphonate compounds as bone-seeking alpha particle-emitting agents. Anticancer Res. 2004;24(1):101–5.

Hoskin P, Sartor O, O'Sullivan JM, et al. Efficacy and safety of radium-223 dichloride in patients with castration-resistant prostate cancer and symptomatic bone metastases, with or without previous docetaxel use: a pre-specified subgroup analysis from the randomized, double-blind, phase 3 ALSYMPCA trial. Lancet Oncol. 2014;15(12):1397–406.

Howell RW, Goddu SM, Narra VR, et al. Radiotoxicity of gadolinium-148 and radium-223 in mouse testes: relative biological effectiveness of alpha-particle emitters *in vivo*. Radiat Res. 1997;147:342–8.

Hsieh B-T, Callahan AP, Beets AL, et al. Ascorbic acid/saline eluant increases ^{188}Re yields after "wet" storage of ^{188}W/^{188}Re generators. Appl Radiat Isot. 1996;47:23–6.

Jadvar H, Quinn DI. Targeted alpha-particle therapy of bone metastases in prostate cancer. Clin Nucl Med. 2013;38:966–71.

Jansen DR, Krijger GC, Kolar ZI, et al. Targeted radiotherapy of bone malignancies. Curr Drug Discov Technol. 2010;7(4):233–46.

Jeong JM, Chung JK. Update: therapy with ^{188}Re-labeled radiopharmaceuticals: an overview of promising results from initial clinical studies. Can Biother Radiopharm. 2003;18:707–18.

Kasalický J, Kraská V. The effect of repeated strontium-89 chloride therapy in bone pain palliation in patients with skeletal cancer metastases. Eur J Nucl Med. 1998;25:1362–7.

Knapp Jr FF. Rhenium-188 – a generator-derived radioisotope for cancer therapy. Cancer Biother Radiopharm. 1998;13:337–49.

Knapp Jr FF. Baum RP. Radionuclide generators – a new renaissance in the development of technologies to provide diagnostic and therapeutic radioisotopes for clinical applications. Curr Radiopharm. 2012;5(3):175–7.

Knapp Jr FF, Callahan AP, Beets AL, et al. Processing of reactor-produced ^{188}W for fabrication of clinical scale alumina-based ^{188}W/^{188}Re generators. Appl Radiat Isot. 1994;45:1123–8.

Knapp Jr FF, Beets AL, Guhlke S, et al. Availability of rhenium-188 from the alumina-based Tungsten-188/rhenium-188 generator for preparation of rhenium-188-labeled radiopharmaceuticals for cancer treatment. Anticancer Res. 1997;17:1783–95.

Knapp FF, Mirzadeh S, Beets AL, et al. Reactor-produced radioisotopes from ORNL for bone pain palliation. Appl Radiat Isot. 1998;49(4):309–15.

Knapp Jr FF, Mirzadeh S, Beets AL. Tungsten-188/rhenium-188 generators using tungsten-188 reactor-produced from irradiation of natural tungsten targets. J Nucl Med. 2000;41(Suppl):149.

Knapp Jr FF, Turner JH, Padhy AK. Issues associated with the use of the Tungsten-188/Rhenium-188 generator and concentrator system and preparation of Re-188 HDD: A report. World J Nucl Med. 2004;3:137–43.

Kyu KD, Abramov AA, Volkova SV, et al. Extraction of Tin-117m from an antimonic target irradiated by protons. Theor Found Chem Eng. 2010;44:600–3.

Lam AS, Kettle AG, O'Doherty MJ, et al. Pentavalent ^{99m}Tc-DMSA imaging in patients with bone metastases. Nucl Med Commun. 1997;18:907–14.

Lam MGEH, de Klerk JMH, van Rijk PP. ^{186}Re-HEDP for metastatic bone pain in breast cancer patients. In: Bombardieri E, Gianni L, Bonadonna G, editors. Breast cancer. Berlin/Heidelberg: Springer; 2008. p. 257–70.

Lambert B, de Klerk JM. Clinical applications of ^{188}Re-labelled radiopharmaceuticals for radionuclide therapy. Nucl Med Commun. 2006;27(3):223–9.

Lange R, de Klerk JM, Bloemendal HJ, et al. Drug composition matters: the influence of carrier concentration on the radiochemical purity, hydroxyapatite affinity and in-vivo bone accumulation of the therapeutic radiopharmaceutical (188) Rhenium-HEDP. Nucl Med Biol. 2015;42(5):465–9.

Lewington VJ. Targeted radionuclide therapy for bone metastases. Eur J Nucl Med. 1993;20(1):66–74.

Lewington VJ. Bone-seeking radionuclides for therapy. J Nucl Med. 2005;46 Suppl 1:38S–47.

Lewington VJ, McEwan AJ, Ackery DM, et al. A prospective, randomized double-blind crossover study to examine the efficacy of strontium-89 in pain palliation in patients with advanced prostate cancer metastatic to bone. Eur J Cancer. 1991;27:954–8.

Li Y, Russell PJ, Allen BJ. Targeted alpha-therapy for control of micrometastatic prostate cancer. Expert Rev Anticancer Ther. 2004;4:459–68.

Liepe K, Kropp J, Knapp Jr FF, et al. Rhenium-188 in comparison to rhenium-186 and strontium-89 in the treatment of bone metastases. Eur J Nucl Med. 1998;25:861.

Liepe K, Hiliscs R, Runge R, et al. Dose calculation and clinical efficacy of rhenium-188-HEDP in bone metastases, European Association of Nuclear Medicine Congress, Barcelona, Spain, Oct. 9–13, 1999. Eur J Nucl Med. 1999a;26:1052.

Liepe K, Kropp J, Knapp Jr FF, et al. Kinetics and therapeutic effect of rhenium-188 in palliative treatment of metastatic bone pain, annual meeting, Society of Nuclear Medicine, Los Angeles, CA, June 6–10, 1999. J Nucl Med. 1999b;40:219P.

Liepe K, Hilscs R, Kropp J, et al. Rhenium-188-HEDP for the palliative therapy of osseous metastases. In: German Nuclear Medicine meeting, Ulm, April 1999c (German).

Liepe K, Hliscs R, Kropp J, et al. Rhenium-188-HEDP in the palliative treatment of bone metastases. Cancer Biother Radiopharm. 2000a;15(3):261–5.

Liepe K, Franke WG, Kropp J, et al. Comparison of Rhenium-188 and Strontium-89 in palliation of painful bone metastases. Nuklearmedizin. 2000b;39:146–51 (German).

Liepe JK, Kropp J, Hlisc R, et al. Radiation dose of ^{188}Re in bone metastases. J Nucl Med. 2000c; 41(Suppl):266.

Liepe K, Hliscs R, Kropp J, et al. Radiation adsorbed dose pf Rhenium-188-HEDP in bone metastases, bone marrow and bone surface. In: EANM Congress, Naples, 24–29 Aug 2001.

Liepe K, Hliscs R, Runge R, Kropp J. Which is the favorable time for the post-therapeutic scan in dosimetry after ^{188}Re HEDP application. J Nucl Med. 2002;43:358P.

Liepe K, Hliscs R, Kropp J, et al. Dosimetry of ^{188}Re-hydroxyethylidene diphosphonate in human prostate cancer skeletal metastases. J Nucl Med. 2003a;44(6):953–60.

Liepe K, Kropp J, Runge R, et al. Therapeutic efficiency of rhenium-188-HEDP in human prostate cancer skeletal metastases. Br J Cancer. 2003b;18:625–9.

Liepe K, Kropp J, Runge R, et al. Therapeutic efficacy of rhenium-188-HEDP in human prostate cancer skeletal metastases. Br J Cancer. 2003c;89:625–9.

Liepe K, Kropp J, Hliscs R, et al. Radiation dosimetry of Rhenium-188-HEDP in human prostate cancer skeletal metastases. J Nucl Med. 2003d;44:953–60.

Liepe K, Kropp J, Hliscs R, et al. Rhenium-188 HEDP dosimetry in bone pain induced by prostate cancer. In: Proceedings of the 11th mediterranean symposium on nuclear medicine and radiopharmaceuticals, Athens, Greece, 28–30 May. Athens: Mediterrea Pub.; 2003e. p. 69–82. ISBN 960-86437-2-4.

Liepe K, Runge R, Kotzerke J. Systemic radionuclide therapy of pain palliation. Am J Hosp Palliat Care. 2005a;22:457–64.

Liepe K, Runge R, Kotzerke J. The benefit of bone-seeking radiopharmaceuticals in the treatment of metastatic bone pain. J Can Res Clin Oncol. 2005b;131:60–6.

Liepe K, Geidel HH, Bergmann R, et al. Autoradiographic studies of Rhenium-188-hydroxyethylidene diphosphonate and osteoblastic bone metastases in a Rat model of metastatic prostate cancer. Nucl Med Commun. 2009;30:693–9.

Lin WY, Lin CP, Yeh SJ, et al. Rhenium-188 hydroxyethylidene diphosphonate: a new generator-produced radiotherapeutic drug of potential value for the treatment of bone metastases. Eur J Nucl Med. 1997;24(6):590–5.

Majkowska A, Neves M, Antunes I, Bilewicz A. Complexes of low energy beta emitters ^{47}Sc and ^{177}Lu with zoledronic acid for bone pain therapy. Appl Radiat Isotopes. 2009;67:11–3.

Mantyh PW. Bone cancer pain: from mechanism to therapy. Curr Opin Support Palliat Care. 2014;8(2): 83–90.

Marques F, Gano L, Paula Campello M, et al. 13- and 14-membered macrocyclic ligands containing methylcarboxyate or methylphosphonate pendate arms: chemical and biological evaluation of their ^{153}Sm and ^{166}Ho complexes as potential agents for therapy or bone pain palliation. J Inorg Biochem. 2006;100: 270–80.

Maslov BD, Ya G, Starodub GY, et al. Production of ^{117m}Sn with high specific activity by cyclotron. Appl Radiat Isot. 2011;69:965–8.

Mathew B, Chakraborty S, Das T, Sarma HD, Banerjee S, Samuel G, Venkatesh M, Pillai MR. ^{175}Yb labeled polyaminophosphonates as potential agents for bone pain palliation. Appl Radiat Isot. 2004;60: 635–42.

Mausner LF, Mirzadeh S, Srivastava SC. Improved specific activity of reactor produced ^{117m}Sn with the Szilard-Chalmers process. Int J Radiat Appl Instrum Appl Radiat Isot. 1992;43:1117–22.

Maxon III HR, Schroder LE, Hertzberg VS, et al. Rhenium-186(Sn)HEDP for treatment of painful osseous metastases: results of a double-blind crossover comparison with placebo. J Nucl Med. 1991;32: 1877–81.

Maxon HR, Schroder LE, Washburn LC, et al. Rhenium-188 (Sn)HEDP for treatment of osseous metastases. J Nucl Med. 1998;39:659.

McGann S, Horton ER. Radium-223 dichloride: a novel treatment option for castration-resistant prostate cancer patients with symptomatic bone metastases. Ann Pharmacother. 2015;49(4):469–76.

Mirzadeh S. Generator-produced alpha-emitters. Appl Radiat Isot. 1998;49:345–9.

Mirzadeh S, Knapp Jr FF, Alexander CW, Mausner LF. Evaluation of neutron inelastic scattering for radioisotope production. Appl Radiat Isot. 1997;48: 441–6.

Mirzadeh S, Mausner LF, Garland MA. Reactor-produced medical radionuclides. In: Vértes A, Nagy S, Klencsár Z, Lovas RG, Rösch F, editors. Handbook of nuclear chemistry. Dordrecht, USA: Springer Science Business Media B.V.; 2011. p. 1857–902.

Mitterhauser M, Togel S, Wadsak W, et al. Binding studies of [(^{18})F]-fluoride and polyphosphonates radiolabeled with [(^{111})In], [(^{153})Sm], and [(^{188})Re] on bone compartments: a new model for the pre *in vivo* evaluation of bone seekers. Bone. 2004a;34:835–44.

Mitterhauser M, Wadsak W, Eidherr H, et al. Labeling of EDTMP (multibone®) with [^{111}In], [^{99m}Tc], and [^{188}Re] using different carriers for "cross complexation. Appl Radiat Isot. 2004b;60:653–8.

Morris MJ, Scher HI. Clinical approaches to osseous metastases in prostate cancer. Oncologist. 2003;8(2): 161–73.

Nilsson S, Larsen RH, Fosså SD, et al. First clinical experience with alpha-emitting radium-223 in the treatment of skeletal metastases. Clin Cancer Res. 2005;11(12):4451–9.

Nilsson S, Franzen L, Parker C, et al. Bone targeted radium-223 in symptomatic, hormone refractory prostate cancer: a randomised, multicentre, placebo-controlled phase II study. Lancet Oncol. 2007;8:587–94.

Ogawa K. Development of radiopharmaceuticals for diagnosis and therapy of metastatic bone cancer. Yakugaku Zasshi. 2012;132:1151–7.

Ogawa K, Washiyama K. Bone target radiotracers for palliative therapy of bone metastases. Curr Med Chem. 2012;19:3290–300.

Ogawa K, Mukai T, Arano Y, Ueda M, et al. Design of a radiopharmaceutical for the palliation of painful bone metastases: rhenium-186-labeled bisphosphonate derivative. J Label Compd Radiopharm. 2004;47: 753–61.

Ogawa K, Mukai T, Arano Y, et al. Development of a rhenium-186-labeled MAG3-conjugated bisphosphonate for the palliation of metastatic bone pain based on the concept of bifunctional radiopharmaceuticals. Bioconjug Chem. 2005;16:751–7.

Ogawa K, Mukai T, Arano Y, et al. Rhemium-186-monoaminemonoamidedithiol-conjugated bisphosphonate derivatives for bone pain palliation. Nucl Med Biol. 2006;33:513–52.

Ogawa K, Kawashima H, Shiba K, et al. Development of ^{90}Y-DOTA-conjugated bisphosphonates for treatment of painful bone metastases. Nucl Med Biol. 2009;36: 129–35.

Oh SJ, Won KS, Moon DH, et al. Preparation and biological evaluation of 188Re-ethylenediammine-N, N, N', N'-tetrakis(methylenephosphonic acid) as a potential agent for bone pain palliation. Nucl Med Commun. 2002;23:75–81.

Orsini F, Guidoccio F, Mazzarri S, Mariani G. Palliation and survival after repeated ^{188}Re-HEDP therapy of hormone-refractory bone metastases of prostate cancer: a retrospective analysis. J Nucl Med. 2012; 53(8):1330–1.

Oster ZH, Som P, Srivastava SC, et al. The development and in-vivo behavior of tin containing radiopharmaceuticals II. Autoradiographic and scintigraphic studies in normal animals and in animal models of disease. Int J Nucl Med Biol. 1995;12:175–84.

Paes FM, Serafini AN. Systemic metabolic radiopharmaceutical therapy in the treatment of metastatic bone pain. Semin Nucl Med. 2010;40:891–904.

Paes FM, Ernani V, Hosein P, Serafini AN. Radiopharmaceuticals: when and how to use them to treat metastatic bone pain. J Support Oncol. 2011;9:197–205.

Palmedo H, Guhlke S, Beets AL, et al. Rhenium-188-HEDP for pain palliation of bone metastases: first clinical results. European Nuclear Medicine Congress, Glasgow, Scotland, August 23–27, 1997. Eur J Nucl Med. 1997;24:962.

Palmedo H, Guhlke S, Bender H, et al. Rhenium-188 HEDP for multiple metastases – a dose escalation study. Nuklearmedizin. 1998a;37:A30 (German).

Palmedo H, Guhlke S, Bender H, et al. Rhenium-188 HEDP for palliation of multiple bone metastases – a dose escalation study. Eur J Nucl Med. 1998b;25:1047.

Palmedo H, Guhlke S, Schoencich G, et al. Pain therapy with Rhenium-188-HEDP of the bone metastases from prostate carcinoma. In: German Nuclear Medicine meeting, Ulm, Apr 1999a (German).

Palmedo H, Guhlke S, Bender H, et al. Dose escalation study with Re-188-HEDP in prostate cancer patients with osseous metastases, annual meeting, Society of Nuclear Medicine, Los Angeles, CA, June 6–10. J Nucl Med. 1999b;40:218P.

Palmedo H, Guhlke S, Bender H, et al. Dose escalation study with rhenium-188-HEDP in prostate cancer patients with osseous metastases. Eur J Nucl Med. 2000;27:123–30.

Palmedo H, Albers P, Guhlke S, et al. ^{188}Re-HEDP in the treatment of bone metastases generating from prostate cancer. J Nucl Med. 2002;43:160P.

Palmedo H, Manka-Waluch A, Albers P, et al. Repeated bone targeted therapy for hormone-refractory prostate carcinoma: randomized phase II trial with the new, high-energy radiopharmaceutical rhenium-188-HEDP. J Clin Oncol. 2003a;21:2869–75.

Palmedo H, Manka-Waluch A, Albers P, et al. Repeated bone targeted therapy for hormone-refractory prostate carcinoma: randomized phase II trial with the new, high energy radiopharmaceutical rheium-188-HEDP. J Nucl Med. 2003b;44:174P.

Pandit-Taskar N, Batraki M, Divgi CR. Radiopharmaceutical therapy for palliation of bone pain from osseous metastases. J Nucl Med. 2004; 45(8):1358–65.

Parker C, Nilsson S, Heinrich D, et al.; the ALSYMPCA Investigators. Alpha emitter radium-223 and survival in metastatic prostate cancer. N Engl J Med. 2013; 369(3):213–23.

Pecher C. Biological investigations with radioactive calcium and strontium: preliminary report on the use of radioactive strontium in the treatment of bone cancer. Univ Calif Publ Pharm. 1942;11:117–49.

Pillai AM, Knapp Jr FF. Evolving important role of Lutetium-177 for therapeutic nuclear medicine. Curr Radiopharm. 2015;8:78–85.

Pillai MR, Dash A, Knapp FF. Rhenium-188: availability from the ^{188}W/^{188}Re generator and status of current applications. Curr Radiopharm. 2012;5: 228–43.

Pirmettis I, Limouris GS, Bouziotis P, et al. Pentavalent rhenium-188 dimercaptosuccinic acid: a New Kit formulation and its initial evaluation in mice. Radiochim Acta. 2001;89:115–8.

Polig E, Jee WS, Kruglikov IL. Hit rates and radiation doses to nuclei of bone lining cells from alpha-particle-emitting radionuclides. Radiat Res. 1992; 131:133–42.

Ponsard B, Srivastava SC, Mausner LF, et al. Production of Sn-117m in the BR2 high-flux reactor. Appl Radiat Isot. 2009;67(7–8):1158–61.

Quilty PM, Kirk D, Bolger JJ, et al. A comparison of the palliative effects of strontium-89 and external beam therapy radiotherapy in metastatic prostate cancer. Radiother Oncol. 1994;31:33–40.

Rasheed R, Lodhi NA, Khalid M, et al. Radio-synthesis, and in-vivo skeletal localization of ^{177}Lu- zoledronic acid as novel bone seeking therapeutic radiopharmaceutical. J Anesth Clin Res. 2015;6:516.

Robinson RG. Radionuclides for the alleviation of bone pain in advanced malignancy. Clin Oncol. 1986;5:39–49.

Robinson RG, Spicer JA, Preston DF, Baxter KG. Treatment of metastatic bone pain with strontium-89. Nucl Med Biol. 1987;14:219–22.

Safarzadeh L. (^{175})Yb-TTHMP as a good candidate for bone pain palliation and substitute of other radiopharmaceuticals. Indian J Nucl Med. 2014;29:135–9.

Sartor O. Overview of samarium Sm-153 lexidronam in the treatment of painful metastatic bone disease. Rev Urol. 2004;6 Suppl 10:S3–12.

Savio E, Gaudiano J, Robles AM, et al. Re-HEDP: pharmacokinetic characterization, clinical and dosimetric evaluation in osseous metastatic patients with two levels of radiopharmaceutical dose. BMC Nucl Med. 2001;1(1):2.

Scheffler J, Derejko M, Bandurski T, Romanowicz G. Application of rhenium-188 HEDP in bone metastases therapy. Nucl Med Rev Cent East Eur. 2003;6(1):55–7.

Schmaljohan J, Guhlke S, Dudczak R, Biersack HJ. Kit preparation of ^{188}Re-HEDP: comparison of three different formulations. J Nucl Med. 2000;41(Suppl): 255P.

Sciuto R, Festa A, Rea S, et al. Effects of low-dose cisplatin on 89-Sr therapy for painful bone metastases from prostate cancer: a randomized clinical trial. J Nucl Med. 2002;43:79–86.

Shirvani-Arani S, Bahrami-Samani A, Meftahi M, et al. Production, quality control and biodistribution studies of thulium-170-labeled ethylenediamine (tetramethylene phosphonic acid.). Radiochim Acta. 2013; 101:37–44.

Silberstein EB. The treatment of painful osseous metastases with phosphorus-32-labeled phosphates. Semin Oncol. 1993;20:10–21.

Silberstein EB. Teletherapy and radiopharmaceutical therapy of painful bone metastases. Semin Nucl Med. 2005;35(2):152–8.

Singh A, Holmes RA, Farhangi M, et al. Human Pharmacokinetics of Samarium-153 EDTMP in Metastatic Cancer. J Nucl Med. 1989;30:1814–8.

Singh J, Powel AK, Clarke SEM, Blower PJ. Crystal structure and isomerism of a tumour targeting radiopharmaceutical: [$ReO(dmsa)_2$]. Chem Soc Chem Commun. 1991;16:1115–7.

Singh J, Reghebi K, Lazarus CR, et al. Studies on the preparation and isomeric composition of [^{186}Re]- and [^{188}Re]- pentavalent rhenium dimercaptosuccinic acid complex. Nucl Med Commun. 1993;14:197–203.

Sinzinger H, Palumbo B, Özker K. The Vienna protocol and perspectives in radionuclide therapy. Q J Nucl Med Mol Imaging. 2011;55:420–30.

Soderquist CZ, McNamara BK, Fisher DR. Production of high-purity radium-223 from legacy actinium-beryllium neutron sources. Curr Radiopharm. 2012;5: 244–25.

Srivastava SC. Bone-seeking therapeutic radiopharmaceuticals. Braz Arch Biol Technol. 2002;45: 45–55.

Srivastava SC, Meinken GE, Richards P, et al. The development and *in vivo* behavior of Tin containing radiopharmaceuticals I. Chemistry, preparation and Biodistribution in small animals. Int J Nucl Med Biol. 1985;12:167–74.

Srivastava SC, Atkins HL, Krishnamurthy GT, et al. Treatment of metastatic bone pain with Tin-117m stannic diethylenetriamine- pentaacetic acid: a phase I/II clinical study. Clin Cancer Res. 1998;4:61–8.

Srivastava SC, Gonzales GR, Howell RW, et al. Dosimetry implant for treating restenosis and hyperplasia. WO. 2009;2009014806:A2.

Stanik R, Svelik J, Benkovsky I. DMSA and its complexes with radioisotopes: review. J Radioanal Nucl Chem. 2012;293:545–54.

ter Heine R, Lange R, Breukels OB, et al. Bench to bedside development of GMP grade Rhenium-188-HEDP, a radiopharmaceutical for targeted treatment of painful bone metastases. Int J Pharm. 2014;465(1–2): 317–24.

Toporov YG, Andreyev OI, Akhetov FZ, et al. Reactor production of high specific activity Tin-117m at RIAR. In: Proceeding of 5th conference on isotopes, Brussels, 25–29 Apr 2005. p. 47–53.

Tu SM, Delpass ES, Jones D. Strontium-89 combined with doxorubicin in the treatment of patients with androgen independent prostate cancer. Urol Oncol. 1997;2:191–7.

Tu SM, Millikan RE, Mengistu B, et al. Bone-targeted therapy for advanced androgen-independent carcinoma of the prostate: a randomized phase II trial. Lancet. 2001;357:336–41.

Turner PG, O'Sullivan J. Radium-223 dichloride for the treatment of metastatic prostate cancer. Expert Opin Pharmacother. 2014;15(14):2105–11.

Turner JH, Martindale AA, Sorby P, et al. Samarium-153 EDTMP therapy of disseminated skeletal metastasis. Eur J Nucl Med. 1989;15:784–95.

Uehara T, Jin ZL, Ogawa K, et al. Assessment of ^{186}Re chelate-conjugated bisphosphonate for the development of new radiopharmaceuticals for bones. Nucl Med Biol. 2007;34:79–87.

Verdera ES, Gaudiano, J, Leon A, et al. Rhenium-188-HEDP-kit formulation/quality control. In: American Chemical Society annual meeting, Orlando, 25–29 Aug 1996.

Verdera ES, Gaudiano J, Leon A, et al. Rhenium-188-HEDP: kit formulation and quality control. Radiochim Acta. 1997a;77:113–8.

Verdera S, Gaudiano J, Leon A, et al. Rhenium-188-HEDP-kit formulation and quality control. Radiochim Acta. 1997b;70:113–7.

Washiyama K, Amano R, Sasaki J, et al. ^{227}Th-EDTMP: a potential therapeutic agent for bone metastasis. Nucl Med Biol. 2004;7:901–8.

Yano Y, Chu P, Anger HO. Tin—117m: production, chemistry and evaluation as a bone scanning agent. Int J Radiat Appl Instrum Appl Radiat Isot. 1973;24: 319–25.

Yousefnia H, Zolghadri S, Shanehsazzadeh S. Estimated human absorbed dose of ^{177}Lu-BPAMD based on mice

data: comparison with ^{177}Lu-EDTMP. Appl Radiat Isot. 2015;104:128–35.

Zeevart JR, Jarvis NV, Louw WK, Jacksom GE. Metal-Ion speciation in blood plasma incorporating the tetraphosphonate, N, N-dimethylenephosphonate-1-hydroxy-4--aminopropylidenediphosphonate (APDDMP), in therapeutic radiopharmaceuticals. J Inorg Biochem. 2001;83:57–65.

Zhang H, Tian M, Li S, et al. Rhenium-188-HEDP therapy for the palliation of pain due to ossesous metastases in lung cancer patients. Can Biother Radiopharm. 2003;18:719–26.

Zolghadri S, Yousefnia H, Jalilian AR, et al. Production, biodistribution assessment and dosimetric evaluation of ^{177}Lu-TTHMP as an agent for bone pain palliation. Asia Oceania J Nucl Med Biol. 2015;3(1):35–42.

Locoregional Radionuclide Therapy for Nonmelanoma Skin Cancer (NMSC)

13

13.1 Introduction

In the USA, for instance, skin cancer is the most common neoplasia with an estimated 3.5 million skin cancers in over two million people (Rogers et al. 2010). In fact, it has been estimated that there are more cases of skin cancer annually in the USA than the combined annual totals for breast, colon, lung, and prostate cancer. In the USA, it is estimated there are approximately ~700,000 cases of SCC and 2.8 million of the most common and typical BCC cases diagnosed annually. The BCCs generally grow slowly and are generally unlikely to spread. Some of these cancers are disfiguring and may metastasize, and for these and other reasons, the availability of effective treatment methods is important. Although relatively recently introduced and not yet widely used, the topical application of therapeutic radioisotopes for the irradiation of nonmelanoma skin cancer (NMSC) offers a practical and expected inexpensive and effective strategy for the therapeutic option. Such technologies are also useful for the treatment of hemangiomas and other superficial skin diseases. These tumors are generally radiosensitive and are thus often good candidates for topical treatment with radioisotopes.

13.2 Radioisotopes for Treatment of Skin Cancer

The use of such radioactive skin patches, molds, and application strategies involves individualized preparation and application to correlate with the patient-specific anatomical requirements. These radioactive materials are only temporarily applied on generally on an outpatient basis for time periods required to deliver the prescribed radiation dose. Although this technology may thus be designated as "topical brachytherapy," the on-site preparation of these materials involving the use of unsealed source radioactive materials is generally conducted in a nuclear medicine facility, as compared to the broader use of sealed sources in brachytherapy which lies under the purview of radiation oncology.

13.3 Strategies for Treatment on NMSC

Although surgery is often the first-line strategy, often tumors cannot be readily removed because of anatomical location, etc., and alternative technologies such as external radiation therapy with neutrons, electrons and X-rays, brachytherapy, and photodynamic therapy, have been widely

F.F. (Russ) Knapp, A. Dash, *Radiopharmaceuticals for Therapy*, DOI 10.1007/978-81-322-2607-9_13

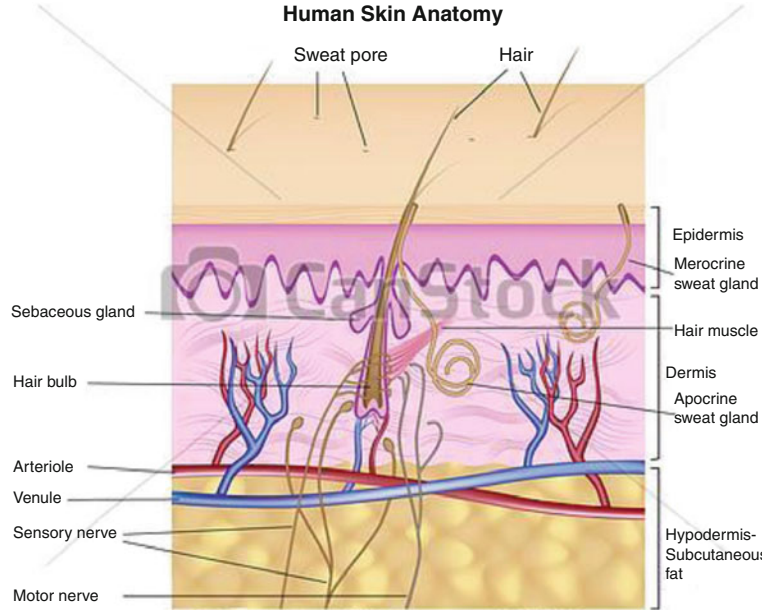

Fig. 13.1 Anatomical cross section illustrating the layers of skin

used. Traditional strategies for treatment of nonmelanoma skin cancers include surgical resection, use of fractionated external X-ray therapy with 116 keV X-rays, and traditional brachytherapy molds (Rustgi and Cumberlin 1993). Although these strategies focus on the therapy of nonmelanoma skin cancers, such approaches have also been used to treat cutaneous malignant melanoma using ^{106}Ru plaques (Anteby et al. 1993) and ^{125}I-seeds on gold plaque. As shown in Fig. 13.1, the maximal treatment depth is determined by the lesion dimensions, and based on the penetration depth of the radioactive emissions of the radioisotope patch used, dosimetry estimates then prescribe the contact time of the radioactive patch.

13.4 Topical Use of Radioisotopes for NMSC Therapy

As an attractive alternative to either surgery or invasive brachytherapy, the topical use of radioisotopes offers an effective, simple approach and expected cost-effective technology in many cases, especially where cosmetic results would be difficult to attain by traditional methods. In addition to radioisotope availability and cost, both total dose and dose rate are also important factors which must be evaluated for dose planning for consideration of using radioisotopes for this application. Because of health costs and other practical issues, the use of radioisotopes with physical half-lives which permit outpatient treatment would be expected to be of increasing interest. Numerous studies have thus established that the use of therapeutic radionuclides for the superficial treatment of skin cancers is an attractive simple and cost-effective strategy, especially when cosmetic issues are considered. Although the best radionuclide(s) of choice have not yet been established, it would be expected that the issue of costs and availability will be important factor which will determine which technology will move forward on a broader scale.

As described in Table 13.1, a variety of radioisotopes, agents, and therapeutic strategies have been evaluated for topical treatment/contact brachytherapy of NMSC and other experimental and natural skin diseases. Although the chemical nature of the materials formulated with these radioisotopes is not sophisticated, the substrates to which the radioisotopes are attached are important to insure good

Table 13.1 Examples of therapeutic radioisotopes which have been evaluated for superficial brachytherapy of skin cancer

Radioisotope	$T_{1/2}$, $E\beta_{max}$, MeV Approx. mm average soft tissue penetration[a]	Agent for application	Reference
Gold-198	2.7 days, β^-_{max} 0.96 ≈4.2 mm	Gold grains	Lock et al. (2011)
Holmium-166	26.8 h, β^-_{max} 1.85 ≈0.8 mm	Polyurethane patch	Chung et al. (2000)
Iodine-131	8.02 days, β^-_{max} 0.606 ≈4.2 mm	Metaiodobenzylguanidine (also emits high-energy gammas)	
Iridium-192	73.8 days, β^-_{max} 0.672 ≈4.1 mm	Afterloader (also emits high-energy gammas)	Rustgi and Cumberlin (1993)
Phosphorus-32	14.29 days, β^-_{max} 1.71 ≈8 mm	Patch	Gupta et al. (2009)
Rhenium-188	16.9 days, β^-_{max} 2.12 MeV ≈9 mm	Cream	Sedda et al. (2008)
Yttrium-90	64.1 h, β^-_{max} 2.3 MeV ≈10 mm	Ferric hydroxide Macroaggregates Immobilized on gauze	Mukherjee et al. (2002) Saxena et al. (2014)

[a]Although many of these radioisotopes decay with emission of multiple beta particles, the energy of the principle beta emission is illustrated

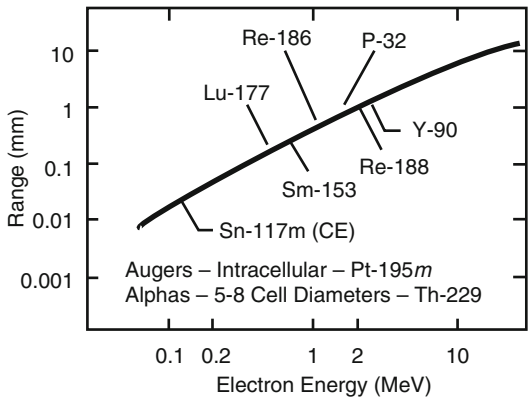

Fig. 13.2 Illustration of approximate maximal beta particle soft tissue penetration as a function of endpoint energy

radiological safety handling, with minimal contamination of patients and staff. Most recent efforts have focused on the use of ^{32}P, ^{166}Ho, and ^{188}Re patches/creams for this application. Although this technology has not yet reached mainstream application, it would be expected that the benefits of these methods and similar approaches using other therapeutic radioisotopes would represent sufficient benefit to propel this technology forward (Fig. 13.2).

A variety of animal studies and clinical trials have demonstrated the usefulness of using the topical brachytherapy approach for treatment of BCC and SCC for which other therapeutic strategies are either difficult or costly. These include cancers of anatomical regions which are not candidates for surgery for cosmetic reason, such as near the lips, eyes, and nose. A number of radioisotopes and applicator strategies have been reported for treatment of BCC and SCC and also for benign hemangiomas.

13.4.1 Holmium-166

The relatively short 26.8 h half-life of ^{166}Ho is attractive for use for high-dose-rate outpatient therapy of skin cancers. Early evaluation of the potential use of ^{166}Ho for skin cancer therapy utilized a patch attached to chemically induced skin cancers (Lee et al. 1997). The ^{166}Ho-labeled patches were produced in situ by reactor irradiation of macroaggregated ^{165}Ho particles embedded on adhesive tape at low thermal flux (1×10^{13} n/cm^{2}s). This is one important example when sufficiently high specific activity can be

obtained for therapeutic applications at relatively low thermal neutron flux. The patches were affixed to the squamous cell carcinomas and keratoacanthoma tumors induced in ICR and hairless mice with TDA. The 5-mm skin patches were attached to the tumors with adhesive tape for 2 h ($n=4$; 22.2 MBq and 29.6 MBq) and for 1 h ($n=5$; 44.4 MBq and 48.1 MBq). The radiation dose at the surface ranged from 42 to 45 Gy. One to two weeks after treatment, the tumors were destroyed and there was no damage to the underlying soft tissues. In the usual manner, ulceration was accompanied by tumor site infiltration by inflammatory cells, edema, and exudate, but complete healing was observed after 7 weeks. The dose–depth distribution from decay of ^{166}Ho has also been for different shaped sources using the VARSKIN3 Code and has confirmed that radiation damage to underlying bone and other tissue is minimized by the rapid depth–dose fall-off (Mowlavi et al. 2010).

A small number of patients with histologically confirmed SCC (3), BCC (1), and Bowen's disease (1) were also treated with the ^{166}Ho topical patches embedded with 273.8–999 MBq (7.4–27 mCi) of ^{166}Ho for periods from 30 min to 1 h (Lee et al. 1997). After a period of 8 weeks, skin biopsy samples from four patients were available for histological examination, and successful tumor destruction was observed in all cases. Acute radiation-induced effects of ulceration, etc., were observed but healed over a one-month period with no adverse reaction or tumor cell recurrence after 8–20-month follow-up. Another clinical study evaluated the efficacy of ^{166}Ho therapy in patients with Bowen's disease (intraepidermal basal cell carcinoma) by treatment of 29 sites in 8 patients (Chung et al. 2000). Informed consent and complete clinical work-up were completed. The applicator in this study involved dissolution of equal amounts of $^{165}Ho(NO_3)_3 \bullet 5 H_2O$ (2.4 g) and polyurethane in 4 mL of dimethylformamide (DMF) at room temperature. The solution was "cast" on an aluminum dish and the DMF removed by evaporation to yield a patch containing uniformly distributed ^{165}Ho from which pieces were removed for reactor irradiation at low thermal neutron flux (1.25×10^{13} n/cm^{2}s) to produce the ^{166}Ho-labeled patch material. The required size and shape of the patch for each individual tumor site could be readily obtained by cutting the urethane preparation. A total dose of 35 Gy (3500 rads) were delivered by attachment to the tumor surface for 30–60 min. The lesions spanned from 3 to 7.2 cm and post-therapy follow-up was from 10 months to 2 years.

13.4.2 Phosphorus-32

Many recent studies have described the development of various application technologies and clinical results of ^{32}P for the treatment of basal and squamous cell carcinomas and hemangiomas. Advantages for use of ^{32}P include its practical radionuclidic properties (Table 13.1) and availability of ^{32}P phosphate and chromic phosphate as approved cGMP-produced radionuclide preparations. The 14.2-day physical half-life provides convenience for preparation of skin irradiation patches at a centralized site for distribution to clinical centers. In addition, the absence of gamma irradiation optimizes radiation protection issues to minimize radiation dose to both staff and patients. Finally, the emission of 1.7 MeV beta particles optimizes dose to the cutaneous dermal layer.

A variety of approaches have been evaluated for preparation of ^{32}P dose applicators for treatment of BSC and SCC and other animal skin disease models. Radioactive "bandages" have been described in which ^{32}P chromic phosphate particles were bound within Millipore filters which were then immobilized and sealed within nitrocellulose membranes (Pandey et al. 2008a; Mukherjee et al. 2003). The sealed membranes were then placed on adhesive bandages which were then placed on the superficial tumors of melanoma-bearing C57BL/6 mice for a 74 MBq single dose evaluation of tumor regression. Another approach focused on (Pandey et al. 2008b) adsorption of ^{32}P orthophosphate on circular sheets of cellulose-based adsorbent paper. These preparations of various shapes and sizes could be readily prepared and contained 37–74 MBq/cm^2 of ^{32}P which were then immobilized/sealed

between plastic sheets. The ^{32}P was uniformly distributed on the paper adsorbent preparations which showed no activity leakage in either water or saline. Complete tumor regression was observed using these brachytherapy molds with a dose rate of 10 Gy/h in C57BL6 mice with cutaneous melanoma tumors. Evidently, this technology has not yet progressed to evaluation in humans presenting with skin cancers.

In another series of studies, both ^{32}P phosphoric acid and chromic phosphate have been evaluated bound to 2×2 cm natural rubber and silicone patches (Salgueiro et al. 2008a). For preparation of natural rubber patches, the ^{32}P phosphoric acid was first bound to a strongly basic anionic resin (HC-D208) which was then mixed with an equal volume of natural rubber to form a patch 1-mm thick which was desiccated at room temperature. The silicone patch was formed using a ^{32}P chromic phosphate powder formulation which was mixed with Silastic® J-White 80 silicone, dird at room temperature to form a 1-mm thick patch. Although the rubber patch showed significant instability and leakage of ^{32}P, the silicone patch showed much less release of ^{32}P (0.6 %) under mild hydrolysis conditions with uniform activity distribution (10.6 MBq/cm^2) determined by autoradiography. For animal studies in the mouse two-stage carcinogenesis model with papillomas and keratoacanthomas induced by sequential DMBA/TBA topical application, the patch was cut into sections corresponding to the tumor dimensions. The exposure time periods for the applied patches corresponded to delivery of 40 Gy. In this study, seven tumors were treated with two total remissions and two partial remissions. In another study, these authors expanded the protocol and observed that the single-dose regimen resulted in a higher number of complete and partial remissions compared to the fractionated dose scheme (Salgueiro et al. 2008b).

These initial studies were further expanded to include a larger number of animals with a control group and a similar two-stage carcinogenesis group which included a single-stage and two-stage ^{32}P silicone treatment regimen (Salgueiro et al. 2009a, b). Animals were evaluated for an endpoint of tumor size for up to 44 days and included histological analysis and hematoxylin-eosin staining and PCNA immunostaining assessment of tissue samples. A dose response was observed, and the single-dose studies resulted in tumor diameter reduction of 60 %, and in the fractionated dose animals, the tumor size was reduced to >95 % over the same time period compared to controls. Although dermatitis, erythema, and skin ulceration were detected in most treated animals, these are typical hypotrophic responses which healed with regeneration of new tissue. The authors conclude that this technology is well suited for preparation and distribution of the ^{32}P silicone patches from a centralized radiopharmacy. No clinical studies with these patches have yet been described, but such work reflects the broad interest in the topical use of ^{32}P for treatment of skin diseases.

Initial clinical evaluation included ten patients treated on an outpatient basis with facial cutaneous basal cell carcinoma who were treated with the ^{32}P patches. The regimen included successive 3-h treatments with the custom ^{32}P patches on days 1, 4, and 7, with accumulative doses of 100 Gy. Follow-up of the patients included biopsy evaluation which showed that 8/10 (80 %) of these patients were cancer-free after three years. Larger patient studies are currently in progress to determine the efficacy of this method for the treatment of basal cell carcinoma and similar superficial cutaneous cancers. In another study, the perfluorosulfonate ionomer Nafion-117® membrane was used because of its excellent mechanical properties and channel structure which facilitates cation uptake. By initial treatment with zirconium salts, the localized Zr then results in formation and strong table retention of Zr phosphate by subsequent treatment with phosphoric acid. The Naion-117® was "activated" by heating at 60–70 °C for 30 min in 3 % H_2O_2 (Saxena et al. 2012). After washing in deionized water, the membrane preparation was then loaded by H^+ displacement with Zr(IV) ions by treatment with 0.1 M $ZrOCl_2$ solution at 60 °C. Following thorough washing with deionized water and vacuum drying, these substrates were then ready for ^{32}P loading. The ^{32}P loading parameters were then optimized by

treatment of various membrane patch sizes with ^{32}P-H_3PO_4. Using this approach, the ^{32}P activity levels adsorbed on a standard patch can be readily adjusted by variation of the ^{32}P solution.

Clinical studies using a ^{32}P-labeled skin patch have been recently reported in which eight patients present with unifocal basal cell carcinoma (Gupta et al. 2009). Sealed patches containing ^{32}P activity levels of 1 mCi/cm^2 were prepared with the required shape for specific tumor application and applied on the tumor site for 3 h. Re-application for 3 h/application was conducted for 4, 5, and 7 days. Three months following completion of the therapy regimen, biopsy samples obtained from the center and lesion margins were negative for any tumor cells. This procedure was acceptable to patients, was easy to perform, and there was minimal scarring at the lesion sites which were close to the nose, eyes, and forehead. The data from this small patient population indicated that this method is a good alternative strategy in cases challenging for surgical or radiotherapeutic intervention.

Hemangiomas are a congenital anomaly and the most common tumors in infancy that usually appear during in the first weeks of life and are generally resolved by the age of ten years. They are generally benign growths involving swelling or growth ("self-involuting tumor") of endothelial cells that line blood vessels and are thus characterized by increased number of blood-filled normal or abnormal vessels. Hemangiomas are the most common benign and vascular proliferative tumors, and if left untreated they can achieve massive growth, can ulcerate, can cause disfigurement, and can interfere with normal function (Shi et al. 2012). Many hemangiomas are cutaneous, and for this reason, the availability of cost-effective methods which can noninvasively obliterate these hemangiomas is of great interest. Phosphorus-32 has been used for hemangioma therapy for a number of years, and the efficacy of using topical application of ^{32}P has been recently reported as an effective strategy for treatment of the strawberry-type hemangiomas. The results of such topical ^{32}P application of a large 316 patient group with strawberry hemangiomas demonstrated disappearance of the lesions within 3 months after a single treatment in 259 cases (82 %). Because of the importance of relating efficacy with contact time and the adsorbed dose of ^{32}P, these values were calculated using established depth–dose distributions, and dose values were verified by the use of stacked Gafchromic film studies. In this manner, the continued dose-rate change as a function of tissue depth was evaluated, and the adsorbed dose (Gy) and dose-rate (Gy/h/MBq/cm^2) values were estimated as a function of distance (depth). Because the hemangiomas primarily develop in the dermal layer (1–2-mm thickness), ^{32}P has excellent radiation properties for dose delivery at a tissue depth of 0.1–2 mm. For the topical applicator, the ^{32}P (4.14 MBq) was applied to a 1.1×1.2 cm^2 section of filter paper which was then dried and sealed in plastic tape. The paper preparation was then cut into the lesion shape and applied to the hemangioma with a contact time appropriately based on the radiation dose prescription. The observed side effects included pigmentation, loss of pigment, and the sensation of burning, and the authors recommend that less radiation be used for treatment of large-area hemangiomas. In these 259 patients, the hemangiomas completely disappeared (82 %), and in the remaining 18 % of patients the tumor mass reduced and no cases were found where the tumor mass continued to grow. More recently, a paper has described the Monte Carlo-based dose calculations for the ^{32}P patch sources for superficial brachytherapy applications (Saho et al. 2015).

13.4.3 Rhenium-188

Recent studies in a significant number of patients have shown the excellent therapeutic efficacy of ^{188}Re for nonmelanoma skin cancer therapy. The advantages of ^{188}Re skin patch use include the short half-life 16.9 and accompanying high dose rate which allows outpatient treatment, and the on-demand availability of no-carrier-added ^{188}Re from the $^{188}W/^{188}Re$ radionuclide generator system (Chap. 7) which has a useful shelf-life of several months. Initial evaluation of the potential use of ^{188}Re for the topical treatment of superficial skin

cancer involved use of ^{188}Re uniformly embedded in nitrocellulose paper (Jeong et al. 2003) and (Mukherjee et al. 2003). Rhenium-188 sodium perrhenate eluted from the ^{188}W/^{188}Re generator (See Chap. 7) was reduced with stannous chloride in 0.1 M HCl and boiled for 2 h to form ^{188}Re-tin colloid, which was filtered by nitrocellulose filter paper. Because the nitrocellulose is dissolved with acetone, the filtered product was adhered to gauze by contact with gauze wetted with acetone. Uniform distribution of ^{188}Re on the preparation was established by phosphorescence imaging and the stability of preparation was confirmed by no loss of ^{188}Re by immersion in saline for 3 days at room temperature. For evaluation of efficacy in mice, BALBc and ICR mice were inoculated by injection in the thigh with either the RT101 mouse skin cancer or sarcoma 180 cell lines (American Type Culture Collection). After 4 days, the tumors were 5–7 mm in diameter and 1–3 mm in thickness. The ^{188}Re-labeled paper preparation was cut into appropriate size for each tumor and attached on the tumors with adhesive plaster. Tumor growth was evaluated after estimated 50 and 100 Gy doses had been delivered. With the RT101 tumor, complete remission of all tumors was observed after 4 weeks, and with the sarcomas, complete remission was seen in 60–75 % of animals. The results of these initial studies demonstrated that noninvasive technique is effective and expected to be economical because of the ready availability of ^{188}Re.

Although not yet widely described in the scientific literature, an approach using a ^{188}Re-impregnated topical application has been recently commercially developed, and the results of reported studies have demonstrated this to be an excellent approach for expected treatment of skin cancers (Sedda et al. 2000, 2003, 2006, 2008). Descriptions of this technology primarily reside in the patent literature, and clinical papers have now been published in traditional academic open literature publication route (Cipriani 2010; Cipriani and Desantis 2011). This approach has been widely discussed in the trade literature as the "ITM Rhenium-SCT™" (Skin *C*ancer *T*herapy) agent. This technique uses an innovative approach which does require pre-preparation of a radioactive applicator to match the anatomy of the therapy site. Instead, the ^{188}Re is embedded in a cream which is then applied to the treatment site, previously covered with surgical tape, with a special applicator (Sedda et al. 2008; Cipriani 2010).

Results have reported treatment of over 700 patients with BCC and SCC has been treated with ^{188}Re using this technique with an overall 85 % success rate. The special cream is prepared based on preparation of a Re nanocolloid which is then mixed with an acrylic resin. The ^{188}Re sodium perrhenate (Na_2ReO_4) was obtained by saline elution of the ^{188}W/^{188}Re generator system (Cipriani 2010; Cipriani and Desantis 2011) and added to a "kit" containing 250-mg thioacetamide (1 mg), polyvinylpyrrolidone (1 mg), and conc. HCl (0.100). The mixture was then heated at 90 C for 30 min to form a nanocolloid (200–800 microns) which was centrifuged and washed with saline, recentrifuged, and then thoroughly mixed with a synthetic acrylic resin material. The ^{188}Re mixture is 98 % homogenously distributed in this "cream." One recent published study enrolled 53 patients who presented with histologically confirmed basal cell (BCC) and squamous cell (SCC) carcinoma (Sedda et al. 2008). The treatment area is outlined visually using dermoscopy epiluminescence to include a margin of typically 2–3 mm, as illustrated in Fig. 13.3.

After application of a protective cream or surgical tape/protective foil to preclude any radioactive contamination of the epidermal skin layer, the ^{188}Re acrylic mixture is then homogeneously applied using a special applicator device (Cipriani 2010). The resin mixture solidifies with shrinkage to the topical brachytherapy mold. Application requires less than 2 min with irradiation periods typically less than 2 h in duration. The dose–depth curves used for these studies are shown in Fig. 13.4 (Sedda et al. 2008) and a typical epidermal radiation dose is 40–60 Gy at 300–600 micron depth.

After irradiation, the mold is readily removed for disposal. Figures 13.5, 13.6, 13.7, 13.8, 13.9, 13.10, 13.11, 13.12, and 13.13 provide illustrations of a number of cases showing the striking therapeutic efficacy of this technique in patients with a variety of nonmelanoma cancers of the head region.

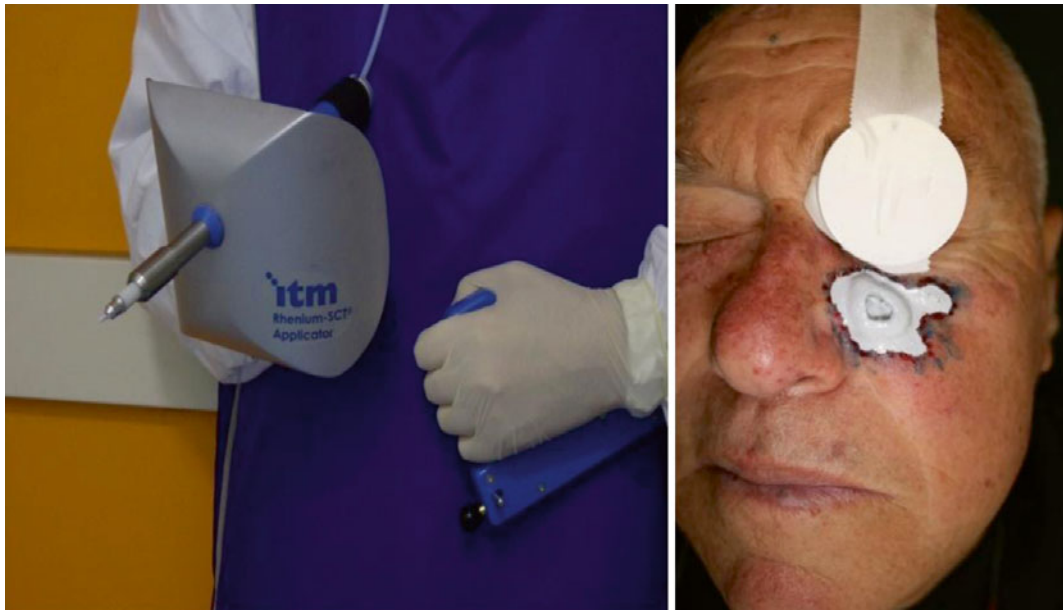

Fig. 13.3 Shielded applicator device and example of the radioactive ^{188}Re resin after tumor resin application (For study illustrated in Fig. 13.9 (Courtesy, A. Sedda and C. Cipriani, Rome/Celano)

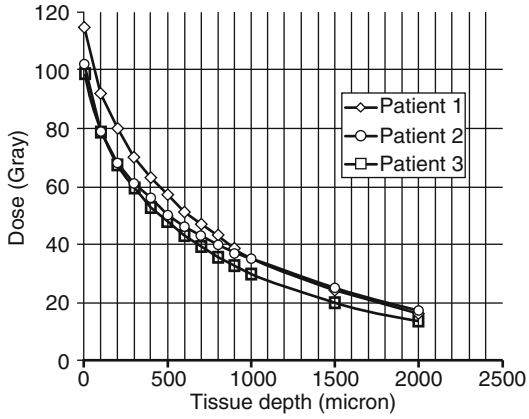

Fig. 13.4 Typical dose adsorption curves in human tissue used for dose prescription for the ^{188}Re-SCT™ system (Courtesy, A. Sedda and C. Cipriani, Rome/Celano)

More recently, the effective use of the ^{188}Re cream for the treatment of Paget's disease in the very delicate area of the male genitalia has also been demonstrated (Carrozzo et al. 2013a, b). This technique using ^{188}Re is now referred to as dermo beta brachytherapy (DBBT). Fifteen patients presenting with histologically confirmed SCC of the penis were treated with the DBBT technique, with 12 patients showing healing. Long-term follow-up has evidently not been reported.

13.4.4 Yttirum-90

Skin patches radiolabeled with ^{90}Y (2.3 MeV beta) have also been evaluated for superficial tumor therapy in mice (Mukherjee et al. 2002). More recently, the physical and chemical parameters affecting incorporation of ^{90}Y into Nafion membranes were studied (Saxena et al. 2014). These studies included an evaluation of pH, Y carrier, reaction volume, ^{90}Y contact time, and other parameters to optimize the labeling process. The patches were then attached melanoma tumors transplanted onto the skin of mice, and under the experimental conditions, complete tumor regression was observed in comparison with control animals. Although the focus of this work is evidently for possible treatment of melanoma, it would also seem appropriate for SCC and BSC therapy. No patient studies had evidently yet been reported.

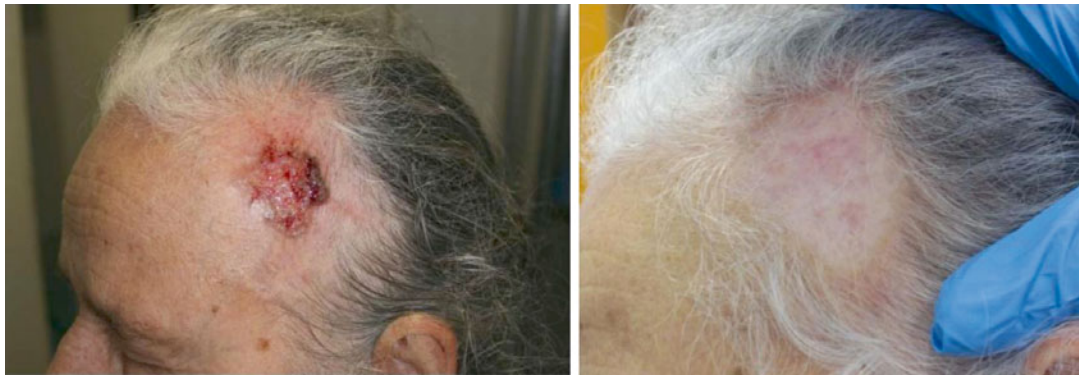

Fig. 13.5 Ulcerated BCC of the scalp and 382 days after a single treatment (Courtesy, A. Sedda and C. Cipriani, Rome/Celano)

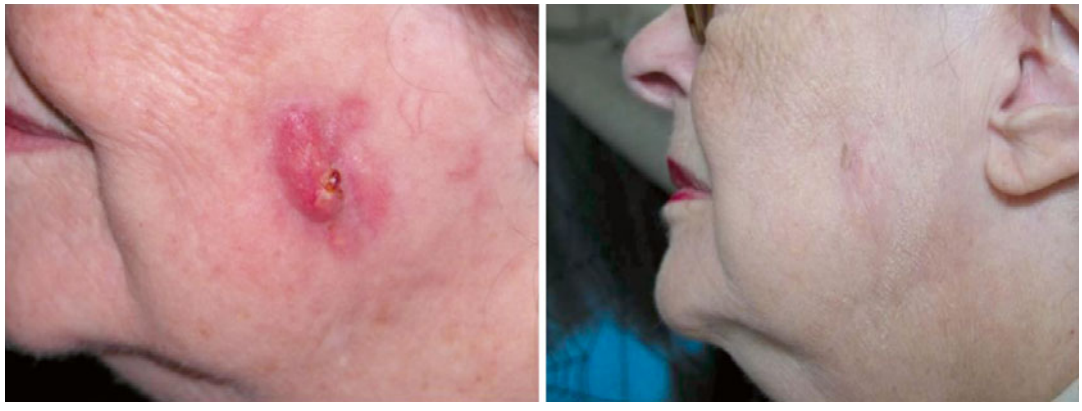

Fig. 13.6 SCC of the face before and 181 days after a single treatment (Courtesy, A. Sedda and C. Cipriani, Rome/Celano)

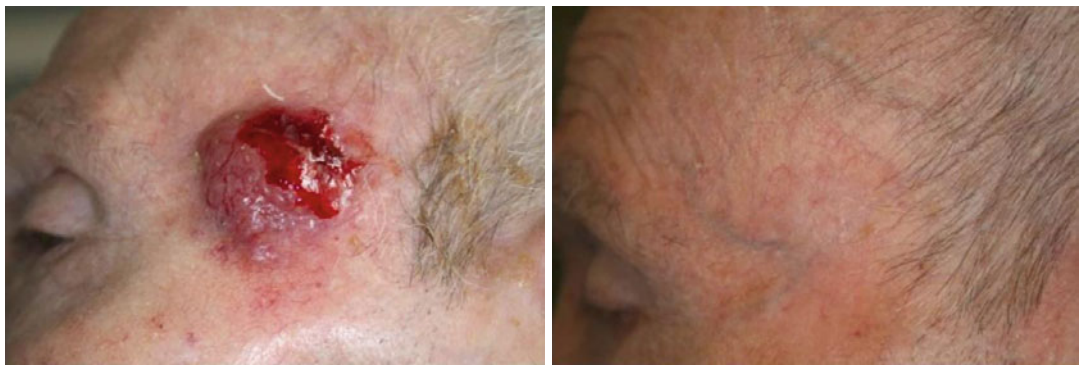

Fig. 13.7 Wide ulcerated SCC of the temple before and 83 days after a single treatment (Courtesy, A. Sedda and C. Cipriani, Rome/Celano)

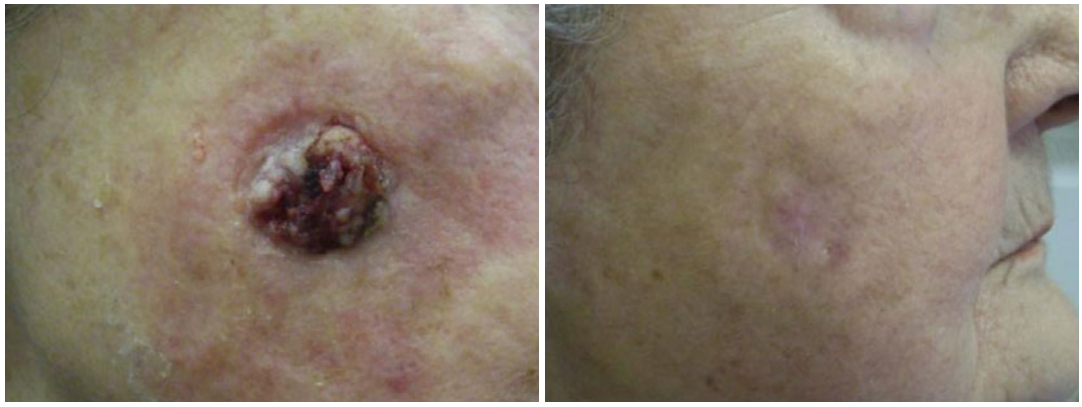

Fig. 13.8 SCC of the face before and 134 days after a single treatment (Courtesy, A. Sedda and C. Cipriani, Rome/Celano)

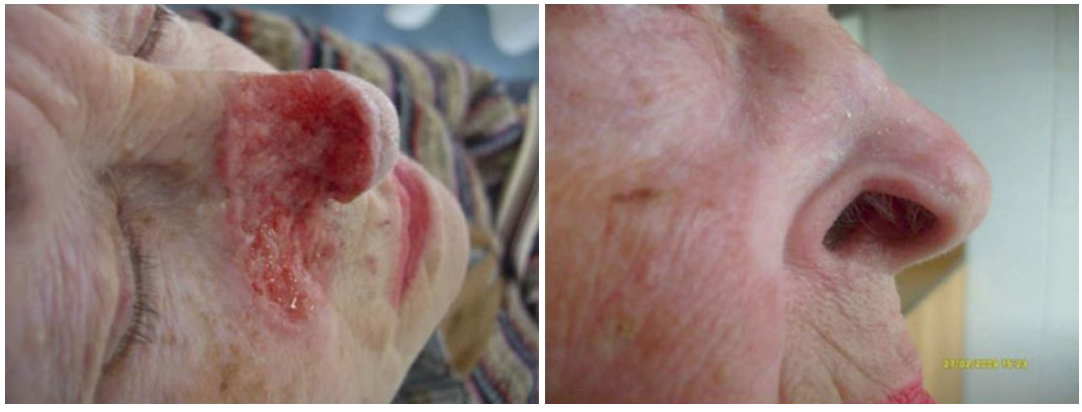

Fig. 13.9 Ulcerated BCC of the nose, extended to the face, before and 151 days after a single treatment (Courtesy, A. Sedda and C. Cipriani, Rome/Celano)

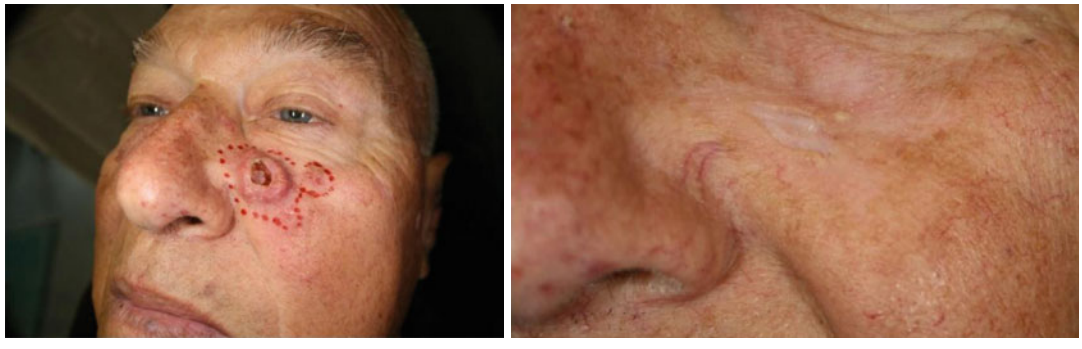

Fig. 13.10 Keratoacanthoma before the treatment, during the treatment, and 180 days after two treatments (Courtesy, A. Sedda and C. Cipriani, Rome/Celano)

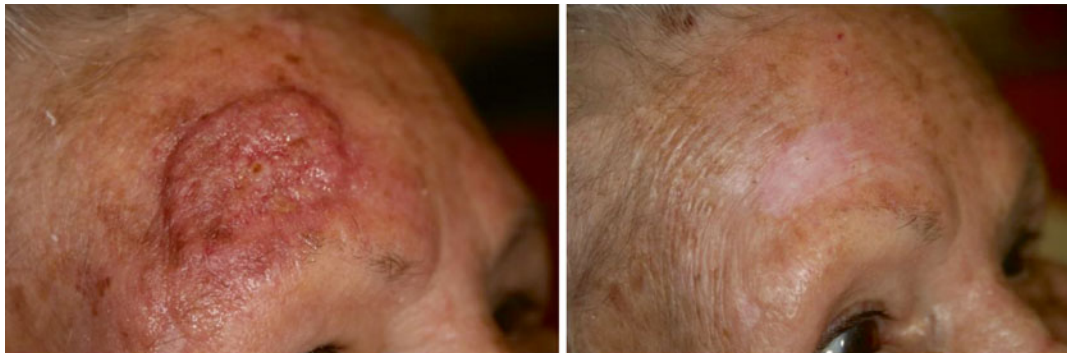

Fig. 13.11 SCC before treatment and 95 days after a single treatment (Courtesy, A. Sedda and C. Cipriani, Rome/Celano)

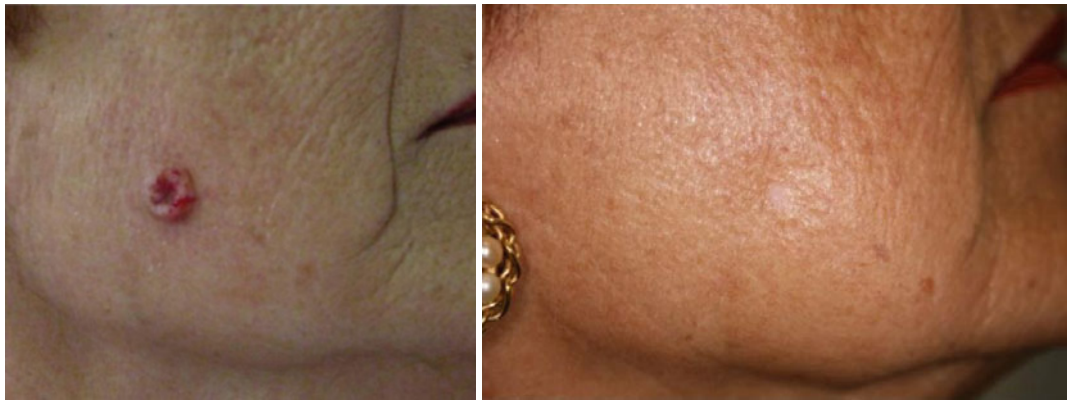

Fig. 13.12 Nodular BCC before treatment and 312 days after a single treatment (Courtesy, A. Sedda and C. Cipriani, Rome/Celano)

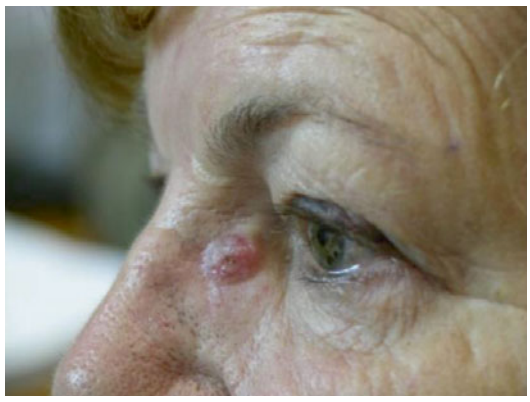

Fig. 13.13 Nodular BCC before treatment and 137 days after a single treatment (Courtesy, A. Sedda and C. Cipriani, Rome/Celano)

13.5 Summary

Although the use of therapeutic radioisotopes for topical brachytherapy has been of interest for some time and has been explored using a variety of beta-emitting radioisotopes, this effectiveness and easy use of this approach have only recently been demonstrated on a broad basis using ^{188}Re and are expected to represent an alternative technology for the effective treatment of nonmelanoma skin cancer and other skin diseases where other technologies are ineffective or difficult to administer.

References

Anteby I, Axer-Siegel R, Pe'er J. Choroidal metastasis of cutaneous malignant melanoma treated by ruthenium-106 plaque irradiation. Ann Opthalmol. 1993;25(9):339–41.

Carrozzo AM, Sedda AF, Muscardin L, et al. Dermo beta brachytherapy with 188-Re in squamous-cell carcinoma of penis: a new therapy. Eur J Dermatol. 2013a;23(2):183–8.

Carrozzo AM, Cipriani C, Donati P, et al. Dermo beta brachytherapy with 188-Re in extramammary Paget's disease. G Ital Dermatol Venereol. 2013b;148:1–2.

Chung YL, Lee JD, Bang D, et al. Treatment of Bowen's disease with a specially designed radioactive skin patch. Eur J Nucl Med. 2000;27(7):842–6.

Cipriani C. Applicator for applying a radioactive substance to a biological sample. US Patent Application 2013/0,006,033, 6 Nov 2010. 2010.

Cipriani C, Desantis M. Brachytherapy method of treating skin tumors using a tailor-made radioactive source. US Patent Application 2011/0,201,866, 18 Aug 2011. 2011.

Gupta P, Malhotra A, Saxena S, et al. Radionuclide therapy of basal cell carcinoma with phosphorus-32 skin patch. J Nucl Med. 2009;50(Suppl):15.

Jeong JM, Lee YL, Kim EH, et al. Preparation of ^{188}Re-labeled paper for treating skin cancer. Appl Radiat Isot. 2003;58:551–5.

Lee JD, Park KK, Lee MG, et al. Radionuclide therapy of skin cancer and Bowen's disease using a specially designed skin patch. J Nucl Med. 1997;38(5):697–702.

Lock M, Cao JQ, D'Souza DP, et al. Brachytherapy with permanent gold grain seeds for squamous cell carcinoma of the lip. Radiother Oncol. 2011;98(3):353–6.

Mowlavi AA, Afzalifar A, Afzalibar N, et al. Depth dose calculation of holmium-166 for different shape by VARSKIN3 code. Iran J Nucl Med. 2010;18(1):32–6.

Mukherjee A, Pandey U, Sarma HD, et al. Preparation and evaluation of ^{90}Y skin patches for therapy of superficial tumors in mice. Nucl Med Commun. 2002;23(3):243–7.

Mukherjee A, Pandhey U, Sarma HD, et al. Bioevaluation of radioactive bandages in a murine model of melanoma. Int J Radiat Biol. 2003;79:839–45.

Pandey U, Saxena SK, Sarma HD, et al. Bioevaluation studies of ^{32}P incorporated mould brachytherapy sources for potential application in treatment of superficial tumors. Nucl Med Comm. 2008a;29(8):717–23.

Pandey U, Sarma HD, Ingle AD, et al. Radioactive skin bandages incorporating ^{32}P for treatment of superficial tumors. Can Biother Radiopharm. 2008b;21(3):257–62.

Rogers HW, Wienstock MA, Harris AR, et al. Incidence estimate of nonmelanoma skin cancer in the United States, 2006. Arch Dermatol. 2010;146(3):283–7.

Rustgi SN, Cumberlin RL. An afterloading ^{192}Ir surface mold. Med Dosim. 1993;18(1):39–42.

Saho S, Palani T, Saxena SK, et al. Monte Carlo-based dose calculation for ^{32}P patch source for superficial brachytherapy applications. J Med Phys. 2015;40(1):13–7.

Salgueiro MJ, Duran H, Palieri M, et al. Design and bioevaluation of a ^{32}P-patch for brachytherapy of skin diseases. Appl Radiat Isot. 2008a;66(3):303–9.

Salgueiro MJ, Duran H, Palmieri M, et al. Bioevaluation of ^{32}P patch designed for the treatment of skin diseases. Nucl Med Biol. 2008b;35(2):233–7.

Salgueiro MJ, Collia M, Barreiro ML, et al. Radioactive treatment of a murine melanoma using a ^{32}P patch. Nucl Med Commun. 2009a;30(9):706–12.

Salgueiro MJ, Collia M, Duran H, et al. Biological effects of brachytherapy using a ^{32}P-atch on the skin of Sencar mice. Appl Radiat Isot. 2009b;67(10):1769–74.

Saxena SK, Kumar Y, Dash A. Nafion-Zirconium phosphate composite membrane: a new approach to prepare ^{32}P patches for superficial brachytherapy applications. Can Biother Radiopharm. 2012;27(4):276–84.

Saxena SK, Pandey U, Kumar Y, et al. On the application of nafion membrane for the preparation of 90Y skin patches, quality control, and biological evaluation of treatment of superficial tumors. Can Biother Radiopharm. 2014;295:200–9.

Sedda AF, Rossi G, Desantis M, et al. DOBBIN (Distribution Optimization for Beta Brachytherapy Intratumor): a program for geometrical optimization of beta brachytherapy interstitial administration. In: V Italian Congress of Nuclear Medicine, Pesaro (Italy) 17–20 Jun 2000. 2000.

Sedda AF, Rossi G, Cipriani C. Beta emitter multilayer for the dermatological brachytherapy of cutaneous tumors. In: European Association of Nuclear Medicine, annual congress, Amsterdam, September 2003. 2003.

Sedda AF, Rossi G, Carrozzo AM, et al. Superficial brachytherapy with beta emitting isotopes for the treatment of basal cell carcinoma. In: 3rd meeting of the European Association of Dermato-Oncology (EADO), Rome, 23–25 June 2006. 2006.

Sedda AF, Rossi G, Cipriani C, et al. Dermatological high-dose-rate brachytherapy for the treatment of basal and squamous cell carcinoma. Clin Exp Dermatol. 2008;33:745–9.

Shi CB, Yuan B, Lu JR, et al. Continuous low-dose-rate radiation of radionuclide phosphorus-32 for hemangiomas. Can Biother Radiopharm. 2012;27(3):198–203.

Radionuclide Synovectomy: Treatment of Inflammation of the Synovial Joints

14

14.1 Introduction

One of the most widely used applications of therapeutic radioisotopes is for the treatment of inflammatory (rheumatoid) joint disease (Fig. 14.1) caused from destruction of diarthrodial or synovial tissues in individuals (Otero and Goldring 2007).

Intra-articular administration of β^- emitting radionuclides in the form of colloidal formulation or radiolabeled particulate (preferably of 1–10 μm size range) into the articular cavity, referred as "radiation synovectomy (RSV)" or "radiosynoviorthesis," has emerged as an effective option of treatment and a viable alternative to surgical synovectomy. RSV is defined as the restoration (orthesis) of the synovia by the local application of radiolabeled particulates or radionuclide-loaded colloid particles. The biological mechanism of RSV essentially involves the absorption of radioactive particulates by superficial cells of the synovium followed by phagocytosis by the macrophages of the inflamed synovium. Beta radiation (Fig. 14.2) results in coagulation necrosis, fibrosis, and sclerosis of the proliferating synovial tissue and leads to destruction of diseased pannus and inflamed synovium (Deutsch et al. 1993). This prevents the secretion of fluid and accumulation of inflammation, causing cellular compounds and the joint surfaces to become fibrotic, offering rapid and sustain pain relief. The effective cytotoxic radiation dose required to be delivered to the joints is determined principally by the size of the joint along with other factors such as synovial thickness, synovial structures (smooth, villous fine/rough edematous), condition of the joint fluid (watery or gelatinous), and inflammatory activity of the synovium (Kitonyi and Kitonyi 2009; Karavida and Notopoulos 2010; Özcan 2014; Dunn et al. 2002) (Fig. 14.3).

14.1.1 Advantages of Radiosynovectomy

- Minimally invasive intervention.
- Radiosynovectomy is generally performed as an outpatient procedure and involves overnight hospital stay.
- No surgical/anesthetic risk.
- Provides an attractive treatment option for inoperable patients.
- Intensity and duration of rehabilitation is minimal.
- Effective radiation dose for the treatment is low.
- Multiple joints may be treated simultaneously or at short intervals.
- Multiple radioactive dose administration to achieve maximum response.
- Relatively free of side effect.

F.F. (Russ) Knapp, A. Dash, *Radiopharmaceuticals for Therapy*, DOI 10.1007/978-81-322-2607-9_14

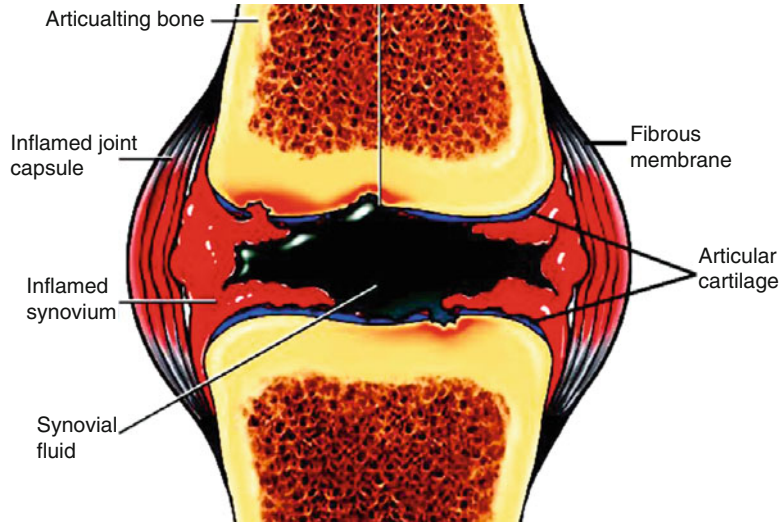

Fig. 14.1 Schematic of the a synovial joint

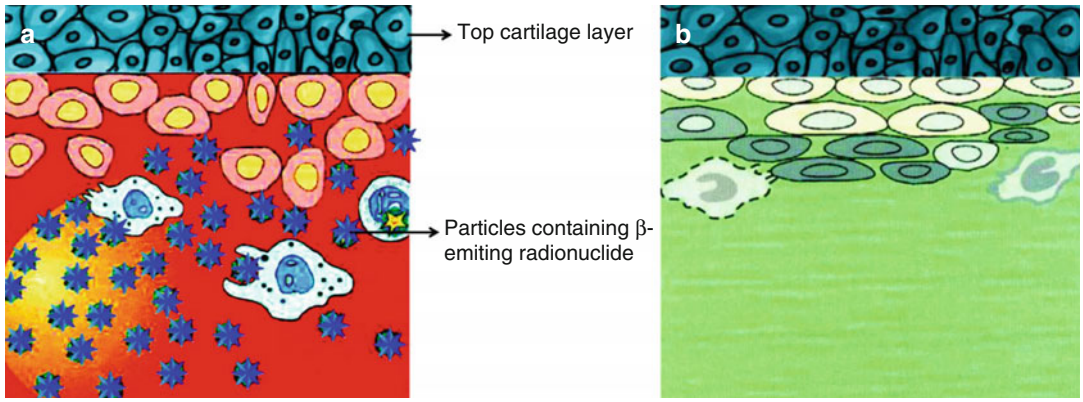

Fig. 14.2 (**a**) Particles containing β^--emitting radionuclide (*blue stars*) phagocytized by inflamed hypertrophic synovial lining with proliferating synoviocytes without affecting top cartilage layer. (**b**) Successive cell damage and sclerosis of synovial membrane

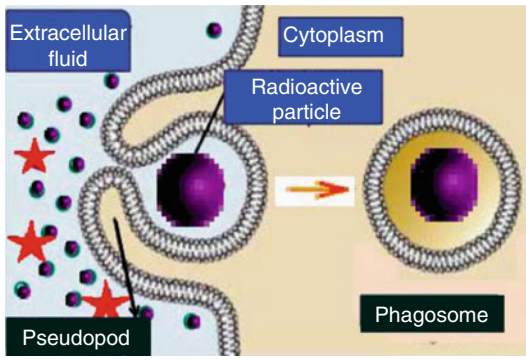

Fig. 14.3 Phagocytosis where cell sequester radioactive particulates by extension of pseudopodia and vesicle formation

14.1.2 Selection of Radionuclides

While a myriad of factors contribute to the utility of RSV, selection of an appropriate β^--emitting radionuclide is critical since the synovial thickness of different joints in the human body (e.g., finger, wrist, knee, etc.) varies substantially. Also, joints at different stages of the disease show different degrees of swelling and may also call for a beta emitter of different penetration. The β^- radiation energy should be sufficient to penetrate and ablate proliferating layer of the inflamed synovium with minimum radiation-induced damaged to the underlying articular cartilage or adjacent bone

underneath (Chakraborty et al. 2015) (Fig. 14.4). The radionuclide dose should be small enough to be phagocytosed, and it should be given in amounts that are limited enough so that leakage does not occur from the joint (Schneider et al. 2005). The radionuclide should have a half-life suffice for adequate, but not excessively prolonged, to deliver cytotoxic radiation dose to the synovium and should be substantially less than the retention time of the radiolabeled particle in the joint to be treated. The penetration depth of the β^- radiation energy should correspond to the thickness of the synovium in the joint to be treated, as inadequate penetration will give an inferior therapeutic effect and excessive penetration depths may constitute a safety hazard. As the thickness of the diseased membrane varies in different joints, treatment of diseased synovium in joints of disparate size requires radionuclide of different β^- particle energies with high-energy beta emitters such as ^{90}Y and ^{188}Re for the large joints such as the knees and the ^{169}Er low beta emitter for treatment of the finger joints. A medium beta energy emitter such as ^{186}Re is useful for irradiation of medium-sized synovial joints such as the elbow. The other important issues are leakage of the radioisotope form the joint, which must be minimized by the characteristics of the preparation, and the gradual particle adsorption by the synovium. The half-life should be long enough to allow good distribution within the synovium and adequate exposure, while being short enough to avoid excessive irradiation and significant leakage from the joint. There is no evidence that the use of radioisotopes is a therapeutic option for the treatment of osteoarthritis (Moskowitz 2007).

Table 14.1 summarizes the principal radioisotopes and preparations which have been evaluated or which are in current use as approved radiopharmaceutical agents for the treatment of rheumatoid arthritis. These agents are approved for clinical use in many countries, but interestingly, radiation synovectomy is not practiced in the USA and these agents have not yet been approved by the regulatory authorities, presumably because of the potential ramifications of joint leakage, although extensive studies as

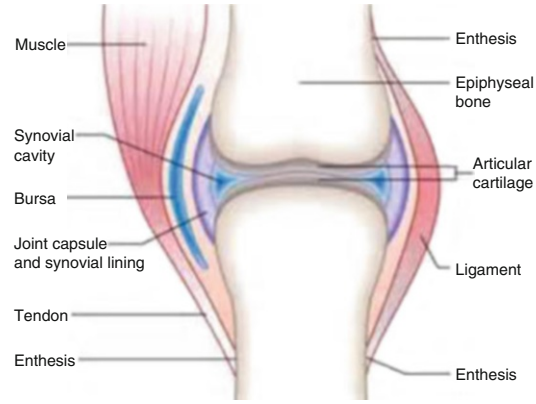

Fig. 14.4 Diagram illustrating the anatomical relationship of the synovial membrane to other structures in the knee joint and needle placement for introduction of radioisotope preparations for synovectomy

discussed later in this chapter have demonstrated the safety and efficacy of this method. The first reports of this last treatment were published as early as 1924 (Ishido 1924) and subsequent later (Fellinger and Schmid 1952) and paved the way for the contemporary broad clinical application of radionuclide synovectomy.

So the challenges in developing a useful agent for the treatment of synovitis include the selection of the appropriate radionuclide(s). In addition to radionuclidic properties, another key issue is availability and radionuclides used for this application decay by beta emission and thus are generally reactor-produced (Table 14.1). One example which can be either reactor or accelerator produced is ^{186}Re (see Chaps. 6 and 7). Key radionuclidic properties include emission of a beta particle with the requisite energy which matches the joint dimensions and required soft tissue penetration requirements (Table 14.2). For radiation safety considerations, these radioisotopes should decay without emission of significant abundance of accompanying high-energy gamma photons. However, the emission of gamma photons which can be imaged is important to substantiate homogeneous distribution within the joint space and to evaluate the possibility of any leakage of activity.

An additional important characteristic is the availability of a particulate preparation which is

Table 14.1 Examples of radioisotope preparations developed and evaluated for treatment of inflammatory (rheumatoid) joint disease

Radioisotope	Half-life Major $E_{\beta max}$ ($Int_{\%}$)	Therapeutic range (X_{90}) in the synovium	Major joints	Radiopharmaceutical (particle size μm)	Key references
Radioisotope preparations which have been evaluated for treatment of synovitis					
Gold-198	2.7 days 0.960 (98 %)	0.39 mm	Large (knee)	High gamma energy	
Dysprosium-165	2.3 h 1.285 (83 %)	0.57 mm	All	Ferric hydroxide macroaggregates (FHMA) (0.8–12) Only low gammas	Hnatowich et al. (1978) McLaren et al. (1990) Sledge et al. (1986)
Holmium-166	26.8 h 1.773 (48 %) 1.854 (51.0 %)		Medium, large	Chitosan FHMA Polylactic acid (PLA) microspheres (1.2–12)	Cho et al. (2012) Argüelles et al. (2003) Makela et al. (2004) Mupmer et al. (1992)
Lutetium-177	6.71 days 0.497 (78.7)	1.3	Small	Hydroxyapatite (HA)	Herrick et al. (1994)
Phosphorus-32	14.29 days 1.701 (100 %)	2.1	All	Chromic phosphate	Sohaib et al. (2011)
Rhenium-188	16.9 h 2.12 (71.4 %)	2.1	Large (knees)	Sulfide/microspheres	Liepe et al. (2011) Wang et al. (2001)
Samarium-153	46.7 h 0.632 (3.1 %) 0.702 (44.1 %)	1.6	Large	HA macroaggregates	O'Duffy et al. (1999a, b)
Approved radiopharmaceuticals for routine clinical treatment of synovitis					
Erbium-169	9.5 days 0.350 (55 %)	0.18	Small	Citrate	
Rhenium-186	3.7 days 1.076 (71 %)	1.2	Medium	Heptasulfide colloid	Klett et al. (2007)
Yttrium-90	2.7 days 2.26 (99.9 %)	2.22	Large (knee)	Citrate/silicate High beta energy (1.5–3.5) No gamma photons	

stable for a sufficient time period after administration prior to synovial resorption. As summarized in Table 14.1, there are many therapeutic radioisotopes which have been evaluated for radionuclide synovectomy. Selection of particulate for use in RSV is primarily based on the ability for facile and reproducible preparation and demonstration of effective synovial targeting/uptake. The particulates should also be sufficiently robust enough to withstand the radiolabeling reaction conditions and should exhibit chemical characteristics which must form a stable complex with the radionuclide and should exhibit good stability to circumvent loss of the radioisotope from radiolysis or during application. The particle chemical characteristics should permit simple and efficient radiolabeling, and they should be nontoxic, nonallergenic, biocompatible, and preferably biodegradable. The binding between the radionuclide and the particle

Table 14.2 European Commission recommended activity doses of approved radiopharmaceutical agents for joint synovectomy

Treated joint	Administered activity, MBq			Recommended volume (ml)
	^{169}Er	^{186}Re	^{90}Y	
Large joints – yttrium-90				
Knee			185–222	3–5
Medium joints – rhenium-186				
Ankle (tibiotalar)		74–185		1–1.5
Elbow		74–111		1.2
Foot (subtalar)		37–74		1.15
Shoulder (glenohumeral)		74–185		4
Wrist		37–74		1–1.5
Small joints – erbium-169				
Fingers (metacarpophalangeal)	20–40			1
Foot (metatarsophalangeal)	30–40			1
Hands/feet (proximal interphalangeal)	10–20			0.5

EANM (2002), van der Zant (2008)

should be irreversible throughout the course of the radiotherapy. Another prerequisite is that the particle must be sufficiently small to be phagocytized; however it should not be too small that would allow joint leakage before phagocytic trapping. The appropriate medium major diameter size range for this application is considered to be from 2 to 10 μm. Following intra-articulation, the radiolabeled particles should be distributed homogeneously in the joint without initiating an inflammatory response.

There are a variety of materials and particulate preparations used for synovectomy, which include preparations based on citrate, sulfide colloids, hydroxyapatite particles, and chitosan (Karavida and Notopoulos 2010; Teyssler et al. 2013; Kasteren et al. 1993; Davis and Chinol 1989; Song et al. 2001; Brecelj et al. 2007). Ideally, the particle size distribution should be in the 2–10 μm range. Depending on the particles, it is possible to incorporate the activity, label throughout the entire volume, or label only in certain structures, such as the surface and the outer or inner wall. The binding of radioactivity to particles can be done by covalent bonds, by chelation, by adsorption processes, or by indirect means. In the light of the perceived need to preclude leakage of the radioactive isotope from the microsphere, the prospect of enclosing the nonradioactive precursor of the radioisotope in the microsphere matrix and subsequent activation in a nuclear reactor shortly before use seemed attractive.

There are of course regulatory guidelines which must be followed for the use of such agents for treatment of synovitis and Table 14.2 summarizes guidelines used in the European community. It is interesting to note that although the first development and the first demonstration of clinical efficacy was reported in the USA (Sledge et al. 1986), radiation synovectomy is not practiced in the USA evidently due to a regulatory concern that potential joint leakage of the radioisotope would expose non-target tissues to unacceptable radiation dose.

14.2 Dosimetry and Dose Rate

Although a detailed discussion of dosimetry is beyond the goal of this presentation, these studies are important and can provide important guidance on the use of radionuclide for synovectomy. In one recent particularly important study, the use of erbium-169 (^{169}Er), phosphorus-32 (^{32}P), rhenium-188 and samarium-153 (^{188}Re and ^{153}Sm), and yttrium-90 (^{90}Y) were analyzed, since these are radionuclides of current major interest for radio-

synovectomy (Torres et al. 2009). The therapeutic range in synovial tissue values and the adsorbed dose values per activity of injected radionuclide (Gy/h*MBq) profiles to the synovial membrane and juxtaposed articular cartilage were evaluated in detail. These useful data provide estimates of the dose expected to be delivered to the synovial membrane and cartilage for joints of different dimensions and for different stages of the arthritic process, which present with different degrees of swelling. In this context, it is recommended in European theater that MRI imaging be initially conducted to determine the tissue volume and the appropriate radionuclide for synovectomy treatment which is dependent on the synovial thickness for treatment and the proximity of the bone and cartilage non-target tissues. The RS procedure demands efforts of a well-coordinated multidisciplinary team of medical specialists, including musculoskeletal physicians, radiologists, nuclear physicians, hematologists, physical therapists, and appropriately trained nurses. In the modality, the role of radiologist represents the key in the assessment of the suitability of the target joint.

14.3 Key Therapeutic Radioisotopes Used for Synovectomy

Many of the radioisotopes described in this section are also used for a variety of other therapeutic applications using unsealed sources described in this book and the production and processing details are included in Chaps. 5, 6, and 7.

14.3.1 Dysprosium-165

In more contemporary times, ^{165}Dy is the first radiopharmaceutical agent which stimulated interest in the more widespread introduction of this technology for the treatment of refractory synovitis as an alternative to surgical intervention (Hnatowich et al. 1978; Sledge et al. 1986; McLaren et al. 1990). It is interesting to note an unusual commentary that the use of 165 Dy as the first therapeutic radioisotope for intra-articulation for this application was developed by Prof. Sledge in Boston. In spite of this pioneering work and effectiveness of this treatment, the US *Food and Drug Administration* (FDA) has not approved such use on the basis of the dosimetric implications of "potential" capsule leakage. Thus, although this use of therapeutic radioisotopes is practiced essentially worldwide except in the USA for effective treatment of such conditions—also in hemophilic patients—it is not routinely practiced in the USA.

14.3.2 Erbium-169

Because of the more abbreviated anatomical dimensions, the use of low-energy beta emitters is indicated for the treatment of synovitis of the small joints in order to minimize any possible radiation damage to the underlying bone or other tissues. The use of reactor-produced ^{169}Er as the citrate is thus the current preferred option for synovectomy of small joints (Kahan et al. 2004; Menkes et al. 1977). A review of the use of ^{169}Er for the treatment of inflamed small joints has been recently published (Karavida and Notopoulos 2010).

14.3.3 Gold-198

The first papers on the use of ^{198}Au in the treatment of arthritis appeared in 1963 in which chronic effusions of the knee was treated with 370 MBq of gold-198 colloids (Ansell et al. 1963). Few studies on the use of ^{198}Au have been reported in the literature (Cayla 1967; Topp and Cross 1970; Van Soesbergen et al. 1988; Visuthikosol and Kumpolpunth 1981). Although used in the early development of the use of therapeutic radioisotopes for synovectomy, ^{198}Au is no longer used for this indication, primarily because of the emission of high-energy gamma photons (411 keV, 95 %).

14.3.4 Holmium-166

One early strategy for the preparation of ^{166}Ho-labeled agents for this application involved preparation of biodegradable neutron-activated

poly-L-lactic acid (PLA) microspheres (2–13 μm) (Mupmer et al. 1992). The microspheres were prepared by combination of PLA and nonradioactive ^{165}Ho-acetyacetonate (^{166}Ho-AcAc) in $ChCl_3$ which was then added to 3 % polyvinyl alcohol. After stirring, the precipitated microspheres (2–13 nm) were centrifuged and the microspheres obtained by 3.0 μm filtration, treated with HCl to remove any excess AcAc, and the solution then repeatedly filtered through 3.0 μm filters. The ^{165}Ho-AcAc microsphere target material was then irradiated at a thermal neutron flux of about 8.88×10^{12} n/cm^2·s. Evaluation after intra-articular injection into the knee joint space of rabbits demonstrated about 98 % retention with no leakage after 120 h. The initial studies in a small patient group with ^{166}Ho-FHMA involved an average 1.11 GBq administration into the knee joints of 22 patients in which 17 patients (71 %) showed complete or partial response (Ofluoglu et al. 2002). Although some joint leakage was observed by detection of low levels of activity in local inguinal lymph nodes in 6 treatments, the authors concluded that this as a safe and effective method for treatment of synovitis.

Hydroxyapatite [HP; $Ca_{10}(PO_4)_6(OH)_2$] is an important natural component of teeth and bones and forms strong complexes by binding with many cations. HP particles labeled with ^{166}Ho has also been widely evaluated for synovitis therapy and are prepared by combining ^{166}Ho-citrate with HA by mixing and agitating at room temperature (Unni et al. 2002). Hydroxyapatite (HA) is a naturally occurring mineral form of calcium apatite with the formula $Ca_5(PO_4)_3(OH)$ but is usually written $Ca_{10}(PO_4)_6(OH)_2$ to denote that the crystal unit cell comprises two entities. Hydroxyapatite is the hydroxyl end member of the complex apatite group. The OH^-ion can be replaced by fluoride, chloride, or carbonate, producing fluorapatite or chlorapatite. It crystallizes in the hexagonal crystal system. Pure hydroxyapatite powder is white. Naturally occurring apatites can, however, also have brown, yellow, or green colorations, comparable to the discolorations of dental fluorosis. Up to 50 % of bone by weight is a modified form of hydroxyapatite. Another approach has been the radiolabeling of the chitosan molecule, which is a linear polysaccharide and consists of randomly distributed deacetylated β-(1-4)-linked D-glucosamine and acetylated *N*-acetyl-D-glucosamine units. It is obtained by sodium hydroxide treatment of shells from shrimp, lobster, and clams and other crustaceans with sodium hydroxide treatment. Because of excellent electrostatic properties, chitosan has high metal cation-binding properties and has been used to bind a variety of therapeutic radioisotopes. The ^{166}Ho-chitosan complex has also been evaluated for treatment of synovitis (Seong et al. 2005; Lee et al. 2003a, b).

14.3.5 Lutetium-177

More recently, the use of ^{177}Lu for synovectomy has been explored. Advantages include the reactor production in very high activity levels and high specific activity (>70 Ci/g ^{176}Lu at a thermal neutron flux of $>1 \times 10^{15}$ n/cm^2/s) ^{177}Lu, the emission of moderate energy beta particle (497 keV), and the emission of relatively low-energy gamma photons (208 keV, 11 %) which permit imaging to evaluate the homogeneity of joint distribution and possible leakage. Moreover, the relatively longer half-life of ^{177}Lu provides logistic advantage for shipment to nuclear medicine centers far away from the reactors. The ^{177}Lu preparations which have been evaluated for synovectomy include hydroxyapatite and liposomes. Increasing use of ^{177}Lu for synovectomy has been impressive and widespread applications of ^{177}Lu therapeutic agents have stimulated progress (Chakraborty et al. 2006, 2014a, b; Kamaleshwaran et al. 2014; Bard et al. 1985; Abbasi et al. 2011; Teyssler et al. 2013).

14.3.6 Phosphorus-32

^{32}P has received attention due to its easy economic availability and reasonably satisfactory nuclear characteristics [$T_{½}$ = 14.3 days; $E_{β\ (Max.)}$ = 1.7 MeV; 3–5 mm of tissue penetration depth, respectively]. ^{32}P chromic phosphate emerged as the current agent of choice in the USA and

Canada. The utility of ^{32}P is thus continually evolving and well entrenched in the arena of radiosynovectomy (Manco-Johnson et al. 2002; Onetti et al. 1982; Rivard et al. 1985, 1994; Siegel et al. 1994, 2001; Silva et al. 2001; Mortazavi et al. 2007). Samarium [^{32}P] phosphate colloid has also recently been exploited as the agent for synovectomy (Prabhakar et al. 2007). The method of preparation involves the reaction of $SmCl_3$ carrier with carrier added [^{32}P]H_3PO_4 in the presence of gelatin. The pure colloid was recovered by dialysis.

14.3.7 Rhenium-186

Rhenium-186 is the radioisotope of choice for the treatment of inflammatory disease of the medium-sized joints such as the shoulder, elbow, wrist, hip, and ankle (Table 14.2). ^{186}Re-sulfide is the radiopharmaceutical used for the treatment (Gedik et al. 2006; Tebib et al. 2004; Göbel et al. 1997; Kavakli et al. 2008). The ^{186}Re-labeled sulfide colloid preparations are available from several commercial supplies as approved radiopharmaceutical preparations for the treatment of inflammatory joint disease (http://www.iba-molecular.com/products/re-186-mm-1). The recommended activity range for RSO with ^{186}Re sulfide colloid is as follows: for the hip, 74–185 MBq; shoulder, 74–185 MBq; elbow, 74–111 MBq; wrist, 37–74 MBq; ankle, 74 MBq; and subtalar joint, 37–74 MBq (van der Zant et al. 2004). When several joints are being treated in a single session, the total activity administered should not exceed 370 MBq (EANM 2003; Farahati et al. 1999). ^{186}Re-sulfide has been widely used in the clinical practice for 25 years in Europe, and its efficacy is well accepted in RA, while adverse effects are minor and infrequent. Reviews describing the clinical use of the ^{186}Re colloid have been recently published (Klett et al. 2007; Koca et al. 2012).

14.3.8 Rhenium-188

Several ^{188}Re-labeled particulates have been developed for this purpose which include polypeptide colloids (Jia et al. 1996), sulfur colloid (Wang et al. 1995; Li et al. 2004), tin colloid (Jeong et al. 2000; Lee et al. 2003a, b; Shin et al. 2003, 2007), hydroxyapatite particles (Grillenberger et al. 1997; Kothari et al. 2003), rhenium colloids (Ures et al. 2002), and microspheres (Yu et al. 2005; Wang et al. 2001). Most of the particles are reported to have suitable biological properties for application in radiosynovectomy as seen in animal experiments.

Although not available as an approved agent, the ^{188}Re tin colloid has shown excellent efficacy for the treatment of inflammation of large joints (Liepe et al. 2011; Shukla et al. 2007; Shamim et al. 2010). The NCA ^{188}Re is obtained from the ^{188}W/^{188}Re radionuclide generator system (Chap. 7). It is prepared by lyophilization of 10 mg $SnCl_2 \cdot 2H_2O$ 0.5 ml, HCl 0.1 N, 2 mg ascorbic acid, and 1 % w/w Tween 80® (Jeong et al. 2000). In addition, ^{188}Re-labeled microspheres prepared using the commercially available B20 human albumin preparation have also been utilized for this application (Liepe et al. 2011). Preparation of these particles involves aseptic preparation of a mixture of 2,5-dihydroxybenzoic acid and potassium sodium tartrate in the lyophilized form each in a separate vial. Prior to use for injection, the content of these vials is dissolved in water. The radiolabeling is performed in the presence of stannous chloride using HSA microspheres B20; 300,000–500,000 particles 2.5 mg using [^{188}Re] $NaReO_4$ was obtained from a ^{188}W/^{188}Re generator (Wunderlich et al. 2000, 2005).

14.3.9 Samarium-153

There is a great deal of interest on the use of ^{153}Sm produced by neutron activation of both natural Sm_2O_3 and 98 % enriched 152 Sm_2O_3 targets. This is attributed to the beta energy of 0.8 MeV of ^{153}Sm that has penetration in average range of 0.8 mm and maximum of 3.1 mm in soft tissues. This is appropriate for synovectomy of median articulations. Several ^{1153}Sm-labeled preparations including hydroxyapatite (Boerbooms 1997; Calegaro et al. 2009, 2014; Chinol et al. 1993; Clunie et al. 1995, 1996;

Santos et al. 2009; Yarbrough et al. 2000; O'Duffy et al. 1999a, b), chitosan (Shin et al. 2001), citrate-hydroxyapatite (Fan et al. 2006), and metallic-hydroxide macroaggregates (Ferro-Flores et al. 1997) have also been prepared and evaluated as candidates for synovectomy. Several clinical studies have also been conducted (Boerbooms 1997; Calegaro et al. 2009, 2014; Dos Santos et al. 2011; Clunie et al. 1996; Santos et al. 2009; O'Duffy et al. 1999a, b).

14.3.10 Yttrium-90

Yttrium-90 has a half-life of 64.1 h and decays to the stable ^{90}Zr daughter product, by emission of high-energy β^- radiation ($E_{\beta max}$=2.28 MeV). The beta rays have a maximum tissue range of 11 mm which is useful for the treatment of large joints such as the knees. Another major advantage is the availability of ^{90}Y from a ^{90}Sr/^{90}Y generator, since the 28.8 years half-life of ^{90}Sr makes it an attractive generator system for long-term usage. The ^{90}Y obtained is "no carrier added" which results in preparations that are more stable than the low specific activity ^{90}Y prepared by (n, γ) activation of ^{89}Y. The ability of the high-energy β^- radiation ($E_{\beta max}$=2.28 MeV) to penetrate deeply into tissue made ^{90}Y an appropriate radionuclide for the knee joint and those with substantially thickened synovia (Schneider et al. 2005; Spooren et al. 1985; Heuft-Dorenbosch et al. 2000; Chatzopoulos et al. 2009; Chrapko et al. 2007; Oka 1975; Stucki et al. 1993; Taylor et al. 1997; Kampen et al. 2007; Badiavas et al. 2006; Jacob et al. 2003; Shabat et al. 2002). In knee joints, the preferred dose range is 5–15 mCi. The tremendous prospect associated with the use of ^{90}Y for treating large joint led to a considerable amount of fascinating clinical research and innovative strategies (Will et al. 1992; Wong et al. 2014; Oztemür et al. 2013; van der Zant et al. 2009; O'Doherty et al. 2014a, b; Jahangier et al. 2006; Chatzopoulos et al. 2009; Dawson et al. 1994; Boerbooms and Buijs 1993; Stucki et al. 1993; Davis and Chinol 1989; Dunscombe and Ramsey 1980; Wiss 1982; Doyle et al. 1977; Dunscombe et al. 1976). By far, ^{90}Y is the radioisotope used most extensively for radiosynoviorthesis in rheumatoid arthritis. Histological studies after ^{90}Y synovectomy have revealed reduction in the number and size of the synovial villi with decreased hyperemia in the early phase (Mödder 1995; Erselcan et al. 2003; Pavelka et al. 1975; Heuft-Dorenbosch et al. 2000). A large number of ^{188}Re-labeled particulates have been developed including silicate (Dunscombe and Ramsey 1980; Markou and Chatzopoulos 2009; van Kasteren et al. 1993; Gumpel 1980; Kasteren et al. 1993), ferric hydroxide colloid (Bayly et al. 1973; Beer et al. 1973; Pandey et al. 2001; Chinol et al. 1990; Dunscombe et al. 1976; Schmid et al. 2006; Teyssler et al. 2013; Turkmen et al. 2007; Voth et al. 2006), hydroxyapatite (Kamaleshwaran et al. 2015; Thomas et al. 2011a, b; Vimalnath et al. 2015; Khalid and Mushtaq 2005), citrate (Bowen et al. 1975; Gumpel et al. 1973), and resin colloid (Oka et al. 1971).

14.4 Summary

The use of beta-emitting radioisotopes for synovectomy is a unique, simple, and effective procedure for palliation and reduction of swelling from synovitis. It is represented as a safe, fast, and patient-friendly therapeutic option in the management of different kinds of arthritis. Compared to the practice of surgical synovectomy, this minimally invasive modality offers better preservation of range of motion, does not necessitate hospitalization, and requires minimal administration with clotting factor. This modality of treatment has been successfully performed through most of the world for over four decades. This technique is widely practiced throughout much of the world. There is extensive accumulated evidence for both the efficacy and safety of this treatment if properly conducted. The theoretical danger arising through exposure to radiation is minimal, and there are no known cases of malignancies caused by radioactive particles. The rate of side effects and patient radiation exposure are minimal. The size of the synovial joint for treatment and the prescribed depth of radiation penetration can be effectively accommodated by the

appropriate choice of radionuclide preparations which are available from commercial manufacturers. The practice of radiation synovectomy is expected to further evolve, with development of new particles as well as the availability of a whole range of radioisotopes.

References

Abbasi I, Ishfaq M, Sohaib M. Preparation and preclinical study of ^{177}Lu-labelled hydroxyapatite for application in radiation synovectomy of small joints. Q J Nucl Med Mol Imaging. 2011;55:458–68.

Ansell BM, Crook A, Mallard JR, Bywaters EGL. Evaluation of intra-articular colloidal gold Au 198 in the treatment of persistent knee effusions. Ann Rheum Dis. 1963;22:435–9.

Argüelles MG et al. Preparation and evaluation of holmium-166 ferric hydroxide macroaggregates for radiation synovectomy. Alasbimn J. 2003;5: AJ19–9.

Badiavas K, Chatzopoulos D, Markou P. Radiation doses from patients undergoing yttrium-90 silicate knee radiosynovectomy. Hell J Nucl Med. 2006;9:65–8.

Bard DR, Knight CG, Page-Thomas DP. Effect of the intra-articular injection of lutetium-177 in chelator liposomes on the progress of an experimental arthritis in rabbits. Clin Exp Rheumatol. 1985;3:237–42.

Bayly RJ, Peacegood JA, Peake SC. ^{90}Y ferric hydroxide colloid. Ann Rheum Dis. 1973;32:41–2.

Beer TC, Crawley JC, Farran HE, Gumpel JM. Preliminary assessment of ^{90}Y ferric hydroxide colloid. Ann Rheum Dis. 1973;32:41–2.

Boerbooms AM. Clinical outcome after one year following samarium-153 particulate hydroxyapatite radiation synovectomy. Scand J Rheumatol. 1997; 26:136–7.

Boerbooms A, Buijs W. Efficacy and safety of radiation synovectomy with Yttrium-90: a retrospective long-term analysis of 164 applications in 82 patients. Br J Rheumatol. 1993;32:1114–5.

Bowen BM, Darracott J, Garnett ES, Tomlinson RH. Yttrium-90 citrate colloid for radioisotope synovectomy. Am J Hosp Pharm. 1975;32:1027–30.

Brecelj J, Gmeiner-Stopar T, Jevsek M, et al. Colloidal ^{90}Y used for radiation synovectomy decreases the viability of chondrocytes in human cadaveric samples. Nucl Med Commun. 2007;28:704–10.

Calegaro JU, Machado J, De Paula JE, et al. Clinical evaluation after 1 year of 153-samarium hydroxyapatite synovectomy in patients with haemophilic arthropathy. Haemophilia. 2009;15:240–6.

Calegaro JU, Machado J, Furtado RG, et al. The use of 185 MBq and 740 MBq of 153-samarium hydroxyapatite for knee synovectomy in haemophilia. Haemophilia. 2014;20:421–5.

Cayla J. Colloidal Au-198 in the treatment of hydrarthrosis in rheumatoid polyarthritis. Rev Rhum Mal Osteoartic. 1967;34:438–41.

Chakraborty S, Das T, Banerjee S, et al. Preparation and preliminary biological evaluation of ^{177}Lu-labelled hydroxyapatite as a promising agent for radiation synovectomy of small joints. Nucl Med Commun. 2006;27:661–8.

Chakraborty S, Vimalnath KV, Rajeswari A, et al. Preparation, evaluation, and first clinical use of 177Lu-labeled hydroxyapatite (HA) particles in the treatment of rheumatoid arthritis: utility of cold kits for convenient dose formulation at hospital radiopharmacy. J Label Comp Radiopharm. 2014a;57: 453–62.

Chakraborty S, Vimalnath KV, Rajeswari A, et al. Radiolanthanide-labeled HA particles in the treatment of rheumatoid arthritis: ready-to-use cold kits for rapid formulation in hospital radiopharmacy. J Radioanal Nucl Chem. 2014b;302:875–81.

Chakraborty S, Sharma KS, Rajeswari A, et al. Radiolanthanide-loaded agglomerated Fe_3O_4 nanoparticles for possible use in the treatment of arthritis: formulation, characterization and evaluation in rats. J Mater Chem B. 2015;3:5455–66.

Chatzopoulos D, Moralidis E, Markou P, Makris V. Yttrium-90 radiation synovectomy in knee osteoarthritis: a prospective assessment at 6 and 12 months. Nucl Med Commun. 2009;30:472–9.

Chinol M, Vallabhajosula S, Zuckerman JD, Goldsmith SJ. In vivo stability of ferric hydroxide macroaggregates (FHMA). Is it a suitable carrier for radionuclides used in synovectomy? Int J Rad Appl Instrum B. 1990;17:479–86.

Chinol M, Vallabhajosula S, Goldsmith SJ, et al. Chemistry and biological behavior of samarium- 153 and rhenium- 186-labeled hydroxyapatite particles: potential radiopharmaceuticals for radiation synovectomy. J Nucl Med. 1993;34:1536–42.

Cho YJ, Kim KI, Chun YS, et al. Radioisotope synoviorthesis with holmium-166-chitosan complex in haemophilic arthropathy. Haemophilia. 2012;16(4):640–6.

Chrapko B, Zwolak R, Nocuń A, et al. Radiation synovectomy with ^{90}Y colloid in the therapy of recurrent knee joint effusions in patients with inflammatory joint diseases. Rheumatol Int. 2007;27:729–34.

Clunie G, Lui D, Cullum I, Ell PJ, et al. Samarium-153-particulate hydroxyapatite radiation synovectomy: biodistribution data for chronic knee synovitis. J Nucl Med. 1995;36:51–7.

Clunie G, Lui D, Cullum I, et al. Clinical outcome after one year following samarium-153 particulate hydroxyapatite radiation synovectomy. Scand J Rheumatol. 1996;25(6):360–6.

Davis MA, Chinol M. Radiopharmaceuticals for radiation synovectomy: evaluation of two yttrium-90 particulate agents. J Nucl Med. 1989;30:1047–55.

Dawson TM, Ryan PF, Street AM, et al. Yttrium synovectomy in haemophilic arthropathy. Br J Rheumatol. 1994;33:351–6.

Deutsch E, Brodack JW, Deutsch KF. Radiation synovectomy revisited. Eur J Nucl Med. 1993;20:1113–27.

Dos Santos MF, Furtado RN, Konai MS, et al. Effectiveness of radiation synovectomy with Yttrium-90 and Samarium-153 particulate hydroxyapatite in rheumatoid arthritis patients with knee synovitis: a controlled, randomized, double-blinded trial. Clin Rheumatol. 2011;30:77–85.

Doyle DV, Glass JS, Gow PJ, et al. A clinical and prospective chromosomal study of yttrium-90 synovectomy. Rheumatol Rehabil. 1977;16:217–22.

Dunn AL, Busch MT, Wyly JB, Abshire TC. Radionuclide synovectomy for hemophilic arthropathy: a comprehensive review of safety and efficacy and recommendation for a standardized treatment protocol. Thromb Haemost. 2002;87:383–93.

Dunscombe PB, Ramsey NW. Radioactivity studies on two synovial specimens after radiation synovectomy with yttrium-90-silicate. Ann Rheum Dis. 1980;39:87–9.

Dunscombe PB, Bhattacharyya AK, Dale RG. The assessment of the body distribution of yttrium-90 ferric hydroxide during radiation synovectomy. Br J Radiol. 1976;49:372–3.

EANM. EANM procedure guidelines for radiosynovectomy. Eur J Nucl Med. 2002;30:BP12–6.

Erselcan T, Bulut O, Bulut S, et al. Lipoma arborescens; successfully treated by yttrium-90 radiosynovectomy. Ann Nucl Med. 2003;17:593–6.

Fan Y, Li G, Yao G, Zhang Q, Li G. A study of ^{153}Sm-citrate-hydroxyapatite synovectomy in knee synovitis with rheumatoid arthritis. Chin J Nucl Med. 2006;2:112–4.

Farahati J, Reiners C, Fischer M, et al. Guideline for radiosynorviorthesis. Nuklearmedizin. 1999;38:254–5.

Fellinger K, Schmid J. Die lokale Behandlung der rheumatischen Erkrankungen (Local therapy of rheumatoid arthritis). Wien Z Inn Med. 1952;33:351–63 (In German).

Ferro-Flores G, García-Salinas L, Pedraza-López M, et al. ^{153}Sm metallic-hydroxide macroaggregates: an improved preparation for radiation synovectomy. J Radioanal Nucl Chem. 1997;222:93–7.

Gedik GK, Uğur O, Atilla B, et al. Comparison of extraarticular leakage values of radiopharmaceuticals used for radionuclide synovectomy. Ann Nucl Med. 2006;20(3):183–8.

Göbel D, Gratz S, von Rothkirch T, et al. Radiosynoviorthesis with rhenium-186 in rheumatoid arthritis: a prospective study of three treatment regimens. Rheumatol Int. 1997;17:105–8.

Grillenberger KG, Glatz S, Reske SN. Rhenium-188 labeled hydroxyapatite and rhenium-188 sulfur colloid. In vitro comparison of two agents for radiation synovectomy. Nuklearmedizin. 1997;36:71–5.

Gumpel JM. Radiation synovectomy with yttrium-90 silicate. Ann Rheum Dis. 1980;39(6):614–5.

Gumpel JM, Hasp R, Loewi G. Comparison of ^{90}Y ferric hydroxide colloid with the citrate and resin colloids. A preliminary animal study. Ann Rheum Dis. 1973;32:11–2.

Herrick J, Siegal BA, James VL, et al. Hemarthrosis and synovitis associated with hemophilia: clinical use of P-32 chromic phosphate synoviorthesis for treatment. Radiology. 1994;190:257–61.

Heuft-Dorenbosch LL, de Vet HC, van der Linden S. Yttrium radiosynoviorthesis in the treatment of knee arthritis in rheumatoid arthritis: a systematic review. Ann Rheum Dis. 2000;59:583–6.

Hnatowich DJ, Kramer RI, Sledge CB, et al. Dysprosium-165 ferric hydroxide macroaggregates for radiation synovectomy. J Nucl Med. 1978;19:303–8.

Ishido C. Über die Wirkung des Radiothoriums auf die Gelenke. Strahlentherapie. 1924;15:537–44.

Jacob R, Smith T, Prakasha B, Joannides T. Yttrium90 synovectomy in the management of chronic knee arthritis: a single institution experience. Rheumatol Int. 2003;23:216–20.

Jahangier ZN, Jacobs KMG, Bijlsma JWJ, Lafeber FPJG. Radiation synovectomy with yttrium-90 for persisting arthritis has direct harmful effects on human cartilage that cannot be prevented by co-administration of glucocorticoids: an in vitro study. Ann Rheum Dis. 2006;65:1384–9.

Jeong JM, Lee YJ, Kim YJ, Chang YS, et al. Preparation of rhenium-188-tin colloid as a radiation synovectomy agent and comparison with rhenium-188-sulfur colloid. Appl Radiat Isot. 2000;52:851–5.

Jia W, Ehrhardt GJ, Zinn K, et al. ^{186}Re/^{188}Re labeled polypeptide microspheres as a potential radiation synovectomy agent. J Radioanal Nucl Chem. 1996;206:107–17.

Kahan A, Mödder G, Menkes CJ, et al. ^{169}Erbium-citrate synoviorthesis after failure of local corticosteroid injections to treat rheumatoid arthritis-affected finger joints. Clinical Exp Rheumatol. 2004;22:722–6.

Kamaleshwaran KK, Rajamani V, Thirumalaisamy SG, et al. Radiosynovectomy of the elbow joint synovitis in rheumatoid arthritis treated with Lutetium - 177 labeled hydroxylapatite (Lu-177 HA) particulates; first case report and image of Lu -177 HA in the elbow joint. Indian J Nucl Med. 2014;29:270–2.

Kamaleshwaran KK, Rajan D, Krishnan B, et al. Use of yttrium-90 hydroxyapatite radiosynovectomy as a primary modality of treatment in diffuse pigmented villonodular synovitis of the knee joint: a first case report. Indian J Nucl Med. 2015;30:47–50.

Kampen WU, Voth M, Pinkert J, Krause A. Therapeutic status of radiosynoviorthesis of the knee with yttrium-90 (^{90}Y) colloid in rheumatoid arthritis and related indications. Rheumatology. 2007;46:16–24.

Karavida N, Notopoulos A. Radiation synovectomy: an effective alternative treatment for inflamed small joints. Hippokratia. 2010;14:22–7.

Kasteren MEE, Novakava IRO, Boerbooms AMT, Lemmens JAM. Long term follow up of radiosynovectomy with yttrium-90 silicate in haemophilic haemarthrosis. Ann Rheum Dis. 1993;52:548–50.

Kavakli K, Aydogdu S, Taner M, et al. Radioisotope synovectomy with rhenium186 in haemophilic synovitis

for elbows, ankles and shoulders. Haemophilia. 2008;14:518–23.
Khalid M, Mushtaq A. Preparation and in vitro stability of (n, gamma) yttrium-90 hydroxyapatite. Appl Radiat Isot. 2005;62:587–90.
Kitonyi GW, Kitonyi JM. Radiation synovectomy: treatment option for haemophilia patients with chronic haemarthrosis: a review. East Afr Med J. 2009;86:S71–5.
Klett R, Lange U, Haas H, et al. Radiosynoviorthesis of medium-sized joints with rhenium-186-sulfide colloid: a review of the literature. Rheumatology. 2007;46:1531–7.
Koca G, Ozsoy H, Atilgan HI, et al. Application of rhenium-186 radiosynovectomy in elbow diffuse pigmented villonodular synovitis – a case report with multiple joint involvement. Nucl Med Mol Imaging. 2012;46:215–7.
Kothari K, Suresh S, Sarma HD, et al. ^{188}Re-labeled hydroxyapatite particles for radiation synovectomy. Appl Radiat Isotopes. 2003;58:463–8.
Lee SH, Suh JS, Kim HS, et al. MR evaluation of radiation synovectomy of the knee by means of intra-articular injection of holmium-166-chitosan complex in patients with rheumatoid arthritis: results at 4-month follow-up Korean. J Radiol. 2003a;4:170–8.
Lee YJ, Lee YJ, Cheon GJ, et al. ^{188}Re-tin-colloid as a new therapeutic agent for rheumatoid arthritis. Nucl Med Commun. 2003b;24:689–96.
Li P, Chen G, Zhang H, Shen Z. Radiation synovectomy by 188Re-sulfide in haemophilic synovitis. Haemophilia. 2004;10(5):422–7.
Liepe K, Zaknun JJ, Padhy A, et al. Radiosynovectomy using yttrium-90, phosphorus-32 or rhenium-188 for rheumatoid arthritis of the knee. Ann Nucl Med. 2011;25(5):317–23.
Makela OT, Pentilla P, Kolehainen E, et al. Effect of radiosynovectomy with holmium-166 ferric hydroxide macroaggregate on adult equine cartilage. J Rheumatol. 2004;31:321–8.
Manco-Johnson MJ, Nuss R, Lear J, et al. ^{32}P radiosynoviorthesis in children with hemophilia. J Pediatr Hematol Oncol. 2002;24:534–9.
Markou P, Chatzopoulos D. Yttrium-90 silicate radiosynovectomy treatment of painful synovitis in knee osteoarthritis. Results after 6 months. Hell J Nucl Med. 2009;12:33–6.
McLaren A, Hetherington E, Maddalena D, Snowdon G. Dysprosium (^{165}Dy) hydroxide macroaggregate for radiation synovectomy animal studies. Eur J Nucl Med. 1990;16:626–32.
Menkes CJ, Gô AL, Verrier P, et al. Double-blind study of erbium 169 injection (synoviorthesis) in rheumatoid digital joints. Ann Rheum Dis. 1977;36:254–6.
Mödder G. Radiosynoviorthesis. Involvement of nuclear medicine in rheumatology and orthopaedics. Meckenheim: Warlich Druck und Verlagsges GmbH; 1995.
Mortazavi SMJ, Asadollahi S, Farzan M, et al. ^{32}P colloid radiosynovectomy in treatment of chronic haemophilic synovitis: Iran experience. Haemophilia. 2007;13:182–8.
Moskowitz RW. Osteoarthritis: diagnosis and medical/surgical management. Baltimore: Lippincott Williams & Wilkins; 2007.
Mupmer RJ, Mills BJA, Ryo UY, Jay M. Polymeric microspheres for radionuclide synovectomy containing neutron-activated holmium-166. J Nucl Med. 1992;33:398–402.
O'Doherty J, Clauss R, Scuffham J, et al. Three dosimetry models of lipoma arborescens treated by ^{90}Y synovectomy. Med Phys. 2014a;41:052501.
O'Doherty J, Clauss R, Scuffham J, Khan A. Lipoma arborescens successfully treated with (^{90})Y synovectomy. Clin Nucl Med. 2014b;39:e187–9.
O'Duffy EK, Clunie GP, Lui D, et al. Double blind glucocorticoid controlled trial of samarium-153 particulate hydroxyapatite radiation synovectomy for chronic knee synovitis. Ann Rheum Dis. 1999a;58:554–8.
O'Duffy EK, Oliver FJ, Chatters SJ, et al. Chromosomal analysis of peripheral lymphocytes of patients before and after radiation synovectomy with samarium-153 particulate hydroxyapatite. Rheumatology (Oxford). 1999b;38:316–22.
Ofluoglu S, Schwameis E, Zehetgruber H, et al. Radiation synovectomy with ^{166}Ho-ferric hydroxide: a first experience. J Nucl Med. 2002;43:1489–94.
Oka M. Radiation synovectomy of the rheumatoid knee with yttrium 90. Ann Clin Res. 1975;7:205–10.
Oka M, Rekonen A, Rvotsi A, Seppala O. Intra articular injection of Y-90-resin colloid in the treatment of rheumatoid knee joint effusions. Acta Rheumatol Scand. 1971;17:148–60.
Onetti CM, Gutierrez E, Hliba E, Aguirre CR. Synoviorthesis with 32P-colloidal chromic phosphate in rheumatoid arthritis – clinical, histopathologic and arthrographic changes. J Rheumatol. 1982;9:229–38.
Otero M, Goldring MB. Cells of the synovium in rheumatoid arthritis: chondrocytes. Arthritis Res Ther. 2007;9:220.
Özcan Z. Radiosynovectomy in hemophilic synovitis. Mol Imaging Radionucl Ther. 2014;23:1–4.
Oztemür Z, Bulut O, Korkmaz M, et al. Surgical synovectomy combined with yttrium 90 in patients with recurrent joint synovitis. Rheumatol Int. 2013;33:1321–6.
Pandey U, Mukherjee A, Chaudhary PR, et al. Preparation and studies with ^{90}Y-labelled particles for use in radiation synovectomy. Appl Radiat Isot. 2001;55:471–5.
Pavelka K, Meier-Ruge W, Müller W, Fridrich R. Histological study of effects of colloidal 90yttrium on knee joint tissues of rabbits. Ann Rheum Dis. 1975;34:64–9.
Prabhakar G, Sachdev SS, Umamaheswari S, et al. Development of samarium [^{32}P] phosphate colloid for radiosynoviorthesis applications: preparation, biological and preliminary clinical studies experience. Appl Radiat Isot. 2007;65(12):1309–13.
Rivard GE, Girard M, Lamarre C, et al. Synoviorthesis with colloidal ^{32}P chromic phosphate for hemophilic

arthropathy: clinical follow-up. Arch Phys Med Rehabil. 1985;66:753–6.

Rivard GE, Girard M, Belanger R, et al. Synoviorthesis with colloidal ^{32}P chromic phosphate for the treatment of hemophilic arthropathy. J Bone Joint Surg Am. 1994;76:482–8.

Santos MF, Furtado RN, Konai MS, et al. Effectiveness of radiation synovectomy with samarium-153 particulate hydroxyapatite in rheumatoid arthritis patients with knee synovitis: a controlled randomized double-blind trial. Clinics (Sao Paulo). 2009;64:1187–93.

Schmid E, Selbach HJ, Voth M, et al. The effect of the beta-emitting yttrium-90 citrate on the dose-response of dicentric chromosomes in human lymphocytes: a basis for biological dosimetry after radiosynoviorthesis. Radiat Environ Biophys. 2006;45:93–8.

Schneider P, Farahati J, Reiners C. Radiosynovectomy in rheumatology, orthopedics, and hemophilia. J Nucl Med. 2005;46:48S–54.

Seong SK, Ryu JM, Shin DH, Bae EJ, Shigematsu A, Hatori Y, Nishigaki J, Kwak C, Lee SE, Park KB. Biodistribution and excretion of radioactivity after the administration of 166Ho-chitosan complex (DW-166HC) into the prostate of rat. Eur J Nucl Med Mol Imaging. 2005;32:910–7.

Shabat S, Kollender Y, Merimsky O, et al. The use of surgery and yttrium 90 in the management of extensive and diffuse pigmented villonodular synovitis of large joints. Rheumatology (Oxford). 2002;41:1113–8.

Shamim SA, Kumar R, Halanaik D, et al. Role of rhenium-188 tin colloid radiosynovectomy in patients with inflammatory knee joint conditions refractory to conventional therapy. Nucl Med Commun. 2010;31:814–20.

Shin BC, Park KB, Jang BS, et al. Preparation of ^{153}Sm-chitosan complex for radiation synovectomy. Nucl Med Biol. 2001;28:719–25.

Shin CY, Son M, Ko JI, et al. DA-7911, ^{188}Rhenium-tin colloid, as a new therapeutic agent of rheumatoid arthritis. Arch Pharm Res. 2003;26:168–72.

Shin K, Lee JC, Choi HJ, et al. Radiation synovectomy using ^{188}Re-tin colloid improves knee synovitis as shown by MRI in refractory rheumatoid arthritis. Nucl Med Commun. 2007;28:239–44.

Shukla J, Bandhopadhyaya GP, Shamim SA, Kumar R. Characterization of Re-188-Sn-microsperes used for synovitis treatment. Int J Pharmaceutics. 2007;338:43–7.

Siegel HJ, Luck JV, Siegel ME, Quines C, Anderson E. Hemarthrosis and synovitis associated with hemophilia: clinical use of 32P chromic phosphate synoviorthesis for treatment. Radiology. 1994;190:257–61.

Siegel HJ, Luck Jr JV, Siegel ME, Quinones C. Phosphate-32 colloid radiosynovectomy in hemophilia: outcome of 125 procedures. Clin Orthop. 2001;392:409–17.

Silva M, Luck JVJ, Siegel ME. ^{32}P chromic phosphate radiosynovectomy for chronic haemophilic synovitis. Haemophilia. 2001;7:40–9.

Sledge CB, Zuckerman JD, Zalutsky MR, Atcher RW, Shortkroff S, Lionberger DR, Rose HA, Hurson BJ, Lankenner PA Jr, Anderson RJ, et al. Treatment of rheumatoid synovitis of the knee with intraarticular injection of dysprosium 165-ferric hydroxide macroaggregates. Arthritis Rheum. 1986;29:153–9.

Sohaib M, Abbasi I, Ishfaq M. In vivo evaluation of Lu-177 hydroxyapatite for application in radiation synovectomy of digital joints. J Nucl Med. 2011;52(Suppl):1384.

Song J, Suh CH, Park YB, et al. A phase I/IIa study on intra-articular injection of holmium-166-chitosan complex for the treatment of knee synovitis of rheumatoid arthritis. Eur J Nucl Med. 2001;28(4):489–97.

Spooren P, Johannes J, Rasker JJ. Synovectomy of the knee with ^{90}Y. Eur J Nucl Med. 1985;10:441–5.

Stucki G, Bozzone P, Treuer E, et al. Efficacy and safety of radiation synovectomy with yttrium-90: a retrospective long-term analysis of 164 applications in 82 patients. Br J Rheumatol. 1993;32:383–6.

Taylor WJ, Corkill MM, Rajapaske CN. A retrospective review of yttrium-90 synovectomy in the treatment of knee arthritis. Br J Rheumatol. 1997;36:1100–5.

Tebib JG, Manil LM, Mödder G, et al. Better results with rhenium-186 radiosynoviorthesis than with cortivazol in rheumatoid arthritis(RA): a two-year follow-up randomized controlled multicentre study. Clin Exp Rheumatol. 2004;22:609–16.

Teyssler P, Taborska K, Kolostova K, Bobek V. Radiosynoviorthesis in hemophilic joints with yttrium-90 citrate and rhenium-186 sulfide and long term results. Hell J Nucl Med. 2013;16:44–9.

Thomas S, Gabriel MB, Assi PE, et al. Radioactive synovectomy with ^{90}Y- citrate in haemophilic synovitis: Brazilian experience. Brazilian Hemophilia Centers. Haemophilia. 2011a;17:e211–6.

Thomas S, Gabriel MC, de Souza SA, et al. A ^{90}Yttrium-hydroxyapatite: a new therapeutic option for radioactive synovectomy in haemophilic synovitis. Haemophilia. 2011b;17:e985–9.

Topp JR, Cross EG. The treatment of persistent knee effusions with intra-articular radioactive gold: preliminary report. Can Med Assoc J. 1970;102:709–14.

Torres M, Ayra E, Albuerne O, Montana Delgado MA. Adsorbed does profiles for ^{32}P, ^{90}Y, ^{188}Re, ^{153}Sm and ^{169}Er: radionuclides used for radiosynoviorthese treatment. Rev Esp Med Nul. 2009;28(4):188–92.

Turkmen C, Ozturk S, Unal SN, et al. The genotoxic effects in lymphocyte cultures of children treated with radiosynovectomy by using yttrium-90 citrate colloid. Cancer Biother Radiopharm. 2007;22:393–9.

Unni PR, Chaudari PR, Venkatesh M, et al. Preparation and bioevaluation of ^{166}Ho labeled hydroxyapatite (HA) particles for radiosynovectomy. Nucl Med Biol. 2002;29:199–209.

Ures MC, Savio E, Malanga A, et al. Physico-chemical characterisation and biological evaluation of 188-Rhenium colloids for radiosynovectomy. BMC Nucl Med. 2002;2:1–9.

Van der Zant FW. Radiation synovectomy of the ankle, knee and upper extremity joints. Proefschrift. The Netherlands: Marcelis Vanderlee-ADU-BV; 2008. ISBN 9789039349281.

Van der Zant FM, Jahangier ZN, Moolenburgh JD, et al. Radiation synovectomy of the ankle with 75 MBq colloidal ^{186}Rhenium-sulfide: effect, leakage, and radiation considerations. J Rheumatol. 2004;31: 896–901.

Van der Zant FM, Boer RO, Moolenburgh JD, et al. Radiation synovectomy with (^{90})Yttrium, (^{186})Rhenium and (^{169})Erbium: a systematic literature review with meta-analyses. Clin Exp Rheumatol. 2009;27:130–9.

Van Soesbergen RM, Hoefnagel CA, Marcuse HR, et al. Radiosynoviorthesis of the knee: a doubleblind trial of 1 versus 5 mCi Gold-198. Clin Rheumatol. 1988;7: 224–30.

Vimalnath KV, Chakraborty S, Rajeswari A, et al. Radiochemistry, pre-clinical studies and first clinical investigation of 90Y-labeled hydroxyapatite (HA) particles prepared utilizing 90Y produced by (n, γ) route. Nucl Med Biol. 2015;42:455–64.

Visuthikosol V, Kumpolpunth S. Intra-articular radioactive colloidal gold (^{198} Au) in the treatment of rheumatoid arthritis. J Med Assoc Thai. 1981;64:419–27.

Voth M, Klett R, Lengsfeld P, Stephan G, Schmid E. Biological dosimetry after yttrium-90 citrate colloid radiosynoviorthesis. Nuklearmedizin. 2006;45: 223–8.

Wang SJ, Lin WY, Hsieh BT, et al. Rhenium-188 sulphur colloid as a radiation synovectomy agent. Eur J Nucl Med. 1995;22:505–7.

Wang SJ, Lin WY, Chen MN, et al. Histologic study of effects of radiation synovectomy with rhenium-188 microspheres. Nucl Med Biol. 2001;28:727–32.

Will R, Laing B, Edelman J, Lovegrove F, Surveyor I. Comparison of two yttrium-90 regimens in inflammatory and osteoarhtropathies. Ann Rheum Dis. 1992;51:262–5.

Wiss DA. Recurrent villonodular synovitis of the knee. Successful treatment with yttrium-90. Clin Orthop Relat Res. 1982;169:139–44.

Wong Y, Cherk MH, Powell A, et al. Efficacy of yttrium-90 synovectomy across a spectrum of arthropathies in an era of improved disease modifying drugs and treatment protocols. Int J Rheum Dis. 2014;17(1):78–83.

Wunderlich G, Pinkert J, Andreeff M, et al. Preparation and biodistribution of rhenium-188 labeled albumin microspheres B 20: a promising new agent for radiotherapy. Appl Radiat Isot. 2000;52:63–8.

Wunderlich G, Drews A, Kotzerke J. A kit for labeling of [^{188}Re] human serum albumin microspheres for therapeutic use in nuclear medicine. Appl Radiat Isot. 2005;62:915–8.

Yarbrough TB, Lee MR, Hornof WJ, et al. Samarium 153-labeled hydroxyapatite microspheres for radiation synovectomy in the horse: a study of the biokinetics, dosimetry, clinical, and morphologic response in normal metacarpophalangeal and metatarsophalangeal joints. Vet Surg. 2000;29:191–9.

Yu J, Häfeli UO, Xia J, et al. Radiolabelling of poly(histidine) derivatized biodegradable microspheres with the ^{188}Re tricarbonyl complex $[^{188}Re(CO)3(H_2O)_3]^+$. Nucl Med Comm. 2005;26:453–8.

Inhibition of Arterial Restenosis Following Balloon Angioplasty

15

15.1 Introduction

The introduction of balloon angioplasty represented the first effective strategy for arterial reflow of vessels obstructed by atheromatous plaque and offered reprieve for many patients who would have encountered morbidity and often mortality and who would not have been candidates for coronary bypass grafting (CABG). These complex atherosclerotic structures inhibit myocardial blood flow and thus significantly reduce the oxygenation required for contraction. They consist of lipids, foam cells, and, in later stages, calcium deposits, resulting from genetic, dietary, and other sequelae. With the vessel lumen held open by the stent framework, the plaque is compressed and reflow established. The first such procedure was performed in Zurich, Switzerland in 1997, and since that time coronary angioplasty and implantation of stent frameworks in patients with unstable angina have become a cornerstone of interventional cardiology. Although even approximate statistics are difficult to identify and although the aggressive use of these interventional procedures has declined, it is well established that several hundred thousand procedures are performed just in the USA annually. In spite of this pivotal advance for care of therapeutic intervention in these patients, however, restenosis of the coronary arteries is still a major issue when vessels are obstructed again in both native vessels treated only by angioplasty and stented arterial segments. In fact, it is common for many patients to have multiple stents deployed in the same vessels after the clinical signs of restenosis are again encountered, and there are even reports of patients in whom over 30 coronary stents have been implanted.

Arterial occlusions before and after angioplasty/stenting reflect two different pathologic processes. The restenosis structure is quite different in composition of the atherosclerotic plaques and consists of smooth muscle cell hyperplasia which is stimulated in response to the vessel damage resulting from the balloon inflation and subsequent stent placement. In terms of adequate flow requirements, this is only an academic difference, since the hyperplastic response still results in reduced blood flow to the heart muscle. The enormous health care costs required for intervention of these patients in conjunction with patient inconvenience are important factors which have stimulated the evaluation of the effectiveness of various methods for the inhibition of the subsequent restenosis which so often observed. Although the early intravenous application of radiation was the first widely acknowledged technology to significantly reduce hyperplasia after angioplasty, the issues associated with the use of radioisotopes in such an environments lead to the development of alternative nonradioactive chemical-based methods. The current standard of care for inhibition of coronary restenosis after angioplasty is thus the deployment of "drug-eluting" stents (DES), such as the sirolimus-eluting "Cypher" and the

F.F. (Russ) Knapp, A. Dash, *Radiopharmaceuticals for Therapy*, DOI 10.1007/978-81-322-2607-9_15

paclitaxel-eluting stents ("Tauxs" stent), which release growth substance inhibitors which inhibit or delay restenosis by inhibiting development of smooth muscle cell hyperplasia.

15.2 Radioisotopes for Intravascular Irradiation (IVRT) of Coronary Vessels

Although the focus of this book is on the use of unsealed radioactive materials for therapy, a brief review of the use of sealed radioactive brachytherapy sources (wires, radioactive stents, etc.) for restenosis therapy is included here as an introduction to the development of the unsealed radioactive source technologies. The first interventional strategy which was effective for restenosis therapy was the use of radioisotopes and related technologies to deliver a sufficient radiation dose to the vessel wall to sterilize those invading cells which release inflammatory substances (chemokines, etc.) which simulate the hyperplastic response as illustrated in Fig. 15.1.

A large number of trials focused on the use of radioactive seeds or sources or even radioactive-coated balloons, and even the intraluminal advance of X-ray generating devices was evaluated in both preclinical studies and clinical trials. Many different radioisotopes decaying by photon, electron, positron, and X-ray emission and various source configurations had been evaluated in both animal models and human trials (Table 15.1). Interesting, even a series of short-lived positron-emitting radioisotopes (^{18}F, ^{68}Ga, ^{11}C, ^{13}N, ^{15}O) had been evaluated for possible effectiveness for restenosis therapy in phantom experiments, and from these studies, ^{68}Ga was selected as the most attractive positron-emitting candidate for this application (Stoll et al. 2001a, b). In addition, the use of other related technologies such as the use of catheter-based X-ray generating devices and photodynamic therapy such as the "PhotoPoint™" device (Waksman et al. 2008) had been evaluated also for vulnerable plaque. Once it had been established in clinical trials that the use of intravascular radiation could effectively inhibit, or at least significantly delay, restenosis, this field moved very quickly with the development, evaluation, and clinical introduction of many different technologies.

15.2.1 Solid Radioactive Sources for Vessel Irradiation

The strategies using sealed radioactive sources, which include various radioactive ribbon coils and seeds, as well as ion-implanted stents and radiation-generating devices, are used under the domain of radiation oncology in conjunction with interventional radiology. The first such radioisotope studies reported—which are discussed in more detail in the next section—for the prevention of restenosis after percutaneous transluminal angioplasty (PTA) used radioactive ^{192}Ir sources for treatment of peripheral vessels (Liermann et al. 1994). One early patent (GE Healthcare) covered the use of low-energy X-ray emitting radioisotopes, such as ^{159}Dy, ^{145}Sm, ^{169}Yb, ^{125}I, and ^{103}Cd (Lewis et al 2006). The radioactive sources are advanced either manually or using HDR afterloader devices. Because under-irradiation stimulates the hyperplastic response, irradiation of the stenoses ends is important, and the overlap of the radioactive source with these sources (5–10 mm) is accomplished to preclude the edge, or the so-called candy wrapper effect, where restenosis occurs at the proximal and distal edges which have not been adequately irradiated (i.e., under-irradiated with insufficient radiation dose), which at least to some extent precludes the effectiveness of the intervention.

15.2.2 Dosimetry of Vessel Wall Irradiation Is an Important Issue

Dosimetry also plays a pivotal role for this therapy since the appropriate radiation dose must be delivered. While over irradiation can cause unintended damage to vessels and surrounding tissue, under-irradiation can actually stimulate the hyperplastic response. Radiation physicists and

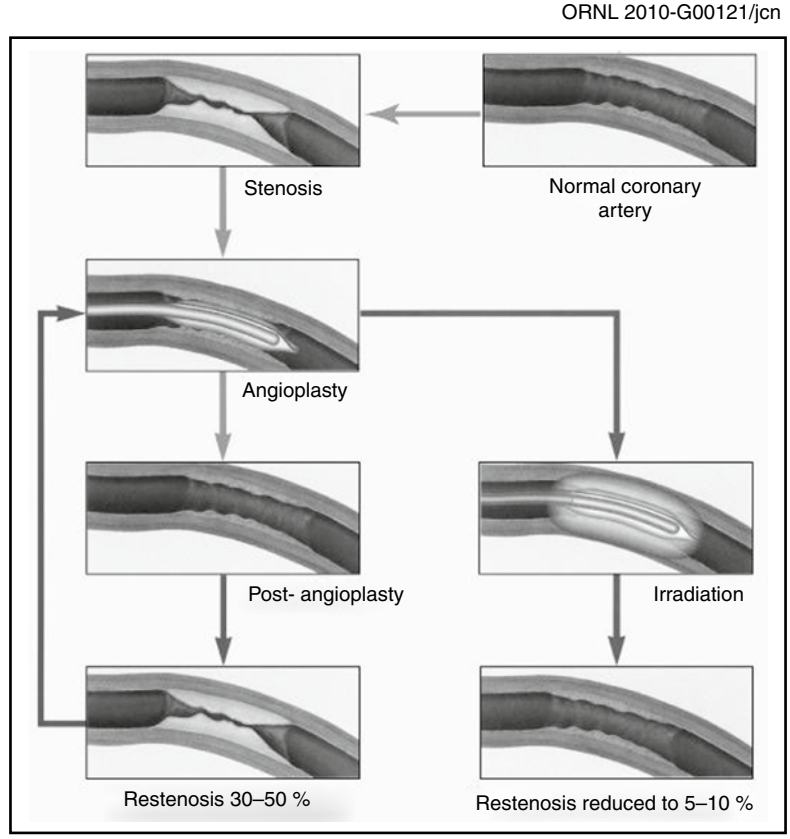

Fig. 15.1 Schematic illustrating the effect of post-PTA irradiation for inhibition of hyperplasia of coronary vessels. Post-balloon angioplasty of coronary stenosis often leads to restenosis resulting from smooth muscle cell hyperplasia resulting from the wound healing response

dosimetrists have thus represented key members of the therapy teams. In addition, dose rate is a key issue, more so for therapy of the coronary vessels, since symptom limited time constraints on vessel occlusion are an important issue. Radioactive catheter-based beta-emitting sources posed serious challenges since the radioactive source must be centered in the lumen. Centering of the source is required because of the rapid dose falloff or decrease of radiation dose with radial distance of the emitted high-energy beta-particles. For this reason, some sophisticated and complex centering strategies were developed, such as a spiral balloon catheter and a CO_2-based centering catheter (Pokrajac et al. 2009). However, liquid-filled balloons offer a convenient self-centering capability requiring no special centering strategy, and routinely available angioplasty balloons can be used for these studies. In this case when liquid-filled balloons are used as the therapeutic intervention, deflation to allow reflow is a common procedure to allow maintenance of adequate oxygenation, and repeated cycling of deflation and re-pressurization/refilling the balloon have been used for delivery of the appropriate prescribed radiation dose to the vessel wall. Although there is some controversy, the target area is the *adventitia*, and the prescribed dose values are within 18–35 Gy. Dose delivery is of course dependent on source "dwell time" (residence time during occlusion) and dose activity. When occlusive radioactive sources are used, as described later for liquid-filled balloons, delivery of the total prescribed radiation dose is often incremental, by removal of the radioactive source and thus permitting reflow during symptom limited periods, with repetitive irradiations until the total prescribed dose has been delivered.

For the coronary vessels, early studies also demonstrated that the use of ^{192}Ir and ^{90}Y seed/wire-based solid sources also worked well for inhibition of hyperplastic cellular response to damage incurred from coronary balloon

Table 15.1 Examples of radioactive solid source strategies which have been evaluated for the transluminal vessel wall therapy for inhibition of arterial restenosis

Radioisotope	$T_{1/2}$: principal therapeutic radiation	Chemical form	Treatment focus	Reference
Solid sources, wires, seeds, etc.: sealed sources/radiation oncology				
Beta/gamma-emitting sources				
Cerium-144	284 days 0.318 MeV	Wire source	30 patients: in-stent restenosis	Bonvini et al. (2003)
Cobalt-55	17.53 h 17.5 h		10 patients	Cervinka et al. (2004)
Holmium-166	26.8 h 1.854 MeV	Coated balloon	Porcine restenosis study	
Iridium-192	74.02 days 316 keV	Wire sources Cordis/best		
Phosphoru-32	14.29 days 1.71 MeV	Coated balloon/catheter Stent: Guidant Wire	Rabbit ileal model 32 patients 332 patients	Herlein et al. (2000) Waksman et al. (2000, 2001)
Rhenium-186	90.64 h 1.076 MeV	Stents		
Rhenium-188	16.9 h 2.12 MeV β_{max}	Coated balloon Self-expanding stent	Sheep model Labeling/stability	Nowak et al. (2001)
Strontium-90 / Yttrium-90	28.6 years 2.283 MeV (from ^{90}Y)	Ribbon, coil: Novoste		
Tungsten-188	69 days 2.12 MeV (from ^{188}Re)	Wire coil "WRIST" study	30 patients: in-stent restenosis	Dilcher et al. (2005)
Yttrium-90	64.1 h 2.283 MeV	Solid source with afterloader	23 swine	Waksman et al. 2000
Xenon-133	5.245 days 0.346 MeV	Gas-filled balloon	Porcine model	

angioplasty. These strategies were based on localized catheter-based delivery of high beta and gamma radiation (Waksman et al. 2001). Use of $^{188}W/^{188}Re$ wire sources for inhibition of coronary restenosis was also evaluated as an interesting candidate for restenosis therapy (Schaart et al. 2002). The ^{188}W decays in situ to the high beta-energy emitting ^{188}Re daughter (see Chap. 7), available from decay of the long-lived reactor-produced ^{188}W parent ($T_{1/2}$ 69 days) (Chap. 5). The use ^{188}Re as a liquid source separated from ^{188}W is described later as a key example of use of radioactive liquid-filled balloons (Sect. 15.2.3).

However, because of the issue of unsymmetrical dose delivery to the vessel wall because of difficulty in centering such sources within the lumen, other self-centering strategies were evaluated which included the use of ^{32}P-coated angioplasty balloons. However, because the exact balloon dimensions required for dilatation are not defined until angioplasty is conducted, maintenance of a spectrum of ^{32}P-coated balloons in advance was a serious disadvantage. The potential use of intracoronary ^{188}Re-labeled stents had also been evaluated (Dinkelborg et al. 2000) and using chelating microfilms (Zamora et al. 2000), but no further reports using these various technique have been published because of the cumbersome requirement for in-house radiolabeling after stent selection following PCTA and the challenges to accurately adjust the activity prescription for optimal radiation dose delivery. Of relevance to the present discussion is the use of radioactive liquid-filled balloons for restenosis therapy, since these

substances are prepared and handled in the nuclear medicine facilities and represent unsealed sources. Generally, following placement of the therapy balloon, the radioactive solution is filled by a nuclear medicine physician. Table 15.2 summarizes information on several key liquid-filled systems which have been evaluated for therapy of the coronary arteries following balloon angioplasty.

15.2.3 Radioactive Liquid-Filled Balloons for Vessel Wall Irradiation

Because of the technical issues associated with optimal source centering, the negative ramifications of rapid radiation dose decrease with radial distance and the effects of overdosing of normal tissue and underdosing of target cells, the development of inherently self-centering liquid-filled balloons was recommended (Knapp et al. 1997a, b, 1998b; 1999a, b, 2001; Weinberger et al. 1999; Weinberger and Knapp 1999) which is initially evaluated using ^{188}Re and later with other candidate (Table 15.2).

The use of ^{188}Re-liquid-filled balloons was envisioned as the most promising approach for uniform vessel wall irradiation, because of in-house availability from the ^{188}W/^{188}Re generator (see Chap. 7), rapid urinary excretion of released chemical species via the urinary bladder, excellent radionuclide properties (half-life, beta radiation, etc.), and optimal radiation dose delivery of liquid-filled balloons. For these reasons, ^{188}Re rapidly gained broad interest and progressed to a large number of clinical trials which demonstrated the simplicity and effectiveness of this technique (Table 15.3). Most reported clinical coronary restenosis therapy studies with liquid-filled balloons have used ^{188}Re, and this technique allows uniform vessel wall irradiation and represents use of an "unsealed radioactive source," which is thus in the nuclear medicine domain, and the studies are conducted in conjunction with interventional cardiologists (Knapp et al. 1997a, b, 1998b, 1999a, b, 2001; Weinberger and Knapp 1999; 2002). The strategy for use of intra-vessel

Table 15.2 Examples of developmental studies with radioactive liquid-filled balloon strategies which have been evaluated for the transluminal vessel wall therapy for inhibition of arterial restenosis used in nuclear medicine/interventional cardiology

Radioisotope	$T_{1/2}$: principal therapeutic radiation	Chemical form	Treatment focus	Reference
Liquid-filled balloons: unsealed sources/nuclear medicine				
Gallium-68	68 min Positron	$GaCl_3$	Coronaries Animals	Stoll et al. (2001a, b)
Holmium-166	26.8 h Beta	DTPA Ethylene dicysteine complex (EC)	Rat excretion	Chakroborthy et al. (2001)
Phosphorus-32	14.3 d Beta,	Sodium phosphate/ NaCl	Animal urinary secretion Rabbits Rabbits/dosimetry Rabbits/in-stent	Walichiewicz et al. (2003, 2004) Wilczek et al. (2002)
Rhenium-186	90.6 h Beta,	Perrhenate	Dosimetry	McGoron et al. 1999
Rhenium-188	16.9 h Beta,	EC complex Perrhenate Perr/MAG3?DTPA	Excretion study Gel dosimeter Dosimetry Rats/excretion	Das et al. (2000, 2001) Wuu et al. (2002, 2003) Lin et al. (2000a, b)
Samarium-153	46.7 h Beta, 0.704 MeV	Liquid	Rabbits Histopathology	Moura et al. (2001)

Table 15.3 Examples of nuclear medicine/interventional cardiology teaming clinical studies with ^{188}Re-liquid-filled balloons for prevention of arterial restenosis after PTCA

^{188}Re agent	Study acronym	Patient population	Dose prescription	Follow-up	Reference
DTPA		30 patients		3 years	Kim et al. (2004, 2005)
EC		187 patients		3 years	Kim et al. (2004)
MAG3		30 patients 50 patients		2 years N/A	Hong et al. (2003a, b)
Perrhenate	POBA TRIPPER-1 DRAIN DIRRT	40 and 15 patients 113 patients 40 patients	15 and 20 Gy at 0.5 mm Nonrandomized 22.5 Gy at 0.5 mm 14 Gy at 0.5 mm	6 months 6 months	Hang et al. (2003a, b) Hoher et al. (2003) Reynen et al. (2004, 2006)

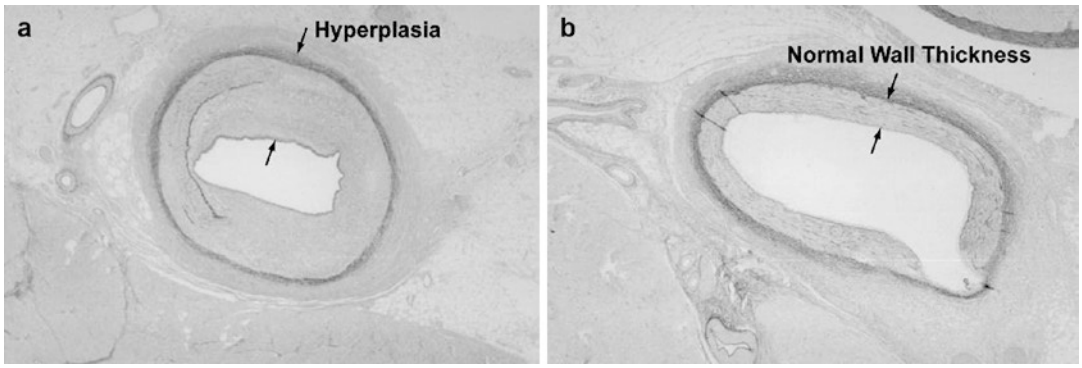

Fig. 15.2 Effectiveness of post-vessel damage irradiation with ^{188}Re in swine model coronary overstretch model (Figure from authors: RK)

radioactive sources to inhibit the hyperplastic response from vessel damage from Percutaneous Coronary Transluminal Angioplasty (PCTA) is illustrated in Fig. 15.2 and is based on the delivery of sufficient radiation (i.e., 25–30 Gy to 0.5 mm) to inhibit the release of substances which would stimulate hyperplasia as a wound healing response to the vessel damage. Use of radioactive liquid-filled balloons is a special approach designed to minimize inhomogeneous vessel irradiation. Figure 15.3 illustrates the effective results of the first animal study using ^{188}Re-liquid-filled balloons.

Because of the rapid falloff of high-energy beta penetration with radial distance, the use of self-centering ^{188}Re-liquid-filled balloons for coronary restenosis therapy was proposed as an alternative for uniform regional radiation dose delivery (Knapp et al. 1997a, 2001) and was first developed at ORNL initially in conjunction with Columbia University and the Cedars-Sinai Hospital in Los Angeles (Knapp et al. 1997a, b, 1998b, 1999a, b, 2001; Eigler et al. 1998; Weinberger and Knapp 1999, 2002; Weinberger et al. 1999). In addition to its on-demand availability from an efficient generator system (Chap. 7) that has a long useful shelf life of several months and the emission of beta-particles with sufficiently high energy to penetrate the vessel wall to the *adventitia*, another unique advantage of ^{188}Re is the rapid renal excretion of perrhenate, MAG3, and DTPA, in the unlikely event of balloon rupture (Lin et al. 2000a, b; Kim et al. 2004, 2005; Knapp et al. 1997b). Early clinical studies with the ^{188}Re-liquid-filled balloon

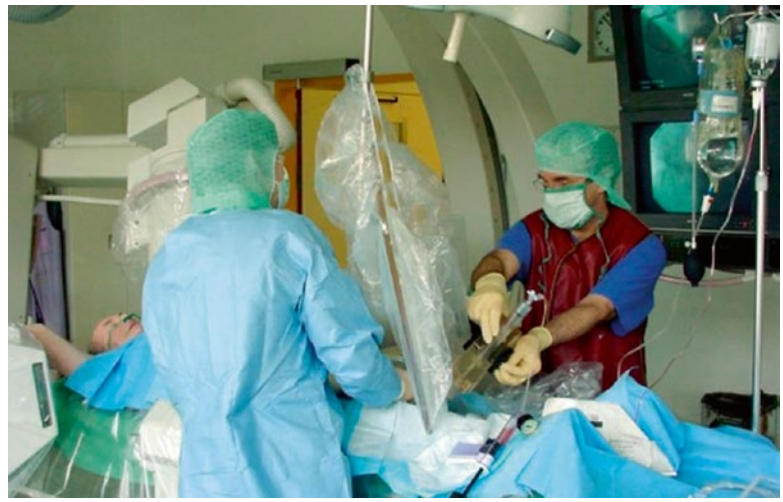

Fig. 15.3 Use of a ^{188}Re delivery device in the catheter laboratory during the DRAIN study. ISAT: isotope (^{188}Re) storage and transfer unit

approach had evaluated this issue and demonstrated rapid urinary excretion (Hausleiter et al. 1999, 2001). There is thus a very high safety margin from a radiological perspective for potential skeletal accumulation of radioactivity and possible marrow suppression which is precluded by the use of ^{188}Re.

One concern was the ramifications of unlikely balloon rupture, although the incidence of balloon rupture is probably <1 in 10,000. Various ^{188}Re chemical species which included DTPA, MAG3, and perrhenate were evaluated identifying those agents which exhibit rapid renal clearance (Table 15.2). The ^{188}Re-DTPA and –MAG3 agents were prepared by well-defined procedures documented for preparation of the ^{99m}Tc-labeled analogs and the Na ^{188}Re–perrhenate is directly obtained by saline elution of the ^{188}W/^{188}Re generator system (Knapp et al. 1998b). The use of sodium ^{188}Re–perrhente for balloon filling was initially evaluated. Animal studies demonstrated rapid renal clearance of the ^{188}Re chemical species which would occur as a result of balloon rupture (Knapp et al. 1998b; Lin et al. 2000a, b). A computer program using Visual Basic software was developed (Stabin et al. 2000) for use to estimate the vessel dwell time based on the ^{188}Re activity concentration (mCi/mL) required for delivery of the prescribed vessel wall radiation dose at a specific tissue depth, based on the vessel anatomy, balloon dimensions. A number of preclinical and clinical studies clearly demonstrated that this technique is physically feasible, readily accessible in the catheterization laboratory, and effective in reducing the incidence of coronary restenosis. In Table 15.3, the details of clinical trials which have been reported with ^{188}Re for coronary restenosis are summarized.

15.3 Examples of Clinical Trials with ^{188}Re-Filled Balloon Sources

As described in Table 15.3, there have been a significant number of clinical trials evaluating the effectiveness of the radioactive liquid-filled balloon technology using ^{188}Re for inhibition of coronary restenosis after balloon angioplasty. The combined results—except in cases where there is improper balloon length or balloon position over the lesion—were not optimal, and a significant reduction in restenosis was observed. There are two key examples of two clinical trials reporting the use of ^{188}Re-liquid-filled balloons for inhibition of arterial restenosis following PTA. In general, intracoronary radiotherapy (IRT) with ß$^-$ and γ-emitting radioisotopes designed as sealed sources has been shown to reduce the rate of restenosis after percutaneous coronary interventions (PCI) and to have a beneficial effect on the clinical outcome of these

patients (Grise et al. 2002). A variety of studies (Table 15.3) were designed to determine whether IRT using radionuclide-liquid-filled balloons is also able to achieve this aim.

15.3.1 The SPARE Trial

In this context, the results of two large clinical studies have been published using the radioisotope-filled balloon system. Because of sustained platelet activation following the vessel damage, long-term IIa/IIB antiplatelet receptor therapy with chlorpedigril is required. These include the *S*eoul National University *P*ost-*A*ngioplasty *Rh*E*n*ium irradiation (SPARE) and the *D*resden prospective, *RA*ndomized, placebo-controlled, double-blind, *IN*-stent restenosis trial (DRAIN). Both systems use the easy-to-handle, self-centering ^{188}Re-liquid-filled standard PTCA balloon either as perrhenate (DRAIN) or ^{188}Re-labeled DTPA (SPARE). Symptomatic patients for CAD (SPARE = 218 and DRAIN = 210) had a mean age of 62 years (253 male, 167 female) with either de novo (re)stenosis or in-stent restenosis and underwent IRT or a sham procedure (SHP) in DRAIN or were case controlled in the SPARE trial. In DRAIN, 180 patients (89 %) had a 6-month quantitative angiographic follow-up, and a subsequent 1-year follow-up was performed in 109 patients. After routine re-PTCA, a second standard balloon was placed into the PTCA area 5 mm longer at each end than the first balloon and filled with ß-emitting liquid ^{188}Re at 3 atm of pressure. Geographical miss was carefully avoided. An irradiation time of 400 ± 122 s (range 240–890 s) to achieve a dose of 30 Gy at 0.5 mm depth of the vessel wall was estimated to be sufficient to suppress the growth of smooth muscle and endothelial cells, which are considered as being primarily responsible for restenosis. In SPARE 190 (87 %) patients had up to 2-year angiographic follow-up. All patients had long-term strong dual antiplatelet therapy after IRT of at least 1 year (Krötz et al. 2002). All procedures were performed successfully and without any problems (Fig. 15.4), and long-term follow-up data have been obtained in most patient studies.

15.3.2 The DRAIN Study

A DRAIN pilot study (Reynen et al. 2004) was conducted consisting of 45 patients separated into two groups. In the first group, 25 patients received only IRT, and in the second group, 20 patients received IRT and a new stent. The restenosis rate in the second group was 63 % compared to the expected rate of 60 %, whereas the rate in the first group was 20 % ($p < 0.03$), which is in agreement with other studies (Cheneau et al. 2003). Therefore, DRAIN IRT and a new stent were avoided in the following randomized study. Almost the same result was found in SPARE by angiography, target lesion revascularization (TLR) and major adverse cardiac event (MACE) in up to 2-year follow-ups. In the DRAIN randomized study, two episodes of stent thrombosis with subsequent MI occurred in follow-up (after 6 days in SHP; after 8 months in IRT). Overall restenosis rate was 35 %, 19/78 (24 %) in IRT and 31/78 (40 %) in SHP ($p < 0.04$). There was no preferred location of the restenosis. Mean diameter stenosis amounted to 44 ± 21 % in IRT and 52 ± 22 % in SHP ($p = 0.02$). The late lumen loss index was 0.29 ± 0.48 in IRT and 0.44 ± 0.44 in SHP ($p = 0.04$). At 1-year clinical follow-up, MACE [death, myocardial infarction (MI), target vessel revascularization (TVR)] occurred in 32 patients more frequently in the SHP group ($p < 0.05$). Overall event-free survival was 87 % in IRT and 74 % in SHP ($p < 0.05$). All other parameters were not significantly different in both groups, but diabetes was even more frequent in IRT patients (44 % vs. 27 %).

In the Seoul study, the overall restenosis rate was 44.6 % in the control group and 21.8 % in the IRT group ($p < 0.001$) at a 2-year follow-up. However, only in the in-stent restenosis group were TVR and MACE reduced significantly ($p < 0.03$), whereas in the other groups (de novo and restenosis), these parameters were not statistically different.

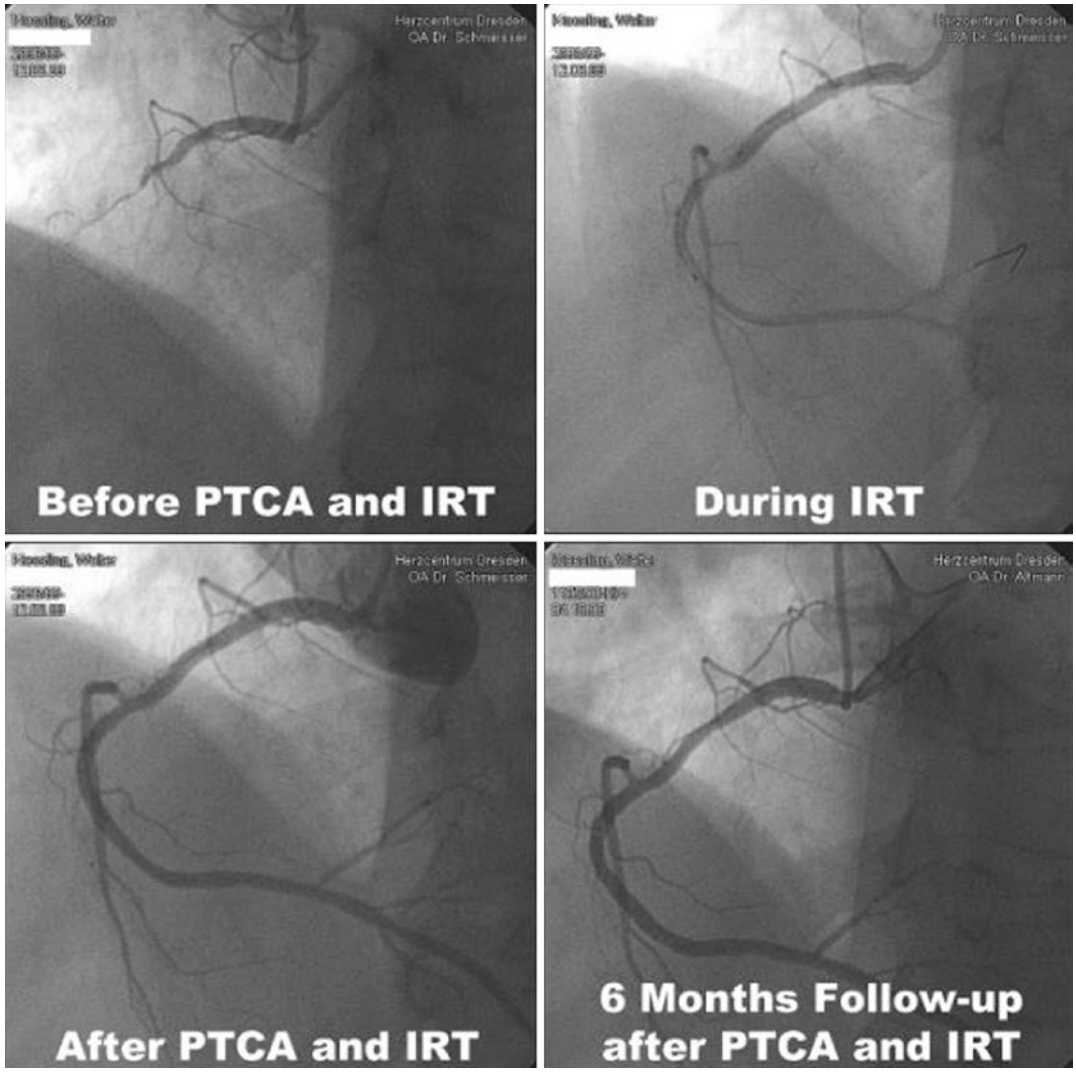

Fig. 15.4 The DRAIN study—*left*—angiogram prior to PCI of in-stent restenosis and IRT; *right*, angiogram 6 months after PCI and IRT (Figure from authors: JK)

These combined studies have clearly demonstrated that in intracoronary radiation therapy using the liquid-filled balloon approach, ß⁻-emitting ^{188}Re is an easy-to-perform, inexpensive, safe, and effective option to prevent re-restenosis in cases of (re)stenosis. It is now generally accepted from meta-analysis that only patients with in-stent restenosis seem to benefit clinically from the procedure during long-term follow-up if MACE (death, MI, TLR, TVR) is considered as endpoints. Data vary in more complex cases in diabetic patients and patients presenting with ostial lesions.

15.4 Radioisotopes for IVRT of the Peripheral Vessels

As discussed earlier, pioneering studies using ^{192}Ir for inhibition of restenosis of the peripheral vessels showed that vessel wall irradiation could prevent restenosis (Schopohl et al. 1996). Late acute thrombotic occlusion (LATO) was also observed similar to observations following coronary irradiation discussed earlier. The results of a larger four-arm study which included 204 randomized patients demonstrated that significant

LATO was only observed in that patients who had stent placement and additional irradiation despite effective antiplatelet medication (Bonvini et al. 2003). Only four patients (16 %) with IVRT showed impaired flow and thus required femoropopliteal arterial target lesion revascularization (Schopohl et al. 1996). The use of ^{188}Re-liquid-filled balloons intraluminal treatment of peripheral vessels with radioactive sources is the earliest example of intravascular radiation therapy to prevent restenosis after PTCA. Initial results were first published by investigators in Germany (Liermann et al. 1994), demonstrating that vessel wall irradiation could prevent restenosis in all but only four patients. In 1996 the same group reported their experience over a 6-year period (Schopohl et al. 1996). Similar to observations following coronary irradiation some years later, late acute thrombotic occlusion (LATO) was observed as a major problem of this therapeutic approach. In a large four-arm randomized study (Bonvini et al. 2003) which included 204 patients, LATO occurred significantly only in patients with stenting and additional irradiation despite effective antiplatelet medication. Only four (16 %) of 25 patients treated with IRT in femoropopliteal arteries showed impaired flow and required target lesion revascularization.

15.5 Use of ^{188}Re Balloons for IVRT of the Peripheral Vessels

Because of large dimensions of femoropopliteal and related vessels of the leg, stents are very large, and restenosis inhibition is unpredictable, and incomplete results using DES for these vessels represented an opportunity to further explore the unique application of the self-centering ^{188}Re-liquid-filled balloon approach. This approach for therapy of the peripheral vessels with ^{188}Re has been demonstrated using a device developed by ITM Flow Medical in Germany (ITM Rhenium-PTA). This system was developed for both intracoronary and peripheral vessel radionuclide therapy. The first results using ^{188}Re in the peripheral vessels were encouraging and demonstrated a 13.6 % restenosis rate after a follow-up period of 16 months. In the meantime, ITM obtained approval for this system, which represents the first instance of approval of an intravascular radionuclide therapy method which is reimbursable, at least in Europe. These seminal trials were first reported using ^{188}Re-liquid-filled balloons during the 1996–2002 period and have been further extended in trials focusing on the post-PTA treatment of peripheral vessels (Wohlgemuth et al. 2008). The percutaneous transluminal angioplasty device filled with ^{188}Re developed by ITM Munich for both rhenium PTA and PTCA received full conversion electrons (CE) certification and approvals in September 2008. More recent papers have further demonstrated the effectiveness of using this approach for restenosis therapy of the peripheral arteries (Leissner et al. 2011; Wohlgemuth et al. 2008, 2010).

15.6 Other Therapeutic Applications of ^{188}Re-Liquid-Filled Balloons

The use of ^{188}Re-filled balloons for therapeutic treatment where access is available has also recently been extended to the treatment of esophageal strictures (Kim et al. 2008). Treatment of recurrent urethral strictures in five patients with ^{188}Re-MAG-liquid-filled balloon dilatation has also proved feasible. The use of ^{188}Re-liquid-filled balloons for endovascular brachytherapy for treatment of recurrent renal artery stenosis was also evaluated (Kotzerke et al. 2002).

15.7 Summary

Although radioisotope methods such as with ^{188}Re-liquid-filled balloons are very effective, the use of such radioisotopic strategies for post-PTCA therapy of the coronary vessels quickly decreased with the introduction and quickly established efficacy of drug-eluting stents. However, as more data from more diverse patient populations have become available, with restenosis rates often approaching those reported for

radioisotope methods, interest in the use of radioisotopes for the acute treatment of arterial stenosis may be expected to be re-explored for comparison with the chronic therapeutic approach. Conceivably, such strategies could be used for delivery of radiation to many tumors which are accessible, such as postsurgical voids for remnant cell killing following resectioning of brain and breast tumors and other solid tumor malignancies. The current status is the use of the ^{188}Re-liquid-filled balloon approach for treatment of peripheral vessels following balloon intervention. This technology has received a "C Mark" in Germany and is quite effective, and time will tell if broader use of this technology will evolve.

References

Bonvini R, Baumgartner I, Do DD, et al. Late acute thrombotic occlusion after endovascular brachytherapy and stenting of femoropopliteal arteries. J Am Coll Cardiol. 2003;41:409–12.

Cervinka P, St'ásek J, Costa MA, et al. The "edge effect" after implantation of beta-emitting (^{55}Co) stents with high initial activity. Acta Medica (Hradec Kralove). 2004;47(1):37–42.

Chakroborthy S, Unni PR, Banerjee S, et al. Potential ^{166}Ho radiopharmaceuticals for intravascular radiation therapy (IVRT)-1: [^{166}Ho] holmium labeled ethylene dicysteine. Bucl Med Biol. 2001;28(3):309–17.

Cheneau E, Wu Z, Leborgne L, Ajani AE, et al. Additional stenting promotes intimal proliferation and compromises the results of intravascular radiation therapy: an intravascular ultrasound study. Am Heart J. 2003;146(1):142–5.

Das T, Banerjee S, Samuel G, et al. ^{188}Re-ethylene dicysteine: a novel agent for possible use in endovascular radiation therapy. Nucl Med Commun. 2000;21(10):939–45.

Das T, Banerjee S, Samuel G, et al. [^{186,188}Re]-Rhenium ethylene dicysteine (Re-EC): preparation and evaluation for possible use in endovascular brachytherapy. Nucl Med Biol. 2001;27:189–97.

Dilcher C, Satler LF, Pichard AD. Intracoronary radiation therapy using a novel beta emitter for in-stent restenosis Tungsten WRIST. Cardiovasc Revasc Med. 2005;6(2):52–7.

Dinkelborg LM, Tepe G, Noll B, et al. ^{186}Re-labeled stents for prophylaxis of restenosis: first animal results. J Nucl Med. 2000;41(Suppl):7P.

Eigler N, Whiting J, Chernomorsky A, et al. RADIANT™ liquid isotope intravascular radiation therapy system. In: Proceedings, second annual symposium on radiotherapy to reduce restenosis. Sponsored by Scripps Clinic and Research Foundation, La Jolla, January 16–17, 1998.

Grise MA, Massullo V, Jani S, et al. Five-year clinical follow-up after intracoronary radiation. Circulation. 2002;105:2737–40.

Hang CL, Fu M, Hsieh BT, et al. Intracoronary beta-irradiation with liquid rhenium-188 to prevent restenosis following pure balloon angioplasty: results from the TRIPPER-1 study. Chang Gung Med J. 2003a;26:98–106.

Hang CL, Fu M, Hsieh BT, et al. Intracoronary beta-irradiation with liquid rhenium-188: results of the Taiwan radiation in prevention of post-pure balloon angioplasty restenosis study. Chest. 2003b;124:1284–93.

Hausleiter J, Li A, Knapp R, Eigler N, Whiting J. Low body exposure in cases of radioactive balloon leakage – a biodistribution and elimination study of rhenium-188 in pigs. J Amer Coll Cardiol. 1999;33(Suppl. A):4A.

Hausleiter J, Li A, Makkar R, Berman D, et al. Leakage of a liquid ^{188}Re-filled balloon system during intracoronary brachytherapy. A case report. Cardiovasc Radiat Med. 2001;2:7–10.

Herlein C, Kovacs A, Wolf GK, et al. A novel balloon angioplasty catheter impregnated with beta-particle emitting radioisotopes for vascular brachytherapy to prevent restenosis. Eur Heart J. 2000;21:2056–62.

Hoher M, Wohrle J, Wohlfrom M, et al. Intracoronary beta-irradiation with rhenium-188-filled balloon catheter: a randomized trial in patients with *de novo* and restenotic lesions. Circulation. 2003;107:3022–7.

Hong MK, Park SW, Moon DH, et al. Extra-stent vascular remodeling in in-stent restenosis after ^{188}Re-MAG3 radiation therapy. Int J Cardiol. 2003a;92:187–91.

Hong MK, Park SW, Moon DH, et al. Intravascular ultrasound analysis of nonstented adjacent segments in diffuse in-stent restenosis treated with radiation therapy with a rhenium-188-filled balloon. Cather Cardiovasc Interven. 2003b;58:428–33.

Kim KI, Bae J, Kang HJ, et al. Three-year clinical follow-up results of intracoronary radiation therapy using a rhenium-188 DTPA-filled balloon system. Circ J. 2004;68:532–7.

Kim K, Bae J, Koo BK, et al. Long-term clinical outcomes of dissections after intracoronary beta-radiation with rhenium-188-diethylenetraimminepentaacetic acid-filled balloon system. Int J Cardiol. 2005;104:190–6.

Kim JH, Shin JH, Song H-Y, et al. Liquid ^{188}Re-filled balloon dilation for the treatment of refractory benign airway strictures: preliminary experience. J Vasc Radiol. 2008;19:406–11.

Knapp FF Jr, Guhlke S, Beets AL, et al. Rhenium-188 – attractive properties for intravascular brachytherapy for inhibition of coronary restenosis after PTCA. J Nucl Cardiol. 1997a;4:S-118.

Knapp Jr FF, Guhlke S, Beets AL, et al. Intraarterial irradiation with rhenium-188 for inhibition of restenosis

after PTCA – strategy and evaluation of species for rapid urinary excretion. J Nucl Med. 1997b;38:124P.

Knapp Jr FF. Rhenium-188 – a generator-derived radioisotope for cancer therapy. Can Biother Radiopharm. 1998;13:337–49.

Knapp FF Jr, Beets AL, Guhlke S, et al. Rhenium-188 liquid-filled balloons effectively inhibit restenosis in a swine coronary overstretch model – a simple new method bridging nuclear medicine and interventional cardiology. J Nucl Med. 1998b;39:48P.

Knapp FF Jr, Beets AL, Mirzadeh S, Guhlke S. Use of a new tandem cation/anion exchange system with clinical-scale generators provides high specific volume solutions of technetium-99m and rhenium-188. In: Proceedings, international trends in radiopharmaceuticals for diagnosis and therapy, Lisbon, Portugal, March 30–April 3, 1998; 1998b.

Knapp Jr FF, Guhlke S, Beets AL, et al. Endovascular beta irradiation for prevention of restenosis using solution radioisotopes: pharmacologic and dosimetric properties of rhenium-188 compounds. Cardiovasc Rad Med. 1999;1:86–97.

Knapp FF Jr, Spencer RH, Stabin M. Use of rhenium-188 liquid-filled balloons for inhibition of coronary restenosis after PTCA – a new opportunity for nuclear medicine. In: Radionuclides for myocardium - current status and future aspects. Mediterra-Publishers, Athens, Greece; 1999b. p. 61–72 (ISBN 960-85227-9-X).

Knapp Jr FF, Spencer R, Kropp J. Intravascular radiation therapy with radioactive liquid-filled balloons for inhibition of restenosis after angioplasty – a new opportunity for nuclear medicine. J Nucl Med. 2001;42:1384–7.

Kotzerke J, Gabelmann J, Hanke H. Recurrent renal artery stenosis – endovascular brachytherapy with a rhenium-188 filled balloon catheter. Rofo Fortschr Geg Rontgentr Neuen Bildgeb Verfahr. 2002;174:1176–178 (German).

Krötz F, Schiele TM, Zahler S, et al. Sustained platelet activation following intracoronary beta irradiation. Am J Cardiol. 2002;90:1381–4.

Leissner GG, Wengenmair H, Sciuk J, et al. Endovascular brachytherapy (EVBT) with Rhenium-188 for restenosis prophylaxis after angioplasty of infrainguinal lesions: early experience. Rofo. 2011;183(8):735–42 (in German).

Lewis DM, Dollimore LA, Powell N, et al. Apparatus and methods for radiotherapy. US Patent 7011619; 2006.

Liermann D, Bottcher HD, Kollath J, et al. Prophylactic endovascular radiotherapy to prevent intimal hyperplasia after stent implantation in femoropopliteal arteries. Cardiovasc Intervent Radiol. 1994;17:12–6.

Lin WY, Tsai SC, Hsieh BT, et al. Evaluation of three rhenium-188 candidates for intravascular radiation therapy with liquid-filled balloons to prevent restenosis. J Nucl Cardiol. 2000a;7(1):37–42.

Lin WY, Hsieh JF, Tsai SC, et al. A comprehensive study of thyroid and gastric uptake of ^{188}Re-perrhenate in endovascular irradiation using liquid-filled balloons to prevent restenosis. Nucl Med Biol. 2000b;27:83–7.

McGoron AJ, Kassing WM, Thomas SR, et al. Intravascular irradiation using Re-186 liquid-filled balloon catheters: correlation between experimental and theoretical studies. Cardiovasc Radiat Med. 1999;1(4):368–75.

Moura A, Yamada A, Hauer D, et al. Samarium-153 for intravascular irradiation therapy with liquid-filled balloons to prevent restenosis: acute and long term results in hypercholesterolemic rabbit restenosis model. Cardiovasc Radiat Med. 2001;2(2):69–74.

Nowak B, Meyer JMA, Goergen T, et al. Dosimetry of a ^{188}Rhenium-labeled self-expanding stent for endovascular brachytherapy in peripheral arteries. Cardiovasc Rad Med. 2001;2:246–53.

Pokrajac B, Kirisits C, Schmid R, et al. Beta endovascular brachytherapy using CO_2-filled centering catheter for treatment of recurrent superficial femoropopliteal artery disease. Cardiovasc Revasc Med. 2009;10(3):162–5.

Reynen K, Kockeritz U, Kropp J, et al. Intracoronary radiotherapy with a Re-188 liquid-filled PTCA balloon system in in-stent restenosis: acute and long-term angiographic results, as well as 1-year clinical follow-up. Int J Cardiol. 2004;95:29–34.

Reynen K, Kropp J, Koeckerits U, et al. Intracoronary radiotherapy with a ^{188}Rhenium liquid-filled angioplasty balloon system in In-stent restenosis: a single-center, prospective, randomized, placebo-controlled, double-blind evaluation. Coron Artery Dis. 2006;17:371–7.

Schaart DR, Bos AJ, Winkelman AJ, Clarijs MC. The radial depth-dose distribution of a ^{188}W/^{188}Re beta line source measured with novel, ultra-thin TLDs in a PMMA phantom: comparison with Monte Carlo simulations. Phys Med Biol. 2002;47:3605–27.

Schopohl B, Liermann D, Jülling L, et al. Ir-192 endovascular brachytherapy for avoidance of intimal hyperplasia after percutaneous transluminal angioplasty and stent implantation in peripheral vessels: 6 years of experience. Int J Radiation Oncology Biol Phys. 1996;36:835–40.

Stabin MG, Konijnenberg M, Knapp Jr FF, Spencer RH. Monte Carlo modeling of radiation dose distributions in intravascular radiation therapy. Med Phys. 2000;27:1088–92.

Stoll H-P, Hutchins GD, Winkle WL, Nguyen AT, Hou D, Appledorn CR, Romeike B, March KL. Liquid-filled balloon brachytherapy with ^{68}Ga is effective and safe because of the short 60-minute half-life. Circulation. 2001a;103:1793–8.

Stoll HP, Hutchins GD, Winkle WL, et al. Advantages of short-lived positron-emitting radioisotopes for intracoronary radiation therapy with liquid-filled balloons to prevent restenosis. J Nucl Med. 2001b;42(9):1375–82.

Waksman R, Bhargava B, Saucedo JF, et al. Yttrium-90 delivered via a centering catheter and afterloader, given both before and after stent implantation, inhibits neointima formation in porcine coronary arteries. Cardiovasc Radiat Med. 2000;2(1):11–7.

Waksman R, Ajani AE, White RL, et al. Two-year follow-up after beta and gamma intracoronary radiation

therapy for patients with diffuse in-stent restenosis. Am J Cardiol. 2001;88:425–8.

Waksman R, McEwan PE, Moore TI, et al. PhotoPoint photodynamic therapy promotes stabilization of atherosclerotic plaques and inhibits plaque progression. J Am Coll Cardiol. 2008;52(12):1024–32.

Walichiewicz S, Petelenz B, Wilczek K, et al. ^{32}P liquid sources – comparison of the effectiveness of postangioplasty versus poststenting intravascular brachytherapy in hypercholesterolemic rabbits. Adjunctly implanted titanium stent does not attenuate the effect of endovascular irradiation. Cardiovasc Radiat Med. 2003;4(2):64–8.

Walichiewicz S, Wilczek K, Petelenz B, et al. Postdilation intravascular brachytherapy trials on hypercholesterolemic rabbits using ^{32}P-phosphate solution in angioplasty balloons. Cardiovasc Intervent Radiol. 2004;27(1):42–50.

Weinberger J, Knapp Jr FF. Use of liquid-filled balloons for coronary irradiation, Chapter 45. In: Waksman R, editor. Vascular brachytherapy. 2nd ed. Armonk: Futura Publishing Co., Inc.; 1999. p. 521–35. ISBN 0-87993-4131.

Weinberger J, Knapp Jr FF. Use of liquid-filled balloons for coronary irradiation. In: Waksman R, editor. Vascular brachytherapy. 3rd ed. Armonk: Futura Publishing Co., Inc.; 2002. p. 753–90.

Weinberger J, Giedd KN, Simon AD, et al. Radioactive beta-emitting solution-filled balloon treatment prevents porcine coronary restenosis. Cardiovasc Rad Med. 1999;1:252–6.

Wilczek K, Walichiewicz S, Petelenz B, et al. Poststenting intravascular brachytherapy trials on hypercholesterolemic rabbits using ^{32}P liquid sources: implications for prevention of in-stent restenosis. Cardiovasc Intervent Radiol. 2002;25(4):307–13.

Wohlgemuth WA, Leissner G, Wegenmair H, et al. Endovascular brachytherapy in the femoropopliteal segment using ^{192}Ir and ^{188}Re. Cardiovasc Intervent Radiol. 2008;31:698–708.

Wohlgemuth WA, Leissner G, Wengenmair H, et al. Endovascular brachytherapy with (192)Ir and (188)Re to treat de novo and recurrent infrainguinal restenoses. J Cardiovasc Surg (Torino). 2010;51(4):573–8.

Wuu CA, Schiff PB, Marylanski M, et al. 3D Dosimetry study of ^{188}Re liquid balloon for intravascular brachytherapy using bang polymer gel dosimeters. Radiat Prot Dosimetry. 2002;99:397–400.

Wuu CS, Schiff P, Maryanski MJ, et al. Dosimetry study of Re-188 liquid-filled balloon for intravascular brachytherapy using polymer gel dosimeters and laser-beam optical CT scanner. Med Phys. 2003;30:132–7.

Zamora PO, Osaki S, Som P, et al. Radiolabeling brachytherapy sources with Re-188 through chelating microfilms: stents. J Biomed Mater Res. 2000;53(3):244–51.

Part V

Looking Ahead: New Radiopharmaceutical Strategies for Therapeutic Applications

16 Moving Forward: Expected Opportunities for the Development of New Therapeutic Agents Based on Nanotechnologies

16.1 Introduction

Targeted radionuclide therapy (TRT) is primarily based on the concept of delivering therapeutic doses of ionizing radiation to disease sites with minimal toxicity to surrounding normal tissues using a target-specific moiety including antibody or antibody fragments, peptides nucleotides, and low molecular weight-specific ligands, linked to an appropriate radionuclide. The expression of intracellular proteins such as nucleolin at the cell surface of tumor cells and tumor endothelial cells emerged as the most common target site because the modality inherently relies on binding to accessible targets on the cell surface rather than overall expression levels. While TRT constitutes a successful paradigm of treating a host of diseases including cancer, the success of this treatment modality is associated with many challenges that include selection and availability of radionuclides with the appropriate half-lives and availability of delivery vehicles capable of incorporating optimal radionuclide activity levels with favorable pharmacokinetics. In addition, suitable tumor biomarkers must be identified which can be used to direct the delivery vehicle to the targeted sites.

Specific tumor-targeting ligands must also be available which can be readily conjugated with the delivery vehicles (Fig. 16.1). Over the years TRT has progressed at a rapid rate and experienced an exponential growth resulting from advances in tumor biology, chemistry, and bioengineered technologies. In order to effectively reach the target site, the radiopharmaceutical must pass through several biological barriers, which include blood vessels, tissues, organs, cells, and even subcellular compartments within the target cell. A targeting strategy based on the specificity of the radiopharmaceutical for the disease site according to its biological function not only precludes the application of every activity levels which are required to achieve sufficient local concentrations, but also must minimize nonspecific toxicity and other adverse side effects.

Some of these systems exploit the overexpression of cancer-related surface markers on diseased cells or the development of a dense, but leaky, vascular system within a tumor, forming the basis of a tumor targeting strategy. It is therefore

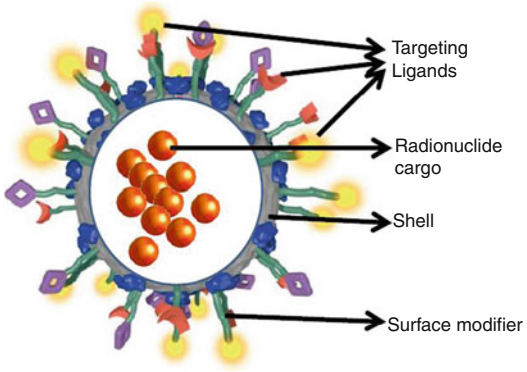

Fig. 16.1 Schematic structural illustration of a nanoparticle comprising the components for radionuclide load delivery

F.F. (Russ) Knapp, A. Dash, *Radiopharmaceuticals for Therapy*, DOI 10.1007/978-81-322-2607-9_16

essential to ensure that the radiopharmaceutical exhibits sufficient stability during administration which is maintained for the required time period in vivo for sufficient radiation delivery to the targeted site before catabolism and eventual excretion. A major problem with many of the currently used tumor-targeting vehicles is that a reagent directed to tumor cells will be impeded by insufficient tumor cell to agents in the vasculature. This challenge is particularly prominent with solid tumors, which have a high interstitial pressure, presumably because the blood vessels can be "leaky" and because of poorly functional lymphatic vessels. Radiopharmaceuticals generally do not penetrate further than three to five cell diameters from blood vessels, which can significantly underexpose more distantly located tumor cells to radiation. This phenomenon can then facilitate the development of resistance. Despite rapid advances, the currently available targeting strategies are often limited by insufficient radionuclide delivery to tumor sites due to relatively low and heterogeneous cell surface receptor expression, as well as dose-limiting toxicity to normal tissues. With a view to maximize the therapeutic index and minimize toxicity, it is crucial to deliver radionuclides to the precise site of action with an adequate dose and with appropriate timing. For these reasons, there is a need to develop novel approaches that offer scope for multiple target recognition on cancer cells, at the same time with the ability to intensify the transport of radionuclides with each target recognition event. There is also the potential to deliver radionuclides selectively to more radiosensitive compartments within the diseased tissue.

In this context this chapter discusses in detail the prospects of using nanoparticles (NPs) as vehicles for targeted radionuclide therapy. Such a strategy has generated widespread interest and is particularly appealing since it offers opportunities to overcome the limitations associated with traditional TRT. At the same time, these methods may permit treating disease at molecular level and capability to diminish unwanted side effects of systemic delivery, by increasing tumor accumulation and improving efficacy. Major advantages of using NPs are the ability to create particles functionalized with a wide variety of targeting ligands and physicochemical properties. This versatility permits the formation of agents that are specifically tailored for each application.

16.2 Therapeutic Strategies Based on Nanotargeting

Radionuclide therapy based on the incorporation of radionuclides with specific emission properties into NPs representing a hybrid science emerging from the ramifications of four powerful scientific domains which include material science, bioscience, radiochemistry, and medical applications may represent a new paradigm in an era of image-based radionuclide delivery and dose delivery. These strategies effectively combine use of biological materials, radionuclide therapy, and tools from the basic sciences of physics, chemistry, bioengineering, physiology, and genetics, etc., to fabricate minute synthetic structures. These combined specialties reflect the increasing ability to investigate beyond the molecular level, whereby generating advantageous results that will have significant impact, for instance, for cancer therapy. It is no longer just a promise, but represents the emergence of a new therapeutic modality. Success of nanotechnology in nuclear medicine relies on tumor targeting specificity.

Delivery of radionuclide to a targeted site from nanocarriers can occur by a variety of mechanisms, which include diffusion, particle fusion and cellular internalization, component (lipid–lipid) exchange and convective flux, biolistics, or a combination of these mechanisms. Major advantages of nanosystems to deliver radionuclide pay loads include the ability for preparation in sizes <100 nm and target a specific site, selectively increase the localization of radiopharmaceuticals in the tumor, and deliver the required localized radiation dose while sparing nontargeted tissue, ensuring minimal leakage of radioactive species during circulation. The ability to synthesize NPs functionalized with a wide variety of targeting ligands and physicochemical properties is also

important, and this versatility permits the creation of agents that are specifically tailored for specific applications. NPs also have the unique capability to gain access to and even to operate within cells (Wang and Cuschieri 2013; Papa et al. 2012; Astolfo et al. 2013) which offers the opportunity of NPs to interact with subcellular structures. Owing to their small sizes, NPs can extravasate from the intravascular space through the endothelial cell layers and interact with the cell structures of various tissues; however, they are also large enough to transport high payloads of therapeutic or diagnostic agents. Use of NPs offers the capability to use radionuclides of lower specific activity owing to large surface areas.

An additional advantage of nanovectors/nanoparticles is their ability to overcome various biological barriers and to localize into the target tissue. The NP delivery platforms provide a multifunctional capacity that offers the scope for loading multiple moieties, such as targeting ligands and therapeutic agents, using multiple reaction steps. A single NP can also be tagged with various radionuclides for imaging as well as therapy with the concomitant attachment of different targeting ligands to introduce selectivity or active groups for nonradioactive monitoring. The ability to load more molecules or radionuclides on a single particle than conventional carriers is a very unique capability of NPs, since sometimes more than one type of therapeutic agent or radioisotope can be attached. The capability to carry multiple, potentially different, targeting ligands on the nanoparticle can thus provide enhanced receptor binding affinity/specificity. The capability of NPs to bypass biological barriers can enhance targeting efficacy. NP delivery platforms allow for interactions with biomolecules on the cell surfaces and within the cells in ways that unaffected the behavior and biochemical properties of those molecules. NPs generally exhibit prolonged blood retention time, ranging from 30 min to more than 24 h, and the radiolabeled NPs remain stable under many physiological conditions and withstand premature degradation. The flexible chemical properties permit surface modifications to enhance their blood circulation half-life and improve their biodistribution profile, and the use of radiolabeled NPs can offer the capability of preventing premature radionuclide release with subsequent interaction with the biological environment. For these reasons, the use of NPs can improve intracellular penetration and enhance uptake of radionuclides into selected tissue sites, such as solid tumors.

NPs also have the ability to control the pharmacokinetic and radionuclide tissue distribution profile, and internalization of receptor targeted NPs leads to a high payload of radionuclide in the target cells, resulting which is expected to result in effective killing of tumor cells which exhibit only a relatively low level of receptor expression. Unique chemical and physical properties of NPs can also include magnetization and photosensitizing, which provide additional capabilities and functions for improving radionuclide delivery, for example, the external application of a magnetic field and for monitoring the therapeutic response. The incorporation of radionuclides into NPs can be achieved by a variety of methods including chemical surface attachment of a radiotracer via the linkage and/or chelating molecule. The synthesis of NPs uses radiolabeled precursors, and diffusion of radioisotopes into the NPs. They can also be prepared by a variety of other methods, including direct neutron activation, direct ion beam activation, and recoil implantation of radionuclides.

16.3 Selection of Radionuclides for NP Therapy

The selection of a method primarily depends on many factors such as the physicochemical and surface properties of the NPs, NP size, the delivery method to be adopted, the duration of the therapy, among others. While the therapeutic utility of nanocarrier lies at the interface of many disciplines, selection of NP is based on various criteria and depends on many factors such as NP size selection, since nanotechnology techniques allow unprecedented control of the material world, at the nanoscale, providing the

means by which materials can be synthesized conforming to desired specifications as well as characteristics. The most desirable size is maintained up to 100 nm to reach tumor affected cells and to provide an opportunity to surpass sinusoid in the spleen and the fenestra of liver Kupffer cells (150–200 nm) and the size of gap junction between endothelial cells of the leaky tumor vasculature (100–600 nm). The chemical composition and structure of NPs are essential to control their interactions. Radiopharmaceutical properties, such as aqueous solubility, stability, etc., can be programmed and loaded. NPs should have an extended circulating half-life, a low rate of aggregation, and a long shelf life. For surface characteristics and functionality, they should exhibit high differential uptake efficiency in the target cells over normal nontargeted cells. For the desired degree of biodegradability and biocompatibility, it is desirable that the NPs are constructed from materials that are biocompatible, well characterized, and easily functionalized. For practicality, the radiation dose delivery profile of the final product should be favorable.

Key properties for radionuclide delivery system using nanocarriers are biocompatibility, proper size and charge to better synergize with the host, high loading and protection of the desired guest molecule, zero premature release before reaching its target, efficient cellular uptake, effective endosomal escape, possible use of ligand on its surface to specifically target tumor cells, stability in circulation, and increasing the fraction of the dose accumulating in the tumor. In order to use a nanocarrier with suitable characteristics for radionuclide therapy, several factors must be considered. These include characterization and extensive evaluation before performing animal experiments since in vivo performance is strongly related to shape, charge, surface modification, and size. The in vivo stability should be scrupulously evaluated using animal experiments since some NPs can be disrupted in the bloodstream. It is also extremely important that the radionuclide chelation with therapeutic agents remains stable over the course of treatment. Therefore, efforts should be focused on preparation of NP-based agents which can allow for efficient, specific in vivo delivery of therapeutic agents without systemic toxicity.

The true power of radioactive therapeutic NPs lies in their ability to interact with disease processes judiciously to deliver the required radiation dose. Radionuclide payload delivery to the target cells from nanocarriers can occur by diffusion, particle fusion and internalization into cells, component (lipid–lipid) exchange and convective flux, biolistics, or some other mechanisms combining these factors. Stability in circulation can be looked up by developing strategies to curtail protein binding and evade the immune system. The efficiency of tumor site accumulation can be augmented by active targeting of the radionuclide delivery system or by increasing extravasation by the enhanced permeation and retention (EPR) effect. The promising attributes of nanomaterials for targeted radionuclide therapy include their ability to concentrate payload of radionuclides for each targeted molecular recognition event in tumors. Two major mechanisms for radionuclide delivery system of NPs to tumor tissue sites are (Allen and Cullis 2004) the site-specific passive tumor targeting and the required molecular affinity and site-specific active tumor targeting for tumor therapy.

16.3.1 Passive NP Targeting

In passive targeting, NPs and radioactive payloads reach the tumor through rich, chaotic, and highly permeable tumor vasculature and are accumulated and subsequently remain in the tumor due to its lack of lymphatic drainage. Accumulation of NPs in tumors takes place due to the pathophysiologic characteristics of tumor blood vessels. When tumor size attains approximately 2 mm^3 volume, the increased interstitial pressure within the tumor appears to hinder the diffusion of metabolites and nutrients necessary for tumor growth. As a consequence, a state of cellular hypoxia initiates along with the sprouting of new blood vessels from the established vasculature or angiogenesis to facilitate the supply of oxygen and nutrients to tumor cells to survive and proliferate. The incomplete tumor

vasculature results in leaky vessels with enlarged gap junctions of 100 nm to 2 μm, depending on the tumor type, its environment, and its localization. When blood components reach the abnormal, discontinuous vascular bed, the fenestrations offer little resistance to extravasation to the tumor interstitium (Hobbs et al. 1998; Yaun et al. 1995). Owing to the lack a well-defined lymphatic system, such tumors have a compound retention time higher than that of normal tissues (Allen and Cullis 2004; Byrne et al. 2008).

These features provide an enhanced permeability and retention (EPR) effect and emerged as an important mechanism for the passive targeting as well as selective accumulation of NPs in the tumor cell interstitial space. In passive targeting, NPs and payloads could reach the tumor and subsequently remain in the tumor due to its lack of lymphatic drainage. NPs with an optimal particle size offer the opportunity to target the tumor vasculature more effectively where the endothelial barrier has an open fenestration, because normal tissues have tight endothelial junction. One of the ways to enhance EPR is strengthening the stability of nanocarrier to lengthen circulation time, so it will have more opportunities to go through the target position and get together (Torchilin 2002). The tumor accumulation levels depend on factors such as the size of NPs and the leaky vascular pore and the blood circulation half-life, since longer half-lives lead to higher accumulation. In addition, the degree of tumor vascularization, since accumulation is less in poorly vascularized tumors, and the degree of angiogenesis, since poor accumulation in small pre-angiogenic tumors or large necrotic tumors, are crucial.

Among the various requirements for and factors influencing the EPR effect, the most important is having a molecular size larger than 40 kDa (Maeda et al. 1994, 1996, 2003; Doi et al. 1996; Wu et al. 1998, 2001; Tanaka et al. 2003; Matsumura and Maeda 1986). Biocompatibility of the NPs also plays a predominate role. The nanocarrier should not have any interaction with blood components or blood vessels, elicit no antigenicity, retained by the reticuloendothelial (REC) system, and undergo no cell lysis. The luminal surface of blood vessels is well known to bear a negatively charged surface owing to the presence of many sulfated and carboxylate sugar moieties (Maeda 1994). This characteristic dictates that nanocarrier with high positive charges will bind nonspecifically to the luminal surface of vascular walls and be rapidly cleared from the blood circulation (He et al. 2010a, b; Lee et al. 2011). Hydrophobicity of the NPs has an important role. An increase in hydrophobicity of NPs would not only result in higher affinity to a cell membrane (Oda et al. 1986), but also exhibit a much faster endocytotic uptake in parallel with an increase of the cell-association constant to about 10–100-fold (Oda et al. 1986; Oda and Maeda 1987).

However, passive targeting approaches suffer from the limitations that would be expected to obstruct the path toward wide-scale utility. Owing to the large variation on the degree of tumor vascularization and porosity of tumor vessels in different tumor type and status, targeting cancer cells using the EPR effect is not feasible in all tumors (Hobbs et al. 1998; Bae 2009). Internalization of NPs is also hampered by the reduced number of specific interactions of cancer cells. As the passive process of accumulation are not optimally designed toward a biological receptor, a long circulation half-life is required to obtain sufficient drug delivery (Holmberg et al. 2012) and depends largely on the size and surface charge of the NPs (Zhang et al. 2014). Thus, passive targeting is sometimes considered as "non-targeting" (Bae and Park 2011), because the NP carrying radioactive payloads are distributed through leaky vasculature, and is determined by the biological environment, rather than active recognition by the tumors.

16.3.2 Active NP Targeting

In order to circumvent the above limitations, active targeting strategy in which NPs are engineered to attach targeting moieties at their surfaces seemed attractive as the NP scaffold containing target-specific biomarker molecules such as antibodies, proteins, peptides, nucleic acids, sugars, and small molecules such as

vitamins provide an opportunity to bind the radionuclide and at the same time offer the scope of targeting the cell surface antigens or membrane receptors that are overexpressed in these cells (Kukowska-Latallo et al. 2005; Weissleder et al. 2005; Liu et al. 2007). While the main mechanism of active targeting lies in the recognition of the ligand by its target substrate, the targeting specificity and the delivering capacity are two important aspects that determine the efficiency of an active targeting system. The targeting specificity is dictated by the ligand as well as NP properties and is decided by the biodistribution of the ligand-functionalized NP and by how the conjugated ligand and the NP system interact with off-target molecules and cells. The delivery of radionuclide payloads to a specific site is directly related to the NP material and structure (Kamaly et al. 2012; Wu and Chu 2013).

Active targeting increases the probability of redirecting long-circulating particles to designated but accessible targets. Unlike passive targeting, in this case, ligands or homing devices that specifically bind to surface epitopes or receptors on the target sites are coupled to the surface of the long-circulating carriers. Strategies for active targeting of tumors primarily involve targeting surface membrane proteins that are upregulated in cancer cells (Huang et al. 2011; Hanahan and Weinberg 2011). Active targeting offers an additional sink for an NP platform since expression of target molecules is usually differential in that the target is highly expressed in tumor cells but expressed at low levels in other cell types in the vascular system. Since the surface area of the vasculature is much larger than the tumor, active binding in tissue can be significant, even for targets that are expressed at relatively low levels. Furthermore, targeting moieties may themselves be targets for receptors on phagocytic cells.

In light of the perceived need to promote and enhance specific interactions between NP and the microenvironment, the surface of particles required to be conjugated with targeting moieties that are recognized specifically by targeted cells. Since NP avidity is dictated by the ligand density, the approaches used to introduce ligands on the surface of the NP represent the cornerstone for the success of actively targeted systems (Gao et al. 2010). The stability of the ligand–NP bond is a key factor that determines how the particle retains the targeting moiety on its surface. While covalent attachment of the ligand is the preferred strategy, physical adsorption using affinity complexes can also be used in case-to-case basis. Owing to the different physicochemical properties of organic and inorganic materials, the type of NP used will determine the difficulty of the ligand conjugation step (Duncan et al. 2005).

16.4 Ligand Conjugation Strategies

Nanoparticles (NPs) can be engineered to target cancer cells for use in therapy. The ultimate goal in the synthesis of multifunctional NPs is the creation of novel NPs for the target-specific therapy. Radiolabeled NPs for radionuclide therapy usually have three major components: core, radionuclide, and targeting biomolecule. The targeting biomolecule serves as a carrier for specific delivery of the radionuclide to the diseased site. With a view to conjugate the ligand to the NP material, both pre-conjugation and post-formulation strategies are being followed. The strategy for the conjugation of biomolecules to nanoparticles generally falls into four classes. Ligand-like binding to the surface of the inorganic particle core is commonly by chemosorptions. Another strategy is electrostatic adsorption of positively charged biomolecules to negatively charged nanoparticles or vice versa. In addition, covalent binding by conjugation chemistry exploits functional groups on both particle and biomolecules, and non-covalent, affinity-based receptor–ligand systems are also exploited.

The choice of the bioconjugation procedure depends strictly on physicochemical and biochemical properties of nanomaterials and ligands. Ligands made by various side chains and residues can interact by multiple coating ligands with the same nanoparticles or even with more nanoparticles. For NP targeting for bioconjugation, one would like to attach the biomolecules to the NPs with control over the following factors,

which include the valence or ratio of biomolecule per NP and orientation of biomolecule on the NP, to achieve specific interactions in the final conjugate. Protein, enzyme, and antibody activities are dependent upon their binding sites having access to the environment. The relative separation distance from the NP and attachment affinity must also be assessed, and optimal function and activity of both participants must be maintained. Ideally, the goal should be to replicate in a facile manner with a variety of biologicals.

16.4.1 Pre-conjugation

Pre-conjugation is relatively straightforward one-step formulation procedure that reduces the risks of side reactions and allows greater control over NP properties. Furthermore, this strategy offers the introduction of multiple types of ligands to NPs and facilitates the purification steps subsequent to NP formulation. Pre-conjugation is used when dealing with small molecules, peptides, and aptamers. It is less adapted to native proteins with complex secondary structures as the conjugation step usually involves exposure to organic solvents.

16.4.2 Post-formulation

In this approach the ligands are reacted with formulated NPs. While this strategy works for all types of ligands including antibody, protein, peptide, aptamer, and small molecules, it is preferably used when the stability of the ligand in organic solvents is an issue, the size of the ligand is too large to promote self-assembly, or when the presence of the ligand changes the physicochemical properties of the NP components.

16.4.3 Bioconjugation Based on Covalent Approaches

The formation of covalent NP–ligand conjugates produces stable hybrid systems that provide control over ligand reactivity and NP aggregation. The most popular approach for covalent coupling is based on the existence on proteins of specific and reactive functional groups such as amino, NH2 (lysine); carboxylic acid, COOH (aspartic, glutamic); hydroxyl, OH (serine, tyrosine; and –SH (cysteine) (Weber et al. 2000). Bifunctional linkers are used to conjugate ligands to NPs through a series of chemical coupling reactions. In this case, NPs are functionalized with functional groups such as carboxylic acid, hydroxyl, sulfhydryl, and amino groups. The formation of a peptide bond between the ligand and the NP surface is one approach that is usually achieved by activating carboxylic groups (using, e.g., N-hydroxysuccinimide (NHS) and 1-ethyl-3-(3-dimethyl-amino-propyl) carbodiimide hydrochloride (EDC)) and reacting it with nucleophilic groups (e.g., amine) on the ligand. While this straightforward conjugation strategy can be carried in both aqueous and organic environments, the selectivity of the conjugation and the final orientation of the ligand both depend on the number of nucleophilic functions on the ligand. Carbodiimide coupling is used to covalently link carboxylic acids to amines via formation of a “zero length” amide bond (Gao et al. 2004). The key advantage of this procedure is that it involves no lengthy linker species, allowing the hydrodynamic radius of the NP to be minimized. Charged NPs may be coupled either with oppositely charged biological and polymeric species (Potapova et al. 2003), or indeed to different oppositely charged NPs (Galow et al. 2000).

Another coupling strategy that merits attention is the coupling of a maleimide group on NP surfaces or polymers with a thiol group present on the ligand (i.e., cysteine residues in proteins or peptides) to form a stable thioether bond. In proteins or peptides, reduction of disulfide bonds to free thiol groups allows the reaction. It should be noted that the reduction retain the three-dimensional structure and affinity of the ligand for its substrate intact. While the introduction of free thiols by reacting 2-iminothiolane to primary amines is also a possible pathway which is widely used, this approach introduces a positive charge on the NP–ligand construct (Shi et al. 2009). Recently, a bioconjugation method called “click

chemistry" was developed which is a single-step reaction that involves heteroatom bonds with or without catalysts (Singh and Lillard 2009). For example, alkyne groups on peptides or small molecules will readily form a bond with the azide group on the NP surface or polymer backbone without side reactions. This method is very selective and provides very good yields.

16.4.4 Bioconjugation Based on Non-covalent Approaches

Pragmatically, non-covalent conjugation provides a complementary strategy to covalent attachment, enabling applications in sensing and delivery. The simplest way to achieve non-covalent conjugates is to exploit the electrostatic interactions between the nanoparticle and the ligand, a particularly useful approach when specificity is not required (Hong et al. 2004). In order to circumvent the inherent nonspecificity of this approach and to avail regiospecific interaction, the NP surface could be strategically modified by fine-tuning its charge and hydrophobicity (Bayraktar et al. 2007). Interaction between avidins and biotin (bio) is a prominent and widely used non-covalent conjugation technique due to the extremely high affinity of avidins to biotin (dissociation constant 10^{-15} M (Gao et al. 2010). Choice of biotin is attractive due to its small molecule size which does not alter the functions of the ligands Fischer 2010). Such a strategy appears to be attractive and has been avidly applied to antibodies, peptides, and aptamers (Park et al. 2011) to establish proof of concepts or to screen different ligands without interference from the conjugation chemistry or to study fundamental ligand decoration parameters (Park et al. 2011; Fahmy et al. 2005). While this method constitutes a step forward to achieve non-covalent conjugation, a major limitation of this method is that it may cause immunogenicity due to the presence of the exogenous protein on the surface and it is not amenable for human use (Yumura et al. 2013). In addition, because avidin can bind biotin in a multivalent fashion, cross-linking between the NP constituents is possible. Another popular conjugation strategy is through carbohydrate–lectin interactions (Jiang et al. 2010). Specific carbohydrate–lectin conjugation facilitates uptake via receptor-mediated endocytosis. The preferential uptake of sugar-capped PEGylated QDs by specific asialoglycoprotein has been reported to be successful for in vivo targeting and imaging (Kikkeri et al. 2009).

16.4.5 Influence of the Architecture of Actively Targeted NPs

The conjugation of ligands on the surface of NPs changes not only the properties of targeting molecules but also the nanomaterial (Kamaly et al. 2012; Shi et al. 2011). The ligands lose the rotational and translational freedom bestowed to free molecules, but the new targeted entity achieves improved avidity because of the increased valency. The size, geometry, surface properties (charge and hydrophobicity), and composition of NPs can also be altered. Efficient ligand–receptor interaction for "active targeting" is dependent upon a variety of factors that include (Capone et al. 1984; Li and Hall 2010) the extent of target cell-selective expression of the receptor relative to nontarget cells and the receptor availability on the target cell surface. Furthermore, the rate of internalization versus shedding of that surface receptor following ligand binding is important as well as the expression of a promising tumor-targeting receptor which may not be homogenously distributed within a tumor or may change in its surface expression over time.

16.5 NP Targeting Groups

Targeting ligands with various types of nanomaterials increased specificity and efficacy as well as reduced toxicity. Significantly, the conjugates exhibit special properties, and targeting ligand-conjugated nanomaterials with diverse characteristics display additional capability for therapy (Fig. 16.2). A wide range of ligands may be used as a basis for targeted delivery. Most important parameters that should be considered while

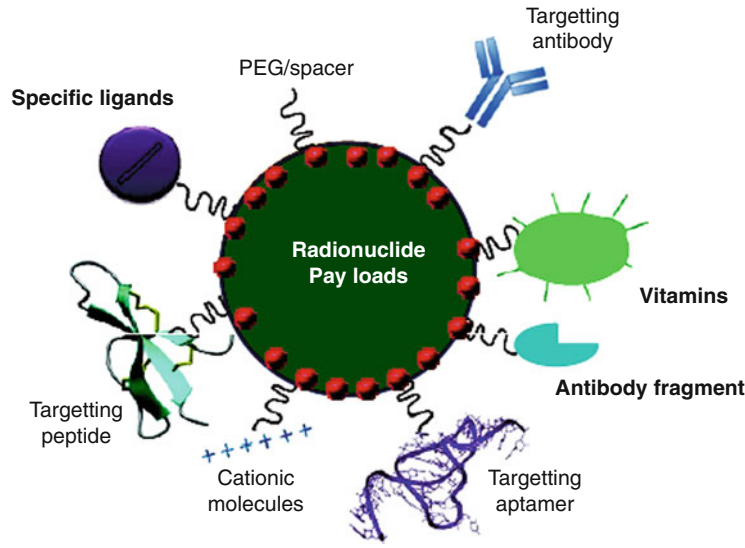

Fig. 16.2 Illustration of the different types of nanoparticle targeting vectors

selecting a ligand for targeted drug delivery are binding affinity, size, immunogenicity, and cost of production. The ligand should be unique to the target cell and be characterized by the highest binding affinity and lowest immunogenicity. It should also enable penetration of the tumor.

16.5.1 Monoclonal Antibodies

Monoclonal antibodies (mAbs) possess many desirable technical attributes and advantages as tools for biomolecular targeting, including molecular homogeneity, specificity of interaction, high binding affinity in the nanomolar range, and ease of selection. mAbs is typically used only as a "hook" that facilitates binding of the larger delivery particle with the site of interest on the target cell. The presence of two epitope binding sites in a single molecule offers an exceedingly high selectivity and binding affinity for the target of interest. mAbs represent a single molecular species that bind to antigens with the same affinity and promote the same effector functions. Therapeutic mAbs are usually completely humanized or produced as chimeric proteins, in order to avoid unwanted immune reactions in patients. The binding (dissociation) constants for antibody–antigen interactions vary over a wide range from 10^{-6} to 10^{-9} M, but can be as high as 10^{-12} M for high-affinity antibodies (Dill et al. 1994), Rituximab (Rituxan®) for non-Hodgkin's lymphoma treatment (James and Dubs 1997), Trastuzumab (Herceptin®) for breast cancer treatment (Albanell and Baselga 1999), Bevacizumab (Avastin®) designed to inhibit angiogenesis (Ferrara 2005), and Cetuximab (Erbitux®) for advanced colorectal cancer treatment (Van Cutsem et al. 2009) have been developed and introduced for clinical therapy.

Antibody-conjugated NPs combine the advantages of NPs with the ability to bind to their target with high affinity and improve cell penetration given by the antibodies. The efficacy of the delivery depends on the ability of each antibody to reach its target in adequate quantities and on the limited amount of nanoparticles trapped by the cell. In order to create a stable linkage, antibodies should be covalently linked to the nanoparticle surface. The physical adsorption method which relies on the affinity of certain functional groups on proteins such as amine and thiol groups and other moieties, for attachment via non-covalent interactions to the particle surface, appeared to be the least stable. In an in vivo environment, or even in cell media, antibodies that are physically adsorbed can be easily displaced. In this premise, the covalent conjugation method which provides a stable linkage between the particle and the antibody and several different chemistries such as

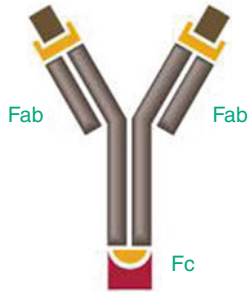

Fig. 16.3 Antibodies are Y-shaped and possess two antigen-binding regions (Fab fragments) and a constant region (F_c region)

N-hydroxysuccinimide (NHS)-coupled NP with 1-ethyl-3-(3-dimethylaminopropyl) carbodiimide (EDC) emerged as the most widely used regime. While the antibody-conjugated NPs is attractive for targeting applications, the F_c region of the antibody can be a disadvantage if it is accessible to F_c receptors on macrophages, which can lead to increased accumulation in the liver and spleen (Allen 2002) (Fig. 16.3).

16.5.2 Antibody Fragments

Although antibodies have proven to be effective targeting agents, there are inherent issues such as decreased receptor affinity due to inadequate conjugation methods, insufficient tumor cell penetration, and nonspecific binding of antibodies to cellular receptors. Being 150 kDa in size, they cleared slowly from the blood pool and lead to significant accumulation in normal organs and relatively limited delivery to lesions such as tumors (Colcher et al. 1998). Antigen-binding sites represent only a small part of the overall size of antibodies. The Fab fragments retain both antigen-binding sites of the antibody coupled by disulfide linkages. Cleavage of the disulfide bond under reducing conditions yields two Fab fragments with sulfhydryl groups that can be used for coupling to the targeting platform. Single chain variable fragments maintain only the variable regions (variable light chain and variable heavy chain) of one arm of an antibody. The use of small fragments of the antibody molecule (Fig. 16.1) such as Fabs (molecular weight MW ~50 kDa; ~6 nm in size) and Fvs (variable region fragments, MW ~25 kDa, ~3 nm in size) offers several advantages over intact antibodies because of the reduced nonspecific binding from F_c interactions (many cells have receptors that bind the F_c region). The ability to control Fc binding to protein A or protein G is important and allows more efficient penetration of tissue sections. Potentially higher sensitivity in antigen detection in solid phase applications results from the reduced steric hindrance from large protein epitopes. This strategy also allows the elimination of Fc-associated effector functions (e.g., complement fixation) in antigen–antibody binding studies and lower immunogenicity than intact antibody. Finally, these species are cleared much faster from the blood than are intact antibody.

The scope of using Fabs and Fvs fragments is enticing as they can be selected by phage display and are engineered more easily than mAbs, to control properties such as affinity (K_D usually lower than 1 nM) or internalization capabilities (Holliger and Hudson 2005). To enable directional attachment, one end of a hetero-bifunctional cross-linker molecule is bound to the F_c region of the antibody. The other end of the linker binds directly to the nanoparticle surface, providing a directional linkage between the antibody and the particle. Using this method, a stable linkage between the particle and the antibody is realized while leaving the variable region (F_v), or antigen interacting site, sterically unhindered and available for binding. The directional nature of the attachment makes characterization of the antibody-to-particle ratio more consistent and also enhances cell labeling efficiency. Labeling efficiency can be increased by seven to tenfold using a directional versus nondirectional attachment method. It is pertinent to point out that all of these antigen-binding fragments usually retain the specific antigen-binding affinity of the parent antibody, but is usually characterized by improved pharmacokinetics with respect to tissue penetration and lack the Fc-antibody region, which is most immunogenic.

16.5.3 Other Proteins

The three-dimensional shape of proteins offers affinity for specific substrates, and therefore the prospect of using non-antibody proteins (both naturally occurring and synthetic) as targeting moieties seemed possible. The scope of using naturally occurring proteins for therapeutic applications is attractive owing to the presence of endogenous targets. In this premise, transferrin (Tf), an 80-kDa glycoprotein, that regulates the supply of iron into cells via receptor-mediated endocytosis merits attentions (Kresse et al. 1998). On the surface of cells, it binds the internalizing transferrin-receptor (Tf-R) with high affinity The transferrin receptor is expressed at low levels in most normal tissues but is overexpressed in many tumor types (Daniels et al. 2012). NPs decorated with Tf could be used for delivering radioactive payloads. Other proteins, such as human serum albumin (HSA) (Quan et al. 2011), bovine serum albumin (BSA) (Wang et al. 2011), concanavalin A (Smiljanic et al. 2006), protamine (Wang et al. 2012), E-selectin (Rana et al. 2012), and avidin (Li et al. 2013) are just a few promising candidates that could be used for targeted delivery. Synthetic proteins such as "affibodies" (Alexis et al. 2008) or ankyrin repeat proteins decorated with NPs have also been exploited as targeting ligands. This approach seemed attractive as it possesses the advantage of using high affinity, artificial ligands which do not have to compete against highly abundant, naturally occurring proteins.

16.5.4 Peptides

Peptides are formed by joining amino acids together through peptide bonds, which are usually composed of less amino acid than proteins. Peptides offer several unique advantages. Their small size minimizes the overall radius of the resulting peptide–NP conjugate while still affording a high valence (number of peptides per NP) and reduces immunogenicity in vivo. Peptides are also economical and facile to produce as they can be easily synthesized commercially or in the laboratory. From a functional perspective, peptides are biocompatible, derived from naturally occurring protein precursors and can be very specific and bind with high affinity to their cognate receptors, often with affinities comparable to those of full-length antibodies (Yao et al. 2009). Multiple different peptide species can be arrayed around the NP to incorporate multifunctionality or produce a 'value-added' material that serves multiple purposes in one NP.

Owing to these attributes, peptides represent a very attractive and useful class of molecules for the development of NPs for targeted delivery. To attach a peptide to an NP and to display peptides uniformly on the NP surface with their active regions all clearly extended away and available for activity, the chemistry involved follows various pathways. These include in a homogenous manner, with control over its final orientation, distance from the NP surface, and the ratio or valence on the NP surface. The strategy used for peptide attachment to an NP will be dictated primarily by a combination of the NP materials themselves, their characteristics, the ligands on their surfaces along with their functional groups, the peptide sequence itself, and the final utility desired.

The most widely investigated peptides in the targeted-delivery applications is probably the integrin-targeting RGD (arginine–glycine–aspartic acid) peptide family (Kamaly et al. 2012; Shi et al. 2011). Integrins $\alpha_v\beta_3$ and $\alpha_v\beta_5$ are overexpressed on tumor endothelium and some epithelial cells during tumor growth, angiogenesis, invasion, and metastasis and constitute an interesting molecular target for a tumor-homing approach. The binding affinities of some of the RGD-containing derivatives for $\alpha_v\beta_3$ range from 3.2 to 100 nM (Huang et al. 2008; Alloatti et al. 2012). The addition of specific amino acid residues to peptide sequence motifs, such as RGD, that induce binding to cell-attachment proteins, strongly enhances the binding affinity of this peptide. In this premise, RGD peptide functionalized Au–Fe2O3 developed by Tang's group for cancer cell-specific apoptosis and real-time imaging merit attention (Gao et al. 2012). Among other targeting moieties, cytokines and typical peptides

released from a variety of cells during an inflammatory response which exhibit broad biological activities should also be mentioned. They are produced by immune cells (such as monocytes, macrophages, T cells, B cells, NK cells, etc.) and some nonimmune cells (endothelial cells, epithelial cells, fibroblasts) after stimulation. Shenoi and coworkers found tumor necrosis factor α (TNF-α), a representative cytokine, has the potential to improve tumor-specific action in combination with locally applied thermal therapy in prostate cancer when conjugated to AuNPs (Shenoi et al. 2013). The agonist or antagonist pharmacologic activity of peptides has been harnessed to alter the fate of NPs decorated with such peptides (Hild et al. 2010). In this study, the targeting of quantum dots to G-protein-coupled receptors using peptide agonists led to the internalization of the nanomaterial.

16.5.5 Aptamers

Aptamers are single-stranded deoxyribonucleic acid (DNA) or ribonucleic acid (RNA) oligonucleotides that can bind to target antigens with high affinity and specificity. Target molecules for aptamers can be virtually any class of substrate ranging from whole cells to large molecules, like proteins, to peptides to drugs and organic small molecules or even metal ions. Aptamers have a molecular weight (10–15 kD) which is one order of magnitude lower than that of antibodies (150 kD) (White et al. 2000) and derive their name from the Latin word "aptus" meaning "to fit." Owing to their small size and similarity to endogenous molecules, aptamers exhibit superior tissue penetration (Hicke and Stephens 2000) and are believed to be less immunogenic than antibodies (Drolet et al. 2000). In comparison with antibodies, these molecules have some advantages because of their molecular nature which offers the scope for storage at room temperature owing to their high stability (especially DNA aptamers). They can be heated to temperatures as high as 95 °C or exposed to various solvents or harsh environments and will return to their original confirmation, providing a long shelf life (White et al. 2000) and low immunogenicity and toxicity. Chemical modifications are also possible to extend their lifetime in biological fluids, to immobilize them on surfaces, to endow them with radionuclide (Jenison et al. 1994; Lee et al. 2006), and to "tune" their half-lives to match the indication (Carlson 2007). The low molecular weights facilitate penetration of these molecules into tissues and cells.

While the attributes of aptamers are appealing, these molecules are susceptible to nuclease degradation or renal clearance in vivo. Therefore, their pharmacokinetic properties need to be enhanced prior to in vivo applications. Although aptamers themselves are typically quite good at homing to their intended targets even in complex solutions including the in vivo milieu, nanoparticles can be used for directing aptamer NPs and radioactive payloads to their target cells. In view of their small sizes, they require attachment to the nanoparticles via linkers sufficiently long to ensure that they are not sterically hindered from contacting their specific targets. Conjugations to nanoparticles have been extensively studied and reviewed (Teply et al. 2006; Farokhzad et al. 2006; Ellington et al. 2007). Aptamer-conjugated NPs target cancer cells of different types, including prostate cancer (Lupold et al. 2002; Farokhzad et al. 2004; Wang et al. 2007; Zhang et al. 2007) and breast cancer (Huang et al. 2009). With specificity for integrins, they can target tumor vasculature (Schiffelers et al. 2004).

16.5.6 Vitamins

Vitamins such as vitamin B_9 (folic acid) and vitamin H (or vitamin B_7, biotin) offer the scope for targeting diseased tissue. In this premise, folic acid (FA), a low-molecular-weight vitamin which plays an essential role in cell survival and binds with high affinity to the folate receptor (FR), a membrane-anchored protein that is overexpressed on the surface of a variety of human tumors including ovarian, brain, breast, colon, renal, and lung cancers merits attention (Low et al. 2008: Hilgenbrink and Low 2005; Markert et al. 2008). The prospect of using folate-conjugated NP is enticing because of low-cost, nonimmunogenic character and ability to conjugate with a wide variety of NP and ability to enter

cells through receptor-mediated endocytosis (Pan et al. 2013). Folate-targeted NPs co-encapsulating paclitaxel and yittrium-90 showed improved survival in a xenograft model of ovarian cancer. Riboflavin is an essential vitamin primarily responsible for cellular metabolism, and the riboflavin carrier protein (RCP) is highly upregulated in metabolically active cells (Foraker et al. 2003). With these data in mind, flavin mononucleotide (FMN), an endogenous RCP ligand, could be used as a targeting ligand for metabolically active cancer or endothelial cells.

16.5.7 Specific Ligands

Biotin is a CO_2 carrier for several important biological reactions, including gluconeogenesis and the synthesis of fatty acids, and the metabolism of amino acids acts as an aid in maintaining blood sugar levels in people and promotes the health of sweat glands, nerve tissue, bone marrow, male sex glands, blood cells, skin, and hair. Conspicuously, biotin levels might be correlated with diseases such as diabetes mellitus, liver and skin disorders, immunological and neurological abnormalities, and epilepsy (Ho and Hung 2008). Biotin has been successfully incorporated into the architecture of carbon nanotube (CNTs) to develop a multifaceted delivery vehicle with high stability, substantial cell viability and targeted specificity toward cancer cells (Brahmachari et al. 2014). Among the synthetic and natural small molecule ligands reported, triphenylphosphonium (TPP) and its derivatives have been used for mitochondria targeting (Marrache and Dhar 2012; Smith et al. 2003). The TPP molecule is a cationic, relatively large, and hydrophobic molecule that can penetrate easily through the cell membrane. Despite the desire to direct therapeutics to the mitochondria, the actual task is more difficult due to the highly complex nature of the mitochondria. The potential benefits of integrating nanomaterials can lead to the development of nanomedical platforms for targeting therapeutics to the mitochondria. An investigation indicated that the positively charged TPP could accumulate several hundredfolds within mitochondria (Marrache and Dhar 2012).

Carbohydrates (Zhang et al. 2010a, b, c) are a large class of small molecule targeting ligands which can selectively recognize cell surface proteins receptors, such as lectin (André et al. 2000). The asialoglycoprotein receptor (ASGP-R) is present on hepatocytes at a high density of 500,000 receptors per cell (Shen et al. 2011; Kim et al. 2005). It has a tendency to bind carbohydrates including galactose, mannose, and arabinose and therefore can thereby serve as an effective liver-targeting ligand (Yang et al. 2010; Cho et al. 2008) Hyaluronic acid (HA), a copolymer of *N*-acetyl D-glucosamine and D-glucuronic acid, can be effectively used for targeting macromolecule that can bind to cluster determinant 44 (CD44), which is overexpressed in various tumors (Gunthert et al. 1991; Platt and Szoka 2008; Bhang et al. 2009).

16.6 Radiolabeling

The ultimate goal in the synthesis of multifunctional NPs is the creation of novel NPs for the target-specific therapy. The radiolabeled nanoparticles for tumor targeting usually have three major components: core, radionuclide, and targeting biomolecule. The targeting biomolecule serves as a carrier for specific delivery of the radionuclide. The radionuclide can be conjugated directly on the surface of nanoparticle core through various labeling methods. In order to obtain optimal therapeutic outcome, appropriate therapeutic radionuclide and radiolabeling strategy must be carefully taken into consideration. Some key factors need to be considered while undertaking radiolabeling of nanoparticle. In designing a radiolabeled nanoparticle several key factors must be considered including radiolabeling integrity. The nanoparticle structure and radiolabeling strategy must both be designed to get robust, stable radiolabeling. The half-life of the radionuclide must be congruent with the binding kinetics of the carrier and target, as well as the in vivo pharmacokinetics of the carrier. The targeting efficiency and radiolabeling-specific activity, for well-designed nanoparticle allows increased loading of targeting ligands

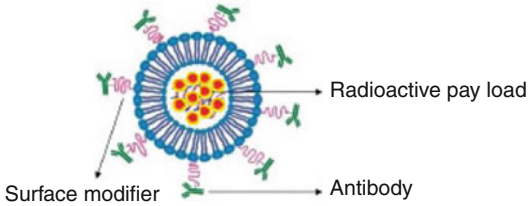

Fig. 16.4 Example of a radioactive payload using an antibody for the nanotargeting

and high radiolabeling-specific activity and can provide elevated binding efficiency to reduce the required administration of nanoparticle to just trace amounts. The radionuclide can be conjugated directly on the surface of nanoparticle core through t various labeling approaches, including (Xing et al. 2014) direct labeling (nucleophilic or electrophilic reactions), indirect labeling (through prosthetic group), coordination chemistry labeling of chelator-functionalized NPs, and nucleophilic halogen exchange chemistry. Among these approaches, complexation reactions of radiometal ions with chelates through coordination chemistry have been widely used (Fig. 16.4).

16.7 Nanoparticles for Therapy

While the successful use of NP resides on its ability to target the disease site, the characteristic of NP is being recognized as an essential part that determines its success.

16.7.1 Particle Size

Particle size and size distribution are the most important characteristics of nanoparticle systems that dictate the in vivo distribution, biological fate, toxicity, and the targeting ability of nanoparticle systems. In addition, they can also influence the drug loading, drug release, and stability of nanoparticles. The size of therapeutic nanomaterials should be in the range of 10–100 nm, as larger particles have limited diffusion in the extracellular space (Dreher et al. 2006) (Fig. 16.5).

16.7.2 Composition

The surface reactivity of nanoparticles is dependent on their chemical composition, which in turn controls particle circulation time, the interaction of nanoparticles with their local environment, and ultimately the efficiency of receptor targeting. The chemical composition of the NP can be tailored in such a way that it can respond either to an internal stimulus (such as the reducing nature of the cytosol compared with the extracellular space or the drop in pH known to occur in endosomes) or to an external stimulus (such as an applied magnetic field or exposure to a specific wavelength of light).

16.7.3 Surface and Ligand Charge

The charge of the NP as well as the ligand is particularly important as the repulsive or attractive forces between the surface of the NPs and the ligand can affect the conjugation yield and the spatial display of the ligand on the surface (Barua et al. 2013; Kocbek et al. 2007: Patil et al. 2009). The final surface charge of the conjugate is a key determinant that dictates efficacy of the targeted NPs. It has been reported that positively charged NPs show increased cellular binding and uptake owing to the interaction between cationic NPs and negatively charged cell membranes (Zhao et al. 2011). In general, neutral particles show lower interaction with the cell membrane than charged (cationic or anionic) nanoparticles of the same size, due to the lower number of electrostatic interactions between NP surface and charged cell membranes.

16.7.4 Surface Hydrophobicity

Apart from the size and surface charge of NPs, their surface hydrophobicity affects the architecture of the ligand display and the nonspecific interactions with cells. Surface hydrophobicity determines the amount of adsorbed blood components, mainly proteins (opsonins). This in turn influences the in vivo fate of NPs (Muller and Wallis 1993; Brigger et al. 2012).

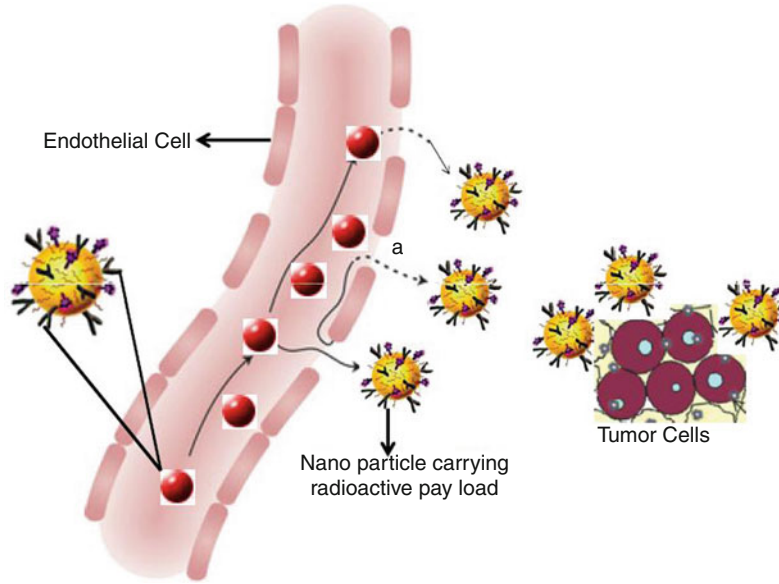

Fig. 16.5 Schematic of the extravasation of nanoparticles carrying radioactive payloads to be retained by specific interaction with tumor cells (Modified from Mier et al. 2014)

16.7.5 Mechanical Properties

To survive within the turbulent dynamics of the bloodstream, an NP requires a certain mechanical integrity. Nanoparticles held together only by charge-based forces would not suffice as they are likely be disrupted rapidly. In this context, cross-linking by covalent bonds seemed to be an effective strategy as it would offer necessary stiffness and cohesion to the NPs not only to survive bloodstream turbulence, but also to ensure their stability at the target site, where stationary accumulation of stable NPs is essential.

16.7.6 NP Surface Coating

The use of polymers to coat NPs to protect them from metabolizing enzymes is an attractive proposition to increase their stability and solubility (Zhang et al. 2011; Tsuchiya et al. 2012; Gregory et al. 2013). The surface layer serves to reduce the surface energy and at the same time acts as the protective coating preventing nanoparticles from agglomerating due to steric repulsion thus increasing their long-term stability to preserve their efficacy. Surface coating offers the following advantages since it provides biocompatibilities that include minimizing toxicity from metallic nanoparticles, modulating interactions between nanoparticles and biomolecules, cells and tissues, together with altering the secretion and biodistribution of the nanoparticles. Protection of the bioconjugate from premature degradation in the biological environment is a major feature, and this approach renders them inert to the body's immune responses.

The polymer coatings can be classified as natural polymers such as chitosan, dextran, and rhamnose or synthetic polymers like polyethylene glycol (PEG), polyvinyl alcohol (PVA), polyethyleneimine (PEI), and polyvinylpyrrolidone (PVP). In some cases other organic molecules including oleic acid, oleylamine, dodecylamine, and sodium oleate are also used to enhance water solubility of NPs. On the other side, there are very less number of inorganic materials available for MNP surface coatings, in which gold (Au) and silica (SiO_2) are the most common used ones due to their biocompatibility. The coating can consist of long-chain organic ligands or inorganic/organic polymers, where these ligands or polymers can be introduced during (in situ coating) or after (post-synthetic coating) synthesis. Among all the coatings, organic coatings, particularly those of polymers, are very attractive as they offer great versatility in the chemical groups that can be incorporated at the surface to control tissue–

biomaterial interactions and possess mechanical properties similar to soft biological tissues and relative ease of processing. The prospect of functionalizing the coating polymers with reactive functional groups, such as –COOH, $–NH_2$, and –SH, is an attractive strategy as it offers the scope for the conjugation of the tumor-targeting ligands. Reactive functional groups also allows for covalent cross-linking or non-covalently incorporating chelates of radioisotopes for carrying and delivering therapeutic radioisotopes.

16.8 Biomedically Important NPs

According to the chemical composition of nanoparticle core, nanoparticles can be broadly classified into organic and inorganic nanoparticles. As shown in the cartoon in Fig. 16.6 for radionuclide therapy of tumor cells using these platforms, tumor-targeting ligands are attached to the nanoparticles, the radioisotope attached, and the whole assembly then targeted to receptors, for instance, which may be specifically overexpressed on the tumor cell membrane (Fig. 16.6).

16.8.1 Organic NPs

Over the last decade, a number of organic NPs such as dendrimers, polymeric micelles, liposomes, and proteins have been used. These organic NPs carrying therapeutic radionuclides have shown potential for radionuclide therapy (Fig. 16.7).

16.8.2 Liposomes

Liposomes are small vesicles consisting of one or more concentric lipid bilayers with an aqueous interior but can be unilamellar, with a single lamella of membrane, or multilamellar, with multiple membranes. The membranes consist of amphiphilic compounds (phospholipids, glycolipids, and aminolipids) (Hofheinz et al. 2003). The unique ability of liposomes to entrap radiopharmaceuticals both in an aqueous and a lipid phase makes it attractive for hydrophilic and

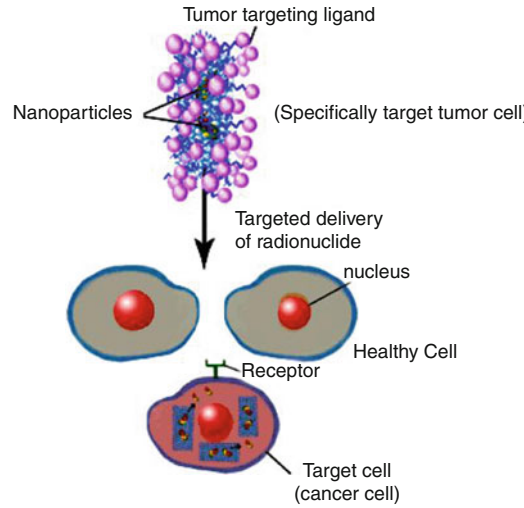

Fig. 16.6 Schematic showing the active targeting of nanoparticles

hydrophobic moieties. Hydrophobic molecules are intercalated within the bilayer membrane, and hydrophilic molecules can be entrapped in the internal aqueous region. The prospect of using liposomes as nanocarriers is attractive since they are generally considered nontoxic, biodegradable, and nonimmunogenic, as they are typically composed of naturally occurring lipids. They can passively accumulate in tumor by extravasation through abnormal leaky tumor vasculature, or actively accumulate by tumor cell-specific targeting, and can carry substances dissolve both in water and lipid. Liposomes can also decrease or even eliminate side and toxic effects. They have versatile modifiability by encapsulating the functional molecules in the inner surface, inserting in the bilayer, or attaching on the bilayer membrane surface and protect it from early degradation, inactivation, and dilution in circulation (Sahoo and Labhasetwar 2003). Association of a radiopharmaceutical with liposomes generally prolongs circulation half-life, reduces volume of distribution, and lowers systemic toxicity. In vivo behavior of liposomes can be easily manipulated by altering their characteristics, such as size, lipid composition, and charge (Ulrich 2002).

These unique properties of liposomes make it an excellent platform for the specific delivery of therapeutic radionuclide moieties. While the

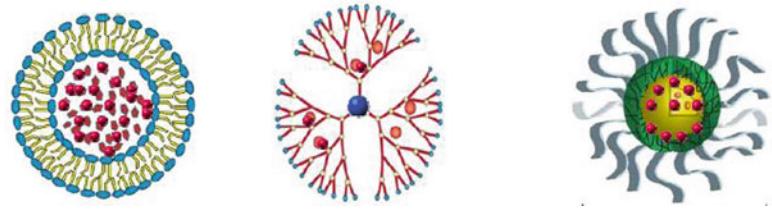

Fig. 16.7 Examples of organic nanoparticles

attributes of liposomes are appealing, its biodistribution is one of the major concerns as they are vulnerable to eliminate from the systemic circulation by the cells of the reticuloendothelial system (RES) (Senior 1987). A number of studies have shown that 50–80 % of liposomes are adsorbed by the RES, primarily by the Kupffer cells of the liver within the first 15–30 min after intravenous administration (Laverman et al. 2001; Litzinger et al. 1994; Allen and Hansen 1991). Other major problems associated with liposomes are their stability, poor batch-to-batch reproducibility, difficulty in sterilization, and low loading capacity of therapeutic radionuclide moieties. Soundararajan et al. have formulated radiolabeled liposomes by directly loading ^{186}Re and DOX into liposome interior for cancer chemoradionuclide therapy (Soundararajan et al. 2009). A large number of radionuclides have been explored to formulate liposome-based theranostic particles, including the beta emitters ^{131}I, ^{177}Lu, ^{90}Y, ^{111}In, ^{166}Ho, and ^{186}Re (Bao et al. 2003; Osborne et al. 1979; Harrington et al. 2001; Hoefnagel 1998; Zweit 1996; Kostarelos and Emfietzoglou 2000; Kostarelos et al. 1999) and the alpha emitters ^{223}Ra and ^{225}Ra (Rojas et al. 2015) and ^{225}Ac (McLaughlin et al. 2014).

16.8.3 Dendrimers

Dendrimers are a novel class of repeatedly branched polymeric macromolecules with numerous arms extending from a center, resulting in a well-defined topological structure (Satija et al. 2007). Dendrimers have three major components: a central core with two or more reactive groups, repeated units covalently attached to the central core and organized in a series of radially homocentric layers as called "generations," and peripheral functional groups on the surface which predominantly determine the physicochemical properties of a dendrimer. The peripheral groups can be modified to obtain both a charged and hydrophilic or lipophilic function for the desired biological and radionuclide delivery application (Bai et al. 2006). Based on the molecular "hooks" attached to the surface, dendrimers can be actively targeted to cancer cells, tumor tissues, and abnormal vessels. Use of dendrimers as a nanocarrier is appealing since they can be synthesized in various sizes, molecular weights, and chemical compositions and designed for specific applications. Through the modification of cores, interiors, and surface groups of dendrimer, the properties of dendrimer can be optimized to reach favorable physical characteristics, biodistribution, and receptor-mediated targeting. They also exhibit non- or low immunogenicity associated with most dendrimer surfaces modified with small functional groups or polyethylene glycol (PEG). A number of peripheral surface groups are amenable for bioconjugation of radionuclide targeting moieties or biocompatibility groups. They also offer the scope for surfaces design with functional groups to augment or resist transcellular, epithelial, or vascular biopermeability. Surface groups can be modified to optimize biodistribution and receptor-mediated targeting. The multifunctional nature of the dendritic network makes it easier to incorporate both the radionuclide and the targeting moieties simultaneously. Due to the high loading capacity and the flexibility of controlling the polymer structure, dendrimers are favorable scaffolds or vehicles for the delivery of radionuclide payload (Khosroshahi et al. 2013; Parrott et al. 2009; Xu et al. 2011; Zhang et al. 2010a, b, c). Nanoscale sizes of dendrimers have similar dimensions to important

biobuilding blocks, e.g., proteins and DNA. An interior void space may be used to encapsulate therapeutic radionuclide moieties. Because the DOTA chelator in the dendrimers can be readily labeled by therapeutic nuclides, such as ^{90}Y and ^{177}Lu, the newly developed dendrimers could afford a potential platform for radionuclide therapy.

16.8.4 Micelles

Micelles are spherical nanostructures ranging from 10 to 100 nm, formed from the self-assembly of amphiphilic-block copolymers in aqueous environments (Kataoka et al. 2001). The hydrophobic core region serves as a reservoir for hydrophobic moiety of radiopharmaceuticals, whereas the hydrophilic shell stabilizes the hydrophobic core and renders the polymer water soluble, making the particle an appropriate candidate for the intravenous administration (Nakanishi et al. 2001). Polymer micelles can be functionalized with targeting ligands for receptor-mediated targeting. Currently, the most commonly used corona-forming polymer is polyethylene glycol (PEG), with a molecular weight range from 2 to 15 kD. Core-forming blocks typically consist of poly(propylene oxide) (PPO), poly(D,L-lactic acid) (PDLLA), poly(ε-caprolactone) (PCL), and poly(L-aspartic acid), and many others. (Sutton et al. 2007). The use of micelles offers a variety of advantages. They are biocompatible, self-assembling, and biodegradable. The hydrophobic cores of micelles provide a natural carrier environment that allows easy encapsulation of poorly soluble radiopharmaceuticals. The non-covalent encapsulation strategy makes it feasible to entrap radiopharmaceuticals without the requirement of reactive chemical groups. Functional modification is facile since the unique chemistry of the polymer constituents does allow for the chemical conjugation of targeting moiety as well as radionuclide. They also offer the scope for controlling the in vivo pharmacokinetics by suitable selections about their size, shape, and surface characters, and the same NP can be used as a carrier for imaging and therapeutic purposes. The size of polymeric micelles, 10–100 nm, can be easily controlled by varying the hydrophobic block of the amphiphilic copolymer (Shuai et al. 2004). This size range also permits for evasion of renal filtration while allowing for increased tumor penetration compared to liposomes (Torchilin 2007). Micelles can also passively accumulate in the areas with leaky vasculature such as tumors, inflammation, and infarction. Despite the positive attributes, micelles are designed to evade from undesired capture by RES system and exhibit prolonged periods of blood circulation. Radioactivity is decreased with distinct half-life of each radionuclide, and time period, which can be effectively used, is limited. Therefore, radionuclide with relatively long half-life period such as ^{177}Lu is suitable for radiolabeling of polymer nanoparticles for therapy.

16.9 Inorganic NPs

Inorganic NPs have recently gained significant attention due to their unique material and size-dependent physicochemical properties, which may not be possible with their organic counterpart. In particular, characteristics such as chemical inertness, good stability, and ease of functionalization make inorganic NPs attractive for radionuclide therapy. While Inorganic NPs offer advantages in function and properties not possible with organic nanoparticle platforms, this is often at the expense of biocompatibility of inorganic nanoparticles.

16.9.1 Gold Nanoparticles

Gold NPs have received special attention in the last few years due to their appealing properties. Synthesis is straightforward and size controllability is an important feature, since the size and shape of the gold NPs can be readily controlled by tuning the synthesis procedure (Lee et al. 2012). These NPs also elicit low immunogenic response. Due to their multivalency and functional versatility, gold nanoparticle conjugates can exhibit increased targeting selectivity, augmented binding

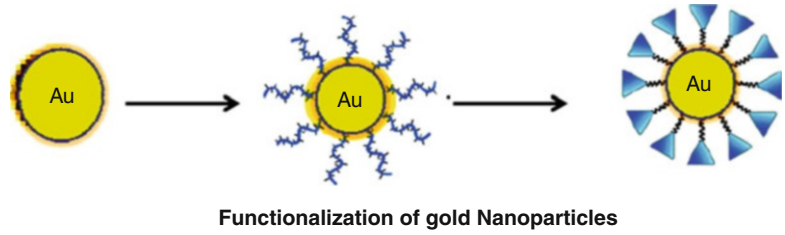

Fig. 16.8 Functionalization of gold nanoparticles

affinity, long circulatory half-life, high biocompatibility, rapid transport kinetics, and size-enhanced tumor uptake. Facile conjugation of gold nanoparticle surface to biomolecules represents one of the most stable and easily functionalized platforms for molecular conjugation. They also exhibit easy surface modification which can be modified to incorporate an array of ligands for multifunctionality such as targeted delivery. Au surfaces can be functionalized with a variety of organic self-assembled monolayers (SAMs) (e.g., thiolates, dithiolates, amines, carboxylates, cyanides, isothiocyanates, phosphines, etc.) to allow stable dispersion of particles in both aqueous and organic media (Fig. 16.8) (Love et al. 2005).

Gold is resistant to oxidation under physiological or ambient conditions, which permit unrestricted interaction of gold with the biological environment (Ying et al. 2010) and gold nanoparticles in the shape of "nanorods" have been demonstrated to actually penetrate the cell membrane. One particular advantage of using gold nanoparticle conjugates is their size-selective accumulation at tumor sites due to the enhanced permeability and retention (EPR) effect (Iyer et al. 2006). Gold nanoparticle conjugates exhibit unique properties from both their parent molecules and their particle scaffolds. They can show increased binding affinity and targeting selectivity when functionalized with multiple targeting groups, as well as tumor-selective uptake due to their size. Their intrinsic size, shape, and surface reactivity can further be exploited to direct and selectively modify cellular processes associated with malignant progression. Their widespread utilization in biological assays relies on the availability of synthetic methods yielding nanoparticles with desired characteristics including high solubility in water, adequate morphology, size dispersion, and surface functionalities.

16.10 Quantum Dots (QDs)

Quantum dots (QDs) consist of a semiconductor core and possess a cap which provides higher solubility in aqueous buffers. Quantum dots can be molded into different shapes and can be conjugated with bio-recognition ligands using the rich surface functionalization chemistry for targeted delivery applications. The QD surface can be decorated with functional groups such as carboxylic acid, primary amine, and thiol, which can be used for conjugation with targeting ligands by using conjugation chemistries such as carbodiimide, maleimide, and succinimide. Various colloidal core/shell usually synthesized are CdSe/ZnS, CdTe/CdSe, InP/ZnS, and CdSe/CdS/ZnS (Cai et al. 2006). While preparing QD formulations for targeted therapy in vivo, some guidelines must be followed. Surface of nanoparticles must be functionalized with targeting ligands for specific delivery to tumor cells and must allow the radionuclide to be delivered together with the carrier. Nanoparticle size is to be minimized to allow excretion from the body. The radionuclide must be confined within the nanoparticle delivery system to prevent any detrimental effects to the normal tissue; however, the radionuclide along with the vehicle must be released at tumor cells after being triggered externally or by local environmental factors. In order to prevent degradation or collapse of the QDs upon encounter with the biological environment, the surface of QDs must be passivated with a biocompatible polymer.

16.11 Iron Oxide Nanoparticles

The iron oxide (IO) NPs used as carrier are typically classified based on their sizes as standard super paramagnetic iron oxide (SSPIO) at 60–150 nm, ultra small, superparamagnetic iron oxide (USPIO) of approximately 5–40 nm, and monocrystalline iron oxide (MION)—a subset of USPIO ranging from 10 to 30 nm. The successful targeted use of IO nanoparticles relies critically on the conjugation with a targeting moieties and a therapeutic radionuclide through a number of conjugation strategies. Among the nanoparticle platforms, magnetic nanoparticle-based systems show particular promise. Due to their magnetic properties IO nanoparticles as carriers have been extensively useful as they facilitate fast extracellular, intracellular, and site-specific/targeted delivery of therapeutic radionuclide under the influence of an external magnetic field. Magnetic nanosystem is enticing due to its ability to become magnetized upon exposure to a magnetic field but have no permanent magnetization (remanence) once the field is turned off. IO nanoparticles can be degraded to Fe ions in the body particularly in the acidic compartments of cells (e.g., lysosomes), alleviating the potential toxicity of long-term residence of nanoparticles.

Parameters such as depth of the target tissue, rate of blood flow, and vascular supply determine the usefulness IO nanoparticles for targeted radionuclide delivery (Sun et al. 2008). Several other criteria that merit attention include NP carriers which should be stable and remain constant in size and magnetic property during the course of treatment (Fang et al. 2009). The nanoparticles must be small so that they can be superparamagnetic in order to avoid agglomeration after stopping magnetic field and to remain in circulation without being removed by the body's natural filters such as the liver or the immune system (Pankhurst et al. 2003). Magnetization of the IO NP carrier must be sufficient in response to the applied magnetic field. At the same time, exterior magnetic fields in terms of magnetic flux density and permeability should be optimized to be strong enough to mediate penetration of biotherapeutics across the biological barriers and sufficient accumulation at target sites while remaining safe to normal tissue (McBain et al. 2008).

Functionalization of IO NPs with amino group, silica, polymer, various surfactants, or other organic compounds not only provided better physical and chemical properties, but also offer good dispersibility and high stability against oxidation and provided the scope for loading appreciable amount of radioconjugate to the polymer shell (Hu et al. 2006). Furthermore, lots of functional groups from polymers on the surface can be exploited for further functionalization for propitious outcome (Parvin et al. 2007). The size of IO with coating should not exceed 100 nm in size to preclude rapid clearance by RES (Shubayev et al. 2009). Coating of IO NPs with polymers is an effective strategy to impact the stability of nanoparticles against oxidation (Faraji and Wipf 2004; Singh and Lillard 2009). The material used for surface coating must not only be nontoxic and biocompatible but also allow a targetable delivery with particle localization in a specific area.

For engineering tumor targeted-IO nanoparticles, ligands targeting the related receptors that are highly expressed in tumor cells are usually conjugated to the surface of IO nanoparticles. Conjugation of radionuclide along with targeting moiety with IO nanoparticles may be achieved by covalent binding electrostatic interactions (Figuerola et al. 2010), adsorption (Yallapu et al. 2011), or encapsulation process (Wu et al. 2010). There remain many challenges which must be addressed for the use of IO nanoparticles (Peng et al. 2008). In light of the limited concentrations of the different cellular cognate receptors expressed on the tumor cell surface, it is crucial to determine the optimal number of targeted ligands on IO nanoparticles. It is pertinent to point out that excessive amounts of targeting ligands on the IO nanoparticles may not necessarily increase binding of the IO nanoparticles to specific cells, but can increase the size of the nanoparticles. The ideal ratio of ligands and IO nanoparticles primarily depends on the number

of receptors on targeted cells, the binding affinity of ligands to receptors and the molecular weight and size of ligands. The fate of targeted IO nanoparticles after cell internalization continue to be contentious, with most reports showing that nanoparticles enter into endosomes and are then degraded in lysosomes, while other studies have shown that they can escape from the endosome and locate in the cytoplasm or around the nucleus. It seems that conjugated ligands and surface coating of IO affect the distribution of particles within the cells. The range of the concentration of IO nanoparticles used for animal studies is large, from 1 to 250 mg of Fe/kg, making it difficult to compare results from different research groups; the quantification of IO nanoparticle levels in vivo continues to be challenging.

16.12 Silica Nanoparticles

In recent years, silica nanoparticles have created interest among which silica-based nanomaterials, mesoporous silica nanoparticles (MSNs), have attracted great attention (Vallet-Regí et al. 2001; Yang et al. 2012; Tang et al. 2012; He and Shi 2011; Manzano and Vallet-Regí 2010) since these substances are chemically inert and easily modified through chemistry. Mesoporous silica nanoparticles (MSNs) have huge surface area (>700 m^2/g), large pore volume (>1 cm^3/g), tunable particle size (10–1000 nm) and pore diameter (2–30 nm), regular mesoporous structure, flexible morphology, and facile surface functionalization. They also possess excellent biocompatibility, biodegradation, and bioresorbability both in vitro and in vivo (He et al. 2010a, b; Liu et al. 2011; Zhang et al. 2014) and offer the scope for embedding of functional materials in mesoporous channels, core-shell structure, and functionalization on the surface of mesoporous silica. The highly stable pore channels prevent encapsulated radiolabeled formulation from degradation in harsh environments during administration. The textural properties of MSNs provide the possibility to load high amount of radionuclides along with carrier moieties within MSN carriers. The presence of silanol groups on the surfaces of mesoporous channels and the outer surfaces of MSNs facilitates surface functionalization to offer better control over radionuclide diffusion kinetics. Coexistence of hydrophilic surface silanol (−Si–OH) and deprotonated silanol (−Si–O–) groups at neutral pH makes MSNs water dispersible, which reduces not only nonspecific binding, but also in vivo aggregation. The external surface of MSNs can be modified with tumor-recognition molecules to increase active targetability through receptor-mediated endocytosis. Size, shape, and surface properties can be tailored to achieve efficient loading of therapeutics, tissue-specific accumulation, high levels of intracellular uptake, favorable intracellular localization, and appropriate release of therapeutics (Tang et al. 2012).

Potential clinical applications of MSNs would depend not only on the core chemistry, but also on the capacity for multiple functionalization, standardization, particle stability, and expense of components. The core–shell structured nanoparticles with magnetic core and mesoporous silica shell are considered as the most important and desirable structure owing to its ability to combine with targeting and/or hyperthermia functions (Wu et al. 2011). While the use of MSNs for the transport of radioactive payload through cell membranes and delivery into cells is appealing, there are still many technical issue which must be answered for practical applications, such as pharmacokinetics and pharmacodynamics, biodistribution, the acute and chronic toxicities, long-term in vivo degradation, and compatibility of MSNs (Chen et al. 2013). Despite the number of in vitro and animal studies (Liong et al. 2009; Rosenholm et al. 2010), the acquired limited evidence thus far on the biocompatibility, targetability, and therapeutic efficiency must be reexamined and further expanded. The reported synthesis methods to prepare functional MSNs with a core–shell structure are currently limited to laboratory scale. Therefore, large-scale synthesis routes needs to be devised for widespread use.

16.13 Summary, Challenges, and Future Directions

Nanoparticle-based targeted delivery of radionuclide as well as localization within the cell provides new opportunities to overcome the limitations associated with traditional radionuclide therapy. Nanotargeted radionuclide therapy has the ability to deliver a high payload of radionuclides to achieve multifunctional and multimodality targeting to tumor cells to enhance the efficacy as well as safety of targeted therapy. The ability of radiolabeled nanoparticles for effective targeted delivery of radioactive payloads to specific cells and subcellular components largely depends on retention, evasion, targeting (recognition), and release. Targeting to tumor cells is primarily based on the combination of a few independent phenomena involving events associated with the enhanced permeability and retention (EPR) effect, properties of nanoparticles, increased retention in the circulation, and the type of ligand–receptor interaction. The specific ligand–receptor interaction for intracellular localization will take place following blood circulation and extravasation steps, and the unique pharmacokinetics of nanoparticle carriers has strong implications in optimizing internal radiation sources with proper consideration of the half-life of the radionuclide, radiation dosages, and treatment regime.

Efficient ligand–receptor interaction is dictated by a number of factors, including the extent of expression of specific receptors on target cells relative to nontarget cells, receptor availability on the surface of the target cells, fraction of cells express a specific receptor at a given time point, expression pattern, tumor heterogeneity, the rate of internalization, and recycling of receptor after binding with ligand and other factors should also be considered for effective tumor treatment. Selection of nanoparticle carriers as well as radionuclide primarily resides on the pharmacokinetics and enhances the delivery of radioactive payloads, their therapeutic effects, and the additional functionalities offered by nanoparticle carriers. The ideal nanocarrier will be one that is size and shape specific, has the ability to incorporate the therapeutic radionuclide, and has the flexibility to be functionalized with surface targeting ligands. Continuous advances in synthetic chemistry and materials chemistry will lead to the development of new NP materials and elucidation of their properties with an aim to incorporate them within bioconjugates as well as radionuclide.

Although great strides have been made on the use of radiolabeled NPs for therapy, most of studies are proof-of-principle and more research efforts are needed to translate radiolabeled NPs to the clinical stage in the near future. As such a strategy moves forward toward clinical applications, several types of challenge emerge. Firstly, the scale/batch size of nanoparticle synthesis must be significantly increased, standardized, and streamlined. Following successful upscaling, there will be of course significant regulatory barriers and costs encountered in preparing these nanoparticles for clinical use. While the development of NP bioconjugates constitutes a successful paradigm for targeted delivery of radioactive payloads, the issue of potential toxicity needs to be thoroughly considered. Development of nanoplatforms for radionuclide therapy requires evaluation in tandem with the assessment of any toxicological side effects. In this context, detailed characterization of the NP preparations is mandatory for the initial stage of toxicity assessment.

The optimization of the nanoparticle compositions and structure, the simultaneous attainment of preferential targeting location, reduction of any immunotoxic effects, and the evasion of sequential biological barriers of the nanoparticles are the major challenges which have to be assessed. The use of multifunctional radiolabeled nanoparticles capable of not only delivering radioisotopes into targeted tumor cells but also real-time imaging for the monitoring and follow-up of the treatment represents an emerging vision and potentially important technical capability. Radiolabeled NP-based theranostic agents are expected to afford accurate and precise assessment of biological signatures in cancer in a real-time manner and, thus, pave the path towards personalized medicine in the near future. The integrated multidiscipline and multi-institute collaboration between academia, research institutes, and industry would accelerate the progression of

research into nanotargeted therapeutic radiopharmaceuticals toward clinical applications for the healthcare field.

Exciting new concepts are being so rapidly developed and many successful studies preparing specially designed molecules and radiolabeling studies have been reported in just the last decade. For these reasons and the di rigueur use of "nano," there is great hope for appropriate specific targeting for therapeutic applications. However, there is also some concern recently expressed in the literature that the expected successful use of these "nano" agents for radionuclide therapy has little likelihood (Mier et al. 2014). The real challenge is targeting, since some authors estimate that even if the transfer through the vessel wall gaps into the interstitial space is successful, the required navigation to the distant targeted tumor cell surfaces still has to be accomplished. Nonetheless, this is an exciting area of research and surely more research and time will sort out the possible clinical applications.

References

Albanell J, Baselga J. Trastuzumab. A humanized anti-HER2 monoclonal antibody, for the treatment of breast cancer. Drugs Today. 1999;35:931–46.

Alexis F, Basto P, Levy-Nissenbaum E, et al. HER-2-targeted nanoparticle–affibody bioconjugates for cancer therapy. Chem Med Chem. 2008;3:1839–43.

Allen TM. Ligand-targeted therapeutics in anticancer therapy. Nat Rev Cancer. 2002;2:750–63.

Allen TM, Cullis PR. Drug delivery systems: entering the mainstream. Science. 2004;303:1818–22.

Allen TM, Hansen C. Pharmacokinetics of stealth versus conventional liposomes: effect of dose. Biochim Biophys Acta. 1991;1068:133–41.

Alloatti D, Giannini G, Vesci L, et al. Camptothecins in tumor homing via an RGD sequence mimetic. Bioorg Med Chem Lett. 2012;22(20):6509–12.

André S, Frisch B, Kaltner H, Desouza D, et al. Lectin-mediated drug targeting: selection of valency, sugar type (Gal/Lac), and spacer length for cluster glycosides as parameters to distinguish ligand binding to C-type asialoglycoprotein receptors and galectins. Pharm Res. 2000;17:985–90.

Astolfo A, Schültke E, Menk RH, et al. In vivo visualization of gold-loaded cells in mice using x-ray computed tomography. Nanomedicine. 2013;9(2):284–92.

Bae YH. Drug targeting and tumor heterogeneity. J Control Release. 2009;133:2–3.

Bae YH, Park K. Targeted drug delivery to tumors: myths, reality and possibility. J Controlled Release. 2011; 153:198–205.

Bai S, Thomas C, Rawat A, Ahsan F. Recent progress in dendrimer-based nanocarriers. Crit Rev Ther Drug Carrier Syst. 2006;23:437–95.

Bao A, Goins B, Klipper R, et al. Re-186-liposome labeling using Re-186-SNS/S complexes: in vitro stability, imaging, and biodistribution in rats. J Nucl Med. 2003;44:1992–9.

Barua S, Yoo JW, Kolhar P, Wakankar A, Gokarn YR, Mitragotri S, et al. Particle shape enhances specificity of antibody-displaying nanoparticles. Proc Natl Acad Sci. 2013;110(9):3270–5.

Bayraktar H, You C-C, Rotello VM, Knapp MJ. Facial control of nanoparticle binding to cytochrome c. J Am Chem Soc. 2007;129:2732–3.

Bhang SH, Won N, Lee T, et al. Hyaluronic acid-quantum dot conjugates for in vivo lymphatic vessel imaging. ACS Nano. 2009;3:1389–98.

Brahmachari S, Ghosh M, Dutta S, Das PK. Biotinylated amphiphile-single walled carbon nanotube conjugate for target-specific delivery to cancer cells. J Mater Chem. 2014;B2:1160–73.

Brigger I, Dubernet C, Couvreur P. Nanoparticles in cancer therapy and diagnosis. Adv Drug Deliv Rev. 2012;54:631–51.

Byrne JD, Betancourt T, Brannon-Peppas L. Active targeting schemes for nanoparticle systems in cancer therapeutics. Adv Drug Deliv Rev. 2008;60:1615–26.

Cai W, Shin DW, Chen K, et al. Peptide-labeled near-infrared quantum dots for imaging tumor vasculature in living subjects. Nano Lett. 2006;6:669–76.

Capone PM, Papsidero LD, Chu TM. Relationship between antigen density and immunotherapeutic response elicited by monoclonal antibodies against solid tumors. J Natl Cancer Inst. 1984;72:673–7.

Carlson B. Aptamers: the new frontier in drug development? Biotechnol Health Care. 2007;4:32–6.

Chen Y, Chen HR, Shi JL. In vivo biosafety evaluations and diagnostic/therapeutic applications of chemically designed mesoporous silica nanoparticles. Adv Mater. 2013;25:3144–76.

Cho CS, Park IK, Cho CS. Galactosylated Poly(ethylene gly-col)-Chitosan – graft- Polyethylenimine as a gene carrier for hepatocyte-targeting. J Control Release. 2008;131:150–7.

Colcher D, Pavlinkova G, Beresford G, et al. Pharmacokinetics and biodistribution of genetically engineered antibodies. Q J Nucl Med. 1998;42: 225–41.

Daniels TR, Bernabeu E, Rodriguez JA, et al. The transferrin receptor and the targeted delivery of therapeutic agents against cancer. Biochim Biophys Acta. 2012;1820:291–317.

Dill K, Lin M, Poteras C, Fraser C, et al. Antibody-antigen binding constants determined in solution-phase with the threshold membrane-capture system-binding constants for antifluorescein, anti-saxitoxin, and anti-ricin antibodies. Anal Biochem. 1994;217:128–38.

Doi KT, Akaike H, Horie Y, et al. Excessive production of nitric oxide in rat solid tumor and its implication in rapid tumor growth. Cancer. 1996;77:1598–604.

Dreher MR, Liu W, Michelich CR, et al. Tumor vascular permeability, accumulation, and penetration of macromolecular drug carriers. J Natl Cancer Inst. 2006;98:335–44.

Drolet DW, Nelson J, Tucker CE, et al. Pharmacokinetics and safety of an anti-vascular endothelial growth factor aptamer (NX1838) following injection into the vitreous humor of rhesus monkeys. Pharm Res. 2000;17:1503–10.

Duncan R, Vincent MJ, Greco F, et al. Polymer–drug conjugates: towards a novel approach for the treatment of endocrine-related cancer. Endocrinol Relat Cancer. 2005;12:S189–S19.

Ellington AD, Ebright J, Chu T, Levy M. Using aptamers for cell-specific labeling and delivery. In: American Association for Cancer Research education book. Philadelphia: American Association for Cancer Research; 2007. p. 51–5.

Fahmy TM, Samstein RM, Harness CC, Saltzman WM. Surface modification of biodegradable polyesters with fatty acid conjugates for improved drug targeting. Biomaterials. 2005;26:5727–36.

Fang C, Bhattarai N, Sun C, Zhang M. Functionalized nanoparticles with long-term stability in biological media. Small. 2009;5:1637–41.

Faraji A, Wipf P. Nanoparticles in cellular drug delivery. Bioorg Med Chem. 2004;17:2950–62.

Farokhzad OC, Jon S, Khademhosseini A, et al. Nanoparticle–aptamer bioconjugates. A new approach for targeting prostate cancer cells. Cancer Res. 2004;64:7668–72.

Farokhzad OC, Karp JM, Langer R. Nanoparticle–aptamer bioconjugates for cancer targeting. Expert Opin Drug Deliv. 2006;3:311–24.

Ferrara N. VEGF as a therapeutic target in cancer. Oncology. 2005;69:11–6.

Figuerola A, Di Corato R, Manna L, Pellegrino T. From iron oxide nanoparticles towards advanced iron-based inorganic materials designed for biomedical applications. Pharmacol Res. 2010;62:126–43.

Fischer MJ. Amine coupling through EDC/NHS: a practical approach. In: Nico NJ, Fisher MJE, editors. Surface Plasmon Reson. New York: Humana Press: 2010:55–73. ISBN 978-1-60761-670-2.

Foraker AB, Khantwal CM, Swaan PW. Current perspectives on the cellular uptake and trafficking of riboflavin. Adv Drug Deliv Rev. 2003;55:1467–83.

Galow TH, Boal AK, Rotello VM. "Building block" approach to mixed-colloid systems through electrostatic self-organization. Adv Mater. 2000;12:576–9.

Gao XH, Cui YY, Levenson RM, et al. In vivo cancer targeting and imaging with semiconductor quantum dots. Nat Biotechnol. 2004;22:969–76.

Gao J, Feng SS, Guo Y. Antibody engineering promotes nanomedicine for cancer treatment. Nanomedicine. 2010;5:1141–5.

Gao WL, Ji L, Li G, Cui K, Xu P, Tang B. Bifunctional combined Au-Fe_2O_3 nanoparticles for induction of cancer cell-specific apoptosis and real-time imaging. Biomaterials. 2012;33:710–3718.

Gregory AE, Titball R, Williamson D. Vaccine delivery using nanoparticles. Front Cell Infect Microbiol. 2013;3:13.

Gunthert U, Hofmann M, Rudy W, et al. A new variant of glycoprotein CD44 confers metastatic potential to rat carcinoma cells. Cell. 1991;65:13–24.

Hanahan D, Weinberg RA. Hall marks of cancer: the next generation. Cell. 2011;144:646–74.

Harrington KJ, Mohammadtaghi S, Uster PS, et al. Effective targeting of solid tumors in patients with locally advanced cancers by radiolabeled PEGylated liposomes. Clin Cancer Res. 2001;7:243–54.

He QJ, Shi JL. Mesoporous silica nanoparticle based nano drug delivery systems: synthesis, controlled drug release and delivery, pharmacokinetics and biocompatibility. J Mater Chem. 2011;21:5845–55.

He C, Hu Y, Yin L, et al. Effects of particle size and surface charge on cellular uptake and biodistribution of polymeric nanoparticles. Biomaterials. 2010a;31:3657–66.

He QJ, Shi JL, Zhu M, Chen Y, Chen F. The three-stage *in vitro* degradation behavior of mesoporous silica in simulated body fluid. Micropor Mesopor Ma. 2010b;131:314–20.

Hicke BJ, Stephens AW. Escort aptamers: a delivery service for diagnosis and therapy. J Clin Invest. 2000;106:923–8.

Hild W, Pollinger K, Caporale A, Cabrele C, Keller M, Pluym N, Buschauer A, Rachel R, Tessmar J, Breunig M, Goepferich A. G protein-coupled receptors function as logic gates for nanoparticle binding and cell uptake. Proc Natl Acad Sci USA. 2010;107:10667–72.

Hilgenbrink AR, Low PS. Folate receptor-mediated drug targeting: from therapeutics to diagnostics. J Pharm Sci. 2005;94:2135–46.

Ho JA, Hung CH. Using liposomal fluorescent biolabels to develop an immunoaffinity chromatographic biosensing system for biotin. Anal Chem. 2008;80:6405–9.

Hobbs SK, Monsky WL, Yuan F, et al. Regulation of transport pathways in tumor vessels: role of tumor type and microenvironment. Proc Natl Acad Sci U S A. 1998;95:4607–12.

Hoefnagel CA. Radionuclide cancer therapy. Ann Nucl Med. 1998;12:61–70.

Hofheinz RD, al-Batran SE, Hartmann F, et al. Stromal antigen targeting by a humanized monoclonal antibody: an early phase II trial of sibrotuzumab in patients with metastatic colorectal cancer. Onkologie. 2003;26:44–4.

Holliger P, Hudson P. Engineered antibody fragments and the rise of single domains. Nat Biotechnol. 2005;23(9):1126–36.

Holmberg RJ, Bolduc S, Beauchemin D, et al. Characteristics of colored passive layers on zirconium: morphology, optical properties, and corrosion resistance. ACS Appl Mater Interfaces. 2012;4:6487–98.

Hong R, Fischer NO, Verma A, et al. Control of protein structure and function through surface recognition by

tailored nanoparticle scaffolds. J Am Chem Soc. 2004;126:739–43.
Hu FX, Neoh KG, Kang ET. Synthesis and in vitro anticancer evaluation of tamoxifen-loaded magnetite/PLLA composite nanoparticles. Biomaterials. 2006; 27:5725–33.
Huang G, Zhou Z, Srinivasan R, et al. Affinity manipulation of surface-conjugated RGD peptide to modulate binding of liposomes to activated platelets. Biomaterials. 2008;29(11):1676–85.
Huang YF, Lin YW, Lin Z-H, Chang HT. Aptamer-modified gold nanoparticles for targeting breast cancer cells through light scattering. J Nanopart Res. 2009;11:775–83.
Huang FY, Lee J, Kao TW, et al. Imaging, autoradiography, and biodistribution of Re- 188-labeled PEGylated nanoliposome in orthotopicglioma bearing rat model. Cancer Biother Radiopharm. 2011;26:717–25.
Iyer AK, Khaled G, Fang J, Maeda H. Exploiting the enhanced permeability and retention effect for tumor targeting. Drug Discov Today. 2006;11:812–8.
James JS, Dubs G. FDA approves new kind of lymphoma treatment. AIDS Treat News. 1997;284:2–3.
Jenison RD, Gill SC, Pardi A, Polisky B. High-resolution molecular discrimination by RNA. Science. 1994;263(5152):1425–9.
Jiang XZ, Housni A, Gody G, et al. Synthesis of biotinylated alpha-D-mannoside or N-acetyl beta-D-glucosaminoside decorated gold nanoparticles: study of their biomolecular recognition with Con A and WGA lectins. Bioconjug Chem. 2010;21:521–30.
Kamaly N, Xiao Z, Valencia PM, et al. Targeted polymeric therapeutic nanoparticles: design, development and clinical translation. Chem Soc Rev. 2012;41: 2971–3010.
Kataoka K, Harada A, Nagasaki Y. Block copolymer micelles for drug delivery: design, characterization and biological significance. Adv Drug Deliv Rev. 2001;47:113–31.
Khosroshahi AG, Amanlou M, Sabzevari O, et al. A comparative study of two novel nanosized radiolabeled analogues of methionine for SPECT tumor imaging. Curr Med Chem. 2013;20:123–33.
Kikkeri R, Lepenies B, Adibekian A, et al. In vitro imaging and in vivo liver targeting with carbohydrate capped quantum dots. J Am Chem Soc. 2009; 131:2110–2.
Kim EM, Jeong HJ, Moon MH. Asialoglycoprotein receptor targeted gene delivery using galactosylated polyethylenimine-graft -poly (ethylene glycol): in vitro and in vivo studies. J Control Release. 2005;108:557–67.
Kocbek PN, Obermajer M, Cegnar J, et al. Targeting cancer cells using PLGA nanoparticles surfacemodified-with monoclonal antibody. J Control Release. 2007; 120:18–26.
Kostarelos K, Emfietzoglou D. Tissue dosimetry of liposome-radionuclide complexes for internal radiotherapy: toward liposome-targeted therapeutic radiopharmaceuticals. Anticancer Res. 2000;20:3339–45.
Kostarelos K, Emfietzoglou D, Stamatelou M. Liposome-mediated delivery of radionuclides to tumor models for cancer radiotherapy: a quantitative analysis. J Liposome Res. 1999;9:407–42.
Kresse M, Wagner S, Pfefferer D, et al. Targeting of ultra small super paramagnetic iron oxide(USPIO) particles to tumor cells *in vivo* by using transferring receptor pathways. Magn Reson Med. 1998;40:236–42.
Kukowska-Latallo JF, Candido KA, Cao Z, et al. Nanoparticle targeting of anticancer drug improves therapeutic response in animal model of human epithelial cancer. Cancer Res. 2005;65:5317–24.
Laverman P, Carstens MG, Boerman OC, et al. Factors affecting the accelerated blood clearance of polyethylene glycol-liposomes upon repeated injection. J Pharmacol Exp Ther. 2001;298:607–12.
Lee JF, Stovall GM, Ellington AD. Aptamer therapeutics advance. Curr Opin Chem Biol. 2006;10(3):282–9.
Lee JS, Ankone M, Pieters E, et al. Circulation kinetics and biodistribution of dual-labeled polymersomes with modulated surface charge in tumor-bearing mice: comparison with stealth liposomes. J Control Release. 2011;155:282–8.
Lee DE, Koo H, Sun IC, et al. Multifunctional nanoparticles for multimodal imaging and theragnosis. Chem Soc Rev. 2012;41:2656–72.
Li YM, Hall WA. Targeted toxins in brain tumor therapy. Toxins. 2010;2:2645–62.
Li LL, Xie M, Wang J, et al. Vitamin-responsive mesoporous nanocarrier with DNA aptamer-mediated cell targeting. Chem Commun. 2013;49:5823–5.
Liong M, Angelos S, Choi E, et al. Mesostructured multifunctional nanoparticles for imaging and drug delivery. J Mater Chem. 2009;19:6251–7.
Litzinger DC, Buiting AM, van Rooijen N, Huang L. Effect of liposome size on the circulation time and intraorgan distribution of amphipathic poly(ethylene glycol)-containing liposomes. Biochim Biophys Acta. 1994;1190:99–107.
Liu Z, Cai W, He L, et al. *In vivo* biodistribution and highly efficient tumour targeting of carbon nanotubes in mice. Nat Nanotechnol. 2007;2:47–52.
Liu T, Li L, Teng X, et al. Single and repeated dose toxicity of mesoporous hollow silica nanoparticles in intravenously exposed mice. Biomaterials. 2011;32: 1657–68.
Love JC, Estroff LA, Kriebel JK, et al. Self-assembled monolayers of thiolates on metals as a form of nanotechnology. Chem Rev. 2005;105:1103–70.
Low PS, Henne WA, Doorneweerd DD. Discovery and development of folic-acid-based receptor targeting for imaging and therapy of cancer and inflammatory diseases. Acc Chem Res. 2008;41:120–9.
Lupold SE, Hicke BJ, Lin Y, CoVey DS. Identification and characterization of nuclease-stabilized RNA molecules that bind human prostate cancer cells via the prostate-specific membrane antigen. Cancer Res. 2002;62:4029–33.
Maeda H. Polymer conjugated macromolecular drugs for tumor-specific targeting. In: Domb AJ, editor.

Polymeric site-specific pharmacotherapy. New York: John Wiley & Sons; 1994. p. 95–116.
Maeda H, Noguchi Y, Sato K, Akaike T. Enhanced vascular permeability in solid tumor is mediated by nitric oxide and inhibited by both new nitric oxide scavenger and nitric oxide synthase inhibitor. Jpn J Cancer Res. 1994;85:331–4.
Maeda H, Akaike T, Wu J, Noguchi Y, Sakata Y. Bradykinin and nitric oxide in infectious disease and cancer. Immunopharmacology. 1996;33:222–30.
Maeda H, Fang F, Inuzuka T, et al. Vascular permeability enhancement in solid tumor: various factors, mechanisms involved and its implications. Int Immunopharmacol. 2003;3:319–28.
Manzano M, Vallet-Regí M. New developments in ordered mesoporous materials for drug delivery. J Mater Chem. 2010;20:5593–604.
Markert S, Lassmann S, Gabriel B, et al. Alpha-folate receptor expression in epithelial ovarian carcinoma and non-neoplastic ovarian tissue. Anticancer Res. 2008;28:3567–72.
Marrache S, Dhar S. Engineering of blended nanoparticle platform for delivery of mitochondria-acting therapeutics. Proc Natl Acad Sci U S A. 2012;109:16288–93.
Matsumura Y, Maeda H. A new concept for macromolecular therapeutics in cancer chemotherapy: mechanism of tumoritropic accumulation of proteins and the antitumor agent SMANCS. Cancer Res. 1986;46:6387–92.
McBain SC, Griesenbach U, Xenariou S, et al. Magnetic nanoparticles as gene delivery agents: enhanced transfection in the presence of oscillating magnet arrays. Nanotechnology. 2008;19(40):405102.
McLaughlin MF, Robertson D, Pevsner PH, Wall JS, Mirzadeh S, Kennel SJ. $LnPO_4$ nanoparticles doped with Ac-225 and sequestered daughters for targeted alpha therapy. Cancer Biother Radiopharm. 2014; 29(1):34–41.
Mier W, Babich J, Haberkorn U. Is nano too big? Eur J Nucl Med Mol Imaging. 2014;41:4–6.
Muller RH, Wallis KH. Surface modification of i.v. injectable biodegradable nanoparticles with poloxamer polymers and poloxamine 908. Int J Pharm. 1993; 89:25–31.
Nakanishi T, et al. Development of the polymer micelle carrier system for doxorubicin. J Control Release. 2001;74:295–302.
Oda T, Maeda H. Binding to and internalization by cultured cells of neocarzinostatin and enhancement of its actions by conjugation with lipophilic styrene-maleic acid copolymer. Cancer Res. 1987;47:3206–11.
Oda T, Morinaga T, Maeda H. Stimulation of macrophage by polyanions and its conjugated proteins and effect on cell membrane. Proc Soc Exp Biol Med. 1986; 181:9–17.
Osborne MP, Richardson VJ, Jeyasingh K, Ryman BE. Radionuclide-labeled liposomes – a new lymph node imaging agent. Int J Nucl Med Biol. 1979;6:75–83.
Pan W, Yang H, Zhang T, et al. Dual-targeted nanocarrier based on cell surface receptor and intracellular mRNA: an effective strategy for cancer cell imaging and therapy. Anal Chem. 2013;85:6930–5.
Pankhurst QA, Connolly J, Jones SK, Dobson J. Applications of magnetic nanoparticles in biomedicine. J Phys D Appl Phys. 2003;36:R167–81.
Papa A-L, Basu S, Sengupta P, et al. Mechanistic studies of Gemcitabine-loaded nanoplatforms in resistant pancreatic cancer cells. BMC Cancer. 2012;12: 419–30.
Park J, Mattessich T, Jay SM, et al. Enhancement of surface ligand display on PLGA nanoparticles with amphiphilic ligand conjugates. J Control Release. 2011;156:109–15.
Parrott MC, Benhabbour SR, Saab C, et al. Synthesis, radiolabeling, and bio-imaging of high-generation polyester dendrimers. J Am Chem Soc. 2009;131: 2906–16.
Parvin S, Matsui J, Sato E, Miyashita T. Side-chain effect on Langmuir and Langmuir–Blodgett film properties of poly(n-alkylmethacrylamide)-coated magnetic nanoparticle. J Colloid Interface Sci. 2007;313: 128–34.
Patil YB, Toti US, Khdair A, Ma L, Panyam J. Single-step surface functionalization of polymeric nanoparticles for targeted drug delivery. Biomaterials. 2009;30: 859–66.
Peng XH, Qian X, Mao H, et al. Targeted magnetic iron oxide nanoparticles for tumor imaging and therapy. Int J Nanomedicine. 2008;3(3):311–21.
Platt VM, Szoka Jr FC. Anticancer therapeutics: targeting macromolecules and nanocarriers to hyaluronan or CD44, a hyaluronan receptor. Mol Pharm. 2008;5:474–86.
Potapova R, Mruk R, Prehl S, Mews A, et al. Semiconductor Nanocrystals with Multifunctional Polymer Ligands. J Am Chem Soc. 2003;125:320–1.
Quan Q, Xie J, Gao H, et al. HSA coated iron oxide nanoparticles as drug delivery vehicles for cancer therapy. Mol Pharm. 2011;8:1669–76.
Rana K, Reinhart-King CA, King MR. Inducing Apoptosis in Rolling Cancer Cells: A Combined Therapy with Aspirin and Immobilized TRAIL and E-Selectin. Mol Pharm. 2012;9:2219–27.
Rojas JV, Woodward JD, Chen N, et al. Synthesis and characterization of lanthanum phosphate nanoparticles as carriers for 223Ra and 225Ra for targeted alpha therapy. Nucl Med Biol. 2015;42(7):614–20.
Rosenholm JM, Peuhu E, Bate-Eya LT, et al. Cancer-cell-specific induction of apoptosis using mesoporous silica nanoparticles as drug-delivery vectors. Small. 2010;6:1234–41.
Sahoo SK, Labhasetwar V. Nanotech approaches to drug delivery and imaging. Drug Discov Today. 2003;8: 1112–20.
Satija J, Gupta U, Jain NK. Pharmaceutical and biomedical potential of surface engineered dendrimers. Crit Rev Ther Drug Carrier Syst. 2007;24:257–306.
Schiffelers RM, Ansari A, Xu J, et al. Cancer siRNA therapy by tumor selective delivery with ligand-targeted sterically stabilized nanoparticle. Nucleic Acids Res. 2004;32(19):e149.

Senior JH. Fate and behavior of liposomes in vivo: a review of controlling factors. Crit Rev Ther Drug Carrier Syst. 1987;3:123–93.

Shen Z, Wei W, Tanaka H, et al. A galactosamine-mediated drug delivery carrier for targeted liver cancer therapy. Pharmacol Res. 2011;64:410–9.

Shenoi MM, Iltis I, Choi J, et al. Nanoparticle delivered vascular disrupting agents (VDAs): use of TNF-alpha conjugated gold nanoparticles for multimodal cancer therapy. Mol Pharm. 2013;10:1683–94.

Shi M, Lu J, Shoichet MS. Organic nanoscale drug carriers coupled with ligands for targeted drug delivery in cancer. J Mater Chem. 2009;19:5485–98.

Shi J, Xiao Z, Kamaly N, Farokhzad OC. Self-assembled targeted nanoparticles: evolution of technologies and bench to bedside translation. Acc Chem Res. 2011;44:123–34.

Shuai X, Ai H, Nasongkla N, Kim S, Gao J. Micellar carriers based on block copolymers of poly(epsilon-caprolactone) and poly(ethylene glycol) for doxorubicin delivery. J Control Release. 2004;98:415–26.

Shubayev VI, Pisanic TR, Jin SH. Magnetic nanoparticles for theragnostics. Adv Drug Deliv Rev. 2009;61:467–77.

Singh R, Lillard JW. Nanoparticle-based targeted drug delivery. Exp Mol Pathol. 2009;86:215–23.

Smiljanic N, Moreau V, Yockot D, et al. Supramolecular control of oligosaccharide–protein interactions: switchable and tunable ligands for concanavalin a based on β-cyclodextrin. Angew Chem Int Ed. 2006;45:5465–8.

Smith RAJ, Porteous CM, Gane AM, Murphy MP. Delivery of bioactive molecules to mitochondria in vivo. Proc Natl Acad Sci U S A. 2003;100:5407–12.

Soundararajan A, Bao A, Phillips WT, et al. [^{186}Re] Liposomal doxorubicin (Doxil): in vitro stability, pharmacokinetics, imaging and biodistribution in a head and neck squamous cell carcinoma xenograft model. Nucl Med Biol. 2009;36:515–24.

Sun C, Lee JSH, Zhang MQ. Magnetic nanoparticles in MR imaging and drug delivery. Adv Drug Deliv Rev. 2008;60:1252–65.

Sutton D, Nasongkla N, Blanco E, Gao J. Functionalized micellar systems for cancer targeted drug delivery. Pharm Res. 2007;24:1029–46.

Tanaka S, Akaike T, Wu SJ, et al. Modulation of tumor-selective vascular blood flow and extravasation by the stable prostaglandin I2 analogue beraprost sodium. J Drug Target. 2003;11:45–52.

Tang FQ, Li LL, Chen D. Mesoporous silica nanoparticles: synthesis, biocompatibility and drug delivery. Adv Mater. 2012;24:1504–34.

Teply BA, Rocha FG, Levy-Nissenbaum E, et al. Nanoparticle-aptamer bioconjugates for targeted anti-neoplastic drug delivery. Am J Drug Deliv. 2006;4:123–30.

Torchilin VP. PEG-based micelles as carriers of contrast agents for different imaging modalities. Adv Drug Deliv Rev. 2002;54:235–52.

Torchilin VP. Micellar nanocarriers: pharmaceutical perspectives. Pharm Res. 2007;24:1–16.

Tsuchiya K, Nitta N, Sonoda A, et al. Evaluation of atherosclerotic lesions using dextran- and mannan-dextran-coated uspio: Mri analysis and pathological findings. Int J Nanomedicine. 2012;7:2271–80.

Ulrich AS. Biophysical aspects of using liposomes as delivery vehicles. Biosci Rep. 2002;22:129–50.

Vallet-Regí M, Rámila A, del Real RP, Pérez-Pariente J. A new property of MCM-41: drug delivery system. Chem Mater. 2001;13:308–11.

Van Cutsem E, Köhne CH, et al. Cetuximab and chemotherapy as initial treatment for metastatic colorectal cancer. N Engl J Med. 2009;360:1408–17.

Wang Z, Cuschieri A. Tumour cell labelling by magnetic nanoparticles with determination of intracellular iron content and spatial distribution of the intracellular iron. Int J Mol Sci. 2013;14:9111–25.

Wang AZ, Bagalkot V, Gu F, et al. Novel targeted aptamer–super paramagnetic iron oxide nanoparticle bioconjugates for combined prostate cancer imaging and therapy. Int J Rad Oncol Biol Phys. 2007;69 Suppl 1:S110–1.

Wang Y, Chen J, Irudayaraj J. Nuclear targeting dynamics of gold nanoclusters for enhanced therapy of HER2+ breast cancer. ACS Nano. 2011;5:9718–25.

Wang C, Ma X, Ye S, et al. Protamine Functionalized Single-Walled Carbon Nanotubes for Stem Cell Labeling and In Vivo Raman/Magnetic Resonance/Photoacoustic Triple-Modal Imaging. Adv Funct Mater. 2012;22:2363–75.

Weber C, Reiss S, Langer K. Preparation of surface modified protein nanoparticles by introduction of sulfhydryl groups. Int J Pharm. 2000;211:67–78.

Weissleder R, Kelly K, Sun EY, et al. Cell-specific targeting of nanoparticles by multivalent attachment of small molecules. Nat Biotechnol. 2005;23:1418–23.

White RR, Sullenger BA, Rusconi CP. Developing aptamers into therapeutics. J Clin Invest. 2000;106:929–34.

Wu J, Chu CC. Water insoluble cationic poly(ester amide) s: synthesis, characterization and applications. J Mater Chem. 2013;B1:353–60.

Wu J, Akaike T, Maeda H. Modulation of enhanced vascular permeability in tumors by a bradykinin antagonist, a cyclooxygenase inhibitor, and a nitric oxide scavenger. Cancer Res. 1998;58:159–65.

Wu J, Akaike T, Hayashida K, Okamoto T, et al. Enhanced vascular permeability in solid tumor involving peroxynitrite and matrix metalloproteinase. Jpn J Cancer Res. 2001;92:439–51.

Wu W, Chen B, Cheng J, et al. Biocompatibility of Fe3O4/DNR magnetic nanoparticles in the treatment of hematologic malignancies. Int J Nanomedicine. 2010;5:1079–84.

Wu H, Liu G, Zhang S, Shi J, Zhang L, et al. Biocompatibility, MR imaging and targeted drug delivery of a rattle-type magnetic mesoporous silica nanosphere system conjugated with PEG and cancer-cell-specific ligands. J Mater Chem. 2011;21:3037–45.

Xing Y, Zhao J, Conti PS, Chen K. Radiolabeled nanoparticles for multimodality tumor imaging. Theranostics. 2014;4:290–306.

Xu X, Zhang Y, Wang X, et al. Radiosynthesis, biodistribution and micro-SPECT imaging study of dendrimer-avidin conjugate. Bioorg Med Chem. 2011;19: 1643–8.

Yallapu MM, Othman SF, Curtis ET, et al. Multi-functional magnetic nanoparticles for magnetic resonance imaging and cancer therapy. Biomaterials. 2011;32:1890–905.

Yang Y, Zhang Z, Chen L, et al. Galactosylated poly(2-(2-aminoethoxy)ethoxy)phosphazene/DNA complex nanoparticles: in vitro and in vivo evaluation for gene delivery. Biomacromolecules. 2010;11:927–33.

Yang P, Gai S, Lin J. Functionalized mesoporous silica materials for controlled drug delivery. Chem Soc Rev. 2012;41:3679–98.

Yao N, Xiao W, Wang X, et al. Discovery of targeting ligands for breast cancer cells using the one-bead one-compound combinatorial method. J Med Chem. 2009;52(1):126–33.

Yaun F, Dellian M, Fukumura D, et al. Vascular permeability in a human tumor xenograft: molecular size dependence and cutoff size. Cancer Res. 1995;55:3752–6.

Ying X, Wen HE, Lu WL, et al. Dual-targeting daunorubicin liposomes improve the therapeutic efficacy of brain glioma in animals. J Control Release. 2010;141:183–92.

Yumura K, Ui M, Doi H, et al. Mutations for decreasing the immunogenicity and maintaining the function of core streptavidin. Protein Sci. 2013;22:13–221.

Zhang L, Radovic-Moreno AF, Alexis F, et al. Co-delivery of hydrophobic and hydrophilic drugs from nanoparticle–aptamer bioconjugates. ChemMedChem. 2007; 2:1268–71.

Zhang H, Ma Y, Sun XL. Recent developments in carbohydrate-decorated targeted drug/gene delivery. Med Res Rev. 2010a;30:270–89.

Zhang Y, Sun Y, Xu X, et al. Synthesis, biodistribution, and microsingle photon emission computed tomography (SPECT) imaging study of technetium-99m labeled PEGylated dendrimer poly(amidoamine) (PAMAM)-folic acid conjugates. J Med Chem. 2010b;53:3262–72.

Zhang Y, Sun Y, Xu X, et al. Radiosynthesis and micro-SPECT imaging of 99mTc-dendrimer poly(amido)-amine folic acid conjugate. Bioorg Med Chem Lett. 2010c;20:927–31.

Zhang F, Lees E, Amin F, et al. Polymer-coated nanoparticles: a universal tool for biolabelling experiments. Small. 2011;7:3113–27.

Zhang Q, Neoh KG, Xu LQ, et al. Functionalized mesoporous silica nanoparticles with muco adhesive and sustained drug release properties for potential bladder cancer therapy. Langmuir. 2014;30:6151–61.

Zhao F, Zhao Y, Liu Y, et al. Cellular uptake, intracellular trafficking, and cytotoxicity of nanomaterials. Small. 2011;7:1322–37.

Zweit J. Radionuclides and carrier molecules for therapy. Phys Med Biol. 1996;41:1905–14.

17 Translation of Radiopharmaceuticals from Bench to Bedside: Regulatory and Manufacturing Issues

17.1 Introduction

Radiopharmaceuticals are administered by parental routes and must comply with strictly controlled sterility requirements and, where relevant, aseptic working conditions are required for the manufacture of sterile medicinal products. The RPh manufacturing process must adhere to Quality Assurance (QA) requirements incorporating Good Manufacturing Practice (GMP) and thus Quality Control (QC) procedures which must not only be well documented, but which must also be effectively monitored (Cox et al. 1994). The cGMP compliance covers the manufacturing process and facility, quality guidelines, and personnel training. The term cGMP is used to define the latest best practice for the manufacture of pharmaceutical and allied products in various countries around the world (Decristoforo et al. 2008; Gouveia et al. 2015). Good manufacturing practice (GMPs) is that part of quality assurance which ensures that RPhs are consistently produced and controlled to the quality standards appropriate to their intended use and as required by the product specification. The GMP is concerned with both production and quality control. In this chapter, the basic concepts of QA, GMP, and QC are interrelated and are described to emphasize their relationships and importance in the endeavor of radiopharmaceutical production and control.

17.2 The Radiopharmaceutical Manufacturing Process Elements

17.2.1 Quality Assurance (QA)

Quality assurance (QA) encompasses all parameters which individually or collectively concern the preparation and control of a finished product (Khurshid and Sadiq 1996). The QA criteria for radiopharmaceuticals include appearance, radiochemical purity/yield, radiochemical stability, radionuclide purity, radionuclide identity, assay for radioactivity, specific activity, pH, chemical purity, residual solvents, bacterial endotoxins (BET), and sterility (Cohen 1975). QA is of paramount importance for the manufacture of radiopharmaceuticals because of their unique characteristics, which include the administration of often very small sub-pharmaceutical mass, which in itself does not illicit a pharmaceutical response. In addition, RPhs are often administered in low volumes, and in some circumstances with ultra-short-lived radioisotopes (i.e., short-lived positron-emitting radioisotopes (^{11}C, $t_{1/2}$ 20 min; ^{18}F, $t_{1/2}$ 110 min, etc.), it is even necessary to administer the product before testing is complete. In these cases, extensive preclinical evaluation has substantiated the product sterility in multiple batches. QA is commonly broadly used for the confirmation and validity of various ways and measurements adopted to obtain

F.F. (Russ) Knapp, A. Dash, *Radiopharmaceuticals for Therapy*, DOI 10.1007/978-81-322-2607-9_17

a high-quality procedure with the objective of ensuring that pharmaceutical products are of the quality required for their intended use.

For these reasons, the manufacture of radiopharmaceuticals should ensure that they are designed and developed in a way that takes account of the requirements of GMP, good laboratory practice (GLP), and good clinical practice (GCP) (Decristoforo and Peñuelas 2009; Woldring 1999; De Vos et al. 2006; Otte and Maier-Lenz Dierckx 2005; Elsinga et al. 2010). The required production and control operations must be available in a clearly documented format and follow GMP requirements. The requirements for responsible individuals must be clearly specified and appropriate arrangements must be in place for the manufacture, supply, and use of the approved raw and packaging materials. All necessary controls must be conducted by well-defined and documented procedures for starting materials, including the radionuclide, intermediate products, and bulk products. These include in-process controls, calibrations, and validations. The radiopharmaceutical product must be correctly formulated and checked, according to defined procedures. Radiopharmaceuticals cannot be approved for commercial availability or supplied for patient use before an authorized individual has certified that each production batch has been produced and controlled in accordance with the requirements of the marketing authorization and any other regulations relevant to the production, control, and release of medicinal products. Satisfactory arrangements must also be developed to ensure, as far as possible, that RPhs are stored, distributed, and subsequently handled so that quality is sustained throughout their specified shelf life. In addition, procedures must be in place for self-inspection and/or quality audit to regularly appraise the effectiveness and applicability of the quality assurance system. Any deviations in any of these requirements are required to be reported, investigated, and recorded, and there are systems in place for approving changes that may have an impact on product quality. Finally, regular evaluation of the quality of radiopharmaceuticals should be conducted with the objective to authenticate the consistency of the process and ensuring its continuous improvement.

17.2.2 Good Manufacturing Practices (GMP) for Radiopharmaceuticals

The GMPs for radiopharmaceutical are the part of quality assurance that ensures that they are consistently produced and controlled in such a way to meet the quality standards appropriate for the intended use, as required by the approved specifications in the market authorization of the radiopharmaceutical in dosage form (Decristoforo et al. 2008; Woldring 1999; Elsinga et al. 2010; Gouveia et al. 2015). GMP basic requirements are as follows. With a view to ensure consistency as well as compliance with approved regulatory specifications, it is essential to clearly define and control the RPh production processes through which they are formulated and produced. In this case, the reproducibility of the production process is a principal criterion for ensuring consistency of quality, efficacy, and safety between different batches. Validation of critical formulation process steps must be carried out regularly as well as for any significant changes brought for processes improvement. The depth and scope of validation depend on the diversity, complexity, and criticality of the production process (Zigler 2009). Scientific and technical judgment should be used to justify the process changes and validation studies. All necessary key elements for GMP must be available, including the necessity of qualified and trained personnel, the availability of adequate premises and space, including appropriate hot cell facilities, remote handling equipment, and services. In addition, only approved radionuclides, excipients, and containers can be used for the formulation. Also, recommended procedures and instructions must be available and up-to-date and proper storage/quarantine facilities must be available.

Personnel involved with the production, quality control, and documentation of RPhs should have adequate training in accordance with

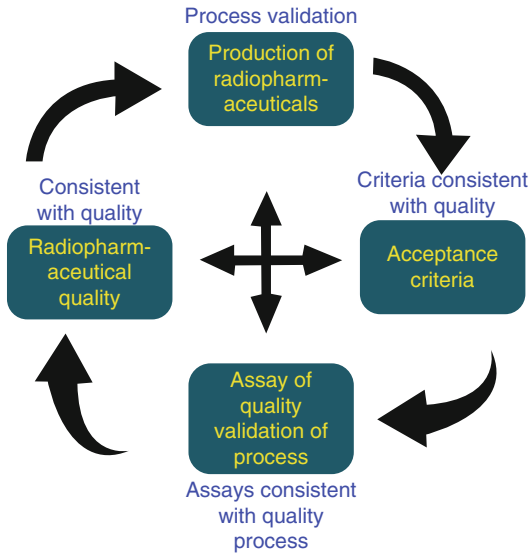

Fig. 17.1 Radiopharmaceutical GMP production

applicable official federal, state, and local laws. Instructions and production procedures are required to be clear and written in unambiguous language. Written procedures should not only specify critical processing steps and factors (such as irradiated target processing time, temperature, and reagent purity, etc.) but must also specify the acceptance criteria, as well as the type of validation to be conducted (e.g., retrospective, prospective, or concurrent) and the product batch number/identification. These records are also required to address the identity of the batch and the amount of activity produced. The GMP facility must insure that all steps required by the recommended procedures and instructions are in place. It is also essential that qualified and competent operators are trained to document procedures. The key elements for GMP radiopharmaceutical production are depicted in Fig. 17.1.

17.2.3 Quality Control (QC)

Quality control is that part of GMP which is concerned with sampling, specifications, and testing and with the organization, documentation, and release procedures which ensure that the necessary and relevant tests are actually carried out and that radiopharmaceuticals are not released for patient use until their quality has been assessed to be satisfactory (Cohen 1975; Cox et al 1994). QC is not confined to laboratory operations, but may be involved in many decisions to ensure the quality of the product. Basic requirements of quality control include that adequate facilities, trained personnel, and approved procedures are available to perform sampling, inspecting, and testing of starting materials, packaging materials, and intermediate, bulk, and finished products, and where appropriate for monitoring environmental conditions for GMP purposes. Samples of starting materials, packaging materials, intermediate products, bulk products, and finished products must be reserved by trained personnel and by methods approved by QC. Of course, all test methods require validation and appropriate records must be prepared and maintained, either electronically or by hard copy, which demonstrate that all the required sampling, inspecting, and testing procedures were actually carried out. Any deviations must be fully recorded and investigated. The final finished products containing the API (i.e., active pharmaceutical ingredient, Sect. 17.4) must comply with the qualitative and quantitative composition requirements for marketing authorization, including the desired purity, and enclosure within a suitably labeled appropriate container. As described earlier, a very important requirement is that records of inspection results are maintained and that testing of materials, intermediate, bulk, and finished radiopharmaceuticals is formally assessed against specification. Product assessment includes a review and evaluation of relevant production documentation and evaluation of deviations from specified procedures. Product batches cannot be released for use, sale, or supply prior to certification by an authorized individual, in accordance with the requirements of the relevant authorizations. Finally, sufficient reference samples of starting materials and products must be retained in the final package, unless exceptionally large packages are required for the product (i.e., large volume, high activity, heavy shielding, etc.), to permit future product examination.

17.3 Personnel

Radiopharmaceutical production is carried out in an interdisciplinary environment, including chemists with radiopharmacists, engineers, clinician-scientists, technologists, and biologists (Duatti and Bhonsle 2013; Lass and Scheffler 2003; Wang 1996). In light of the perceived need to establish and maintain a satisfactory quality assurance system, a staff of qualified and competent personnel is required to perform production, control, and supervision. These individuals must have the appropriate motivation, education, knowledge, and professional skills necessary to support the establishment and to perform the required tasks. Availability of well-trained skilled personal is critical to a viable RPh production program which must be conducted under the active direction and supervision of competent technical staff with prescribed qualifications and practical experience with competence in radiation protection. All responsible staff should have specific duties recorded in written descriptions and adequate authority to carry out their responsibilities without any gaps or unexplained overlaps. Personnel involved in the production of the radiopharmaceutical should receive training appropriate to the duties and responsibility assigned to them to ensure the safe manufacture of radiopharmaceuticals and radiation safety procedures, and regular in-service training is also required. Activities between radioactive and non-radioactive areas are permitted only if the safety rules of radiation control (health physics/radiation safety control) are respected, and only the minimum number of personnel required should be present in clean and aseptic areas when work is in progress. Access to these areas should be restricted during the preparation of radiopharmaceuticals, kits, or sterile set-ups. The number of personnel employed must also be adequate and in direct proportion to the workload and personnel involved in QA and QC operations must of course be suitably qualified and experienced. The duties of technical and quality control personnel must be defined, documented, and strictly adhered to. In order to avoid potential conflicts of interest, the individual responsible for the quality control laboratory must have responsibilities and activities which are independent of the manufacturing unit.

17.4 Active Pharmaceutical Ingredient (API)

Any substance or mixture of substances intended to be used in the manufacture of radiopharmaceuticals and used in the production of a radiopharmaceutical is defined as an API (Cervera-Padrell et al. 2012; Kumar et al. 1992). Such substances are intended to provide pharmacological activity or other direct effect in the diagnosis as well as treatment of disease or to affect the structure and function of the body. All radionuclides used in the manufacture of a radiopharmaceutical without a purification of the final preparation before administrations are considered an API. For radiopharmaceutical kits—which are targeting agents to which the radioisotope is attached—the active ingredient is considered to be that part of the formulation that is intended to carry or bind the radionuclide or to permit its binding.

Starting materials used in the radiolabeling reaction for the manufacture of RPhs which are purified after the radiolabeling process are not active pharmaceutical ingredients but are API starting materials. Because of this distinction, several rules need to be applied. For instance, all starting materials used in radiolabeling reactions for the preparation of radioactive pharmaceutical ingredients (APIs) that are not isolated and/or fully analyzed before incorporation in the final radiopharmaceutical preparation have to be analyzed according to a monograph of pharmacopoeia and must comply with the requirements of the pharmacopoeia. In case the substance is not described in a pharmacopoeia, it must be analyzed using validated methods. All analyses have to be performed in accordance with national regulations. If starting materials which are to be considered as APIs are produced by a

foreign GMP-certified facility, a copy of the certificate of GMP production must be submitted to the competent authority of the user country for mutual recognition. Excipient starting materials used in the preparation of radiopharmaceuticals such as solvents, buffers, stabilizers, additives, antimicrobial agents, etc., must be of pharmaceutical l quality (as indicated on the label), be accompanied by a certificate of analysis, or be analyzed using validated methods and in accordance with national regulations.

The manufacture of all APIs should be carried out under general GMP requirement and although aseptic is not necessarily required to curtail the risk of contamination (i.e., US Food and Drug Administration). The emphasis on quality is most prominently manifested by the fact that all equipment, instruments, technologies, and accessories associated in the production of API must fulfill preset criteria and the product obtained has to meet strict specifications. Written and approved protocols specifying critical steps, acceptance criteria, must be in place. Confirmation of appropriate regulatory conditions for aseptic processing and its supportive activities are often mandatory.

17.5 Radionuclide Production

The procedure for the production of the radionuclide (see Chaps. 5, 6, 7, and 8) clearly describes major parameters, such as target material, nuclear reactions, construction and target holder material, and irradiation data—such as beam energy and intensity or neutron flux, etc. In addition, typical radionuclidic contaminants for the adopted procedure of separation/purification of the desired radionuclide and the effects on the efficiency of the production in terms of quality and quantity of the produced radionuclide must be evaluated. Radionuclide production for RPh formulation involves adherence to regulations on radiation protection. Therefore, the principles of qualification and validation should be applied to radionuclidic production, and a risk management approach should be used to determine the extent of qualification/validation, focusing on a combination of GMP and radiation protection.

17.6 Radiopharmaceutical Manufacture

The production of radiopharmaceuticals is a very specific and complex task required to meet quality standards to ensure product quality during all stages of the production process (Decristoforo et al. 2008). While undertaking the production of radiopharmaceuticals for human use, the availability of standard operating procedures (SOPs) must be considered at the RPh production site to ensure the regularly required reviews are kept up to date (Callahan et al. 2007). The purpose of an SOP is to carry out the operations correctly and always in the same manner. Specifications for starting materials used for the preparation of RPhs should include details of source, origin, methods of manufacture, and the controls used to ensure suitability for the intended use. Release of starting materials for the preparation of an RPh should be conditional and solely based on satisfactory results being obtained in the tests on starting materials. Adequate consideration must be given to the validation of sterilization methods. A list of critical equipment used for RPh production must be available, calibrated, or tested at regular intervals and should be checked before the initiation of production. In the case of radiolabeling kits, freeze drying must be carried out as an aseptic procedure, and the dispensing, packaging, and transportation of RPhs should comply with the relevant national regulations and international guidelines.

17.6.1 Sterile Production

Within the strictest definition of sterility, a specimen would be considered sterile only when the substance or material can be demonstrated to be completely absent of viable microorganisms (Brown and Baker 1996; Castronovo 1992; Chen et al. 1974). While a wide range of methods such

as steam, dry heat, and filtration can be used for sterilization, it is important to note that the method used must both sterilize and maintain the strength, purity, and packaging integrity. Sterile RPhs may be divided into those which are manufactured aseptically and those which are sterilized at a terminal stage of the process. With a view to maintain sterility of an RPh which has been assembled from components, careful attention must be given to the environment, personnel, critical surfaces, container/closure sterilization and transfer procedures, the holding period of the RPh before dispensing into the vial, and any other key factors which may compromise sterility.

17.6.2 Terminal Sterilization

A RPh can also be sterilized in the final container after preparation and dispensing. This process is referred to as terminal sterilization and not only minimizes upstream bio-burden, but also reduces the challenge to the subsequent sterilization process. Terminal sterilization through membrane filtration is a process for the removal of any viable microorganism. In this process, the RPh formulation solution is filtered through one or two sterilizing-grade (0.22 μm) membrane filters into a sterilized receiving vessel located in a traditional clean room with an ISO Class 5 unidirectional airflow, isolator, or restricted access barrier system (RABS) to produce sterile effluent. For effective sterilization, the integrity of the sterilized filter must be verified and confirmed immediately after use by appropriate methods such as a Bubble Point, Diffusive Flow, or Pressure Hold Test (Belanger et al. 2009; Hayashi et al. 2014; Jornitz 2001).

17.6.3 Aseptic Sterilization

In this aseptic process, the RPh, containers, and closures are sterilized separately and then assembled under an extremely high-quality environmental condition designed to reduce the possibility of any nonsterile components. Aseptic sterilization presents a higher risk of microbial contamination of the product than terminal sterilization, and the principles of cGMP must be carefully observed during sterilization. In particular, the involvement of qualified personnel with appropriate training is required, along with adequate facilities, suitable production equipment—designed for easy cleaning and sterilization—adequate precautions to minimize bio-burden prior to sterilization, validated procedures for all critical production steps, environmental monitoring, and in-process testing procedures. Process validation includes appropriate regular checks on the process, by means of process simulation tests using microbial growth media that are then incubated and examined for microbial contamination (media fill tests). In addition, a suitable sample of each batch of any product that is sterilized by filtration and/or aseptically processed must be tested for sterility before the batch is released.

In this regard, several points need to be taken into account while undertaking RPh sterilization. First of all, the appropriate level of environmental cleanliness of the facility must be maintained. For the manufacture of sterile products where the working zone in which the products or containers may be exposed to the environment, cleanliness requirements should be complied. An essential aspect of contamination prevention is the adequate separation of areas of operation, and it is vital for rooms of higher air cleanliness to have a substantial positive pressure differential relative to adjacent rooms of lower air cleanliness. In addition to these points, a risk assessment analysis should be carried out to determine that appropriate pressure differences, air flow direction, and air quality are maintained in the clean room where radiopharmaceuticals are produced. The number of personnel in an aseptic processing room should be minimized, and both personnel and material flow should be regulated and minimized to prevent potential for the introduction of contaminants. The design of the equipment used in aseptic processing should limit the number and complexity of aseptic intervention by personnel, and the equipment should be appropriately designed to facilitate ease of sterilization. It is also important to ensure ease of installation to facilitate aseptic setup. Appropriate training should be conducted before an individual is permitted to enter the aseptic manufacturing area. Under the cGMP

regulations, equipment must be qualified, calibrated, cleaned, and maintained to prevent contamination and mix-ups. The cGMP regulations place as much emphasis on process equipment as on testing equipment while most quality systems focus only on testing equipment.

Sterilization of RPhs by filtration must be conducted in a grade C environment, and if filtration sterilization is not performed, RPh preparation should then be carried out in a grade A environment with grade B in the background. Another important operational factor is minimization of the time between the initiation of RPh preparation and the filter sterilization or filtration stage through a microorganism retaining filter. There must also be a set maximum permissible time periods for each product that takes into account the composition and method of storage mentioned in the Master Formula record. In addition, all steps of the sterilization process should be appropriately validated and the validity of the process verified at regular predetermined intervals. Periodic bio-burden monitoring of products before terminal sterilization must also be performed and controlled to limits specified for the product in the Master Formula. Verification of the sterilized filter integrity is also a key point which must be confirmed immediately after use by appropriate methods such as Bubble Point, Diffusive Flow, or Pressure Hold Test. Record keeping at this stage is also important, and sterilization records must be maintained for each sterilization process. These processes may also include thermographs and sterilization monitoring strips, and all of these data must be maintained as part of the batch release procedure.

Any closures, containers, and stoppers should be designed to simplify cleaning and also to insure airtight seal of the RPh. The closures and stoppers should also be of such quality to avoid the risk of toxicity. As with any aseptic processing operation, it is critical that product contact surfaces should be sterile. A validated steam-in-place cycle, or equivalent process, should be used to sterilize the equipment path through which the product is conveyed. Prior to RPh production, assembly of sterilized equipment and consumable materials such as tubing, sterilized filters, and sterile closed and sealed vials to a sealed fluid path must be performed under aseptic conditions. While the manufacturing of sterile radiopharmaceuticals remains at the interface of various disciplines, sterility testing is a crucially important component and includes following microbiological laboratory controls, sampling and incubation, and investigation of sterility positives. The identification of organisms by sterility testing is important. The documentation of laboratory tests and deviations, monitoring of production area environment and personnel, product presterilization bio-burden, and production record review are also key components.

Microbiological controls and bacterial endotoxin testing (BET) must be performed according to written policies and procedures for specific compounded RPh (i.e., radiopharmacy preparation) when these tests are required as release criteria. Retrospective sterility testing—as in the case for use of ultra-short-lived radioisotopes—and BET should be conducted on randomly selected batches of the product to evaluate adequacy of the aseptic technique employed. These tests should also be conducted at regular periodic intervals, depending on historic results and trends, and should be completed more frequently when new personnel are involved. Sterility testing and BET should be performed according to locally accepted test methodology. The endotoxin limit for intrathecal RPh administration radiopharmaceuticals is significantly less than values allowed for intravenously administered RPhs (maximum administration of 14 EU vs. 175 EU, respectively). For this reason, a BET appropriate for detecting endotoxin concentrations at this lower limit should be performed by qualified personnel for each compounded radiopharmaceutical intended for intrathecal administration.

17.6.4 Sanitation and Hygiene

In the light of the perceived need to prevent possible contamination and cross contamination, a high level of sanitation and hygiene which is clearly outlined in SOPs must be practiced in every aspect of RPh production. Any residues

and contaminants from previously manufactured products can cross-contaminate subsequent products from equipment or from the cleaning procedure (detergents/sanitizers) or degradation products resulting from the cleaning process itself. A high level of sanitation and hygiene insures product safety and purity and assures the quality of the process from an internal control and compliance points of view. The range of sanitation and hygiene includes personnel, premises, equipment and apparatus units, starting materials used for RPh production, products used for cleaning, de-sanitation and disinfection, and all other issues which could become a source of product infection or contamination. An integrated comprehensive sanitation and hygiene program must therefore be instituted to preclude potential sources of contamination.

Because of all these crucial issues and potential dangers, it is obligatory to insure that the RPh production facilities are free from any accumulated waste, dust, debris, and even other similar material RPhs. The facilities must be cleaned and maintained in an orderly manner which requires the availability of validated procedure which is maintained to assure the effectiveness and consistency of a cleaning process. RPh production areas should not be used as a general thoroughfare and not used for storage of materials, except for the material being processed. A routine sanitation program should cover both the specific areas to be cleaned and cleaning intervals. Cleaning procedures include equipment and materials to be used, and personnel assigned to and responsible for the cleaning operation must be properly recorded. The working and in-process storage spaces must be adequate to permit orderly and logical positioning of equipment and materials which necessary to reduce the risk of cross contamination. While undertaking RPh production, effective control of microbial contamination and particulate contamination are thus a critically important aspect of for production documentation. A cleaning validation program must thus be instituted in order to demonstrate that any residues of substance previously manufactured are consistently reduced to levels that are acceptable and that the cleaning procedure itself does not contribute unacceptable levels of residual materials to equipment. Written, approved, and routinely reviewed procedures are thus required which clearly define the assignment of responsibilities for sanitation. The cleaning schedules, methods, equipment, and materials to be used in cleaning and records should be available in sufficient detail and should be maintained. The cleaning documentation should include detailed description of the levels of cleaning as well as methods necessary to inspect and verify equipment and SOP. Where microbial contamination may be an issue, consideration should be given to the integrity of the vessel prior to manufacture.

17.7 Documentation

Documentation constitutes an indispensable component of a QA system related to all aspects of GMP and is intended to preclude the risk of error that purely verbal communication may introduce. The aim is to account traceability of each RPh preparation and provide an audit to trace an individual product for suspected defects. It ensures that all personnel concerned with manufacture are intimately aware of this information necessary to decide whether or not to release an RPh batch for patient use. The instructions and standard operating procedures (SOPs) of RPh preparation should be written and independently approved for each procedure or activity associated with the production. A specification should be available for each material used as well as for the final, dispensed radiopharmaceutical. All documents related to RPh manufacture should be prepared, reviewed, approved, and distributed according to written procedures. In order to achieve regulatory compliance, it is essential to have a full documentation system providing traceability of radiopharmaceuticals that include the following.

17.7.1 Site Master File

This document provides a general description of the activities that occur at the production site and contains a general description of the site and information on processes, facilities, equipment,

and instruments. It also describes the production site quality management system, responsibilities of key personnel, and organizational charts**.**

17.7.2 Drug Master Files (DMF) for Individual Batches

A Batch Processing Record must be available and archived for each product which is primarily based on the relevant parts of the currently approved procedures.

17.7.3 Validation Master File

This document constitutes a comprehensive overview describing the applicable validation requirements for the radiopharmaceutical facility and provides a plan for meeting those requirements. It is an essential part of GMP that provides a high degree of assurance that a production process will consistently produce an RPh that meets its encoded specifications and quality attributes. It permits the reviewer to understand the scope of the validation and so avoid misconceptions.

17.7.4 Specifications for Materials

Each batch of raw material used at any stage for RPh preparation must be tested to ensure that it complies with the following specifications.

17.7.4.1 Operating Procedures

Standard operating procedures and records must be prepared for the RPh production facility, for each instrument, equipment, and accessories used, and for any precautions which should be observed to avoid contamination of the material or any quality deterioration. A written report should summarize the operating procedures required to be prepared, documented, and maintained.

17.7.4.2 Batch Processing Records

A batch record based on the relevant sections of the currently approved Master Formula must be maintained and archived for each batch or part of the batch processed. Each action of processing operation and major equipment used should be recorded.

17.7.4.3 Staff Training

It is essential to provide training in accordance with a written program for all personnel associated with RPh production and control laboratories. Continuing training should also be given, and its practical effectiveness periodically assessed. An approved training program should be available and training records should be maintained.

All records should be maintained either at the RPh facility or at another accessible location. The records must be legible, appropriately stored to prevent deterioration or loss, and be readily available for review when required. These records should be maintained for the legally required period and include receipt dates for all ingredients and expedients, including the radionuclides. Information on radiopharmaceutical preparation must include batch numbers, activity and volume added, and results of quality control and release. Documentation of laboratory and processing facility maintenance and radioactivity-measuring equipment, calibration, and maintenance must be maintained. Training of personnel and transport of radioactive materials must be also considered as well as any information about radioactive contamination monitoring and radioactive waste disposal, product defects, and events of nonconformity to SOPs.

Although data may be recorded by electronic or hard copy means, the advantages of electronic documentation include real-time massive and complex processing, minimization of human vulnerability and errors, remote control and assay, prompt decision making, and electronic encryption. Limitations of electronic documentation include dedicated hardware and software, electronic literacy, sensors network, electricity supply dependent, systematic error proliferation, and increased massive data loss risk. Although limited data monitoring, low cost, flexibility, simplicity, and authenticity are appealing, hard copy documentation has its own limitations that include uncomfortable handling in radiation and aseptic environments, operator distraction from

further functions, lengthy data transfer for processing, subjective errors probability, fire, water, and atmosphere sensitive, and spacey storage. In the current environment, it would seem appealing that both hard copy and electronic files are both maintained.

17.8 Container Labeling

Each RPh preparation must comply with labeling requirements established under GMP, since consistent and legible labels are absolutely necessary for identification of the drugs and their use. All containers and equipment used for RPh preparation must have appropriate labels. Printing can be conducted legibly in bright colors and the label must include all prescribed RPh detail. The label on the primary container should include a radioactivity symbol, name of the manufacturer, the name of the RPh preparation, the batch number, radioactivity content at a stated date and time, radioactive concentration (in MBq per mL of the solution), solution identifier (i.e., saline, etc.) and total volume, intended purpose (diagnostic or for therapeutic), and administration route. Radiopharmaceutical preparations that are intended for parenteral use should be kept in a glass vial, ampule, or syringe that is sufficiently transparent to permit the visual inspection of the contents. In addition to meeting pharmaceutical GMP regulations, manufacturers undertaking regular production of radiopharmaceuticals in the USA, for instance, must generally be licensed by a Nuclear Regulation Authority (NRA). In the USA this is the Nuclear Regulatory Commission (NRC), but the national laboratories are operated by the Department of Energy and are exempt from NRC regulations. In India and major Asian countries, the national laboratories are also exempt for NRA regulations. In this context, it is mandatory for the manufacturer to demonstrate that the facility used for RPh production is adequate to protect health and minimize danger to life and property. Additionally, the manufacturer is required to be qualified to use radioactive material, has an established radiation protection program, as well as controls and procedures for management, record keeping, accounting, and use of radioactive materials.

17.9 Centralized Radiopharmacy (CRPh) Concept

Because of the rapidly growing interest in radionuclide therapy, the supply of therapeutic radiopharmaceuticals has attracted attention from the industry. Radiopharmaceuticals, similar to normal medicines, are required to undergo total quality control assessment before patient administration to insure patient safety (Kowalsky 1989; Harapanhalli 2010). Some of these major requirements include those relating to establishment of chemical, radiochemical, and radionuclidic purity of therapeutic RPhs (Woldring 1999). In addition, the granting of marketing authorization is dependent on the condition that these agents are manufactured under conditions of GMP. Formal RPh "Approval or Registration" involves screening by competent national authorities for GMP compliance and is a necessity before the RPhs are released to end-users as therapeutic products (Norenberg et al. 2010). In this context, GMP compliance of each RPh must be overseen by a state-registered pharmacist or "Authorized person/Qualified person" to establish and a dossier which must be submitted as a prerequisite for patient use (Otte and Maier-Lenz Dierckx 2005). To address these requirements, RPh production strategy is migrating in many countries toward the use of centralized radiopharmacies (CRPhs). These highly specialized nuclear pharmacies are able to prepare and distribute calibrated, GMP-compliant, and safe single RPh doses to nuclear medicine (NM) facilities within their geographical area in routine and scheduled timetables (Norenberg et al. 2010; Ramírez de Arellano et al. 1999; Gnau and Maynard 1973). In the USA, for instance, there has been a significant decrease in the availability of hospital-based radiopharmacies, and there are about 135–150 centralized radiopharmacies in operation.

To address cGMP requirements, the prospect of RPh production using a CRPh service for dose

formulation and distribution through CRPhs is very appealing and has major benefits. For instance, it is well known in the nuclear medicine field that the major challenges in this field are not the initial investments for installation and operation of radiochemical facility with the required radiation protection tools, but rather the routine cost of RPhs and cold kits due to the irregular flow of patients, radioactive waste handling and disposal, and more recently the requirement for cGMP manufacture of all patient radiopharmaceutical products. The CRPh can effectively utilize the available radionuclide activities for the preparation of a wide range of RPh without significantly incurring decay loss. A CRPh can overcome the limitation on high RPh costs, in addition to irregular radionuclide availability. In many countries, NM facilities are generally unable to provide the proper radiopharmacy QC tests due to the lack of instruments and trained professionals. With mandatory and basic configuration, a CRPh can easily provide high-caliber, safe, and up to standard patient doses which are fulfilling the international drug safety demands, as has been demonstrated with over 150 CRPh in the USA and many more throughout the world. The radiation protection issues during RPh production in a CRPh can be effectively handled by using state-of-the-art processing facilities and highly skilled personnel. These capabilities will not only reduce the radiation exposure but also decrease the probability of radioactive contamination (Heller 1996). The CRPh concept is being highly appreciated and encouraged by many governing and regulating authorities. A central radiopharmacy can also decrease the number of highly skilled staff directly involved in RPh preparation and thus can also act as an efficient key factor in mitigating the adverse effects on the shortage of skilled professionals. Regulatory and GMP compliance of RPh production is a tedious process and requires time and high costs, elaboration of a complete dossiers, including optimization of manufacturing and analytical methods, establishment of pharmacological, and radiation safety. CRPhs simplify the regulatory and practice-based paperwork and can also be utilized for training, research, and education in the field of nuclear pharmacy and radioisotope production, owing to the ready availability of professional teams comprised of radiopharmacists, radiochemists, and technologists. These facilities can also provide guidance and technical advices to the concerned facilities for proper standardization of NM procedures and related dosimetry features. Finally, concern regarding the management of radioactive waste is negligible owing to the availability of efficient and well-maintained radioactive waste storage system for returning waste to a central site.

The existing practice of radiopharmacetical dose formulation in nuclear medicine centers is expected to converge, making it likely that future supplies will take place through CRPhs set up to achieve the compliance with cGMP (Elliot et al. 1993). Although the central radiopharmacy concept is not widely practiced on an international basis, the large number of such centralized radiopharmacies currently operating in the USA provides a model for further expansion to other regions/countries of this important concept to reduce costs. While the establishment of CRPhs are driven more by needs in meeting regulatory demands than by commercial interests alone, it is anticipated that nuclear medicine facilities will look to the CRPh model for an increasing portion of their radiopharmaceutical needs, with manufacturers ready and able to meet demands in a safe, timely, and cost-efficient manner.

17.10 Infusion of Automation in Radiopharmaceutical Production

In light of the explicit need to handle radioactivity during the production of radiopharmaceuticals, the prospect for using automated radiochemical processing system is expected not only to expand the scope and utility, but would also represent a stepping stone toward achieving cGMP compliance. In this context both semiautomated and fully automated radiochemical processing system should be given further serious consideration. One advantage in adopting semiautomated radiochemical processing system is that it will be

better able to meet regulatory needs and introduced to the market. But if the semiautomated radiochemical processing system is used to satisfy regulatory demands, conversion of semiautomated to automated unit will be strategic and can delay the requirement to invest more capital for an automated radiochemical processing system. While the use of semiautomated radiochemical processing system whereby the operator still has to interfere in the process of isolating generator-produced radionuclide has tangible benefits, availability and use of fully automated system using a computer controlled interface is very desirable.

The advantages of using fully automated radiochemical processing system include the capability without user intervention which leads to reduction of RPh production time, decline in radiation exposure to the operator, and elimination of human error. Dedicated units also preclude the possibility of cross-contamination and improve robustness of the production process as well as the capability for online documentation of the process thus improving GMP compliance. Use of these units also assures reproducibility in production yield as well as consistency in product quality. The ability to handle multiple GBq level of radioactivity safely is also important for enabling the manufacturer to produce and distribute the required RPh quantities for therapy. Automation also offers low operational variability as regards to purity and yield are concerned and use of these systems guarantees robustness. In addition to providing the scope of maintaining a data base of steps performed including documentation of all process parameters and functions during production of radiopharmaceuticals, electronic record keeping is not only accurate and complete but also helps in accomplishing regulatory compliance. In addition, an automated radiochemical processing system can guarantee better control of sterility and apyrogenicity of radiopharmaceuticals because of minimal human intervention. Use of these systems also facilitates regulatory compliance through manufacturer installation qualification/operational, qualification/performance, and qualification and scheduled maintenance protocols performed for radiopharmaceutical production by trained personnel. While automation holds promise and offers numerous advantages, it is associated with the challenge of reconfiguring the radiochemical processing technology that requires integration of several steps while maintaining full automation. The tremendous prospects associated with the use of automated radiochemical processing system have led to the development of a number of products by commercial manufactures of which Eckert & Ziegler, Germany; Isotope Technologies Dresden (ITD) GmbH, Germany; and IBA Radiopharma, South Africa, which have had leading roles. Examples of these commercial products are illustrated in Fig. 17.2.

17.11 Constraints in the Transition of Radiopharmaceuticals from Bench to Bedside

The route that a radiopharmaceutical takes from development to mass-production and availability for patient care is called the Critical Path and is illustrated in Fig. 17.3.

The research, development, and the transition of radiopharmaceuticals from "bench to bedside" is a continuous but lengthy process (Lipsky and Sharp 2001). The transition of radiopharmaceuticals from "bench to bedside" as well their industrial translation and encompasses several steps broadly classified in three categories, as tracer discovery/development, regulatory aspects, and clinical development. Initially, identification of specific target for the disease of interest is of pivotal importance, and evaluation of functional characterization of the disease process, the target density, and thus the radiopharmaceutical uptake representative of the extent and progression of the disease are important factors. The selection of a target for a given disease, and thus the development of a new radiopharmaceutical, is dependent on sound physiological, molecular, and cellular biological information base. Integration of genomic and proteomic information facilitate the selection of new targets. Subsequently, the selection of a lead molecule represents an important aspect (e.g., an enzyme, receptor ligand, peptide,

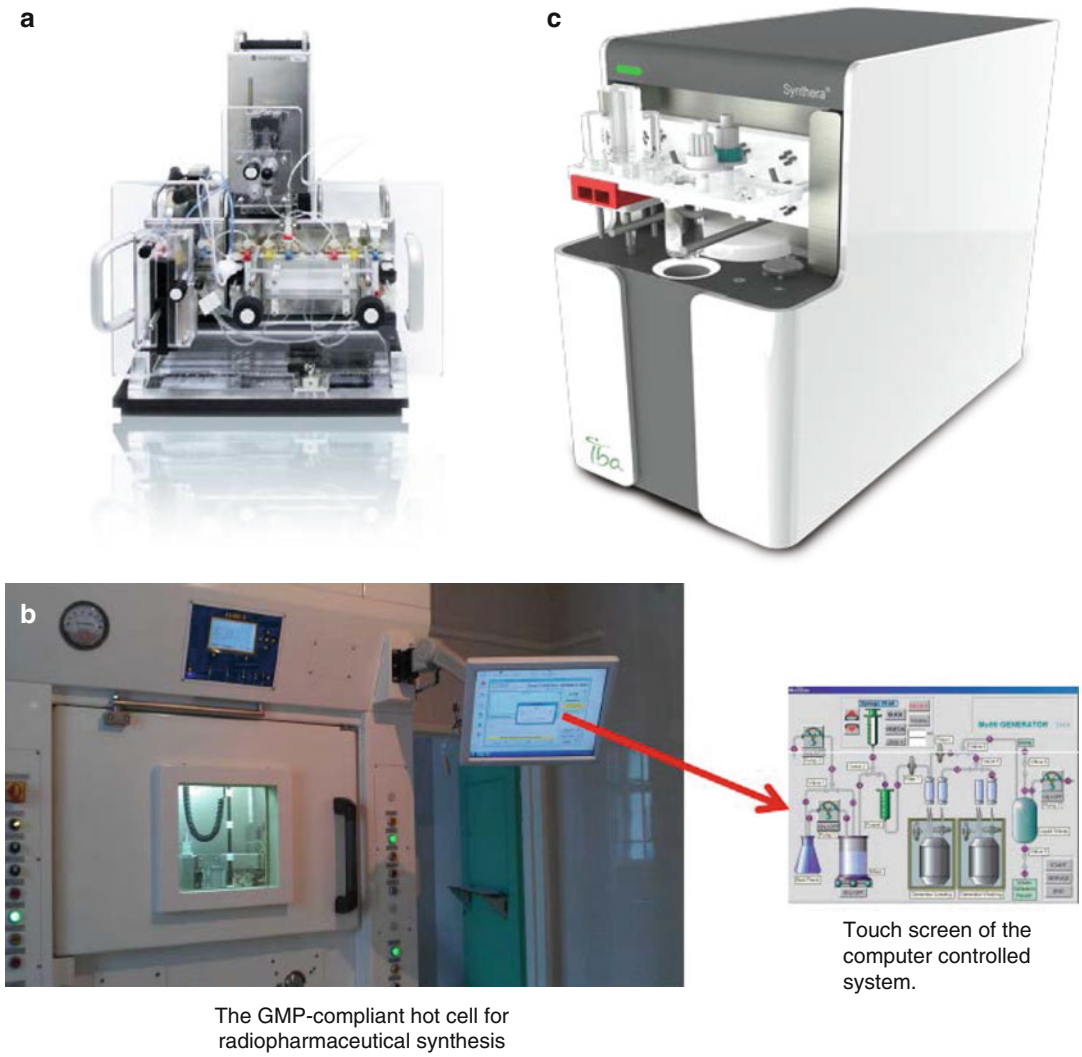

Fig. 17.2 Examples of commercial automated radiopharmaceutical synthesizers. (**a**) Fully automated and GMP-compliant synthesis ^{177}Lu- and ^{90}Y-labeled DOTA-conjugated peptides. Synthesizer of Eckert & Ziegler. (**b**) GMP-compliant hot cell housing automated radiopharmaceutical synthesis of ITG Germany. (**c**) Synthera®, a multipurpose fully automated radiopharmaceutical synthesizer of IBA Radiopharma of South Africa

Fig. 17.3 The journey of a radiopharmaceutical from research and development to full-scale production and marketing

antibody, etc.) with relevant target affinity and suitability to serve as a lead for the development of a radiopharmaceutical. The protein expression pattern on tissue samples collected can often be used to identify and select a lead antigen/antibody targeting molecules, for instance. Organic synthesis and combinatorial chemistry, solid-phase peptide syntheses, and phage display

are all key techniques generally exploited for generating potential high-affinity binding agents for a selected target. Selection of a radionuclide apart from radiation emission characteristic is primarily dictated by the physiochemical behavior of the radiopharmaceutical in vivo which should correspond with the radionuclide half-life. The radiopharmaceutical must bind to the therapeutic target or to a corresponding molecule without initiating any adverse effect. Thus the structural requirements for radioisotope binding present challenges for the synthesis, validation, and testing of these targeting molecules, and this is major aspect for the development of new agents. Assessment of the possibility to modify and optimize the lead molecule is important to perform radiolabeling, in vivo stability evaluation, clearance route and kinetics, specificity of binding, and background radioactivity levels. Evaluation and validation of the correlation of radiopharmaceutical in vivo accumulation with the biochemical process is crucial. This most relevant validation and final preclinical milestone have to be evaluated in suitable animal models, often with human tumor xenografts, potentially serving as the first relevant proof of the hypothesized target/tracer concept. Safety and efficacy studies in animals usually reveal a lead candidate that will be taken through the clinical phases of development.

Translational development and validation involves use of animal models into clinical models to population level. One initial step can involve toxicity validation in animals as a preliminary indication of the absence of expected subsequent patient toxicity. Validation in humans can also require independent assays on tissue samples obtained from biopsies and surgical specimens. Validation of clinical models is required for the purpose of prognosis, diagnosis, staging of disease, and selection and monitoring of therapy. Positive initial preclinical results then pave the way for clinical trials which follow the principal I, II, and III clinical trial phases. Phase I "safety" trials are focused to demonstrate absence of toxicity in a small group of generally human volunteers. Phase II trials are directed to demonstrate efficacy and to choose the most adequate dose in patients on the scale of 50–100. Finally, appropriately designed and blinded phase III studies confirm the efficacy and absence of side effects at the selected dose. The practice of studying the distribution of radiation resulting from the systemic or loco-regional patient administration of therapeutic radiopharmaceuticals is termed "dosimetry" which requires not only a thorough understanding of the radiopharmaceutical biodistribution and pharmacokinetics but also a methodology for translating total number of radionuclide disintegration in a particular anatomical volume to the absorbed dose to the volume (Eberlein et al. 2011; Bacher and Thierens 2005).

The preclinical phase of radiopharmaceutical development is highly dependent on the hope to identify new lead molecules which can target a specific disease. These chemical and radiopharmaceutical development and initial animal and human evaluation efforts can consume up to 5 years. Clinical testing is the most expensive and time-consuming aspect of radiopharmaceutical development, often requiring the enrollment of large numbers of volunteers and patients and the collection of massive amounts of data. The first clinical trial involving a minimum of 15–30 patients can take up to 12–18 months, and phase II studies can require up to three years. Phase III studies will require, dependent on the types of studies and endpoints, 300–1000 patients recruited over 2–4 years. If the radiopharmaceutical is then of potential clinical/commercial interest, preparation of the NDA dossier and its evaluation can require at least one year. Once sufficient evidence of safety and efficacy is available, the results of testing will be compiled in an application to regulatory authorities for marketing approval. In the USA, manufacturers submit a new drug application (NDA) or a biological license application (BLA) to the FDA for review and approval.

The clinical success of any radiopharmaceutical largely depends on the purpose of its use—including expected patient throughout and the market potential—the cost associated with its GMP production, and the process of validation through clinical trials. If a radiopharmaceutical requiring either a rare and expensive radionuclide

or a biomolecule and its application is too specific and would unable to reach a large population, this generally constitutes an unsuccessful venture from commercial and clinical point of views. The successful development of a therapeutic radiopharmaceutical is strongly dependent on the three issues: (a) availability, (b) capability, and (c) in vivo characteristics. Availability includes radionuclide production capabilities, availability and costs, and the development and technical realization of efficient syntheses of radiopharmaceutical. Capability is predominantly determinate by a proper selection of the molecular targets. The optimization of the "in vivo biodistribution and metabolism characteristics" of a radiopharmaceutical includes catabolic stability, clearance rate, excretion route, specificity of uptake, accumulation, retention, etc., which must be adequately fine-tuned.

Radiopharmaceutical development does not end with discovery and publication, which are prerequisite for radiopharmaceutical development. Transformation into clinical application is the ultimate goal of research and has many hurtles and challenges. The success story of a therapeutic radiopharmaceutical is a complex multidisciplinary tortuous process, associated with diverse, unforeseeable challenges, and basically consists of three research stages. Basic research is the earliest stage of research, carried out for the advancement of knowledge with particular reference to human disease and biology. Translational research is the transfer of knowledge gained from basic research to new and improved methods of preventing, diagnosing, or treating disease, as well as the transfer of clinical insights into hypotheses that can be tested and validated in the basic research laboratory (Hall 2002). And finally, clinical research is research in human subjects that determine the safety and effectiveness of radiopharmaceutical for prevention, treatment, diagnosis, or relieving symptoms of a disease.

Of these three, the translational research represents the interface between basic science and clinical medicine and primarily dictates the transition of radiopharmaceutical not only from bench to bedside, but also from the bedside to clinical practice, to general policies and, finally, to public health. Despite decades of scientific and technological advances, many basic discoveries are of scientific interest and importance, but do not move further into the therapeutic development pipeline because of irrelevance as clinical therapeutic tools, or because of lack of funding, incentives, and technical expertise to advance any further. That translational gap has been called previously as the "valley of death" which was used to describe the chasm separating two significant challenges, i.e., between biomedical researchers and patients requiring new treatment options (Butler 2008). Both bench-to-bedside and bed-to-bench bridges are necessary to bridge the gap. But as translational science evolved so too has the image of this valley topography: rather than one valley, two distinct mountains of despair lag between clinical knowledge and patients have emerged. The first involves regulatory and business model issues that may delay marketing of a successful solution, and the second one involves education of stakeholders (physicians, healthcare professionals, healthcare decision-makers, patients, etc.) and policies that allow widespread implementation of the solution across socioeconomic and geographical barriers. For these reasons, tunnels are required to surmount these mountains of despair, as depicted in the cartoon illustrated in Fig. 17.4.

17.12 Barriers to Success

While new therapeutic radiopharmaceuticals are required to offer new opportunities and rejuvenate the practice of nuclear medicine for improving patient outcomes, technology transition of new therapeutics from laboratory to market is a long and winding road with multiple road blocks and detours. Commercialization and marketing strategies pathways extend beyond startup development and can include the willingness of industry to act as partners, invest in new product development, and enter the marketplace and assure on return of investment. Although a large number of radiopharmaceutical have been developed in the research community as well as national invest-

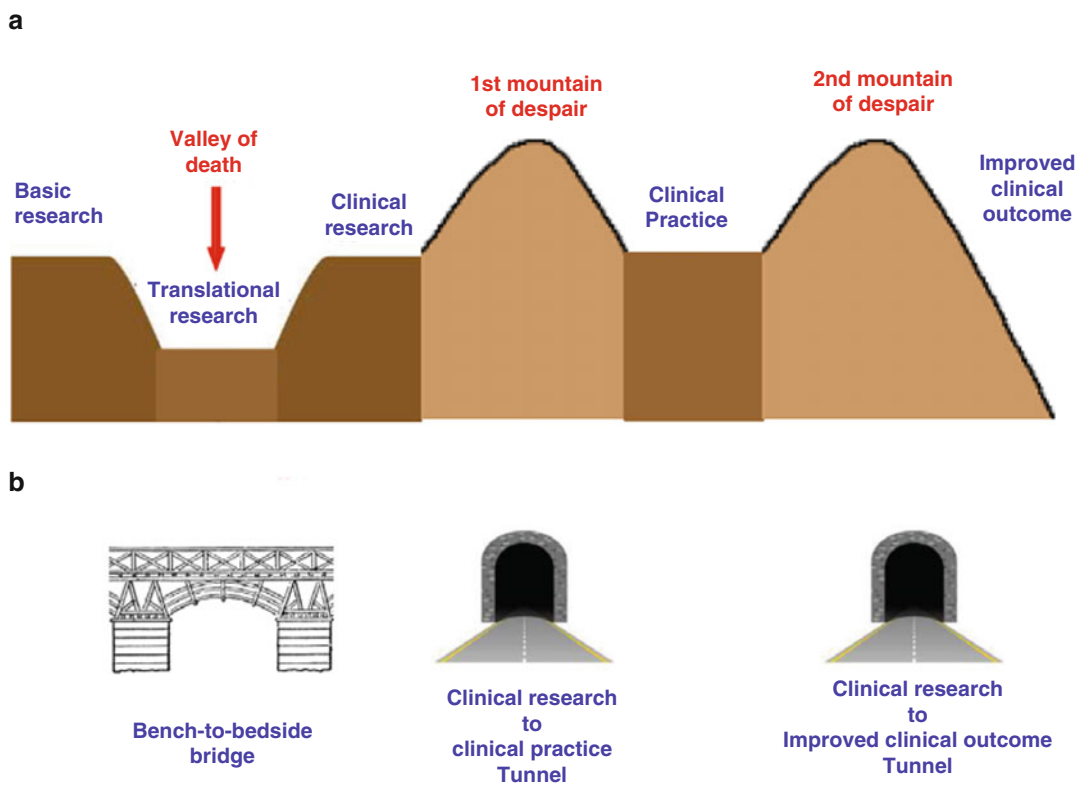

Fig. 17.4 "Valley of death" and "mountains of despair" of a radiopharmaceutical on its journey from basic scientific discoveries into full-scale production, marketing, and patient therapies. (**a**) Major challenges encountered during development of radiopharmaceutcials for approval for human use. (**b**) Hurtles which must be overcome during transition from radiopharmaceutical development to clinical trials and routine clinical use

ment in federal research and development, only a small number have reached the market. In fact, as an example, only three radiopharmaceuticals have been approved in the USA during the last decade. A number of novel, unique, or esoteric laboratory discoveries which offer benefits fail in the next stage of development for a variety of reasons. If investment is available, these radiopharmaceutical products can be further developed and made available. Of course, the industrial sector will invest in the development of a new radiopharmaceutical generally if intellectual property (IP) protection is insured and only if convinced about the chance of success and a positive financial outcome. A guaranteed profit in a predefined limited development timeframe with a minimized risk must be assured. A variety of major constraints in the industrial translations of new radiopharmaceutical include the following.

- *Negative Image Provided by Radioactivity*. Despite innumerable positive benefits for radiopharmaceutical use, if there is a choice between the use of alternative technologies—including conventional pharmaceutical drugs to RPhs—priority will generally be given to the non-radioactive solution, even if it could prove less efficient, slightly more toxic, or much more expensive (Freudenberg and Beyer 2011). This reality involves several realities, including the issues associated with radiation safety, exposure, and waste, and the fact that nuclear medicine has not yet shown a radiopharmaceutical with blockbuster potential (Schelbert 2011). The limited acceptance of new tracers by referring physicians is a barrier, due to lack of training, familiarity, and understanding of the unique strengths of RPhs. Nuclear medicine physicians must have

positive and proactive interaction with referring physicians and educate them about the unique benefits of RPhs, the benefits of combined imaging technologies (PET/CCT PET/MRI, etc.), and the positive impact on clinical utilization of radiopharmaceuticals.

- *Limited Research Funding*. While nuclear medicine research funding from the major federal agencies (for instance, in the USA, NIH, DOD, and DOE) has increased over the last decade, the amount of funding has not kept pace with the overall growth of the nuclear medicine field and the cost to bring a radiotracer from the bench to the bedside. According to a recent study (Nunn 2006), the cost of new tracer development has been estimated to be as high as $100–200 million, and research funding is insufficient to bring these tracers through the full development process.
- *Prolonged Development Time*. The average time required to move a new radiopharmaceutical from discovery through development and the three phases of clinical trials to obtain full Food and Drug Administration (FDA) approval to market the drug can take up to 15 years (Dickson and Gagnon 2004; DiMasi et al. 2003). The most time-consuming aspects of the process are the early discovery phase involving screening a large numbers of candidate compounds to define a lead class or classes of molecules and phase III clinical trials that involve sizeable cohorts of patients in multicenter trials (Seddon and Workman 2003; Reichert 2003).
- *Limited Success Rate*. The development of successful radiopharmaceuticals and eventual clinical introduction can never be guaranteed. The failure and dropout incidences at all stages of development is quite high. As an example, it is estimated that for every 5,000–10,000 compounds that enter the research and development (R&D) pipeline, ultimately only one will receive marketing approval (Reichert 2003). This is largely due to the inability of the radiopharmaceutical agents to obtain adequate concentrations in target tissues, the inability to bind to a receptor in vivo, or demonstrate inappropriate absorption, distribution, metabolism, and excretion (ADME) characteristics. However, it has been reported that up to 25 % of all entities entering the clinical phases reach the approval stage (DiMasi and Grabowski 2007).
- *Adequate Protection for Intellectual Property*. While academic investigators strongly object to patent inventions, viewing this process as anti-ethical to the free exchange of knowledge, adequate protection for intellectual property (IP) is in reality inextricably linked to the potential for commercial success and thus is a key consideration for the private sector when deciding whether to invest in a project. Moreover, the period of commercial exclusivity was seen as a potential step forward for raising the capital required to convert inventions into promising radiopharmaceutical products, because there would be no incentive to invest in expensive radiopharmaceutical development programs if a competitor could wait for a radiopharmaceutical to show its commercial success and then offer it with competing pricing (Herrling 2007).
- *Low Clinical Acceptance*. In addition to promising patient benefits, clinical acceptance constitutes a potential hurdle that impedes development progress. Successful promotion and marketing of new radiopharmaceuticals require high investment and the expected profit can only justify the investments. The nuclear medicine community is not yet sufficiently influential and much too small to persuade the medical community that radiopharmaceuticals could so easily replace the existing alternative treatment modalities.
- *Slow Return on Investment*. Although radiotracer development is significantly different from therapeutic drugs, the same routes to obtain regulatory approval are followed. The major cost areas for developing radiopharmaceuticals lie in the discovery portion and in phase II/III clinical trials and filing. While the time periods required for RPh development are estimated to be shorter by at least two years compared to conventional drugs, with development costs which are almost five times less, the expected revenues are much lower by the same

order of magnitude. A full therapeutic toxicology package on a single entity may currently be expected to cost up to $200–400 million. Globally, the clinical development of a radiotherapeutic agent will take about 9–11 years and cost €20–40 million more (Nunn 2007). To initiate a development program, a company must be assured that peak year sales will equal development costs. Such a return is required not only to recover the development costs of a successful program but also to cover the costs of other unsuccessful ventures. Current therapeutic radiopharmaceutical pricing does not allow a reasonable investment return. To remain commercially viable, the industrial sector tends to concentrate efforts in areas where financial returns appear likely. This means that new agents that are scientifically interesting and useful are not being developed, and potential targets are not being addressed. Companies already specialized in radiolabeled compounds will give priority to diagnostics rather than therapeutics due to smaller development costs and a more rapid return.

- *Small Market Size*. The size of the "real" market and the level of competition are the two important issues to address. The radiopharmaceutical market is very small compared to the conventional pharmaceuticals market, and thus the number of companies specifically engaged in radiotracer development has been limited. Presently, there are a limited number of players—some of which are also players in pharmaceutical—although there are other companies which are also medical device manufacturers (i.e., Siemens, GE, Iba, AAA). The domination of new drug development process of these companies comes from the tradition of medical device manufacturer, which unique principles must be considered as well.
- *Lack of Reimbursement or Inadequate Reimbursement***.** To insure the clinical relevance and use of a radiopharmaceutical, it obviously must be approved by the FDA or a similar authority; however, it is just as important that it will generate a much larger income if it is reimbursed. Although radiopharmaceuticals may hold great promise for therapy, reimbursement costs will be crucial for the eventual widespread clinical utilization. The decision of obtaining reimbursement is based on state healthcare authorities after the drug obtains market authorization. The medical economics requirement tests must demonstrate that the radiopharmaceutical is able to cost less than a certain amount per quality year of life saved. In terms of return on investment (which corresponds to the returns gained relative to the amount of money invested), the impact can be huge. It is not possible to predict the level to radiotracer reimbursement as healthcare policies of countries differ from one another in a number of ways.

Maximizing returns from national investment in federal research and development on radiopharmaceutical is essential to ensure as many taxpayer-funded technologies as possible to make the transition from lab to market. In this context, government bodies have a role to develop a framework to streamline administrative processes and facilitate academia and business partnerships that encourage commercialization of federally funded research and development. In an attempt to address the above challenges, radiopharmaceutical industry and professional institutions in the USA, for instance, such as National Institutes of Health (NIH) or the National Cancer Institute (NCI), have played a major role for bringing new players into industry. These institutions are inviting either active substance (API) or finished product and/or technology manufacturers to participate in clinical trials of new radiopharmaceuticals. Their efforts in this direction have been successful as the clinical studies are being funded by these institutions, and according to the results of the studies, institutions apply for the marketing authorization of the new drug. During the preparation of the application file, both API manufacturers (as Type II Drug Master File, DMF) and finished drug (as Type I DMF) add their own subfiles. Such an attempt constitutes a step in the right direction as the clinical trials, the longest and most costly stage of new product development, are financed by institutions instead of these companies that cannot afford the

finance of this huge amount; on the other hand, all of these companies can be licensed with a single application.

In order to ensure the availability of new radiopharmaceuticals for patient care, in March 2004, the FDA released a document entitled, "Innovation/Stagnation: Challenge and Opportunity on the Critical Path to New Medical Products," focused to improve the product development process and thereby to contribute to the success rate of new radiopharmaceuticals that will benefit the public. In this document, the FDA outlines possible changes that will facilitate the drug development process from inception to approval. The document constitutes a step in right direction to stimulate the process in bringing more new drugs into the approval pipeline by reducing the time for approvals and leveraging scientific advancements. Although the Critical Path Initiative (CPI) is still in its infancy, it has holds the potential to break down barriers between regulators and industry and to expedite the often complicated journeys of lifesaving medical innovations from researchers to regulators to patients. Within the CPI framework, two new steps deemed worthy of consideration. The first is introduction of the Exploratory Investigational New Drug (Exploratory IND) application based on micro-dosing concept and the second is the identification of lead radiolabeled therapeutic agent as to facilitate medical product development.

The current revolution in biomedical science has raised new hope for the development of effective and safer radiopharmaceuticals for the treatment of a wide range of diseases including cancers. In drug regulation, the regulatory body acts as the public guardian by controlling products available from private entities for public purposes. While the regulation of radiopharmaceuticals is the cornerstone to ensure safety, both quality and efficacy are sensible ideals also for the scientific community, but have emerged as major hurdles for research conducted in academia. Under the banner of public health protection, regulatory bodies have been accused of using the evaluation tools of earlier time periods to ensure safety and effectiveness of radiopharmaceuticals developed using more recent advances. The efforts of the regulatory bodies for patient protection outweigh the promotion of new radiopharmaceuticals as depicted in Fig. 17.5.

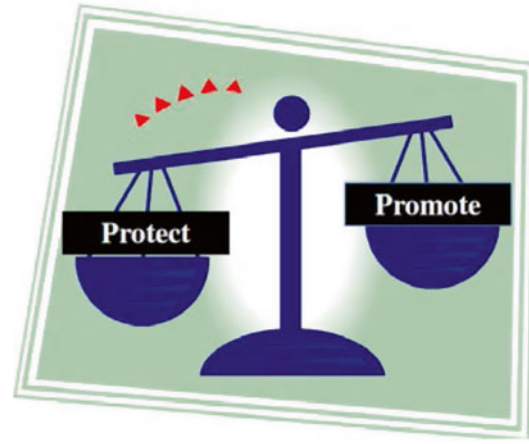

Fig. 17.5 Cartoon representing efforts by regulatory bodies to protect the patient may outweigh the promotion of new radiopharmaceuticals

In order to mitigate such consequences, appropriate structures must be established and appropriate activities consistent with to put in place the intended course of actions. Comprehensive and up-to-date laws, competent human resources, freedom from political and commercial influence, clear and transparent standards and procedures, outcome-oriented implementation, and systematic monitoring and evaluation are critical components expected to contribute for effective radiopharmaceutical regulation. Government agencies are required to encourage entrepreneurial teams to identify and pursue market applications for new radiopharmaceuticals through direct engagement with industry, entrepreneurs, and investors. Translation of scientific discoveries into effective radiopharmaceuticals for patient care is one of the most exciting, satisfying, and complex challenges. The opportunity to translate these developments will have benefits not only for patients, but also for providers and payers and also the industrial and economic sectors that traditionally have not been associated with radiopharmaceuticals. This critical path must be finely orchestrated to infuse innovation for radiopharmaceutical production and market stabilization

through novel means with long-term viability and practices in order to make industry investments worthwhile from a business perspective.

17.13 Summary

The goal of this final chapter was to navigate the reader through the complex maze of regulatory and marketing authority requirements for introduction of a radiopharmaceutical drug for human use. From "bench to bedside" is a catchy phrase, but really very accurately describes in a simple manner the early efforts at the chemical bench which must precede in general by many years the introduction of a radiopharmaceutical into clinical practice for patient use. The navigation of a newly developed and promising radiopharmaceutical through the required regulatory maze in the current environment of GMP production, marketing and clinical acceptance and implementation, is a timely and expensive task. From a purely technical perspective, frustration is encountered when promising new radiopharmaceutical agents drop from the developmental chain early in the scenario because of issues which are unrelated to the expected, or proven, efficacy of the new agent. Of course in the contemporary climate, it is an absolute necessity to have patent protection (IP), so the very high costs of commercialization, regulatory, and marketing authority can be justified. In may seem unreasonable that radioisotopes/radiopharmaceuticals which are administered at very high specific activity and well below any pharmacological threshold still must meet the same standards as for all other drugs, but in reality, there must be this safety net for patient protection.

References

Bacher K, Thierens HM. Accurate dosimetry: an essential step towards good clinical practice in nuclear medicine. Nucl Med Commun. 2005;26(7):581–6.

Belanger AP, Byrne JF, Paolino JM, DeGrado TR. Use of pressure-hold test for sterilizing filter membrane integrity in radiopharmaceutical manufacturing. Nucl Med Biol. 2009;36(8):955–9.

Brown S, Baker MH. The sterility testing of dispensed radiopharmaceuticals. Nucl Med Commun. 1996; 7(5):327–36.

Butler D. Translational research: crossing the valley of death. Nature. 2008;453:840–2.

Callahan RJ, Chilton HM, Ponto JA, Swanson DP, Royal HD, Bruce AD. Procedure guideline for the use of radiopharmaceuticals. J Nucl Med Technol. 2007;35(4):272–5.

Castronovo Jr FP. Audits of radiopharmaceutical formulations. Am J Hosp Pharm. 1992;49(3):584–90.

Cervera-Padrell AE, Skovby T, Kiil S, Gani R, Gernaey KV. Active pharmaceutical ingredient (API) production involving continuous processes – a process system engineering (PSE)-assisted design framework. Eur J Pharm Biopharm. 2012;82(2):437–56.

Chen M, Rhodes BA, Larson SM, Wagner Jr HN. Sterility testing of radiopharmaceuticals. J Nucl Med. 1974; 15(12):1142–4.

Cohen Y. Views on quality tests of radiopharmaceuticals. J Radioanal Chem. 1975;26(2):317–25.

Cox JA, Hesslewood SR, Palmer AM. A mechanism for professional and organizational audit of radiopharmacy departments. Nucl Med Commun. 1994;15(11):890–8.

De Vos FJ, De Decker M, Dierckx RA. The good laboratory practice and good clinical practice requirements for the production of radiopharmaceuticals in clinical research. Nucl Med Commun. 2006;26(7):575–9.

Decristoforo C, Peñuelas I. Towards a harmonized radiopharmaceutical regulatory framework in Europe? Q J Nucl Med Mol Imaging. 2009;53(4):394–401.

Decristoforo C, Elsing P, Faivre-Chauvet A, Farstad B, Meyer G, Mikolajczak R, Penuelas I, Unak P, Wester G. The specific case of radiopharmaceuticals and GMP – activities of the Radiopharmacy Committee. Eur J Nucl Med Mol Imaging. 2008;35(7):1400–1.

Dickson M, Gagnon JP. Key factors in the rising cost of new drug discovery and development. Nat Rev Drug Discov. 2004;3:417.

DiMasi JA, Grabowski HG. Economics of new oncology drug development. J Clin Oncol. 2007;25:209.

DiMasi JA, Hansen RW, Grabowski HG. The price of innovation: new estimates of drug development costs. J Health Econ. 2003;22(2):151–85.

Duatti A, Bhonsle U. Strengthening radiopharmacy practice in IAEA Member States. Semin Nucl Med. 2013;43(3):188–94.

Eberlein U, Bröer JH, Vandevoorde C, Santos P, Bardiès M, Bacher K, Nosske D, Lassmann M. Biokinetics and dosimetry of commonly used radiopharmaceuticals in diagnostic nuclear medicine – a review. Eur J Nucl Med Mol Imaging. 2011;38:2269–81.

Elliot AT, Hilditch TE, Murray T, McNutty H. The design and construction of a central radiopharmacy. Nucl Med Comm. 1993;14:328–34.

Elsinga P, Todde S, Penuelas I, Meyer G, Farstad B, Faivre-Chauvet A, Mikolajczak R, Westera G, Gmeiner-Stopar T, Decristoforo C. Guidance on current good radiopharmacy practice (cGRPP) for the small-scale preparation of radiopharmaceuti-

cals. Eur J Nucl Med Mol Imaging. 2010;37(5): 1049–62.
Freudenberg LS, Beyer T. Subjective perception of radiation risk. J Nucl Med. 2011;52:29S–35.
Gnau TR, Maynard CD. Reducing the cost of nuclear medicine: sharing radiopharmaceuticals. Radiology. 1973;108(3):641–5.
Gouveia BG, Rijo P, Gonçalo TS, Reis CP. Good manufacturing practices for medicinal products for human use. J Pharm Bioall Sci. 2015;7:87–96.
Hall JE. The promise of translational physiology. Am J Physiol. 2002;283(2):E193–4.
Harapanhalli RS. Food and Drug Administration requirements for testing and approval of new radiopharmaceuticals. Semin Nucl Med. 2010;40(5): 364–84.
Hayashi K, Douhara K, Kashino G. Evaluation of the bubble point test of a 0.22-μm membrane filter used for the sterilizing filtration of PET radiopharmaceuticals. Ann Nucl Med. 2014;28(6):586–92.
Heller SL. Radiation safety in the central radiopharmacy. Semin Nucl Med. 1996;26(2):107–18.
Herrling P. Patent sense. Nature. 2007;449:174–5.
Jornitz MW. Integrity testing. Adv Biochem Eng Biotechnol. 2001;98:143–80.
Khurshid SJ, Sadiq MZ. Quality assurance in nuclear medicine-biological quality control of radiopharmaceuticals. Pak J Pharm Sci. 1996;9(1):43–54.
Kowalsky RJ. A basic overview of radiopharmaceuticals and their relationship to nuclear pharmacy practice. J Pharm Pract. 1989;2(3):139–47.
Kumar V, Sunder N, Potdar A. Critical factors in developing pharmaceutical formulations–an overview. Part 2. Pharm Technol. 1992;16:86–8.
Lass P, Scheffler J. Undergraduate teaching of nuclear medicine in European universities. Eur J Nucl Med Mol Imaging. 2003;30(7):1018–23.
Lipsky MS, Sharp LK. From idea to market: the drug approval process. J Am Board Fam Pract. 2001;14(5):362–7.
Norenberg JP, Petry NA, Schwarz S. Operation of a radiopharmacy for a clinical trial. Semin Nucl Med. 2010;40(5):347–56.
Nunn AD. The cost of developing imaging agents for routine clinical use. Invest Radiol. 2006;41(3):206–12.
Nunn AD. The cost of bringing a radiopharmaceutical to the patient's bedside. J Nucl Med. 2007;48:169.
Otte A, Maier-Lenz Dierckx RA. Good clinical practice: historical background and key aspects. Nucl Med Commun. 2005;26(7):563–741.
Ramírez de Arellano I, Piera C, Pavia J, Setoain J. Experiences in setting up the first centralized radiopharmacy in Spain. Nucl Med Commun. 1999;20(3):279–85.
Reichert JM. Trends in development and approval times for new therapeutics in the United States. Nat Rev Drug Discov. 2003;2:695.
Schelbert HR. Nuclear medicine at a crossroad. J Nucl Med. 2011;52:10S–5.
Seddon BM, Workman P. The role of functional and molecular imaging in cancer drug discovery and development. Br J Radiol. 2003;76(Spec No 2):S128.
Wang SC. Nuclear medicine training in china. Eur J Nucl Med. 1996;10:1405–7.
Woldring MG. Radiopharmaceuticals and good radiopharmacy practice. Pharm Weekblad Sci Ed. 1999;3(1): 1285–301.
Zigler SS. Instrumentation and radiopharmaceutical validation. Q J Nucl Med Mol Imaging. 2009;53(4): 402–10.

Glossary: Definitions and Terminology

Active Pharmaceutical Ingredient (API) refers to a substance or substance combination that is used as an active substance or excipient for the preparation of radiopharmaceuticals for human use. It may be used as such or as a starting material for subsequent formulation to prepare radiopharmaceutical. API also refers to the active or central ingredient in the radiopharmaceutical which causes the direct effect for diagnosis or treatment.

Antibody (Ab) is an immunoglobulin molecule that is produced in response to an antigen and forms a specific complex with it. By becoming attached to antigens on infectious organisms, antibodies can render them harmless or cause them to be destroyed.

Aseptic Technique consists of a set of scrupulous specific practices or rules and procedures conducted under controlled conditions to prohibit or minimize the chance of contamination. It is adopted during the preparation of radiopharmaceuticals to maximize and maintain asepsis, the absence of pathogenic organisms.

Bacterial Endotoxin (BET) Test is used to detect or quantify any endotoxins which may be present from gram-negative bacteria using amebocyte lysate from the horseshoe crab (*Limulus polyphemus* or *Tachypleus tridentatus*). Endotoxins are only permitted at very low levels because of high fevers which they cause.

Batch is defined as the quantity radiopharmaceutical or radiochemical obtained in one production. The units are often expressed either in mass (mg or gram), volume (mL or L), total radioactivity (Ci or GBq), or total number of vials or doses.

Becquerel (Bq) is the unit of radioactivity. One becquerel is equal to 1 disintegration per second.

Biological Half-Life is the time required for half the radioactive material to be excreted by the body by natural processes.

Carrier-Free (CF) refers to radionuclides having maximum theoretical specific activity values when all the atoms contain one isotope of the element. Carrier-free thus denotes a radionuclide having 100 % isotopic abundance, i.e., free from any stable isotopes.

Chelating Agent is a compound whose molecules can form several coordinate covalent bonds to a single metal ion.

Chemical Purity is defined as the fraction of the chemical of interest in the specified chemical form. It is the measure of the degree to which a chemical substance is undiluted or unmixed with extraneous material. In monographs, radiopharmaceutical preparation chemical purity is controlled by specifying limit on chemical impurities.

Clean Room is a controlled environment, typically used for the production of radiopharmaceuticals, where concentration of dust, airborne microbes, aerosol particles, and chemical vapors are controlled to specified very low limits.

Cold Kits are freeze-dried injectable substrates ready for radioisotopic labeling which do not need refrigeration, which are prepared by lyophilization. They can be stored at ambient temperatures, have a long shelf life, and can be completely instantly reconstituted with radioactive solution.

F.F. (Russ) Knapp, A. Dash, *Radiopharmaceuticals for Therapy*, DOI 10.1007/978-81-322-2607-9

Critical Organ is also referred to as the physiological system that is functionally essential for the body and would receive the highest radiation dose from a radioactive material after administration of radioactivity.

Curie (Ci) is the unit of radioactivity that is defined as 3.7×10^{10} disintegrations per second.

Dispensing is the process of aliquoting bulk radioactive solution into unit dose forms, subject to release before medical administration.

Dosage is a general term for the activity level of a radiopharmaceutical administered, generally defined in millicurie (mCi) or millibecquerel units (mBq).

Freeze Drying (Lyophilization) is a drying process in which water is sublimed from a product after it is frozen and placed under a vacuum allowing the ice to change directly from solid to vapor without passing through a liquid phase. This drying process is applicable for the manufacture of certain pharmaceuticals and biologicals that are thermolabile or otherwise unstable in aqueous solution for prolonged storage periods, but that are stable in the dry state.

Half-Life ($t_{½}$) is the time required for one half quantity of a radionuclide to decay to half its initial value. It is a unique characteristic of a radionuclide and related to the decay constant (λ) by $t_{½} = 0.693/\lambda$.

Hot Cells are shielded nuclear radiation containment chambers equipped with remote handling accessories designed to control and manipulate the equipment during the radioisotope processing and during preparation and dispensing of radiopharmaceuticals.

Isotope is an element with similar chemical makeup and the same atomic number, but different atomic weights to another or others. The atoms of isotopes have the same number of protons in the nucleus, but different number of neutrons.

Isotopic Carrier is a stable isotope of the element either present or added to the radioisotope of the same element. It differs only in *isotopic* composition from the radioisotope with which it is mixed and dilutes the SA.

Isotope Dose Calibrator is an instrument used for the activity measurements of radiopharmaceuticals administered in nuclear medicine. The displayed activity readout is based on the ionization current measured as photons emitted by a radioactive source that interacts with the gas in a sealed, gas-filled ionization chamber which has a convenient shape and capacity for various-size vials, syringes, and other containers.

Kit for Radiopharmaceutical Preparation is a set of nonradioactive reagents which are reconstituted and/or combined with a radionuclide following the protocol suggested by the manufacturer for preparing the final radiopharmaceutical formulations or radiolabeled derivative which then allows it to be easily administered to the patient for diagnosis or therapy. Such kits are also often referred to as "cold kits," as they are devoid of radioactivity.

Labeled Compound is a chemical compound in which part of the molecules are *labeled* with a radionuclide or radioisotope. The radionuclide is as an integral component of the molecule.

No Carrier Added (NCA) radionuclide is characterized as no carrier added (NCA or n.c.a.) in which no carrier atoms have been added and for which precautions have been taken to minimize contamination with stable isotopes of the element in question. It does not necessarily mean, however, 100 % isotopic abundance.

Nuclide (from nucleus) is the specific constitution of an atom characterized by its mass number "A," its atomic number "Z," and by its nuclear energy state.

Parenteral is a term indicating the drug administration route other than oral intake. Parenteral radiopharmaceutical dosage forms are intended for administration as an injection or infusion. Common injection routes are intravenous (into a vein), subcutaneous (under the skin), and intramuscular (into muscle). Infusions typically are given by the intravenous route.

Radiopharmaceutical is any radioactive pharmaceutical or compound in a form suitable for administration to humans for diagnostic imaging or therapy.

Radiopharmaceutical Precursor is a chemical compound or ligand used as a starting material for the radiolabeling process for preparation of the radiopharmaceuticals. It

could either be an inactive chemical compound, API, or a radiolabeled intermediate produced for the preparation of radiopharmaceutical formulation prior to administration.

Radioactivity is defined as the spontaneous emission of particles (alpha, beta, neutron) or radiation (gamma, K capture), or both at the same time, from the decay of an unstable nuclide.

Radioactive Concentration (RAC) refers to the number of nuclear disintegrations per unit time (the radioactivity) of a radionuclide per unit volume of the radioactive preparation.

Radiochemical Purity is defined as the fraction of radioactivity of the radionuclide of interest in the desired chemical form to the total radioactivity of that radionuclide present in the preparation.

Radiolysis is a process by which radiolabeled compounds or radiopharmaceuticals are unstable in a radiation field and decompose.

Radionuclide is an unstable form of a nuclide that is radioactive and decays by the emission of nuclear radiation (alpha, beta, gamma, neutron, or K capture) to attain stability. The initial unstable nuclide is referred to as the "parent radionuclide" and the nuclide after transformation as the "daughter nuclide."

Radionuclide Generator is a self-contained system housing an equilibrium mixture of a parent–daughter radionuclide pair and designed to specifically remove the daughter radionuclide formed by the decay of a parent radionuclide which is free from the parent.

Radionuclide Precursor is any radionuclide produced for the radiolabeling of another substance prior to patient administration.

Radionuclidic Purity is defined as the fraction of the radioactivity of the desired *radionuclide* to the total radioactivity of the stated radionuclide. Any extraneous radioactivity is considered as an impurity.

Specific Activity (SA) is defined as the activity of a radionuclide divided by the mass (or molar amount) of the sum of all radioactive and stable nuclides (present in the same chemical and physical form) isotopic with the element involved. Effective specific activity is used to describe the mass or molar quantity of a single species radiotracer relative to the total mass or molar quantity of the radiotracer and nonradioactive compound(s) that has similar biochemical properties. Units are often mCi/mg, Ci/gm, etc.

Sterility specifies the absence of any viable bacteria or microorganism in a radiopharmaceutical preparation. All radiopharmaceuticals for human administration must be sterilized by suitable means.

Total Radioactivity is defined as the fraction of the radioactivity of the radionuclide per unit volume of the dispensed formulation (vial, capsule, ampoule, generator, etc). It constitutes an important parameter in dispensing and patient administration of radiopharmaceuticals as well as from regulatory requirements for the safe handling of radiopharmaceuticals in a radiopharmacy and hospital setting.